Fluides et instabilités sismiques : implications pour le comportement mécanique de la croûte supérieure

Jean-Robert Grasso

THESE

présentée par

Jean-Robert GRASSO

Pour obtenir le titre de DOCTEUR ES SCIENCES de

l'UNIVERSITE JOSEPH FOURIER - GRENOBLE I

Fluides et instabilités sismiques : implications pour le comportement mécanique de la croûte supérieure

---

Date de soutenance : 26 février 1993

Composition du jury :

M.	R.	MADARIAGA	Président
M.	Y.	GUEGUEN	Rapporteurs
M.	A.	McGARR	
M.	M.	ZOBACK	
M.	P.	VIALON	Directeur de thèse
M.	M.	CAMPILLO	Examinateurs
M.	D.	SORNETTE	
M.	V.	MAURY	Invité

LGIT / IRIGM - Observatoire de Grenoble
FRANCE

THESE de DOCTORAT

Titre de l'ouvrage :

FLUIDES ET INSTABILITES SISMIQUES : IMPLICATIONS POUR LE COMPORTEMENT MECANIQUE DE LA CROUTE SUPERIEURE

Nom de l'auteur :

Jean-Robert GRASSO

Etablissement :

Université Joseph Fourier - Grenoble I

RESUME

Sur la base des faibles variations de contraintes poroélastiques qui sont à l'origine de la séismicité déclenchée localement par la baisse de pression du gisement de Lacq, on tente dans le chapitre 3 d'évaluer les échelles spatiales des connections fluides dans la croûte supérieure à l'aide de la migration des fronts de pression induits. Les séismes associés à la mise en eau d'une retenue artificielle (M 4-5, Monteynard, Vercors, France) permettent par exemple de cartographier des failles sismiques potentielles au sud de l'agglomération grenobloise, les séismes induits jouant alors le rôle de jauges de contrainte. Dans la région de Lacq, à l'aide de modélisations analytiques des transferts de contraintes visco-élastiques et poro-élastiques, on montre qu'on ne peut rejeter a-priori des interactions entre l'extraction du champ de Lacq, les séismes majeurs de la faille Nord-Pyrénéenne distants d'une trentaine de kilomètres, et les séismes locaux à l'aplomb du champ d'hydrocarbure.

Le chapitre 4 constitue une synthèse des mécanismes d'instabilités sismiques déclenchées par les exploitations d'hydrocarbures. On isole trois classes de mécanismes de déclenchements des séismes correspondant à des types d'exploitations et à des réponses sismiques (taille-temps-espaces) bien différenciés : augmentation de pression due à l'injection de fluide ; baisse de pression due à extraction de fluide, déficit de masse lors d'extraction massive. Les mécanismes de ruptures sont en accord avec les lois de contraintes effectives, et s'expliquent soit par des transferts poroélastiques soit par des compensations isostasiques. Si la sismicité induite par les extractions de fluides reste marginale par rapport au nombre de gisements exploités, la surveillance sismique fine effectuée sur les gisements montre que de nombreux petits séismes (M < 3) sont présents et permettent un suivi in-situ du comportement des réservoirs au cours de l'exploitation.

Notre approche de la séismicité à l'aide des séismes induits par des activités humaines montre les limites des lois de la mécanique classique qui, si elles permettent de comprendre et d'évaluer les seuils critiques qui déclenchent les instabilités sismiques, ne peuvent expliquer ni la durée des phénomènes d'instabilités qui sont entretenus durant de nombreuses années ni la taille des instabilités sismiques (Mmax 7). Sur la base des cas mondiaux de séismicité induite on propose la notion de Systèmes Critiques Auto-Organisés Induits où l'on peut observer la genèse, la pérennité et la disparition de systèmes critiques dans un contexte, proposé par ailleurs, d'état critique auto-organisé pour l'ensemble de la croûte supérieure.

MOTS CLES

Fluides et failles ; Fractales ; Gazli ; Hydrocarbures ; Lacq ; Mécanique de la croûte ; Monteynard ; Sismicité induite.

THESE

présentée par

Jean-Robert GRASSO

Pour obtenir le titre de DOCTEUR ES SCIENCES de

l'UNIVERSITE JOSEPH FOURIER - GRENOBLE I

Fluides et instabilités sismiques : implications pour le comportement mécanique de la croûte supérieure

---

Date de soutenance : 26 février 1993

Composition du jury :

M.	R.	MADARIAGA	Président
M.	Y.	GUEGUEN	Rapporteurs
M.	A.	McGARR	
M.	M.	ZOBACK	
M.	P.	VIALON	Directeur de thèse
M.	M.	CAMPILLO	Examinateurs
M.	D.	SORNETTE	
M.	V.	MAURY	Invité

LGIT / IRIGM - Observatoire de Grenoble
FRANCE

A Marion

...Vous verrez par vous même qu'on peut tirer du miel des pierres et de l'huile des rochers les plus durs.
(St Bernard de Clairvaux, 1133)

REMERCIEMENTS

co-auteurs

-R. **Bossu** (LGIT-Grenoble)
-J.C. **Chatelain** (ORSTOM-Nouméa)
-D. **Fabre** (LGM-Grenoble)
-B. **Feignier** (Queen's University-Canada)
-J. **Fréchet** (LGIT-Grenoble)
-D. **Fourmaintraux** (Elf-Pau)
-M. **Frogneux** (IPGS- Strasbourg)
-J.F. **Gamond** (LGIT-Grenoble)
-J.P. **Gratier** (LGIT-Grenoble)
-F. **Guyoton** (CapGeophys-Grenoble)
-V. **Maury** (Elf-Pau)
-B. **Nurtiev** (ISL-Tashkent)
-Y. **Orengo** (LGM-Grenoble)
-J.C. **Paumier** (Maths Appli., Grenoble)
-L.M. **Plotnikova** (ISL-Tashkent)
-P. **Segall** (Stanford Univeristy- Californie)
-P. **Volant** (LGIT-Grenoble)
-G. **Wittlinger** (IPGS- Strasbourg)

réalisation technique- direction scientifique -arrangements divers

-M. **Lambert**
-R. **Guiguet**
-L. **Jenatton**

P. **Vialon** (LGIT-Grenoble)

J. Blanchet (LGIT-Grenoble)
M. Prot (LGIT-Grenoble)

support financier

-Elf
-INSU (programmes DBT-Instabilités et Tectoscope)
-Pôle Grenoblois Risques Naturels
-Académie des sciences d'Ousbékistan

remerciements spéciaux à Georges Poupinet, Directeur du LGIT et responsable du Pool Lithoscope, pour sa confiance et ses encouragements constants

INTRODUCTION

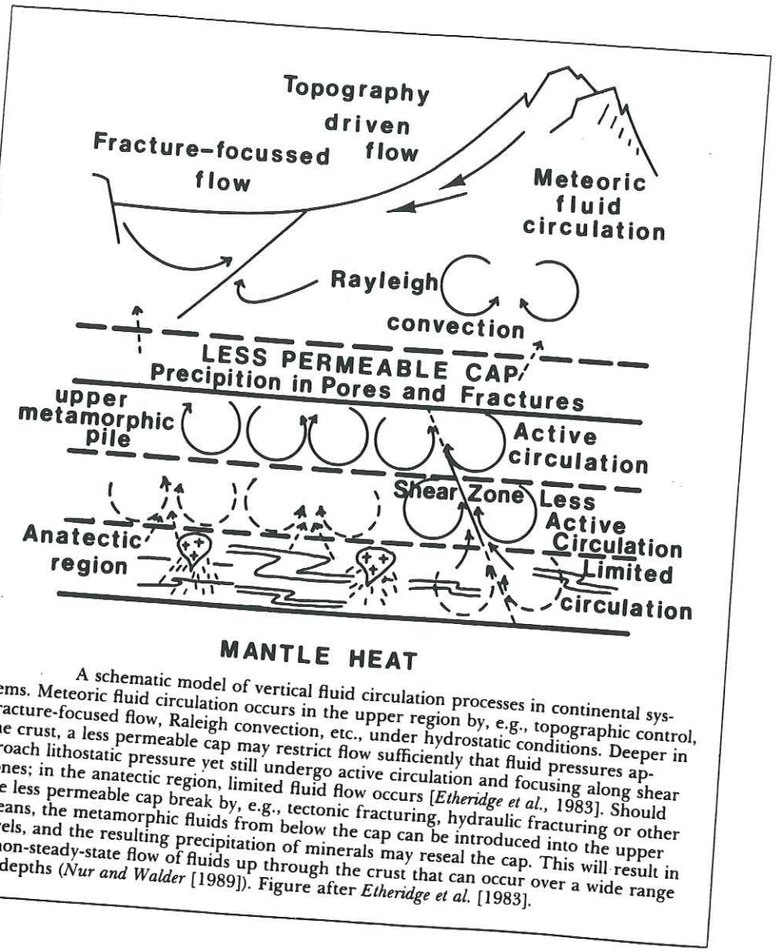

A schematic model of vertical fluid circulation processes in continental systems. Meteoric fluid circulation occurs in the upper region by, e.g., topographic control, fracture-focused flow, Raleigh convection, etc., under hydrostatic conditions. Deeper in the crust, a less permeable cap may restrict flow sufficiently that fluid pressures approach lithostatic pressure yet still undergo active circulation and focusing along shear zones; in the anatectic region, limited fluid flow occurs [*Etheridge et al.*, 1983]. Should the less permeable cap break by, e.g., tectonic fracturing, hydraulic fracturing or other means, the metamorphic fluids from below the cap can be introduced into the upper levels, and the resulting precipitation of minerals may reseal the cap. This will result in a non-steady-state flow of fluids up through the crust that can occur over a wide range of depths (*Nur and Walder* [1989]). Figure after *Etheridge et al.* [1983].

FLUIDES ET INSTABILITES SISMIQUES: IMPLICATIONS POUR LE COMPORTEMENT MECANIQUE DE LA CROUTE SUPERIEURE

FLUIDES ET RUPTURES

Dans le domaine de la mécanique de la croûte terrestre, pour les sciences de la terre, les dernières décennies ont été dominées par deux concepts: la dynamique des plaques et les lois de pression effective. Si le premier concept a été très médiatisé et est maintenant perfectionné et modifié pour permettre des études à plus petites échelles, en particulier dans les domaines définis comme intraplaque, la rentabilité, en terme d'impact scientifique, du concept de pression effective s'avére d'années en années grandissante.

La séismicité induite par la mise en eau de retenue artificielle et les injections de fluide avait dans les années 1960-1970 permis de vérifier in-situ a Denver (Colorado) les lois de pression effective, les critères de Coulomb et les propriétés des coefficients de friction (Figure 1 d'aprés Gough, 1979). La population géophysicienne avait alors admit le rôle des fluides dans les modifications du comportement mécanique des roches de la croûte terrestre. On notera que lors de l'expérience de Denver la corrélation entre l'augmentation de la pression du fluide injectée et le nombre de séismes est très satisfaisante tant spatialement que temporellement sur une période de 5 années (Figure 2, Grasso, 1993). Toutefois si l'on s'intéresse à la corrélation entre l'énergie libérée par les séismes, donc la taille des séismes déclenchés, et la pression du fluide, il est clair que les plus gros événements, 3 séismes de magnitudes ≥ 5, ont eu lieu respectivement, 14, 18, 21 mois après la fin des injections et à des distances du puits injecteur d'un ordre de grandeur supérieures à celles des petits séismes situés au voisinage du puits. Ces informations furent publiés plus tardivement (Hsieh et Bredehoft, 1981) et n'ont pas sensibilisé de façon significative les sismologues dont la structuration en terme de fluide est principalement construite à partir de la corrélation entre la pression et les petits séismes de Denver en négligeant les effets distants dirigés par des contraintes apparemment trop faible.

L'idée fédératrice de l'ensemble des travaux qui sont rassemblés dans cette thèse est l'étude d'instabilités sismiques déclenchées par de faibles perturbations de contrainte avec une attention particulière sur le rôle des fluides dans ces instabilités, soit en tant que vecteur de transfert de contrainte soit par leur rôle en terme de pression effective.

Dans un contexte plus généraliste, les fluides comme vecteur de transfert de contrainte sont utilisés pour expliquer à la fois les phénomènes pré- et post-

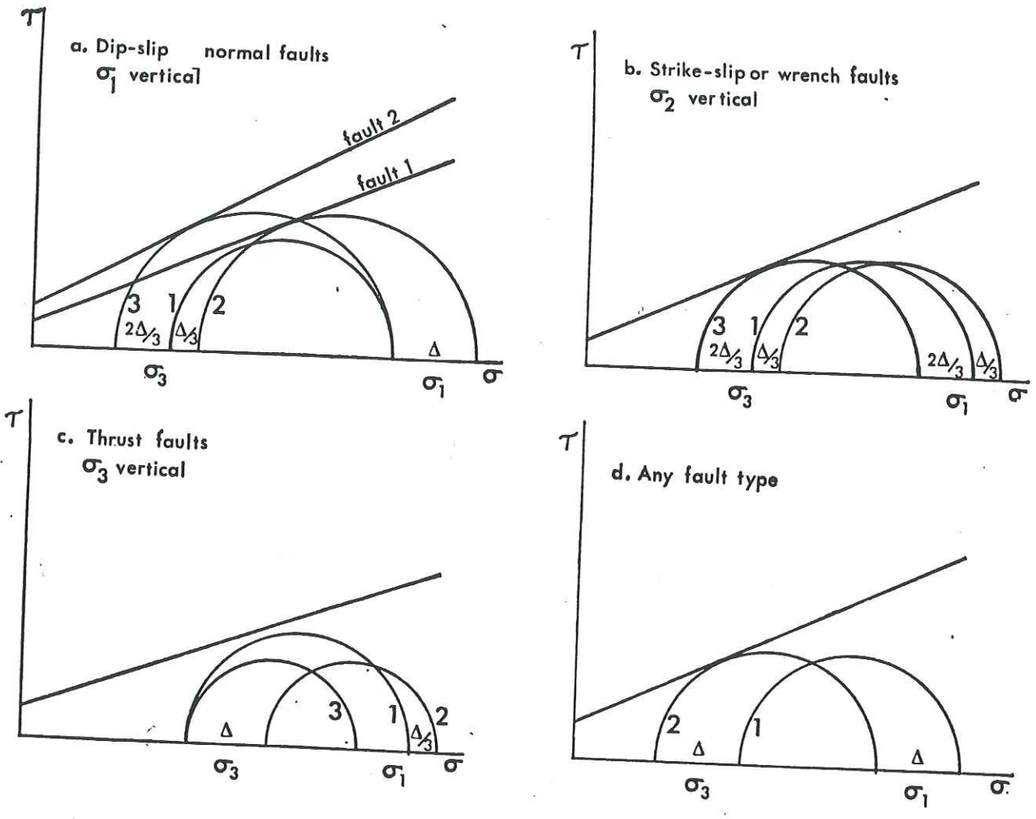

Mohr failure criterion for faults having Coulomb friction.

a, *b*, *c*; faults under a large reservoir of depth h. $\Delta = \rho g h$. In case *a*, earthquakes are trigge on fault 1 by the increment to the elastic stresses, on fault 2 by the later rise of water-pre in pores and cracks. Circles 1, initial stress; Circles 2, initial stress + elastic load; Circ (initial + elastic load) stress − increase of water pressure.

d, Initial stress (circle 1) and effective stress (circle 2) after rise in water pressure in rock either by rise in the water-table near a reservoir, or by increase of water pressure near an well.

Figure I1

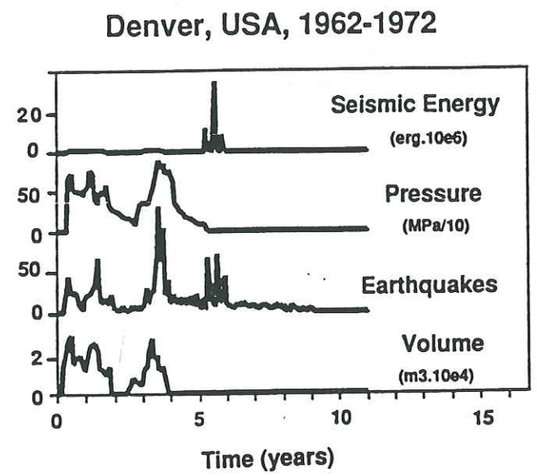

Denver earthquakes and fluid injection. From bottom to top: a) History of injected fluid volume; b) history of number of locally induced earthquakes; c) fluid pressure history; d) history of seismic energy release. Note the correlation between pressure history and the number of induced events during the first five years. Nevertheless, the correlation fails regarding seismic energy and pressure history. These major shocks ($M \approx 5-5.5$) occur respectively 18, 21 and 24 months after the injection ended, at larger distances from the injection well than the earliest small shocks (adapted from HEALY *et al.*, 1968).

Figure I2

Mohr circle representation of stress states

(Illustrated as critical for *strike-slip* failure in the vertical fault zone and for *thrust* failure in the adjacent crust)

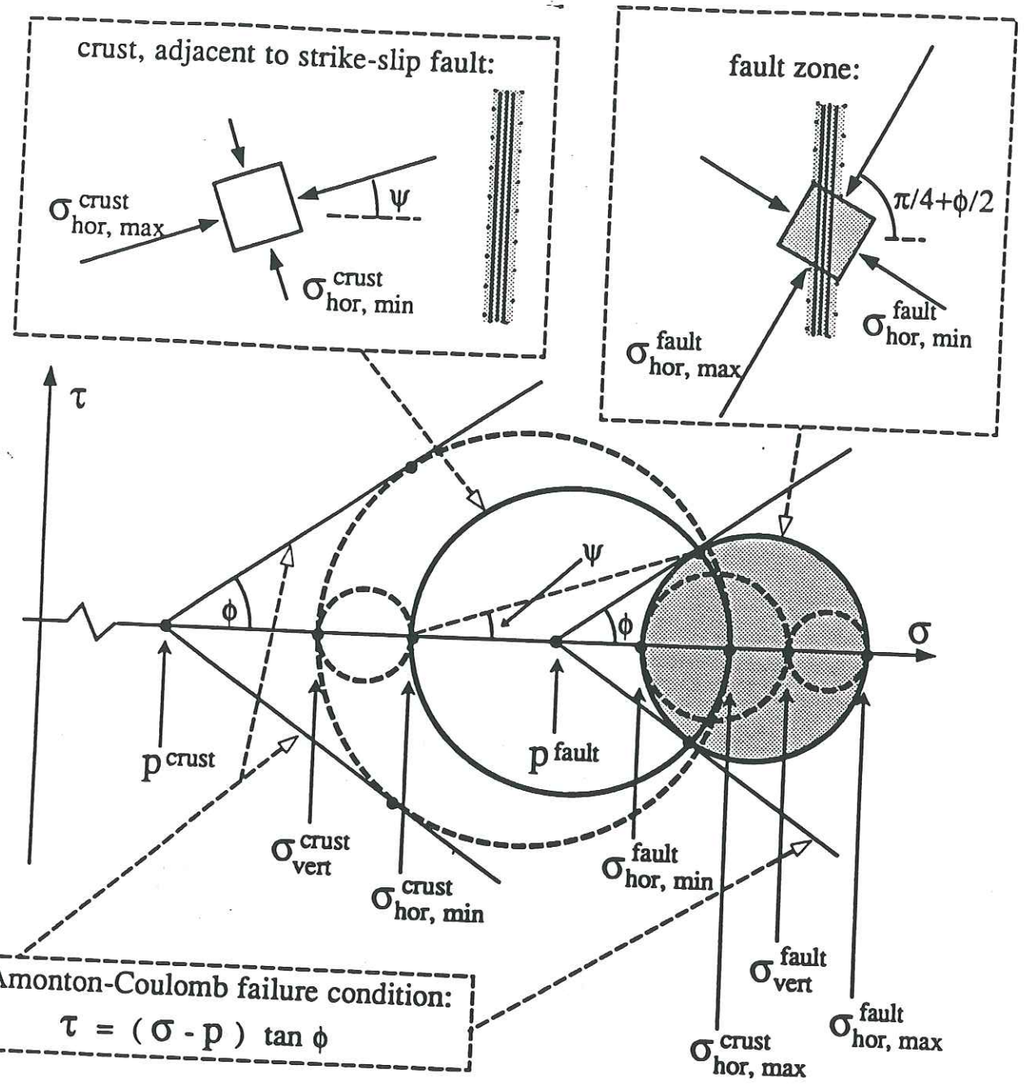

[drawn for $\phi = 35°$ ($\tan\phi = 0.7$) and $\psi = 18°$]

FAULT STRESS STATES, PORE PRESSURE DISTRIBUTIONS, AND THE WEAKNESS OF THE SAN ANDREAS FAULT

James R. Rice

To be published in *FAULT MECHANICS AND TRANSPORT PROPERTIES OF ROCK: A Festchrift in Honor of W. F. Brace* (based on June 1990 symposium at MIT), edited by Brian Evans and Teng-fong Wong, Academic Press, 1991:

Figure I3

An earthquake mechanism based on rapid sealing of faults

Michael L. Blanpied, David A. Lockner & James D. Byerlee

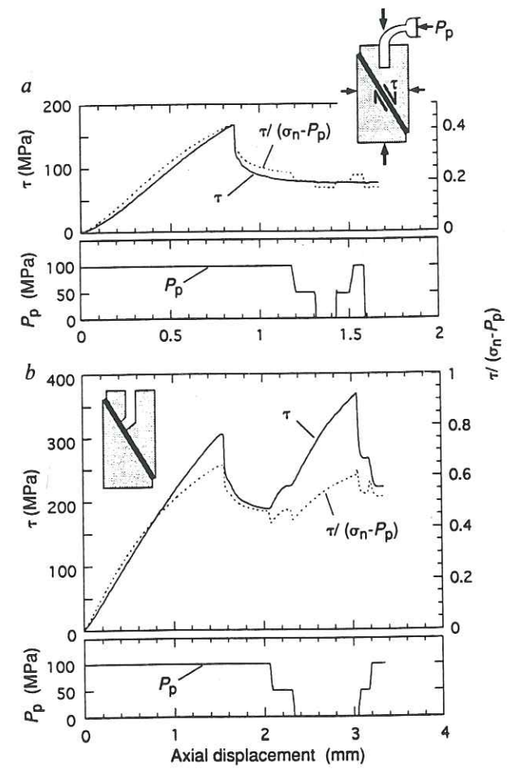

FIG. 1 Shear stress (τ), apparent friction ($\mu_{app} = \tau/(\sigma_n - P_p)$) and imposed H_2O pore pressure (P_p) in sliding tests on granite at 600 °C. Cross-section sketches of cylindrical granite samples (19 mm diameter by 38 mm long) show principal stress directions and sense of sliding. Sawcut 'fault' at 30° to the loading axis contains a 0.5-mm layer of granite powder. Bore hole in the upper forcing block admits H_2O. (For more on the method, see ref. 37.) *a*, Sample with blind bore hole shows elastic loading to a low peak stress. Onset of shear is accompanied by rapid decay of strength to a remarkably low level. Shear stress does not respond to large, imposed steps in P_p, showing that the sample has become sealed. Apparent friction responds because we calculate it assuming P_p in the fault is known. *b*, Sample with hole through to fault shows the expected higher peak and residual strengths. Shear stress responds strongly to steps in P_p, demonstrating fluid communication.

NATURE · VOL 358 · 13 AUGUST 1992

Figure I4

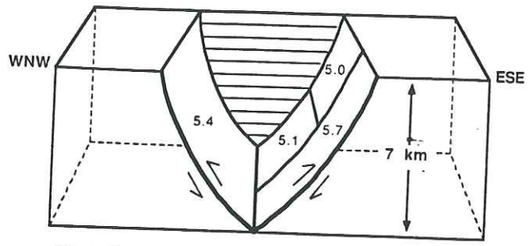

Block diagram, viewed looking NNE, of the V-shaped pattern defined by the main rupture planes in the Miramichi earthquake sequence (after Wetmiller *et al.* 1984).

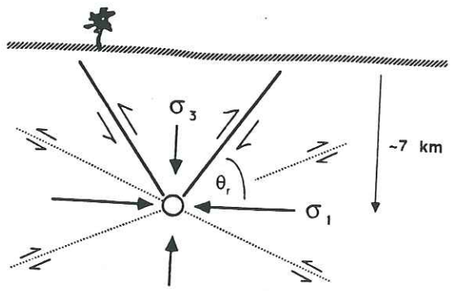

Schematic WNW–ESE section through the Miramichi ruptures showing the reactivation angle, θ_r, in relation to the inferred stress trajectories. Light dotted lines delineate expected orientation of thrusts formed by shear failure of intact rock in the same stress field.

Figure I5

sismiques. Ces observations et modèles furent utilisés pour comprendre par exemple la migration des répliques après un séisme majeur. Des variantes plus complexes sont mis en œuvre actuellement pour tenter d'expliquer la faible contrainte de cisaillement qui parait mobiliser les rejeux de failles majeures (figure 3, d'aprés Rice 1990). Certains auteurs proposent que les fluides piégés dans la zone faillée, avec une pression supérieure à la pression hydrostatique, permettent une réactivation des déplacements sur la faille par de faibles contraintes effectives. Dans le cas de la faille de San Andreas, référence de discontinuité réactivée, le problème qui actuellement se pose, est la réalimentation en fluide de la faille lors du cycle sismique. Des poches isolées dans la zone faillée semblent pouvoir exister sur la base d'expérience de laboratoire (Figure 4, d'aprés Blanpied et al. 1992). Dans le domaine intraplaque des processus analogues sont proposés pour expliquer la réactivation de failles mal-orientées par rapport aux directions déduites du critère de rupture de Coulomb. Les surpressions de fluide permettent alors, par diminution du coefficient de frottement le rejeu de faille inverse par exemple avec des angles de plus de 50° (Figure 5, d'aprés Sibson 1989). Une revue synthétique du rôle des fluides dans les mécanismes d'instabilités de la crôute supérieure est proposé dans la partie 1 de cette thèse comme une introduction volontairement qualitative.

ECHELLES ET MECANISMES DES DEFORMATIONS SISMIQUES ET ASISMIQUES INDUITES PAR LES FLUIDES

Dans les chapitres 2 à 5, le rôle des fluides dans les mécanismes de ruptures de la croûte superficielles est abordé en utilisant les séismes déclenchés par des activités humaines. Cet approche donne accès à un domaine privilégié où les évaluations des perturbations qui dirigent les instabilités sont à priori connu. La quantification en terme de contrainte gagne donc en précision, par comparaison avec les cas de séismicité naturelle. Les objets étudiés ont une taille décakilométrique et le cas de Lacq détaillé dans le chapitre 2 constitue un des cas mondiaux les mieux cernés où de faibles contraintes (<1 MPa) ont déclenché une activité sismique modérée (1000 événements de magnitudes comprises ente 1 et 4.2) en 20 ans. Cette activité sismique est par ailleurs maintenue durant plus de 20 ans par des perturbations de l'ordre de 0.1 MPa, soit un ordre de grandeur inférieur aux perturbations qui ont déclenché le début de la séquence sismique.

Sur la base des faibles variations de contraintes effectives qui sont à l'origine de la séismicité du champ de lacq, on tente dans le chapitre 3 d'évaluer les échelles spatiales des connections fluides dans la croûte supérieure.

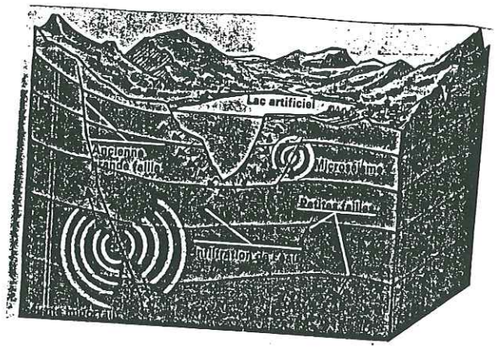

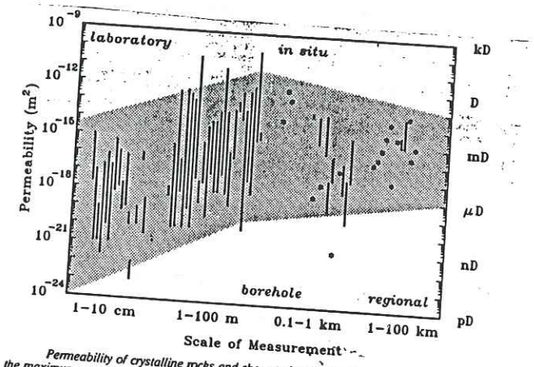

Permeability of crystalline rocks and characteristic scale of measurements: Bars mark the maximum permeability range when several individual values are reported, stars represent single values. The shaded region is a personal view of the data trend. (Table 1 identifies both geographic location and references for all data by their relative position in the plot, from left to right.)

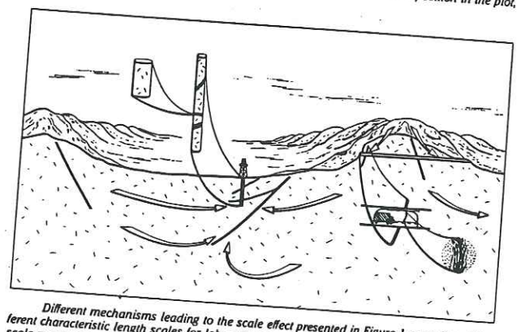

Different mechanisms leading to the scale effect presented in Figure 1 as well as different characteristic length scales for laboratory measurements, borehole tests, and regional scale measurements (illustrated here in a motorway tunnel).

Figure I6

La première partie de ce chapitre chapitre 31 montre comment la surpression de fluide liée à la mise en eau de retenue artificielle peut déclencher des instabilités sismiques dont les distances à la retenue augmentent avec le temps. Les mécanismes proposés pour expliquer ces séismes, qui constitue historiquement les séismes majeurs de la région grenobloises (Mmax =5.3), font appel à des migrations du fluide, donc du front de pression associé à la mise en eau de la retenue. Cette modélisation de la croûte superficielle par un milieu à comportement poro-élastique permet une extension du concept de pression effective. Bien que l'absence de forages profonds empêche un contrôle in-situ des propriétés hydrauliques de la croûte supérieure, déduites de l'activité sismique, la séquence sismique qui s'est développé au sud de la région grenobloise dans la période 1962-1984, permet d'une part, d'estimer des diffusivités hydrauliques en accord avec les valeurs proposés sur d'autres sites (Figure 6, from Clauser Eos, May 1992) sur la base soit de mesure in-situ soit sde la migration des séismes (diffusivités de quelques m^2/s, pour des permabilités variant entre 10^{-13} et 10^{-16} m^2), mais aussi de cartographier les failles sismiques régionales potentielles. En effet les séismes induits se localisent sur des accidents tectoniques qui semblent s'organiser et définir une nouvelle zone potentiellement sismique proche de la mégapole grenobloise. Ces séismes induits permettent alors de jouer le rôle de jauge de contrainte.

En tenant compte des connections spatiales proposées sur différents sites de barrage entre la mise en eau et le déclenchement de séismes, une réflexion sur la quantification des effets distants (>dizaine de km) de l'extraction d'hydrocarbure est proposé dans le chapitre 32 sur la base du cas de Lacq. On montre alors qu'on ne peut rejeter a-priori des interactions entre l'extraction du champ de Lacq, les séismes majeurs de la faille Nord-Pyrénénne, et les séismes locaux à l'aplomb du champ d'hydrocarbure. En effet on peut ajuster les paramètres de modéles analytiques des transferts de contraintes visco-élastiques et poro-élastiques pour expliquer le déclenchement de séismes sur la Faille Nord-Pyrénénne par l'activité industrielle d'une part, et d'autre part, considérer que ces séismes majeurs pyrénéens peuvent eux aussi renforcer l'activité sismique locale sous le champ de Lacq. Les modéles utilisés sont monodimensionnels et très conceptuels, et les résultats sensibles aux paramètres géomécaniques (viscosité du sel en particulier). Toutefois, une combinaison des paramètres géomécaniques appartenant aux intervalles de valeurs réalistes, permet par exemple de concevoir que les changements de contrainte induits par les séismes pyrénéens majeurs peuvent atteindre le champ de Lacq avec un délai d'environ

8 MARDI 16 FEVRIER 1993

lioration du plan social qui accompagne les suppressions d'emplois.

PETROLE. Elf-Aquitaine signe un protocole de coopération avec l'Ouzbékistan. Le pétrolier français prévoit la conclusion rapide d'un contrat pour la production d'hydrocarbures. A moyen terme, il est question de coopération dans le raffinage et le commerce international des produits pétroliers.

survien

M

d

L

m

LIBERATION

deux ans et expliquer ainsi l'augmentation de l'activité sismique au voisinage du champ en 1969, 1981 et 1984

Enfin dans la troisième partie de ce chapitre (Chapitre 33) on tente d'éclairer la géométrie et la cinématique des ruptures sismiques de la région de Gasli où 3 séismes de magnitude supérieure à 7 se regroupent en moins de dix ans autour d'un gisement de gaz du désert du kyzyl-koum (Ousbékistan, Asie Centrale), dans une région considéré comme intraplaque et peu sismique. La géométrie du réseau portable dense mis en oeuvre durant 2 mois en 1991, permet de montrer que l'activité régionale est très faible excepté une concentration de séisme sur des géométrie proche des plans ruptures définies par les séismes majeurs. En particulier la répartition concentrique des pendages des plans de ruptures vers le gisement est un argument important pour contraindre et comprendre les mécanismes de déclenchement de cette séquence. Les informations de cette campagne sont utilisées dans le chapitre suivant qui constitue une synthèse des mécanismes d'instabilités sismiques déclenchées par les exploitations d'hydrocarbures.

Lors de cette synthèse (chapitre 4), sur la base des cas mondiaux, on choisit d'analyser les phénomènes où le couplage entre les différents mécanismes est le plus faible, c'est à dire, les cas où les mécanismes peuvent être clairement individualisé. Cette démarche simplificatrice permet de proposer une synthèse des mécanismes de déclenchements des ruptures sismiques aux voisinages d'exploitations d'hydrocarbures, 17 années après les travaux de Yerkes and Castle (1976). Ces auteurs avaient alors proposés sur la base des cas connus jusqu'alors 2 processus pouvant déclenchés des séismes au voisinage d'extractions d'hydrocarbure: l'injection de fluide, utilisée pour favoriser la récupération secondaire, et les cisaillement induits par les fortes subsidences (de l'ordre de plusieurs métres). La taille des séismes restaient dans la plupart des cas faible (Mmax~3). Les 3 classes de mécanismes que je propose dans le chapitre 4 correspondent à des types d'exploitations et à des réponses sismiques (temps et espaces) bien différenciés: augmentation de pression due à l'injection de fluide et pour la récupération secondaire; baisse de pression due à extraction de fluide, déficit de masse lors d'extraction massive.

Dans le cas des séismes induits par l'injection de fluide, notre contribution principale se situe au niveau des échelles de temps et d'espace à prendre en compte autour d'une exploitation. Les effets d'une injection de fluide sont maintenant clairement démontrer comme n'étant plus confinés temporellement à la période d'injection ni spatialement au proche voisinage des points d'injections. L'effet de la baisse de pression pour le déclenchement de ruptures

Hydromechanical setting of earthquakes triggered by poroelastic stressing caused by hydrocarbon extraction. Average reservoir characteristics are defined as follows: T, thickness; ϕ, porosity; φ, matrix permeability; μ, shear modulus; ν Poisson's ratio; α is a coefficient related to the bulk moduli of saturated rock (K) and the grains in the rock (K_s) by $\alpha = 1 - K/K_s$. Displacement and pressure history are defined by: the onset of production and the date of the first induced event; P_{init} the initial pressure in the reservoir; ΔP, the pressure drop at the onset of seismicity; pressure values are from the yearly bottom of well measurements, with a few bars of accuracy; ΔH is the maximum depth of the subsidence bowl; m_1 is the magnitude of the first reported induced event and m_2 is the maximum magnitude of induced events. $\Delta\sigma_{max}$, the order of magnitude of the induced stress at the onset of the seismicity, is estimated using the poroelastic stress model as follows: (i) For the 8 fields we reported a rough value depending on pressure drop and reservoir geometry: $\Delta\sigma_{max} \approx \alpha[(1-2\nu)/2\pi(1-\nu)] \cdot T/D \cdot \Delta P \cdot F_{max}$ where ΔP, F_{max} are respectively the reservoir pressure drop and a dimensionless function of position and reservoir geometry. A maximum stress change value above the reservoir is $F_{max} \sim 3$ (SEGALL, 1989); for limestone reservoir rocks of fields 1–2 and 4 we assume that $\alpha[(1-2\nu)/2\pi(1-\nu)] \sim 0.1$. (ii) If the subsidence and shear modulus of the rocks involved are known (field 3, 6–7), we check the above estimates by using $\Delta\sigma_{max} \approx [4\mu/(1-\nu)\pi D] \cdot \Delta H_{max}$), where μ, ν, D, H_{max} are respectively the shear modulus, the Poisson's ratio of the rock matrix, the depth of reservoir and the maximum depth of the subsidence bowl

Area or field Country	Strachan[o] Alberta	Fashing[a] Texas	Imogene[a] Texas	Lacq[b] France	Grozny[c] Tchecheny	Assen[d] Netherland	Groningen[d] Netherland	Ekofisk[e] Norway	Dan[f] Danemark
reservoir characteristics									
Size (km^2)	25	10	20	150	70	50	900	130	24
Depth (km)	3-5	3.4	2.4	3.5	4.0	3.0	2.9	3.0	1.8
T (km)	0.1	.05	0.03	0.25	0.4	0.2	0.15	0.2	0.15
Φ (%)	–	15	17	3	4	15	18	30	30
φ (mD)	–	13	7	0.5	–		$0.1\text{-}10^3$	$1\text{-}10^2$	0.1–1
μ (GPa)	–	–	–	23	–	10	10	0.07	–
ν	–	–	–	0.25	–	0.25	0.26	0.3	(0.3)
α	–	–	–	0.25	–	0.9	0.9	1.	(1.)
displacement and pressure history at the onset of Eqs									
Onset Prod. (year)	1971	1958	1944	1959	1964	1972	1964	1973	1972
Onset Eqs (year)	1976	1974	1973	1969	1971	1986	1991	1982	1985
Pinit (MPa)	50	35	25	66	69	37	35	48	26
ΔP (MPa)	25	23	13	30	25	30	15	24	18
ΔH (m)	–	–	–	0.05	–	–	0.16	3.5	–
$m1$	3.0	3.1	2.2	4.0	3.5	2.8	2.5	2.2	4.0
$\Delta\sigma_{max}$ (MPa)	0.25	0.1	0.05	0.6	0.7	0.5	0.2	0.4	0.45
$m2$	3.4	3.4	3.9	4.2	4.1	2.8	2.5	3.4	4.0

[o]from WETMILLER (1986); [a]from PENNINGTON *et al.* (1986); [b]from GRASSO and WITTLINGER (1990); [c]from SMIRNOVA (1977); [d]from NAM (pers. commun., 1992); [e]from PHILLIPS (pers. commun., 1992)

sismiques est par contre nouvellement reporté. Les modéles simples permettent de montrer que le transfert poroélastique de contraintes des niveaux réservoirs vers les niveaux environnant est en accord avec les localisations des ruptures sismiques au dessus et au dessous des réservoirs déplétés. Nous montrons qu'il n'est pas nécessaire d'avoir une subsidence importante pour déclencher et maintenir sur plus d'une dizaine d'années une activité sismique notable (de nombreux séismes de magnitudes comprises entre 3 et 4). Enfin la dernière classe d'instabilités potentiellement déclenchées par l'extraction massive de fluide est basée sur un nombre plus faible d'observations, en accord avec les lois d'échelles qui régissent sur notre planète la fréquence des ruptures par rapport à leur taille (loi de Gutenberg-Richter pour les sismologues). Ces séismes majeurs posent de nombreuse questions sur la mécanique de la croûte terrestre mais rejoignent la taille des grands séismes reliés à la mise en eau de certaines retenues artificielles. Si les deux premiers mécanismes sont indépendant du contexte tectonique et génèrent des ruptures qui restent modérées (M<5) le troisième type nécessite un état de contrainte où la contrainte principale est horizontale et peut, par contre, déclencher des ruptures majeurs (M>6). Cette analyse montrent aussi que la sismicité induite par les extractions de fluides reste marginale par rapport au nombre de gisements exploités et qu'une des questions d'avenir sera de comprendre l'aséismicité (M>3) qui existent sur plus de 90% des champs exploités. Cependant la surveillance sismique du site de lacq, ainsi que les campagnes temporaires effectuées sur quelques autres gisements (Canada, Texas, Hollande) montrent que de nombreux petits séismes (M<3) sont présents et permettent de suivre le comportement des réservoirs au cours de l'exploitation.

Si la synthèse des mécanismes de ruptures aux voisinages des exploitations d'hydrocarbures est une des conclusions de cette thèse en terme de géophysique appliquée, les faibles changements de contraintes mis en jeu et la taille des séismes majeurs proposés comme potentiellement déclenchés par des extractions d'hydrocarbures, posent des questions qui sont d'actualité pour la sismologie fondamentale. Les faibles variations de contraintes induites sont accord avec celles proposés actuellement pour expliquer les effets coséismiques à quelques centaines de kilométres de l'hypocentre (voir par exemple les effets du séisme Californien de 1992 sur l'activité sismique au Nevada ou en Californie du Nord). Notre approche de la séismicité à l'aide des séismes déclenchés par des activités humaines nous permets de rejoindre et de renforcer le courant d'idées actuel sur l'état quasi-critique de la croûte supérieure.

Lacq fait trembler la terre

Depuis 1969, l'exploitation du gisement de gaz a induit une micro-sismicité très locale

24 novembre 1969. La petite commune de Lacq est agitée par un séisme de faible magnitude. D'autres suivront.

L'exploitation de Lacq, cause de séismes

Une thèse que les services géologiques d'Elf-Aquitaine estiment «aberrant».

SCIENCES

L'exploitation du gaz de Lacq provoquerait des mini-séismes

Les étranges tremblements de terre des Landes

Plus de 800 secousses, certaines assez importantes, ont ébranlé la région depuis 20 ans. Une enquête, restée secrète depuis 1982, met en cause l'exploitation du gisement de gaz.

BAYONNE

CHEVAUCHEMENT FRONTAL (INACTIF)

QUAND L'HOMME FAIT TREMBLER LA TERRE

Legere secousse tellurique hier en Bearn

Séismes : Lacq montré du doigt

Le tremblement de terre de faible ampleur enregistré hier en Béarn risque de relancer une polémique.

En pompant du pétrole ou du gaz, en injectant un liquide dans le sous-sol ou en remplissant un barrage, il est possible de provoquer des tremblements de terre. A Lacq par exemple, Elf cache depuis sept ans que les séismes qui se sont produits sur le gisement étaient artificiels.

N'aurait-il pas fallu prévenir les habitants, sans les affoler, au lieu de les prendre pour des bambins attardés ?

Pétrole et séismes

Séisme: l'épicentre était situé à Lacq

Arthez-de-Béarn

Masiacq

Lacq

Champ d'exploitation du gaz

Chaque point sur cette carte de la région représente une secousse sismique, enregistrée sur les deux seules annees 1978-1979, due [illegible] du gisement de gaz de Lacq. Toutes les secousses [illegible] d'énergie, mais sur l'exemple [illegible]

Vendredi 5 janvier 1990 - Page 3

Dans ce sens dans la partie 5 deux applications montrent comment à différentes échelles spatiales et temporelles des connexions entre séismes peuvent être utilisés pour comprendre le comportement mécanique de la croûte terrestre. On utilise alors soit les lois classiques de la mécanique des matériaux, soit le concept plus récent de chaos organisé. Dans un cas, la simultanéité de l'activité sismique sur une distance de plus de 150 km de part et d'autre de la subduction au Nlles Hébrides, permet de proposé que le fort couplage local des deux plaques crée une entité mécanique dont le comportement mécanique peut être expliquer par des phénomènes de flambage (chapitre 51). La seconde partie de ce chapitre, montre les limites des lois de la mécanique classique pour expliquer les phénomènes d'instabilités et l'on se sert des cas mondiaux de séismicité induite pour appuyer le concept théorique d'état critique Auto-orgnisé pour la croûte superficielle. Il est important de noter que les objets géologiques que nous étudions ici constituent des structures de tailles intermédiaires entre les études en laboratoires et la tectonique des plaque. En terme d'étude de mécanique de la rupture ces objets sont fondamentaux. Les sites de sismicité induites (mines, barrages, extractions d'hydrocarbure et volcans) sont de tailles décakilométriques où les sollicitations aux bornes de l'objet sont connus et plus rapides que les sollicitations tectoniques. Sur ces sites les échelles des processus de ruptures sont elles aussi intermédiaires entre les expériences de rupture en laboratoire, où les régimes chaotiques auto-organisés ne sont pas observés (dès la localisation de la déformation, une macro-rupture de la taille de l'échantillon se propage, et l'on ne peut observer que le régime transitoire correspondant à la mise en place de l'état critique organisé), et le milieu naturel où l'on possède des observations sur des états critiques auto-organisés déjà établis. On peut ainsi parler de Systémes Critiques Auto-Organisés Induits où l'on peut observer la genèse, la pérennité et la disparition de systémes critiques (chapitre 52).

Lacq: Laboratoire de séismologie

Une des contribution majeures des recherches présentées dans cet ouvrage, consiste en l'analyse du cas mondial actuellement le mieux contraint pour évaluer le lien entre perturbation de l'état de contrainte et séismes. Tant les données géomécaniques fournie par le groupe Elf, que les données des mouvements sismiques (réseau d'acquisition de données en vitesse et accélérations du sol) et les déplacements de surface mesurés par les nivellements successifs permettent des quantifications géomécanique de l'état de la structure de Lacq . En effet la séismicité associée à l'extraction de gaz du gisement de Lacq, Aquitaine, France est observée de façon instrumentale continue depuis 1974. L'étude d'objet

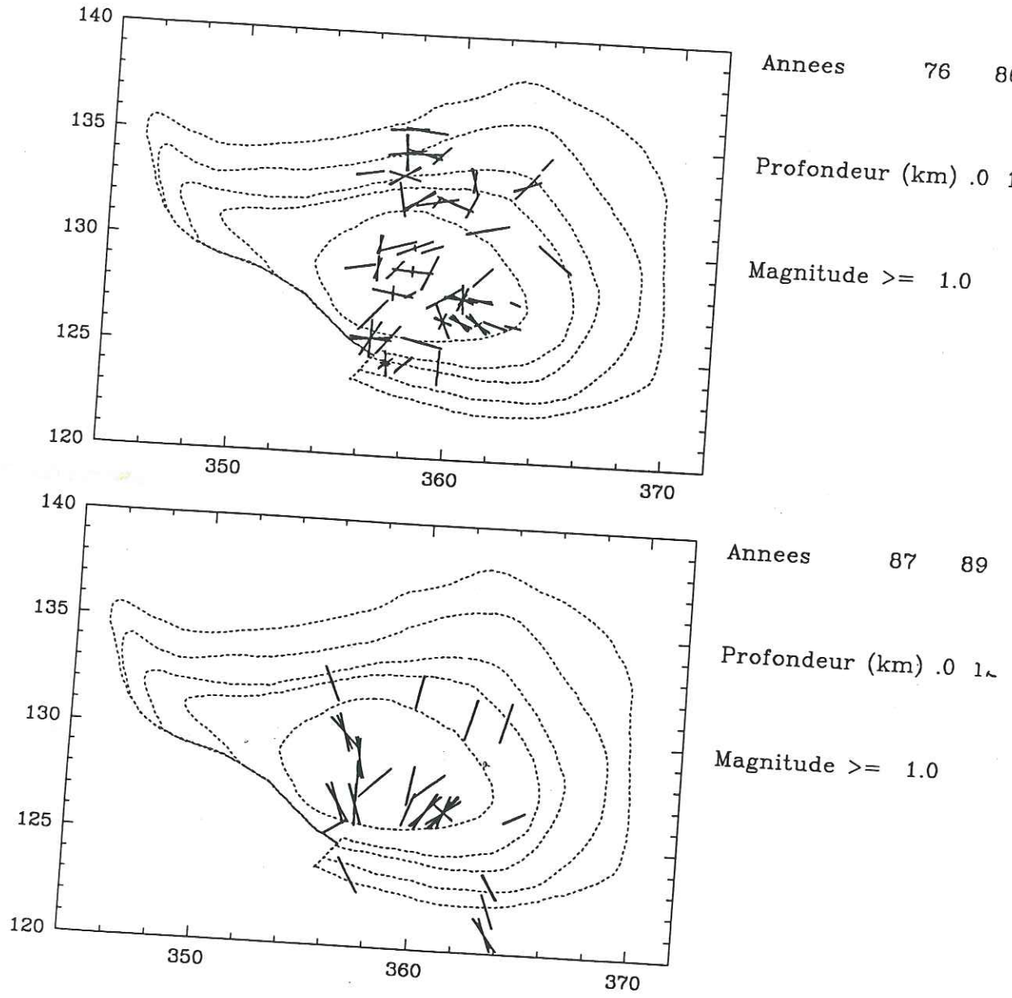

Figure I7

géologique isolée est une opportunité pour le géophysicien, pour lequel de nombreuse informations restent habituellement inaccessibles, pour la compréhension des mécanismes de déformations de la croûte terrestre. L'étude du cas Lacq a permis de mettre en évidence que des perturbations très faible des contraintes étaient suffisantes pour déclencher des ruptures. La base de cette étude est constitué par une analyse de la séismicité historique du site et la mise en oeuvre de localisation fine de séismes. Les localisations furent successivement obtenues à l'aide d'inversion simultanées des foyers et des vitesses sismiques, d'utilisation de données d'une station de fond de forage à 3500 m de profondeur, d'inversion des hypocentres dans un milieu 3D complexes définis sur la base de plus de 40 forages profonds, des nombreux carottages sismiques et profils sismiques locaux. L'ensemble de ces localisations a permis de montrer que la seule perturbation due à l'exploitation qui ait une échelle spatiale et temporelle compatible avec celle de la séismicité est la baisse de pression du réservoir de Lacq profond. Or en accord avec les lois de la pression effective, la diminution de la pression de fluide stabilise le milieu où les contraintes effectives augmentent, donc éloigne le milieu de seuil critique de rupture. Le site de Lacq nous a permis de tester in-situ l'effet d'une déplétion importante (30-60 Mpa) et de montrer que le paradoxe précédemment décrit s'explique par un transfert de contrainte de la zone dépressurisée vers les niveaux environnant. Cette mise sous contrainte poro-élastique s'appuie sur le fait que les ruptures sismiques du dôme de Lacq sont, pour leur grande majorité, localisées au dessus où au dessous des niveaux réservoir. Les directions des axes de compression déduites des séismes les mieux contraints sont complexes et peuvent être compatible avec une organisation axisymétrique autour du réservoir de gaz (Grasso et Feignier, 1990), (Figure 7 d'aprés Volant 1993). Les modéles analytiques que nous mettons en oeuvre pour évaluer les variations de contraintes qui ont déclenchés les ruptures (Segall and Grasso,1991 & 1993) utilisent les données poroélastiques qui contraignent la déformation du réservoir de Lacq, permettent de proposer des variations de l'ordre de quelques bars. Ces variations très faibles dirigent les ruptures sismiques si on admet un contexte tectonique régional en compression et un critère de rupture de type Mohr-Coulomb (Segall, Grasso et Mossop, 1993). Ce modéle qui explique aussi la subsidence observée en surface, ne rend pas compte de la diversité des types de mécanismes aux foyers observés. On peut alors proposer (Chapitre 4), que le modéle poroélastique est satisfaisant pour décrire la mise en charge du site avant l'occurrence de la séismicité. L'apparition des ruptures sismiques est alors interprété comme une phase de localisation de la

Stress Orientations

Stress generated breakouts have been identified with difficulty in approximately 100 wells, and their mean orientations measured. There is a large amount of borehole ovalisation, but much of it is geometrically related to well deviation, even in wells where departures from vertical inclinations are minimal. Focal mechanisms have been determined for 3 recent earthquakes along the northern edge of the Pyrenees, and for more than 100 microearthquakes generated locally by gas production. Regionally consistent stress orientations have been measured by strain release techniques and by hydraulic fracturing in basement rocks to the northeast. Focal mechanisms of Pyrennean earthquakes yield a confused picture. No well-defined regional stress trajectories are evident within the Aquitaine Basin, except on its northern margin (Fig 4).

Stress Magnitudes

Stress magnitudes have been measured by hydrofracturing and strain relief techniques in basement rocks surrounding the Aquitaine Basin. In the basin itself there is little data except for indications of σ_v magnitudes provided by leak-off tests in a few wells (Fig 5). These suggest that σ_h is approximately 80% of σ_v.

Geomechanical Setting

The Aquitaine basin contains a varied assemblage of Paleozoic sediments overlying basement and attached to it. Above are widespread Triassic and Lower Jurassic evaporite sequences containing salt. These units are overlain by Mesozoic and Tertiary carbonates and clastics, which are effectively detached from basement everywhere except in the northern part of the basin around Bordeaux. Local salt ridges disrupt the overlying sediments and there is considerable Mesozoic faulting adjacent to the Pyrenees.

Tectonic History.

Following a period of widespread evaporite deposition in early Mesozoic time, sedimentation became restricted to two centres by Late Jurassic. Rifting began in early Cretaceous time and was succeeded by local subsidence and, in mid-Cretaceous time, salt diapirism. The Pyrenean orogeny began in late Cretaceous time and gave rise to flysch troughs along the southern margin of the basin. During the Eocene, the Iberian plate collided with the European plate and caused folding, reverse faulting and trough inversion in the latter area. Few structural effects were felt to the north and orogenic activity ceased in Eocene time. During Late Tertiary and Quaternary time, uplift of the Pyrenees took place and molasses deposits prograded widely to the north and west.

Interpretation

The Aquitaine Basin is a rebounding foreland basin - that has been affected by transpressional tectonics along its southern margin. The axial sediments are entirely underlain by salt and thereby detached from basement. Their horizontal stress signature is very weakly defined and there are strong grounds for believing that differences in horizontal principal stress magnitudes are minimal. Local structure seems to determine preferred stress orientations. Along the northern margin, stress trajectories conform to those of the European Plate and the section is interpreted as being attached to basement. The degree of horizontal stress anisotropy is believed to be greater here, but this has not been confirmed.

Bell, J.S., 1993. The Global Sedimentary Basin Stress Project of the International Lithosphere Program. Poster P-71, 55th Meeting of European Association of Exploration Geophysicists, Stavanager, Norway, June 7-11, 1993.

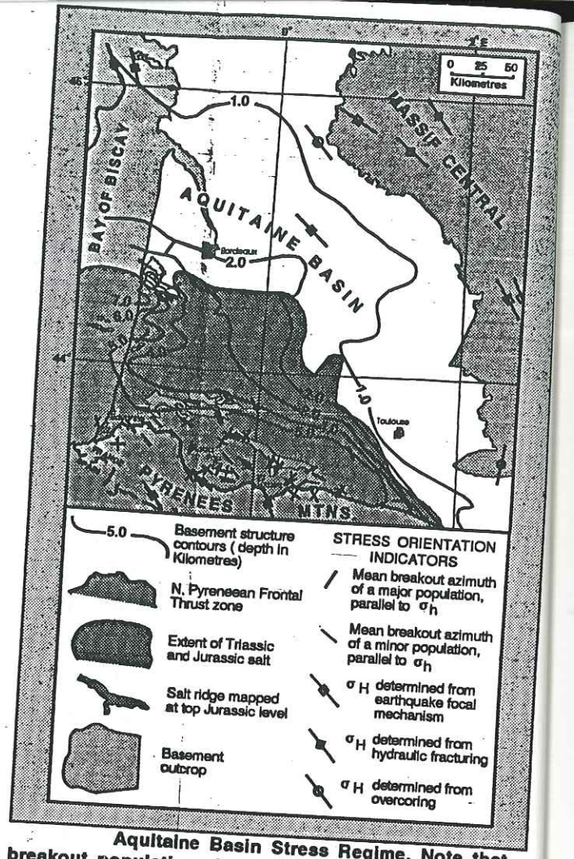

Aquitaine Basin Stress Regime. Note that breakout populations in sediments overlying salt have semi-random orientations.

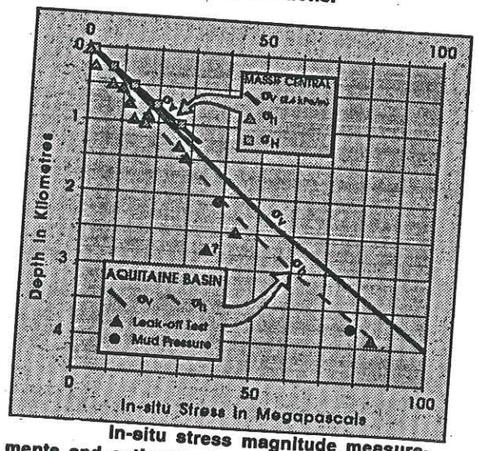

In-situ stress magnitude measurements and estimates in and around the Aquitaine Basin, France.

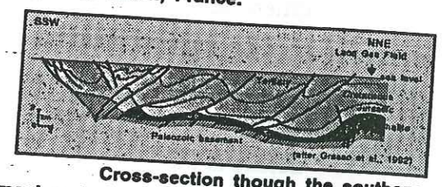

Cross-section though the southernmost part of the Aquitaine Basin. Note the salt interval that separates the Paleozoic basement from the Mesozic and Cenozoic sediments.

Figure I8

déformation sur des accidents préexistants, et la perte d'un comportement élastique. Les glissements sismiques sont alors dirigés par la géométrie de mouvements entre blocs, cette cinématique expliquant la variété observée dans les mécanismes aux foyers. Une tentative d'homogénéisation des informations déduites des rejeux sismiques (Volant, 1993) permet d'obtenir des tenseur de contraintes différents sur deux périodes de temps sans pouvoir déterminer la réalité physique de ces solutions. Un état avec S1~Sv, dans un premier temps permutant avec un état où S1~SH. On remarquera toutefois qu'une telle évolution des contraintes avec la profondeur est proposée dans certains bassins sédimentaires où des surpressions de fluides sont présentes (Bell 1989), même si sur le site de Lacq l'influence de la profondeur ne parait pas déterminante pour les mécanismes traités (Volant 1993). On peut aussi remarqué que l'état de contrainte dans le bassin Aquitain parait faiblement anisotrope (Bell et Caillet 1992), ce qui impliquerait l'absence de déviateur de contrainte (Figure 8, d'aprés Bell 1993). Ainsi, la diversité des mécanismes observés (normaux et inverses) peut être attribuer soit aux géométries des failles préexistantes, soit au fait que sur le site de Lacq les déplacements et déformations sont principalement élastiques donc aséismiques (Grasso et Feignier, 1990; Volant , Grasso, Chatelain et Frogneux 1992). Les ruptures séismiques sont alors des ajustements du second ordre en réponse à des glissement non séismiques. Des observations récentes lors de séismes induits par des injections de fluides, montrent aussi que les orientations de contraintes déduites des séismes sont en accord, non pas avec la tectonique régionale ou les contraintes induites par l'injection, mais avec les hétérogénéités de contraintes induites par le glissement aséismique suite à l'injection de fluide (Scotti et Cornet, communi. pers. 1992)

FLUIDES ET RUPTURES : PROCESSUS PHYSICO-CHIMIQUES OU COMPETITON ENTRE DEFORMATION PLASTIQUE ET FRAGILE

Si le modéle poro-élastique homogéne, même grossier, permet de comprendre l'apparition de séismes, (sur les différents cas disponibles, la variation de la perturbation de la contrainte poroélastique est toujours comprise entre 0,1 et 0,7 MPa (Table 1)), il est fondamentale de noter que les déformations et déplacements observés sur les champs d'hydrocarbures *séismogéniques* restent dominer par des mécanismes lents, c'est à dire n'émettant pas d'ondes sismiques. En effet une estimation de la taille maximale des séismes potentiels sur la base des déplacement observés lors des déplétion de gisement ($Mo \sim \mu \Delta v$, V étant la perte de volume liée à l'extraction et μ le module de rigidité du milieu)

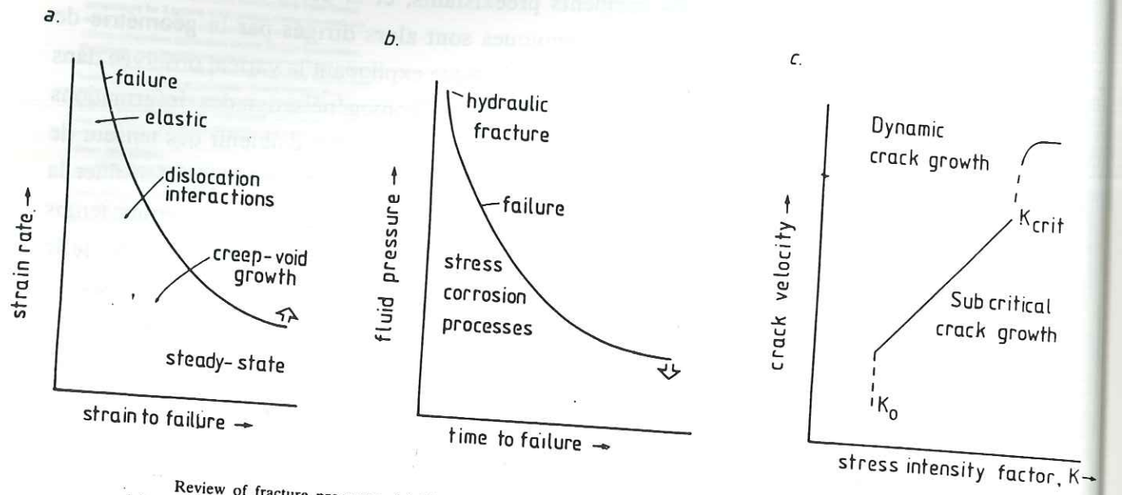

Review of fracture processes. (a) The range of pre-failure processes which may operate during fluid-absent deformation under different strain rate conditions. The arrow represents the change in the failure line position associated with an increase in temperature or confining pressure. (b) illustrates the possibility of additional slow crack growth processes such as stress corrosion in a fluid present situation. The arrow indicates the movement direction of the fluid chemistry to a more corrosive during an increase in the stress intensity factor (see c) and/or the alteration of the time to failure line composition. (c) is the fracture mechanisms associated with different crack velocities and stress intensity factors. The stress intensity factor (K) can be considered to be the driving force for crack propagation. It describes the stress system around a crack tip and is dependent upon the loading conditions and the material properties. The values of K range from K_0, below which sub-critical crack growth ceases, to K_{crit} when propagation accelerates to approach the velocity of sound in the material.

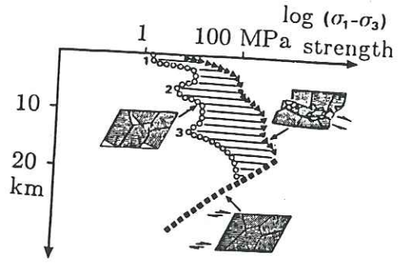

Fig. 8. Strength profile through the upper crust taking into account the two (observed) deformation mechanisms: cataclastic deformation (law derived from Mohr–Coulomb behaviour, triangles), and pressure solution creep (laws derived from theoretical, experimental and natural observations, circles), at geological strain-rate: 10^{-14} s^{-1}, (equivalent to a change in length of 3 mm a^{-1} for an element of 10 km size). Dislocation creep mechanisms (squares) operate within the lower crust. The model of the typical crustal section is composed of different rocks, (see Fig. 7): from top to bottom, sediments with high porosity (1), limestones, slates (2), metamorphic rocks (gneisses then schists (3)), granitic rocks. The strength values vary considerably with depth, depending on various parameters (possibility of mass transfer, solubility of solid in fluid, mean displacement rate at the boundaries of the system, etc.).

Figure I9 Figure I10

GASLI MAY-JUNE 1991: NW-SE CROSS SECTION

NOBS>6 GAP<360°

RMS< 0.3s ERH<5 KM

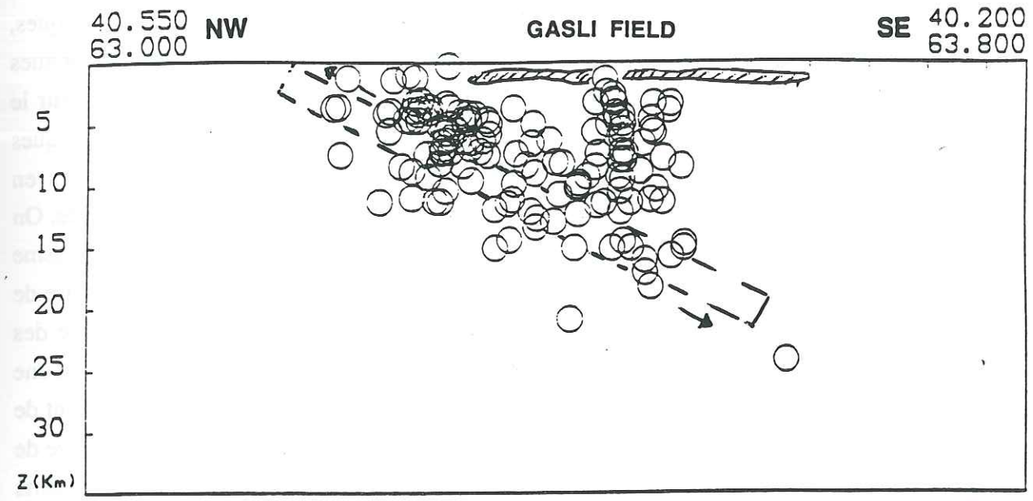

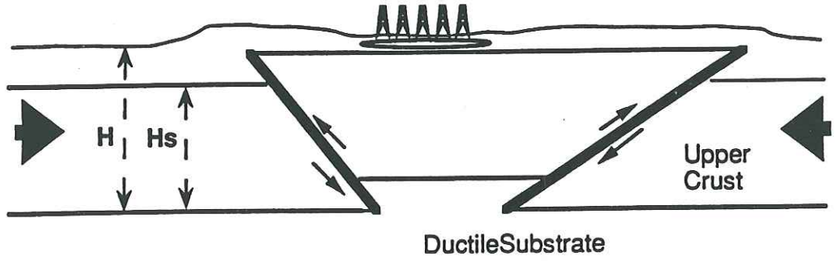

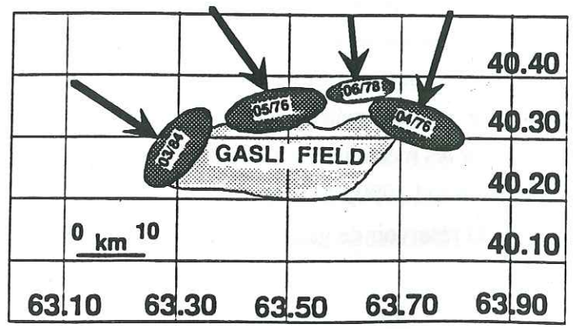

Figure I11

est de plusieurs ordre de grandeur supérieurs à la taille des séismes effectivement observés. Cette compétition entre rejeux sismiques, donc ruptures dynamiques, et déplacement asismiques, c'est à dire quasi-statiques, reste une des inconnues majeures pour la prévision du potentiel de séismicité induite d'un site. Sur le champ de Lacq, on montrent comment des déplacement sismique et asisimiques sur les mêmes accidents peuvent expliquer les déplacements observés en surface, la séismicité représentant seulement 10% des déplacements cumulés. On doit remarquer que ces mouvements lents se rapprochent de la notion de séisme lent proposé pour expliquer les séismes basses fréquences présents à la base de lithosphére fragile. Dans les terrains plastiques de la croûte superficielle des phénomènes semblables prennent place et sont souvent ignorés à cause d'une instrumentation inadaptée. Pourtant des observations in situ de cisaillement de forage en quelques minutes ou heures (Maury et Sauzay, 1989) en l'absence de séismicité (i.e. M>3) et de rares mesures de séismes superficiels lents (Kanamori et Haukson 1992) montrent que de tels mécanismes existent. Ces observations et modéles attestent que la transition entre 2 types de comportements distincts, plastique-elastique n'est pas brutale mais continue. Ces comportements peuvent être la base phénoménologique des nombreux écarts reportés entre déformations et déplacements, déduits de données géodésiques et déformations et déplacements, déduits de données sismiques, ainsi que par exemple les cas de fausses alarmes lors de tentatives de prévisions de séismes. Le déplacement principale est aséismques avec des précurseurs ou répliques sismiques. Les mécanismes de déformations peuvent aller des phénomènes de solution cristallisations pour les plus lents, a la croissance de fissure en régime sous critique (Figure 9).

Dans le but d'estimer le risque sismique induit localement par les séismes déclenchés par l'extraction de gaz sur le site industriel de Lacq, les contributions respectives des comportements fragiles et plastiques ont été quantifiées. La subsidence de surface (un maximum 6 cm sur zone anomalique de 10 km de rayon) correspond environ à un rejeu en faille normale d'un séisme de magnitude 6 localisé à 8-10 km de profondeur. Le moment sismique cumulé des séismes de lacq n'atteint pas l'équivalent d'un séisme de magnitude 5. De plus, les rejeux "aséismiques" localisés sur des failles définies par la microséismicité expliquent les profils de nivellement. Ces processus aséismiques (3 cm en 10 ans pour un objet de taille décakilométriques) sont compatibles avec les ordres de grandeur proposés pour les mécanismes de dissolution-cristallisation (Figure 10, d'aprés Gratier et Gamond 1990). Si dans ce cas le moteur de déformation est la chute de pression du réservoir de gaz, les micro-mécanismes de mis en jeu

lors des déplacements non sismiques (M<1, seuil de magnitude pour lequel le catalogue est complet localement) sont des transferts de masse liés au processus de dissolution-cristallisation. On notera que des instabilités *aséismiques* (que nous définissons comme des mouvement ayant des durées de l'ordre de quelques minutes à quelques heures) ont cisaillés de nombreux forages pétroliers en l'absence de seismicité ($M \geq 3$). Ces instabilités posent la question de la transition entre rejeu sismique et asismique tels que définis par les études de paléoséismes (les stries sont présentent dans les 2 cas, l'énergie sismique libérée donc le facteur risque seulement dans un seul).

A une autre échelle des transferts de masse, macro-mécanisme gravitaire, sont proposées pour expliquer la sismicité induite par surcharge ou décharge en fonction du contexte tectonique. Pour tester ces concepts nous avons analysé l'activité sismique actuelle dans la région de Gasli (Ousbékistan) où 3 magnitudes 7 se concentrent temporellement et spatialement autour d'un gisement d'hydrocarbure. Les géométries définies tant par l'activité microséismiques, que par les mouvements coséismiques (Figure 11) rendent plausible le liens entre la masse perdue par extraction et les moments sismiques des séismes qui plongent sous le gisement. En plus de leurs effets gravitaires, la modification de la pression des fluides ou de leurs circulations (Figure 12, d'aprés Koons and Craw 1991) peut contribuer à expliquer anomalie des axes P de ces séismes majeurs repartis de façon concentrique autour du gisement. Dans cet exemple les processus moteurs de transfert de masse serait localement associés à des micro-mécanismes impliquant des anomalie de pression fluide. Il semble en être de même pour le séisme de Coalinga (USA) qui est associé lui aussi à la fois à un déficit de masse dans un contexte tectonique en compression, pour des failles mal orientés. Ici les anomalies de pression fluides sont mise évidence indirectement avec des zones à moindre vitesse sismique (Figure 13, d'aprés Sibson 1991).

D'une façon plus globale nous avons dans les chapitres 3-4 tenté d'éclairer divers mécanismes possibles de déclenchements de rupture (Figure 9, d'aprés Knipe 1987) et de tester la plausibilité de distances de connection rejetées jusqu'alors sur une base a priori de niveau de contrainte trop faible. Ces distances de connections entre perturbations fluides et instabilité sismiques, sont reportés depuis plusieurs décennies lors de la mise en eau de retenues artificielles. Sur une base observationnelle, de nombreux séismes, de magnitude comprise entre 3 et 6, sont associés à des réponses poro-élastiques des structures géologiques locales sous l'effet de la charge hydraulique que représente une retenue. Les mécanismes hydrauliques, en milieu drainés ou non

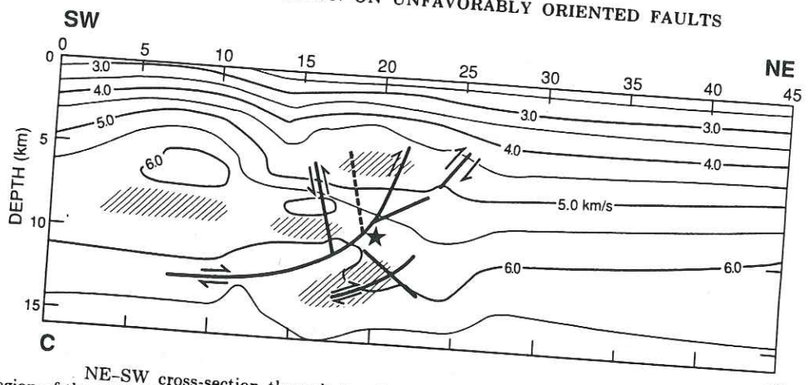

NE–SW cross-section through the three-dimensional velocity model in the hypocentral region of the 1983 *M*6.7 Coalinga earthquake (after Eberhart-Phillips, 1989), showing the main shock rupture and subsidiary faults inferred from aftershock relocations, and their relationship to localized low-velocity zones (cross-hatching).

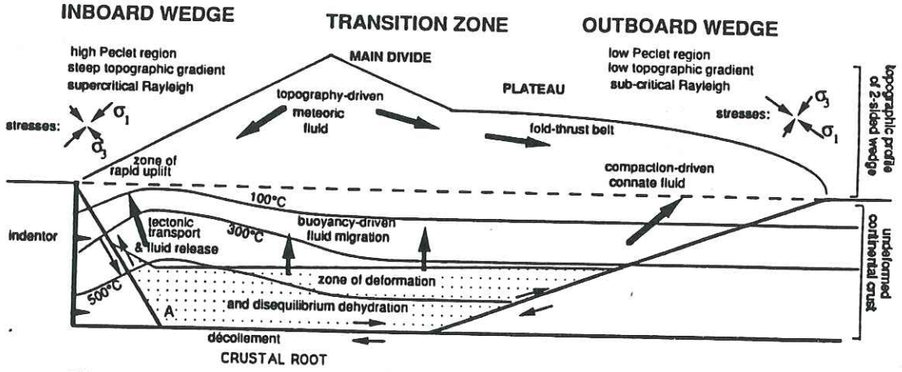

Diagram of a two- sided collisional orogen summarizing the thermal and topographic character orogen. The stress orientations for the inboard and outboard wedges are derived from the Mohr circle [1986]. The thermal and topographic patterns come from Koons [1987, 1989].

Figure I12 Figure I13

drainés impliquent deux types de réponses temporelles. Une analyse géomécanique des séismes de la région de Monteynard, Sud de Grenoble, montre comment une région à faible taux de séismicité historique peut être activée par la faible perturbation que constitue la retenue. Sur ce site, le développement temporel et spatial de l'activité sismique est en accord avec des valeurs de diffusivité hydraulique qui varient selon le contexte géomécanique (milieu fracturé, présence de failles, orientations des contraintes tectoniques...) mais restent en accord avec les valeurs déduites de la sismicité d'autre retenue artificielle ou de forage (Figure 6). On notera que les valeurs nécessaires pour lier la séismicité de Lacq et celles des pyrénnées sont elles aussi du même ordre de grandeur.

INSTABILITES SISMIQUES INDUITES PAR LES FLUIDES: IMPLICATIONS SUR LE COMPORTEMENT MECANIQUE DE LA CROUTE SUPERIEURE

Lorsque les mécanismes moteurs dans le déclenchement d'une rupture sont isolables, l'occurrence de ces ruptures est une jauge de contrainte pour évaluer l'état local de la croûte, à partir du déviateur qui déclenche la rupture. Sur le site de Monteynard, on voit combien l'étude de la séismicité déclenchée par une perturbation mécanique peut être utile pour cartographier les discontinuités potentielles, hétérogénéités de contrainte et l'état d'instabilité d'un site. D'un autre point de vue, étant donnée le faible déviateur de contrainte à l'origine du déclenchement de ces ruptures, des distances séismes-retenues atteignant la vingtaine de kilomètres, pour des hauteurs de retenue de l'ordre de 100 m, impliquent des variations de pressions à peine supérieures aux marées terrestres, sont des arguments pour un état quasi-critique de la croûte même loin des frontières de plaques.

La présence de fluide dans la croûte est utilisée tant pour expliquer les signatures hydrauliques des séismes (augmentations de débits des rivières après des rejeux en failles normales; Figure 14, d'aprés Wood et King 1992) que pour expliquer les phénomènes précurseurs des séismes. Les échelles des circulations horizontales dans le contexte de la croûte superficielle sont encore mal connues et peu quantifiées. Toutefois les faibles variations de contraintes qui semblent diriger les instabilités sismiques et aséismiques induites dans de la croûte superficielle (chapitre 5) peuvent permettre de comprendre les anomalies que constituent actuellement les phénomènes précurseurs. Ces anomalies n'étant définies que par rapport à l'état actuel de nos modéles (Figure 15 from Roeloffs, 1988; Figure 16 from Silver and Silver 1992, comme exemple) et de nos connaissances quantitatives des pressions fluides crustales. On notera que

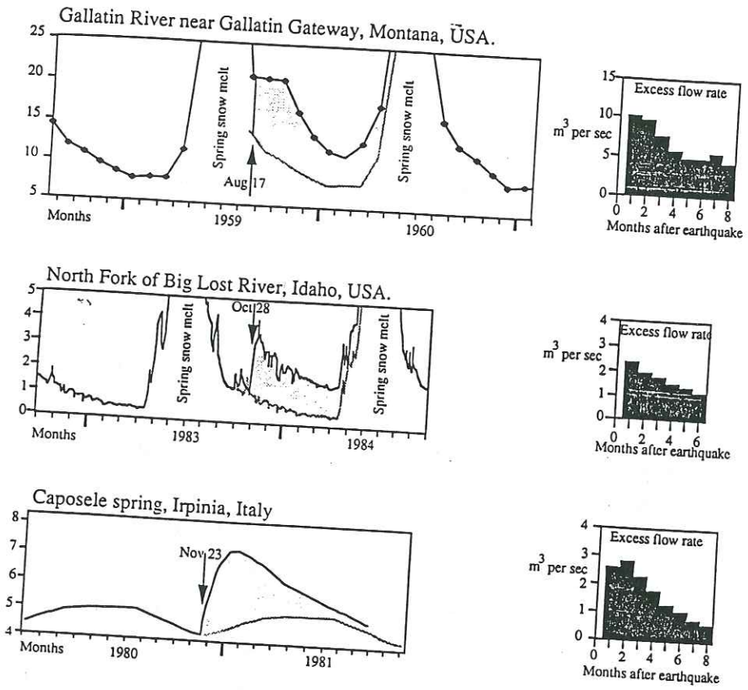

Hydrological Signatures of Earthquake Strain

Robert Muir Wood
BEQE
Cambridge
England

Geoffrey C.P. King
Institut de Physique du Globe
5, rue René Descartes,
67084 Strasbourg, Cedex,
France.

Figure I14

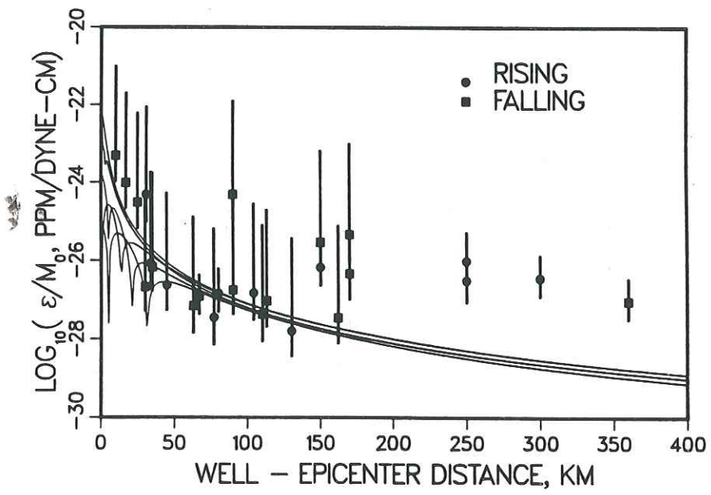

Comparison of strain represented by water level anomalies with predicted maximum coseismic volume strain. Symbols: strain represented by the water level anomalies listed in Table 2, converted to strain using equation (6), and divided by the moment of the subsequent earthquake. Curves: Absolute value of volume strain as a function of distance along the azimuth of maximum volume strain, for several source mechanisms: vertical strike slip, at surface, and 9 km deep; 45 degree dip slip, at surface, and 9 km deep, and 20 degree dip slip, 20 km deep. Curves represent strain per dyne-cm of moment, assuming a shear modulus of 3×10^{11} dynes/cm^2.

Figure I15

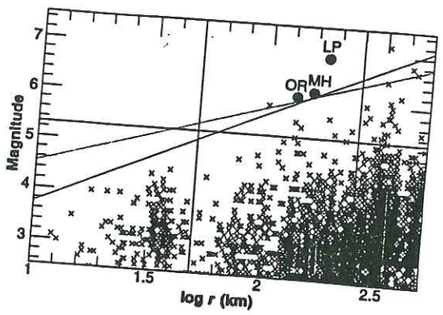

Fig. 2. Plot of seismicity from the NEIC catalog as a function of distance r (<500 km) from the geyser and magnitude M (>2.5). Filled symbols denote the three large events studied. Also shown are vertical lines $r = 50$ km and $r = 250$ km, horizontal line giving magnitude cutoff (5.3) in Fig. 1, and two inclined lines that approximately correspond to constant static (solid line, proportional to r^{-3}) and dynamic (dashed line, proportional to r^{-2}) strain at the geyser.

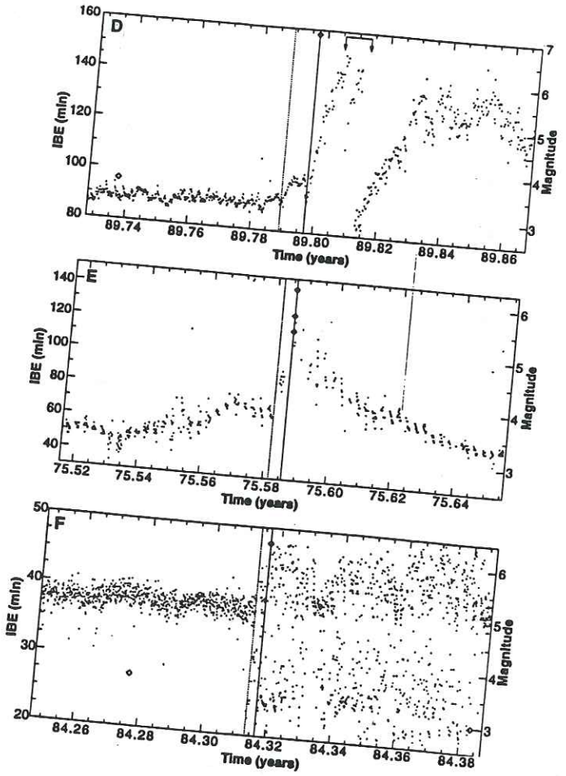

. **(D)** Fifty days of raw IBE data centered on the Loma Prieta earthquake. Interval lengthening began ~60 hours (0.0068 year) before the event (dashed line). Rapid drops in IBE after the earthquake are coincident with the largest 4-day period of precipitation of the year (arrows), suggesting that they are rain-related. **(E)** Same as (D) except for the Oroville earthquake. Interval lengthening begins about a day before the event (dashed line). **(F)** Same as (D) except for the Morgan Hill earthquake. The change from unimodal to multimodal behavior occurred ~1 day before the earthquake.

Figure I16

l'anomalie de potentiel spontané mesurés par le groupe VAN nécessite une différence de pression de pore d'environ 100 MPa (Figure 17, d'aprés Bernard, 1992), ordre de grandeur de la pression initiale du gisement de Lacq ...

Dans une tentative de synthèse, nous montrons comment l'ensemble des observations de séismicité induites peut être utiliser comme argument dans le concept d'état crique auto-organisé de la croûte superficielle. En effet une analyse des cas mondiaux admis par la communauté scientifique comme une séismicité non naturelle permet de dégager les points suivants. Un faible déviateur de contrainte (< 1 MPa) suffit pour déclencher des ruptures sismiques dont la taille n'est pas fonction de la valeur de la perturbation. De plus l'activité sismique, une fois déclenchée, est maintenue pendant de nombreuses années par des variations de contraintes d'un ordre de grandeur inférieures à celles qui ont permis l'apparition des ruptures. Enfin les distribution spatiales ou de type fréquence-taille de ces instabilités sismiques obéissent à des lois puissances. L'ensemble de ces remarques constituent les ingrédients nécessaires au concept de systémes critiques Auto-organisés proposés à plus grande échelles pour caractériser le comportement mécanique de différents processus en sciences de la terre (la mécanique de la lithosphére, activité volcanique, hydrologie de surface, précipitation..). Ces systémes critiques auto-organisés déclenchés par des activités humaines donnent accès à des analyses quantitatives de ces systémes instables où les limites du domaine de validité des comportements fractals, par exemple, sont reliés aux caractéristiques géomécaniques du site (chapitre 52). Ceci ouvre des opportunités interprétatives et dans ce sens les plus gros séismes induits auront potentiellement lieu sur les sites où des couches épaisses et compétentes seront proche de la surface, c'est à dire dans les boucliers et cratons, zone où le taux de séismicité naturelle est faible. Ceci est en accord avec les observations actuelles (Table 2) mais le faible nombre de données ne permets pas une conclusion définitive.

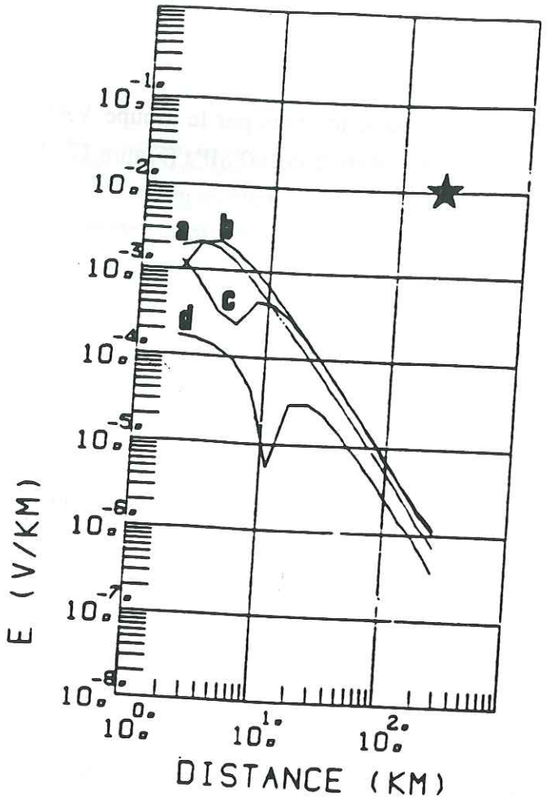

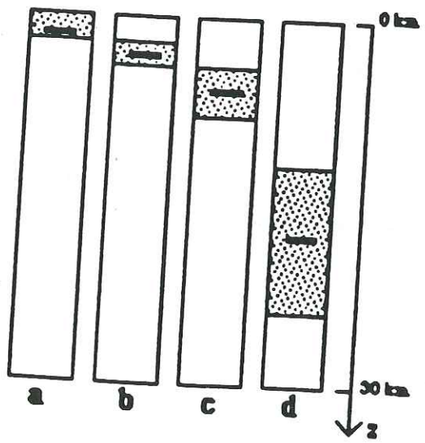

Champ électrique horizontal de surface, produit par un dipole électrique de 1 km de long dans lequel circule 100 A, correspondant à un phénomène d'électrofiltration mettent en jeu une différence de pression de pore de 1MPa. Le milieu conducteur est un demi espace coupé d'une couche de conductivité 100 fois plus grande, et contenant le dipole, située à diverses profondeurs (zone pointillée). L'étoile correspond aux mesures d'anomalie de potentiel spontanés par le groupe VAN.

Bernard, 1991.

Figure I17

Table 2: M > 5.0 induced earthquakes

Dam/reservoir or hydrocarbon field	ΔP (MPa)	ΔM (10^{11}kg)	Maximum Magnitude	Regional seismicity	σ1 orientation (from induced eqs) and Tectonic setting.
Gazli field, EIS Uzbekistan	≤0.	-2.	M=7.3	low	Horizontal - Midplate,
Koyna, RIS India	+1.	+27.	M=6.5	low	Horizontal - Midplate,
Coalinga field, EIS USA	≤0.	-2.7	M=6.5	high	Horizontal - Plate boundary
Kremasta[D], RIS Greece	+1.6	+47.	M=6.3	high	Vertical - Back arc extension
Hsinfengkiang, RIS China	+1.	+1.0 10^2	M=6.1	low	Horizontal - midplate
Kettleman field, EIS USA	≤0.	-1.2	M=6.1	high	Horizontal - Plate boundary
Montebello field, EIS USA	≤0.	-1.3	M=5.9	high	Horizontal - Plate boundary
Oroville, RIS USA	+2.4	+43	M=5.9	low	Vertical - Sierra Nevada foothills
Kariba, RIS Zambia/Zimbabwee	+1.3	+1.7 10^3	M=5.8	low	Vertical - Midplate
Marathon[D], RIS Greece	+0.7	+0.4	M=5.7	high	n.a - Plate boundary
Aswan[D], RIS Egypt	+1.1	+1.6 10^3	M=5.5	low	Vertical - Midplate
Eucumbene, RIS Australia	+1.1	+47	M=5.5	low	n.a - Midplate
Hoover, RIS USA	+2.2	+3.7 10^2	M=5.5	low	Vertical - Colorado plateau
Denver, IIS USA	+3.5*	+10^{-3}	M=5.5	low	Vertical - Colorado plateau
Caviaga, EIS Italy	≤0.	-??	M=5.5	low	Horizontal - midplate
Lake County, IIS USA	+0.5**	~0.	M=5.3	low	Horizontal - midplate
Monteynard, RIS France	+1.3	+2.7	M=5.3	low	Vertical - Alps foothills
El Reno, EIS USA	≤0.	-??	M=5.2	low	Horizontal - midplate
Snipe Lake, EIS Canada	≤0.	-??	M=5.1	low	Horizontal - midplate

n.a., no-available information;
RIS, EIS and IIS are respectively reservoir, extraction and injection induced seismicity.
see references for RIS, EIS and IIS, respectively within Gupta 1985, Grasso 1993 and Nicholson 1993;
[D] Disagree with decision diagramm for Corps of Engineers study of RIS (Meade, 1990);
* Modeled fluid pressure increase (Hsieh and Brehoeft, 1981);
** Modeled fluid pressure increase (Nicholson et al. 1988);

1

CONTEXTE ET VUE D'ENSEMBLE

Ce chapitre d'introduction rappelle les concepts qui sont utilisés pour décrire et comprendre le rôle des fluides dans les mécanismes de rupture de la croûte superficielle. Il présente les concepts, lois spécifiques et modèles de base qui sont détaillés dans cet ouvrage tant du point de vue de leurs bases observationnelles que de leurs supports méthodologiques. Cette introduction reste volontairement qualitative.

PREMIERE ITERATION: A la première représentation d'un phénomène fractal n'apparaissent que de rares indices de la structure mathématique sous-jacente.
(Ian Malcolm)

Bull. Soc. géol. France, 1992, t. 163, n° 1, pp. 27-36

Le rôle des fluides dans les mécanismes d'instabilités de la croûte supérieure : l'exemple des exploitations d'hydrocarbures

par JEAN-ROBERT GRASSO*, DOMINIQUE FOURMAINTRAUX** et VINCENT MAURY**

Mots clés. – Fluide, Instabilités sismiques et asismiques, Séismes intraplaques, Séismes induits, Exploitations d'hydrocarbures, Environnement.

Résumé. – Nous proposons une analyse des différents cas observés d'instabilités mécaniques en terme de comportement sismique et asismique. Nous montrons que les différents paramètres d'exploitation peuvent déclencher des instabilités de différentes échelles en terme de quantité d'énergie impliquée ou de distance au gisement. Trois types d'instabilités mécaniques sont proposées en association avec les observations et mesures effectuées au voisinage d'exploitation d'hydrocarbures : réponses locales type fracturation hydraulique à des injections de fluide; ajustement de la structure géologique aux perturbations des champs de contraintes liées à la déplétion (échelle kilométrique) ; réajustement à l'échelle crustale (décakilométrique) liés au transfert de fluide. Si dans la plupart des cas le risque sismique est mineur pour l'environnement (ruptures sous le réservoir, énergie libérée faible), l'occurrence tardive de séisme majeur à une distance notable du gisement est un phénomène qui doit être analysé en fonction du contexte tectonique et des méthodes d'exploitation.

Fluid induced instabilities of the upper crust in the neighbouring of hydrocarbon extraction

Key words. – Fluid induced instabilities, Intraplate earthquakes, Induced seismicity, Hydrocarbon extraction.

Abstract. – This paper analyses different observed cases of mechanical instabilities in terms of seismic and aseismic behaviour. It is shown that the production parameters can trigger instabilities of different scales measured in terms of involved energy and distance from the reservoir. Three types of instability mechanisms are proposed on different scales, corresponding with observations in the neighbourhood of oil and gas production fields : local hydraulic fracturing due to fluid injection, large adjustment of the geological structure to perturbations related to how the reservoir is depleted, crustal readjustments on a regional scale related to the fluid transfers. In most cases seismic impact on the environment was minimal (fractures beneath the reservoir, low level of energy release). Nevertheless, the late occurrence of a major event far from the reservoir is a phenomenon that must be analysed as a function of the tectonic setting and the exploitation methods.

I. – INTRODUCTION

La plupart des ruptures, à l'échelle du globe, résultent de mouvements relatifs entre des plaques supposées rigides et se concentrent aux frontières de ces dernières. Par contre les processus qui causent les instabilités sismiques intraplaques, à l'intérieur des continents, sont peu compris même si différentes mesures indiquent un état assez uniforme de contrainte horizontale majeure, [Sykes et Sbar, 1973 ; Zoback et Zoback, 1980 ; Fredich *et al.*, 1988] suggérant que dans ces régions, la croûte supérieure agit comme un guide de contrainte de compression. En particulier on ne peut déterminer si les failles intracontinentales sismiques sont des zones faibles potentiellement plus sensibles, ou des zones sous fortes contraintes régionales induites ou concentrées. Le rôle des fluides a été pris en compte par plusieurs auteurs pour expliquer ces ruptures, Byerlee [1967], Nur [1972], Bell et Nur [1978], Gold et Soter [1985], Costain *et al.* [1987], Sibson [1989], sans toutefois les restreindre aux séismes intraplaques.

Yerkes et Castle [1976] présentèrent une synthèse des cas de sismicité induite observés au voisinage d'exploitations d'hydrocarbures. Ces événements de faible magnitude (magnitude < 3), sont associés à des exploitations induisant de forte subsidence (quelques mètres). Le manque d'observations sismiques de qualité n'a pas permis leur étude dans un contexte géomécanique. Grasso [1990], présente de récentes observations d'instabilités sismiques au voisinage d'exploitations d'hydrocarbures sur divers sites mondiaux. Ces séismes induits ou déclenchés par les manipulations de fluides couvrent une gamme énergétique en moyenne largement inférieure à celle des séismes naturels (magnitude ≤ 4). Dans des contextes structuraux et sismo-tectoniques particuliers, certains modes d'exploitation de gisements semblent cependant être associés à des manifestations différées plus énergétiques (magnitude ≥ 6).

La compréhension des conditions d'apparition de tels mécanismes d'instabilité sismique est nécessaire tant pour appréhender fondamentalement l'origine de la sismicité intracontinentale que pour gérer et contrôler l'impact possible des exploitations d'hydrocarbures sur l'environnement.

II. – INJECTION DE FLUIDE, AUGMENTATION DE LA PRESSION DE FLUIDE ET RUPTURE SISMIQUE

Historiquement l'augmentation de la pression du fluide a été le premier mécanisme invoqué pour comprendre le rôle des fluides dans le déclenchement de séismes. Deux principaux types ont été relatés et concernent, soit les séismes survenus après la mise en eau de certaines retenues artificielles [e.g. Gough et Gough, 1970 ; Simpson, 1976 ; Gupta et Rastogi, 1976 ; Simpson, 1986 ; Simpson *et al.*,

* LGIT/IRIGM, Observatoire de Grenoble, Grenoble, France.
** Expertise Mécanique des Roches Elf Aquitaine, Pau, France?
Manuscrit déposé le 28 janvier 1991, accepté le 20 juin 1991.

1988], soit les séismes associés à des injections de fluides [e.g. Evans, 1966; Healy *et al.*, 1968; Raleigh *et al.*, 1972]. Dans cette étude nous n'envisageons pas un inventaire exhaustif des différentes observations, mais une présentation de différentes ruptures types en fonction, à la fois de l'échelle des processus déclencheurs et de celle des phénomènes observés en nous concentrant sur les manipulations souterraines de fluides, proches des phénomènes naturels.

L'injection de fluide localisée (un ou quelques puits) est souvent utilisée par les producteurs, tant pour évaluer les propriétés hydrauliques des réservoirs, que pour stimuler la production en modifiant ces mêmes caractéristiques (fracturation hydraulique). Les événements sismiques correspondant à ces ruptures appartiennent au domaine des microséismes (magnitude maximale < 2, dimension des sources décimétrique). Le délai en temps entre l'injection et les microruptures est fonction du temps de montée en pression au fond du puits. Ces microruptures, utilisées de façon standard sur les champs géothermiques pour évaluer les capacités du réservoir et l'évolution spatio-temporelle de ses caractéristiques, commencent à l'être sur des champs d'hydrocarbures [Cassel *et al.*, 1990]. Des observations semblables, [e.g. Cold Lake, Alberta, Canada, $-2{,}0 < Ml < 1{,}3$, Kapotas et Kanasewitch, 1989], montrent que ce type de mécanisme joue lors d'injection d'eaux polluées en vue de l'évacuation de déchets. Ce mécanisme est susceptible de générer des fractures nouvelles de dimension métrique à pluridécamétrique, dans des roches initialement intactes.

Lorsque ces injections sont utilisées de façon massive, en particulier comme technique de récupération secondaire sur des gisements d'huile, l'échelle des phénomènes observés change d'un ordre de grandeur. En effet de nombreux séismes de magnitude comprise entre 3 et 4 sont reportés au voisinage de gisements stimulés par injection de fluide, dans des régions précédemment considérées comme asismiques [Colorado, Raleigh *et al.*, 1972; Nebraska, Evans *et al.*, 1987; Ohio, Nicholson *et al.*, 1988; Texas, Doser *et al.*, 1991]. Le mécanisme fondamental du déclenchement de tels événements a été suggéré puis vérifié sur deux exemples types au Colorado, Denver et Rangely. Sur le champ de Rangely (réservoir d'huile à 1 700 m de profondeur), une approche en contrainte effective utilisant un critère de rupture de type Mohr-Coulomb, conduit à prévoir à une pression fluide critique de 27 Mpa (Plitho/Pfluide ≈ 1.5), concordant bien avec les variations du nombre de séismes [Raleigh *et al.*, 1972] : 1 000 microséismes d'octobre 1969 à novembre 1970 de magnitude $-0{,}5 < Ml < 3{,}5$. A Denver ce sont plus de 1 500 séismes de 1962 à 1969. Lors d'injection de fluide à Dale, New-York, pour le lessivage et l'extraction de sel un taux mensuel de 80 séismes fut observé contre un taux naturel de 1 séisme par mois [Fletcher et Sykes, 1977]. La pression de fond oscillait entre 5,2 et 5,5 Mpa à 450 m (Plitho/Pfluide ≈ 1,9). Lorsqu'elle tombait sous 5 Mpa l'activité sismique cessait.

Par contre les trois séismes majeurs, $Ml > 5$, survenus à Denver, 14, 18 et 21 mois après la fin des injections, à des distances, du seul puits injecteur, supérieures à 5 km ne sont pas directement expliquables par le mécanisme évoqué précédemment. Le lien entre ces événements et l'injection de fluide conduit à envisager un mécanisme de report spatio-temporel de contrainte par propagation de pression de fluide le long de l'accident préexistant sur lequel se positionnent les microséismes observés antérieurement et ces 3 événements majeurs tardifs [Hsieh et Bredehoeft, 1981]. Plus récemment, l'exemple d'une séquence de séismes en Ohio, [Nicholson *et al.*, 1988], localisés entre 5 et 10 km du puits injecteur, montre que des variations de pression de fluide de l'ordre de quelques Mpa (fig. 1), furent suffisantes pour déclencher des ruptures sismiques ($Ml \approx 3$-4), dans un milieu initialement soumis à un état de contraintes tectoniques qui favorisa les ruptures. La possibilité de connexion régionale, sur des distances horizontales de l'ordre de la dizaine de kilomètres, peut être envisagée selon la dimension et les caractéristiques hydro-mécaniques des fractures préexistantes, les volumes et les pressions de fluides injectés. Pour ces derniers cas, Colorado, Ohio, les directions de contraintes mesurées *in situ* ou déduites des analyses sismiques, [Raleigh *et al.*, 1972; Evans, 1987; Nicholson *et al.*, 1988], sont en accord avec les directions régionales estimées ou mesurées *in-situ*. L'augmentation de la pression de fluide ne représente donc, dans ces exemples, que la perturbation de contrainte, relativement au chargement initial principal tectonique, qui déclenche les instabilités sismiques. Ces instabilités ainsi déclenchées sont donc localisées sur des accidents tectoniques préexistants à la différence des nouvelles ruptures provoquées à plus petite échelle lors de certaines fracturations hydrauliques.

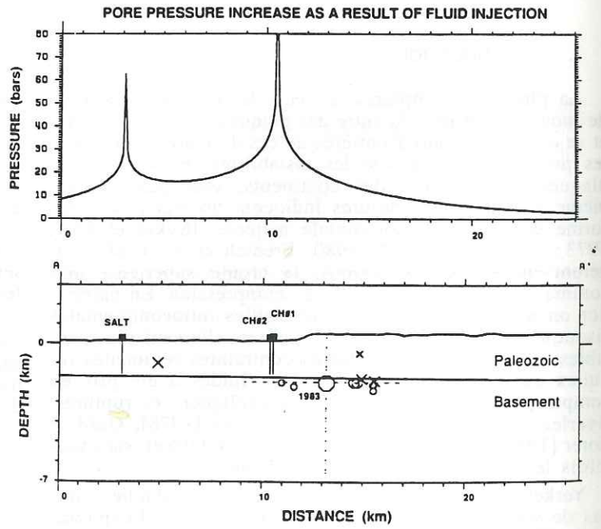

FIG. 1. – (Haut) Variations maximales de pression fluide estimées avec les hypothèses de flux radial pour les 3 puits injecteurs (Perry nuclear power plant, Ohio, USA).
(Bas) Coupe verticale positionnant les séismes associés aux injections sur ce même site. Croix : séismes superficiels ; ronds : séismes dans le socle ; [adapté de Nicholson *et al.*, 1988].

FIG. 1. – *Maximum increase in pore pressure resulting from fluid injection assuming radial flow at the Perry Power Plant injection wells Ohio, USA. [adapted from Nicholson* et al. *1988].*

Les ruptures induites par injection de fluide sont comprises comme résultant de l'augmentation de la pression interstitielle, cette dernière, en diminuant la contrainte normale effective sur le plan de faille en permet le mouvement sous l'effet de la contrainte de cisaillement inchangée (à contrainte tectonique constante).

III. – Extraction de fluide, redistribution des contraintes et instabilités sismiques

Par opposition au mécanisme présenté précédemment, l'extraction de fluide diminue la pression de pore ; la même argumentation suggère donc que ce processus augmente la contrainte effective normale et bloque le rejeu des fractures existantes.

Les observations et études menées sur les événements sismiques survenus autour du champ de Lacq (France), enregistrés avec précision [Grasso et Wittlinger, 1990] et la caractérisation du contexte géomécanique local [Grasso et Feignier, 1990], ont permis de montrer que ce type d'instabilités n'avait pas lieu dans les niveaux dépressurisés du réservoir où la pression du gaz diminue (fig. 2), mais sont dans leur grande majorité localisés au-dessus et au-dessous du réservoir. La présence de niveaux imperméables au-dessus du réservoir réduit les possibilités de connection de fluide entre le réservoir et les niveaux supérieurs. Le mécanisme des ruptures survenues dans ces niveaux ne peut être dû à une propagation rapide de pression fluide. L'orientation des axes de contrainte maximales *in situ* ($\approx \sigma 1$), déduits des interprétations des mécanismes aux foyers des séismes induits, indique une répartition radiale autour du gisement, très différente de l'orientation régionale des contraintes *in situ* déterminées par ailleurs à partir de mécanismes aux foyers des séismes régionaux naturels et de mesures d'ovalisations de forages [Grasso et Feignier, 1990].

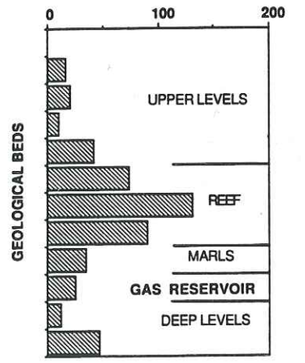

FIG. 2. – Microséismes induits par la déplétion du réservoir de gaz de Lacq (France), période 1976-1982. Chaque colonne du diagramme représente le nombre d'événements localisés dans les différentes entités géomécaniques de la structure en dôme du champ. L'épaisseur de chaque entité est d'environ 500 m. Le réservoir est localisé à 3 500 m de profondeur. Le report poroélastique des contraintes de part et d'autre du réservoir est bien visualisé par les ruptures sismiques.

FIG. 2. – *Induced seismicity on Lacq gas field (France), 1976-1982. Number of events per geological bed are reported on the diagram, in order to take into account the local 3D dome structure. Note that few events occur within the gas reservoir (pore pressure decrease). Events occur above and below reservoir induced by poroelastic stress transfer.*

Pour expliquer ces observations, il faut faire appel à une redistribution des contraintes associée à la déplétion des niveaux réservoirs. Ces ruptures sont ainsi induites dans une zone qui n'est pas en contact direct avec l'extraction de fluide (présence de barrière imperméable nécessaire à l'existence même du gisement), par opposition aux ruptures déclenchées sur une discontinuité par la diminution de la contrainte effective normale s'exerçant sur ce même accident (cas de l'injection détaillée dans le paragraphe précédent). En terme de mécanismes, (fig. 3) ces distinctions correspondent dans un cas à un effet de contrainte (cercle de Mohr dilaté par variation du rayon), dans l'autre à un effet de pression de fluide (cercle de Mohr translaté à rayon constant). Le volume perturbé par le report poroélastique de contraintes définit la zone d'influence du processus de déformation poroélastique du réservoir. Sur le site de Lacq, où ces événements sont observés et étudiés de façon fine depuis de nombreuses années, les déformations sismiques se sont manifestées jusqu'à des distances du réservoir atteignant 5 km : la zone d'influence s'avère plurikilométrique (fig. 4). Des modélisations de ce phénomène, utilisant une formulation linéaire dans un milieu biphasique poroélastique [Biot, 1941 ; Rice et Cleary, 1976], ont été proposés par Geertsma [1973], Segall [1989]. Sur le champ de Lacq, la subsidence maximale mesurée a été de 6 cm pour une déplétion du réservoir de gaz de 50 Mpa à 3 750 m en 30 ans [Maury *et al.*, 1990] : une telle modélisation simplifiée permet dans ce cas une estimation de l'amplitude de la variation de contrainte induite dans les niveaux situés au-dessus du réservoir : celle-ci est de l'ordre du Mpa (Segall comm. pers., 1989). Cet ordre de grandeur est le même que celui de l'amplitude des relâchements cosismiques de contraintes déduits de l'analyse spectrale des événements sismiques survenus dans ces mêmes niveaux [Feignier et Grasso, 1991]. Il est important de noter qu'aucune entrée d'eau naturelle ou artificielle n'est rapportée pour ce gisement, attestant pour ces variations de contrainte une origine induite par une redistribution poroélastique. Ces simples modèles poroélastiques, permettant d'évaluer l'ordre de grandeur des variations de contraintes induites, ne prennent pas en compte les propriétés hydrauliques et mécaniques des niveaux environnants ni les caractéristiques des discontinuités présentes dans la structure géologique. Ces paramètres déterminent cependant la part respective des déformations sismiques et asismiques (fig. 5), ainsi que la localisation des ruptures sismiques [Grasso et Feignier, 1990 ; Feignier et Grasso, 1990]. Sur d'autres sites, où la précision insuffisante des mesures ne permet pas des conclusions aussi détaillées qu'à Lacq, on observe toutefois que les déplétions de réservoir, de l'ordre de 30 Mpa, à 3-4 km de profondeur, peuvent être associées à des événements sismiques de magnitude maximale atteignant 3 à 4, et ce dans des contextes tectoniques régionaux très variés (stable : Hollande [Grasso, 1990], Texas [Pennington *et al.*, 1986] ; extension : mer du Nord, Norvège, Danemark

[Grasso, 1990] ; compression ; Canada [Wetmiller, 1986], Azerbaïdjan [Grasso, 1990]. La taille des accidents structuraux environnant le site (souvent constitutif du type de piège créant le réservoir d'hydrocarbures) ainsi que les propriétés mécaniques des matrices rocheuses sont déterminantes pour comprendre et évaluer la possibilité d'apparition de ce type d'instabilités sismiques.

La sollicitation du milieu poroélastique que constitue le réservoir n'est pas limitée à la seule chute de pression correspondant à la déplétion : des manipulations de fluides plus complexes peuvent provoquer des réponses plus variées.

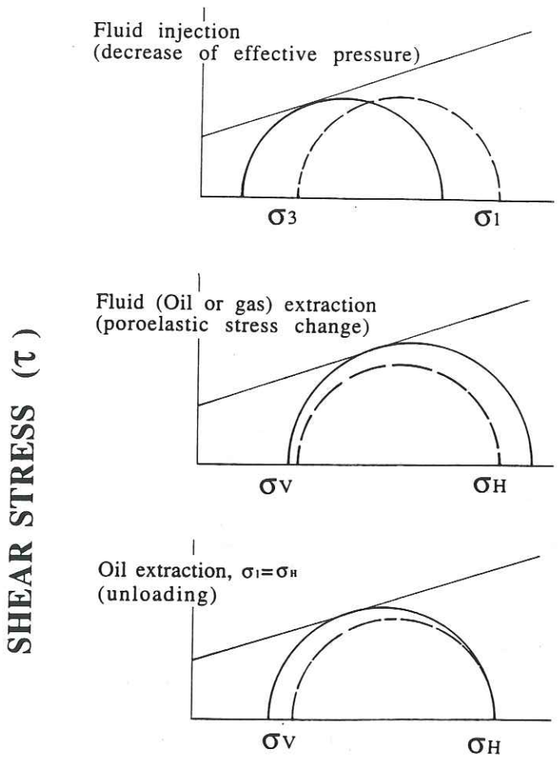

FIG. 3. – Représentation sur le cercle de Mohr des différents mécanismes proposés pour comprendre le rôle des manipulations de fluide dans le déclenchement d'instabilités sismiques. On notera que lors de l'effet poroélastique (schéma central), la pression du fluide intervient de deux façons : par un effet de contrainte mécanique (charge ou décharge), dilatation du rayon du cercle de Mohr, similaire à celui visualisé sur le schéma du bas; par un effet de pression fluide, translation du cercle de Mohr, similaire à celui visualisé sur le schéma du haut. En fonction du contexte géomécanique, les deux effets peuvent se cumuler ou s'opposer. Les orientations des failles préexistantes et des contraintes principales déterminent les contraintes induites efficaces.

FIG. 3. – *Mohr circle interpretation of the 3 type of mechanisms associated with subsurface fluid manipulations.*

IV. – TRANSFERT DE MASSE ET CIRCULATION DE FLUIDE : EFFET MÉCANIQUE, HYDRAULIQUE, PHYSICO-CHIMIQUE ET RUPTURE SISMIQUE

Les cas observés de sismicité déclenchée par des manipulations de fluides au voisinage d'exploitations d'hydrocarbures ne sont pas souvent aussi facilement classifiables et identifiables que ceux analysés ci-dessus. En effet, une troisième catégorie de perturbations, liée au mode d'extraction, est observée sur les gisements où, pour améliorer la récupération secondaire, on injecte un fluide en périphérie du gisement dans le but de « balayer » le fluide intéressant vers le puits producteur tout en « maintenant » une pression de gisement. Le déséquilibre résultant entre zone déplétée et zone soumise à injection, conduit à des ruptures localisées au niveau des contrastes maxima (Caucase : Smirnova [1975] ; Ontario : Mereu *et al.* [1986] ; Texas : Davis *et al.* [1989]). Le report de contrainte accentue l'effet de l'augmentation de pression fluide et peut ainsi expliquer la localisation des ruptures sismiques (zones où les deux effets se cumulent). D'un point de vue temporel, le report des contraintes autour du réservoir expliquerait les délais entre le début de l'exploitation et l'apparition des ruptures. Davis *et al.* [1989] proposent un tel cumul pour certaines observations sur des champs texans : la mise en charge du milieu environnant due à la redistribution de contraintes provoquée par la déformation du réservoir dépressurisé amène localement des conditions proches d'un état critique sur une discontinuité. A ceci s'ajoute la réduction de la contrainte effective normale, provoquée sur cette même discontinuité par l'augmentation de la pression interstitielle. Une instabilité sismique peut ainsi être déclenchée ; sinon, seule une déformation asismique sera observable. On peut donc assister à des réponses sismiques ou asismiques plus ou moins différées selon le contexte tectonique et la rhéologie des matériaux.

Leurs observations dépendent à la fois des moyens de mesures mis en œuvre sur le site et de la taille des ruptures induites. Dans certaines régions les instabilités sont probablement exclusivement asismiques, et de larges déformations sont induites par de fortes déplétions sans aucun séisme. Ces déformations peuvent être reprises par l'ensemble du massif (Groninguen, Hollande) ou être plus ou moins localisées (Buena Vista, Californie [Nason *et al.*, 1968]. Cet aspect n'est pas développé ici, bien que ces mouvements asismiques soient fondamentaux pour l'exploitant [Maury *et al.*, 1987 ; Maury et Sauzay, 1988, 1989].

Si l'on revient au cas où des ruptures sismiques ont été observées, la zone d'influence de la perturbation de contrainte reste kilométrique et les particularités géologiques des différents sites mènent à des réponses locales variées. Le cas du champ de Grozny, Caucase, Azerbaïdjan, est intéressant car d'un point de vue purement sismologique, il représente bien les concepts de faille forte/faille faible, la notion de zone de faiblesse préexistante et l'effet d'une connexion des activités d'extraction d'hydrocarbures avec le fonctionnement d'un accident tectonique sismique-

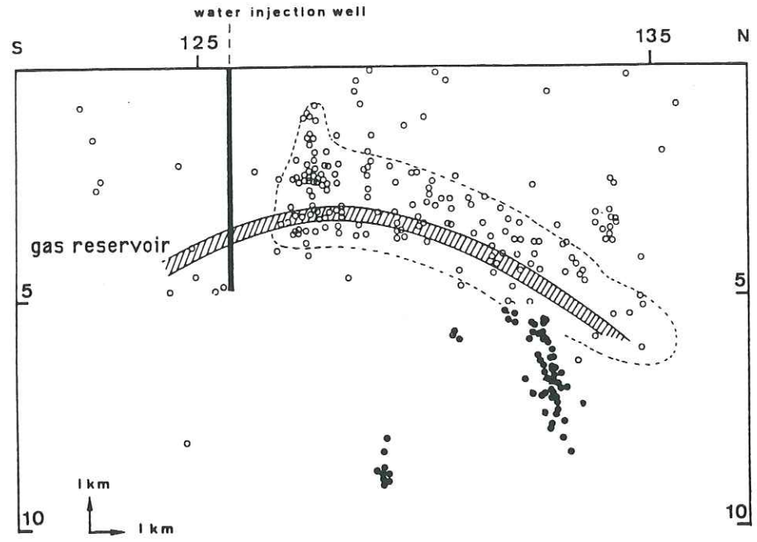

FIG. 4. – Projection sur un plan vertical des événements sismiques du dôme de Lacq (France) associés à la déplétion du réservoir de gaz. 1959, début de l'extraction ; 1969 premier séisme ressenti ; 1969-1981 les microséismes sont localisés exclusivement au-dessus des niveaux déplétés (rond blanc) ; depuis 1982 apparition d'événements profonds (rond noir), localisés sous le réservoir de gaz [adaptée de Grasso et Wittlinger, 1990].

FIG. 4. – *Vertical cross section of the hypocentres located in Lacq area. White circles are induced sismicity in the 1969-1980 period. Black dots are induced events which occur below the reservoir since 1982. [adapted from Grasso et Wittlinger, 1990].*

ment actif. Dans un premier temps (6 ans), la baisse de pression de fluide, 30 Mpa pour le réservoir de gaz, stabilise les instabilités sismiques de la région (fig. 6), ces dernières sont localisées sur une faille proche du gisement (distance < 4 km). Mais ce blocage de la faille ne peut s'effectuer que sur une portion finie de l'accident. Il en résulte une accumulation de contraintes tectoniques aux extrémités de la partie ainsi verrouillée de la faille. Après 6 ans, le seuil critique de résistance au cisaillement est atteint et les séismes réapparaissent. Cette activité a pu être renforcée ultérieurement par des injections périphériques qui débutèrent un an plus tard.

Sur l'ensemble des cas étudiés, il apparaît que ces variations de contraintes relativement faibles (de l'ordre de quelques Mpa), semblent suffisantes pour déclencher des ruptures sismiques dans les formations environnantes. De la même façon ce seraient des variations de pression fluide aussi faibles, liées à des variations de niveaux de retenues artificielles, qui pilotent le rejeu de discontinuités, en fonction de leurs géométries [Roeloffs, 1988].

Il faut évoquer également les connexions possibles entre séismes majeurs (Ms > 6) et certaines exploitations d'hydrocarbures. Tant en Californie [McGarr, 1991] qu'en Ousbékistan [Plotnikova *et al.*, 1989], (la liste n'est pas exhaustive et des cas analogues sont actuellement envisagés en Equateur : Grasso et Chatelain [1991]), des événements majeurs sont corrélés aux perturbations hydromécaniques de la croûte supérieure dues aux extractions de fluides souterrains dans les niveaux supérieurs. Dans ces cas, les accidents stimulés sont des failles cachées, situées sous des anticlinaux ayant piégé le gisement. En Californie, région tectoniquement en compression, McGarr [1991] propose une corrélation entre le moment sismique des séismes (couple des forces élastiques relâchées lors de la rupture) et la variation, positive ou négative, de masse dûe à l'extraction d'huile, corrigé de l'épaisseur de la partie sismogénique de la croûte régionale, sur la base de l'analyse des récents séismes de Coalinga (1983, Ms = 6,5), Kettleman North Dome (1985, Ms = 6,1) et Whittier Narrows (1987, Ms = 5,9). Pour le séisme de Coalinga, le mécanisme de report poroélastique semble trop faible ($\Delta\sigma$ = 0,02 Mpa, augmentation de la contrainte efficace sur le plan de faille du séisme) pour expliquer le déclenchement de la rupture [Segall, 1985], si on le compare à la chute de contrainte cosismique ($\Delta\sigma$ = 10 Mpa). Le problème peut être considéré comme ouvert du fait de la très forte indétermination inhérente au calcul de la chute de contrainte cosismique dans les différents modèles sismologiques. Pour les séismes de Gasli, dans une région considérée jusqu'alors comme peu sismique (Ouest Ousbékistan), on peut retrouver la relation proposée par McGarr : l'excès de masse (entrée d'eau) est aussi corrélable au moment sismique. De plus le flux d'eau vers le champ perturbe l'équilibre hydrostatique régional. Le gisement est envahi avant chaque instabilité par plus de 300 millions de tonnes d'eau de l'aquifère. Même si une alimentation s'effectuant partiellement à partir d'aquifères superficiels (z < 5 km) peut être également envisagée, les connexions hydrauliques avec les discontinuités régionales majeures sont possibles compte tenu des anomalies hydrauliques observées sur ce site (Plotnikova, commu. pers.,

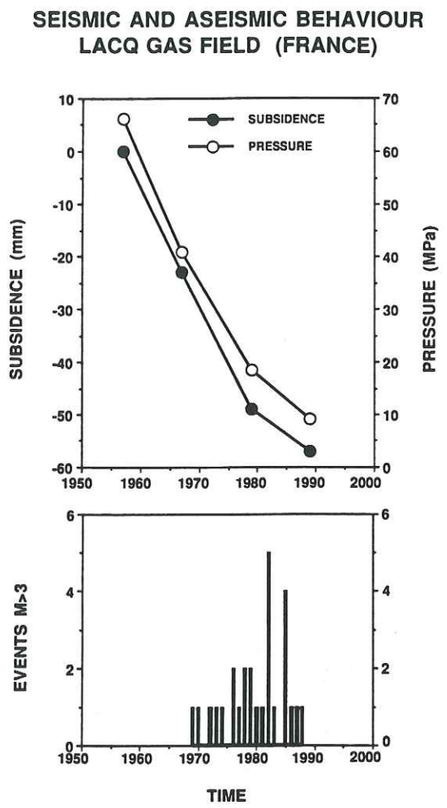

FIG. 5. – Sismicité et affaissement de surface observés sur le site de Lacq (France), en fonction de la baisse de pression du réservoir de gaz. Seul les événements dont Ml ≥ 3 sont reportés sur le diagramme inférieur (période 1950-1989).

FIG. 5. – *Seismic and aseismic behaviour of the Lacq Gas Field (France).*

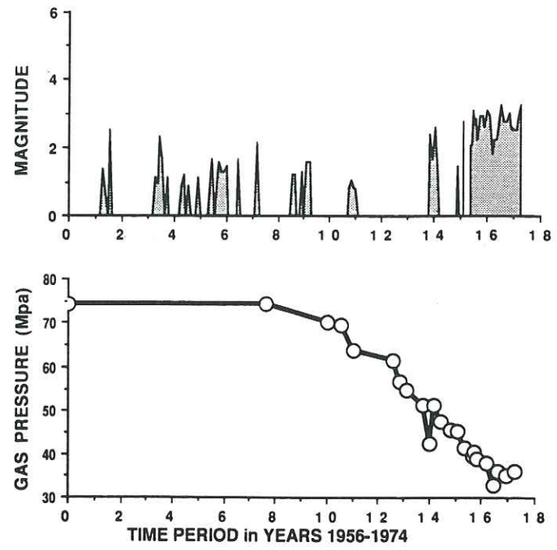

FIG. 6. – Sismicité et baisse de pression induites par l'exploitation du champ de Grozny (Azerbaïdjan), période 1956-1974, [adaptée de Smirnova comm. pers. 1990).

FIG. 6. – *Seismicity and reservoir pore pressure drop induced by the Grozny Gas field, (Azerbaïdjan), period 1956-1974, [adapted from Smirnova comm. pers., 1990].*

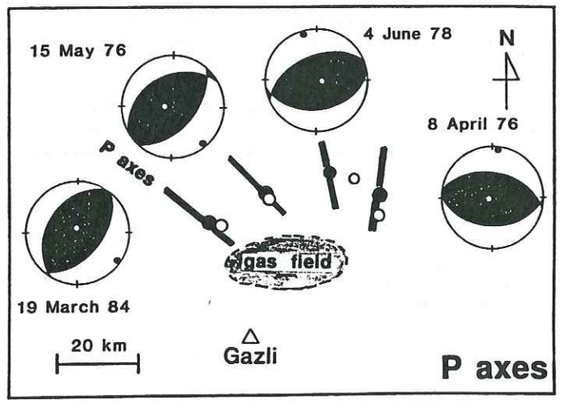

FIG. 7. – Carte des séismes majeurs de la région de Gasli (Ousbekistan), Ms ≥ 7, excepté pour le séisme de 1978 (Ms = 5,9). Les ronds noirs sont les relocalisations des séismes effectuées en prenant l'évenement de 1984 comme référence [adapté de Eyidogan *et al.*, 1985]. Les barres noires schématisent localement la direction de la contrainte principale majeure estimée in situ à partir des mécanismes aux foyers [Eyidogan *et al.*, 1985; Besrodny, 1986].

FIG. 7. – *Seismicity map for the major events in Gasli area Ms ≥ 7, excepted june 4 event with magnitude = 5.9 Black lines are the orientation of the major horizontal stress. These orientations are estimated in situ by [Eyidogan* et al., *1985; Besrodny, 1986] with Paxes of focal mechanism analysis.*

1990). On rejoint ainsi l'idée proposée plus généralement par Gold et Soter [1985] pour les séismes naturels, de déclenchements de ruptures dûs à l'envahissement, par un milieu fluide, d'un massif soumis à un fort état de contraintes. On notera sur la période 1976-1984 le caractère anormal des axes de contraintes des séismes majeurs (fig. 7), en désaccord avec les orientations régionales [Zoback *et al.*, 1989]. De telles orientations anomaliques peuvent être caractéristiques de la présence de failles faibles, d'anomalie locale de contrainte (répartition radiale autour du gisement provoquée par l'importance de la zone déplétée), ou des indices du rôle des fluides dans le déclenchement de ces ruptures.

V. – CAS DES SÉISMES NATURELS

Dans le cas des séismes naturels des pressions de fluides anormales, surpressions par rapport au régime hydrostatique, ont d'abord été invoquées pour expliquer la propagation des ruptures qui suivent spatio-temporellement les séismes majeurs. Ces surpressions, créées par le déséquilibre mécanique localement induit aux extrémités de la rupture principale, expliquent les migrations spatio-temporelles des ruptures secondaires, en accord avec les valeurs de diffusivité hydraulique [Nur, 1972]. Plus récemment, ces mêmes surpressions ont été proposées pour comprendre des séquences de ruptures intraplaques [Gold et Soter, 1985], des géométries de ruptures anormales [Sibson, 1989] ou des anomalies de contraintes au voisinage de failles majeures [San Andreas : Byerlee, 1990 ; Rice, 1990].

Gold et Soter [1985] invoquent le rôle prépondérant que doivent jouer les fluides lors de séquence spatio-temporelle courte de séismes majeurs (New-Madrid, USA, 3 magnitudes 8 en 3 mois, 1911-1912 ; Sungpan-Pingwu, Chine, M = 7,2, 6,8, 7,2, la même semaine en moins de 40 km, août 1976 ; Tenant Creek, Australie, 3 magnitudes 6, à 12 h d'intervalle près d'une zone de pompage d'eau, 1988) telle celle de Gasli (Ms = 7,1, 7,1, en moins de 40 jours, distants de 20 km, suivi par Ms = 7 à moins de 20 km 8 ans plus tard). On pourrait imaginer que les ruptures, lors du premier séisme de chaque série aient déchargé la plupart de l'énergie de déformation emmagasinée sur la faille et les accidents voisins. La continuation de la lente accumulation de contrainte tectonique, qui nécessite un minimum d'une centaine d'années pour déclencher de telles ruptures, ne peut donc pas être le processus à la base d'une telle performance quelques jours ou mois plus tard. La nécessité d'une constante de temps plus courte mène à impliquer la pression de fluide par son effet poroélastique. Deux autres mécanismes à constantes de temps plus lentes peuvent aussi être impliqués. Une diffusion de contrainte visco-élastique est possible soit au niveau du couplage lithosphère-asthénosphère [e.g. Rice, 1983 ; Rydelek et Sacks, 1990], soit pour des séismes plus superficiels au niveau des décollements socle-sédiments [Grasso *et al.*, 1991]. Il convient d'envisager également qu'un effet physico-chimique (dissolution-cristallisation, Gratier [1984]) puisse modifier les propriétés mécaniques des accidents préexistants et ce mécanisme, plus lent, serait à prendre en compte comme processus de déclenchement de la première instabilité de la série.

Dans un domaine proche, des orientations anormales des plans de ruptures de séismes majeurs pose le problème de la réactivation ou de la nucléation de la rupture sur ces discontinuités. De telles géométries sont déduites de mécanismes au foyer de séismes bien contraints. En désaccord avec les lois de mécaniques des roches (fig. 8), coefficient de friction < 0,55, alors que le critère de Byerlee est vérifié sur la majorité des séismes, ces ruptures sismiques correspondent à des angles d'environ 60° pour les rejeux en failles inverses et des angles inférieurs à 30° pour des failles normales. Bruhn *et al.* [1982], démontrent que pour des failles normales à faible pendage, la réactivation implique soit un coefficient de friction inférieur à 0,35 soit une contrainte effective principale mineure négative. Dans ce sens Sibson [1983, 1989] propose que l'activation répétée de telles géométries nécessite une pression de fluide supérieure à la contrainte principale mineure, c'est-à-dire une contrainte effective négative, en accord avec différentes observations [Sibson 1981, 1990]. La recharge en pression de fluide permet de réinitialiser le système avec des pressions de fluide proche de la pression lithostatique. Ainsi la nucléation des ruptures sur des accidents fortement mal orientés dépend d'une pression critique de fluide dans un milieu soumis à un niveau suffisant de contrainte de cisaillement. Ce cycle, gouverné par la dépendance entre la pression de fluide et la résistance au cisaillement peut être très variable.

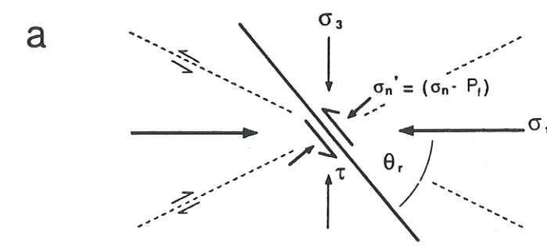

FIG. 8. – a) Schéma présentant le problème de la réactivation d'une faille « mal orientée » (en trait gras) et les orientations optimales pour des coefficients de friction respectant la loi de Byerlee (trait pointillé). b) Coupe verticale illustrant les relations entre les failles inverses raides de Oak ridge, Red mountain (RMF) et l'anticlinal de Ventura, Santa Barbara, Californie. On notera qu'un rapport Pf/σv proche de 0.9 est mesuré dans cette région à 4 km de profondeur [d'après Yeats *et al.*, 1988].

FIG. 8. – a) *Condition for fault reactivation. Misoriented preexisting faults are labelled using black lines. Dotted line faults agree with the Byerleelaw for friction coefficient.* b) *Vertical cross section showing relation between strip reverse faulting and anticline structure, Santa Barbara USA. Note that a ratio fluid pressure/vertical stress = 0.9 is reported at 4 km depth in this area [after Yeats* et al., *1988].*

VI. – Conclusions

1) Nous montrons dans cette étude que des manipulations de fluides souterrains sont susceptibles d'induire ou de déclencher des instabilités sismiques habituellement situées dans une gamme de faible niveau énergétique ; dans certains contextes géologiques et industriels, l'énergie libérée pourrait atteindre le niveau de séismes naturels majeurs.

2) Les ruptures sismiques résultent de la création locale d'un état critique proche de la rupture par variation de contrainte ou par variation de la pression de fluide. La variation de contrainte peut, elle-même, être due à un transfert de masse fluide. A l'échelle d'un champ d'hydrocarbure, l'augmentation locale de pression fluide par injection, cas historiquement le plus étudié, est un processus secondaire tant du point de vue des énergies libérées, que par sa capacité à amener le milieu vers un état critique. La diminution de pression fluide, par la diversité des mécanismes qu'elle déclenche et de leur localisation spatio-temporelle selon les contextes, doit être prise en compte par les producteurs à la fois comme un outil d'exploitation du réservoir, mais aussi comme un outil de contrôle des effets sur l'environnement.

3) Les paramètres contrôlant les types de comportements (sismique, asismique) et la taille des phénomènes observés, sont liés aux propriétés géomécaniques et hydrauliques des milieux ainsi qu'au type de perturbation hydraulique appliquée. Les variations de contraintes effectives susceptibles d'induire de telles instabilités sont faibles, de l'ordre de quelques Mpa.

4) Des processus de redistribution de contrainte et de pression fluide sont quantitativement en accord avec les échelles des connexions observées. Les processus poroélastiques ont une zone d'influence limitée à quelques kilomètres autour de la zone perturbée. Les transferts de fluide, et leurs effets de masse et/ou physico-chimique ont une zone d'influence pouvant atteindre plusieurs dizaines de kilomètres. Les constantes de temps expérimentalement observées varient de quelques années à la dizaine d'années.

5) Ces observations et mécanismes confirment, à une échelle charnière entre le laboratoire et les blocs tectoniques, l'importance et la variété du rôle des fluides pour le déclenchement d'instabilités sismiques (en particulier dans le domaine intraplaque), et pour expliquer les différences de comportements entre ces instabilités.

Remerciements. – Cette étude n'a pu être réalisé qu'avec la collaboration de nombreux partenaires KNMI (Hollande), British Geological Survey (Scotland), Académie des Sciences d'Ousbékistan. Nous remercions D. Doser, D. Haak, Art McGarr, Leila M. Plotnikova, M.N. Smirnova, pour la fourniture de leurs travaux en cours de publication. Les critiques constructives de J.-P. Gratier, N. Kessler, P. Vialon et des 2 rapporteurs Y. Guegen, G. Vasseur ont permis d'améliorer la version finale du manuscrit.

Références

Bell M.L. & Nur A. (1978). – Strength changes due to reservoir-induced pore pressure and stresses and application to lake Oroville. – *J. Geophys. Res.*, **83**, 4469-4483.

Besrodny E.M. (1986). – The source mechanism of the Gazly earthquakes of 1976-1984. *In* : Gazly earthquakes of 1976 and 1984, Tashkent, Fan, 94-105.

Biot M.A. (1941). – General theory of a 3-dimensional consolidation. – *J. Appl. Phys.*, **12**, 155-164.

Bruhn R.L., Yusas M.R. & Huertas F. (1982). – Mechanics of low angle normal faulting : an example from Roosevelt hot springs geothermal area, Utah. – *Tectonophysics*, **2**, 345-356.

Byerlee J.D. (1967). – Frictional characteristics of granite under high confining pressure. – *J. Geophys. Res.*, **72**, 3639-3648.

Byerlee J.D. (1990). – Friction, overpressure and fault normal compression. – *Geophys. Res. Let.*, **17**, 2109-2112.

Cassel B., Bol G.M. & Stewart L. (1990). – Acoustic emission monitoring during hydraulic fracturing. – SPE 20970, Europec 90, The Hague 1990.

Costain J.K., Bollinger G.A. & Speer J.A. (1987). – Hydroseismicity : a hypothesis for the role of water in the generation of intraplate seismicity. – *Seismol. Res. Lett.*, **58**, 41-63.

Davis S.D. & Pennington W.D. (1989). – Induced seismic deformation in the Cogdell oil field of West Texas. – *Bull. Seism. Soc. Am.*, **79**, 1477-1494.

Doser D.I., Baker M.R. & Mason D.B. (1991). – Seismicity in the War-Wink gas field, Delaware basin, West Texas, and its relationship to petroleum production. – *Bull. Seism. Soc. Am.*, **81**, 971-996.

Evans M.D. (1966). – Man made earthquakes in Denver. – *Geotimes*, **10**, 11-17.

Evans K. (1987). – *In situ* stress discontinuity across the Appalachian plateau decollement. – AGU Spring Meeting, 1987.

Evans D.G. & Steeples D.W. (1987). – Microearthquakes near the Sleepy Hollow oil field, southwestern Nebraska. – *Bull. Seism. Soc. Am.*, **77**, 132-140.

Eyidogan H., Nabelek J. & Tolsoz N. (1985). – The Gazli, USSR, 19 march 1984 earthquake : the mechanism and tectonic implications. – *Bull. Seism. Soc. Am.*, **75**, 661-675.

Feignier B. & Grasso J.R. (1990). – Seismicity induced by a gas depletion ; I Correlation of focal mechanisms and dome structure. – *Pure Appl. Geophys.* **134**, 405-426.

Feignier B. & Grasso J.R. (1991). – Characteristics of seismic fractures as a function of geomechanical setting. – *Pure Appl. Geophys.* (sous presse).

Fletcher J.B. & Sykes L.R. (1977). – Earthquakes related to hydraulic mining and natural seismic activity in western New-York State. – *J. Geophys. Res.*, **82**, 3767-3780.

Fredrich J., McCaffrey R. & Denham D. (1988). – Source parameters of seven large Australian earthquakes determined by body waveform inversion. – *Geophys. J.R. astr. Soc.*, **95**, 1-13.

Geertsma J. (1973). – Land subsidence above compacting oil and gas reservoir. – *J. Petrol. Techn.*, **25**, 734-744.

Gold T. & Soter S. (1985). – Fluid ascent through the solid lithosphere and its relation to earthquakes. – *Pure Appl. Geophys.*, **122**, 492-530.

Gough D.I. & Gough W.I. (1970). – Stress and deflection in the lithosphere near lake Kariba. – *Geophys. J. Roy. Astro. Soc.*, **21**, 65-101.

Grasso J.R. (1990). – Hydrocarbon extraction and seismic hazard assessment. – *Eos transactions*, Am. Geophys. Union, **71**, 1454.

Grasso J.R. & Chatelain (1991). – Anomalous seismicity in the Lago-Agrio area, Equateur : Fluid-induced earthquakes ? – Report to Elf-Aquitaine company, 10 p., (non publié).

Grasso J.R. & Feignier B. (1990). – Seismicity induced by gas depletion : II Lithology correlated events, induced stresses and deformations. – *Pure Appl. Geophys.*, **134**, 427-450.

Grasso J.R., Gratier J.P., Gamond J.F. & Paumier J.C. (1991). – Stress diffusion triggering of earthquakes in the upper crust. – Int. Conference on Mechanical Instabilities In Rocks and Tectonics, Montpellier, France (Abst.).

Grasso J.R. & Wittlinger G. (1990). – Ten years of seismic monitoring over a gas field area. – *Bull. Seism. Soc. Am.*, **80**, 450-473.

Gratier J.P. (1984). – La déformation des roches par dissolution-cristallisation. – Thèse Doct. Etat, Univ. Grenoble, 316 p.

Gupta H.K. & Rastogi B.K. (1976). – Dams and earthquakes. – Elsevier, Amsterdam, 229 p.

Healy J.H., Rubey W.W., Griggs D.T. & Raleigh C.B. (1968). – The Denver earthquakes? – *Science*, **161**, 1301-1310.

Hsieh P.A. & Bredehoeft J.D. (1981). – Reservoir analysis of the Denver earthquakes. The case of induced seismicity. – *J. Geophys. Res.*, **86**, 903-920.

Kapotas S. & Kanasewitch E.R. (1989). – Microseismicity and stress orientations in Cold lake, Alberta. – Report to Esso Ress. Canada Cy. (non publié).

MacGarr A. (1991). – On a possible connexion between three major earthquakes in California and oil production. – *Bull. Seism. Soc. Am.*, **81**, 948-970.

Maury V., Fourmaintraux D. & Sauzay J.M. (1987). – Approche géomécanique de la production pétrolière. Problème essentiels, premiers résultats. – Proc. Int. ISRM Meeting, Montréal, 1987.

Maury V., Grasso J.R. & Wittlinger G. (1990). – Lacq gas field (France). Monitoring of induced subsidence and seismicity : consequences on gas production and field operation. – SPE 20887, Europec 90, The Hagen, October 1990.

Maury V. & Sauzay J.M. (1988). – Borehole instability : case history, rock mechanics approach and results. – Proc. SPE/IADC Conf. paper ; SPE/IADC 16051.

Maury V. & Sauzay J.M. (1989). – Oil well collapse due to fault shearing : a case study and some comments. *In* : V. Maury & D. Fourmaintraux Eds., Proc. of the Int. Symp. I.S.R.M. Rock at great depth, Pau. – Balkeman, Amsterdam, 871-880.

Mereu R.F., Brunet J., Morrissev K., Price B. & Yapp A. (1986). – A study of the microearthquakes of the Gobles oil field area of southwestern Ontario. – *Bull. Seism. Soc. Am.*, **76**, 1215-1223.

Nason R.D., Copper A.K. & Tocher D. (1968). – Slippage on the Buena Vista thrust fault. – 43rd annual meeting guidebook, AAPG, SEG, SEPM. – Am. Ass. Pet. Geol., Pac. Sect., 100-101.

Nicholson C., Roeloffs E. & Wesson R.L. (1988). – The northeastern Ohio earthquake of 31 january 1986 : Was it induced ? – *Bull. Seism. Soc. Am.*, **78**, 188-217.

Nur A. (1972). – Dilatancy, pore fluids, and premonitory variation of ts/tp travel times. – *Bull. Seism. Soc. Am.*, **62**, 1217-1222.

Pennington D.W., Davis S.D., Carlson S.M., Dupree J. & Ewing T.E. (1986). – The evolution of seismics barriers and asperities caused by the depressuring of fault planes in oil and gas fields of south Texas. – *Bull. Seism. Soc. Am.*, 939-948.

Plotnikova L.M., Flynova M.G. & Machmudova V.I. (1989). – Induced seismicity in gas field region. – Proc. XXV IASPEI general assembly, Istambul, august 1989.

Raleigh C.B., Healy J.H. & Bredehoeft J.D. (1972). – Faulting and crustal stress at Rangely, Colorado. – A.G.U., *Geophys. Monog.*, **16**, 275-284.

Rice J.R. (1983). – Earthquake aftereffects and triggered seismic phenomena. – *Pure and Appl. Geophys.*, **121**, 187-219.

Rice J.R. (1990). – Fault stress states, pore pressure distributions, and the weakness of the San Andreas fault. – *Eos* transactions, Am. Geophys. Union, **71**, 1652.

Rice J.R. & Cleary M.P. (1976). – Some basic stress diffusion solution for fluid saturated elastic porous media with compressible constituents. – *Rev. Geophys. Space Phys.*, **14**, 227-241.

Roeloffs E. (1988). – Fault stability changes induced beneath a reservoir with cyclic variations in water level. – *J. Geophys. Res.*, **93**, 2107-2124.

Rydelek P.A. & Sacks I.S. (1990). – Asthenospheric viscosity and stress diffusion : a mechanism to explain correlated earthquakes and surface deformations in the NE Japan. – *Geophys. J. Int.*, **100**, 39-58.

Segall P. (1985). – Stress and subsidence resulting from subsurface fluid withdrawal in the epicentral region of the 1983 Coalingua earthquake. – *J. Geophys. Res.*, 6801-6816.

Segall P. (1989). – Earthquakes triggered by fluid extraction. – *Geology*, **17**, 942-946.

Sibson R.H. (1981). – Fluid flow accompanying faulting : field evidence and models. *In* : Earthquake prediction : an international review. – Am. Geophys. Union, *M. Ewing series*, **4**, 593-603.

Sibson R.H. (1989). – High-angle reverse faulting in northern New-Brunswick, Canada, and its implication for fluid pressure levels. – *J. Struct. Geol.*, **11**, 873-877.

Sibson R.H. (1990). – Rupture nucleation on unfavorably oriented faults. – *Bull. Seism. Soc. Am.*, **80**, 1580-1604.

Simpson D.W. (1976). – Seismicity changes associated with reservoir loading. – *Engineer. Geol.*, **10**, 123-150.

Simpson D.W. (1986). – Triggered earthquakes. – *Ann. Rev. Earth Planet. Sci.*, **14**, 21-42.

Simpson D.W., Leith W.S. & Scholz C.H. (1988). – Two types of reservoir-induced seismicity. – *Bull. Seism. Soc. Am.*, **78**, 2025-2040.

Smirnova M.N., Navitskaya N.A. & Shebalin N.V. (1975). – Earthquake swarm caused by intensive exploitation of an oil field. – I.U.G.G., I.A.S.P.E.I., Abstracts, 39.

Sykes L.R. & Sbar M.L. (1973). – Intraplate earthquakes, lithospheric stresses and the driving mechanism of plate tectonics. – *Nature*, **245**, 298-302.

Wetmiller R.J. (1986). – Earthquakes near Rocky Mountain House, Alberta, and relationship to gas production. – *Can. J. Earth Sci.*, **32**, 2, 172-181.

Wittlinger G. (1980). – Etude de la sismicité en chap proche par un réseau sismologique à faible ouverture : application au frioul (Italie) et au gisement de Lacq (France). – Thèse doct. Etat, Univ. Strasbourg, France, 261 p.

Yeats R.S., Huftile G.J. & Grigsby F.G. (1988). – Oak ridge fault, Ventura fold belt and the Sisar decollement, Ventura bassin, California. – *Geology*, **16**, 1112-1116.

Yerkes R.F. & Castle R.O. (1976). – Seismicity and faulting attribuable to fluid extraction. – *Engineer. Geol.*, **10**, 151-167.

Zoback M.D. & Zoback M. (1980). – State of stress in the conterminous United States. – *J. Geophys. Res.*, **85**, 6113-6156.

Zoback M.L. & 29 co-auteurs (1989). – Global patterns of tectonic stress. – *Nature*, **341**, 291-298.

2

LE DOME DE LACQ : OBJET GEOLOGIQUE ISOLE MIS SOUS CONTRAINTE PAR LA DEPLETION D'UN RESERVOIR DE GAZ

Le gisement de Lacq constitue un objet d'échelle intermédiaire entre d'une part, les échantillons de roches de taille décimétrique dont le comportement mécanique est étudié en laboratoire avec des conditions aux limites contrôlées par l'expérimentateur et d'autre part les entités tectoniques dont les caractéristiques spatiales et temporelles de leurs domaines d'études sont des domaines de recherche à part entière. La mise en charge du dôme de Lacq (10.10.10 km^3) par déplétion du gisement de gaz et les déplacements sismiques et asismiques induits sont analysés pour (1) montrer la marginalité de ces instabilités sismiques par rapport au contexte sismo-tectonique régional; (2) comprendre leurs localisations dans la structure en dôme qui piège le réservoir de Lacq; (3) évaluer leur comportement spatio-temporel et quantifier les rôles respectifs des différents modes de déformations (fragile, plastique).

DEUXIEME ITERATION: Dans les représentations suivantes de brusques changements peuvent apparaître. (Ian Malcolm)

21

DIX ANS DE SURVEILLANCE SISMIQUE AU VOISINAGE D'UN CHAMP DE GAZ: EVIDENCE D'UN NOUVEAU TYPE DE SEISME INDUIT: ASPECT PHENOMENOLOGIQUE.

Bulletin of the Seismological Society of America, Vol. 80, No. 2, pp. 450–473, April 1990

TEN YEARS OF SEISMIC MONITORING OVER A GAS FIELD

By J. R. Grasso and G. Wittlinger

Abstract

Ten years of seismic recording allows us to locate more than 800 tremors with magnitudes ranging from 1.0 to 4.2, in a small (10 by 10 by 5 km) volume near a major gas field (Lacq, France). The seismic activity began 10 yr after gas extraction began. Nearly all of the epicenters are located within the lateral extent of the gas field. The only perturbation of the stress or strain fields, which has the same spatial and temporal scale as the seismicity, is the 500-bar drop in gas pressure due to 20 yr of gas exploitation, demonstrating that these events are induced. The network, established to monitor this activity, consists of eight telemetered stations including a well-bottom geophone located at 3200 m depth. Using three-dimensional relocation techniques, we computed new hypocenter positions for more than 280 events. These better-located hypocenters form a diffuse zone that mimics the local dome structure. Taking the regional tectonic stresses into account, we suggest that these ruptures may be the result of unfolding of the dome structure.

Introduction

The study of small- or moderate-size earthquakes in oil and gas fields provides a unique opportunity to relate earthquakes to the physical environment in which they occur. Many cases of induced seismicity have been reported in the literature (e.g., Calloi *et al.*, 1956; Kovach, 1974; Smirnova *et al.*, 1975; Yerkes and Castle, 1976; Smirnova, 1977; Rothé and Lui, 1983; Simpson and Leith, 1985; Pennington *et al.*, 1986). The local monitoring of the seismic activity, however, is often poor or operated on a short time scale (a few months). As a result, the data obtained can seldom be studied in a geomechanical context. We present here the specific seismic pattern deduced from 10 yr of seismic recording over a hydrocarbon field. First, we demonstrate the geographical correlation between the earthquakes and the lateral extent of the gas field. Then, we use three-dimensionally relocated events, selected for their high-quality data, and show that the hypocenters define a geometry which is close to the well defined local dome structure. The only possible forcing which has the same length and time scale as the ruptured area is the 500-bar drop in gas pressure over 20 yr, strongly suggesting these events are induced. According to regional tectonic stresses, we suggest that these ruptures correspond to the unfolding of the anticline structure.

Geological Setting

The hydrocarbon field (Lacq, France) is located near the western edge of the Pyrenean chain in the northern foreland. Different interpretations of the geodynamic evolution of the Pyrenees have been proposed by Boillot and Capdevilla (1977), Choukroune (1976), Choukroune and Mattauer (1978), and Daigniéres *et al.* (1982). The seismically active zone in the Western Pyrenees defines an east–west strip no more than 10 km wide associated with the North Pyrenean fault (Gagnepain *et al.*, 1980; Gagnepain–Beyneix *et al.*, 1982; Olivera, 1983; and Gallart *et al.*, 1985). The northern folded foreland, the site of the gas field, is located outside of the currently active areas. The seismicity map (Fig. 1) and the N–S section (Fig. 2) illustrate these patterns.

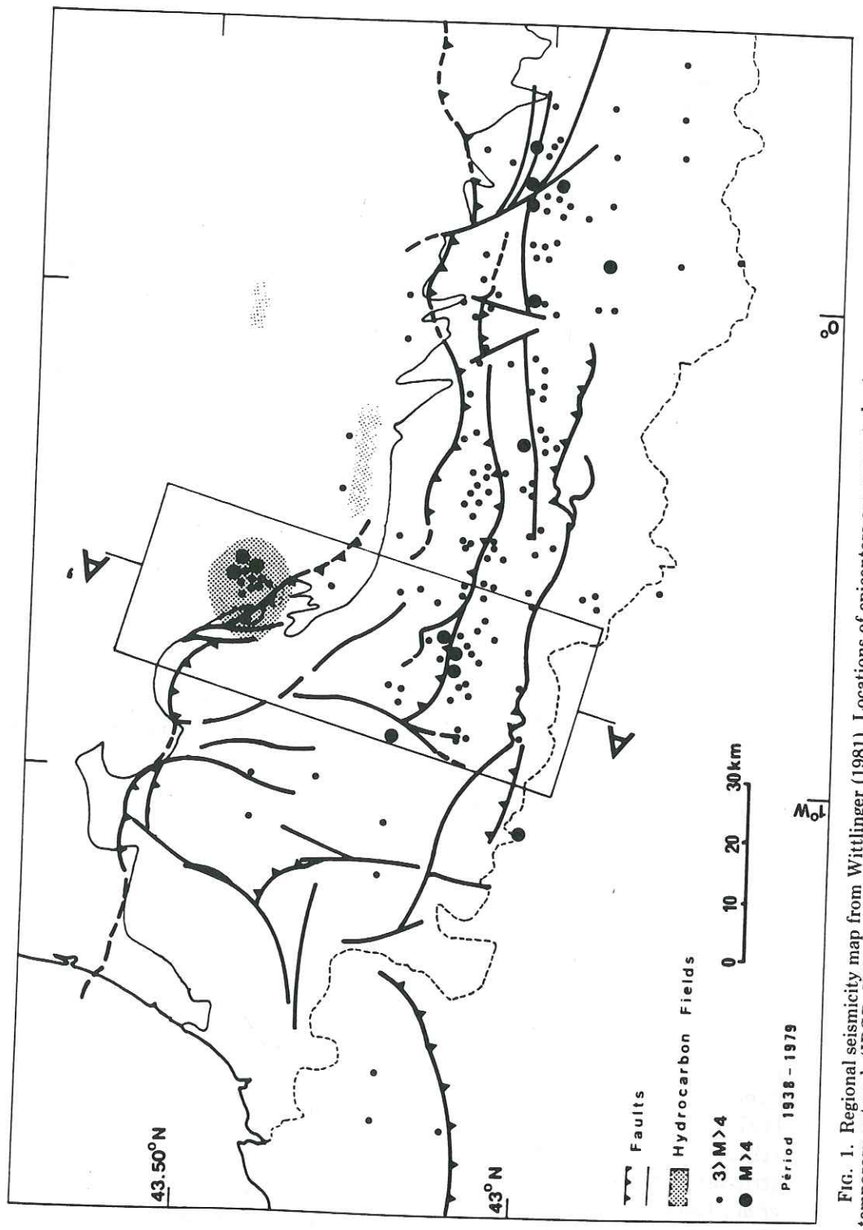

FIG. 1. Regional seismicity map from Wittlinger (1981). Locations of epicenters are computed using permanent French network and local temporary network (IPGP, IPGS, O.G.: Institut de Physique du Globe de Paris, Strasbourg et Grenoble). These data cover the period from 1938 to 1979. The epicenter accuracy is 10 km.

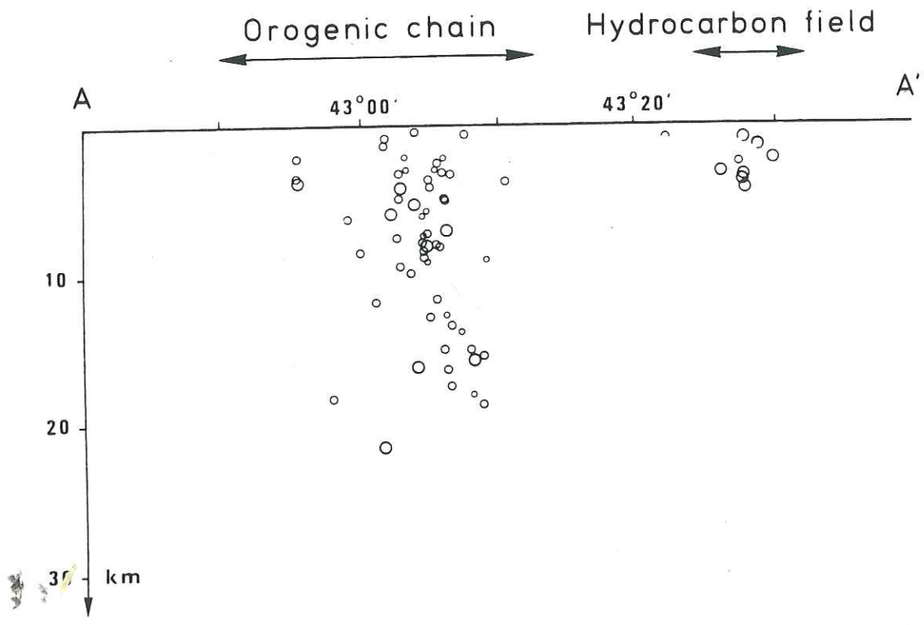

FIG. 2. N–S vertical cross section showing hypocenter projections. The largest open circles plot the hypocenters with $M_L > 3$. These data are from 3 months of observation using portable stations (September through December, 1982). Each event is located using at least 20 observations (from Gallart *et al.*, 1985). The location of this section and the lateral extension of the box are shown by the line AA′ on Figure 1.

Excluding the seismically active North Pyrenean fault, which lies 25 km to the south of the hydrocarbon area, the most significant structure in the neighborhood is the aseismic North Pyrenean thrust, which overlays the western part of the field along a curved thrust plane (Fig. 3). The autochthonous series are widely folded at the frontal thrust, especially above it (Fig. 4).

Numerous wells in the area and geophysical exploration data clearly define the local structure. It forms a dome (Fig. 3), the southern part of which is limited by a faulted area oriented S60°E. Another faulted strip, oriented in the N10°E direction, is recognized on the western face of the dome. An Upper Cretaceous reef lies above the dome, but this formation is absent on the western side of the structure. The thrust sheet, situated on the W and SW faces of the dome, trends approximately S30°E (Fig. 3) and is linked to several steep faults dipping toward the S or SW and striking from S50°E to S10°E. On all these faults, the displacements are of the reverse faulting type and are associated with dextral strike slip, whose amplitude grows going north.

RESERVOIR CHARACTERISTICS

The hydrocarbon field, located in an anticline structure, has two producing levels. The shallowest is an oil field having its top at 495 m depth, being composed of rocks from Upper Cretaceous age (fractured dolomites and limestones). The oil overlays a large fractured aquiferous reef, the thickness of which can be greater than 2000 m. The second producing level is a gas field which lies at a minimum depth of 3100 m. Its rock matrix consists of dolomitic sandstones and limestones of

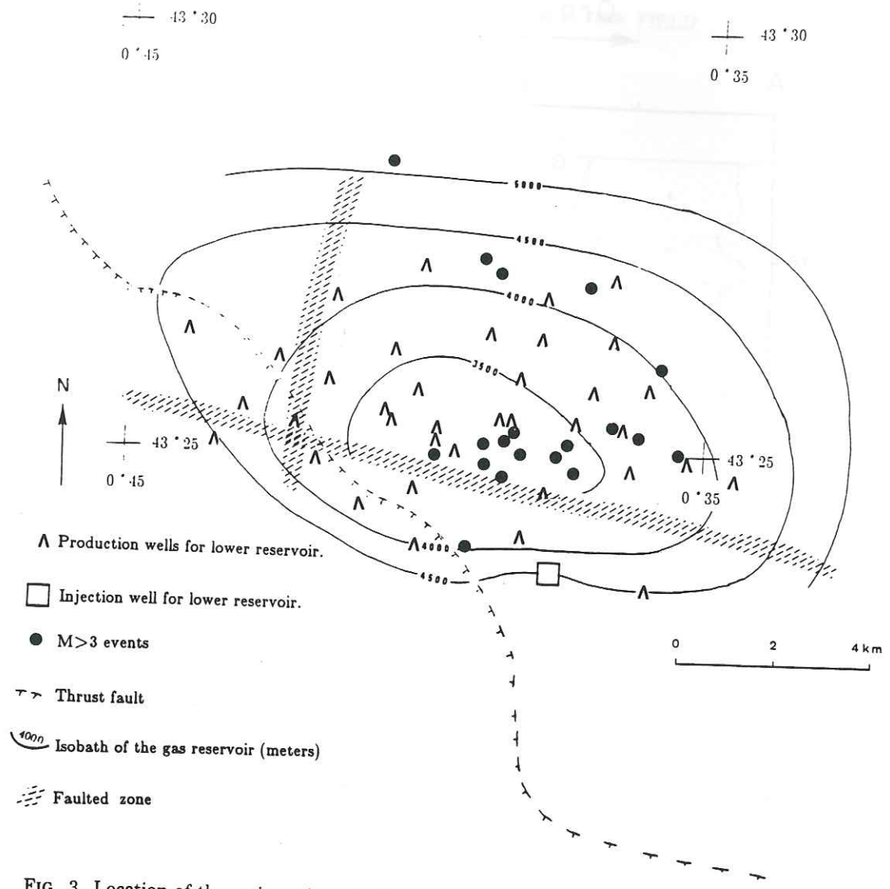

FIG. 3. Location of the major epicenters $M_L > 3$. Only the 19 events by the local network (1974 to 1983) are reported with dots. The dotted line indicates the surface trace of the main fault of the area. The curved lines are isobaths for the reservoir levels. These standard locations performed by (IPGS) Institut de Physique du Globe de Strasbourg are obtained using half-space velocity model.

late Lower Cretaceous and Upper Jurassic ages, with a producing area of 100 km^2. A thick marly level of lower Aptien age traps the anhydrous gas.

Since oil production began in 1950, all of the water produced from the oil field has been reinjected in the oil reservoir. Since 1957, however, additional injection of waste water has affected the oil field pressure. The initial pressure at 625 m depth was 61 bars; it dropped to 59 bars in 1959 and reached 65 bars in 1975. The injection of waste water in the oil field stopped in 1980. The stabilized pressure has been 67 bars since 1980. The gas production of the lower reservoir began in 1957, and since 1963 the field has produced more than 7×10^9 m^3 /yr (gas volume at standard conditions). The cumulative production for each well shows that the best producing area is located near the top of the structure.

Water has been injected in only one well (Fig. 3) since 1974. This injection takes place at a depth of 4800 m, within the productive levels. Its site lies about 1 km down dip from the likely trace of the S60°E-striking fault, which is recognized on

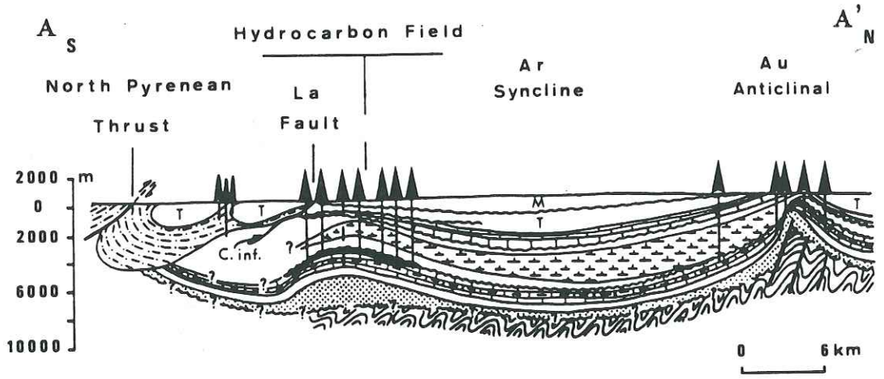

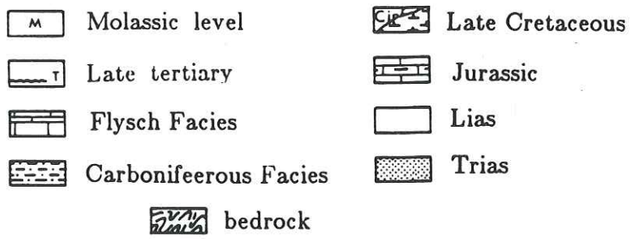

FIG. 4. N–S vertical cross section of the local geological structure. The location of this section is shown by line AA′ on Figure 1.

the southern flank of the dome (Fig. 3). Since 1976 the volume of water injected in the lower reservoir has been 7.2×10^5 m^3/yr. The injected volumes, however, are negligible compared with those of the gas withdrawn. Thus, there is a substantial depletion of the gas reservoir pressure: 660 bars at 3700 m depth in 1957 and 350 bars in 1969 (Fig. 5b) when the seismicity began, at the same depth. The reservoir responds to depletion as a homogeneous matrix. No compartments with different relative pressures have been observed during gas extraction (Jenner and Dienesh, 1965). At this stage, we simply note that the characteristics of the two field exploitations are dominated by the progressive 500-bar depression of the lower reservoir over the last 20 yr (Fig 5b).

SEISMICITY PATTERNS FROM TEN YEAR OF SEISMIC RECORDING

The initial seismic sensor geometry consisted of four geophones. Three instruments were deployed in the production area, and one was located 7 km away from the site. Between 1976 and 1981, seven seismic stations were operated. In 1982 a three-component unit, located at the bottom of a 3800-m-deep borehole was added to the seismic monitoring system (Fig. 12). The geophones have a bandwidth of 1 to 30 Hz. Signals from the geophones are relayed to the central site by UHF/FM radio telemetry. The analog data relayed from the subsurface sensors are digitized using a multichannel PCM modulator. A "transient" recorder was activated by a coincidence trigger unit, which used an amplitude threshold within a specified time window as a comparator. Preliminary locations were based on an equivalent homogeneous half-space velocity model. The value of the equivalent velocity was

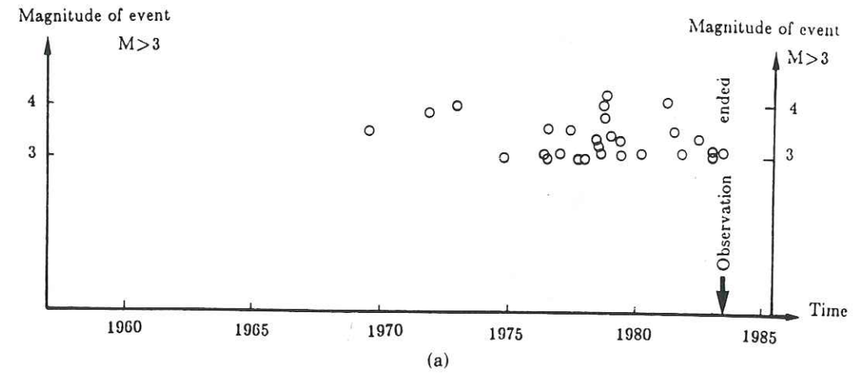

(a)

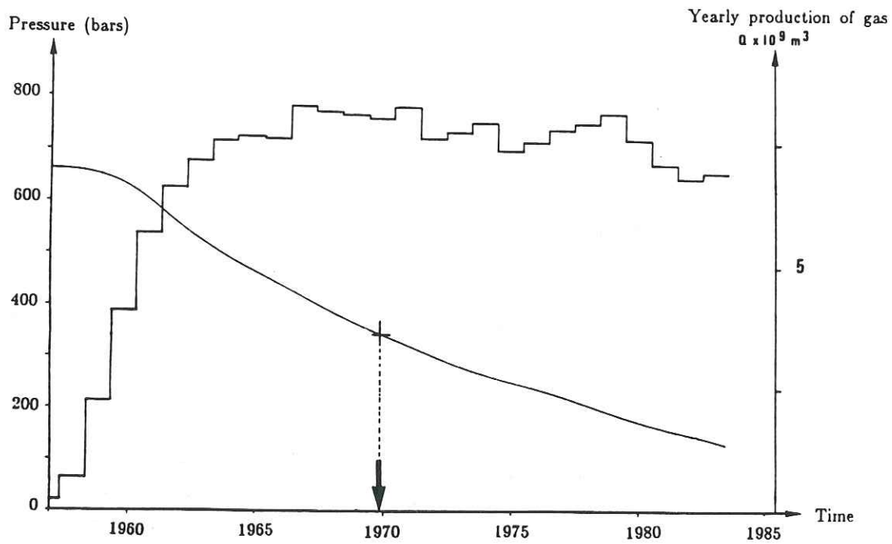

(b)

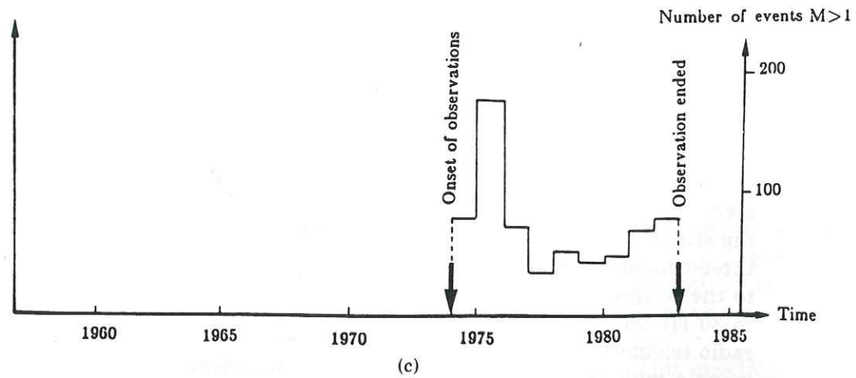

(c)

FIG. 5. History of the field as a function of time: number of events (a, c), production rate, pore pressure (b). (a) $M_L > 3$ events are plotted versus time. (b) The evolution of the pressure of the gas field versus time. The broken line is the yearly production of gas for the same period. (c) Number of $M_L > 1$ events are plotted versis time between 1974 (onset of the local monitoring) and 1983 (end of this study).

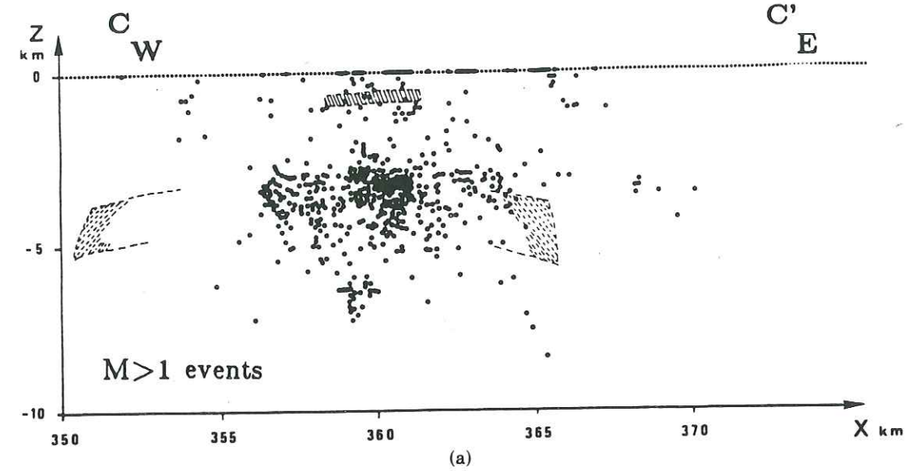

(a)

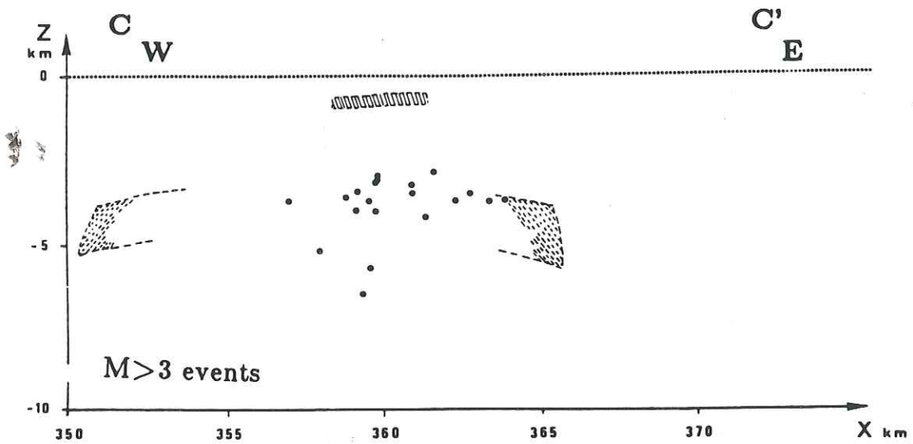

(b)

FIG. 6. Standard locations for hypocenters of the period from 1974 to 1983. (a) Projection of the hypocenters on a W–E vertical cross section. The events of the period from 1974 to 1983 are plotted. (b) Major earthquake $M_L > 3$: Projection of the hypocenter on a W–E vertical cross-section. The events of the period from 1974 to 1983 are plotted. The shaded areas are the lateral extension of the gas field (the deepest one) and the oil field (the shallowest one). The location of the cross section is shown by CC′ line on Figure 12.

checked using artificial sources at different depths (Wittlinger, 1980). Between April 1974 and December 1983, more than 800 events were recorded. The selected events have local magnitudes greater than 1.0.

More than 90 percent of the epicenters are located in the hydrocarbon fields (Wittlinger, 1980). Although the seismicity extends beyond the lateral limits of the oil field, the correlation with the estimated gas field extension (Haas *et al.*, 1972) is quite good, particularly for the eastern part of the gas field. The error in hypocenter location is numerically estimated from least-square solution to be 1 km. We used $M_L > 3$ events to estimate the temporal evolution of the seismicity and to synthesize the characteristics and features of the ruptures. Twenty-eight events of $M_L \geqq 3$ were located in this area. Three occurred in the 1969 to 1972 period, before the local

network was installed, and were located by the French national network. Comparisons between epicenters using local network, regional network location, and macroseismic observations of intensity (Fig. 7) allow us to evaluate the accuracy of the data prior to installation of the local network. These data convincingly show that these $M_L \geqq 3$ events are well located by intensity pattern, and that national network locations are in good agreement with those determined by the local network for these *three* epicenter locations. We have looked for events as far back as 1940 (Annales IPGS, Rothé, 1941, 1956, 1967, 1972). A recent report on the historical seismicity of the Pyrenees (Vogt, 1979, 1982) suggests that the north Pyrenean

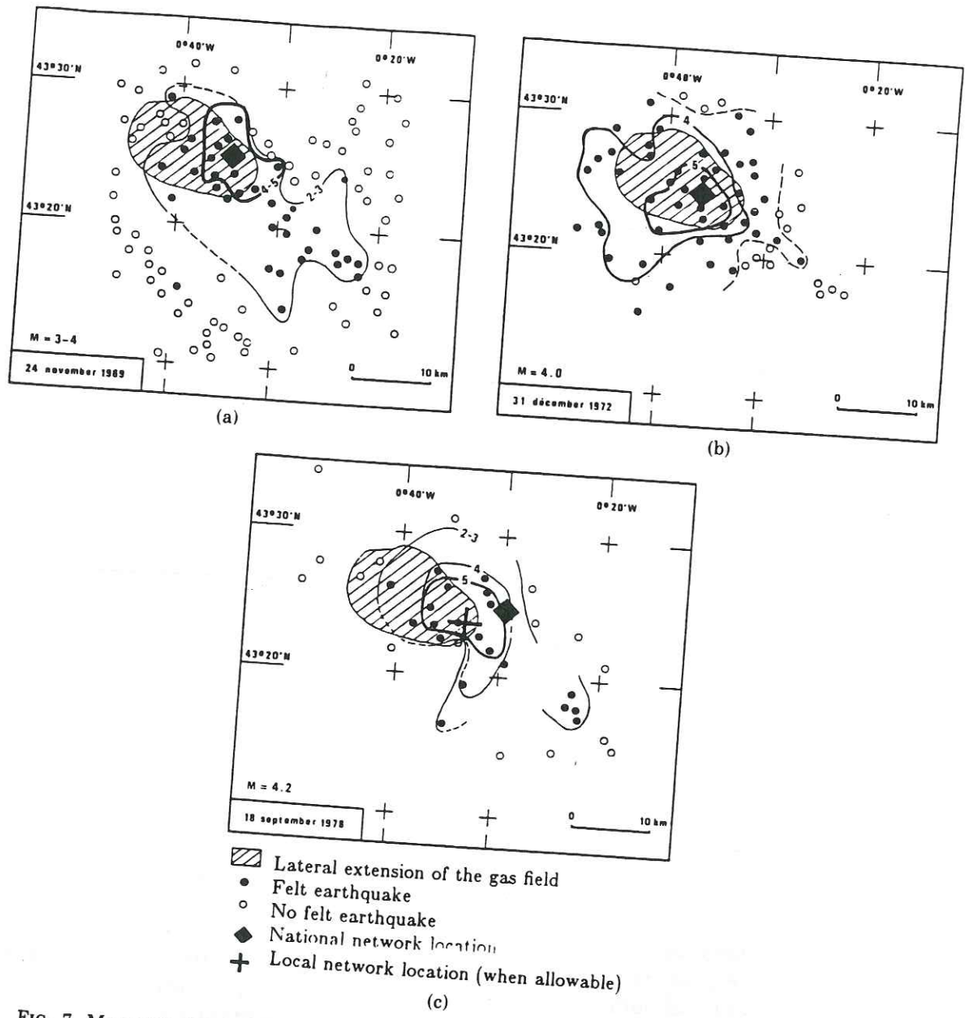

FIG. 7. Macroseismic maps adapted from Rothé (1972) and Vogt (1982). Thick line is the isoseismal line for 5 Modified Mercalli intensity. Thin line is the isoseismal line for 2 to 3 Modified Mercalli intensity. Magnitude and date of the events are in the lower left-hand corner of the figure. Black diamond is the event location computed with national network data. Cross is the event location computed with local network data (when allowable). (a) 24.11.1969 event, (b) 31.12.1972, (c) 18.09.1978 event.

foreland has been aseismic for several centuries. The first $M_L > 3$ event occurred in November 1969. Since 1969, one event of this magnitude has been felt (intensity $\geqq 5$) each year (Fig. 5). It is therefore possible to place, with a good degree of confidence, the beginning of seismic activity in 1969, roughly 10 yr after the gas exploitation started.

All the epicenters of major ($M_L > 3$) events located with local network data lie within the gas field (Fig. 3), which is similar to the pattern indicated by all events ($M_L > 1$). Their depths, however, differ from the image deduced from lower magnitude events. The major earthquakes occur between depths of 3 and 5 km (Fig. 6b), whereas $M_L > 1$ events occur between 0 and 7 km (Fig. 6a). The two events located between 6 and 7 km depth are linked to a new seismic pattern which began in late December 1982. This clustered activity, consisting of more than 35 events ($1 < M_L < 3.5$) over a 2-wk period, is concentrated in a volume of less than 1 km^3 below the gas reservoir. Taking into account the error in hypocenter location (less than 1 km) and the average slope of the dome (25°), the majority of major events coincides with the Aptien levels, the roof of the gas reservoir, and some formations within the gas reservoir itself. To the contrary, the oil reservoir and the neighboring formations are not associated with any major seismic phenomena.

During the period 1974 to 1983, no spatial or temporal migration can be clearly defined. The annual rate of seismic activity for $M_L > 1$ events is presented in Figure 5. The small yearly variations are not correlated with either the production rate of the fluid withdrawal (Fig. 5b) or the technical operating cycle of the network (Wittlinger, 1980).

In conclusion, the seismicity pattern deduced from the preliminary locations is stable to first order over time and coincides with the lateral extension of the gas field. The geographical correlation between epicenter locations and the gas field is strong. However, more accurate data are needed to understand the exact significance of the hypocenter locations and the mechanism of the seismicity.

RELOCATED EVENTS

In this section we present the results of three-dimensional event relocations. Each residual, $t_{obs} - t_{cal}$, is modeled by both velocity perturbations relative to an initial velocity model and hypocenter movements relative to initial locations. The velocity and hypocenter parameters are solved simultaneously using the techniques described in Grasso (1983) and Grasso *et al.* (1983). In a first step we selected 60 events in the period May 1978 to May 1979 with at least six arrival times. We discretized the anticline structure using constant velocity blocks. We use a flat-layered initial velocity model for the inversion (Fig. 8b). The main discrepancy between the initial model and the velocity structure determined by refraction studies and borehole seismic surveys (Fig. 8a) is the low-velocity zone (LVZ), just above the gas reservoir. This LVZ is not present in the initial velocity model used for three-dimensional relocations, but intermediate constant velocity layers were introduced to give more freedom to the calculated response. The initial residuals are computed using the tabular velocity model of Figure 8b. The purpose of this preliminary test is to check the quality of the information included in the initial residuals. One way to evaluate this information is to compare the residual variance with the reading error variance. The reading error is taken to be a centered random variable. In this example, $T^2_{\text{residual}} = 0.063$ and $T^2_{\text{error}} = 0.025$. Thus, more sophisticated models are justified inasmuch as the residual variance is greater than that of the reading error.

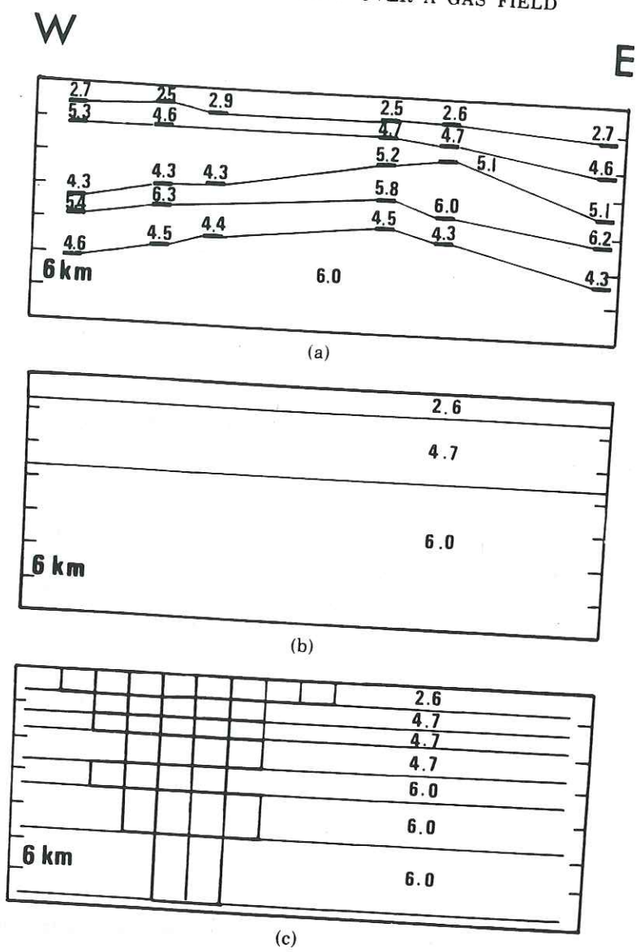

FIG. 8. Velocity models linked to the different location techniques. (a) Velocity structure derived from refraction experiments and borehole seismic shots. Velocity values are in km/sec. This section is a E–W section of structure. (b) Homogeneous layer model with parallel interfaces we used as an initial model for the inversion process. (c) The E–W vertical cross section of geometrical discretization. The block size presented here is 1 km × 1 km × *e*. *e* moving from 0.5 km to 1.4 km according to each layer thickness. The minimum block size used to test the stability of the solution is 0.5 km × 0.5 km × *e*. We used seven geometrical layers linked to the three velocity layers defined on the (b) model.

. Two numerical controls were used to estimate the relative influence of the two unknown sets (velocity blocks and focal parameters) in fitting the data. In one case, we kept the hypocenters fixed while the velocity parameters were forced to move between *a priori* bounds based on the known geological structure (Fig. 8a). Such a computation explains 32 percent of the initial residuals. The other case used both velocity perturbations and hypocenter movements to explain the data. In this latter case, we fit the data with an 80 percent confidence level using the same stochastic approach as before. The bounds on hypocenter parameters were chosen so that the average travel-time delay is the same as the one attributed to velocity perturbations.

These statistical considerations require hypocenter displacements to explain the residuals due to standard locations. In order to minimize the correlation between velocity and hypocentral parameters, we used different discretization units (size of velocity blocks). The solutions obtained were stable to the first order. All these controls show that the information in the initial residuals is consistent with the parameters we chose to fit the data, a result that was not known *a priori*.

According to the initial test discussed above, we attempt to compute reliable relocated hypocenters with quantified errors; i.e., we want to estimate the degree of confidence of the new hypocenter location. We first look for a detailed three-dimensional representation of the seismic velocity structure suitable for yielding a model close to the real structure. To this end, we use 525 parallel-piped velocity blocks. The block size is $0.5 \times 0.5 \times e$ km, where e is the thickness of the element, ranging from 0.5 to 1.4 km. The resulting solution is in good agreement with the velocity model deduced from local seismic sounding (Wittlinger, 1980). According to the linearized inversion techniques some velocity constants are smoothed, but it is important to notice that the LVZ layer, present at the top of the gas reservoir, is well defined by our solutions (Fig. 9).

The next step was to test the stability of earthquake displacements using events in the period May 1978 to May 1979. On Figure 10a, 65 event displacements are plotted. Forty-nine additional events occurring in the periods from 1976 to May 1978 and July 1979 to July 1980 are relocated on Figure 10b. Figure 10c shows the same N–S section when the 45 + 69 events are relocated simultaneously. Comparisons between these three solutions indicate the stability of the relocations. In the first computation, the associated linear system that we have to solve is underdetermined (364 data/800 unknowns). The unknowns are separated as follows: 523 are linked to block velocity perturbation, and 65×4 are associated with X, Y, Z, T focal parameters. When the 113 events are computed together, the 49 new hypocenters balance the linear system with 382 additional data, compared with 196 unknown linked to new hypocenters. The same computations were performed on the whole data set (227 events). As before, only events with at least six arrival times in the period 1976 to 1982 were selected. The largest initial residuals were rejected later in the relocation routines. For this reason, some of the events have less than six observations when computing the dispersion of hypocenter parameters (Fig. 11). Three additional computations involved the simultaneous relocations of all 227 events, the 129 events selected with seven observations and with the 175 events relocated with at least six arrival times. The largest discrepancy between the three solutions allows us to define ΔX, ΔY, ΔZ as the quantitative uncertainty of the location parameters as estimated using this technique (Fig. 11). For events with less than six arrival times in the final data set, the errors were arbitrarily bounded with the *a priori* statistical values used in the inversion techniques (lateral and vertical errors being equivalent to 0.1 and 0.15 km, respectively).

The principal feature of the depth relocation is the differential earthquake movements. These displacements are due to the change in location technique. The new location set is not a simple depth translation applied to the old data set. We observe in Figure 10 that the depth displacement of the shallower earthquakes is larger than the movement of earthquakes initially located at greater depth. The seismicity pattern displayed by the 227 relocated events occurring from 1976 to 1982 is stable to the first order over the time period considered and coincides (Fig. 12) with the estimated contour of the gas field defined by Haas *et al.*, 1972. The seismicity is diffuse and not part of a well defined fault system, unlike the regional seismicity. All earthquakes outside the gas field occur well to the south and

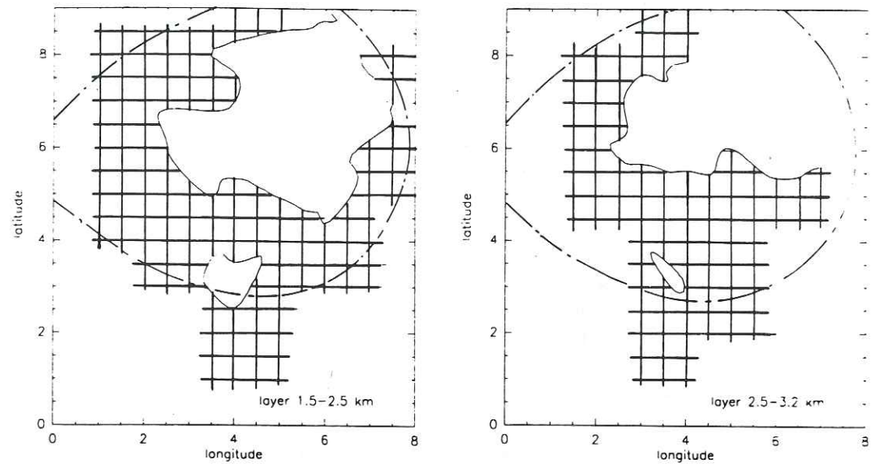

FIG. 9. Velocity image deduced from three-dimensional inversion techniques. (a) Average velocity between 1.5 and 2.5 km depth. (b) Average velocity between 2.5 and 3.2 km depth. (c) Average velocity between 3.2 and 4.6 km depth. Relative low velocity images are shaded. The dotted line bounds the lateral extenstion of the gas field. Because of the dome structure, the center of the image has to have a relatively high velocity value due to velocity increasing with depth ((a) to (b)). The marls image is a well-defined low-velocity contrast in the center of (c) and with a high-velocity area in the surrounding volume.

are associated with well known tectonic features (Figs. 1 and 2) (Gallart *et al.*, 1985; Gagnepain *et al.*, 1980; Gagnepain-Beyneix *et al.*, 1982). The local seismic activity appears rather as a spatially distinct, roughly irregular concentration of epicenters. While the regional Pyrenean earthquakes are located up to 20 km depth by the local permanent network of the Institut de Physique du Globe de Paris, 75 percent of the relocated events of the hydrocarbon field area range in depth from 1.5 to 5.5 km (Fig. 13).

Several other features of the seismicity of the field area deserve mention. In the western part relocated events are absent. This confirms the aseismic behavior of

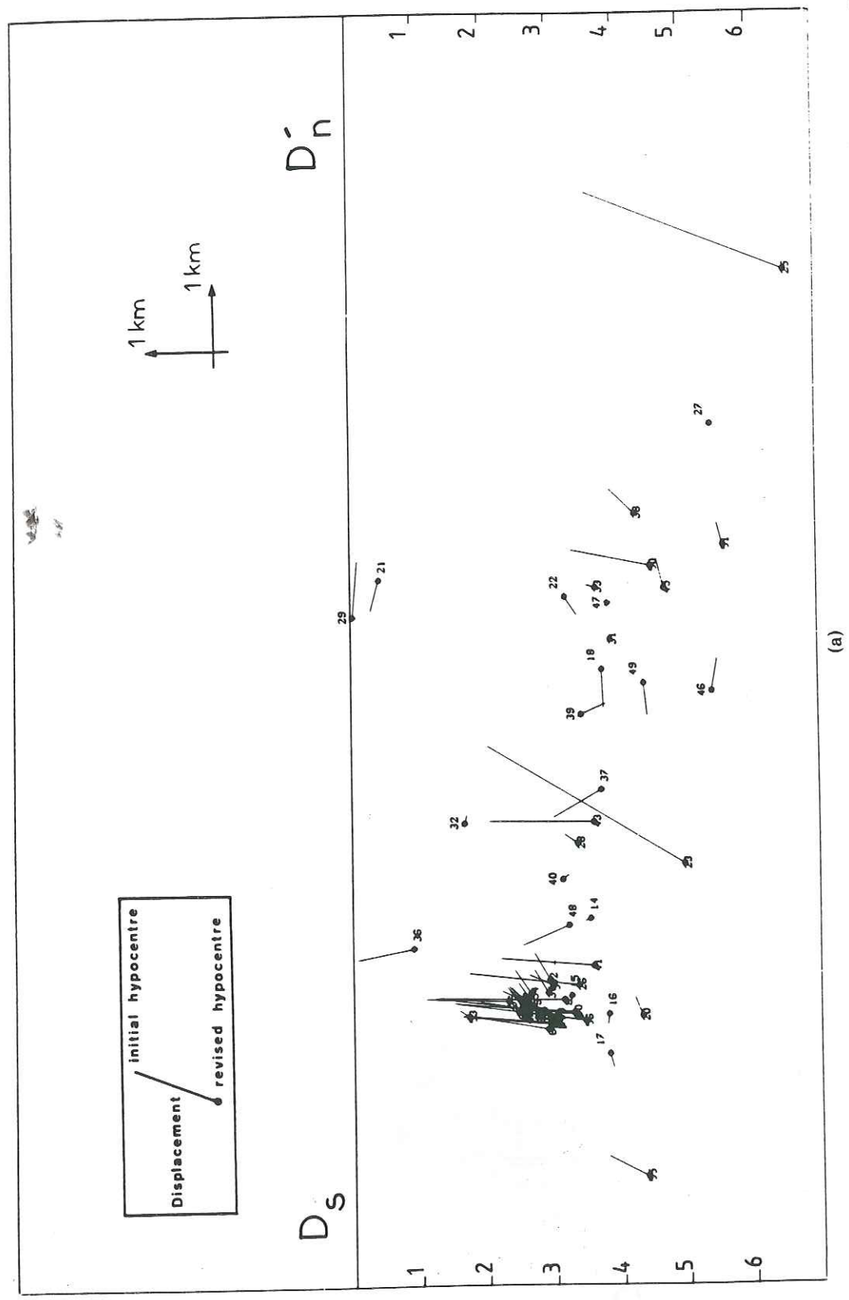

FIG. 10. Comparison of initial hypocenters and revised hypocenters obtained with three-dimensional relocation techniques. For each hypocenter we plot the projection of the displacement vector on a vertical N–S section. These results correspond to the simultaneous inversion of velocity structure and hypocenter parameters. The velocity structure is mapped in Figure 9. One end of each straight line is the revised hypocenter and the other one (full circle) is the initial hypocenter. (a) Displacement vectors for 65 relocated events corresponding to the seismic activity of the period from June 1978 to June 1979. (b) Displacement vectors for 49 additional events in the period from June 1976 to June 1978, and from July 1979 to July 1981. (c) Displacement vectors for the 65 + 49 events of data set (a) and (b). In case (c) the (65 + 49) events are relocated simultaneously. The results presented on Figures (a), (b), and (c) are associated to three independent computations. The location of this section is mentioned with DD′ line on the Figure 12.

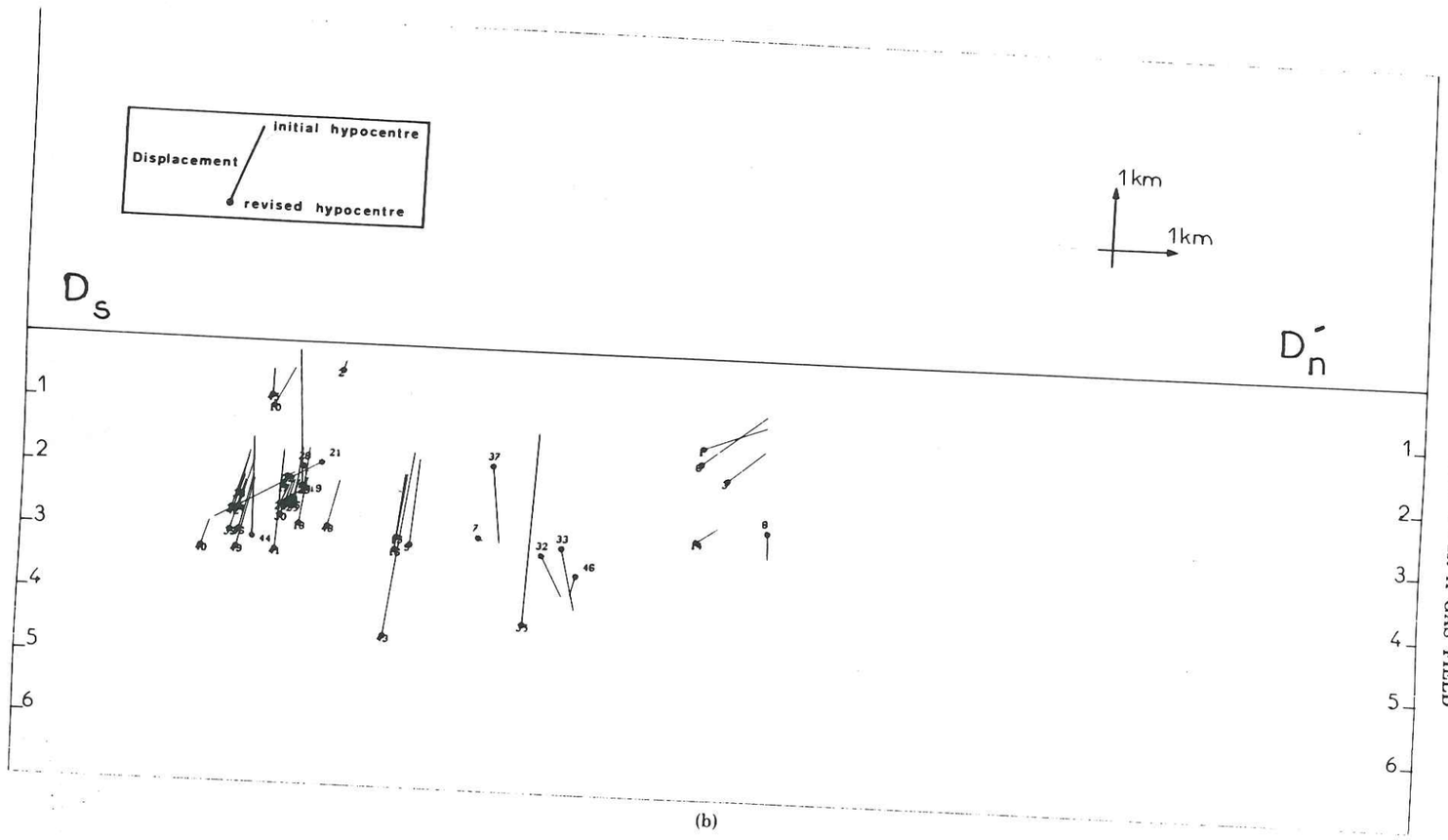

(b)

FIG. 10. (*Continued*).

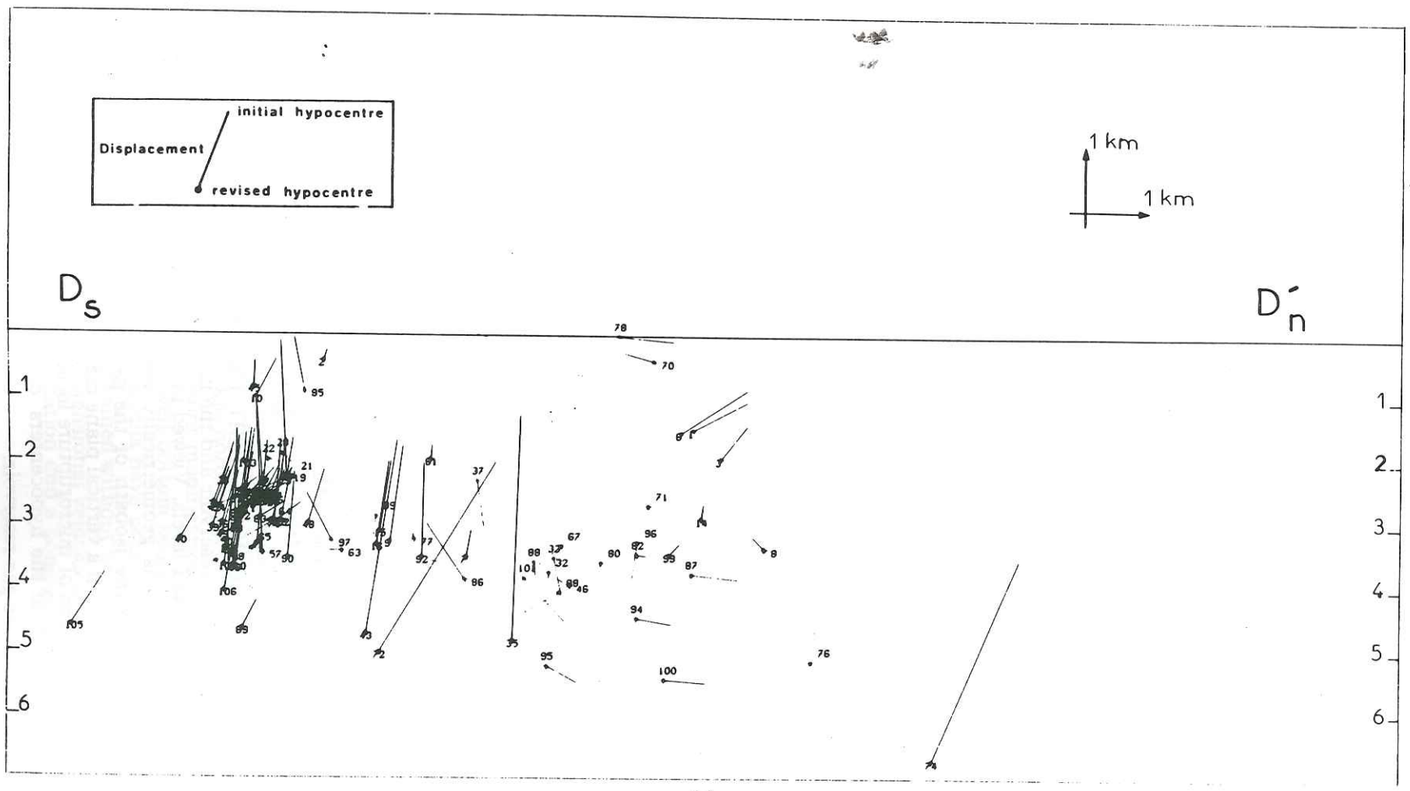

(c)

FIG. 10. (*Continued*).

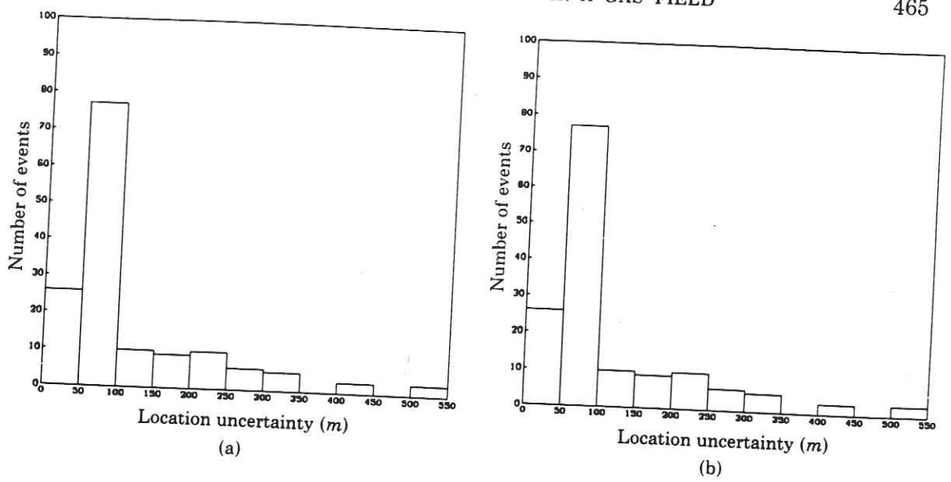

FIG. 11. Frequency distribution of the errors. (a) ΔX is the error in the N–S direction in m. (b) ΔY is the error in the E–W direction in m. (c) ΔZ is the error of the focal depth in m. These errors are computed when the main data set is partitioned in three subdata. Then the maximum location perturbation of three relocation processes allow us to define the location discrepancies presented on diagram a, b, c.

this area. South of the field a cluster activity is clearly defined (Fig. 12). The location of these events coincides with a possibly pre-existing fault, the first evidence of which came from well data (Coustau, 1965). Its apparent geometry is consistent with that of a subvertical normal fault. A recent reflection profile confirms the presence of such a fracture (Kothé, 1981). Using these two sets of independent information, the top of the reservoir and the impermeable marly level overlaying it seem to be the only affected levels. Viewed in cross-section (Fig. 13), the envelope of the hypocenter depths is geometrically well constrained, indicating a dome structure comparable to the isobath of the gas reservoir formations. The global projection of hypocenters on a vertical plane may not be the best way to display the three-dimensional pattern of microrupture locations. Nevertheless, such a drawing shows the homogeneity of the hypocenters' distribution on a geometrical feature: the dome structure of the gas reservoir.

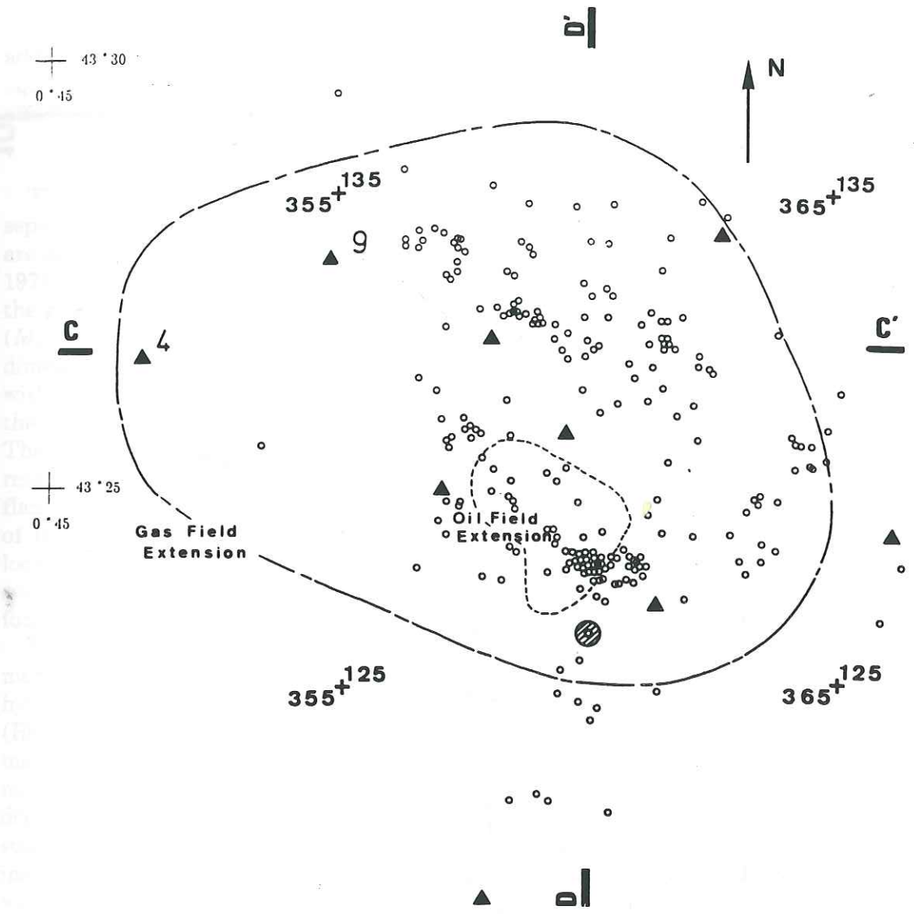

FIG. 12. Final epicenter map of the 227 relocatd events using three-dimensional inversion techniques. The epicenters are plotted using open circle. The dashed line is the lateral extension of the gas reservoir. The dashed circle is the position of the water injection well. Scale numbers are in kilometers.

In the northern part of the field, a marginal cluster of events occurred in December 1982. The well controlled location of this new activity ranges in depth from 6 to 7 km. These earthquakes lie below the gas reservoir and seem to be a new feature of the seismicity since late 1982. The relocation techniques previously described give new positions for the 82 events of 1982 (Fig. 14). The cross-section (Fig. 14b) shows slight vertical movement, except for ten events, indicating good initial depth determinations, in contrast to the previous results. Moreover, horizontal displacements exhibit a systematic 1 km northern movement. These surprising results are associated with the latest network modifications. In July 1981, the western station 4 (Fig. 12) was replaced by a well-bottom seismometer at 3.2 km depth (station 9, Fig. 12). Thus, the initial locations have better depth constraint than before. The 1982 relocated events were obtained without western constraint on the X, Y, and Z positions, but with a three-dimensional velocity structure, while the initial location used the western subsurface station and a homogeneous half-space velocity model.

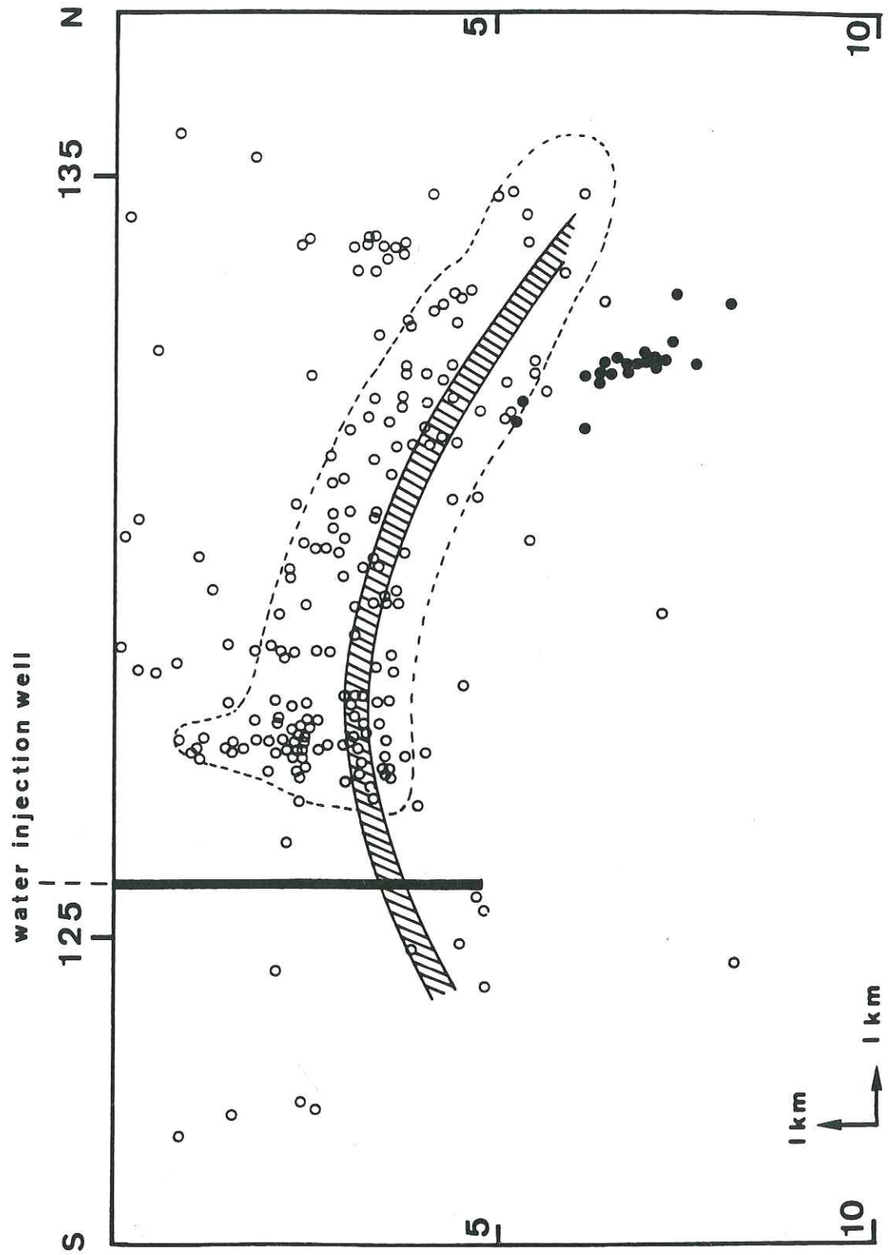

FIG. 13. Final hypocenter positions of the 227 relocated events using three-dimensional inversion techniques. The open circles are the projections of the hypocenter on a verticle N-S cross section. The black circles are the hypocenter projections of the December 1982 crisis events. The shaded area is the roof of the gas reservoir. The thick vertical line is the location of the water-injection well. The dashed line is the envelope of the main seismic area. The location of this section is mentioned with DD' line on Figure 12.

The slight vertical displacement of the relocated hypocenters shows that the additional information linked to the well-bottom station (data acquisition effort) is equivalent to the use of more sophisticated inversion techniques (data treatment effort) to constrain the depth of events.

POSSIBLE CAUSES OF AN INDUCED SEISMICITY

The gas field seismicity is isolated in an otherwise aseismic region, with 25 km separating these epicenters from the regional Pyrenean seismic zone. These events are always shallower than the tectonic shocks. The location of the events, between 1974 and 1983, extends beyond the oil field area but coincides with the bounds of the gas field. This correlation is also clear for the largest earthquakes in the area ($M_L > 3$). The correlation is confirmed and enhanced by the result of three-dimensional relocation techniques. More than 95 percent of the events relocated with this technique fall within the area of the gas field. The events are located on the eastern part of the field, with an aseismic zone near the top of the structure. The envelope of the event hypocenters mimics the dome structure of the gas reservoir. Two large dip features disrupt this geometry, however. One on the south flank of the structure is over the reservoir and has been active since the beginning of the monitoring (Wittlinger, 1980). The second one, on the northern area, is located below the gas reservoir and has been active only since 1982. This northern swarm contrasts with the diffuse seismicity present in the northern area in the formation overlaying the gas reservoir.

There have been many studies of the cause-effect relation of reservoir impoundment (Simpson, 1976) or fluid injection (Healy *et al.*, 1968) and seismicity. The first hypothesis proposed to explain the seismicity described here as fluid injection (Rothé, 1970, 1977). The injection in the upper reservoir can be discarded as the major cause of this seismicity because of the small quantity of injected fluid, the minor pore-pressure change and the minor seismic activity present at this shallow depth. The only injection well in the lower gas reservoir, located close to the southern swarm, also appears to be of little consequence regarding the seismicity, inasmuch as the southern swarm preceded the beginning of the injection. Moreover, we notice that large variations of the injected volume (breakpoint in November 1975 and restart in December 1975; Grasso *et al.*, 1985) were not followed by measurable seismicity changes.

Another possible cause of localized seismicity may involve lenses at the top of the reservoir containing natural gas originally at a much higher pressure than found in the main reservoir. Production of gas from the main reservoir, with an attendant decline in pore pressure, would lead to an augmented pressure differential between the lenses (Grasso *et al.*, 1985) and the main reservoir. Because the lenses are of the order of 100 m or less in dimension, any associated seismicity would almost certainly be correspondingly localized.

In contrast to the causes just described, which would be consistent with small-scale seismicity, the pressure drop has much the same extension as the area defined by the seismicity (of the order of a few kilometers). The seismicity involves the entire dome structure, and its physical cause is likely to have the same dimensions. The 500-bar depletion of the gas field stimulates a structure which has the same scale as the area which is microfractured by the seismic events.

Because the production parameters appear to be homogeneous throughout the gas field, the inhomogeneity of the seismicity could be a consequence of variations in the rheological response of the dome to the deformation induced by the exploi-

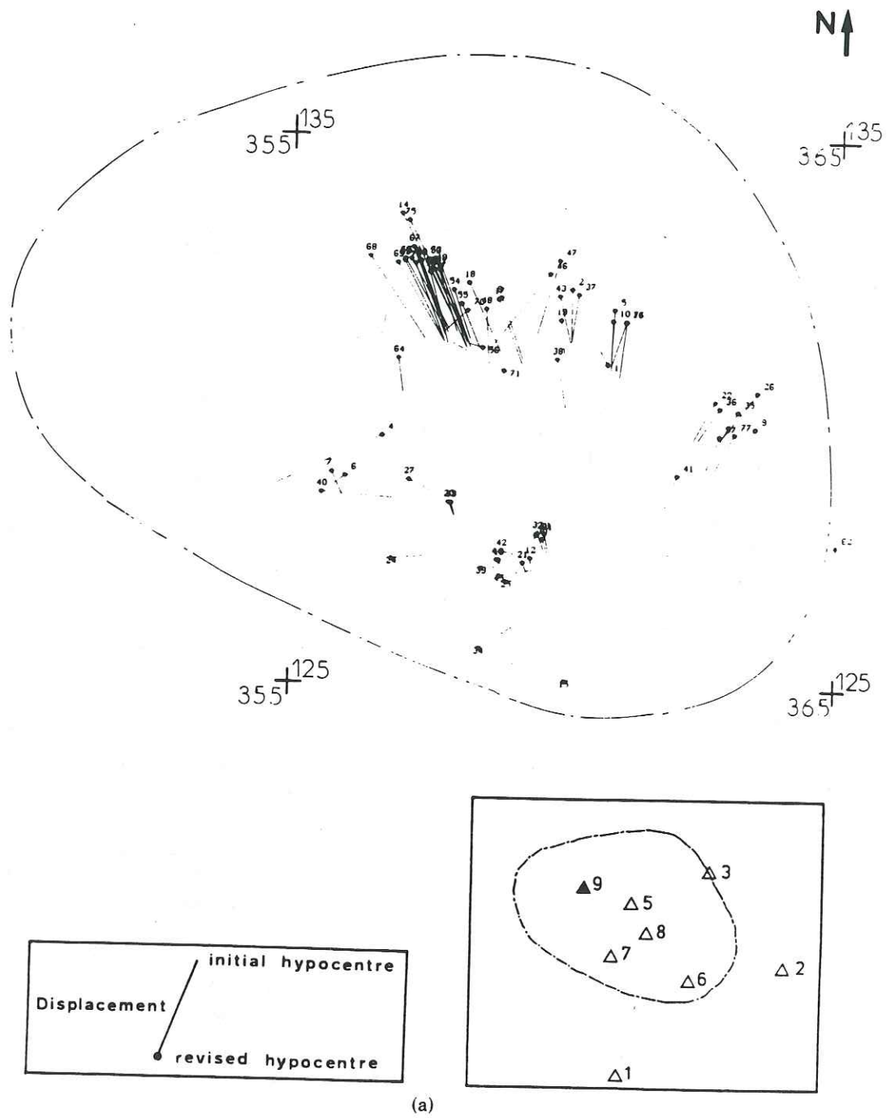

(a)

FIG. 14. Comparison of initial and relocated events obtained with three-dimensional techniques for the 82 events of the 1982 years. The straight line visualizes the discrepency between the two locations. One end is the initial location, the full circle at the other end is the revised position. (a) The displacement vectors, between initial event location and relocated event location for the 82 events of the 1982 years, are projected on an horizontal plane. In the window, open triangles are the station sites used with relocation techniques. The solid triangle is the bottom of well additional station site which is only used with preliminary locations. The extension of the gas field is present in the window using dashed line. (b) Comparison of preliminary hypocenter location and revised hypocenter locations for the 82 events of the 1982 year. The displacement vectors are projected on a N–S vertical cross section. The location of this section is mentioned with DD′ on Figure 12.

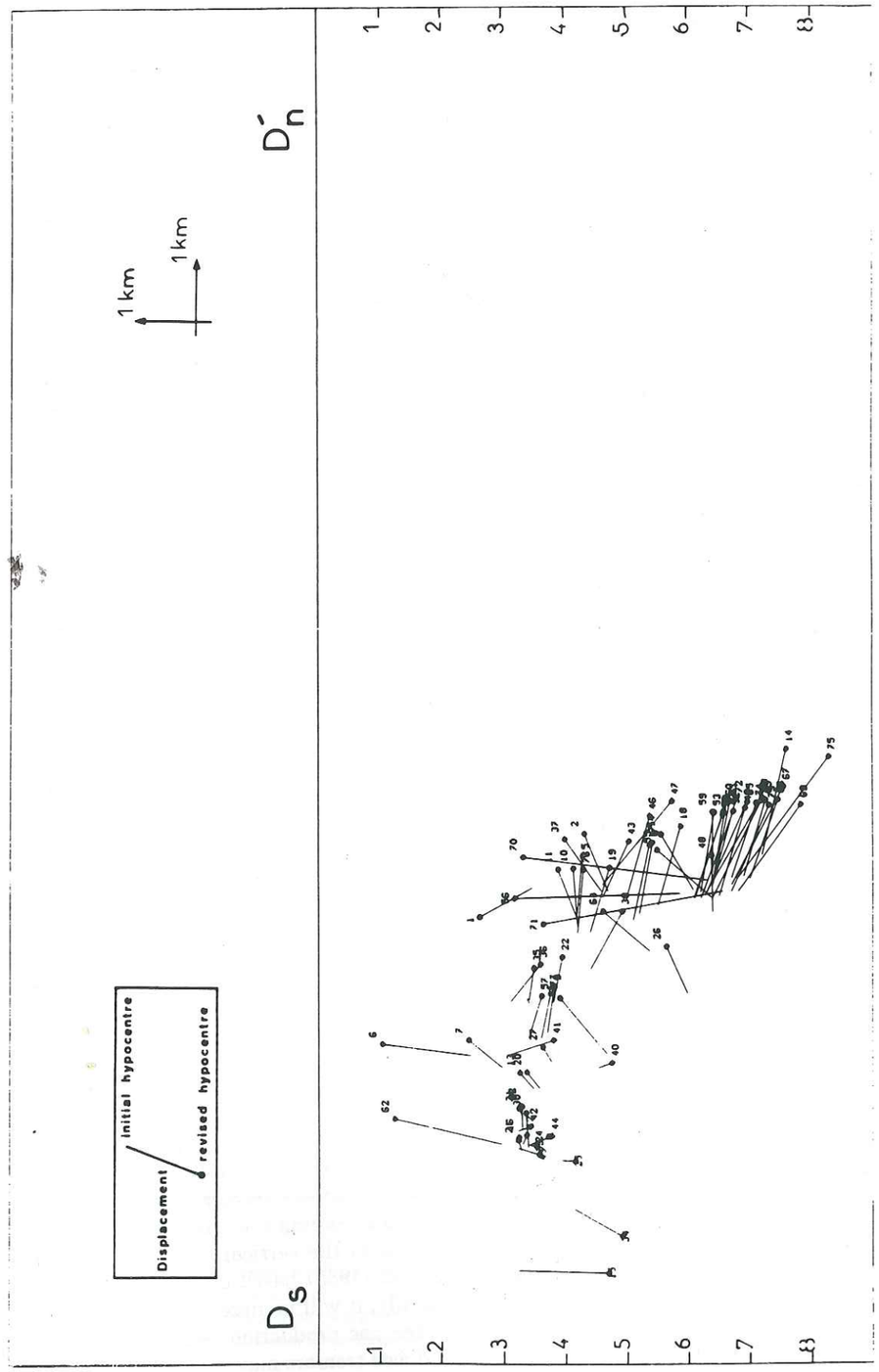

(b)

FIG. 14. (*Continued*).

tation. The seismic deformation would be concentrated in the strong brittle formations, whereas within the more ductile rocks much or all of the induced deformation is presumably aseismic (Grasso and Feignier, 1989). Moreover, the induced deformation may be controlled to some extent by pre-existing planes of weakness, including the faults (e.g., Fig. 3) and bedding planes.

The deformational response of the dome to gas exploitation most in accord with the seismic observations (Fig. 13) seems to be relaxation, or unfolding, of the anticline. This anticline probably formed under the influence of a compressional state of stress for which the maximum horizontal stress is oriented at an azimuth of approximately N30°E, consistent with the North Pyrenean thrust fault (Fig. 1), which was active until the late Tertiary period. In contrast, the present regional stress state (Hoang and Rouland, 1971; McKenzie, 1972; Tapponnier, 1977; Gagnepain *et al.*, 1980; Modiano, 1980; Gagnepain-Beyneix *et al.*, 1982; Philip, 1983) is one for which the maximum horizontal stress is oriented N60°W, which is approximately parallel to the axis of the anticline. This 90° rotation of the maximum horizontal stress may augment the tendency of the dome to "unfold," and thus extend in the northeast direction, in response to the pore pressure depletion due to gas production.

Discussion

Induced earthquakes are associated with water filling of artificial lakes, the subsurface injection of fluids, and, in fewer reported cases, fluid extraction. Earthquakes in the first group are the result either of increases in the shear stress acting on faults or decreases in the effective normal stress due to increased pore pressure (Simpson *et al.*, 1988). Crustal earthquakes associated with the second group are commonly thought to result from increased pore fluid pressure (Healy *et al.*, 1968; Raleigh *et al.*, 1972, 1976). Seismic observations are important in developing an understanding of the mechanics of earthquakes induced under conditions of decreasing pore pressure.

Yerkes and Castle (1976) had reported the characteristics of earthquakes associated with fluid extraction to be shallow depth and relatively small events, accompanied by massive land subsidence with surface faulting. Recent studies (e.g., Smirnova, 1977; Simpson and Leith, 1985; Pennington *et al.*, 1986; Wetmiller, 1986) show that deeper and larger earthquakes occur in conjunction with modest amounts of surface subsidence. In these case studies, a deep gas reservoir, a strong decrease in pore pressure (around 50 percent), and high strength rock formations are the factors leading to a strong seismic response.

In this work, we demonstrate that the pore pressure reductions induced by gas extraction began to trigger seismic ruptures above the gas reservoir 10 yr after the onset of gas production (300 bars or 45 percent of gas pressure drop). At least 10 additional yr of gas extraction were necessary to reach the critical threshold at which events were triggered below the reservoir structure, only 1 km deeper than previous events (Fig. 13) (450 bars or 70 percent of gas pressure drop).

We anticipate that further progress in understanding the seismic response of the gas field to exploitation will involve modeling of the vertical and horizontal deformation using techniques developed by Segall (1985) based on the mechanics of a poroelastic medium (Biot, 1941). Additionally, it will be necessary to take account of the response of pre-existing faults to the gas production (e.g., Roeloffs, 1988). Precise focal mechanisms for a suite of induced tremors may provide useful insights on the nature of the deformation and its relationship to exploitation.

Acknowledgments

This study was undertaken on behalf of, and with financial support from, the Societe Nationale Elf Aquitaine (Production). The authors acknowledge and appreciate the cooperation, contributions, and exchanges of data provided by a number of SNEA(P) groups involved in this study. This study benefitted greatly from the seismic monitoring carried out by the IPG Strasbourg. We are grateful to Art McGarr for many hepful comments and suggestions in reviewing the manuscript. We thank Paul Segall and David Boore for constructive comments on the manuscript. We are also very grateful to the following persons for assisting with various aspects of this study : M. Bouchon, A. Cote, J. Delvaux, D. Fabre, J. Fréchet, M. Gaillard, A. Guénot, H. Haessler, V. Maury, M. Mollier, H. Taussac, A. Toreilles, and P. Vialon.

References

Biot, M. A. (1941). General theory of 3-D consolidation, *J. Appl. Physics* **12,** 155–164.

Boillot, G. and Capdevilla, R. (1977). The Pyrenees: subduction and collision?, *Earth Planet. Sci. Lett.* **35,** 151–160.

Calloi, P., DePanfilis, M., DeFilippo, D., Marcelli, L., and Spadea, M. C. (1956). Terrimoti della Val Padana del 15–16 Maggio 1951, *Ann. Geophys.* **9,** 63–105 (with summary in English).

Choukroune, P. (1976). Structure et evolution tectonique de Ia zone nord-pyreneenne, *Memoire Societé Géophysique de France, Nouvelle Serie*, Fr., N. S. LV **127,** 1–116.

Choukroune, P. and Mattauer, M. (1978). Tectonique des plaques at Pyrenees: sur le fonctionnement de Ia faille transformante nord-pyreneenne; comparison avec les modeles actuels, *Bull. Soc. Geol. Fr.* **7,** XX, 689–700.

Coustau, R. (1965). Premiers resultats de l'etude tectonique du gisement de Lacq profond, Report to SNEA(P), RG/cg, 65/2277.

Daignieres, M., Gallart, J., Banda, E., and Hirn, A. (1982). Implications of the seismic structure for orogenic evolution of the Pyrenean range, *Earth Planet. Sci. Lett.* **57,** 88–100.

Gagnepain, J., Cisternas, A., Ruegg, J. C., Vadell, M., Modiano, T., Hatzfeld, D., and Mezcua, J. (1980). Sismicite et mecanisme au foyer de Ia region d'Arette, *Ann. Geophys.* **36,** 499–508.

Gagnepain-Beyneix, J., Haessler, H., and Modiano, T. (1982). The Pyrenean earthquake of February 29, 1980: an example of complex faulting, *Tectonophysics* **85,** 273–290.

Gallart, J., Daignieres, M., Gagnepain-Beyneix, J., and Hirn, A. (1985). Relationship between deep structure and seismicity in the western Pyrenees, *Ann. Geophys.* **3,** 239–248.

Grasso, J. R. (1983). Three-dimensional velocity image of a barrier associated with moderate Pyrenean (France) earthquake, *Geophys. Res. Lett.* **10,** 229–232.

Grasso, J. R., Cuer, M., and Pascal, G. (1983). The use of two inverse techniques: application to a local structure in the New Hebrides Island arc, *Geophys. J. R. Astr. Soc.* **75,** 437–472.

Grasso, J. R. and Feignier, B. (1990). Seismicity induced by gas depletion: I. Lithology correlated events, induced stresses and deformations, *Pure Appl. Geophys.* (in press).

Grasso, J. R., Vialon, P., and Fabre, D. (1985). Etude géomécanique de la sismicité dans la région de Lacq, Report to the SNEA(P) Compagny, 400 pp.

Haas, A., Mollier, M., and Taussac, R. (1972). Etude sur l'extension du gisement de Lacq profond, SNEA (P), D. 9983.

Healy, J. H., Rubey, W. W., Griggs, D. F., and Raleigh, C. B. (1968). The Denver earthquakes, *Science* **181,** 1301–1310.

Hoang, T. and Rouland, D. (1971). Mécanisme au foyer du seisme d'Arette (P.A.), *Comptes-rendus Academie des Sciences, Paris* **272,** 3249–3251.

Jenner, P. and Dienesh, J. (1965). Histoire géophysique du champ de Laqc, *Geophysical Prospecting* **13,** 518–540.

Kothé (1981). Interpretation de la campagne sismique 81LAQ, S.N.E.A. (P) internal report, MF.EXPLO, no. 81.14212.

Kovach, R. L. (1974). Source mechanisms for Wilmington oil field, California, subsidence earthquakes, *Bull. Seism. Soc. Am.* **64,** 699–711.

McKenzie, D. (1972). Active tectonics of the Mediterranean region, *Geophys. J. R. Astr. Soc.* **30,** 109–185.

Modiano, T. (1980). Sismotectonique des Pyrénées Occidentales. Etude détaillée du contenu spectral des ondes de volume dans la région focale. *Thése 3'éme cycle*, University of Grenoble, Grenoble, France.

Olivera, C. (1983). Estudis de sismicitat i sismotectonica local. Applicacio als Pirineus, *Ph.D. Thesis*, Univeristy of Barcelona, Barcelona, Spain, 263 pp.

Pennington, D. W., Davis, D. D., Carlson, S. M., DuPree, J., and Ewing, T. E. (1986). The evolution of seismic barriers and asperities caused by the depressuring of fault planes in oil and gas fields of south of Texas, *Bull. Seism. Soc. Am.* **76,** 939–948.

Philip, H. (1983). La tectonique actuelle et récente dans le domaine Méditerranéen et ses bordures. Ses relations avec Ia sismicité, *Thèse de Doctorat d'Etat*, Université de Montpellier, Montpellier, France, 240 pp.

Raleigh, C. B., Healy, J. H., and Bredehoeft, J. D. (1972). Faulting and crustal stress at Rangely, Colorado, in *Flow and Fracture of Rocks* (Griggs Volume), H. C. Heard, I. Y. Borg, N. L. Carter, and C. B. Raleigh (Editors), American Geophysical Union Monograph **16,** 275–284.

Raleigh, C. B., Healy, J. H., and Bredehoeft, J. D. (1976). An experiment in earthquake control at Rangely, Colorado, *Science* **191,** 1230–1237.

Roeloffs, E. A. (1988). Stability changes induced beneath a reservoir with cyclic variations in water level, *J. Geophys. Res.* **93,** 2107–2124.

Rothé, G. H. and Lui, C. Y. (1983). Possibility of induced seismicity in the vicinity of the sleepy hollow oil field, southwesern Nebraska, *Bull. Seism. Soc. Am.* **73,** 1357–1367.

Rothé, J. P. (1941). *Annales de l'Institut de Physique du Globe, Nouvelle Serie*, Troisième Partie, vol. 5, Géophysique, Strasbourg.

Rothé, J. P. (1956). *Annales de l'Institut de Physique du Globe, Nouvelle Serie*, Troisième Partie, vol. 7, Géophysique, Strasbourg.

Rothé, J. P. (1967). *Annales de l'Institut de Physique du Globe, Nouvelle Serie*, Troisième Partie, vol. 8, Géophysique, Strasbourg.

Rothé, J. P. (1970). Séismes artificiels, *Techtonophysics* **9,** 215–218.

Rothé, J. P. (1972). *Annales de l'Institut de Physique du Globe, Nouvelle Serie*, Troisième Partie, vol. 9, Géophysique, Strasbourg.

Rothé, J. P. (1977). Séismes artificiels et exploitations pétrolières: l'exemple de Lacq (France), *Annali de Geoficicia* **30,** 369–383.

Segall, P. (1985). Stress and subsidence resulting from subsurface fluid withdrawal in the epicentral region of 1983 Coalinga earthquake, *J. Geophys. Res.* **90,** 9801–9816.

Simpson, D. W. (1976). Seismicity changes associated with reservoir loading, *Engineering Geology* **10,** no. 2–4, 123–150.

Simpson, D. W. and Leith, W. (1985). The 1976 and 1984 Gazli, USSR, earthquakes were induced?, *Bull. Seism. Soc. Am.* **75,** 1465–1468.

Simpson, D. W., Leith, W. S., and Scholz, C. H. (1988). Two types of reservoir-induced seismicity, *Bull. Seism. Soc. Am.* **78,** 2025–2040.

Smirnova, M. N. (1977). Vliyanie inzhenernoj deyatel'nosti na sejsmicheskii rezhim, ed. "Nauka," Moscow, 128–140.

Smirnova, M. N., Shebalin, N. V., Navitskaja, N. A., and Miatockin, V. J. (1975). Earthquake swarm caused by exploitation of an oil field, *IUGG* **16,** Gen. Assembly, Grenoble.

Tapponnier, P. (1977). Evolution tectonique de systeme alpin en Méditerranée: poinconnement et écrasement rigide-plastique, *Bull. Soc. Geol. Fr.* **58,** 399–4165.

Vogt, J. (1979). Les tremblements de terre en France, *Mém B.R.g.M., no. 96.*

Vogt, J. (1982). Les séismes pyrénéens: 19.05.1765, 28.10.1835, 5.12.1855, 1858, 1859, 27.02.1924, Technical note B.R.G.M. no. 15-20-24-25/1982.

Wetmiller, R. J. (1986). Earthquakes near Rocky Mountain House, Alberta, and their relationship to gas production facilities, *Can. J. Earth. Sci.* **23,** 172–181.

Wittlinger, G. (1980). Etude de la sismicité en champ proche par un réseau sismologique à faible ouverture: application au Frioul (Italie) et au gisement de Lacq (France), *Thèse de Doctorat d'Etat*, University of Strasbourg, Strasbourg, France, 261 pp.

Yerkes, R. F. and Castle, R. O. (1976). Seismicity and faulting attributable to fluid extraction, *Engineering Geology* **10,** 151–167.

LABORATOIRE DE GEOPHYSIQUE INTERNE ET TECTONOPHYSIQUE
OBSERVATOIRE DE GRENOBLE
UNIVERSITÉ JOSEPH FOURIER
LGIT IRIGMBP 53X
38041 GRENOBLE CEDEX FRANCE
(J.R.G.)

LABORATOIRE DE SISMOLOGIE
INSTITUT DE PHYSIQUE DU GLOBE DE STRASBOURG
5 RUE RENÉ DESCARTES
64084 STRASBOURG CEDEX FRANCE
(G.W.)

Manuscript received 23 August 1988

22

LE ROLE DES DISCONTINUITÉS GÉOMÉTRIQUES ET MÉCANIQUES SUR LA LOCALISATION DES RUPTURES SISMIQUES.

PAGEOPH, Vol. 134, No. 3 (1990)

0033–4553/90/030427–24$1.50 + 0.20/0

Seismicity Induced by Gas Production: II. Lithology Correlated Events, Induced Stresses and Deformation

JEAN-ROBERT GRASSO[1] and BRUNO FEIGNIER[1]

Abstract—A 3D relocation technique permits precise locations of induced earthquakes. Geostatistical processing using the data of 87 boreholes provides the basis of a precise 3D structure, with a dome geometry. Conventional laboratory mechanical tests performed on deep rock samples (1000 m to 5000 m) define the rock properties at depths similar to those of the seismic events ($1 < M_L < 4.2$) that range from 1 to 7 km.

In the studied period, most (85%), of the events were located above the gas reservoir, with very few located in the reservoir itself. Because the production parameters (50 MPa depletion of the gas pressure reservoir) are homogeneous throughout the gas field, the lateral inhomogeneity of the seismic rupture locations are a consequence of variations in the rheological response of the dome to the deformation induced by gas production.

Here a ratio of two is found between the elastic modulus of the seismic rock matrix and the elastic modulus of the aseismic rock matrix. The contrast in strength is at least as great, if not greater. Repeated measured surface deformations involve the whole structure. Spatial and temporal deformations indicate that aseismic deformation is quantitatively the main process of this structural deformation. The heterogeneous stress pattern inferred from *P*-axes of induced earthquakes disagrees with the tectonic regional stress field. The radial distribution of *P*-axes towards the gas reservoir probably reflects the production induced deformation. The inferred deformation of the dome occurs in response to weak induced stresses.

Key words: Induced seismicity, gas production, rock mechanic, regional stress field, Pyrenees.

Introduction

The regional seismicity of the western Pyrenean area is characterized by a narrow strip, less than 10 km wide. Earthquake occurrence, 30 km to the north of this strip clearly set apart a cluster of seismic activity with a 10×10 km^2 lateral extension. The spatial and temporal patterns of these tremors are well correlated to the patterns of the Lacq gas field exploitation (GRASSO and WITTLINGER, 1990).

A review of earthquakes associated with fluid extraction was presented in YERKES and CASTLE (1976). Additional observations (e.g., ROTHE and LUI, 1983;

[1] Observatoire de Grenoble, Laboratoire de Geophysique Interne et Tectonophysique, IRIGM, BP 53X, 38041 Grenoble, France.

MEREU *et al.*, 1986; WETMILLER, 1986) were published but the number of recording stations, time scale of the observation, location procedures and geological knowledge of the area do not allow the analysis of seismic fractures in a geomechanical context.

Recent mechanical models have been used to assess either the effects of field exploitations on the pore fluid pressure and stress field (see, for example, SEGALL, 1985, 1989) or the possible mechanism of induced faulting (e.g., PENNINGTON *et al.*, 1986). But for some previous reasons, poor connections exist between these modeling approaches and the observed fractures.

In our case, ten years of seismic recording with a local network, have led to the location of more than 800 induced earthquakes above a natural gas field (GRASSO and WITTLINGER, 1990). The beginning of the seismicity can be defined in 1969 by the first felt $M_L = 3.0$ event, ten years after the beginning of the gas field exploitation. Since this date at least one $M_L > 3$ event has occurred every year.

In a companion study, FEIGNIER and GRASSO (this issue), use focal mechanism techniques to understand the kinematics of induced fractures. The geometry of the fracture planes and the displacements of these planes imply a model with a collapsed block at the top of the dome structure. Lateral boundaries of this block are the preexisting faults, recognized using numerous boreholes.

3D relocation techniques, performed by GRASSO and WITTLINGER (1990), provide precise locations for these earthquakes. In this study, geostatistical processes using the data of 87 boreholes allow the modeling of a precise 3D structure, with a dome geometry. Conventional laboratory mechanical tests performed on deep rock samples (1000 m to 5000 m) by GRASSO *et al.* (1985) define the rock properties. These data sets are used to perform geomechanical localization of hypocenters, i.e., the event occurrence within rock of known mechanical properties.

In this context we investigate the mechanics of fractures induced by the gas extraction. The main purpose of this study is to understand the rheological response of a known geological structure when triggered by a gas extraction. Because induced events seem to be physically identical to natural earthquakes (GRASSO and WITTLINGER, 1990; FEIGNIER and GRASSO (this issue)), the results of this study are important with regard to the understanding of natural crustal earthquakes. The scale of the involved structure ($10 \times 10 \times 5$ km^3) and the available data are crucial to the interest of this natural laboratory. The first two sections review the exploitation characteristics and the seismic patterns. In the third section the procedure of geomechanical earthquake location is detailed. Furthermore, we first study seismic fractures according to properties of the rock matrix in which they are located. Thereafter a global deformation of the involved dome structure is analysed, using repeated leveling, in order to assess the relative importance of the tectonic background (preexisting fractures and the state of stress) versus stresses and deformation induced by the gas extraction.

Characteristics of Oil and Gas Fields

Lacq hydrocarbon fields (Figure 1a) are located in an anticline structure of the French Pyrenean foreland. Production of the oil field, or upper reservoir (average depth of 600 m), began in 1950, in an upper-Cretaceous level containing water and oil. The initial fluid pressure in the field was 6.1 MPa. Slight perturbations of this fluid pressure are reported (less than 1 MPa), due to waste water injections. Since 1975, the pressure has been stabilized at 6.7 MPa. Because of the lack of significant changes in the geomechanical parameters of the oil field and its small lateral extension, the hypothesis that earthquakes are triggered by the exploitation of the upper reservoir cannot be applied in this case study (GRASSO and WITTLINGER, 1990).

The producing horizons of the gas field (lower reservoir) are late Cretaceous and upper Jurassic limestones. The field has an average thickness of 550 meters and a depth of 3.2 to 6.0 km due to the anticline structure. Averaged porosity is less than 5% in the 250 m of thickness of the effective reservoir and average transmissivity of a so-called fractured reservoir is 50 darcy.m. Structural traps are formed by impermeable marly levels which bound the reservoir. An upper-Cretaceous reef overlays the eastern part of the gas field. This reef seems fractured and cavernous, i.e., there was a loss of tools during prospection drills. The reef laterally vanishes and marly levels take over (Figure 1b).

Since its discovery in 1958, 1.8 10^{11} m^3 of gas have been extracted from the lower reservoir. The average extraction rate of 7.5 10^9 m^3 per year is nearly constant from 1961 to 1983. No major faults or preferential orientation has been identified in the structure from the seismic reflection data or "well-logs".

The 68 MPa initial gas pressure indicates a reservoir overpressured with respect to the 32 MPa hydrostatic state. The lithostatic stress at the same 3.2 km depth is 82 MPa (Figure 2). It can be reported that borehole operations reveal the presence of high-pressure lenses at the top of the reservoir horizons and at the base of the marly layers overlaying it (pressure lenses up to 90 MPa). These lenses have no hydraulic communication with the reservoir: in 1979, a 45 MPa pressure lens was perforated during the drilling and at this date, reservoir pressure was 20 MPa (Figure 2).

If the vertical stress can be taken as to the lithostatic stress, the direction of maximum and minimum horizontal regional stresses is often determined from the data of natural focal mechanisms. In the surrounding area, focal mechanisms of natural earthquakes located 25 km southward from the gas field are consistent with N120° orientation of $|S_1| = |S_H|$ and N30° orientation of $|S_3| = |S_h|$ (GAGNEPAIN-BEYNEIX *et al.*, 1982; GALLART and DAIGNIÈRES, 1985), which are the accepted regional orientations (HOANG and ROULAND, 1971; MCKENZIE, 1972; TAPPONNIER, 1977; MODIANO, 1980; DAIGNIÈRES *et al.*, 1982; PHILIP, 1983). Data deduced from borehole breakouts in neighbouring gas field are less convincing. Even between 4 and 5 km in depth, only 50% of breakouts analysed in more than 32 wells, agree with

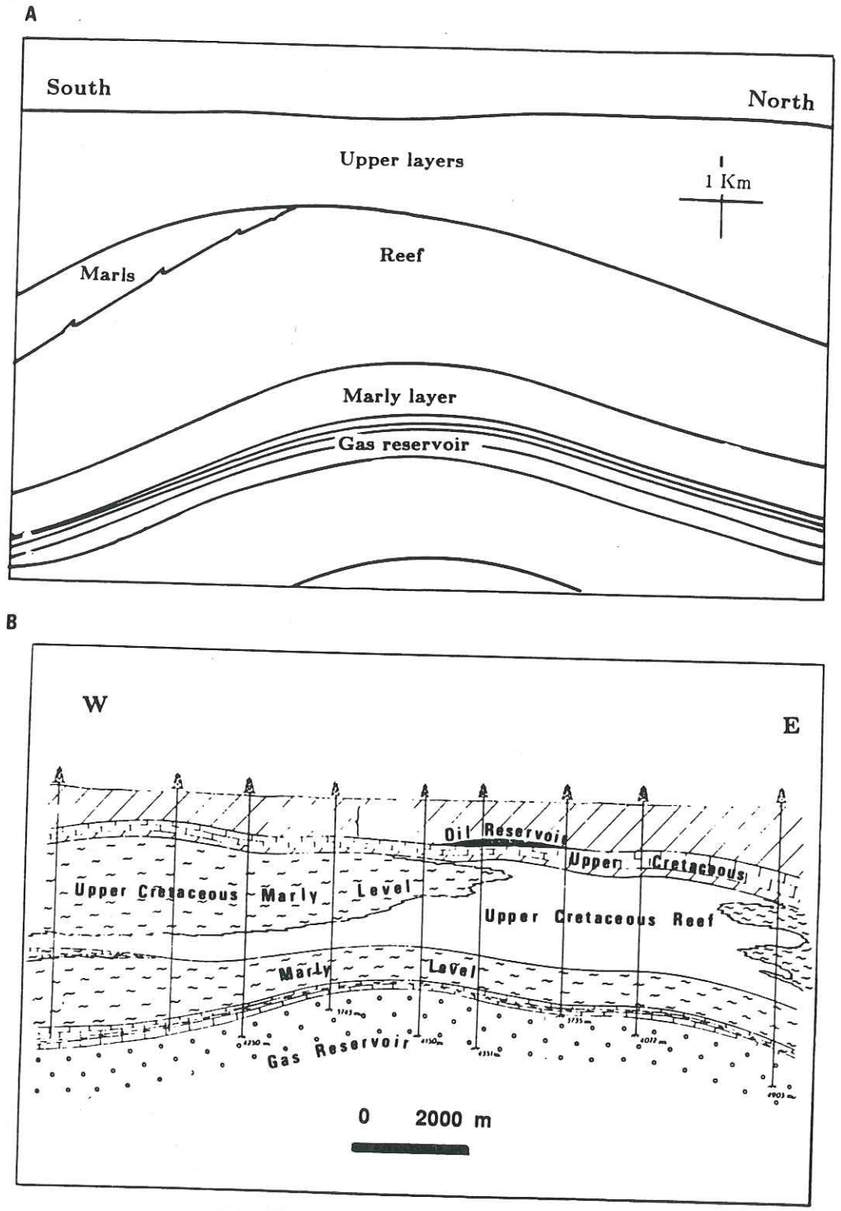

Figure 1
Structural vertical cross-sections of the hydrocarbon fields. (a) North-South direction, (b) East-West direction.

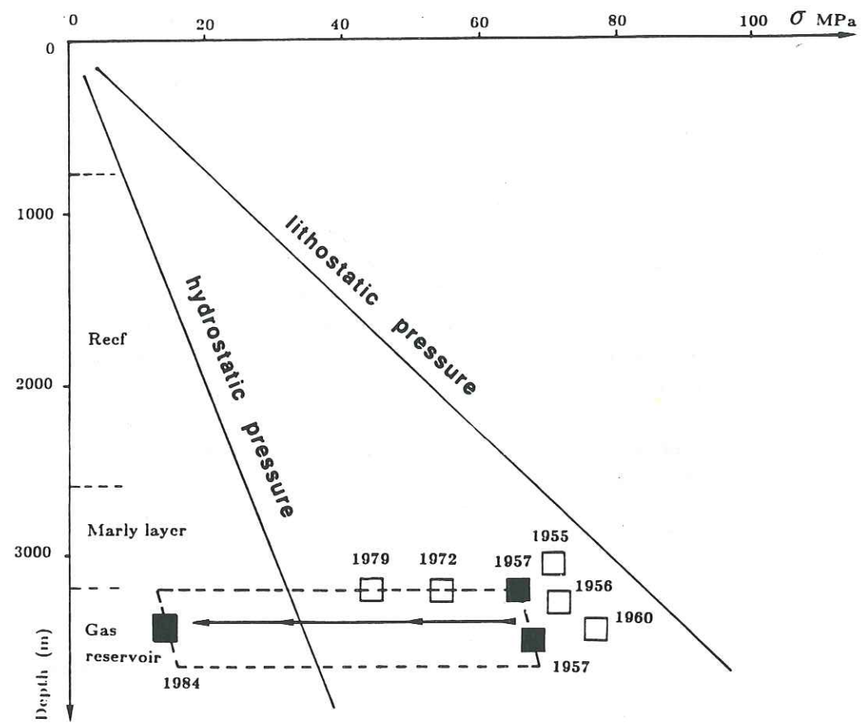

Figure 2
Pressure versus depth. Black squares are the pressure of the reservoir with corresponding dates. Open squares are the values of the overpressured lenses. Horizontal arrow is the time evolution of the gas pressure of a borehole located at the top of the structure. On the depth axis, schematic lithology is reported from a borehole located at the top of the dome structure.

the N120° orientation of the major horizontal stress (GUÉNOT, 1987). 90° rotations of the breakouts have been observed in a part of the field, like the eastern part of the Meillon field (Figure 10). The analysis of borehole breakouts which have been performed on other fields in the area agree with the accepted regional orientation. The effect of this tectonic stress on the shallow complex structure of the fields is one of the major interests of this study.

Seismic Patterns

The most striking feature of the seismic activity of the area is the spatial coherency of the seismic cluster in time. GRASSO and WITTLINGER (1990) have shown that this clustering activity is correlated with the lateral extension of the gas

reservoir and that neither spatial nor temporal migration can be discerned in the 1974–1983 period. The energy release in the 1969–1983 period, using $M_L > 3$ events, confirms the temporal stability of the rupture (Figure 3).

Data from this 4-year-long period represented in Figure 4, show the roughly circular pattern of the events, in association with the geometry of the local dome structure by GRASSO and WITTLINGER (1990). The seismic gap in the central part of the cluster is located at the top of the structure. The behaviour of the rock matrix in the western part of the field is undoubtedly defined as an aseismic zone in Figure 4. Because the production parameter seems to be homogeneous throughout the gas field the inhomogeneity of the seismicity could be a consequence of variations in the rheological response of the dome to deformation induced by production. Southwest-northeast and northwest-southeast cross-section views of the data indicate that the depth of most of the earthquakes is less than 5 km (Figures 5 and 6). Although a geometry close to the anticline of the field structure is prominent in the southwest-northeast cross-section, the distribution of focal depths remains complex. Its understanding needs further investigations which are proposed in the following sections. Large events seem to cluster in the 1976–1979 study period. In order to understand the fracture induced by gas exploitation, we choose to work with 220 relocated events, the same data as FEIGNIER and GRASSO (this issue).

Relationship Between Seismicity and Lithology

The survey of the gas field gives us a unique data set with regards to the study period duration and the quality of both the recording network and the hypocenter location. A local network has been installed on the field since 1974. Seven seismological stations have operated in the 1976–1979 period and 8 since 1982. The depths of the earthquakes play an important role in this analysis, because the respective geomechanical properties of rocks and structures are both functions of depth. An unusually complete set of seismological data and geomechanical measurements has been collected in this gas field (WITTLINGER, 1980; GRASSO *et al.*, 1985; GRASSO and WITTLINGER, 1990; FEIGNIER and GRASSO, this issue). In order to use the seismological data set in this optimum geomechanical context, we used the 3D relocated events of GRASSO and WITTLINGER (1990).

The accuracy of geographical earthquake parameters was determined according to the location discrepancy obtained between 3 different data sets. Three independent relocations, linked to these 3 data sets, gave outputs for the earthquake parameters [X, Y, Z and Ho, (origin time)]. *A priori* bounds were respectively: $\delta X = \delta Y = 0.1$ km, $\delta Z = 0.15$ km, $\delta Ho = 0.5$ s. *A posteriori* errors are calculated as $\max(X_i - X_j, Y_i - Y_j, Z_i - Z_j, Ho_i - Ho_j)$ for $i = 1, 3$ and $j = 1, 3$; the Z values are presented in Figure 7b. On the other hand, geostatistical methods allow the discovery of determination in 3D of each geological level. The data are well-logs for

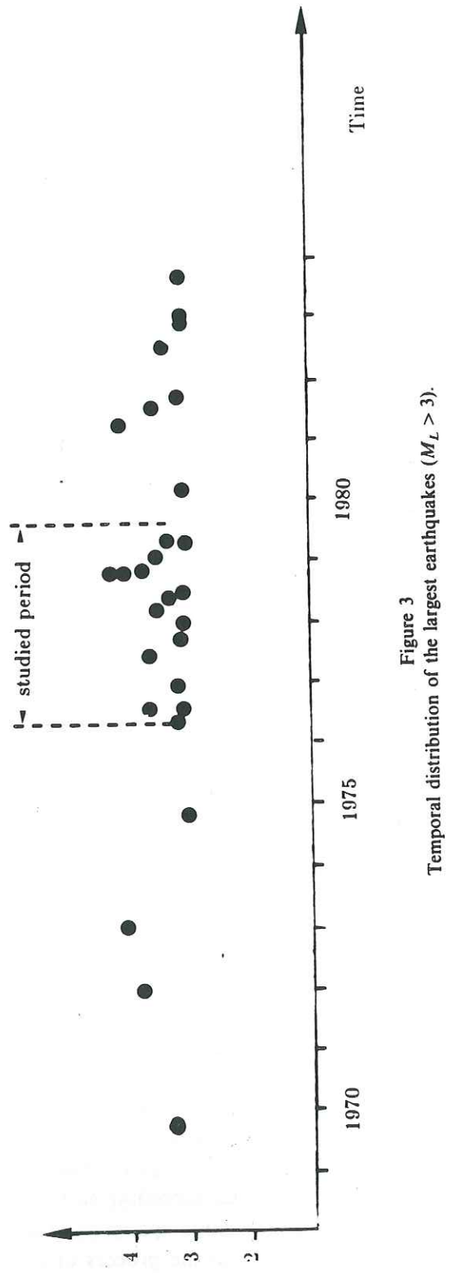

Figure 3
Temporal distribution of the largest earthquakes ($M_L > 3$).

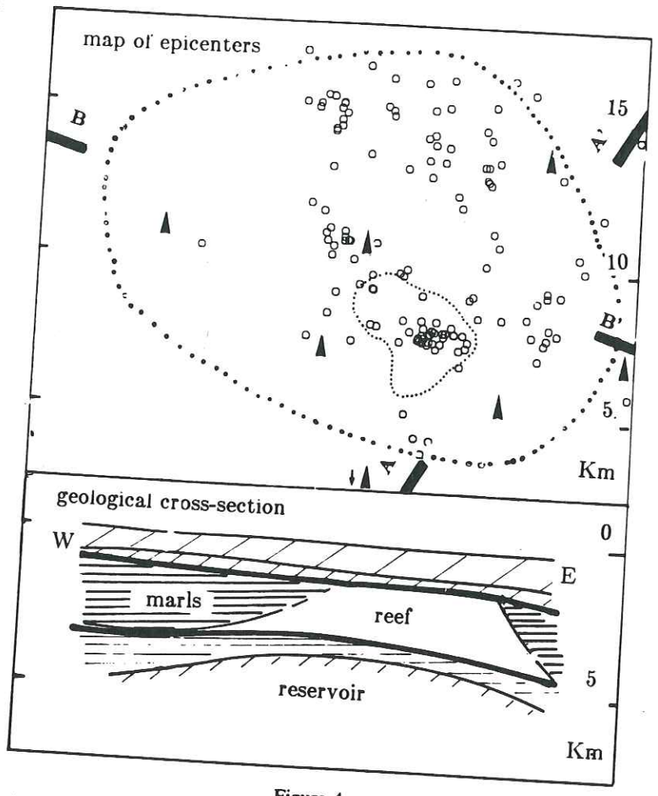

Figure 4

Upper box: epicentral map of the events and the 7 station network used in this study. Open circles are epicentres. Large dotted line is the lateral extension of the gas reservoir. Small dotted line is the lateral extension of the oil field. Arrows are the seismological stations. The southern station is located 5 km southward of the star position on the map. *Lower box*: schematic E-W structural cross-section.

the 32 boreholes of the lower reservoir and 55 additional wells for the upper layers. These two data sets can be correlated and the diagram of Figure 7a shows the relative distribution of seismic activity for the main structure entities. A triangular probability law defines the linkage of an earthquake position to a specific formation when event occurrence within a level is greater than 50%. For a synthetic presentation, the 14 initial layers are reduced to 5 specific groups: layers located below the gas reservoir, gas reservoir horizons, marly levels, reef, upper horizons. These synthetic entities are defined according to the layer thickness (2 times greater than the average earthquake location accuracy) and to the properties which are mechanically distinct with regard to the process of earthquake generation.

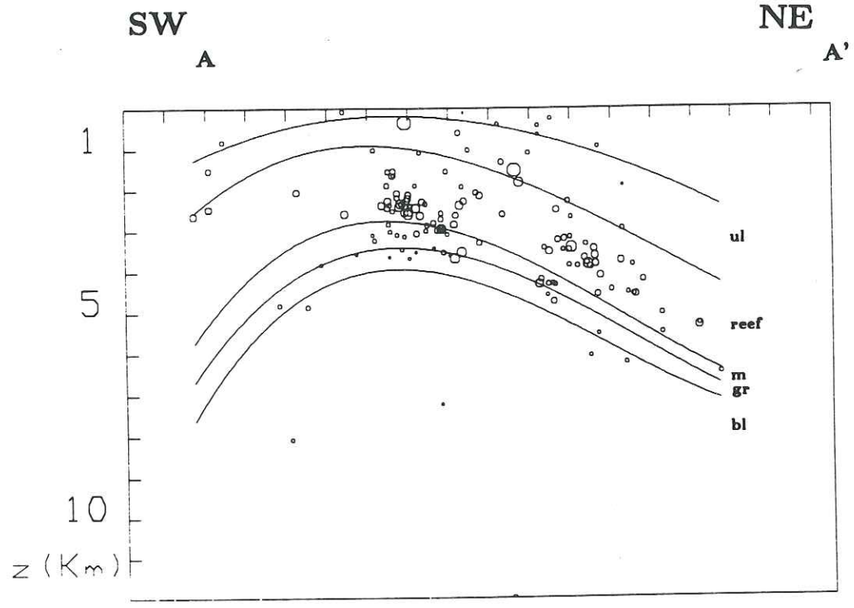

Figure 5

Cross-section in the SW-NE direction with projection of the whole hypocentre data set. Circles are functions of the event magnitudes. The curved lines show, with decreasing depth, the gas reservoir (gr), the marly level (m), the reef formation (reef), and the upper calcareous layers (ul). The location of the section is given on Figure 4 by *AA'* line.

The mechanical behaviour of these 5 groups are analysed, in order to understand their respective responsibility in the seismic activity and the global deformation of the gas field. The histogram of Figure 7 exhibits the major role of the reef layer in the global seismicity (60%). One may further notice the great asymmetry between the activity in the layers above (more than 85% of total seismicity) and below the reservoir (less than 5% of seismicity). Only 8% of the events are located within the gas reservoir itself. The layers below the reservoir have a weak seismic activity. Their mechanical properties are not well known but this relative aseismicity allows two interpretations: there is no differential motion below the reservoir (i.e., reservoir is not at lithostatic equilibrium) or the internal deformation is ductile. The lack of geological knowledge prevents the choice at interpretation. Moreover, only 4% of the seismicity occurs in these levels which poorly contribute to the comprehension of gas field response in the period of study. The reservoir (500 m thick and 250 m of effective thickness for gas matrix) is made up of dolomites and limestones from Portlandian to Barremian age (140 to 120 Ma); these are overlain by a stack of thin layers (50 to 150 m thick). Thus, their physical properties are very

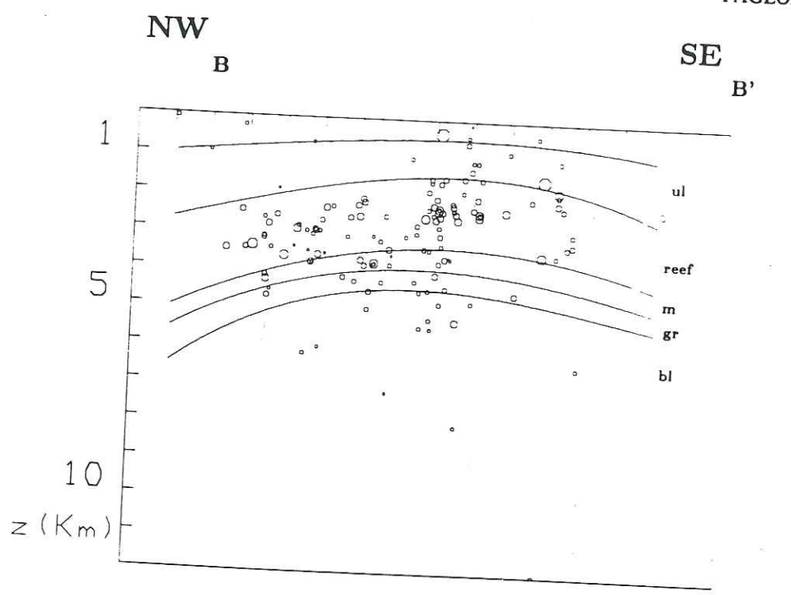

Figure 6
Cross-section in the NW-SE direction with projection of the whole hypocentre data set. Circles are a function of the event magnitudes. The curved lines refer to Figure 5. The location of the section is given on Figure 4 by *BB'* line.

heterogeneous with uniaxial compressive strength increasing from 84 MPa to 213 MPa for 11 samples (GRASSO *et al.*, 1985) and successive ductile and brittle mechanical behaviour in the temperature and stress conditions of the field (FABRE *et al.*, 1989). Only 8% of the total seismicity occurs within these layers where the depressurization effect (50 MPa) is the most important. The assumed induced strains and the weak seismic activity of the reservoir horizons, indicate a ductile process in response to reservoir compaction. In this context of rock matrix compaction the reservoir behaves continuously as a closed cavity (the gas pressure/gas compressibility ratio is constant over more than 20 years), according to the most recent drill holes which perforated the top of the dome until 1979.

The value of 15% of seismic activity in the marly levels may seem high. In fact, the so-called "marls" present local lithological variations of calcareous facies. This is particularly true at the reef base where seismic fractures are located (Figure 7). Figure 8 indicates this trend, and events with magnitudes greater than 3 in the middle of the marls are linked to these calcareous banks (BARTHE and REVERDY, 1958). This is also compatible with the wide range of the uniaxial compressive strength deduced from laboratory tests (GRASSO *et al.*, 1985): from 40 up to 90 MPa. The global behaviour of marls is ductile. With an elastic modulus 1.5 times

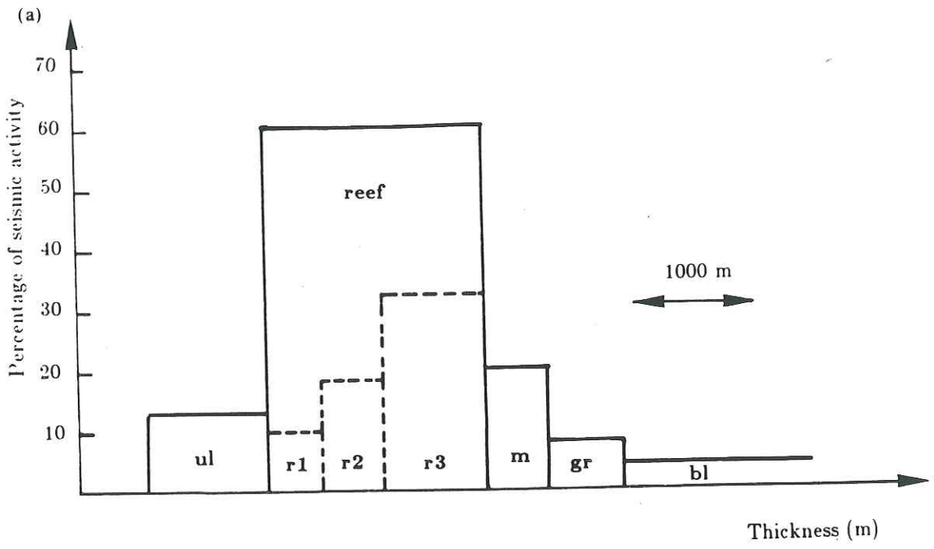

Figure 7a
Histogram denotes the percentage of seismic activity for the 5 main entities of the structure: ul, upper layers; reef, rl r2 r3, reef formations gr, gas reservoir; bl, layers below the reservoir. The widths are linked to layer thicknesses.

lower than that of the gas reservoir rocks, they act as a filter smoothing possible differential displacements of the reservoir to a quite regular curve, as shown by the leveling profile of Figure 9. Measurements were made in 1967 and 1979. The values show a maximum vertical motion of 3 cm between these years. This maximum is centred over the top of the dome and its lateral extension has the same scale as the gas field. These measures are coherent with the values computed by RYAN *et al.* (1983) and SEGALL (1985) when studying respectively magma and oil reservoir subsidence mechanics. Additional measurements exist if we use the 1887 data set. The similarity between the 1887–1967 and 1967–1979 curves indicates a subsidence of 3 cm per 10 years of gas exploitation since the beginning of the extraction operations in 1959. Thus, the first 10 years of subsidence (1959–1969) are entirely due to an aseismic process (pressure solution process, e.g., GRATIER, 1984), associated with this seismic quiescence until 1969.

The reef characteristics are those of a very brittle, water-saturated and prefractured medium. About 60% of the seismicity is located inside this reef, including events of the largest magnitude. Uniaxial compressive strength ranges from 130 to 160 MPa. An important result in the understanding of the reef deformation would be to ascertain whether preexisting fractures or brittle behaviour is more important in concentrating the seismicity in the reef layers. In the western part of the gas field,

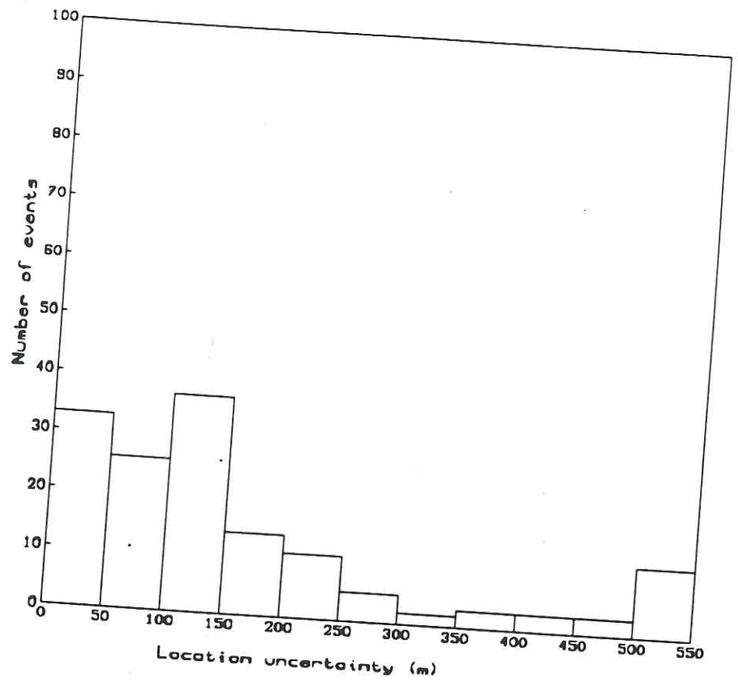

Figure 7b

Location uncertainties in the Z direction. Most of the error margins are less than 200 m (adapted from GRASSO and WITTLINGER, 1990).

marls replace the calcareous reef. The epicentre map shows a corresponding lateral change (Figure 4) and the aseismicity of the western part is thus related to rheological lateral variations (Table 1). No significant seismicity (11.5%) affects the layers located above the reef, despite the presence of stiff limestone. Several explanations are proposed here: a great distance from the gas reservoir (at least 2.5 km), a prefracturation state different from the reef, or the lack of energy to initiate new fractures in an unprefractured medium.

Therefore we may conclude that a leading factor for the seismic fracture localization is the lateral and vertical change in the lithology which transforms a massive, water-saturated, prefractured calcareous entity into marly levels with important (30% to 50%) clay minerals increasing its ductility. Moreover conventional rock properties deduced from uniaxial compression tests strongly differentiate the rock matrix behaviours (Table 1). A ratio of two for Young's modulus characterizes the lateral and the vertical change from seismic calcareous reef to relatively aseismic marly levels. Compressive strengths of the rocks are at least

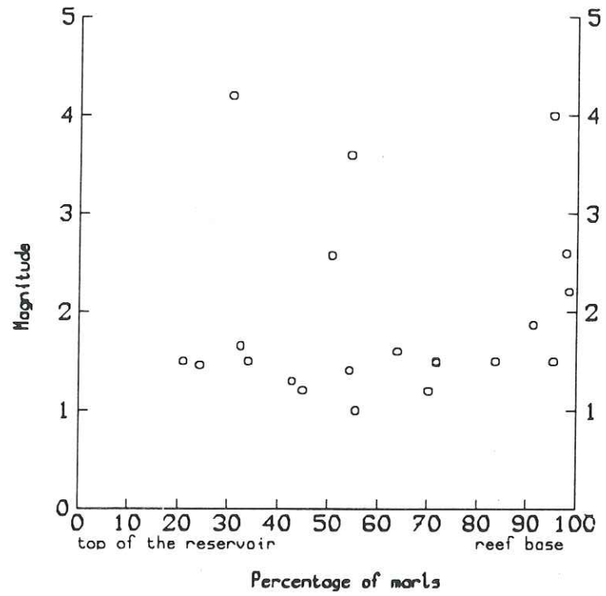

Figure 8

Seismicity of the marls. Circles are drawn according to the event location in this level. The use of percentage inhibits lateral variation of thickness.

70 MPa higher for the seismic area than for the relatively aseismic area. Such a pattern was presented by MCGARR *et al.*, (1975), where a 40% change in strength is considered as the primary factor in the asymmetric distribution of seismic sources about the plane of the reef in a dry mining environment of intact rock. In our study a major change in both the strength of the rock matrix and the elastic modulus correlated with a change in seismic response on a scale of the order of a few kilometers, demonstrates that the mechanical properties of the rock matrix are appropriate parameters to define the large-scale behaviour of a geological structure. Second-order effects must be mentioned. The strength of the rock matrix seems to be directly correlated to the seismicity rate. The lowest strengths characterize the aseismic lateral marls. The intermediate strengths characterize the sparse 15% of the seismic activity of the marls located below the calcareous reef and the highest strengths characterize the main seismic entity, i.e., the calcareous reef. Even if another mechanical parameter can influence the seismic localization of this case study (fluid circulation in the reef, rock heterogeneity of the sedimentary environment) we show that material strength is a powerful parameter for understanding the seismic deformation.

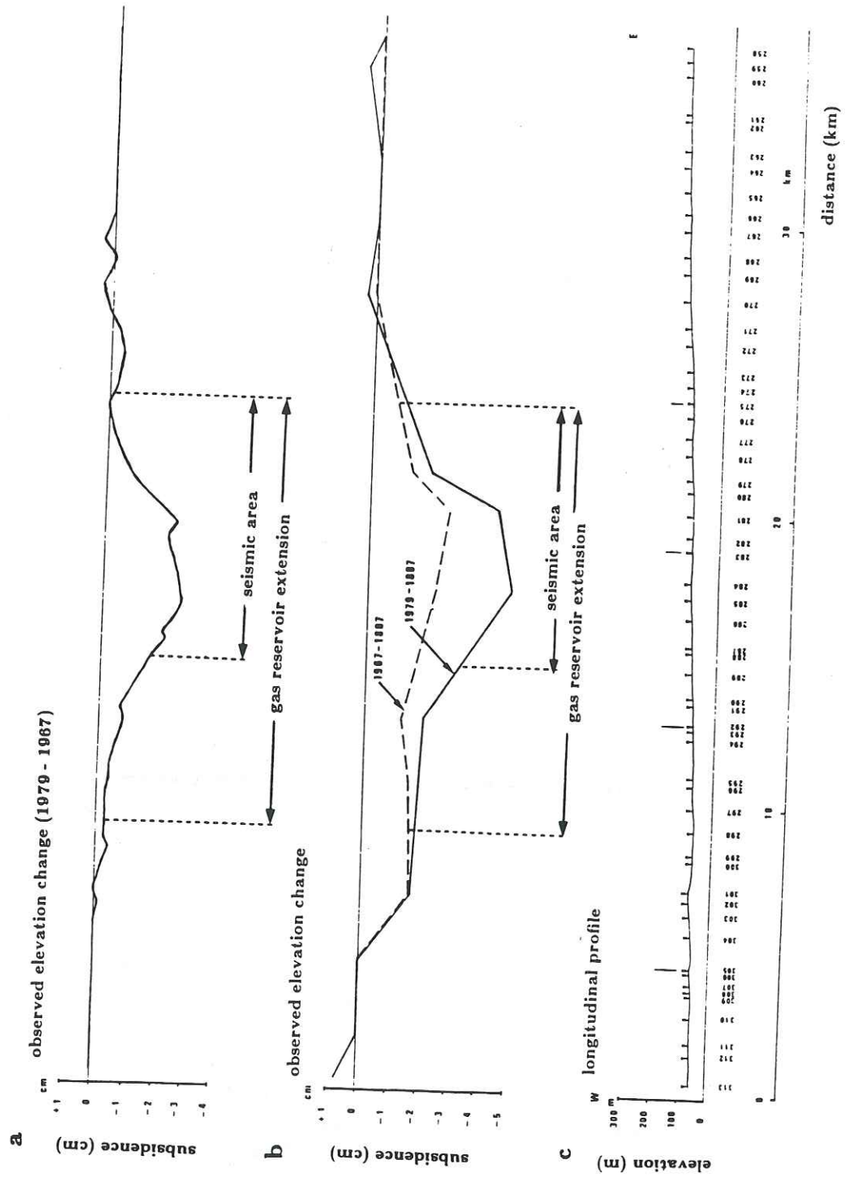

Table 1

Mechanical Properties of the Lithological Layers

	Specimen No.	Depth km	Strength MPa	Young's modulus 10^3 MPa	Poisson's ratio
Calcareous reef					
	113.3.31	1.00	158	54	0.25
	106.8.14	2.60	129	64	0.32
	106.8.16	2.60	136	63	0.32
	Average		141	60	0.30
Marls at same level but laterally displaced					
	106.7.47	2.40	45	35	0.24
	106.7.48	2.40	52	30	0.30
	Average		49	33	0.27
Marls (below the reef)					
	113.5.33	2.70	93	44	0.4
	143.1.4	2.90	64	—	—
	104.23.41	3.30	43	—	—
	106.13.1	3.30	95	—	—
	102.16.3	3.63	62	22	0.25
	Average		71	33	0.33
Reservoir					
	Average	4.0	142 (11)	54 (8)	0.25 (6)

According to the leveling profile, the eastern calcareous seismic deformation and the western aseismic marly deformation cannot be distinguished. These results suggest that the seismic energy is released preferentially in the stronger calcareous reef because the higher material strength can store more strain energy before failure for a constant strain than the marly formations.

Discussion: Global Behaviour of the Structure

The kinematic fracture process deduced from seismic data is not correlated with lithology. No particular response of an individual level can be isolated using focal mechanism techniques (GRASSO *et al.*, 1985). In terms of fracture geometries, the

Figure 9

Subsidence profiles. Vertical displacements are in cm. (a) Observed elevation changes between 1967 and 1979. 55 measurements points are used. (b) Comparison between the 3 observed profiles. The dotted line is the observed elevation change between 1887 and 1967. The continuous line is the observed elevation change between 1887 and 1979. Sixteen measurement points are allowable. Lateral extension of the seismic activity and gas reservoir, are reported with vertical marks. (c) Longitudinal profile of the measurement line with the benchmark used in 1967 and 1979 measurements. The location of the profile is given on the Figure 4 by *BB'* line.

response to gas reservoir depletion appears to be that of the whole structure. Using the composite focal mechanism technique, the complex organisation of the fault planes is consistent with the block displacement model presented by FEIGNIER and GRASSO (this issue). Laterally, normal faulting on the western part of this block and reversed faulting on the eastern part, indicate brittle strain responses. Reverse faults occur on the south and north flank. Diffuse seismicity on the north flank, associated with a nonprefractured medium, gives fault planes consistent with layer over layer slips, i.e, across stratigraphic discontinuities. The lower Aptian marly level and the upper Aptian calcareous horizon form the most active geological interface. The reversed faulting observed for these layer over layer slips implies a vertical gradient for the horizontal strain boundary conditions (Figure 12). The complex organization of these fault planes is coherent with the restoring of the dome structure. This differential restoring model of the dome structure in the N30° direction emphasizes the structural deformation in the direction perpendicular to the anticline axes. This model of the whole structure fits with observed reservoir strains. Assuming that the values given in Table 1 are valid for large-scale, slow deformations, we find Young's modulus for the gas reservoir rock to be 54,000 MPa, and a Poisson's ratio for these same rocks to be 0.25, and we directly obtain a bulk modulus (incompressibility) of 36,000 MPa. If we assume, now, that the reservoir is compressed equally in all directions in response to the increase in effective pressure (confining pressure minus pore-fluid pressure) of 45 MPa, the reservoir-pressure drop over 20 years, we will find that the change in vertical thickness is 0.04%. Using the effective thickness of the gas reservoir of 250 m, we find a change in thickness of 0.10 m. It is likely that the lateral strain is less than the vertical strain (one could easily work out a reasonable yet simple model), so this compression in a vertical direction is probably a minimum value. It is clear from the releveling surveys reported in Figure 9 that a considerable amount of this compression is supported by the elastic deformation in the overlying rocks, but the seismicity also clearly indicates that there is considerable brittle failure of the rocks as well. The absence of seismicity in the presence of deformation (western part of the gas field) does not necessarily imply ductile deformation. It can imply elastic deformation or aseismic slip as well. There is every reason to suspect that all mechanisms are active in this area and the seismicity represents a certain component of the deformation in the regions where the rocks are sufficiently brittle.

The *P*-axis directions for the focal mechanisms during the 1976–1979 period, (FEIGNIER and GRASSO, this issue) (Figure 10) indicate no preferred orientation. This suggests that either the stress field is extremely heterogeneous or that *P*-axes are controlled by the orientation of reactivated faults. Alternatively, the *P*-axis directions can also be defined in Figure 10 as a roughly radial orientation towards the gas reservoir location. A difference of 10° to 20° between the calculated *P*-axis direction and the real maximum horizontal stress orientation is inherent to this approach (SCHEIDEGER, 1964; CÉLÉRIER, 1988). This error margin is due to the

difference between double-couple mechanisms which place the *P*-axis at 45° of the fault plane and old fractures which can be reactivated by various *P*-axis directions. Accordingly, we infer here a radial symmetry of the stress field components around the gas reservoir. Furthermore, the NE-SW cross-section and map (Figures 11 and 10a) show the dip patterns of these *P*-axes. The dip of the *P*-axis is linked to the fracture locations relative to the dome structure of the gas field. Maximum dip values (the symbol scaling of the map decreases as a function of the dip value) are associated with events near the top of the dome.

This stress interpretation is enhanced by the theory of reservoir deformation where direction of principal stresses are orthogonal and tangent to the separation surface (e.g., ANDERSON, 1936; FUNG, 1965; JAEGER, 1969; PIPER and GIBSON,

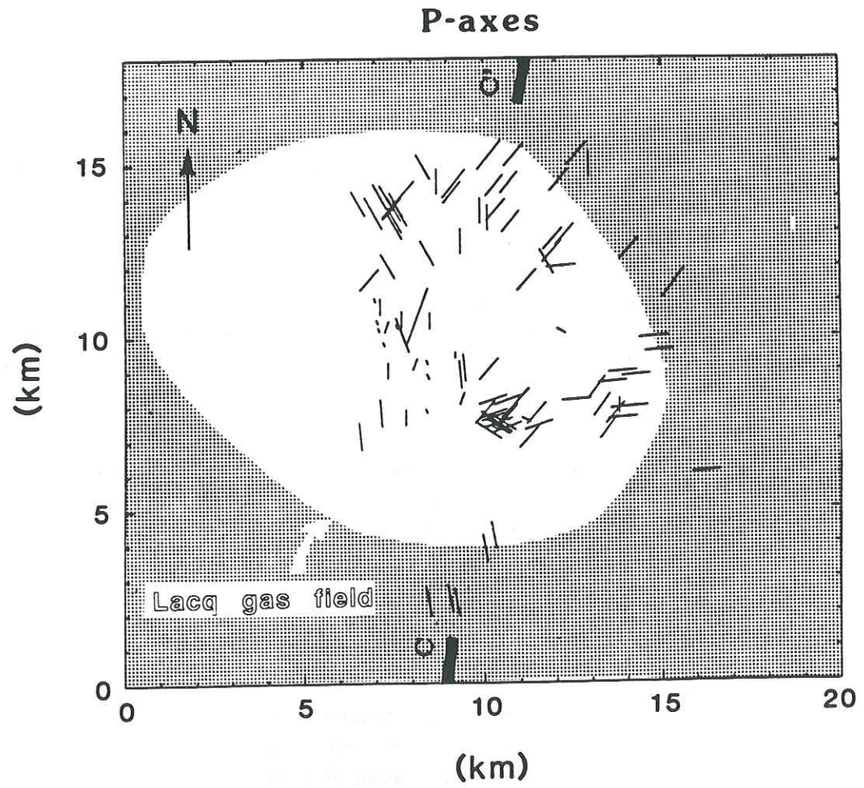

Figure 10a
P-axis map. *P*-axis orientations are reported for each event, but because of composite mechanism use, several events have the same azimuth value. Symbol scaling of the *P*-axis orientation decreases as a function of the *P*-axis dip value.

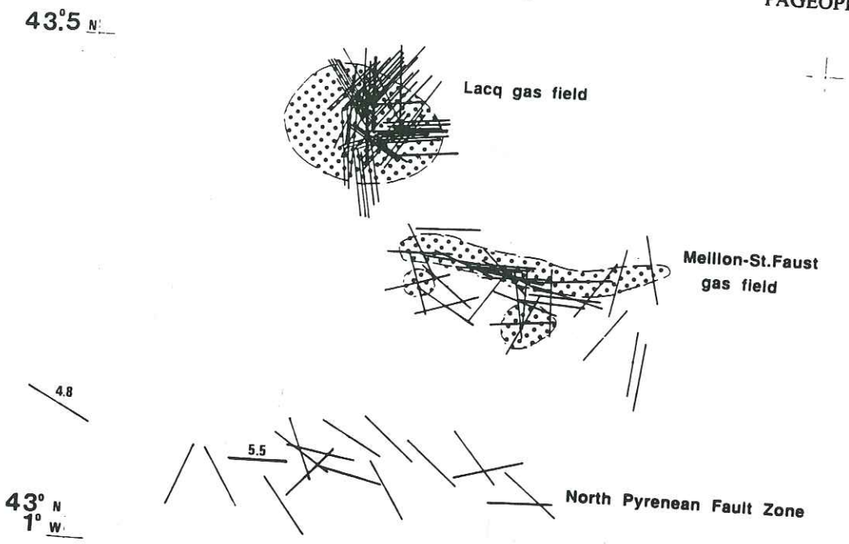

Figure 10b

Regional $S_{H\,max}$ orientations, 1976–1985. This map is built with three independent data set: A, northern area, composite focal mechanism for earthquakes induced by gas extraction, $1.5 < M_L < 4.2$, depth ranging from 0 to 6 km (this study). B, central area, borehole breakouts between 4 km and 5 km in a neighbouring gas field (after GUÉNOT, 1987). C, south area, composite and individual ($M_L > 4.8$) focal mechanism for natural Pyrenean earthquakes, $1.5 < M_L < 5.5$, depth ranging from 0 to 20 km (after, GAGNEPAIN-BEYNEIX, 1987). Lateral extension for gas reservoirs are stippled.

1972). Recent strain measurements on similar active hydrocarbon fields exhibit a radially oriented deformation towards the dome structure of producing reservoirs (TEUFEL, 1989). Such a strain and stress pattern is in accordance with the strain and stress images deduced from the theoretical poro-elastic model of SEGALL (1989), when analysing stresses and strains induced by fluid extraction. At this time we notice that this stress field could characterize the initial state of stress of a dome structure as reported by several authors (e.g., BRADLEY, 1978; MAURY and SAUZAY, 1987) that recognized, using borehole breakout analysis that the major horizontal stress was oriented radially with respect to salt domes.

Because the orientation of induced P-axes are heterogeneous but in 3D oriented towards the gas reservoir (location of normal and reversed faulting in a few km^3 volume) there are four possible explanations for such a pattern. The first possibility consists of a large induced stress relative to the regional tectonic stresses. This assumption implies a scale order of induced stresses greater than the hundred of

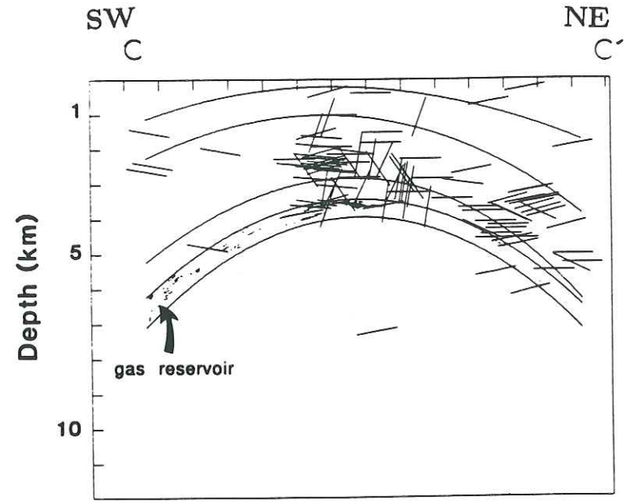

Figure 11

Projection of the hypocentres on a NE-SW vertical cross-section. Small bars are the projected of the P-axis orientation deduced from the focal mechanism study. The main entities of the structure are reported using curved lines.

MPa order of the initial stress tensor ($|Sv| \simeq 100$ MPa at 3 km depth). These values disagree with the numerical results of the poro-elastic model developed by SEGALL (1985, 1989). For this case study, comparison of our field characteristics with those of the Coalinga field, suggests an induced stress of about 1 MPa (SEGALL, personal communication, 1989). Alternatively, how a nondeviatoric stress tensor, which is the expected state of stress in the absence of applied forces (MCGARR, 1988) could be sufficiently destabilized by perturbations transmitted by the reservoir depletion to attain critical deviatoric stresses? Clearly this second possibility is also unrealistic.

In our case study a previous seismically quiescent area has been brought to activity by the destabilizing stress and strain changes induced by the gas depletion.

Attempts to explain seismic events on the basis of calculated induced stresses must admit both an initial steady state orientation of principal stresses close to the induced one (third possibility), and an initial near-critical stress difference (ROELOFFS, 1988). The small induced perturbations alone cannot cause slips even on preexisting discontinuities of this case study. But similarly small perturbations have triggered numerous small earthquakes in cases of reservoirs with induced seismicity related to a water height variation of only a few meters (SIMPSON, 1986). Also such a situation is described in the study of NICHOLSON *et al.* (1988), for earthquakes triggered by well activity.

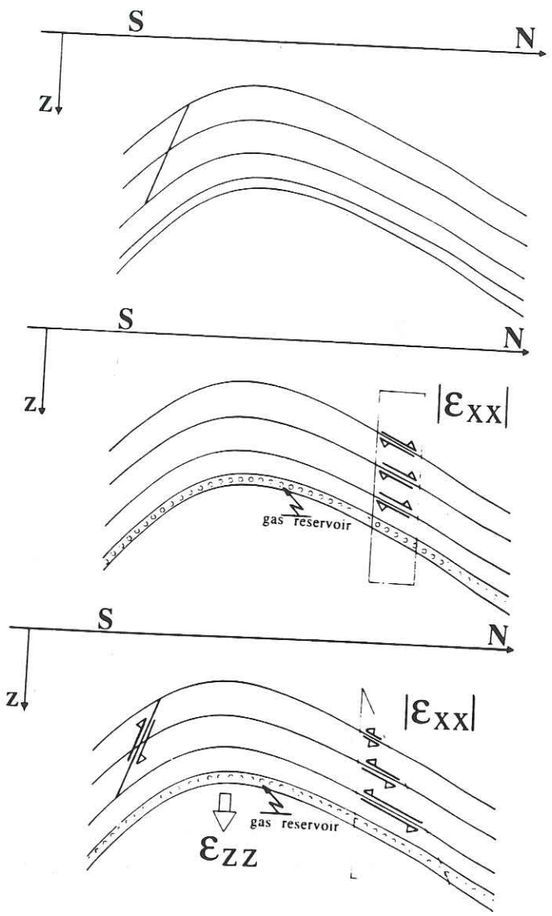

Figure 12
Schematic restoring model for the dome structure of the gas field. This model fits the observed displacements of the diffuse seismicity on the north flank of the field. This section is a supposed N30° vertical cross-section. (a) Initial regional steady state. (b) Horizontal homogeneous restoring model would imply normal movements on the interfaces. It disagrees with focal mechanisms. (c) Differential horizontal strain in N30° vertical plane restoring model is needed to explain the observed reverse layer over layer slips.

Because the inferred radially organised orientation of the initial stress field is characteristic of the structural effect of the dome geometry, the task of determining whether this structure, submitted to a lithostatic load and an initial relative pressured gas (Figure 2) can generate a near-critical stress field, or whether a horizontal loading is needed at the boundaries of the structure (i.e., horizontal

tectonic background), necessitates stress measurements which would monitor the temporal evolution of such a geological structure triggered by a fast process. The fourth possibility involves the idea that the *P*-axes, are controlled by weak faults and preexisting discontinuities drive their orientations. The two first possibilities seem unlikely because the expected values induced for the stress are too large. Both the third and fourth possibilities emphasise the importance of the structural effect in the understanding of strains and stresses at low depth.

Conclusion

The various observations and analyses discussed here allow us to draw a few definite conclusions:

(1)—Seismic zones and aseismic areas are correlated with strong lithologic changes. These lithologic changes were defined using data from more than thirty deep boreholes (up to 6 km in depth) in a 10 km × 10 km area. This correlation of hypocenters and lithology is either lateral (West-East) or vertical. Seismic areas coincide with calcareous, water saturated and prefractured media, with a brittle matrix behaviour. Aseismic areas involve marly media which have ductile behaviour in the pressure and temperature field conditions reported by GRASSO *et al.* (1985), and by FABRE *et al.* (1989). Here, a ratio of two is found between the elastic modulus of the seismic rock matrix and that of the aseismic rock matrix. The contrast in strength is at least as great, if not greater. This suggests that the rheological behaviour of the dome structure, seismic or aseismic, is controlled by mechanical properties of rock matrix.

(2)—Repeated measured surface deformations involve the entire structure. In contrast, the seismicity exhibits an asymmetric distribution relative to the extension of the gas reservoir. Because homogeneous gas production parameters are important in triggering the deformation of this dome structure (GRASSO and WITTLINGER, 1990), the seismicity is a consequence of variations in the rheological behaviour of the dome. Thereafter, strong asymmetric seismicity (with seismic moment ranging from 10^{17} to 10^{20} dyne.cm (FEIGNIER, 1989)), with regard to the symmetric deformation curve, cannot explain the deformation. Moreover for the first 250 bars depletion (10 years of production) the structure showed purely aseismic behaviour.

(3)—The heterogeneous stress pattern inferred from *P*-axes of induced earthquakes disagrees with the tectonic regional stress field. Such nonparallel trajectories for the principal stresses have been associated with perturbations of shallow structures, due to localized processes (e.g., volcanic structure or geothermal area, ODE, 1957; MULLER and POLLARD, 1977; FOULGER, 1988). Here, they could be driven by the deformation induced by gas extraction. It agrees with a heterogeneous stress pattern deduced both from the analysis of numerous breakouts in a neigh-

bouring active gas field and from another gas field deformation (e.g., TEUFEL, 1989). These observations, radial patterns towards the center of the gas reservoir, if confirmed by the more constrained focal mechanism study, cannot be quantitatively explained by the small stress change (maximum 1 MPa) deduced from numerical poro-elastic modeling for a homogeneous medium (SEGALL, 1989). Although such small stress changes are apparently sufficient to trigger the seismic activity, they cannot control stress trajectories in an active tectonic context, unless the regional deviatoric stress is exceedingly low.

Acknowledgements

The authors gratefully thank the Société Nationale Elf-Aquitaine for providing all the characteristics of the gas field which were essential for this work. We would also like to thank M. Bouchon, P. Segall and P. Vialon who reviewed the initial manuscript. Constructive comments and reviews by Art McGarr and Wayne Pennington greatly improved the final paper. This study was supported by the Société Nationale Elf-Aquitaine under contract 915/9/549.

REFERENCES

ANDERSON, E. M. (1936), Proc. Roy. Soc. Eding. *56*, 128.

BARTHE, A., and REVERDY, X. (1958), *Le recif de Lacq*, R.G. 325, a report to the SNEA(P) company.

BRADLEY, W. B. (1978), *Borehole Failure near Salt Domes*, SPE 7503 presented at the 53rd Annual Fall meeting of the SPE, Houston.

CÉLÉRIER, B. (1988), *How Much Does Slip on a Reactivated Fault Plane Constrain the Stress Tensor*, Tectonics *7*, 4182–4198.

DAIGNIÈRES, M., GALLART, J., BANDA, E., and HIRN, A. (1982), *Implications of the Seismic Structure for Orogenic Evolution of the Pyrenean Range*, Earth and Planet. Sci. Lett. *57*, 88–100.

FABRE, D., GRASSO, J. R., and ORENGO, Y. (1989), *Analysis of the Failure Behaviour of Deep Rock Core Samples during Triaxial Testing: Application to Field Conditions*, submitted to Int. Journ. Rocks. Mech. and Min. Sci. and Geomech. Abs.

FEIGNIER, B., and GRASSO, J. R. (1990), *Seismicity and Deformation Induced by Gas Production I. Correlation of Focal Mechanisms and Dome Structure*, Pure Appl. Geophys. *134*, 405–426.

FEIGNIER, B. (1989), *Comportement à la source de séismes induits: caractérisation géomécanique*, Ph.D. Thesis, University of Grenoble.

FOULGER, G. R., Hengill triple junction, SW Iceland (1988), *Tectonic Structure and the Spatial and Temporal Distribution of Local Earthquakes*, J. Geophys. Res. *93*, 13493–13506.

FUNG, Y. C., *Foundations of Solid Mechanics* (Prentice Hall, New Jersey 1965).

GAGNEPAIN-BEYNEIX, J., HAESSLER, and H., MODIANO, T. (1982), *The Pyrenean Earthquake of February 29, 1980: An Example of Complex Faulting*, Tectonophysics *85*, 273–290.

GAGNEPAIN-BEYNEIX, J. (1987), *Etude expérimentale des tremblements de terre, Exemple de la région d'Arette (France)*, Thèse d'Université, Université de Paris, 210 pp.

GALLART, J., DAIGNIÈRES, M., GAGNEPAIN-BEYNEIX, J., and HIRN, A. (1985), *Relationship Between Deep Structure and Seismicity in the Western Pyrenees*, Annales Geophysicae *3*, 239–248.

GRASSO, J. R., VIALON, P., and FABRE, D. (1985), *Etude géomécanique de la sismicité dans la région de Lacq*, Report to the SNEA(P) Company, 400 pp.

GRASSO, J. R., and WITTLINGER, G. (1990), *Ten Years of Seismic Monitoring over a Gas Field Area*, Bull. Seismol. Soc. Am. *80*, 450–473.

GRATIER, J. P. (1984), *La déformation des roches par dissolution-cristallisation*, Thèse de Doctorat d'Etat. U, de Grenoble, 316 p.

GUÉNOT, A., *Borehole breakouts and stress field.* In *Proc. Int. Workshop on Forced Fluid Flow Through Strong Fractured Rock Masses*, 1 (CNRS, Paris 1987) pp. 219–233.

HOANG Van, T., and ROULAND, D. (1971), *Mécanisme au foyer du séisme d'Arette (P.A.)*, C.R.A.S. *272*, 3249–3251.

JAEGER, J. C., *Elasticity, Fracture and Flow with Engineering and Geological Applications*, (Science paperbacks, Methuen's Monographs on Physical Subjects, 1969).

MAURY, V., and SAUZAY, J. M. (1987), *Borehole Instability: Case History Rock Mechanics Approach and Results*, Proc. SPE/IADC Conf. Paper; SPE/IACC 16051, New Orleans.

MCGARR, A. (1988), *On the State of Stress in Absence of Applied Tectonic Forces*, J. Geophys. Res. *93*, 13609–13617.

MCGARR, A., SPOTTISWOODE, M., and GAY, N. C. (1975), *Relationship of Mine Tremors to Induced Stresses and to Rock Properties in the Focal Region*, Bull. Seismol. Soc. Am. *65*(4), 981–993.

MCKENZIE, D. (1972), *Active Tectonics of the Mediterranean Region*, Geophys. J. R. Astr. Soc. *30*, 109–185.

MEREU, R. F., BRUNET, J., MORRISSEY, K., PRICE, B., and YAPP, A. (1986), *A Study of the Microearthquakes of the Globes Oil Field Area of Southwestern Ontario*, Bull. Seismol. Soc. Am. *76*, 1215–1223.

MODIANO, T. (1980), *Sismotectonique des Pyrénées Occidentales. Etude détaillée du contenu spectral des ondes de volume dans la région focale*, Thèse 3ème cycle, Grenoble.

MULLER, O. H., and POLLARD, D. D. (1977), *The Stress State near Spanish Peaks, Colorado, Determined from a Dyke Pattern*, Pure Appl. Geophys. *115*, 69–86.

NICHOLSON, C., ROELOFFS, E., and WESSON, R. L. (1988), *The Northeastern Ohio Earthquake of 31 January 1986: Was It Induced?*, Bull Seismol. Soc. Am. *78*, 188–217.

ODE, H. (1957), *Mechanical Analysis of the Dyke Pattern of the Spanish Peaks Area, Colorado*, Bull. Geol. Soc. Am. *68*, 567–576.

PENNINGTON, D. W., DAVIS, D. D., CARLSON, S. M., DUPREE, J., and EWING, T. E. (1986), *The Evolution of Seismic Barriers and Asperities Caused by the Depressuring of Fault Planes in Oil and Gas Fields of South Texas*, Bull. Seismol. Soc. Am. *76*, 939–948.

PIPER, J. D. A., and GIBSON, I. L. (1972), *Stress Control of Processes at Extensional Plate Margins*, Nature *238*, 83–86.

PHILIP, H. (1983), *La tectonique actuelle et récente dans le domaine méditerranéen et ses bordures. Ses relations avec la sismicité*, Thèse de Doctorat d'Etat, U. de Montpellier, 240 pp.

ROELOFFS, E. A. (1988), *Fault Stability Changes Induced Beneath a Reservoir with a Cyclic Variation in Water Level*, J. Geophys. Res. *93*, 2107–2124.

ROTHE, G. H., and LUI, C. Y. (1983), *Possibility of Induced Seismicity in the Vicinity of the Sleepy Hollow Oil Field, Southwestern Nebraska*, Bull. Seismol. Soc. Am. *73*, 1357–1367.

RYAN, M. P., BLEVINS, J. Y. K., OKAMURA, A. T., and KOYANAGI, R. (1983), *Magma Reservoir Subsidence Mechanics: Theoretical Summary and Application to Kileaua Volcano, Hawaii*, J. Geophys. Res. *88*, 4147–4181.

SCHEIDEGGER, A. E. (1964), *The Tectonic Stress and Tectonic Motion Direction in Europe and Western Asia as Calculated form Earthquake Fault Plane Solutions*, Bull. Seismol. Soc. Am. *54*, 1519–1528.

SEGALL, P. (1985), *Stress and Subsidence Resulting from Subsurface Fluid Withdrawal in the Epicentral Region of 1983 Coalinga Earthquake*, J. Geophys. Res. *90*, 9801–9816.

SEGALL, P. (1989), *Earthquake Triggered by Fluid Extraction*, Geology *17*, 942–946.

SIMPSON, D. W. (1986), *Triggered Earthquakes*, Ann. Rev. Earth. Planet Sci. *14*, 21–42.

TAPPONNIER, P. (1977), *Evolution tectonique du système alpin en Méditerranée: poinçonnement et écrasement rigide-plastique*, Bull. Soc. Geol. Fr. *58*, 399–4165.

TEUFEL, L. (1989), *On Recent in situ Stress Measurements in EKOFISK Gas Field*, Proc. Int. Symp., Rock at Great Depth, PAU, 1989, 08, 28–31.

WETMILLER, R. J. (1986), *Earthquakes near Rocky Mountain House, Alberta, and their Relationship to Gas Production Facilities*, Can. J. Earth. Sci. *23*, 172–181.
WITTLINGER, G. (1980), *Etude de la sismicité en champ proche par un réseau sismologique à faible ouverture: application au Frioul (Italie) et au gisement de Lacq (France)*, Thèse de Doctorat d'Etat, U. de Strasbourg, 261 pp.
YERKES, R. F., and CASTLE, R. O. (1976), *Seismicity and Faulting Attributable to Fluid Extraction*, Eng. Geol. *10*, 151–167.

(Received January 12, 1989, revised December 26, 1989, accepted February 4, 1990)

23

PROPRIÉTÉS MÉCANIQUES DES ROCHES À GRANDES PROFONDEURS ET ESSAIS EN LABORATOIRES.

PAGEOPH, Vol. 137, No. 3 (1991)

0033–4553/91/030201–19$1.50 + 0.20/0

Mechanical Behaviour of Deep Rock Core Samples from a Seismically Active Gas Field

D. FABRE,[1] J.-R. GRASSO[1] and Y. ORENGO[1]

Abstract—This study concerns the laboratory testing of core samples from massive sedimentary rocks from an oil and gas field. The depth of extraction of the samples analysed varies between 1000 and 5000 metres. In all, 65 tests were performed, most of which included systematic measurement of acoustic activity during loading. The aim of the testing was to determine which types of fracture could occur in the rock matrix under field-stress conditions by examining in particular the relationship between confining pressure and the transition from brittle to ductile behaviour. The results of the laboratory tests are used to predict the occurrence of seismic activity resulting from the depletion of the gas reservoir which has been monitored during the last twenty years.

Key words: Gas field, induced seismicity, rock mechanics, acoustic emission, brittle-ductile transition, sedimentary rocks, porosity, triaxial test.

Introduction

Conventional laboratory mechanical tests are rarely performed on deep rock core samples, not only because of the high cost of recovery but also because of the effects of stress relief and environmental changes. Such changes may lead to irreversible modification of the rock properties, by inducing fractures, by modifying the system of micro-cracking or by allowing chemical transformations (hydration, oxidation) to take place. Consequently, there is little hope of being able to perform representative tests on all types of rock encountered in oil exploration boreholes (case of clays, for example). However, for certain low-porosity or well-cemented rocks, it should be possible to obtain representative mechanical parameters (Young's modulus of deformability, yield stress under confining stress, etc.) by replicating, at least in part, the field conditions.

This study concerns the examination of massive sedimentary rock core samples (limestones, dolomites, calcareous marls, anhydrite layers) from the Lacq oil and gas field. The depth of extraction of the samples analysed varies between 1000 and 5000 metres, with more than 80% coming from five distinct geological levels situated at depths of between 2500 and 4000 metres.

[1] IRIGM, BP 53X, 38041 Grenoble Cedex, France.

The Lacq field is located in an anticline on the northern side of the Pyrenees in France. Production began in 1950 for the oil and in 1959 for the gas.

On November 24th, 1969 an earthquake of magnitude $M = 4.1$ was recorded in the area. It was later attributed to movement resulting from extraction. In the following twenty years other seismic events with local magnitude ranging from 1 to 4.2 have been located and observed in detail for more than ten years using high-accuracy geophysical methods (GRASSO and WITTLINGER, 1990). In addition, a few centimetres' subsidence have been observed on the surface above the hydrocarbon field (GRASSO and FEIGNIER, 1989).

The aim of the mechanics study carried out in the laboratory has been to determine the mechanical behaviour of the rock formations with a view to preparing a model of the field. In order to do this, it was necessary to simulate possible failure mechanisms under *in situ* stress conditions.

Collectively 65 samples of fairly massive rock were analysed. The samples were 40 mm diameter and 80 mm long. Most of them were cut from old cores obtained during the exploration of the field (1960–72). For one of the geological facies (the massive micaceous marls) a new core was drilled especially for this study in 1981.

All samples were saturated with water before testing. It has been assumed that the mechanical behaviour of these massive rocks has not been substantially modified by the effects of coring and subsequent storage.

Apart from traditional compression tests (21 uniaxial and 39 triaxial tests), 5 hydraulic fracture tests were also performed in order to investigate the possibility of fracture from a trapped, overcompressed fluid lens. Most of the tests included systematic measurement of acoustic activity during loading. The brittle-ductile transition was examined for the main rock facies analysed as a function of confined pressure. The implications of the results to the development of large-scale rupture occurring in the field during gas extraction are discussed.

1. Geotechnical Identification of the Rocks Forming the Geological Structure

Figure 1 shows a vertical cross section through the reservoir and overlying strata. The structure is a dome covering some 100 km^2 in the horizontal plane. The gas reserves are located in limestones and dolomites at depths of between 3200 and 4800 metres in a series of highly contrasted geological formations (Upper Jurassic to Lower Cretaceous). Since 1974 some 800 seismic events of magnitude $1 < M_l < 4.2$, have occurred in 10 years of precise observation, mainly above the reservoir (GRASSO and FEIGNIER, 1989), in a formation of micaceous marls (15% of the events) and reef limestones (60%). A further 10% of the events have been traced to the reservoir itself and 5% in deeper levels (depth > 6000 m); very little is known about the latter, since no borehole has been drilled to this depth.

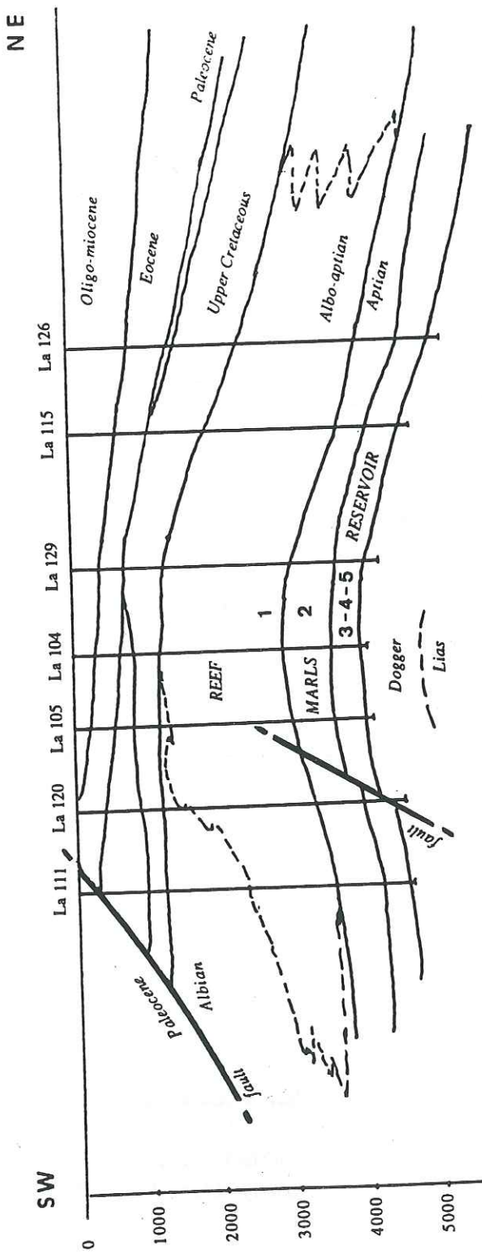

Figure 1
Cross section through the Lacq field. La 105 indicates the reference of a well. Numbers 1 to 5 indicate the location of the five geological levels tested for this study.

Some 40 wells tap the deep gas reservoir. Core samples have been obtained from a few of these and were used in the tests. They represent the main massive rock families found in the deposits.

While the two formations located immediately above the reservoir (marls and limestones) display a certain lithological homogeneity over several hundred metres' depth, the same is not true of the reservoir itself, where several facies must be distinguished, namely:

- massive limestones,
- anhydrite layers,
- schistous clay,
- dolomites containing varying degrees of sandstone.

For the reasons given previously, it was not possible to obtain any representative sample of the schistous clay layers.

Table 1 summarises the main geotechnical properties of the five units studied, based on the tests undertaken. The following information is given:

- the dry density, which, combined with the mineralogical features, gives an indication of the porosity of the rock;
- the wave propagation velocity of the sample, measured in the laboratory; this enables the continuity index to be defined and provides further information on the type of porosity (pore porosity, crack porosity: FOURMAINTRAUX, 1975);
- the ultimate strength σ_c obtained during a uniaxial compression test; this parameter serves as a basis for most geotechnical rock classifications:
- the Young's modulus of deformability, E, obtained from the stress-deformation curve of the compression test. The modulus ratio E/σ_c indicates the position of the rock in the standard Deere and Miller classification (DEERE, 1968). The stress-deformation curve also indicates the predominant mechanical behaviour of the rock (DAYRE *et al.*, 1978).

According to their identification parameters, the reef limestones are weakly porous (1–4%) but display significant microcracks. The feature also occurs on a large scale, as can be seen from the extensive fracturing and high overall permeability of the aquifer formed by the reef.

The micaceous marls are hardly porous ($n < 1\%$). The average mechanical strength is appreciable (70 MPa) but is generally lower than that of the overlying limestones. Given the high percentage of clay minerals (30–50%), there is considerable deformability, as can be seen from the fairly low modulus of elasticity.

There are alternating facies in the reservoir and levels with consistent lithology are generally of no more than a few dozen metres thick. The following have been encountered:

- virtually impervious limestones that are very brittle when subjected to uniaxial compression and extremely strong ($\sigma_c > 200$ MPa);

Table 1

Geotechnical identification of deep rocks studied (the numbers between brackets indicate the number of measurements made)

Name	Depth (m)	Thickness (m)	Dry density	*P*-wave velocity (m/s)	σ_c (compression) (MPa)	*E* (modulus) (GPa)
1: Reef limestones	1100–3200	1500–2300	2.58–2.64 (22)	4200–5400 (26)	45 158 (5)	30 64 (5)
2: Micaceous marls	2600–4100	600–900	2.65–2.70 (11)	300–5200 (6)	43 95 (5)	22 44 (5)
3: Massive limestones	3200	three levels: 30–100	2.69–2.73 (17)	5400–6200 (17)	89 213 (4)	55 65 (3)
4: Anhydrite levels	to	several levels: 1–100	2.78–2.94 (6)	5100–5900 (6)	98 (1)	50 (1)
5: Dolomites containing sandstone	4900	150–300	2.60–2.83 (11)	4100–6200 (11)	64–189 (5)	45 69 (5)

- a dolomite unit with extremely variable porosity (0–20%), in which fairly deformable beds containing sandstone alternate with extremely massive, strong levels;
- a few clay layers several metres thick that were not sampled, making the reservoir a fairly heterogeneous system in which the relatively thin individual layers display marked differences in mechanical behaviour.

2. Study of Brittle-ductile Transition

The brittle-ductile transition, according to classical definition (PATERSON, 1978), was examined by means of conventional triaxial compression tests. The confining pressure was varied from 10 to 100 MPa, which corresponds approximately to the lithostatic pressure occurring to depths of 4000 metres.

In the reef limestones (Figure 2), the transition between brittle behaviour (with axial fracturing and significant loss of strength after peak) and ductile behaviour (with inclined cracking and significant residual strength) occurs between $\sigma_3 = 20$ MPa and $\sigma_3 = 50$ MPa.

The curves obtained during triaxial tests on the marls (Figure 3) show that the material is more deformable. The sample tested at $\sigma_3 = 20$ MPa, already showed some inclined cracking at failure. This pressure is therefore within the transitional

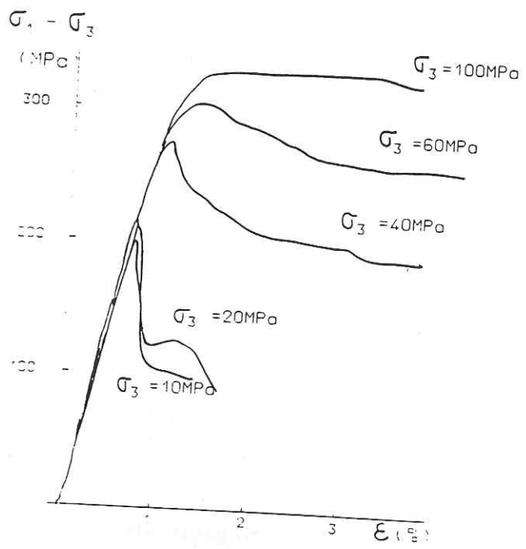

Figure 2
Reef limestones (depth 2660 metres): stress-deformation curves for triaxial tests with variable σ_3.

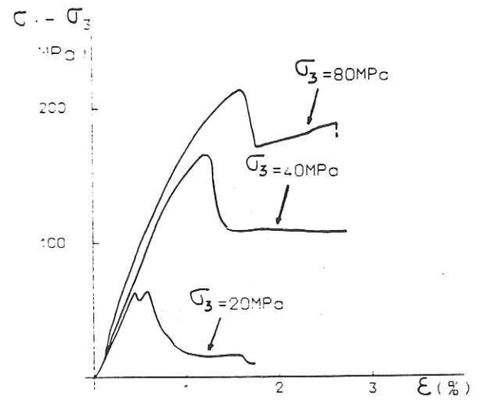

Figure 3
Micaceous marls (depth 2950 metres): stress-deformation curves for triaxial tests with variable σ_3.

brittle-ductile range. It is estimated that the transition for this formation must be between $\sigma_3 = 10$ MPa and $\sigma_3 = 30$ MPa.

In both cases, the transition occurred at a confining pressure equivalent to about a quarter of the uniaxial compressive strength.

Figure 4 shows the results of tests on samples from the massive limestone levels (depth = 3660 m) within the reservoir. The samples failed in a brittle mode at confining pressure up to $\sigma_3 = 90$ MPa.

Other samples from a similar depth of slightly less massive limestone (for which the curves are not shown) display a transition between $\sigma_3 = 60$ MPa and $\sigma_3 = 80$ MPa. The anhydrite layer exhibits a ductile behaviour at failure under lateral stresses of $\sigma_3 = 20$ MPa, whereas in the case of the sandstone dolomites the transition occurs between 40 MPa to 70 MPa, depending on the porosity.

Generally speaking, it might be concluded that failure is of the distinctly brittle type in all the rocks studied, whenever the confining pressure is less than a quarter of the unconfined compressive strength σ_c, and of distinctly ductile type when the confining pressure exceeds $\sigma_c/2$.

3. Compression Tests Including Measurement of Acoustic Activity During Loading

In order to study the relationship between mode of failure and microseismic activity during a compression test, a small piezo-electric acoustic sensor (Dunegan S 1000 BM, with wide pass-band of 200 kHz–2.5 MHz at +10 dB) was used. The sensor was linked up to a Dunegan S 3000 specialised measuring system which filters the acoustic emissions (filter pass-band 100 kHz–2 MHz), amplifies them

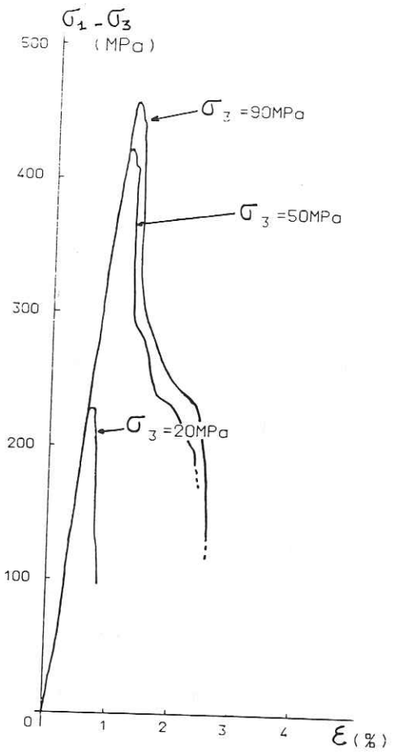

Figure 4
Massive reservoir limestones (depth 3660 metres): stress-deformation curves for triaxial tests with variable σ_3.

(gain of 40–100 dB) and then processes them in a digital form for later manipulation (spectrum analysis, deconvolution, etc.).

A simple form of measurement of "acoustic activity" was used, which involved counting the number of times the signals exceeded a given amplitude (1 Volt for a gain of 80 dB in this study).

The first series of acoustic measurements was carried out during the uniaxial compression tests on the reservoir formations (Table 2). As mentioned above, certain layers (massive limestones and dolomites) display a very brittle type of behaviour, while in others (anhydrite or sandstone layers) the rupture is more ductile.

It is clear from the tests that the acoustic activity is a good indication of the energy involved during the creation and development of cracks, thus enabling a degree of brittleness to be quantified quite accurately. The only slightly porous

Table 2

Uniaxial compression tests including measurement of acoustic activity (reservoir rocks)

Samples	Depth	σ_c (compression) (MPa)	E (modulus) (GPa)	Acoustic activity at 50% of σ_c	Acoustic activity at 100% of σ_c
Massive limestone	3620	191	65	1550	230.000
Massive limestone	3670	89	55	3100	86.000
Massive dolomite	3505	99	19	32.000	>300.000
Massive dolomite	3526	87	45	16.500	189.000
Sandstone dolomite	4925	117	48	745	15.000

sample on which measurements were undertaken was sandstone dolomite (Table 2): here, the less brittle nature of the rupture is probably not best indicated by the ultimate strength, modulus or even shape of the stress-deformation curve but indeed by the acoustic activity values. This technique was therefore applied during a series of triaxial tests reproducing the field conditions in order to investigate the type of fracture likely to occur *in situ*. The value $\sigma_3 = 90$ MPa was adopted in the triaxial tests as an average value for the confinement stress in the area where many earthquakes were identified by seismic methods at between 3000 and 3500 metres depth.

At these depths, the rock temperature varies between 100°C and 120°C. Since this could not be reproduced with the triaxial cells used, the tests were run at ambient temperature. Studies concerning the influence of temperature on the mechanical behaviour of rocks (HOMAND-ETIENNE, 1986) show that an increase in temperature from 20°C to 120°C only affects uniaxial compressive strength (σ_c) to a slight extent (5% difference in the case of sandstones and 12% for limestones) and that the effect is only actually perceptible above 300°C. However, the effects of temperature on acoustic activity and type of fracturing could be greater and should be studied further.

Table 3 shows the results of the triaxial tests at a confining pressure of $\sigma_3 = 90$ MPa where acoustic activity was measured. In contrast to the uniaxial compression tests, where the sensor was attached to the sample, it was fixed to the piston of the triaxial test cell. The piston-rock interface significantly attenuated the signal amplitude, and this effect therefore has to be countered by an appropriate increase in gain.

Generally, failure in triaxial tests was found to be less brittle than that seen during uniaxial compression. The test curves (Figures 5, 6, 7) for three of the samples presented in Table 3 clearly indicate that certain failures in the ductile zone (Figure 5) are accompanied by only slight acoustic activity. In contrast, a distinctly brittle mode of failure such as that in Figure 6 gave rise to considerable acoustic activity as soon as the elastic limit was reached, at approximatively 85% of the

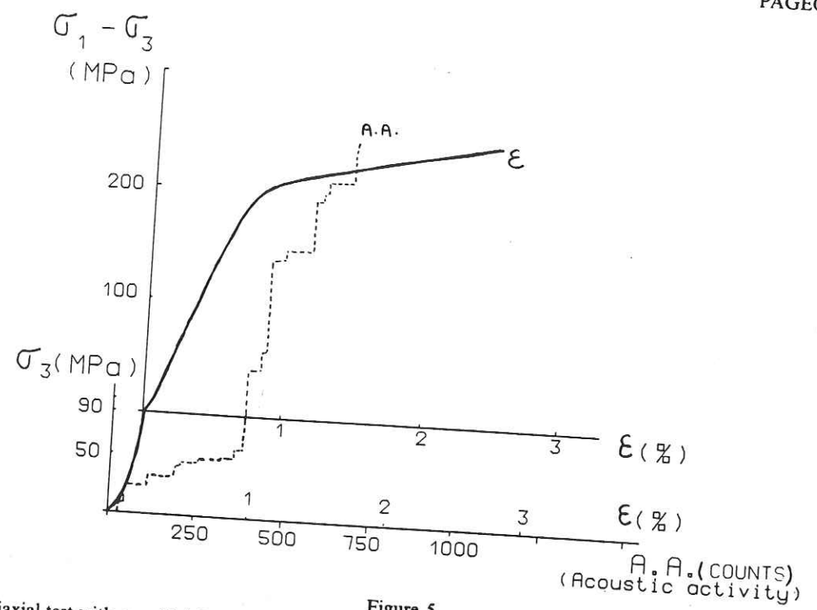

Figure 5
Triaxial test with $\sigma_3 = 90$ MPa and measurement of acoustic activity with a sample of reservoir anhydrite (3700 metres depth): example of ductile fracturing.

Table 3
Triaxial tests ($\sigma_3 = 90$ MPa), including measurement of acoustic activity (reservoir rocks)

Samples	Depth (m)	$(\sigma_1 - \sigma_3)_{max}$ (MPa)	Acoustic activity (counts) Rising to σ_3	at 50% of peak	at 100% of peak
Anhydrite level	3700	212	380	475	630
Massive limestone	3640	412	509	521	13,000
Massive dolomite	3553	515	210	2875	95,000
Sandstone dolomite	3552	417	1170	1290	1510

maximum deviatoric stress. Finally, transitional failure may still be observed, such as that in the sandstone dolomite layer shown in Figure 7. In this case, there was little noise during the elastic stage, but a significant amount of energy was released, especially after the peak deviatoric stress was reached, when a shear plane formed in the sample.

Both the triaxial tests carried out on the reservoir rocks during the brittle-ductile transition study and those including measurement of acoustic activity under the field conditions show that certain formations (such as the anhydrite levels—and

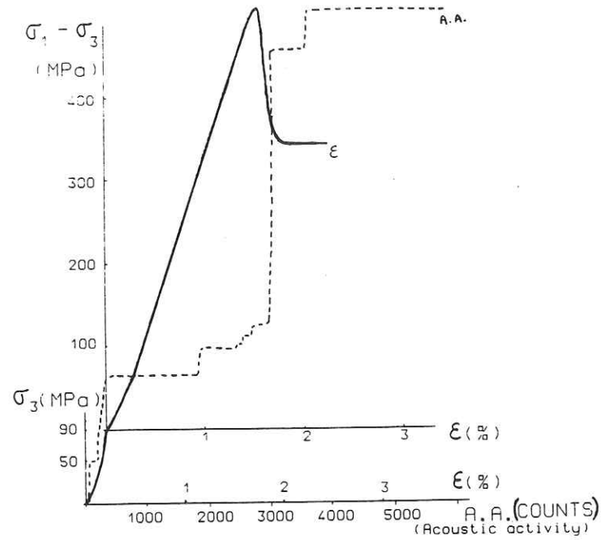

Figure 6
Triaxial test with $\sigma_3 = 90$ MPa and measurement of acoustic activity with a sample of reservoir dolomite (3553 metres depth): example of rather brittle fracturing.

this would also be true of the clay levels) can probably not give rise to fractures suddenly freeing energy in the form of microseisms. In contrast, the massive limestone and dolomite formations behave in a brittle mode under the pressure (and probably also temperature) conditions found in the reservoir. With regard to the porous levels with strong mineral matrices, such as the sandstone dolomites, the study was not sufficiently comprehensive to define in detail the type of rupture occurring in the field. The only test performed (Table 3) indicated a hybrid type of behaviour, with features of both brittle and ductile fracturing. However, with this kind of material containing interstitial fluid, it is essential to carry out tests where the interstitial pressure is also monitored.

4. Hydraulic Fracturing Tests

When the interstitial pressure distribution within the oil and gas deposits was examined, lenses of overcompressed fluid were observed; i.e., levels where the fluid pressure was distinctly higher than the hydrostatic pressure. Occasionally, the lens pressure almost equalled the lithostatic pressure (Figure 8).

Exploitation of the reserves naturally causes a drop in gas pressure within the reservoir. At Lacq, the pressure dropped by more than 50 MPa over a period of 30

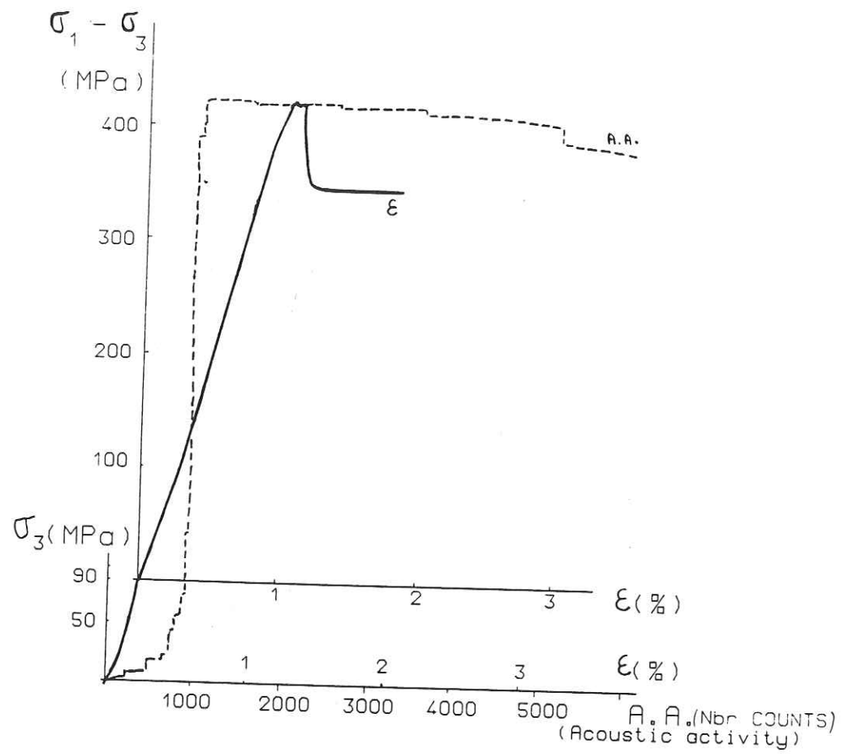

Figure 7
Triaxial test with $\sigma_3 = 90$ MPa and measurement of acoustic activity with a sample of reservoir limestone (3640 metres depth): example of transitional fracturing.

years. This results in an increase in the difference between global pore pressure in the field and local pressure in the trapped lenses (GRASSO *et al.*, 1985).

In the case studied here, gas lenses were discovered while drilling exploratory boreholes or production wells in the micaceous marls and in the clay levels of the reservoir. It therefore appeared interesting to consider the eventuality of a fracture occurring during exploitation between a trapped lens and a well drained area of the reservoir, where the pressure would be equal to the present global pore pressure.

In order to construct a model of this phenomenon, a series of five hydraulic fracturing tests was carried out with an apparatus developed in the I.R.I.G.M. laboratory (MORALES, 1981) on samples of marls and limestones, using a confining pressure of 75 or 90 MPa. The axial stress σ_1 was 100 MPa. A 10 mm diameter axial hole is drilled in samples, 75 mm in diameter and between 150 and 200 mm high. The shape of the sample is: 75 mm in diameter, 150 to 200 mm high and an axial hole, 10 mm in diameter.

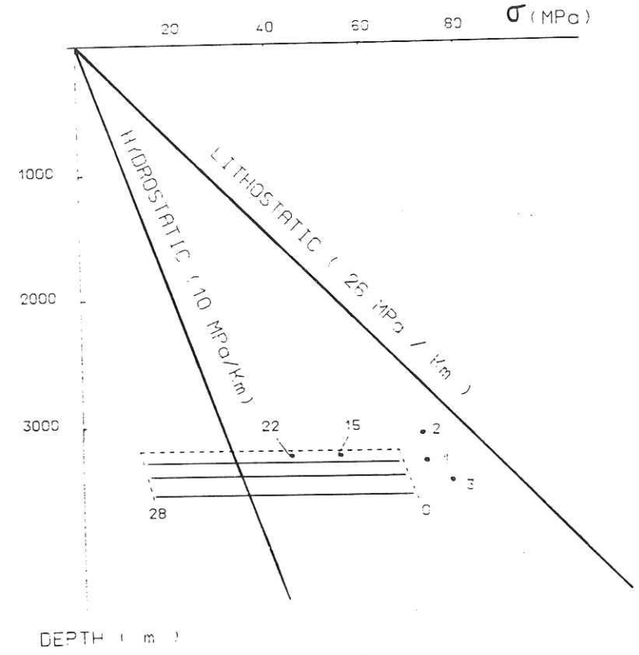

Figure 8
Changes in hydrostatic and lithostatic pressure with depth (corresponding to the top of the anticline). Reservoir depletion is indicated by the shaded area. The points correspond to pressures measured in the overcompressed fluid lenses encountered by the boreholes. The figures indicate the number of years' exploitation of the deposits (adapted from [12]).

Two small, perforated circular aluminium plates are set between the ends of the sample and the base plate and piston. These plates ensure that the central injection hole is perfectly sealed and limit the reinforcement required. The sample is surrounded with a rubber membrane and placed in a triaxial cell.

The normal test procedure is as follows:

- position the sample in the cell,
- apply a slight deviatoric stress to the piston (5–10 MPa) to maintain contact between the ends of the sample and the piston and base plate as pressure rises,
- increase the confining pressure by injecting oil into the outer circuit of the cell,
- apply the required deviatoric stress,
- increase the water pressure (pi) in the central hole until the sample breaks under the effect of hydraulic fracturing.

Throughout the tests, acoustic activity is measured using the same procedure as used in the small-diameter triaxial compression tests.

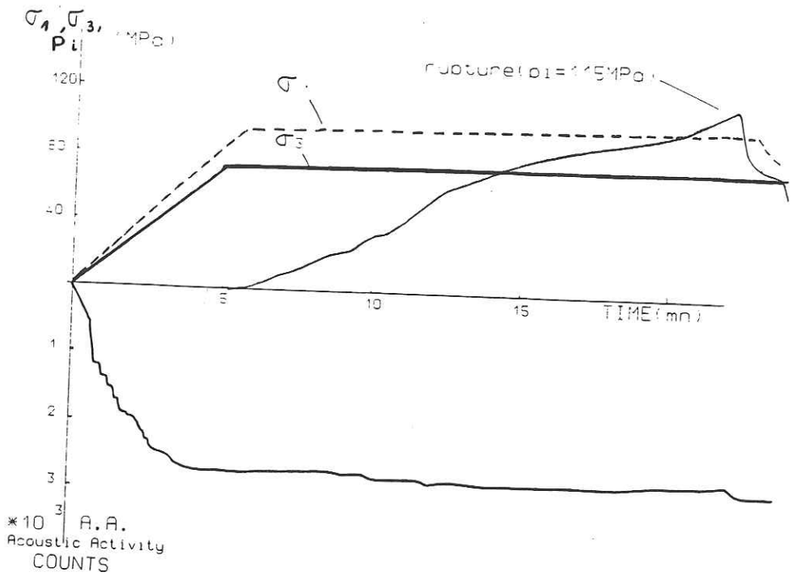

Figure 9
Hydraulic fracturing test with $\sigma_3 = 75$ MPa and $\sigma_1 = 100$ MPa on a marl sample (3220 metres depth): example of progressive fracturing with very little acoustic emission.

Figure 9 shows the results of a test carried out on a sample of the micaceous marls from a core obtained at a depth of 3320 metres. At this point the marls have fairly clayey facies, with a measured uniaxial compressive strength of 43 MPa. Monitoring of the acoustic activity indicated little energy release during cracking. During the initial pressure rise in confining and deviatoric stress, the slight but noticeable activity corresponds to compression of the sample (closure of microcracks perpendicular to σ_1, i.e., parallel to the direction of anisotropy of the rock). During injection, cracking parallel to the core axis seems to occur with even less activity, which would indicate that failure is progressive and in a ductile mode. This was not observed during the tests carried out with limestone samples. The most massive sample (Figure 10) shows a very brittle type of fracturing, with considerable acoustic activity occurring suddenly at the end of the test. This suggests sudden failure (which is usual in this type of test).

If these tests may be considered representative of the behaviour of the rocks under field conditions, it must be concluded once again that the marl level above the reservoir does not appear capable of producing new brittle fractures involving a sudden release of energy under the pressure conditions obtained in the deposits. In contrast, it may be noted that brittle failure occurs with limestone samples subjected to a pressure differential across lenses comparable to that existing in the field.

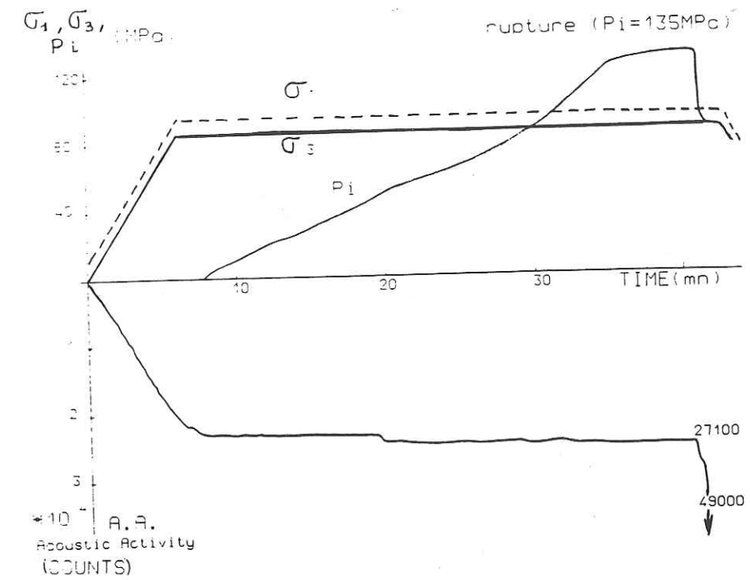

Figure 10
Hydraulic fracturing test with $\sigma_3 = 90$ MPa and $\sigma_1 = 100$ MPa on a sample of massive reservoir limestone (3850 metres depth): the final fracturing occurs with considerable acoustic emission (brittle behaviour).

It may therefore be concluded that, under the existing geomechanical conditions, localised seismic events in the reservoir (GRASSO and FEIGNIER, 1990) could be the result of the local "hydraulic" fracture of a limestone bed held between an overcompressed lens trapped in a clay level and a well-drained porous area of the reservoir.

5. Application to Geomechanical Interpretation of Deep Fractures

In parallel with the sample study, an analysis was made of geomechanical data relating to localised fractures near the deep gas exploitation area. This included:

- a study of the structural geology, with a view to determining the precise geometry of the structure and its principal faults and the state of stress in the deposits prior to exploitation;
- a detailed seismic-acoustic study of the fractures in each geological horizon and, in particular, a study of focal mechanisms, including the likely geometry of the fracture plane, or zone, and the movement associated with it (AKI and RICHARDS, 1980).

Analysis of the structural geology data (GRASSO *et al.*, 1985) reveals dissymmetry in the structure, seen in terms of a southern stress area, where the major principal stress σ_1 is N120° horizontal, and a northern area, where the difference between the stress σ_1 and the lithostatic stress is smaller (this area is further from the mountain range). The dome structure is distinct but also asymmetric, with the northern side sloping more gently than the southern. The southern and western flanks are broken by several steeply sloping faults that cross the reservoir levels and gradually disappear in the overlying marl formation.

Detailed analysis of the seismic events (GRASSO and WITTLINGER, 1990) and associated mechanisms (GRASSO and FEIGNIER, 1989; GRASSO *et al.*, 1985) reveals a distinct absence of correlation between the geometrical pattern of cracks and their location in any particular geological level. The above references demonstrate that the seismic behaviour is governed primarily by complex stress conditions due to the presence of fractures on the one hand and exploitation of the resources on the other. The overall deformation of the structure therefore conceals the individual response of each geological level and it is mainly the lithological unconformities (slips along the stratification of the northern side) and tectonic nonconformities (faulted areas on the southern, eastern and western sides of the anticline) that govern fracture locations (FEIGNIER and GRASSO, 1990).

By inducing a significant drop in pressure of more than 50 MPa (see Figure 8), exploitation of the resources has noticeably increased the effective stresses in the deposits (GRASSO and WITTLINGER, 1990; SEGALL, 1989). Adopting a large-scale view and applying conventional soil mechanics principles, it may be deduced that an increase in the effective stresses will result in a major settlement within the reservoir itself. This has mechanical repercussions on the underlying and overlying layers. The structure therefore adapts to the deformation of the reservoir, but in the same way as would a heterogeneous rock mass, i.e., either by readjustment of the blocks, with movement occurring along existing discontinuities whenever their orientation with respect to the direction of the main stresses allows, or, more rarely, by the appearance of new cracks when the stress reaches the failure threshold of the rock matrix at certain points.

Within this general context, it is possible to predict the most likely fracture mechanisms in each geological layer:

- The reef limestones, are the origin of a significant proportion of the seismic events (60%). The absence of events on the western slope is explained by a variation in the facies of the reef limestones, which in this sector turn laterally into marls (GRASSO and FEIGNIER, 1990). Laboratory tests show that the limestones may behave in a brittle manner under field conditions. However, the extensive fracturing observed indicates rather reactivation of the blocks along existing unconformities. All the various movements revealed by the seismological analysis are consistent with the unfolding of the dome structure and a general downwards displacement of a unit located above the reservoir (FEIGNIER and GRASSO, 1990) resulting from settlement within the reservoir itself.
- A significant proportion (15%) of the seismic activity was noted in the micaceous marls. According to the laboratory tests, brittle cracking cannot occur in the marl matrix under present field conditions. The predominant quake mechanism would therefore appear to be linked with reactivation of geological faults, and particularly, as indicated by detailed studies, with fractures inside more calcareous layers or, mainly, with movement on the faulted southern part of the anticline along a major faulted zone (see Figure 1). Judging by the magnitude of seismic events, the seismic deformation within the marls is negligible compared to the aseismic one (FEIGNIER and GRASSO, 1991).
- In the reservoir itself, there are few seismic events. Given the heterogeneous structure and highly contrasting mechanical properties of the rocks, all fracture mechanisms could be possible here. Due to the huge pore pressure drop within the reservoir, the increase of effective stress prevents a failure process. Nevertheless, according to the previously discussed rock sample tests, seismic fracture located in the reservoir can be understood as a result of a similar mechanism to hydraulic fracturing between an area of trapped gases and a more effectively drained part of the reservoir.

Conclusions

This experimental study using deep core samples from a partially depleted gas field provides a number of results concerning the real properties of deep geological strata under stress conditions similar to those assumed to exist in the field. Firstly, it was possible to deduce certain aspects of the mechanical behaviour of the rock which enabled the behaviour of the structure to be modelled. A study of surface subsidence is in progress. However, the main point of the study was to identify the various modes of rupture of the rock that can occur under field conditions and to determine in which way these affect seismic activity in the area, as a result of the drop in gas pressure within the deep reservoir. The analysis led to the identification of two distinct types of behaviour:

- Seismic events are localised in geological levels where the conditions for brittle failure are satisfied. In this case, the only way of ascertaining whether the fracture is a new matrix fracture or the reactivation of an old fault is to analyse the kinematic and dynamic fracture parameters obtained by the seismological study.
- Seismic events occur at levels where only ductile behaviour is currently possible (with virtually no acoustic activity, as shown by certain laboratory tests). In this case, the movements can only have taken place along existing

discontinuities and the major deformation process is aseismic. This would appear to be the case in the marls, located at about 3000 metres depth, above the gas deposits and also within the whole western side of the dome structure where the Albian deposits have a clayey facies.

Finally, it is clear that, while it is possible to recreate in the laboratory the effective stress conditions of a fracture occurring at depths of 1000–5000 metres, this knowledge alone is not sufficient to provide prediction or replication of seismic and aseismic movements that may occur in hydrocarbon fields. However, it is an essential component in the multidisciplinary study (including geology, geophysics and mechanics) that needs to be carried out to understand all the phenomena governing the behaviour of a rock mass at great depth.

Acknowledgements

The authors are pleased to thank the Société Nationale Elf-Aquitaine for providing authorization to publish this work. This study was supported by D.E.L. Elf-Aquitaine under contract 915/6/982. We are also grateful to Dr. H. St. John for his assistance in reviewing the English text.

References

AKI, K., and RICHARDS, P. G., *Quantitative Seismology Theory and Methods* (W. H. Freeman, San Francisco 1980) 984 pp.

DAYRE, M., FABRE, D., LETOURNEUR, J. ANTOINE, P., and ORENGO, Y. (1978), *Eléments pour une classification géotechnique des terrains*, Proc. 3rd IAEG Congress, Madrid, Sec. II, Vol. 2, pp. 131–139.

DEERE, D. U., *Geological considerations*. In *Rock Mechanics in Engineering Practice* (eds. Stagg and Zienkiewicz), (John Wiley, London 1968) pp. 1–20.

FEIGNIER, B., and GRASSO, J. R. (1990), *Seismicity Induced by Gas Production: 1. Correlation of Focal Mechanisms and Dome Structure*, Purc and Appl. Geophys. *134* (3), 405–426.

FEIGNIER, B., and GRASSO, J. R. (1991), *Relation between Seismic Source Parameters and Mechanical Properties of Rocks: A Case Study*, Pure and Appl. Geophys., in press.

FOURMAINTRAUX, D. (1975), *Quantification des discontinuités de la roche et du massif rocheux. Méthode et application*, Bull. Liaison Labo. P. et Ch. *75*, 69–76.

GRASSO, J. R., FABRE, D., and VIALON, P. (1985), *Etude géomécanique de la sismicité de la région de Lacq*, IRIGM/SNEA(P) in-house Report, Grenoble, 400 pp.

GRASSO, J. R., and FEIGNIER, B., *Geomechanical behaviour and structural effect induced by the depletion of a gas field dome*. In *Rockburst and Seismicity in Mines, II* (ed. Fairhurst, C.), (Balkema, Rotterdam 1989) pp. 53–60.

GRASSO J. R., and FEIGNIER, B. (1990), *Seismicity Induced by a Gas Production; II: Lithology Correlated Events, Induced Stresses and Deformation*, Pure and Appl. Geophys. *134* (3), 427–450.

GRASSO, J. R., and WITTLINGER, G. (1990), *Ten Years of Seismic Monitoring over a Gas Field*, Bull. Seismol. Soc. Am. *80* (2), 450–473.

HOMAND-ETIENNE, F. (1986), *Comportement mécanique des roches en fonction de la température*, Doctoral thesis, Mémoires Sc. de la Terre, Nancy, 46, 261 pp.

MORALES, R. (1981), *Etude expérimentale au laboratoire de la fracturation hydraulique des roches. Analyse des pressions d'injection*, Doctoral thesis, Grenoble University, 175 pp.

PATERSON, M. S., *Experimental Rock Deformation: The Brittle Field* (Springer, Berlin 1978) 254 pp.

SEGALL P. (1989), *Earthquake Triggered by Fluid Extraction*, Geology *17*, 9801–9816.

(Received December 19, 1990, revised November 11, 1991, accepted November 12, 1991)

24

LES SÉISMES INDUITS COMME INDICATEUR DU COMPORTEMENT DES RÉSERVOIRS D'HYDROCARBURES.

Engineering Geology, 32 (1992) 123–135
Elsevier Science Publishers B.V., Amsterdam

Monitoring of subsidence and induced seismicity in the Lacq Gas Field (France): the consequences on gas production and field operation[1]

V.M.R. Maury[a], J.-R. Grasso[b] and G. Wittlinger[c]

[a]*Elf-Aquitaine, France*
[b]*LGIT/Institut de Recherches Interdisciplinaire de Géologie et de Mécanique, Grenoble, France*
[c]*Institut de Physique du Globe de Strasbourg, Strasbourg, France*

(Received January 30, 1991; revised version accepted November 26, 1991)

ABSTRACT

Maury, V.M.R., Grasso, J.-R. and Wittlinger, G., 1992. Monitoring of subsidence and induced seismicity in the Lacq Gas Field (France): the consequences on gas production and field operation. Eng. Geol., 32: 123–135.

Between 1957, when the Lacq gas field was first put into production, and 1967, 2.5 cm of subsidence occurred. This corresponded to a period in which the pressure had been depleted by 30 MPa. Further depletion from 1967 until 1989, of 25 MPa induced an additional subsidence of 3.0 cm, which coincided with more than 1000 earthquakes; 44 with magnitudes greater than 3, and 4 with magnitudes greater than 4. The strain energy release rate by seismic events increased for the period 1969–1979 and now decreases yearly.

The method used for processing and interpreting the seismological data takes into account the lithologies and the mechanical properties of the rocks and the source parameters. The regional mechanism of the gas field deformation appears to be the lowering of a rigid block located at the top of the structure by a succession of movements along pre-existing fractures and faults in the reverse direction to the original. From spectrum analysis of seismic recordings, the amplitude of the fault slips has been calulated to be of the order of millimetres. This may be the reason why there has been no damage to the wells. The radii of the sources may give an indication about the size of the blocks to be considered in the reservoir engineering models.

In spite of the obvious non-elastic behaviour of the seismic events, the regional response of the rock mass is an elastic one. The rock mass can be modeled as a block assembly, with localized movements between some blocks being responsible for the induced seismicity. The size of the induced events is, therefore, limited by the pre-existing fractures.

Close monitoring of subsidence and seismic events is a new and useful aid to understanding the reservoir response to fluid withdrawal, the practical consequences with regard to safety and gas production, and a contribution to our knowledge of reservoir behaviour over the course of time.

Introduction

Human and industrial activities are known to trigger or produce seismic events, for example, surface or underground nuclear explosions and large quarry blasts. The problem becomes more complex when fluid or gas extraction or injection are concerned. The three main types which can cause problems are: fluid injection, injection of fluid (or pore pressure increase) due to surface damming, and fluid or gas extraction.

Triggering seismic events by fluid injection has been proven to be a straightforward phenomenon as shown by the observations and tests performed in Colorado (Healy et al., 1968). The effects of dam and reservoir filling sometimes can be straightforward, such as when seismic events occur very close to the dam or the reservoir during the initial filling (Hoover dam, U.S., 1939; Hsingfengkiang, China, 1962; Monteynard, France, 1963; Kremasta, Greece, 1966; Nurek, U.S.S.R., 1972). More

[1]*Correspondence to*: J.-R. Grasso, Université Joseph Fourier, LGIT/IRGIM, B.P. 53X, F-38041 Grenoble, France.

0013-7952/92/$05.00

questionable are the cases where events occur after several fillings (for example: Marathon, Greece, 1938; Kariba, Zambia, 1962; Koyna, India, 1967; Oroville, U.S.A., 1975, Aswân, Egypt, 1981). In these cases, Newtonian effects of the weight of the water in the reservoir have been invoked as the possible cause of triggering the seismic events. The pore pressure increase in depth (I.C.O.L.D, 1973; I.C.O.L.D., 1979), and the corresponding effective normal stress decrease, allowing fractures and faults to slip, have also been invoked as a possible cause of seismic activity (Raleigh et al., 1972, 1976; Simpson et al., 1988).

Fluid extraction (water, oil or gas) is the most questionable of these three cases. Up to now, most oil and gas fields have been operated without inducing any noticeable seismic event. In some cases, however, production has been found to initiate seismic activity. For example, during the 1920s, a series of earthquakes were observed to coincide with production from the Goose creek oil field in Texas (Pratt and Johnson, 1926). In Italy, the production of gas from the Caviaga field caused an earthquake of magnitude 5.5 in 1951. Caloi et al. (1956) assumed, and Caloi was able to confirm in 1970 (Caloi, 1970), that the gas production was the main cause of the earthquake.

Several cases were also reported at the First International Symposium on Induced Seismicity (Banff, Canada, 1975), and others in Texas, California and Canada were described by Yerkes and Castle (1976), Pennington et al. (1986), and Wetmiller (1986). Several minor events were noticed at Wilmington, California (Frame, 1952; Kovach, 1964), where many wells were sheared by horizontal displacements of up to 23 cm, at a depth of 400–600 m. The production of the oil field at Buena Vista Hills in California is known to have played a key role in the accelerated movements of a local fault (Nason et al., 1968).

In the U.S.S.R., Smirnova (1976) studied the Staro Groznenskoï field and the possible influence of its production on natural regional seismicity. More recently (also in the U.S.S.R.), Simpson and Leith (1985) and Grasso (1990) gave some details about 3 events of magnitude 7 observed at the Gazli gas field (2 in 1976 and 1 in 1984) for a gas depletion less than 10 MPa (Grasso, 1990).

These observations, among others, have raised several questions:

(1) Is the extraction of fluids able to initiate seismic events?

(2) Are the fluid movements in underlying levels (aquifers) or overburden associated with gas or oil production another possible cause of seismicity?

(3) Is there a possibility of predicting a range of magnitudes once the mechanism has been more clearly identified?

The case of the Lacq gas field, intensively studied since 1973, provides some answers to these questions. This paper presents a brief description of the Lacq gas field, a description of the seismic activity since 1974, the local network of seismological stations and the process of interpretation. The method used is derived from large-scale interpretation methods in seismology and adapted for this case. The mechanism of deformation of the gas field is then described and practical conclusions are drawn for operation.

Background

The Lacq gas field, 200 km southeast of Bordeaux (France), has already been described in several papers (Jenner and Dienesh, 1965; Winnock and Pontalier, 1968; Nicolai et al., 1991). The gas field is on the northern border of the Pyrenees mountain chain (Figs. 1, 2 and 3), very close (2 km) to the shallow and inactive "North Pyrenean overthrust". It is about 40 km from the "North Pyrenean fault", which is active and responsible for the seismic activity in the Pyrenees down to a depth of 20 km. The reservoir consists of Jurassic dolomite, with levels of low porosities (4–6%) alternating with levels of very low porosities (< 1%). The migration of the gas is the result of fracturing, which is responsible for the high permeability of the rock. The gas field is located in an anticline that extends 16 km east–west and 8–9 km north–south (Fig. 4). The thickness of the reservoir is about 500 m and the top is located 3240 m below the surface. At the beginning of 1990, the pressure at the top of the reservoir was measured at 9 MPa, a significant drop from an initial pressure of 64 MPa (Fig. 5). The initial capacity of the gas field was 269×10^9 m^3. At a

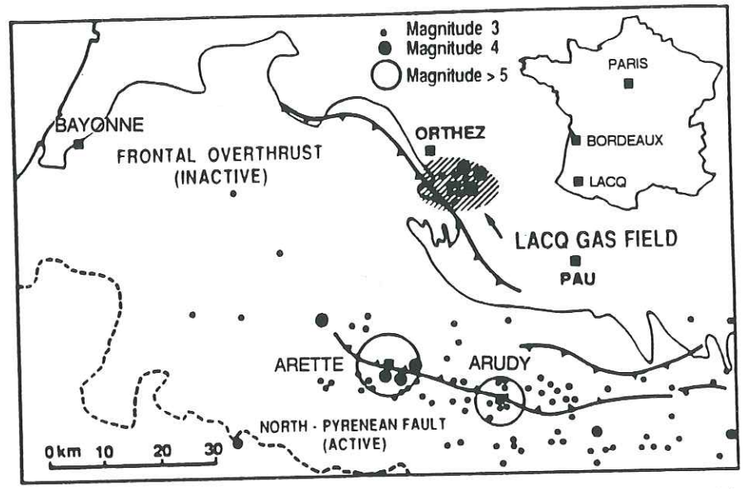

Fig. 1. General location of the gas field (shaded area), seismicity (black dots: Ml < 5; open circle: Ml > 5) and local geologic structure (heavy line).

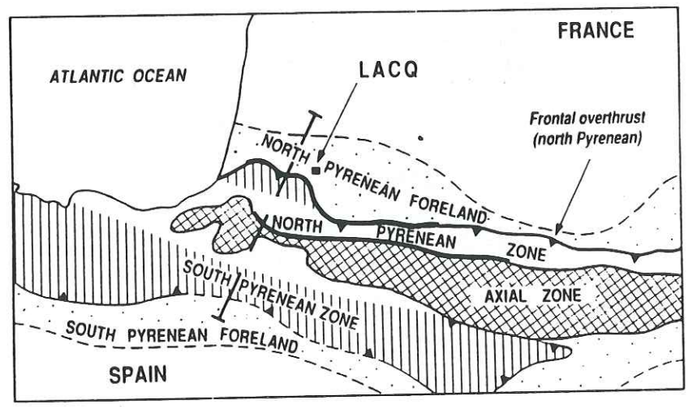

Fig. 2. Main geological units (adapted from Mattauer and Henry).

depth of 900 m in the Senonian Limestones (upper levels), there is a small oil field (called "Lacq Supérieur"), which was discovered prior to the underlying gas field. The production of this oil field started in 1950 and had produced 3.8×10^6 t by early 1990.

Injection of water was started in the oil field in 1968, increasing the initial pressure (reference level at 525 m) from 6.1 MPa to 6.4 MPa in 1978; it then decreased to 6.25 MPa in 1989. In 1975, water injections were initiated in the gas field. An overpressure of 13 MPa above the present reservoir pressure is now observed in some of the injection wells (wells La 102 and La 109). Injection of water into the shallow oil field approximately corresponded to the start of seismic activity. The question of the possible local role of these injections has not yet been resolved. The possible link between the presence of overpressured fluid and the reactivation of unfavourably oriented faults, rather than the nucleation of new fractures, could be investigated.

In addition, it was important to consider how the structure of the reservoir was developed. This study was based on all the geological data and studies carried out on similar structures. Figure 6

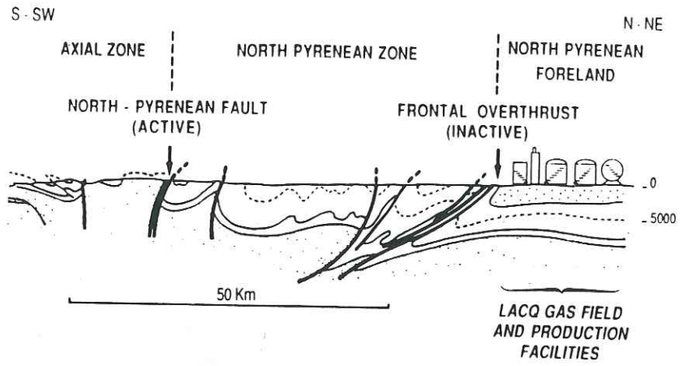

Fig. 3. Schematic tectonic cross section SSW–NNE.

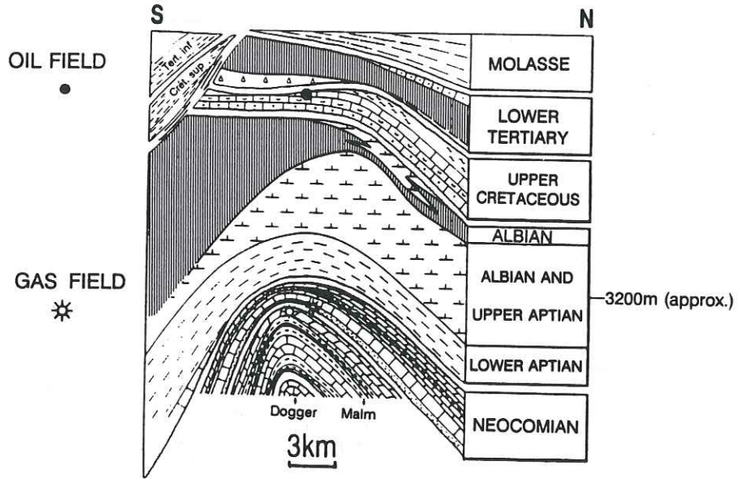

Fig. 4. Cross section of the Lacq anticline showing stratigraphic units (vertical scale exagerated).

illustrates how, during the Cretaceous (Albanian–Cenomanian), salt doming caused an uplift and normal faulting (faults F1 and F2, Fig. 6a). During the Tertiary (Eocene–Lutetian), compressive forces created the reverse fault F3 (North Pyrenean overthrust, Fig. 6b), twisted the F2 fault and reactivated the F1 system. From the beginning of gas production (1959) until 1969, which corresponded to a pressure drop of 30 MPa, no sign of seismic activity was detected. On the 24th of November, 1969, a seismic event was felt, followed by two events in January and December, 1972. The magnitudes of these events were estimated at 3–4, and were localized directly above the gas field (Rothé, 1970, 1977). It was then decided to install a local network of seismographs, under the guidance of the Institut de Physique du Globe de Strasbourg (I.P.G.S.). This network (Fig. 6) has been in operation since 1974. The interpretation was carried out by the Institut de Rechèrches Interdisciplinaire de Géologie et de Mécanique de Grenoble (I.R.I.G.M.).

Seismicity patterns and location of hypocentres

The initial seismic network consisted of four geophones. Three instruments more were later deployed in the production area, and one was

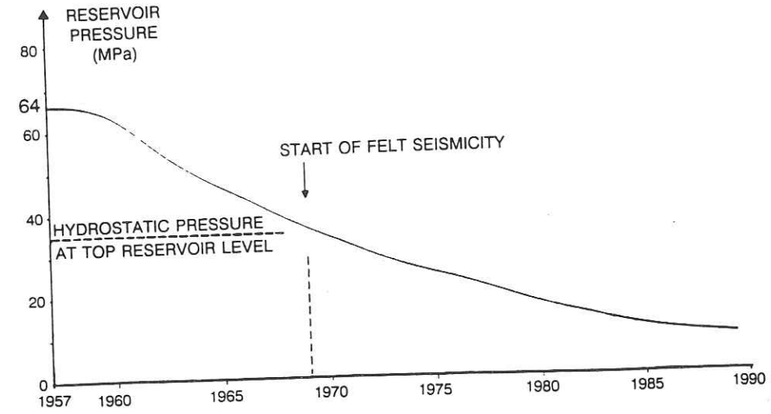

Fig. 5. Plot of pressure with time showing point of felt seismicity.

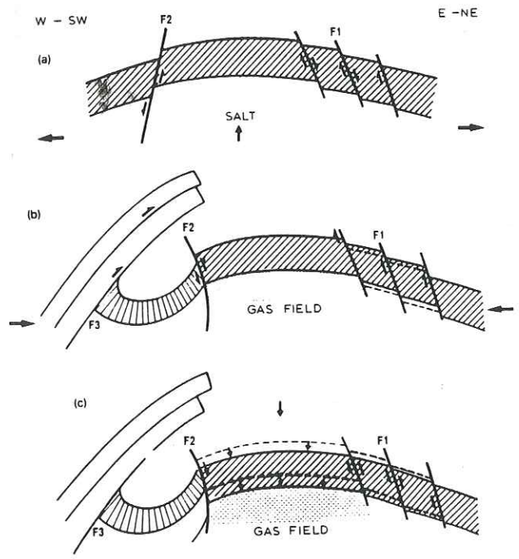

Fig. 6. General scheme of deformation. (a) During Cretaceous (Albo–Cenomanain 100 MA), uplift and normal faulting faults F1–F2 were caused by salt doming and extensional tectonics. (b) Tertiary-(Eocene 60 MA) Compression created the reverse fault F3 (overthrust), twisted the F2 fault system, and reactivated the F1 normal fault. (c) The depletion of the gas field is presently lowering the top, through movements on existing faults. The motions are reversed: F1 is "pseudo-reverse", F2 is "pseudo-normal". The overthrust is inactive.

located 7 km away from the site. Between 1976 and 1981, seven seismic stations were operational. In 1982 a three-component unit, located at the bottom of a 3800 m deep borehole in the western part of the field, was added to the seismic monitoring network (Fig. 7). The whole system has a flat response between 1 and 40 Hz. Signals from the geophones are relayed to the central site by UHF/FM radio transmission. Until 1982, the analog data relayed from the subsurface sensors were digitized using a multichannel modulator. A "transient" recorder was activated by a coincidence trigger unit, which used an amplitude threshold within a specified time window as a comparator. Since 1982 digital recordings have been made. Preliminary event locations are computed on the basis of a homogeneous half-space velocity model. The selected events have local magnitudes greater than 1.0. Between April 1974 and December 1989 more than 900 events were recorded (Fig. 8).

More than 90% of the epicentres are inside the gas and oil field limits. Although the seismicity extends beyond the lateral limits of the oil field, the correlation with the estimated gas field extension is quite good, particularly for the eastern part of the gas field. The error in the standard hypocentre location is numerically estimated (from least-square solutions) at 1 km. Events of $M_l > 3$ were used to estimate the temporal evolution of the seismicity and to assess the main features of the ruptures. In the following sections we present the results of three-dimensional event locations, using the techniques described in Grasso et al. (1983) and Grasso and Wittlinger (1990). This method allows definition of DX, DY and DZ as

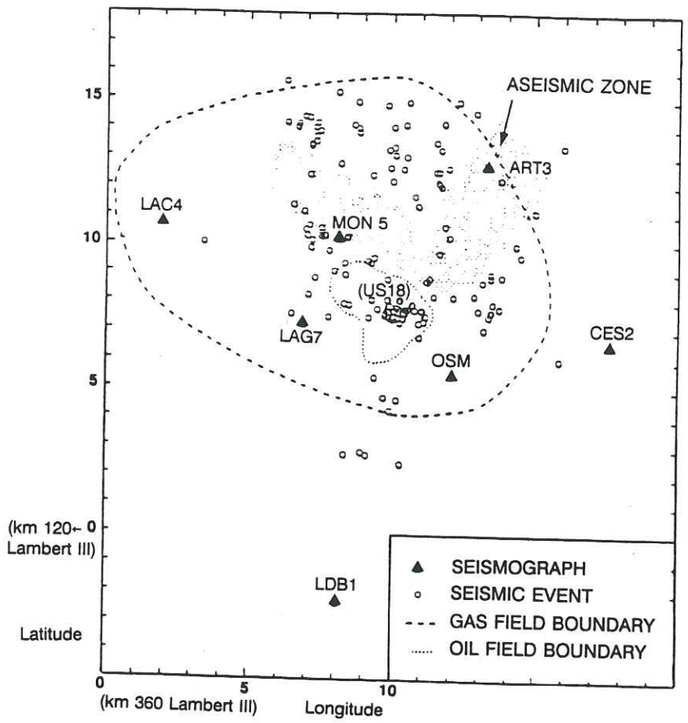

Fig. 7. Map showing location of seismic stations (black triangle) and seismic events (open circle) in the time period 1976–1979. Relative coordinates are in km. Boundaries of gas and oil field are shown.

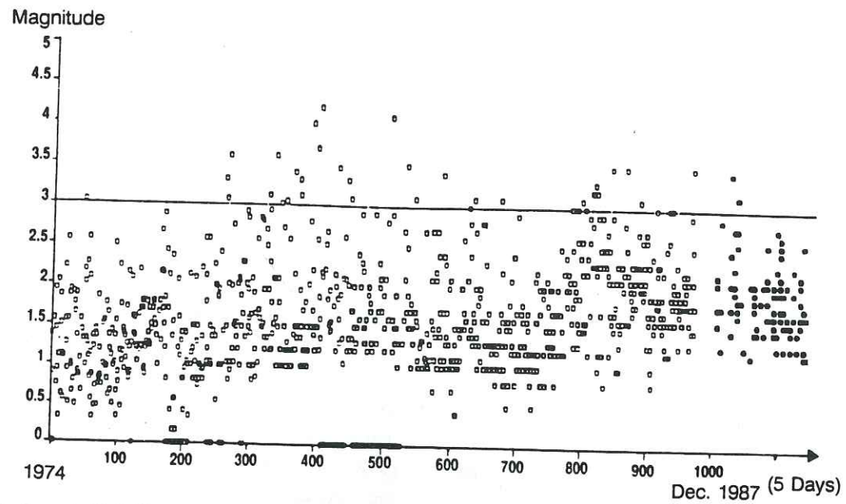

Fig. 8. Seismicity in period of 1974–1987. The numbers on the horizontal axis are the cumulative number of events.

the uncertainties for the event location parameters, that is, with the average lateral and vertical errors equivalent to 0.1 and 0.15 km, respectively (Grasso and Wittlinger, 1990).

At this scale, with the depth of events ranging from 2 to 7 km, the seismicity pattern displayed by the 227 well-located events occurring between 1976 and 1982, can be analyzed with respect to their geomechanical setting.

Characteristics of induced seismicity

The gas field seismicity is in an otherwise aseismic region, with 25 km separating the epicentres from the active North Pyrenean fault which is the northern limit of limits the regional Pyrenean seismic zone. The gas field seismic events are always shallower than the regional tectonic shocks (Gagnepain-Beyneix et al., 1982; Grasso and Wittlinger, 1990). The locations of the events between 1974 and 1989 extend beyond the upper oil field area but coincide with the area of the lower gas field. This correlation is also clear for the largest earthquakes in the area ($M_l > 3$). The correlation is confirmed and enhanced by the results from three-dimensional location techniques. More than 95% of the events located using this technique fall within the area of the gas field. The events are located on the eastern part of the field, with an aseismic zone on the western part of the field and near the top of the structure. The envelope of the 227 hypocentres fits closely with the dome structure of the gas reservoir (Grasso and Wittlinger, 1990).

The seismicity involves the entire dome structure. The 50 MPa depletion of the gas field pore pressure has activated structures that have the same area as the area that is microfractured by the seismic events.

From the production data, the depletion in the period 1960–1980 can be considered as homogeneous throughout the field. The presence of seismic and aseismic zones is, therefore, mainly governed by rock heterogeneities (lithologies, geomechanical properties and preexisting fractures).

Identification of fractures responsible for seismic events

The eastern seismic zones and western aseismic areas correlate with lithologic changes. These lithologic changes are known from data from more than 30 deep boreholes (up to 6 km in depth) in a 10×10 km area. The correlation of hypocentres and lithology is either lateral (west–east) or vertical. Seismic areas are located in a calcareous, water saturated, fractured and permeable medium, with a stiff and brittle matrix behaviour (Albian–Aptian reef limestones). Aseismic areas are located in marls that exhibit a ductile behaviour at the pressure and temperature conditions present (Grasso and Feignier, 1990). A ratio was obtained between the elastic modulus of the limestones (seismic rock matrix, 60,000 MPa) and the elastic modulus of the marls (aseismic rock matrix, 33,000 MPa). This ratio was also obtained from the uniaxial compressive strength of these rocks (140 MPa and 50–70 MPa, respectively). As far as the gas reservoir rocks are concerned, they exhibit similar seismic properties to the overburden. As only 10% of the seismic activity occurs in the reservoir rocks, the reduction in pore pressure in these levels increases the effective normal stress on the fractures and is, as expected, a stabilizing factor (it is assumed that fracture behaviour is mainly governed by the geomechanical properties of their walls).

Kinematics of displacements associated with seismic events

The kinematic study of micro-earthquakes induced by the exploitation of the Lacq gas field allows a deformation model to be built using focal mechanism techniques (Feignier and Grasso, 1990). The analysis of seismic displacements in the eastern, western and southern zones indicates movements in the sense of normal and reverse faulting. The geometry of the faulting coincides with pre-existing fractures described previously (compare Figs. 6 and 9). Figure 9 shows, schematically, that the inferred rupture geometry defines the blocks and that the main faults (in terms of the number of earthquakes) define the boundaries of the blocks. From the movements along these faults, the block may be identified as a "collapsing zone" at the centre of the area. This zone is located at the top of the anticlinal structure and its downward motion is consistent with reservoir strain due

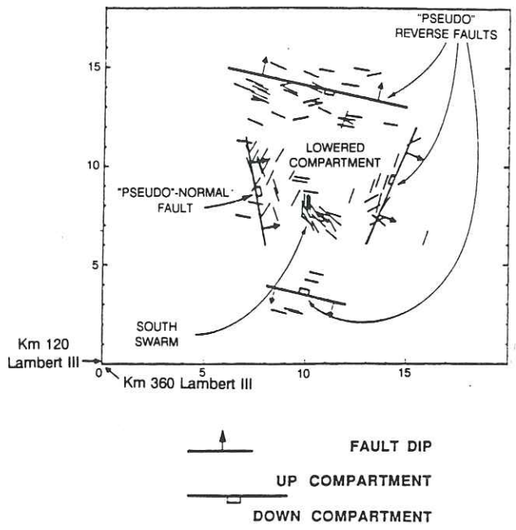

Fig. 9. Schematic deformation map. Shorts lines denote event locations, their orientation are associated with their fault plane azimuths. Large lines underscores the main faults that define the collapsing blocks (adapted from Feignier and Grasso 1990).

to compaction (a swarm of events located inside this block (Fig. 9) locally complicates the collapsing area). This mechanism explains 97% of the data sets in the 1976 –1981 period.

Another interesting feature is the northern flank response to depletion. The composite mechanisms in this area indicate fracture planes moving parallel to the bedding plane. We interpret this seismicity as the response of a known unfractured medium where motions are localized along planes of weakness (bedding). The direction of motion is found to coincide with the direction of least regional stress (Feignier and Grasso, 1990). This supports the argument that movement along pre-existing fractures and bedding planes is activated by the gas production in this field.

Surface displacement measurements

Surface displacements have been recorded by levelling measurements obtained in 1887, 1967, 1979, 1989, as shown in Figs. 10 and 11. A maximum displacement of about 60 mm was registered from the last survey in 1989. The levelling reveals that the whole structure of the gas field is involved. The first 25 MPa depletion (after 10 years of production) did not give rise to seismic (felt) events: the behaviour of the structure was either elastic or (aseismic) plastic. Further seismic events, triggered by depletion, show a strong asymmetric distribution of events. This asymmetry does not coincide with the symmetric curve of subsidence. The regional response of the structure is, therefore, mainly governed by the elastic or plastic behaviour of the rocks which make up the structure. The size of the blocks or the presence of pre-existing fractures limits the size of the events.

Dynamic characteristics of seismic fractures

Recent developments in seismology and in seismic data acquisition allow us to understand the source of brittle fractures more clearly (Aki and Richards, 1980). A source is characterized in terms of seismic moment, size of the fault, post-fracture stress drop, dislocation and seismic energy release. These parameters may be computed from either a dynamic or kinematic point of view (Brune, 1970; Madariaga, 1976; Aki and Richards, 1980).

Data were obtained from 149 earthquakes, which ranged in magnitude from 1.0 up to 4.2, recorded between August 1976 and June 1979 by the 7 station seismic network. This time frame corresponded to the most active seismic period. Seismograms were digitized at a rate of 111 points/sec; 401 of them gave a signal-to-noise ratio greater than 2, which was the selection threshold (for details see Feignier and Grasso, 1992).

Basically, this study uses the characteristics of the displacement spectrum in the frequency domain. The spectrum is computed from ground velocity (displacements of the soil recorded by the seismogram), by a Fourier transform and an integration in the frequency domain to obtain the displacement spectrum (seismometer and recording system response deconvolved, Feignier and Grasso, 1992). Thus, the displacement spectrum is characterized by three independent parameters: a low-frequency plateau, a high-frequency decay and their intersection, the "corner" frequency. These patterns are predicted by most of the dynamic or kinematic source models, relating the high-frequency decay to the finiteness of the fault size

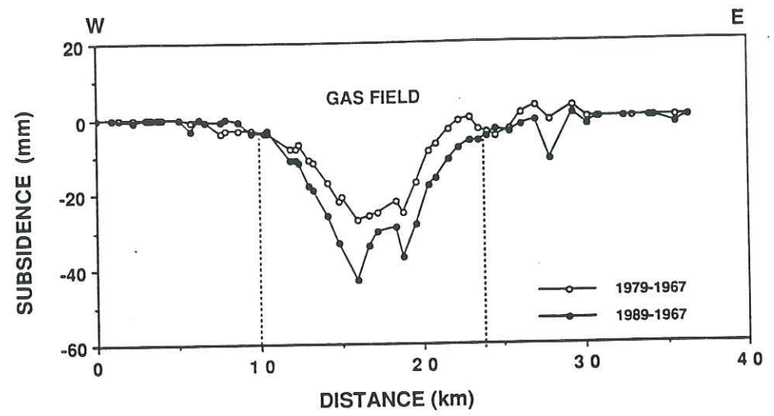

Fig. 10. West–east plot of subsidence. The deepest subsidence curve (open circles) corresponds to elevation changes between 1967 and 1979. The black dot curve corresponds to elevation changes between 1967 and 1989. Vertical dotted lines are schematic boundaries of gas reservoir.

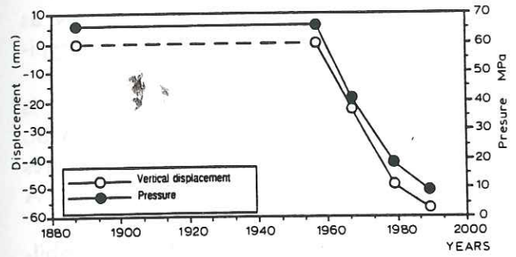

Fig. 11. Subsidence and pressure drop with time.

and fracture velocity. The slope of this decay is specific to the fracture itself. The corner frequency is related to the size of the fault and the low-frequency plateau gives information about the magnitude of the seismic moment.

Investigations of seismicity induced by mining (Gibowicz et al., 1977; Gibowicz, 1989), have demonstrated that the dynamic circular source model of Madariaga (1976) provides the most appropriate values for the fault size for micro-earthquakes ($M_l < 3$). Moreover, recent investigations on seismic spectra (Gibowicz et al., 1977; Gibowicz, 1984) have indicated that this model is the most realistic way of describing the fracture movement. This model assumes a circular fault plane, with a fracture front growing from the centre to the edge at a fixed velocity. In fact, it may be qualified as a "quasi-dynamic" model since the effective stress is specified at the fault.

The seismic moment, corresponding to the equivalent force couple, is defined (Aki and Richards, 1980) by: $M_o = \mu SD$, where: μ = the modulus of rigidity, D = the average dislocation over the fault, S = the fault surface area.

This seismic moment is an evaluation of the magnitude of an earthquake and is more closely related to the mechanical fracture process than the usual magnitude scale. It is the elastic couple of forces that disappear when seismic fractures occur.

Source radii are evaluated by means of: $R = 0.32 V_s / f_{cp}$, where: V_s = the S wave velocity, f_{cp} = the corner frequency for P waves.

Seismic moments and source radii allow us to evaluate the stress drops according to Brune's formula (1970): $D_s = (7/16) M_0 / R^3$.

This value represents the uniform reduction in the shear stress which produces the seismic slip over the fault. D_s can be considered as an estimate of the static stress drop, defined as the difference between initial and final stress values (see for details Del Pezzo et al., 1985; De Natale et al., 1987; Feignier and Grasso, 1991).

Regarding the geomechanical analysis of the source parameters, it can be pointed out that (Fig. 12):

(1) The event distribution is correlated with lithology except for the reservoir. A high proportion of events is located in the strongest beds: 60% of the seismicity occurs in limestones, 15% in

marls. The horizon with the highest seismicity rate is the calcareous layer located just above the gas-trapping marls.

(2) Average and maximum values of the seismic moment are correlated to the number of seismic events (Fig. 12). Seismic moments are considered to represent the strain energy release. The major seismic moments released in this period of time are localized in the reef base (Aptian Superior level). This level appears to be the most active as regards seismic fracturing, in terms of number of events and in the intensity of seismic moments.

(3) Source radius distribution is basically different. Average values are roughly constant (80 m) above the gas reservoir in limestones and marls and decrease sharply (40 m) in and below the reservoir. Again, strong levels above the reservoir appear to contain the largest sources.

Three factors can explain this discrepancy:

(a) The size range of pre-existing fractures and bed thicknesses (40 to 200 m in limestones, 500 m in marls).

(b) The role of pore pressure depletion, which increases the effective normal stress on the fractures, as seen previously.

(c) The possible different conditions for the in situ state of stress.

The lack of data on this last point prevents us from drawing more conclusions.

(4) Correlation can be observed between the magnitude of stress drop and geomechanical properties of different beds. As expected, the highest stress drop (up to 4 MPa) occurs in the strongest limestones (overburden). It is up to 2 MPa in the reservoir. Again, the lack of knowledge of the in situ state of stress does not enable us to draw more definitive conclusions at present.

(5) The slip averages 2.5 mm in the overburden, again with a maximum value of 6 mm in the strongest limestones of the overburden. The average is 5 mm in the reservoir. These results are very model-dependent but allow us to compare seismic fractures within different geomechanical settings.

Comments

The relationship between the deformation and the seismic activity for the Lacq field is a particular one that deserves special attention. The depletion in the reservoir induces an increase in normal effective stress on the fractures, faults, and joints (discontinuities), which tends to stabilize them. At the same time, the stress redistribution in the reservoir, as well as in the overburden and the underlying beds, causes deformation. In fractured media, this deformation occurs very quickly as small slips along discontinuities. Two extreme typical cases may then be encountered:

(1) If the overburden is very permeable, as it is for the overburden of Lacq (except the seal by St. Suzanne marls), the opening of joints and fractures and the pressure build-up will be simultaneous. A low level seismicity can be generated.

(2) If the overburden has a very low permeability, the build-up of pressure in fractures or joints does not occur immediately but is delayed, relieving normal effective stresses on faults, possibly on much larger surfaces. The magnitudes of events triggered by this mechanism are much more important than those triggered by the direct stress release. An example of this mechanism on a small scale has been identified as the cause of spontaneous collapse of certain room and pillar arrangements in mines (Maury, 1979).

A build-up of pressure in joints and fractures can be caused by abnormal pressure transmission through cementation of well bores, or through the opening of joints due to quiet subsidence, with or without felt seismicity. It is a very important phenomenon for the oil industry. It has been proven to be the cause of the loss of well bores

Fig. 12. (a) Distribution of events within the geomechanical bed of the structure. The location of each bed are given by the key (f) and the schematic cross section on figure 4. The average thickness of each bed is 500 m. (b) Distribution of the seismic moments within the geomechanical bed of the structure. Dotted lines are minimum and maximum value envelope. Continuous line are average values. The number of events within each beds are plotted on the left of each diagram. Small dot areas localize the gas reservoir levels. (c) Same as (b) for the sources radii of seismic events. (d) Same as (b) for the shear stress drop of seismic events. (e) Same as (b) for the dislocation of seismic events (adapted from Feignier and Grasso 1992).

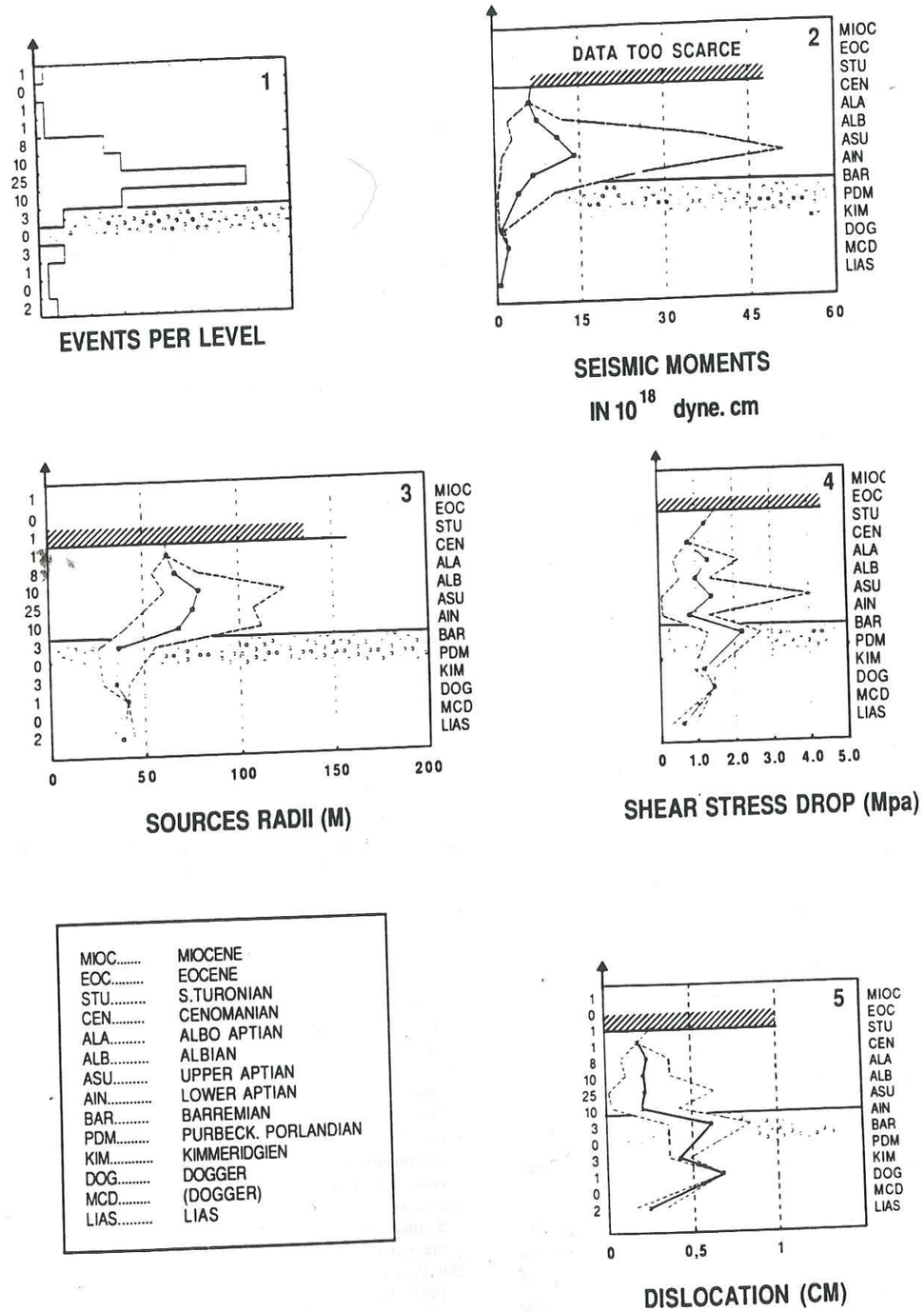

(Maury and Sauzay, 1989) and can be without any associated seismicity. This can also occur under drilling conditions, making it possible to destabilize a hole by increasing the mud weight. The case of Wilmington field, California, should be re-examined bearing this mechanism in mind.

Conclusions

The studies undertaken revealed the following results and conclusions:

(1) Detailed and precise location of seismic events made possible by the installation of a seismological network, show that a man-induced seismicity exists due to the production of gas (most of magnitudes lower than 3, 40 events of magnitudes 3–4, and 4 events of 4–4.2).

(2) The mechanism of deformation is the lowering of a summital block, which is limited by the pattern of pre-existing fractures.

(3) The spectrum analysis of the seismic recordings gives a large quantity of information on the geometrical and mechanical parameters of the seismic sources. The following are of importance for producers:

(a) The amplitude of the movements (so-called "fault slips" in seismology) is of the order of millimetres. This may be the reason why no damage has occurred to the wells.

(b) The exact locations of the events allows some parameters to be correlated with the geomechanical properties of the different beds.

(c) The radii of the sources can give an indication of the size of the blocks to be considered in the reservoir engineering models.

(4) The gas production and induced stresses have reactivated movements on the boundaries of pre-existing blocks and on discontinuities. No seismic movements have been observed along the North Pyrenean overthrust.

(5) The strain energy release rate by seismic events increased for the period 1969–1979 and now decreases, more regularly, yearly.

(6) There is an exact correlation between recorded surface movements and depletion rates. In spite of the obvious non-elastic behaviour of the seismic events, the regional response of the rock mass is an elastic response. The rock mass can be modeled as a block assembly, with localized movements between some blocks responsible for the induced seismicity. The size of the induced events is, therefore, limited by the pre-existing fractures.

(7) The absence of weak rocks, such as undercompacted clays, in the overburden and the reservoir, enables us to rule out the possibility of large aseismic movements, such as are encountered in the North Sea or in California.

(8) The movements along these fractures were analyzed using focal mechanism methods developed in seismology. The movements are in the reverse direction to the original ones: initial normal faults move as reverse faults, and initial reverse faults move as normal faults.

Acknowledgements

The cooperation of the staff of I.P.G.S., who were in charge of the design and installation of the local seismological network, and of the I.R.I.G.M., for the interpretation of data and geomechanical tests, and of the Lacq gas field, for maintenance of the network, is gratefully acknowledged. We would also like to thank P. Volant for much help during the manuscript preparation. Constructive criticism from an anonymous reviewer and A. McGarr greatly improved the final paper. The authors also wish to thank the management of Elf-Aquitaine for permission to publish this work.

References

Aki, K. and Richards, P.G., 1980. Quantitative Seismology: Theory and Methods. W.H. Freeman, San Francisco, Calif., USA.

Brune, J.N., 1970. Tectonic stress and the spectra of seismic shear waves from earthquakes. J. Geophys. Res., 75: 4997–5009.

Caloi, P., 1970. How nature reacts on human intervention: responsibilities of those who cause and who interpret such reactions. Ann. Geofis., 23: 283–305.

Caloi, P., de Panfilis, M., di Filippo, D., Marcelli, L. and Spadea, M.C., 1956. Terremoti della Val Padana del 15–16 maggio 1951. Ann. Geofis., 9: 63–105.

Del Pezzo, E., De Natale, G., Scarcella, G. and Zollo, A., 1985. Qc of three component seismograms of volcanic microearthquakes at Campari Flegrei volcanic area, Southern Italy. Pure Appl. Geophys., 123: 683–696.

De Natale, G., Madariaga, R., Scarpa, R. and Zollo, A., 1987. Source parameter analysis from strong motion records of the Friuli, Italy, earthquake sequence, 1976–1977. Bull. Seismol. Soc. Am., 77: 1127–1146.

Feignier, B. and Grasso, J.R., 1990. Seismicity induced by gas depletion: I. Correlation of focal mechanisms and dome structure. Pure Appl. Geophys., 134: 405–426.

Feignier, B. and Grasso, J.R., 1992. Characteristics of seismic fractures as a function of geomechanical setting. Pure Appl. Geophys. (in press).

Frame, R.G., 1952. Earthquake damage, its cause and prevention in the Wilmington oil field. Californian Oil Fields, 38(1): 5–15.

Gagnepain-Beyneix, J., Haessler, H. and Modiano, T., 1982. The Pyrenean earthquake of February 29, 1980: an example of complex faulting. Tectonophysics, 85: 273–290.

Gibowicz, S.J., 1984. The mechanism of large mining tremors in Poland. In: N.C. Gay and E.H. Wainwright (Editors), Rockbursts and Seismicity in Mines. S. Afr. Inst. Min. Metall. Symp. Ser., 6: 17–28.

Gibowicz, S.J., 1989. The mechanism of seismic events induced by mining: A review. In: C. Fairhurst (Editor), Rockbursts and Seismicity in Mines, II. Balkema, Rotterdam (in press).

Gibowicz, S.J., Cichowicz, A. and Dybe, T., 1977. Seismic moment and source size of mining tremors in upper Silesia, Poland. Acta Geophys. Pol., 25: 201–218.

Grasso, J.R., 1990. Hydrocarbon extraction and seismic hazard assessment. EOS, Trans. Am. Geophys. Union., 71: 1454.

Grasso, J.R. and Feignier, B., 1990. Seismicity induced by a gas depletion: I. Lithology correlated events, induced stresses and deformation. Pure Appl. Geophys., 134: 427–450.

Grasso, J.R. and Wittlinger, G., 1990. Ten years of seismic monitoring over a gas field area. Bull. Seism. Soc. Am., 80: 450–473.

Grasso, J.R., Cuer, M. and Pascal, G., 1983. The use of two inverse techniques: application to a local structure in the New Hebrides Island arc. Geophys. J. R. Astron. Soc., 75: 437–472.

Haskell, N.A., 1964. Total energy and energy spectral density of elastic wave radiation from propagation faults. Bull. Seism. Soc. Am., 54: 1811–1841.

Healy, J.H., Rubey, W.W., Griggs, D.T. and Raleigh, C.B., 1968. The Denver earthquakes. Science, 161: 1301–1310.

I.C.O.L.D., 1973. Question 40. Proc. 11th I.C.O.L.D. Congr. (Madrid). I.C.O.L.D., Paris, France, Vol.1.

I.C.O.L.D., 1979. Question 51. Proc. 13th I.C.O.L.D. Congress, (New-Delhi). I.C.O.L.D., Paris, France, Vol. 2.

Jenner, P. and Dienesh, J., 1965. Histoire géophysique du champ de Lacq. Geophys. Prospect., 13: 518–540.

Kovach, R.L., 1964. Source mechanisms for Wilmington oil field, California, subsidence earthquakes. Bull. Seismol. Soc. Am., 54: 699–711.

Madariaga, R., 1976. Dynamics of an expanding circular fault. Bull. Seismol. Soc. Am., 66: 639–666.

Mattauer, M. and Henry, J., 1973. The Pyrenées. In: Data for Orogenic Studies. Geol. Soc. London.

Maury, V.M.R., 1979. Effondrements spontanés, synthèse d'observations et possibilité de mécanisme initiateur par mise en charge hydraulique. Rev. Ind. Minér., Oct.

Maury, V.M.R. and Sauzay, J.-M., 1989. Rupture de puits provoquée par glissement sur faille: cas vécu, mécanisme, remèdes, conséquences. In: V.M.R. Maury and D. Fourmaintraux (Editors), Proc. Int. Symp. Int. Soc. Rock Mechanics, Rock at great depth (Pau, France). Vol. 2, pp. 871–880.

Nason, R.D., Copper, A.K. and Tocher, D., 1968. Slippage on the Buena Vista thrust fault. 43rd Ann. Meet. Guidebook, AAPG, SEG, SEPM. Am. Assoc. Petrol. Geol., Tulsa, Okla., pp. 100–101.

Nicolai, A., Pacaud, M. and Sitbon, A., 1992. Atlas of oil and gas fields—Lacq gas field Aquitaine Basin—France. Am. Assoc. Petrol. Geol., Tulsa, Okla.

Pennington, D.W., Davies, D.D., Carlson, S.M., Dupree, J. and Ewing, T.E., 1986. The evolution of seismic barriers and asperities caused by the depressuring of fault planes in oil and gas fields of south Texas. Bull. Seismol. Soc. Am., 76: 939–948.

Pratt, W.E. and Johnson, D.W., 1926. Local subsidence of the Goose Creek field. J. Geol., 34 (1): 577–590.

Raleigh, C.B., Healy, J.H. and Bredehoeft, J.D., 1972. Faulting and Crustal stress at Rangely, Colorado. A.G.U. Geophys. Monogr., 16: 275–284.

Raleigh, C.B., Healy, J.H. and Bredehoeft, J.D., 1976. An experiment in earthquake control at Rangely, Colorado. Science, 191: 1230–1237.

Rothé, J.P., 1970. Seismic artificials. Tectonophysics, 9: 215–218.

Rothé, J.P., 1977. Séismes artificiels et exploitattions pétrolières: l'exemple de Lacq, France. Ann. Geophys., 30: 369–383.

Simpson, D.W. and Leith, W., 1985. The 1976 and 1984 Gazli, USSR, earthquakes—Were they induced? Bull. Seism. Soc. Am., 75 (5): 1465–1468.

Simpson, D.W., Leith, W.S. and Scholz, C.H., 1988. Two types of reservoir-induced seismicity. Bull. Seism. Soc. Am., 78 (6): 2025–2040.

Smirnova, M.N., Navitskaya, N.A. and Shebalin, N.V., 1975. Earthquake swarm caused by intensive exploitation of an oil field. I.U.G.G.–I.A.S.P.E.I. Meet. (Grenoble, France), Abstr. 39.

Wetmiller, R.J., 1986. Earthquakes near Rocky Mountain House, Alberta, and relationship to gas production. Can. J. Earth Sci., 32(2): 172–181.

Winnock, E. and Pontalier, Y., 1968. Lacq gas field, France. In: Geology of giant petroleum field. Pap. presented 53rd Annu. Meet. AAPG. AAPG Mem., 14: 370–387.

Yerkes, R.F. and Castle, R.O., 1976. Seismicity and faulting attributable to fluid extraction. Eng. Geol., 10 (2–4): 151–167.

25

EVOLUTION DES RUPTURES SISMIQUES : ASPECTS METHODOLOGIQUES ET REALITE PHYSIQUE.

GEOPHYSICAL RESEARCH LETTERS, VOL. 19, NO. 7, PAGES 705-708, APRIL 3, 1992

INTERRELATION BETWEEN INDUCED SEISMIC INSTABILITIES AND COMPLEX GEOLOGICAL STRUCTURE.

Fabrice Guyoton, Jean-Robert Grasso and Philippe Volant

Laboratoire de Géophysique Interne et Tectonophysique, Observatoire de Grenoble, France.

Abstract: From 1982 to 1989, more than 520 local seismic events were recorded by a permanent network of 9 telemetered stations over an active gas field (Lacq, France). The geological data of 46 boreholes coupled to several tens of kilometers of seismic profiles, concentrated in a small volume of 15 x 15 x 10 km^3, allow the development of a very precise velocity structure, exhibiting a dome geometry limited by faulted strips. The discretized velocity model includes almost 20000 blocks with 500 m x 500 m x 250 m minimum dimensions. A relocation technique using this a priori detailed 3D velocity model allows precise locations of induced earthquakes. 351 relocated hypocenters show that of the seismic activity concentrated on geometrical discontinuities of the local dome structure. The locations of seismic events are correlated with geomechanical layers of the structure. Spatial and temporal migration of seismic ruptures mimics the different permeability rings of the reservoir which are progressively depleted by gas extraction. Most of these events are at present confined close to major thrust planes which limit the dome structure laterally, and in depth onto pre-existing faults in the basement below the gas field. The occurence of these deep clusters demonstrates that fluid manipulation in the sedimentary covers can activate pre-existing basement faults. This result changes previous assessments of local seismic risk and provides new insights into fault mechanisms in areas with complex geological structure.

Introduction

Accurate location of earthquake hypocenters is one of the fundamental data analysis problems in seismology. A great deal of effort is devoted to solve this problem, either by improving the algorithm or by increasing significantly the number of seismological data. Usually, relocations of seismic events in complex geological structures are obtained using a three-dimensional inversion technique which solves simultaneous changes in block velocities and hypocenter locations (e.g. Aki and Lee, 1976). The estimated accuracy of hypocenter location (3D problem) is expected to increase with the amount of surface data (fundamentally 2D data set) . In this study, we use 3D a priori information on the subsurface velocity to constrain hypocenter locations, with a limited amount of surface information (maximum of arrival times: 9). Only hypocentral parameters are minimized, in a least squares sense, from a priori 3D velocity model constructed by compiling the whole set of geological and geophysical data (Guyoton, 1991). Numerous producing wells and geophysical exploration data define the local dome structure limited by faulted strips. Such a strong seismic inhomogeneity motivates the need for a precise 3D velocity model to accurate earthquake locations. Relocations are carried out by the modified REL3D program (Roecker, 1982) which uses travel time data in a given three-dimensionally varying structure.

Paper number 92GL00359
0094-8534/92/92GL-00359$03.00

Geophysical characteristics

The Lacq hydrocarbon fields are located in an anticline structure of the French Pyrenean foreland. The autochtonous series including the asymmetrical dome of Lacq (Figure 1) are widely folded at the north pyrenean frontal thrust. The local dome structure is limited to the south by a major fault oriented N120°, and to the west by a faulted strip N10°. The area around the site of hydrocarbon extraction has been aseismic for numerous centuries, since no historic events are known except the active seismic zone of the North Pyrenean Fault which lies 25 km to the south of the field (Grasso and Wittlinger, 1990). The gas producing horizons are dolomitic sandstones and limestones of Portlandian to Barremian age (Vp≈5700 - 6000 m/s, 54 x 10^3 MPa Young's modulus) (Figure 1). An impermeable layer (Sainte-suzanne marls) of lower Aptian age (Vp≈4400 m/s, 33 x 10^3 MPa) about 500 meters thick traps the anhydrous gas. Above these marls lies an Albo-Aptian calcareous reef (Vp≈5800 - 6000 m/s, 60 x 10^3 MPa) 2000 meters thick. This reef is capped by the oil reservoir (with average depth of 600 m) which is covered by molassic Tertiary strata (Vp≈2700 - 3000 m/s). The reef formation is absent on the western and southern flanks of the structure where marls (Vp≈4200-4500 m/s) take place up to 6 km in depth. The figure 3 shows the isobaths of the top of the gas reservoir recently reviewed by new seismic and structural studies (J. de Lanlay, 1990). We note a clearly asymmetry between the north and the south. According to recent exploitation parameters (accumulation, permeability, pressure) producers define different rings within the gas reservoir. These rings range in depth from 3200 m to at least 6000 m with decreasing permeability values. From 1957 to 1989, the total gas pressure drop in the reservoir (first ring) was about 60 MPa.

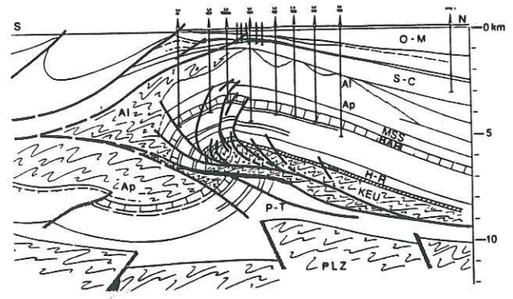

Fig. 1: N-S vertical cross-section of the local geological structure deduced from borehole observations and seimic profiles. O-M: Oligo-Miocene; S-C: Senonian, Cenomanian; Al: Albian; Ap: Aptian; MSS (Marls of Sainte-Suzanne): lower Aptian; BAR: Barremian (reservoir); H-R: Hettangian, Rhetian; Keu: Keuper; P-T: Trias and permian; PLZ: basement.

Dome structure modeling

In order to take into account the local dome structure and the large lateral inhomogeneities described previously, we introduce into the processing of hypocenter location a precise 3D velocity model based on the whole geological and geophysical data set. Lithologic data of more than 46 wells drilled a maximum depth of 6549 m clearly define the asymmetrical geometry of the dome. Numerous seismic profiles (several tens kilometers) allow interpolation between subsurface borehole data and the estimation of the deep structure down to bedrock at more than 10 km depth. From well shootings we assign one average velocity at nineteen geomechanical layers. The block structure (15 x 15 x 10 km^3) is specified by a series of varying perpendicular interfaces. The horizontal block sizes range from 0.5 km x 0.5 km inside the dome structure to 1 km x 1 km outside the structure (Figure 2). Block thicknesses range from 0.250 m between 0 and 6.5 km depth, to 0.500 m underneath. The resulting three-dimensional model is made of about 20000 blocks. It accounts for the following main features of the geological and geophysical sitting: (1) non-consolidated shallow deposits; (2) strong thickness variations of molassic levels; (3) dissymmetrical structure of the dome; (4) 4 low-velocity zones (LVZ) located on the top of the gas reservoir (marls levels), under the dome beds (salt rock), laterally on the western and southern flanks of the dome structure (marls levels); (5) geometry of the layers boundary which mimic the main fault strips.

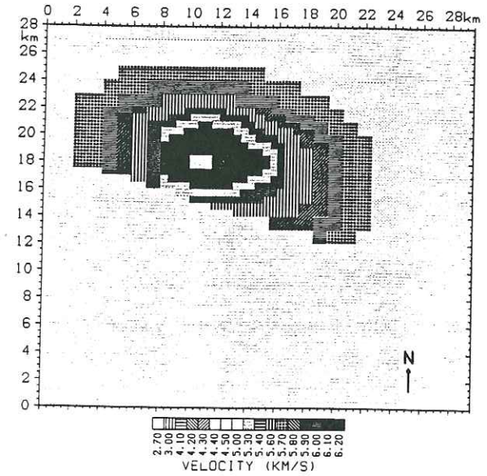

Fig. 2: Map view of the 3D velocity model. This example shows P wave velocity between 5250 and 5000 m at depth.

Seismological patterns

From 1982 to 1989, more than 520 earthquakes with magnitudes ranging from 1 to 3.5 were recorded by a local permanent seismic network of 9 telemetered stations above the gas field. Only 351 events were selected in this study according to the following criteria: (1) the event is recorded by at least 6 stations; (2) the rms residual of the arrival times must be less than 0.2 s; (3) the location algorithm must converge with less than 0.5 km change in location on the final iteration; (4) the condition number (i. e., the ratio of largest to smallest eigenvalues) of the matrix of partial derivatives must be less than 50. We obtain for the relocated events an average rms residual of arrival times of 0.07 s. In the 3D process, the final rms residual has been divided by 2 with respect to the end of the first iteration. It is worth noting that we obtained the same rms values with the 1D and 3D velocity models. It confirms that the rms only allows the estimation of the coherence of travel-times with respect to one model of propagation for a given solution, without allowing any estimation of the accuracy of the absolute locations.

Most of the relocated events are in high velocity sedimentary rocks and on pre-existing geometrical discontinuities within the boundaries of the gas field (Figure 3). The correlation with the estimated extension of the gas field is clear, particularly in the eastern part. A geometry close to the asymmetric dome field structure (Figure 1) is prominent in the S-N section where all the seismicity has been projected (Figure 4). Initial locations obtained with a homogeneous half-space velocity model (Figure 4a) and relocations worked out with a three-dimensional velocity structure (Figure 4b) exhibit the principal features of depth relocations. The main discrepancy between the two location processes is associated with the low-velocity zones above the gas reservoir (500 m thick), below the reservoir (Trias saliferous levels, up to 1500 m thick) and on the flanks of the dome. The LVZ led to migrations in depth and lateral directions (3 km average *X Y Z* change). The seismicity map brings out numerous seismic clusters. Only one cluster has been previously activated in the central part of the field. The location of this central cluster coincides with a possibly pre-existing fault (Feignier and Grasso, 1990). In the northern part of the field a deep cluster of events occured at the end of 1982. Since 1987 another deep cluster appeared in the SE part of the gas field. These new seismic patterns are located into the basement under the gas reservoir (Figure 5) on pre-existing faults determined from reflection studies (see Figure 1). In the S-N cross-section (Figure 5a) only hypocenters with epicentral distances smaller than 1 km are projected regard to the BB' line on Figure 3. Figure 5b shows the same cross-section than figure 5a through the three-dimensionnal velocity model used. In the southern part of the field, well-controlled hypocenters ranging in depth from 2 to 8 km appear to be a new feature of the seismicity since 1985. This swarm underlines a main tectonic fault bounding the dome structure to the South. In the NE part of the field, the

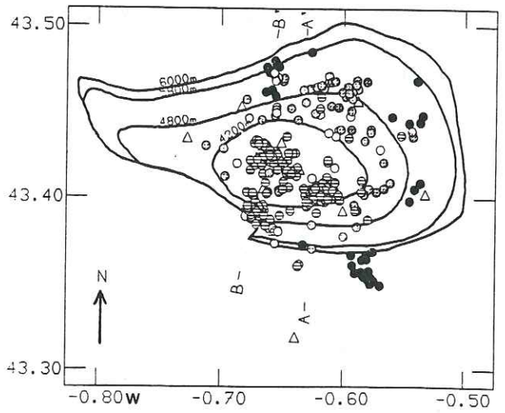

Fig. 3: Epicenter map of the 351 relocated events from 1982 to 1989. The shading scale indicates locations according to depth between 0 km (white circles) and 12 km (dark circle) with a step of 3 km. Open triangles are locations of seismic stations. The curved lines delimite the lateral extension of the gas reservoir.

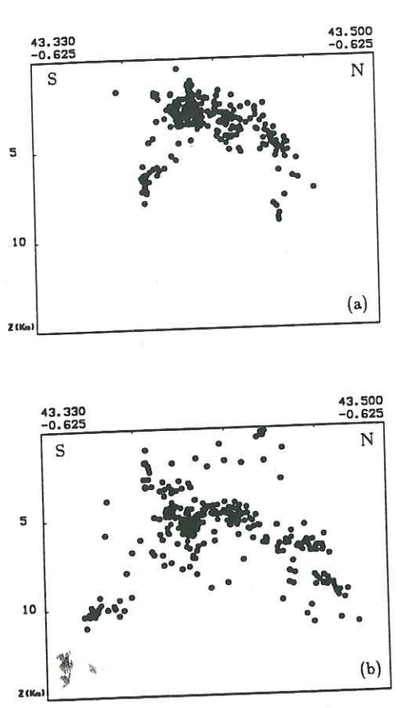

Fig. 4: cross-section in the N-S direction with projection of the whole hypocenter data set: (a) initial locations obtained with a homogeneous half-space velocity model; (b) relocations obtained using the three-dimensional velocity structure. The location of this section is given on figure 3 by AA' line.

seismicity appears more diffuse, while the western part is aseismic. Because no important rheological variations exist at depth below the reservoir between the eastern and the western parts of the field, the inhomogeneity of the seismicity could be result from the reservoir shape, differences in the parameters of production throughout the gas field and the existence of pre-existing planes of weakness.This assumption is reinforced by levelling profiles (Grasso and Feignier, 1990) which exhibit a dissymetric subsidence with respect to the gas reservoir extension. Mechanical modeling using the boundary elements technique shows that the induced deformation can be controlled by pre-existing planes of weakness in the eastern part of the field alone (Grasso et al., 1991). A great vertical asymmetry appears between the activity in the layers above and below the gas reservoir. Plotting of the percentage of events versus the geological layers where they are located (Figure 6) allows us to investigate the 3D pattern of seismicity and the global deformation of the gas field. In the period 1982-1989, the majority of the events is concentrated between the reservoir and the low-velocity zone of the saliferous Trias (P-T). The histogram of Figure 6 exhibits the major role at depth of the calcareous and anhydritic Hettangian-Rhetian (H-R) levels which deaden more than 30 % of the seismic deformation from 1982 to 1989. Less than 2 % of the activity occur above or within the gas reservoir. These events are located along the southern side of the dome structure and underline the overthrust level towards the South . Within the reservoir itself, the effective normal stress increased due to a 60 MPa pore pressure depletion and thus inhibit faulting.

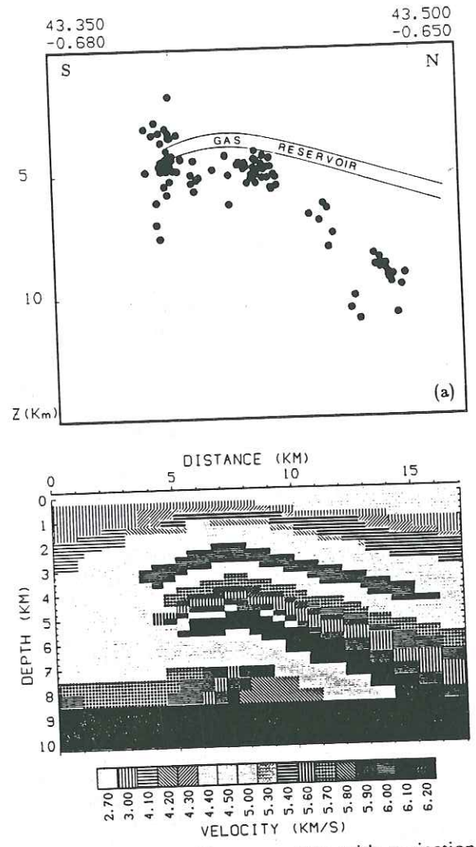

Fig. 5: (a) vertical S-N cross-section with projection of hypocenters 1 km away from BB' line which is plotted on Figure 3; (b) same cross-section as (a) but through the 3D velocity structure used for the relocations of events.

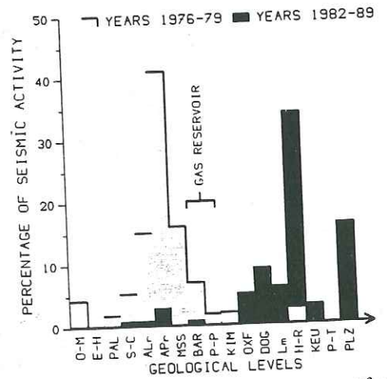

Fig. 6: Histogram represents the percentage of seismic activity in the main geomechanical layers of the local structure above and below the gas reservoir. Full columns show seismic events relocated from 1982 to 1989 and shading columns events relocated between 1976 and 1979 (Grasso and Wittlinger, 1990). The main geomechanical layers are mentioned on Figure 1.

Spatiotemporal migration

The first earthquake was felt during 1969, ten years after the beginning of gas production in a place where no historic seismicity had been reported for at least several centuries (Grasso and Wittlinger, 1990). From 1974 to 1982 more than 800 tremors were recorded by a local network with magnitudes greater than 1.0. Between 1976 to 1982, 220 relocations of seismic events with magnitudes up to 4.2 were obtained using a three-dimensional inversion technique which solves simultaneously changes in block velocities and hypocenters locations (Grasso and Wittlinger, 1990). During this period most of the seismic ruptures had occurred within the stiff part of the overburden above the gas reservoir (Figure 6) and with a highly diffuse location pattern. Since 1982, our results displays essentially deep events occurring below the depleted zone which define numerous organized clusters on large pre-existing faults. The most striking fact in the Lacq field is the migration of the seismic activity towards deeper levels in the 1976-1989 period (Figure 6). However it is worth noting that the distances from the hypocenters to the reservoir remain smaller than 5 km. Note that the 1982 crisis was located below the reservoir both by our technique and the Grasso and Wittlinger technique, attesting for the lack of bias in migration of the activity. The stress changes around the reservoir induced by pressure drop in the gas reservoir (60 MPa at 3750 m), were modeled from poroelastic stressing (Segall and Grasso, 1991) and agree with the observed migrations of the seismic activity during the last 30 years. From 1976 to 1989 the seismic activity spreads along the external part of the central ring of the field. At first, events are more or less concentrated inside the first ring-shaping of the gas reservoir . Subsequently, the seismic activity is more sprawling, according to the new size of the implied reservoir. The time delay to reach this rupture threshold is twice as large below the reservoir than above it. Another feature of the seismicity of the field area is the clustering of earthquakes on pre-existing faults. This clustering activity could be associated to crack coalescence models which are proposed to explain the temporal b value evolution (Volant et al., 1992, submitted). Such pattern as well as the deep migration on basement fault are key parameter to local seismic risk assessment.

Discussion

This paper shows the importance of considering a precise 3D model in a complex geological structure in order to compute accurate seismic locations. The exceptional number of subsurface data available in the hydrocarbon field of Lacq allows us to build an a priori velocity model , which cannot be obtained by standard inversion techniques. We obtained by this process a great coherence between hypocenter locations and preexisting discontinuities. This result emphasizes the interrelation between geophysical structures and instability processes in the earth crust. In this study, seismic instabilities are closely related to high velocity sedimentary rocks and preexisting geometrical discontinuities. At smaller scale the importance of fluid on seismic failure is demonstrated. Seismic and aseismic zone correlate with decreasing and increasing effective stress respectively. In the Lacq field, the main consequence of using of a 3D velocity structure is to move hypocenters towards depth and laterally (3 km average change in position) due to the existence of low-velocity zones and geological discontinuities. The spatial and temporal variations of seismicity are driven by the gas reservoir behaviour. The most striking fact in the Lacq field is the migration of the seismicity to depth in the 1976-1989 time period. Since 1982, deep events defining numerous clusters have occured below the reservoir and are concentrated on major discontinuities of the dome structure and on pre-existing faults in the basement. The fact that deep earthquakes in Lacq area are at present localized on basement faults proves that fluid induced seismicity is not restricted to sedimentary beds. The preliminary study of Segall and Grasso (1991) shows that the implied stress change is less than 1 MPa. The size of pre-existing faults limiting the size of potential earthquakes, the mobilization of basement means sizes of faults potentially more important and less known than faults around the reservoir linked to local dome build up. For the geological structure neighbouring the reservoir, the initial fault sizes could have limited the rupture sizes according to low stress amplitude induced by the depressurization. The knowledge of fault sizes in basement and the regional stress deviator are necessary to assess a new local seismic risk.

Acknowledgements: The authors gratefully thank the Société Nationale Elf-Aquitaine for authorizing this publication. This study benefitted greatly from the seismic monitoring carried out by the IPG Strasbourg. This study was supported by the Société Nationale Elf-Aquitaine under contract 915/9/829.

References

Aki, K. and W.-H.-K. Lee, Determination of three-dimensional velocity anomalies under a seismic array using first P arrival times from local earthquakes. 1. A homogeneous initial model, J. Geophys. Res., 81, 4381-4399, 1976.

Feignier, B. and J.-R. Grasso, Seismicity and deformation induced by gas production: I. correlation of focal mechanisms and dome structure, Pure Appl. Geophys., 134, 405-426, 1990.

Grasso, J.-R., and B. Feignier, Seismicity induced by gas reservoir: II. lithology correleted events induced stresses and deformation, Pure Appl. Geophys., 134, 427-450, 1990.

Grasso, J.-R., and G. Wittlinger, Ten years of seismic monitoring over a gas field area, Bull. Seismol. Soc. Am., 80, 450-473, 1990.

Grasso, J.-R., Ph. Volant, D. Fourmaintraux and V. Maury, Relation between hydrocarbon extraction, local triggered earthquakes and major regional earthquakes: example of the Pyrenean area, 32nd U. S. Symposium on Rock Mechanics, Oklahoma, 1991.

Guyoton, F., Sismicité et structure lithosphérique des Alpes occidentales, Doctorat thesis, U. J. F. of Grenoble, 290 pp., 1991.

J. de Lanlay, Lacq profond: calage de l'historique sur modele, Report to SNEA(P), EP/S/PRO/GIN E.90.020, 1990.

Roecker, S. W., Velocity structure of the Pamir-Hindu Kush region: possible evidence of subducted crust, J. Geophys. Res., 87, 945-959, 1982.

Segall, P. and J.-R. Grasso, Poroelastic stressing and induced seismicity near the Lacq gas field, EOS Trans. AGU, 72, 44, 331, 1991.

F. Guyoton, J.-R. Grasso and Ph. Volant, Laboratoire de Géophysique Interne et Tectonophysique, Observatoire de Grenoble, B.P. 53X, 38041 Grenoble Cedex, France.

received: November 12, 1991
revised: February 3, 1992
accepted: February 4, 1992

26

COMPÉTITION ENTRE LES REJEUX SISMIQUES ET ASISMIQUES DE FAILLE.

GEOPHYSICAL RESEARCH LETTERS, VOL. 19, NO. 11, PAGES 1149-1152, JUNE 2, 1992

b-VALUE, ASEISMIC DEFORMATION AND BRITTLE FAILURE WITHIN AN ISOLATED GEOLOGICAL OBJECT : EVIDENCES FROM A DOME STRUCTURE LOADED BY FLUID EXTRACTION

Philippe Volant[1], Jean-Robert Grasso[1], Jean-Luc Chatelain[1,2] and Michel Frogneux[3]

Abstract. Studies of b-values are usually performed either at rock sample scale (laboratory experiments) or at crustal scale (earthquakes). But interpretations at crustal scale are extrapolated from small scale experimental laws with well defined boundary conditions, to a larger object with no clear boundary conditions. We examine variations of the b-value in time and space at spatial (10x10x10 km^3) and temporal (20 years) scales intermediate between laboratory analyses and tectonic processes, in a dome structure that is an isolated geological object with defined boundaries and known geomechanical properties. Seismic activity (about 1000 events with magnitude ≤ 4.5) and aseismic displacements (6 -7 cm of cumulative subsidence) have been induced by gas extraction in an area where no displacement had previously been reported. We find no agreement between temporal variations in b-values and results from laboratory experiments : there is no correlation between b-values and stress histories, nor between b-values and the spatial migration of seismicity. Aseismic slips introduce anomalies in b-value behaviour when seismic instabilities are a second order process compared to the whole deformation. These observations imply that when changes in b values have been used for earthquake forecasting, false alarms can be explained by the occurrence of aseismic displacement.

Introduction

In b-value studies made using acoustic emission (AE) in laboratory experiments the characteristic parameters (degree of sample homogeneity, stress increase, space - time development of microfractures, size of microfractures, etc.) are known. In natural conditions it is difficult, even impossible, to have a precise knowledge of these parameters, because the size of the studied object cannot be clearly defined. Forecasting of major events using changes in b-values are thus either empirical or ineffective.

For earthquakes, the frequency of occurrence is a log-linear function of the magnitude [Gutenberg and Richter, 1949], corresponding to a power-law distribution of seismic moment or fault length. Mogi [1962, 1985] found the same frequency-magnitude relationship for microcracks as for earthquakes. Mogi [1980] and Hirata [1987], investigating b-values of microcracks in rock samples, noted that the b-value decreases before macroscopic failure caused by a constant or even a decreasing external stress.

Scholz [1968] repeated Mogi's initial laboratory experiments on rock deformation, using a larger frequency range, and showed that b-value is inversely proportional to the stress applied to the rock sample. A study of b-values in the Denver hydrocarbon field by Wyss [1973] local earthquakes in the vicinity of a water injection well, is consistent with Scholz's results [1968].

[1] Laboratoire de Géophysique Interne et Tectonophysique
[2] Office de la Recherche Scientifique et Technique Outre-Mer
[3] Institut de Physique du Globe de Strasbourg

Paper number 92GL01074
0094-8534/92/92GL-01074$03.00

McGarr [1976] using magnitude-frequency relationship of mine tremors argued that there is no simple correlation between b-value and stress changes up to 100 bars. He suggested that a change of 500 bars or more would be necessary to obtain significant results in his case study.

Main *et al.* [1990] show that b-values in laboratory experiments is anticorrelated to stress intensity K [e.g., Lawn and Wilshaw, 1975], which combines stress and crack length. They propose that it is a critical value of K rather than that of the stress which determines the rupture time, using a damage theory based on fracture-mechanics.

In this paper we study a cluster of seismicity located in a place that was historically aseismic before the beginning of a perturbation in the stress field due to gas extraction. The gas field is located 30 km north of a regional area of seismicity defining a narrow east-west strip along the North Pyrenean Fault. Spatial and temporal distributions of earthquakes in the gas field are correlated with the gas field deformation and pressure history [Grasso and Wittlinger, 1990]. Because of the gas extraction, the underground geomechanics is well known (boreholes associated with oil and gas exploration, seismic profiles, preexisting faults, effective stress variations deduced from gas pressure drop, etc.). All these data create a situation close to laboratory experimental conditions, but on a larger scale. We analyse spatial and temporal variations in b-values behaviour during a 17-year period (1974-1990) and test the models discussed above at an intermediate scale between laboratory experiments and regional crustal observations.

Space-time Patterns of Stress and Induced Seismicity

Seismicity began in the Lacq gas field in 1969, 10 years after gas extraction started. No historic seismicity had been reported here for at least several centuries [Grasso and Wittlinger 1990]. The local induced seismic activity is well defined, 30 km away from the strip of the regional seismicity in the Western Pyrenees. The hypocenter distribution of induced events, deduced from the local seismic network operating since 1974, confirms that there is no seismically active zone connecting seismicity induced by fluid extraction in the Lacq area and that occurring on the North Pyrenean Fault system. The envelope of the induced hypocenter locations mimics the dome structure within the gas reservoir stand [Grasso and Wittlinger, 1990 ; Guyoton *et al.*, 1992]. All these observations allow us to consider the 10x10x10 km^3 volume defined by the envelope of the induced seismicity as acting as a closed system. This assumption is enhanced by the results obtained from numerous levelling profiles conducted in the area [Grasso and Feignier, 1990]. These profiles exhibit a subsidence of few centimeters correlated in both space and time with the gas pressure drop (Figure 1), implying that the regional deformation is elastic to first order. At a smaller scale Grasso *et al.* [1991] have shown that the behaviour of the subsidence is consistent with aseismic slip on three major faults. The sizes of the induced seismic sources, estimated by spectral analysis of seismic waves, show that seismic instabilities have only a second order effect on the displacement (maximum dislocations < 2 centimeters, maximum radius < 300 meters) [Feignier and Grasso, 1992].

Two phases of seismic activity have been observed. From 1974 to 1982 most of the seismic activity occurred within the stiffest part of the overburden, with highly diffuse locations (Figure 2a) [see also Grasso and Wittlinger, 1990]. Since

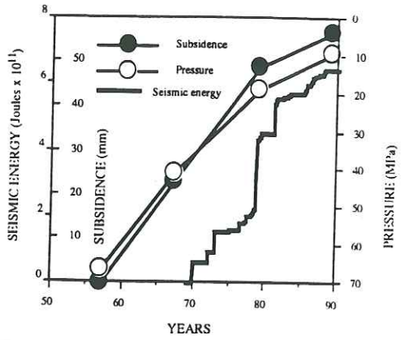

Fig. 1 : Temporal evolution of seismic energy, subsidence and gas pressure drop, since the beginning of gas extraction (1957). Subsidence is the maximum displacement measured at the top of the subsidence bowl. Gas pressure drop is averaged over several wells with a standard deviation ≤ 1 MPa.

1983, deep events have occurred below the reservoir and are more organized on large preexisting faults, defining several clusters (Figure 2b) [see also Guyoton *et al.*, 1992].

The forces applied at the boundaries of such a system are (1) tectonic forces and (2) gas reservoir pressure. Over a time scale of tens of years, we consider that tectonic forces are constant and that possible earthquake after-effects of regional seismicity are short-period phenomena [Grasso *et al.*, 1992]. Thus, the main perturbation of the medium over the 30-year time period of this study has been induced by the pore pressure decrease of the gas reservoir.

Stress changes in the overburden, as well as within the bed below the reservoir, were modeled using pororelastic stressing by Segall and Grasso [1991]. The basic result is that stress changes outside the reservoir (where seismic instabilities occur) are proportional to the pore pressure drop within the gas reservoir itself, despite the fact that there is no direct fluid connection between the reservoir and the overburden. The same critical stress threshold is necessary to explain both the rupture above and below the reservoir, except that due to the free surface a time delay to reach this threshold is two times smaller above the reservoir than below it. The calculated change in shear stress, which triggered shallow seismic activity in 1969 and deeper activity in 1983, is in both cases less than 1 MPa. Even if such stress changes are small, they are of the same order of magnitude as those recognized to drive seismic instabilities in the neighbourhood of artificial water reservoir [Roeloffs, 1988].

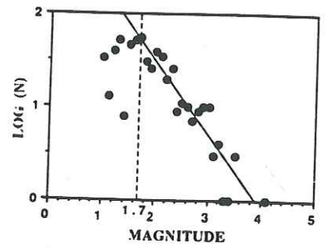

Fig. 2 : Temporal evolution of seismicity across the gas field. The events are plotted on vertical cross-sections. The coordinates of the end points of the cross section are indicated on both ends of the figure. (a) Activity from 1976 to 1982, [data from Grasso and Wittlinger, 1990]; (b) Activity from 1983 to 1989, [data from Guyoton *et al.*, 1992]. The distribution of the seismicity is diffuse during the first time period, while clusters appear during the second time period.

Study of the magnitude frequency relationship

Since 1974, when a local network was installed, we have observed induced seismic activity and computed b-values in order to understand its physical meaning at a scale intermediate between (1) laboratory measurements on rock core samples, where each parameter is controlled, and (2) a large tectonic area where boundary conditions are difficult to isolate. The Lacq local network has operated continuously with only one interruption between July 1979 and December 1979. Starting in 1974, 4 stations were installed and 5 more stations were added between 1974 and 1979. Between 1974 and 1990, about 1000 induced events were detected with a local magnitude ranging from 1.0 to 4.2. Seismicity during the period 1974-1979, in numbers of both low and high magnitude earthquakes, was higher (while the network was smallest), than since 1979 (complete network). We can thus assume that during the first period no significant events were missed. The cutoff magnitude determined by the log-linear portion of the discrete frequency magnitude plot is 1.7 (Figure 3). About 500 events are selected according to this criteria.

As we have a magnitude range spanning less than 2 units, we used the general maximum likelihood estimation of b, where b'=b/log10 [e.g., Page, 1968] :

$$b = \log_{10} e \left[\overline{m}_l - \frac{m_{lmin} - m_{lmax} e^{-b'(m_{lmax} - m_{lmin})}}{1 - e^{-b'(m_{lmax} - m_{lmin})}} \right]^{-1}$$

We calculated the b-value using windows of N events. Windows of N events was preferred to windows of N months in which the difference in the number of events would give heterogeneous results because the seismic activity was not steady. We computed variations in b-values using several windows (between 60 and 100 events) and different increments (between 1 and the window value). Despite some high frequency variations, the general trend is the same. The smoothest variations in b-values were obtained with a window of 87 events. As we are interested in long term b-value variations, we chose this value for the study. Two distinct stages in the behaviour b-value are observed (Figure 4a and

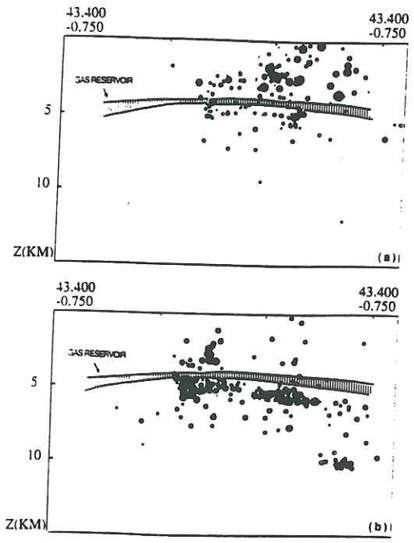

Fig. 3 : Discrete frequency distribution of magnitudes. The dotted line shows our cutoff magnitude (M_l = 1.7).

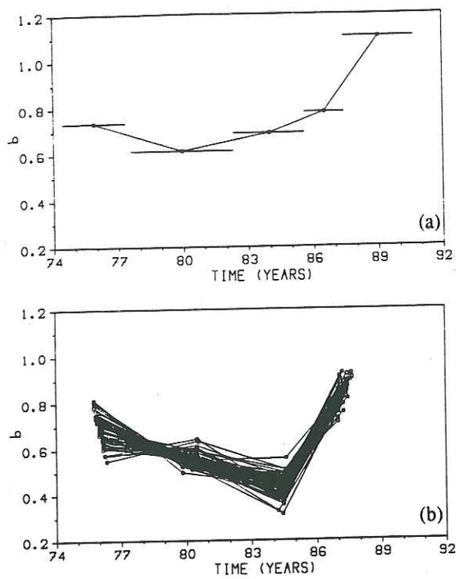

Fig. 4 : Temporal b-value evolution from 1974 to 1990. (a) using a window of 87 events, with an increment of 87 events. Horizontal bars represent the time necessary to obtain a sample of 87 events. (b) using a window of 87 events, with an increment of 87 events. The range of uncertainty on the magnitude is ± 0.1. To obtain the slope b, we added a random value ranging from -0.1 to 0.1 to the magnitudes.

Figure 4b) : a decrease between 1974 and 1982 followed by an increase from 1983 to 1990. The goal of this paper is to relate the b-value variations to the local stress and seismicity history.

Discussion

The Lacq gas field area is considered as a well defined geological object, at a scale intermediate between a rock sample and a tectonic feature, with well defined boundaries and a recent seismological history. In this geological object five facts are observed : (1) a decrease of b-values between 1974 and 1982, followed by an increase from 1983 to 1990 ; (2) a decrease of the gas pressure between 1974 and 1990 that drives the induced stresses in rock above and below the gas reservoir, according to poroelastic stressing [Biot, 1941; Segall and Grasso 1991]; (3) a migration of the seismicity in depth starting in late 1982 - early 1983 ; (4) a change in hypocenter distribution, from diffuse to clustered and (5) a continuous subsidence starting in the 60's correlated with pressure drop, i.e. to stress increase. Mechanical modeling using the boundary elements technique shows that the shape of the subsidence profile can be controlled by aseismic slips on pre-existing faults [Grasso et al., 1991].

Observations (1) and (2) are inconsistent with Scholz's [1968] observations, which predict a continuous decrease of b-values with monotonically increasing stress. A possible explanation is that the stress increase is too small, although it is big enough to trigger and to sustain seismicity. There is thus a paradox : the motor of induced seismicity is pressure change (i.e. stress), but the observed b-value variations are not correlated to this key parameter.

As we observed a migration in the depth of the seismicity (observation 3), we have computed b-values separately for events located above (z < 5 km) and below the reservoir (z > 5 km). The differences between each data set are not significant. The observed b-value variations of the two data subset and that observed from the whole data set are the same. Thus, the contrast in geomechanical properties of rock matrices located above and below the reservoir, within which seismic fractures occur, does not affect the b-value. This is in contradiction to studies on rock samples [e.g. Mogi 1962, 1985], as well as Talwani's [1981] interpretation of b-values from earthquakes around an artificial reservoir, based on differences in rock properties.

Thus, given the first 3 observations, neither the increase of effective stress nor the rock mechanical properties can explain the temporal change in b-value behaviour.

The space-time evolution of the distribution of hypocenters exhibits two patterns (observation 4). During the first period (1974-1982), the seismicity is diffuse with neither aftershocks nor clustering, although the more energy is released during this period than later. In the second period (1983-1990) most of the seismicity in concentrated in several clusters. This change can be interpreted as pre-coalesence or coalescence of cracks. This process would imply a strong decrease in b, as predicted by studies of rock samples [Main *et al.* 1990]. This is opposite to what we observed.

Thus, the variations in b-values that we observed do not support published models obtained from rock mechanics experiments : we find no correlation with stress or stress intensity factor changes, nor with rock property changes. Nevertheless recent laboratory results [Main, personal communication 1992] propose that an increase in b-value might be associated with stable crack coalescence during experiments on wet core samples. They observed a stable b-value increased during crack coalescence and associated strain softening, due to a controlled drop in pore fluid pressure because of dilatant microcracking. The other difference between rock sample experiments and our study (the main difference is these variations in b-value) is the aseismic subsidence (observation 5) occurring simultaneously with seismicity [Grasso et al., 1991], while in rock mechanics experiments, acoustic emission from microcracks is mainly observed after elastic deformation is completed. Moreover, the subsidence is correlated with stress changes (figure 1) and accounts for a large part of stress release in the gas field area [Grasso and Feignier, 1990]. This could explain the discrepancies in b-value behaviour between rock experiments and our study. b-value variations alone would be insufficient to understand seismic instabilities because it does not include aseismic events, as also proposed, at a larger scale, by Robinson [1979]. In some case study b-value variations, deduced from seismic instabilitiy studies, a major event is predicted, but if this event is aseismic, a false prediction might result. On the other hand, when foreshocks of large seismic events (earthquakes) are mainly aseismic processes (slow and silent earthquakes), the b-value variations are inefficient to predict this kind of instability.

Conclusion

Our study of b-value behaviour of induced earthquakes within an isolated geological object shows that laws deduced from rock sample experiments fail to explain our observations. Neither stress changes, although they trigger the seismicity, nor migration of seismic activity control b-value changes. A key factor to explain these discrepancies is the simultaneous occurrence of both aseismic slips and earthquake fractures. Depending of the mechanical behaviour of the studied area we can observe either aseismic foreshocks of earthquakes or earthquake fractures as foreshocks of large aseismic instabilities.

On the basis of both Scholz's report [1968] and observations of b-value decrease prior to large earthquakes [e.g. Suyehiro *et al.*, 1964 ; Li *et al.*, 1978], changes in b-values have been proposed as a precursor of major earthquakes, although

correlation between b-value variations and occurrences of large earthquakes is not always observed. b-value interpretations for earthquake processes using results of rock sample analyses remain ambiguous if only stress interpretation is used, except of specific cases [e.g. Wyss, 1973]. In particular, false alarms of main earthquakes might be explained by occurrence of a main aseismic event. Therefore, in order to use variations in b-values to forecast major earthquakes in regions where significant aseismic deformation takes place, we should somehow include aseismic slip, slow earthquakes etc. in b-value calculations and certainly monitor other parameters (Q^{-1}, wich seems more simply related to creep than the b-value [Sato 1988; Jin and Aki, 1989]).

In our case study we now observe a clustering of seismicity, a decrease of seismic energy release and a locking of subsidence. From a classical seismological point of view this information can lead to a forecast of a major event. The question remains wether we know if the event will be seismic or aseismic. In addition, this information can be interpreted to forecast the end of gas production. In any case, the social and economical impact of these phenomena will be important : for instance for anticipating the shearing of wells in the first case (seismic or aseismic slip within the area where boreholes are situated), and for anticipating termination of the gas production and its social impact in the second case.

Acknowledgements. This study was supported by Université Joseph Fourier and ORSTOM. We thank Dr. Ian G. Main and two anonymous reviewers for constructive comments on the manuscript. Dr. Friedrich Heller provided very helpful editorial assistance. We thank Elf Aquitaine for permission to publish this work. The views expressed are the authors' own and not necessarily those of Elf Aquitaine.

References

Biot, M.A., General theory of a 3-dimensional consolidation, *Appl. Phys., 12*, 155-164, 1941.

Feignier, B. and J.R. Grasso, Seismicity Induced by Gas Production: I. Correlation of focal Mechanisms and Dome Structure, *Pure Appl. Geophys., Vol. 134, No. 3*, 405-426, 1990.

Grasso, J.R. and B. Feignier, Seismicity Induced by Gas Production: II. Lithology Correlated Events, Induced Stresses and Deformation, *Pure Appl. Geophys., Vol. 134, No. 3*, 427-450, 1990.

Grasso, J.R. and G. Wittlinger, Ten years of seismic monitoring over a gas field, *Bull. Seism. Soc. Am. 80*, 450-473, 1990.

Grasso, J.R., J.P. Gratier, J.F. Gamond and J.C. Paumier, Stress diffusion triggering of earthquakes in the upper crust, *Special Issue Mechanical Instabilities in Rock and Tectonics, J. Struc. Geol.*, 1992 in press.

Grasso, J.-R., P. Volant, D. Fourmaintraux and V. Maury, Relation between hydrocarbon extraction, local triggered earthquakes and major regional earthquakes : example of the Pyrenean area, *32nd U. S. Symposium on Rock Mechanics*, Oklahoma, 1991.

Gutenberg, B. and C.F. Richter, Seismicity of the Earth, *Princeton Univ. Press.*, 1949.

Guyoton, F., J.R. Grasso and P. Volant, Interrelation between induced seismic instabilities and complex geological structure, *Geophys. Res. Lett. 19, 7*, 1992.

Hirata, T., Fractal structure of spatial distribution of microfracturing in rock, *J. Geophys. Res. 90*, 369-374, 1987.

Jin, A. and K. Aki, Spatial and temporal correlation between coda Q^{-1} and seismicity and its physical mechanism, *J. Geophys. Res. 94*, 14041-14059, 1989.

Lawn, B. R., and Wilshaw, T. R., Fracture of brittle solids, *Cambridge University Press, Cambridge 1975* 204 pp.

Li, Q. et al., Time and space scanning of the b-value, *Acta Geophysi. Sini. 21*, 101-124, 1978.

McGarr, A., Dependance of magnitude statistics on strain rate, *Bull. Seism. Soc. Am. 66*, 33-44, 1976.

Main, I.G., P.G. Meredith, P.R. Sammonds and C. Jones, Influence of fractal flaw distributions on rock deformation in the brittle field, *Geol. Soc. Spec. Publi. 54*, 71-79, 1990.

Mogi, K., Study of the elastics shocks caused by the fracture of heterogeneous materials and its relations to earthquake phenomena, *Bull. Earthquake Res. Inst., Tokyo Univ. 40*, 125-173, 1962.

Mogi, K., Review of "Rock friction and earthquake prediction" edited by J. D. Byerlee and M. Wyss. *Tectonophysics, 65*, 378-379 1980.

Mogi, K., Earthquake prediction, Earthquake Resarch Institute University of Tokyo, *Academic Press*, 1985.

Page, R., Aftershocks and microaftershocks of the great Alaska earthquake of 1964, *Bull. Seism. Soc. Am. 58*, 1131-1168, 1968.

Robinson, R., Variation of energy release, Rate of occurrence and b-value of earthquakes in the main seismic region, New Zealand, *Phys. Earth Plan. Sci.*, 18, 209 - 220, 1979.

Roeloffs, E. A., Stability changes induced beneath a reservoir with cyclic variations in water level, *J. Geophys. Res. 93*, 2107-2124, 1988.

Sato, H., Temporal change in scattering and attenuation associated with the earthquake occurrence - A review of recents studies on coda waves, *Pure Appl. Geophys., 126*, 465-498, 1988.

Scholz, C. H., The frequency-magnitude relationship of microfracturing in rock and its relationship to earthquakes, *Bull. Seism. Soc. Am. 58*, 399-415, 1968.

Segall, P. and J.R. Grasso, Poroelastic stressing and induced seismicity near the Lacq gas field, *EOS, Trans. Am. Geophys. Union*, 72, p. 331, 1991.

Suyehiro, S. T. Asada, and M. Ohtake, Foreshocks and aftershocks accompagnying a perceptible earthquake in central Japan, *Paper Meteorol. Geophys. 15*, 17-88, 1964.

Talwani, P., Earthquake Prediction studies in South Carolina, in *Earthquake Prediction : An International Review, Maurice Ewing Ser. vol. 4*, edited by D. W. Simpson and P. G. Richards, 381-393, AGU, Washington D. C., 1981.

Wyss, M., Towards a physical understanding of the earthquake frequency distribution, *Geophys. J. R. Astr. Soc. 31*, 341-359, 1973.

P. Volant, J.-R. Grasso, J.-L. Chatelain LGIT-IRIGM BP 53X 38041 Grenoble Cedex France.
J.-L. Chatelain ORSTOM BP A5 Nouméa New Caledonia.
M. Frogneux IPGS 5 rue René Descartes 67084 Strasbourg Cedex France.

(Received : March 16, 1992
Revised : May 5, 1992
Accepted : May 6, 1992)

3

ECHELLE REGIONALE DES CONNECTIONS FLUIDES

Les effets des fluides sur le déclenchement des ruptures, analysés en termes de variations des contraintes effectives, sont souvent étudiés in-situ à une échelle kilométrique. Les travaux les plus connus, soit en terme d'augmentation de la pression de fluide (Denver, Colorado) soit dans le cas de diminution de la pression de fluide (Lacq, Aquitaine) ont principalement analysé les ruptures qui se produisent à des distances proches des perturbations de pression de fluides (≤5 km). Pourtant à Denver les séismes majeurs (M~5) sont localisés à plus de 8 km du puits injecteur, 14, 18 et 24 mois après l'arrêt des injections. Ici nous proposons 3 études types de connections possible. Le premier cas, classique dans son analyse, est le cas d'une sismicité déclenchée par la mise en eau d'un réservoir artificiel, le barrage de Monteynard, France. L'intérêt géographique de cette étude se situe au niveau des implications potentielles sur la cartographie et le comportement des failles dans les massifs sub-alpins et plus particulièrement au voisinage des mégapoles. Les variations du niveau de la retenue, situé à une vingtaine de kilomètres de l'agglomération grenobloise, semble influencer le comportement sismique régional sur des distances de 15-30 km. Le deuxième cas, sur notre terrain d'expérimentation favori, étudie les connections possibles entre l'extraction du gaz de Lacq, les séismes de la faille nord pyrénéenne, et la réponse sismique au voisinage du gisement lui-même. Enfin, le troisième cas s'attache à étudier des connections verticales plus que horizontales, en tentant de comprendre les séismes majeurs (M~7) survenus sous le gisement de Gasli (Ousbékistan). Une étude microsismique permet de définir les géométries des zones sismiques jusqu'à 20 kilomètres de profondeur.

TROISIEME ITERATION: Inévitablement, des instabilités sous-jacentes commencent à se dessiner. (Ian Malcolm)

31

ACTIVITE SISMIQUE DE LA FAILLE NORD PYRENEENNE ET DEPLETION DU GISEMENT DE LACQ: QUELS LIENS POSSIBLES?

Journal of Structural Geology, Vol. 14, No. 8/9, pp. 915 to 924, 1992
Printed in Great Britain

0191-8141/92 $05.00+0.00

Stress transfer and seismic instabilities in the upper crust: example of the western Pyrenees

J.-R. GRASSO, J.-P. GRATIER and J. F. GAMOND

Observatoire de Grenoble, LGIT, IRIGM. B.P. 53X, F-38041 Grenoble Cédex, France

and

J.-C. PAUMIER

Applied Mathematics Department, Grenoble University, F-38041 Grenoble Cédex, France

(*Received* 9 *October* 1991; *accepted in revised form* 28 *April* 1992)

Abstract—When the regional state of stress is close to the condition for earthquakes to occur, small stress and strain changes could trigger seismic instabilities. Stress diffusion ($\Delta\sigma$ = 1–2 MPa) has been suggested to explain, at lithospheric scale, space and time correlated earthquakes and surface deformations in subduction zones (100–200 km, 10–40 years). We test the possible regional mechanisms, at the upper crustal scale, in the western Pyrenees, where major regional events (M_{max} = 5.7), locally induced events and subsurface fluid pressure fluctuations are temporally and spatially correlated.

In a first phase, fluid withdrawal (decrease of pore pressure of the aquifer at the gas–water interface) affects the natural regional seismicity rate. The locked fault inhibits small events for a time, during which tectonic stresses accumulate. Major regional events then occur on the Pyrenean Fault, when the energy of deformation is large enough to allow seismic instabilities to occur. These major events ($M_l > 5$) trigger seismic instabilities ($M_l = 4$), in the vicinity of the gas extraction area, 30 km away. As a result of gas extraction, the Lacq field zone has local weakness characteristics similar to the neighbouring main active fault. The Pyrenean earthquakes lead the gas field events by 2 years. This correlation is consistent with a viscoelastic model, where salt rock acts as a viscoelastic channel, below an elastic bed.

The possible connections proposed here may give a new insight worldwide in understanding the role of fluids in seismic instabilities and seismic risk assessment in the neighbouring of man-made fluid pressure fluctuations, when natural seismic activity is high.

INTRODUCTION

SEISMIC instabilities induced by increasing pore water pressure have been reported for many years. When injection of water takes place, the effective stress value decreases and the Mohr–Coulomb failure criterion seems to be verified *in situ* in different places for small pressure fluctuations (Raleigh *et al.* 1972, Fletcher & Sykes 1977, Nicholson *et al.* 1988). It was shown that connected distances in the upper crust can reach a tenth of a kilometre scale, with a time delay for pore pressure migration of a few years (cf. Hsieh & Bredehoeft 1981). Recent modelling of the water reservoir pore pressure effect on local seismicity shows that a small stress change (<0.1 MPa), could trigger or inhibit seismic instabilities depending on the orientation of pre-existing discontinuities in the vicinity of a storage dam (cf. Simpson 1986, Roeloffs 1988, Simpson *et al.* 1988a). Moreover, coseismic stress perturbations after moderate earthquakes are reported to affect creep on a fault 30 km away (cf. Simpson *et al.* 1988b). Associated stress changes are small (<0.01 MPa). All the previous observations and models attest the possible effect of small stress changes induced by increased pore pressure on seismic or aseismic displacements.

Elsewhere Grasso *et al.* (1992) reported numerous cases of newly recognized instabilities. They are induced by underground fluid pressure fluctuations with decreased pore pressure. These instabilities are triggered or induced by fluid extraction. The driving stress changes involved, modelled using either poroelastic stress transfer or mass effects, are of the same order as described previously; i.e. 0.1–1.0 MPa (cf. Segall 1989, McGarr 1991).

In the Lacq area of the French Pyrenees, accurate determination of the location of seismic events shows that few events, if any, occur within the gas reservoir itself, in agreement with the increase in effective normal stress (Grasso & Wittlinger 1990, Guyoton *et al.* in press). Two seismic activity phases were observed. In a first period (1974–1980) most of the seismic ruptures occur within the stiff part of the overburden, with a highly diffuse location pattern (Grasso & Wittlinger 1990). Since 1982, deep events have occurred below the reservoir and are more organized on large pre-existing faults, defining numerous clusters (Guyoton *et al.* in press). The stress change in the overburden and in the beds below the reservoir have been modelled by Segall & Grasso (1991) using poroelastic stressing. The basic result is that stress changes outside the reservoir (where seismic instabilities occur) are proportional to the decrease in pore pressure within the gas reservoir, despite the fact that no fluid connection exists between the reservoir and the overburden. The calculated change in

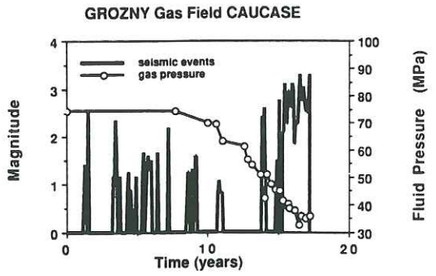

Fig. 1. Seismicity and gas pressure decrease due to gas extraction (Grosny field, Tchechen Republic. Caucasus) from 1956 to 1974 (Smirnova personal communication, 1990). Zero value on the time axis corresponds to year 1956. Pressure values are the average gas reservoir pressure. Earthquake magnitudes are local magnitude.

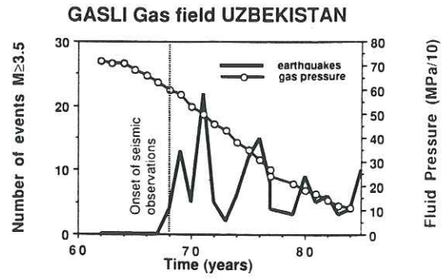

Fig. 2. Seismicity and gas pressure decrease due to gas extraction (Gasli field, Uzbekistan) from 1960 to 1984 (adapted from Plotnikova *et al.* 1989). Zero value on the time axis corresponds to year 1960. Pressure values (MPa/10 = bars) are the average gas reservoir pressure. Earthquake magnitudes are local magnitude.

shear stress for a 25 MPa pressure drop after 10 years of extraction, which corresponds to the onset of seismic activity in 1969, is less than 1 MPa. The same critical stress thresholds are necessary to explain both the rupture above and below the reservoir, except that, due to the free surface, the time delay to reach this threshold is twice as long below the reservoir as above it. Even if such stress changes are small, they are of the same magnitude as those known to drive seismic instabilities in the vicinity of artificial water reservoirs (Roeloffs 1988).

When reported, the seismic instabilities induced by fluid extraction are regional patterns in most of the observed cases: when induced seismic activity occurs within one field, it is also reported in the neighbouring ones (cf. North Sea, Holland, France, Uzbekistan; Grasso 1991). This could imply that a continental plate in mechanical equilibrium and faulted over its entire surface, corresponds to a state of the crust in which the rupture criterion is almost reached everywhere (cf. Sornette *et al.* 1990). This condition is intimately related to the observation at another scale of active faults almost everywhere within the plate. From the above setting, the possible relations between fluid pressure fluctuations, local triggered events and regional seismicity patterns can be analyzed. While the local seismic instabilities sustained in the Lacq area over more that 20 years are driven by the monotonic poroelastic stressing alone, the onset of the two seismic phases in the Lacq area, i.e. 1969—first $M_l > 3$ event above the reservoir, 1982—first $M_l > 3$ event below the gas reservoir, may have been triggered by the combined effects of both the local poroelastic stressing and the stress transfer due to the major regional earthquakes.

In this paper, it is proposed to investigate, at a regional scale, the possible effects of local fluid pressure fluctuation. It is interesting to note that the possible connection between regional seismicity patterns and the history of decrease in pore pressure in hydrocarbon reservoirs is observed in different regions, cf. Grozny field (Fig. 1), Tchetchen Republic, Caucasus, Gasli and Tchurtan fields (Figs. 2 and 3), Uzbekistan, Lacq field, Pyrenees, France (Fig. 4). Although processes explaining the local instabilities induced in the vicinity of fluid pressure fluctuations were recently proposed and reviewed by Grasso *et al.* (1992), the regional effect at upper crustal scale has not yet been investigated. Here it is proposed to test the possible regional mechanisms, at the upper crustal scale, in the western Pyrenees where natural seismicity ($M_{max} = 5.7$) is located 20–30 km from the seismicity triggered by hydrocarbon extraction. In this area, geological and hydrological data fix the limits of the estimates of pore pressure, and stress and strain changes. At the upper crustal scale, the geometry of the layers involved is governed by décollement levels and rocksalt beds. If these processes are verified, these pressure changes must be considered in order to understand the role of fluids in fault mechanics and medium-term seismic prediction.

PRINCIPLES OF METHODS AND APPLICATION IN THE WESTERN PYRENEES

The accurate geomechanical analysis of the Lacq gas field response to fluid pressure fluctuations is performed using levelling data and induced seismicity (Grasso & Feignier 1990). The gas field induced swarm is located 25 km north of a high seismicity area (Fig. 5). This seismicity defines a narrow strip, well defined over several hundred kilometres as the main seismic fault of the Pyrenees (the North Pyrenean Fault). Only a few large earthquakes have originated in this pre-existing zone of weakness over the past centuries ($M_l = 5.7$ in 1967; $M_l = 5.3$ in 1980; $M_l = 5.0$ in 1982). All these events occurred within 30 km of the gas field. Two possible connection mechanisms between the two seismic areas can be investigated. The corresponding processes are water pressure diffusion and viscoelastic stress transfer.

Water pressure drop

Looking at the Grosny, Gasli, Tchurtan and Lacq examples, the first part of this paper suggests that gas extraction changes the hydrological state of the area.

(i) When fluid connection is geologically possible (i.e. water flow along décollement level), the decrease in gas pressure induces a decrease in water pressure around

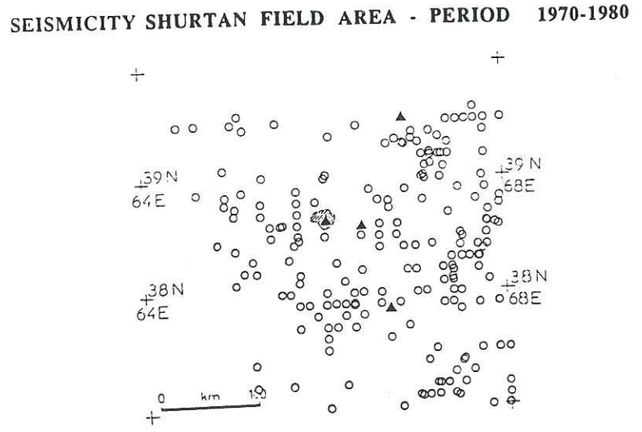

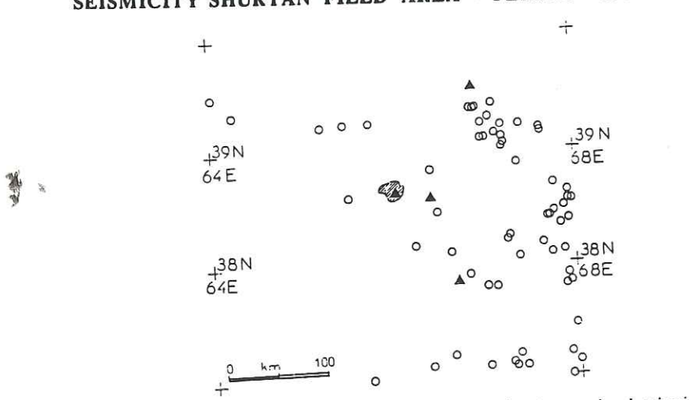

Fig. 3. Siesmicity map of Shurtan gas field area, Uzbekistan. Black triangles are local seismic stations. (a) Period 1970–1980. (b) Period 1980–1990. Note that the gas extraction began in 1979, with an initial gas pressure of 30 MPa. The gas pressure decrease since 1979 is 2 MPa for a production of 20% of the known reserves (Plotnikova personal communication, 1991).

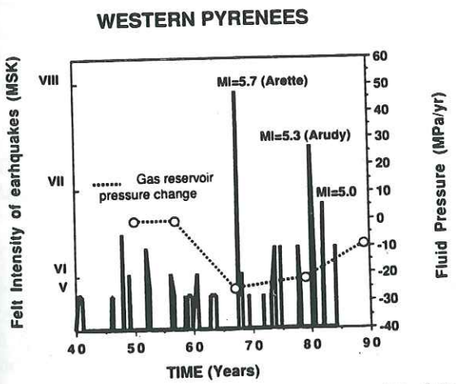

Fig. 4. Historic seismicity of the western Pyrenees and the Lacq gas field, France; pressure drop (dotted line).

the neighbouring faults. Such an increase in effective pressure inhibits seismic fractures in the area during the first years of extraction.

(ii) In a second step, these locked faults inhibit deformation and increase the seismic energy potential. This energy of deformation is released in a second phase at a greater magnitude than before. This classical asperity model is checked at greater scale by numerous seismic cycle observations. At laboratory scale, the damage theory explains the increase in seismic energy after a quiescent period (cf. Main *et al.* 1990).

Viscoelastic stress transfer

In the second part of the paper, the after-effects of these major regional events on the Lacq gas field seismicity are tested. The seismic history of the Lacq field ($M_l > 3$ in 1969, first felt earthquake; $M_l = 4.4$ in 1981, strongest induced event; deep events first observed in

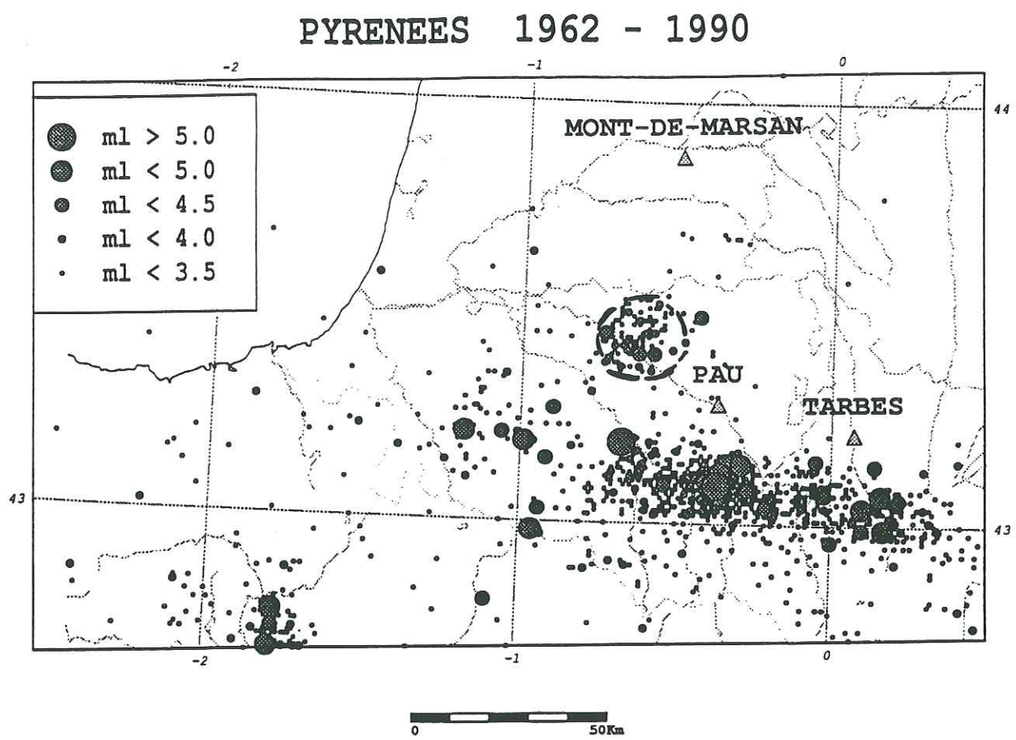

Fig. 5. Seismicity map of the western Pyrenees, France, 1962–1990 (from LDG, CEA French national network). Earthquake magnitudes are local magnitude. The seismically active zone in the Western Pyrenees defines an E–W strip no more than 15 km wide, in the lower part of the map, which is associated with the North Pyrenean Fault. The swarm located 20–25 km north of the main Pyrenean fault (circular outline) has been active since 1969 and is correlated in time and space with extraction from the major Lacq gas field in France (Grasso & Wittlinger 1990).

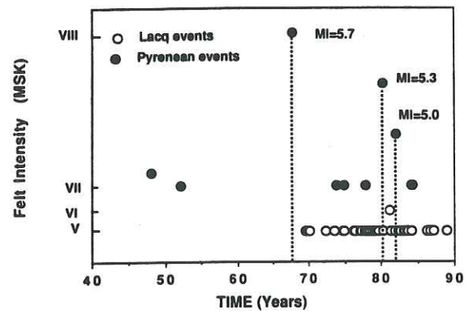

Fig. 6. Regional seismicity of the Western Pyrenees and local triggered earthquakes in the Lacq gas field area. Zero value on the time axis corresponds to year 1940. Earthquake magnitudes are local magnitude.

late 1982 with $M_l > 3$) is connected with the major seismic energy release affecting the North Pyrenean Fault (Fig. 6). As a result of increasing stress induced by gas extraction, the Lacq field zone is close to the critical failure threshold as well as the seismically active regional faults. Around this threshold, small perturbations can trigger instabilities. Earthquake after-effects and triggered seismic phenomena were reviewed by Rice & Gu (1983). One of the mechanisms tested in the Pyrenean area was proposed by these authors at a larger scale. They study major events (magnitude >7) and stress alteration over distances ranging from 100 to 500 km. The entire lithosphere and asthenosphere are used in a sense to channel stress alteration depending on the physical mechanisms of earthquake after-effects. In our model we test the same viscoelastic stress transfer model at the scale of the sedimentary cover.

The manner in which geological, mechanical and hydrological data can limit the effect of each process in this particular case study is investigated. The studies are based on simple models and anticipate that important lessons remain to be learned from first-order models. It is important to note that such possible connections are observed in different areas where fluid manipulations trigger seismic instabilities, cf. Gasli field, Uzbekistan and Monteynard dam, France. If verified, such changes must be considered for medium-term prediction.

WATER PRESSURE CHANGE RESULTING FROM WATER DISCHARGE AROUND GAS FIELD EXPLOITATION

During discharge from a well, water is removed from the aquifer, and this produces a cone of depression in the water table. Following Darcy's law, this hydraulic gradient induces a flow of water. The change in water head (Δh), is governed by various relations depending on the reservoir geometry (cf. Nicholson *et al.* 1988).

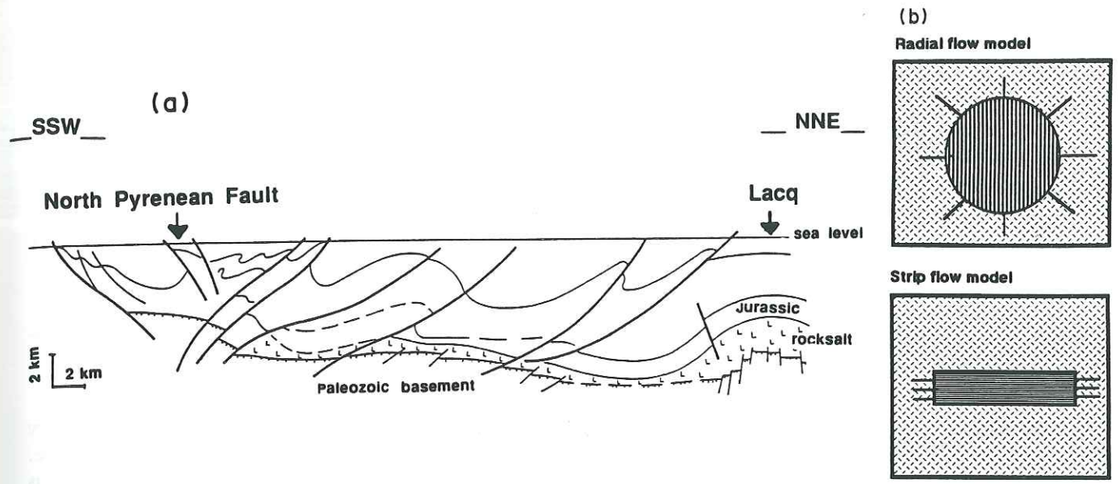

Fig. 7. (a) Geological cross-section between the Lacq field and the North Pyrenean Fault. Rock salt is indicated by small ticks below the Jurassic level and above the Paleozoic basement. The Lacq gas reservoir is located within Jurassic beds, and the aquifer is assumed to follow the décollement level above the basement. (b) Schematic models of the aquifer.

As a result of a constant flow rate (Q), from an isotropic reservoir of infinite area (with radial flow into the well), the change of head at distance r and time t is given by the Theis equation:

$$\Delta h(r,t) = \left(\frac{Q}{4\pi T}\right)\int_u^\infty \frac{e^{-\xi}}{\xi}\,d\xi$$

with T equal to transmissivity (hydraulic conductivity multiplied by aquifer thickness, $T \sim L^2 T^{-1}$), S equal to storativity (amount of fluid released per unit column of aquifer, for a unit decline of head, S is dimensionless), Q equal to out-flow rate and

$$u = r^2 S/4Tt \quad \text{(Freeze \& Cherry 1979).}$$

If fluid flow is confined to a narrow reservoir (strip aquifer model), the head change at a given distance is higher than for the radial flow model (cf. Hsieh & Bredehoeft 1981). For discharge from a well situated at the centre of a strip of width w and infinite extent in the x direction, a constant discharge rate induces a head change given by the following relation (cf. Hsieh & Bredehoeft 1981):

$$\Delta h(x,y,t) = \left(\frac{Q}{4\pi T}\right)\sum_{m=-\infty}^{m=\infty}\int_{u_m}^\infty \frac{e^{-\xi}}{\xi}\,d\xi$$

with

$$u_m = (x^2 + (y + mw)^2)\, S/4Tt.$$

y being the distance from the centre of the strip in the direction perpendicular to x, w is the width of the strip. The length of the strip is infinite in the x direction.

To introduce more clearly this head change in the mechanical behaviour of the deep rocks, most authors use a relation between head change and fluid pressure change (p) as follows:

$$p = \Delta h \rho g,$$

with ρ = density of the fluid.

Such relations were applied to the largest gas field in France (Lacq gas field, Nicolai *et al.* in press), in order to test a possible correlation between the gas production and the regional seismic activity in the nearby mountain chain of the Pyrenees (25–35 km). Since the distance between the gas field wells is rather small compared to the distance from the gas field to the Pyrenees, the cluster of wells were modelled as a single point source of 100 m in diameter.

Using more than 40 deep boreholes in the area, as well as numerous deep seismic soundings from Elf (SNEA(P)) and the preliminary results of Ecors Arzaq seismic profile (Fig. 7), the limit values for the geometry and hydromechanical characteristics of the medium between the Lacq gas field and the North Pyrenean Fault can be determined.

The gas producing reservoir includes limestones and dolomitic formations (Cretaceous and Jurassic), with average thickness of 500 m, but with heterogeneous permeability values (Nicolai *et al.* in press). Using the simplified geological cross-section in Fig. 7, a continuous aquifer through these formations was assumed from the root of the Lacq field to the Pyrenees. Initial gas pressure was 66 MPa at 3.2 km depth. A gas–water contact was never found but was estimated from the abnormally high gas pressure to be located at least at 7 km depth. As a result, this gas reservoir is known as a dry reservoir. The estimated horizontal aquifer is presumed to be down-bounded by the well-known décollement level of the area. A mean thickness of 200 m, a mean porosity of 3%, and a mean hydraulic conductivity of 10^{-8} ms^{-1} were assumed within the aquifer according to the geomechanical data from deep boreholes (Grasso & Feignier 1990).

For given values of the storativity and transmissivity,

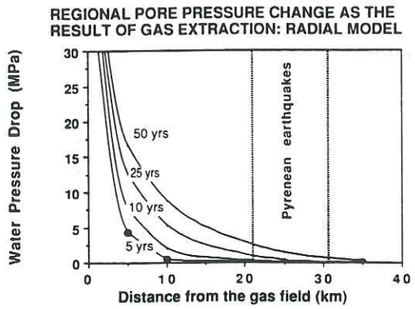

Fig. 8. Radial flow model. Pressure drop of the aquifer as a function of time delay after gas extraction began. Each curve corresponds to a time delay after gas extraction began.

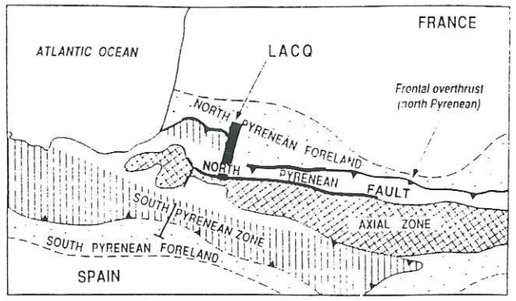

Fig. 9. Geological sketch map of the western Pyrenees. The rectangular box shows the geometry of the strip model used to compute pore pressure changes in Fig. 10.

the value of the water discharge rate must be estimated. The gas pressure drop associated with gas extraction is not isotropic but from an initial pressure of 66 MPa, the gas pressure drop is about 60 MPa at the single point source and 50 MPa at distances ranging from 5 to 10 km, and 35 MPa from 7 to 15 km (Elf (SNEA(P)) company personal communication 1991). According to the production data, with a 60 MPa gas pressure drop, the decrease in water pressure is fixed at 60 MPa at the centre of the gas field, after 25 years of extraction (Grasso & Wittlinger 1990). This means that at this point the water head is presumed to be equal to the gas head. The other boundary condition assumes that the maximum value of the water pressure decrease remains below the initial gas pressure, 66 MPa, after a long time interval (50–100 years). With these constraints, water flow rate (Q) must be close to 16×10^{-3} m^{3}s^{-1}. This corresponds to a total water inflow volume of 12.6×10^6 m^3 over the last 25 years, a relatively small value vs the 9×10^9 m^3 reservoir volume. Note that the depth of major events located on the North Pyrenean Fault —Arette, Arudy Gagnepain (1987)—is of the same order as the depth of the estimated aquifer which is bounded by the knowledge of décollement level. Consequently, the question of downward migration of pressure effects does not need to be tackled.

Assuming a constant water flow rate, the change in head, and thus the change in pressure in the confined aquifer, were calculated using the above relations. The water pressure change is calculated using the radial flow model, and the values are plotted in Fig. 8, on a distance vs time diagram. After 25–50 years a decrease of less than 1 MPa (a few bars) may be obtained between distances ranging from 25 to 35 km.

The water pressure change is also calculated for the strip aquifer model. A strip zone of 5 km in width is used in order to represent an area of fractured rocks from the Lacq anticline to the North Pyrenean Fault. The location of this strip is shown on Fig. 9 with the main tectonic structure of the area. Note that according to a N–S geological discordance, the strip is located in an area where the North Pyrenean Thrust disappears. In this case the transmissivity value is assumed to be 2.5×10^5 m^2 s^{-1} and the porosity is assumed to be 3.75% to account for the fault zone effect. The same boundary conditions are used as for the radial flow model, i.e. after 25 years delay, a 60 MPa water pressure decrease is reached at the single discharge source (100 m diameter) and, after a long period (50–100 years), the maximum decrease value remains below the initial pressure of the reservoir (66 MPa). To fit these limit values a 43×10^{-3} m^3 s^{-1} discharge rate has to be used. This corresponds to a total water flow volume of 3.4×10^7 m^3 since the beginning of gas extraction. In this case the water pressure decrease value is significantly higher, especially over a period ranging from a few years to 10 years (Fig. 10). Water pressure changes greater than 1 MPa can occur at 20–30 km distance from the reservoir within a period of 2 years. The seismicity patterns of the North Pyrenean Fault is compared to the water pressure change in Fig. 11(a). Such an estimation is checked using near-field data close to the gas reservoir. During the past 14 years, deep injection of waste water has occurred below the gas reservoir, with a total estimated injection volume of 3.8×10^6 m^3. Producers estimate that, after 20 years of production, gas volumes are trapped on the southern flank of the field due to the progressive effect of water injection. In Fig. 11, the estimated water pressure value in this area is locally greater than the gas pressure value. The progressive trapping of gas reserves, initially thought to be induced by artificial water injection, could be indicative of natural water inflow. This possibility is added to show that the parameters used to compute water pressure change at great distance from the field are realistic even for the local reservoir behaviour.

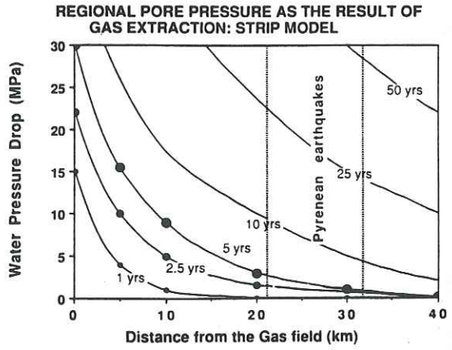

Fig. 10. Strip flow model. Pressure drop of the aquifer as a function of the distance from the gas field. Each curve corresponds to a time delay after gas extraction began.

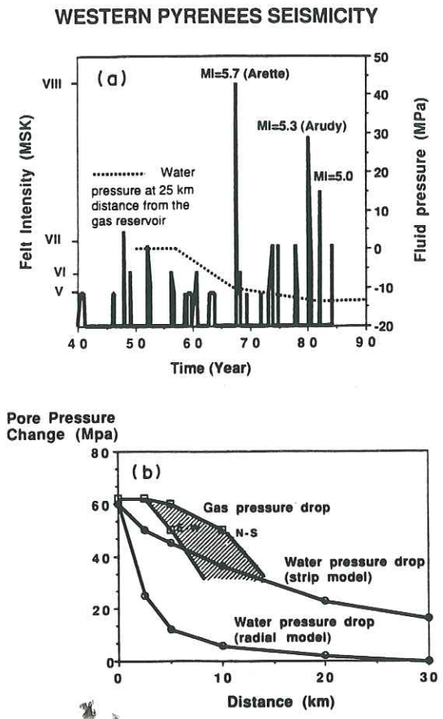

Fig. 11. (a) Historic seismicity of the western Pyrenees and the estimated pressure change on the North Pyrenean Fault (dotted line), estimated with the value calculated with the strip flow model. Zero value on the time axis corresponds to year 1940. Earthquake magnitudes are local magnitude. (b) Gas pressure drop and water pressure drop vs distance in the neighbouring region of the gas reservoir, after 25 years of extraction. Curves labelled with open squares are the gas pressure change within the gas reservoir deduced from well data. The two curves correspond, respectively, to E–W and N–S pressure profile. Curves labelled with open circles are the water pressure changes modelled by strip model and isotropic radial model. Intersection between water pressure drop (strip model) and depletion of gas reservoir can be interpreted as water inflow into the gas reservoir.

ROCKSALT AS A VISCOELASTIC STRESS DIFFUSION CHANNEL IN THE UPPER CRUST

The mechanical connection between earthquakes by a modified Elsasser (1969) model was first proposed by Rice (1980) and further analysed by Lehner *et al.* (1981). Investigations at lithospheric scale were performed (cf. Thatcher *et al.* 1980, Rice & Gu 1983, Li & Kisslinger 1985, Melosh 1988, Linker & Rice 1991). Rydelek & Sacks (1990) discovered an apparent correlation between earthquakes in the subduction zone of northeast Japan and earthquakes in the overthrust block. The land earthquakes precede the events at sea by 36 years and their epicentres are located, on average, 200 km apart. Plate convergence causes the overthrust block to buckle, resulting in the occurrence of thrust events on land. The stresses released by the land earthquake slowly diffuse toward the subduction zone due to viscoelastic coupling between the brittle upper crust and the ductile asthenosphere. The diffusing extensional deformation pulls the overthrust block away from the subducting slab, thus reducing friction and triggering an earthquake. The extensional deformation also reduces the shear stress between the slab and the overthrust block.

The 'Elsasser'-like model which Rydelek & Sacks (1990) employ to investigate stress diffusion has one dimension of freedom with all displacements being horizontal. An elastic layer (30 km thick lithosphere) lies over a viscoelastic layer (30 km thick asthenosphere). The upper layer is displaced by an edge dislocation while the bottom of the lower layer is rigid. This basic first-order model is much simpler than the three-dimensional viscoelastic finite-element technique used to model stress transfer and deformation associated with large earthquakes, when geodetic measurements and fault plane geometry fix the limits of the model (cf. Linker & Rice 1991).

Use of an 'Elsasser'-like model is proposed here to test the possibility of stress transfer at upper crustal scale when moderate shallow earthquakes are used as an initial stress and strain pulse. If the elastic medium (sedimentary level within which shallow earthquakes occurred) lay on a viscous medium (rocksalt beds and décollement level below frontal overthrust in the vicinity of a mountain chain), wave diffusion is delayed, due to the coupling effect with the viscous material. If the diffusing strain wave encounters a locked fault, it can reduce the frictional force, when well oriented, thus unlocking the fault and triggering an earthquake.

As the strain pulse is propagating, its maximum value and velocity decrease with increasing distance from the source. The velocity of the strain pulse is equal to the distance x of a point from the source divided by the rise-time of the pulse at this point. The standard definition of the rise-time (T) is the time taken by the strain, at the distance x from the source, to reach 63% of its maximum value. The expression of strain as a function of x and t can be derived from the equations of Rydelek & Sacks (1990):

$$\varepsilon(x,t) = \frac{U_0}{\sqrt{\pi}\, H_e} \sqrt{\frac{\tau}{t}}\, e^{-x^2\tau/4H_e^2 t}$$

with u_0 the horizontal component of displacement at the source, and

$$H_e = \sqrt{\frac{Y_e}{\mu_v}(H_1 H_2)},$$

where H_e is the effective elastic thickness, Y_e is the Young's modulus of the elastic sedimentary cover, H_1 and H_2 are the thickness of the layers and $\tau = \eta/\mu_v$, ratio of viscosity to shear modulus of the viscous layer. It yields the rise-time T as a function of the distance x from the source:

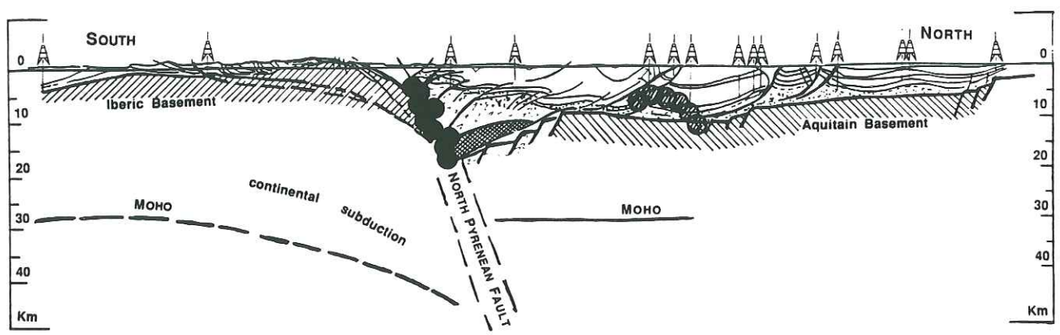

Fig. 12. Tectonic cross-section of the western Pyrenees area (adapted from Ecors Arzacq Program). Black dots are Pyrenees seismicity and hatched dots are induced events in the Lacq gas reservoir area.

$$T(x) = \frac{1}{6}\tau\frac{x^2}{H_e^2}.$$

Since

$$\sigma_{xx} = Y_e\varepsilon_{xx}$$

the corresponding stress drop for 1 m horizontal displacement component of the fault is:

$$\Delta\sigma(x) = \frac{1}{x}\frac{63}{100}Y_e\sqrt{\frac{2}{\pi\rho_E}}.$$

Using numerous borehole and seismic profiles a geomechanical cross-section of the western Pyrenees area was built (Figs. 7 and 12). The corresponding mechanical model is an elastic layer (8 km thick sediments) over a viscoelastic channel (0.2–2 km thick salt bed). This model raises several questions when applied to the upper crustal scale. Can a diffusive deformation in the upper crust stimulate the occurrence of a shallow seismic instability? Are faults between the site of the natural earthquakes and the gas field likely to be excited to rupture?

To check these questions, the $T(x)$ value is calculated at distance ranging from 10 to 60 km. The values of $T(x)$ and $\Delta\sigma(x)$ obtained (Fig. 13) must be considered only as orders of magnitude, since the geological structure is not perfectly horizontal, the evaporites probably have a variable thickness and also because the behaviour of the upper crust is not perfectly brittle (Gratier & Gamond 1990).

As the elastic sedimentary cover is mainly limestones, the Young's modulus Y_e is taken to be 6×10^{10} Pa.

The shear modulus of the viscous Triassic layer is calculated with the relation $\mu_v = 2Y_v/5$. Using $Y_v = 5 \times 10^9$ Pa for evaporites (Carmichael 1982), this gives $\mu_v = 2 \times 10^9$ Pa. The viscosity η of evaporites is considered as ranging from 10^{17} to 10^{19} Pa.s according to both experimental laboratory studies and numerical values used in geomechanics (cf. Last 1988, Spiers *et al.* 1990).

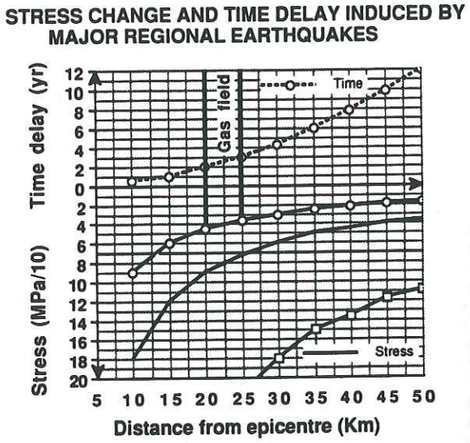

Fig. 13. Time delay (dotted line with open circles) and stress changes (continuous line with open circles) induced by stress transfer from the Arette (M_l = 5.7) Pyrenean events at different distances from the epicentre. A 0.5 m horizontal source displacement is used to model the M_l = 5.7 earthquake after-effects (open circle). The two other stress curves represent stress changes induced by a 1 m source displacement (thick line), and a 3 m source displacement (M ~ 7 event), (open square).

Using a salt viscosity of 10^{17} Pa.s (Last 1988, Spiers *et al.* 1990) and a 0.2 km thickness, the theoretical 2 years $T(x)$ diffusion time of the major Pyrenean earthquake at a distance ranging from 20 to 25 km is of the same order of magnitude as the 25-month time interval between the Arette Pyrenean earthquake and the first event in the Lacq area. Using a salt viscosity of 10^{19} Pa.s, the diffusion time is about 200 years for the same thickness of rocksalt bed. Using a viscosity of 10^{18} Pa.s and a 2 km thickness for the viscous bed, the same theoretical 2 years $T(x)$ diffusion time is obtained for the major Pyrenean earthquake after-effect to reach the Lacq gas field. Thus, within the range of plausible viscosity, the Lacq earthquake could be considered to have been triggered by the stress diffusion from the Pyrenean

event. The estimated implied stress change is less than 1 MPa (Fig. 13) and the same order of magnitude as that deduced from the poroelastic stressing, locally induced by gas reservoir depletion (Segall & Grasso 1991). The onset of seismic instabilities in the Lacq area could thus be triggered by two effects. The first effect is a monotonic increase in poroelastic stressing proportional to the gas pressure drop (25 MPa depletion between 1959 and 1969), without any seismicity, resulting in an increasing shear stress around the reservoir of 0.2 MPa. The second stress change could be the Arette shock after-effect given on Fig. 13 which, in a shorter time period, gives an equivalent stress increase. Note that the same time delay is observed between the Arudy shock and the first deep seismic swarm (events below the gas reservoir) in the Lacq area. Segall & Grasso (1991) show that the poroelastic stress changes below the reservoir where the deep events have occurred since late 1982, are half those above the reservoir. The earthquake after-effect of the 1980 Pyrenean event, could therefore have the same role in triggering the deep Lacq seismicity as the 1967 Arette event for the shallow Lacq seismicity.

Using a salt viscosity of 10^{17}–10^{18} Pa.s and a 0.2–2 km viscous bed, a Pyrenean shock will generate a strain wave that affects the weakened fault at the gas field area 2 years later. Despite the absence of measurements of surface deformations resulting from strain wave migration, which would give an independent estimate of the viscosity, the estimated time delays show that major Pyrenean events and major Lacq field earthquakes can be correlated by a viscoelastic model, In this way, a strain wave from a Pyrenean earthquake should trigger the release of locally accumulated induced strain. The triggering model is not investigated in this preliminary study. If the mechanism proposed here has any veracity, further studies on other areas, where the upper crust is locally weakened either by man-made manipulations or by natural tectonic processes, will check the proposed connections and investigate in more detail the mechanism of triggering events using fault geometry analysis.

CONCLUSIONS

It has been shown that major regional events, locally induced events and subsurface fluid pressure fluctuations in the western Pyrenean area are temporally and spatially correlated. In a first phase, gas withdrawal induces a decrease of water pressure in the aquifer at the gas–water interface and then affects the natural regional seismicity rate. The locked fault inhibits small events for a time, during which tectonic stresses accumulate. Large events then occur on the Pyrenean Fault, when the energy of deformation is large enough to allow seismic instabilities to occur. These large events ($M_l > 5$) trigger seismic instabilities ($M_l = 4$), in the vicinity of the gas extraction area, 30 km away. As a result of gas extraction, the Lacq field zone has weakness characteristics similar to the neighbouring main active fault. The Pyrenean earthquakes lead the gas field events by 2 years. this correlation is consistent with a viscoelastic model, where salt rock acts as a viscoelastic channel, below an elastic bed.

If connections of tens of kilometres are confirmed, major tectonic features located in the vicinity of hydrocarbon fields can be affected by development-induced fluid flows and deformations. Major induced earthquakes should be found on such tectonic features located in the vicinity of fluid pressure fluctuations such as hydrocarbon fields or artificial water reservoirs. Since the role of salt in fold and thrust belts (cf. Davis & Engelder 1985) and the effect of fluids on deformation of rocks (cf. McCaig 1988, Carter *et al.* 1990) are accepted, the possible connections proposed here may give a new insight into understanding the role of fluids in seismic instabilities and seismic risk assessment in the vicinity of fluid pressure fluctuations, when natural seismic activity is high.

Acknowledgements—We gratefully acknowledge, N. B Ulumov, A. McGarr, J. R. Rice and L. M. Plotnikova for fruitful discussion and encouragements. We thank two anonymous reviewers for their constructive comments. This research was partially supported by Grenoble University, Uzbek Academy of Sciences, Elf company and DBT-INSU Instability Program, contribution No. 458.

REFERENCES

Carter, N. L., Kronenberg, A. K., Ross, J. V. & D. V. Wiltschko 1990. Control of fluids on deformation of rocks. In : *Deformation Mechanisms, Rheology and Tectonics* (edited by Knipe, R. J. & Rutter, E. H.). *Spec. Publs geol. Soc. Lond.* **54**, 1–13.

Carmichael, L. J. 1982. *Handbook of Physical Properties of Rocks*. CRC Press, Boca Raton, Florida.

Davis, D. M. & T. Engelder 1985. The role of salt in fold and thrust belts. *Tectonophysics* **119**, 67–88.

Elsasser, W. M. 1969. Convection and stress propagation in the upper mantle. In : *The Application of the Modern Physics to the Earth and Planetary Interiors* (edited by Runcorn, K.). Wiley Interscience, New York, 223–246.

Fletcher, J. B. & L. R. Sykes 1977. Earthquakes related to hydraulic mining and natural seismic activity in western New York State. *J. geophys Res.* **82**, 3767–3780.

Freeze, R. A. & Cherry, J. A. 1979. *Ground Water*. Prentice-Hall, Englewood cliffs, New Jersey.

Gagnepain, J. 1987. Sismicité de la région d'Arette. Unpublished thèse, Université de Paris VI.

Grasso, J.-R. & Feignier B. 1990. Seismicity induced by a gas depletion: II Lithology correlated events, induced stresses and deformation. *Pure & Appl. Geophys.* **134**, 427–450.

Grasso, J.-R. & Wittlinger G. 1990. Ten years of seismic monitoring over a gas field area. *Bull. seism. Soc. Am.* **80**, 450–473.

Grasso, J.-R. 1991. Fluid induced instabilities of the upper crust: Application to seismic risk assessment in the neighbouring of hydrocarbon extraction. Paper presented at Int. Conf. on Earthquake Prediction. State of the Art, held in Strasbourg, France.

Grasso, J.-R., Fourmaintraux, D. & Maury, V. 1992. Le role des fluides dans les instabilitiés de la croute supérieure: L'exemple des exploitations d'hydrocarbures. *Bull. Soc. geol. Fr.* **163**, 27–36.

Gratier, J.-P. and Gamond J. F. 1990. Transition between seismic and aseismic deformation in the upper crust. In: *Deformation Mechanisms, Rheology and Tectonics* (edited by Knipe, R. J. & Rutter, E. H.). *Spec. Publs. geol. Soc. Lond.* **54**, 461–473.

Gupta, H. K. & Rastogi, B. K. 1976. *Dams and Earthquakes*. Elsevier, Amsterdam.

Guyoton, F., Grasso, J.-R. & Volant, P. In press. Interrelation between induced seismic instabilities and complex geological structure. *Geophys. Res. Lett.*

Hsieh, P. A. & Bredehoeft, J. D. 1981. A reservoir analysis of the Denver earthquakes: A case of induced seismicity. *J. geophys. Res.* **86**, 903–920.

Last, N. C. 1988. Deformation of a sedimentary overburden on a slowly creeping substratum. In: *Numerical Methods in Geomechanics* (edited by Svoboda, G.). Balkema, Rotterdam, 577–585.

Lehner, F. K., Li, V.C. & Rice, J. R. 1981. Stress diffusion along plate boundaries. *J. geophys. Res.* **86**, 6155–6169.
Li, V. C. & Kisslinger, C. 1985. Stress transfer and nonlinear stress accumulation at subduction plate boundaries—application to the Aletians. *Pure & Appl. Geophys.* **122**, 812–830.
Linker, M. F. & Rice, J. R. 1991. Models of stress transfer and deformation associated with the Loma Prieta earthquake. Paper presented at the USGS Asilomar Workshop on the Loma Prieta Earthquake, held in San Francisco.
Main, I. G., Meredith, P. G., Sammonds, P. R. & Jones, C. 1990. Influence of fractal flaw distributions on rock deformation in the brittle field. *Spec. Publs. geol. Soc. Lond.* **54**, 71–79.
McCaig, A. M. 1988. Deep circulation in fault zones. *Geology* **16**, 867–870.
McGarr, A. 1991. On a possible connexion between three major earthquakes in California and oil production. *Bull. seism. Soc. Am.* **81**, 948–970.
Melosh, H. J. 1988. Action and delayed reaction. *Nature* **336**, 205.
Nicholson, C., Roeloffs, E. & Wesson, R. L. 1988. The northeastern Ohio earthquake of 31 January 1986 : Was it induced? *Bull. seism. Soc. Am.* **78**, 188–217.
Nicolai, A., Pacaud, M. & Sitbon, A. In press. *Atlas of Oil and Gas Fields—Lacq gas Aquitaine Basin – France. Am. Ass. Petrol. Geol.*
Plotnikova, L. M., Flynova, M.G. & Machmudova V. I. 1989. Induced seismicity in gas field region. *Proc. XXV IASPEI General Assembly*, Istambul.
Raleigh, C. B., Healy, J. H. & Bredehoeft, J. D. 1972. Faulting and crustal stress at Rangely, Colorado. *Am. Geophys. Un. Geophys. Monogr.* **16**, 275–284.
Rice, J. R. 1980. The mechanics of earthquake rupture. In: *Physics of the Earth's Interior* (edited by Dziewonski, A. & Boschi, E.). North Holland, Amsterdam, 555–649.
Rice, J. R. & Gu, C. 1983. Earthquake after effects and triggered seismic phenomona. *Pure & Appl. Geophys.* **121**, 187–219.
Roeloffs, E. 1988. Fault stability changes induced beneath a reservoir with cyclic variations in water level. *J. geophys. Res.* **93**, 2107–2124.
Rydelek, P. A. & Sacks, I. S. 1990. Asthenospheric viscosity and stress diffusion: a mechanism to explain correlated earthquakes and surface deformations in the N.E. Japan. *Geophys. J. Int.* **100**, 39–58.
Segall, P. 1989. Earthquakes triggered by fluid extraction. *Geology* **17**, 942–946.
Segall, P. & Grasso J.-R 1991. Poroelastic stressing and induced seismicity near the Lacq gas field (France). *Eos* **72**, 293.
Simpson D. W. 1986. Triggered earthquakes. *Annu. Rev. Earth & Planet. Sci.* **14**, 21–42.
Simpson, D. W., Leith, W. S. & Scholz, C. H. 1998a. Two types of reservoir-induced seismicity. *Bull. seism. Soc. Am.* **78**, 2025–2040.
Simpson, R. W., Schultz, S. S., Dietz, L. D. & Budford, R. O 1988b. The response of creeping parts of the San Andreas fault to earthquakes on nearby faults: two examples. *Pure & Appl. Geophys.* **126**, 665–685.
Sornette, D., Davy, P. & Sornette A. 1990. Structuration of the lithosphere in plate tectonics as a self-organised critical phenomena. *J. geophys. Res.* **95**, 17,353–17,361.
Spiers, C. J., Schutjens, P. M. Brzessowsky, Peach, C. J., Liezenberg & Zwart, H. J. 1990. Experimental determination of constitutive parameters governing creep of rocksalt by pressure solution. In : *Deformation Mechanisms, Rheology and Tectonics* (edited by Knipe, R. J. & Rutter, E. H.). *Spec. Publs. geol. Soc. Lond.* **54**, 215–227.
Thatcher. W., Matsuda, T., Kato, T. & Rundle, J. B. 1980. Lithospheric loading by the 1896 Riku-u earthquake, northern Japan: implications for plate flexure and asthenosphere rheology. *J. geophys. Res.* **85**, 6429–6435.

32

FAILLES SISMIQUES CACHEES DANS LES PREALPES GRENOBLOISES: CARTOGRAPHIE A L'AIDE DES SEISMES DECLENCHES PAR LA RETENUE DE MONTEYNARD.

PAGEOPH, Vol. 139, No. 3/4 (1992)

0033-4553/92/040579-27$1.50 + 0.20/0

Triggered Earthquakes as Stress Gauge: Implication for the Uppercrust Behavior in the Grenoble Area, France

J.-R. GRASSO,[1] F. GUYOTON,[2] J. FRÉCHET[1] and J.-F. GAMOND[1]

Abstract—A sequence of moderate shallow earthquakes ($3.5 \leq M_L \leq 5.3$) was located within the Vercors massif (France) in the period 1961–1984. This subalpine massif has been a low seismic area for at least 5 centuries. During the period 1962–1963, 12 shallow earthquakes occurred in the neighborhood ($\Delta \leq 10$ km) of the Monteynard reservoir, 30 km south of the city of Grenoble. The latest four $M_L \geq 4.0$ earthquakes occurred in 1979–1984 either at larger distance (35 km) or greater depth (≥ 10 km) from the reservoir. Two triggering mechanisms are suggested for this sequence: (i) the direct effect of elastic loading through either increased shear stress or strength reducing by increased pore pressure at depth; (ii) the pore pressure diffusion induced by poroelastic stress change due to the reservoir filling.

The weekly water levels, local balanced geological cross sections, and focal mechanisms argue for two types of mechanical connection between the earthquake sequence and the filling cycles of the Monteynard reservoir. The seismic sequence started with the 1962–1963 shallow earthquakes that occurred during the first filling of the reservoir and are typical of the direct effect of elastic loading. The 1979 deeper earthquake is located at a 10 km depth below the reservoir. This event occurred 16 years after the initial reservoir impoundment, but one month after the previous 1963 maximum water level was exceeded. Moreover the yearly reservoir level increased gradually in the period 1962–1979 and has decreased since 1980. Accordingly we suggest that the gradual diffusion of water from reservoir to hypocentral depths decreases the strength of the rock matrices through increased pore pressure. The transition between the two types of seismic response is supported by the analysis of $M_L \geq 3.5$ earthquakes which all occurred in the period 1964–1971, ranging between 10 and 30 km distance from the reservoir. The three other delayed earthquakes of the 1961–1984 seismic sequence ($M_L \geq 4$ during the 1979–1984 period) are all located 35 km away from the reservoir. Based on the seismic activity, the estimates for the hydraulic diffusivities range between 0.2–10 m^2/s, except for the first event that occurred 30 km north of the reservoir, the filling just started. The lack of *in situ* measurements of crustal hydrological properties in the area, shared by most of the Reservoir-Induced-Seismicity cases, prevents us from obtaining absolute evidence for the triggering processes. These observations and conceptual models attest that previous recurrence times for moderate natural shocks ($4.5 \leq M_L \leq 5.5$) estimated within this area using historical data, could be modified by 0.1–1 MPa stress changes. These small changes in deviatoric stress suggest that the upper crust is in this area nearly everywhere at a state of stress near failure. Although the paucity of both number and size of earthquakes in the French subalpine massif shows that aseismic displacements prevail, our study demonstrates that triggered earthquakes are important tools for assessing local seismic risk through mapping fault zones and identifying their possible seismic behavior.

Key words: Induced seismicity, faulting, fluid, artificial reservoir, pore pressure, poroelasticity.

[1] Observatoire de Grenoble, LGIT/IRIGM, BP53X, 38041 Grenoble Cedex, France.
[2] Now at CapGeophy, 131 chemin des Oiseaux, 38330 Monbonnot, Grenoble Cedex, France.

Introduction

A sequence of moderate earthquakes (1 $M_L \geq 5.0$, 10 $M_L \sim 4.0$) occurred in the French alpine Foreland in the period 1961–1979. The seismic sequence is situated in the central part of the external zone of the western Alps (subalpine chains), where no historical seismicity ($M_L \geq 3.0$) had been reported for at least five hundred years (FRÉCHET, 1978; VOGT, 1979).

The map of the historical seismicity from 1500 to 1990 (Figure 1) shows earthquakes with $M_L \geq 3.0$. The relatively low seismicity level, with a lack of large

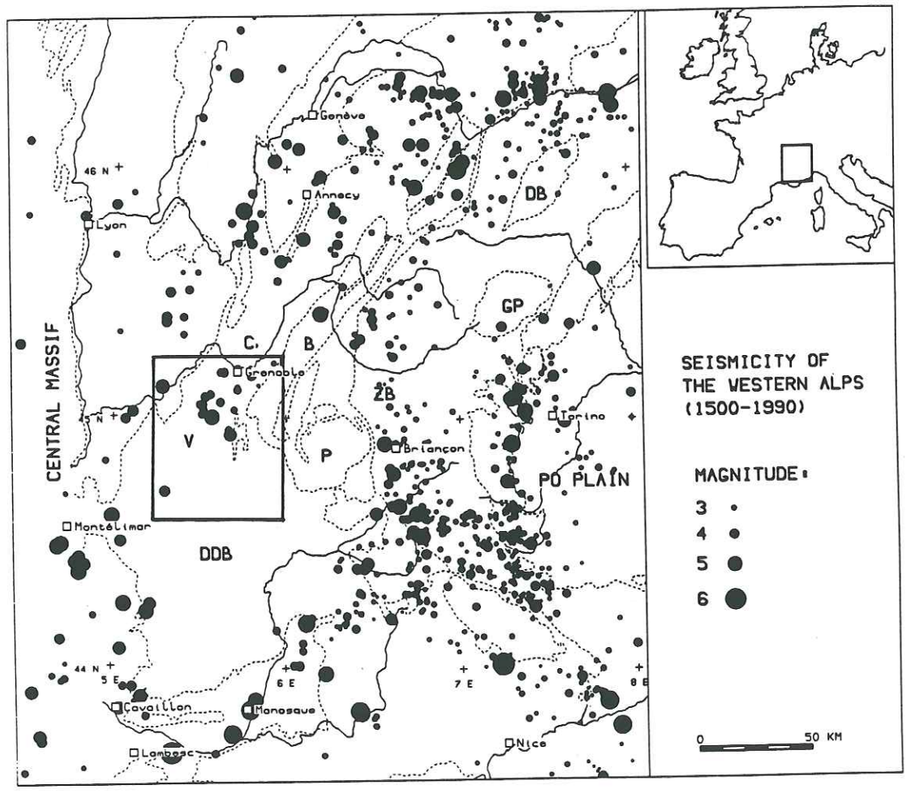

Figure 1

Map of the historical seismicity (earthquakes with magnitude $M_L > 3$) in the western Alps during the 1500–1990 period. The box indicates the sequence that occurred south of Grenoble. All the earthquakes in the box occurred in the 1961–1984 period. Massif toponyms from North to South: DB—Dent Blanche; GP—Grand Paradis; C—Chartreuse; B—Belledonne; ZB—Zone Briançonnaise; V—Vercors; P—Pelvoux and Grandes Rousses; DDB—Diois, Devoluy, Baronnies. The seismic Canavese Line is located west to Torino; the seismic Frontal Pennic Thrust is defined by the Nice-Briançon-East to Geneva alignment; the Durance fault extends from Manosque to Briançon Durance; The Rhône valley is defined by the Cavaillon-Montelimar axis.

events, is the main feature of the western Alps (FRÉCHET, 1978; NICOLAS *et al.*, 1990). In the western Alps, the largest shock in the 1500–1990 period is the $M \sim 6.2$ Lambesc earthquake, Provence on June 11 1909 (LEVRET *et al.*, 1988). Another feature that deserves mention is the presence of two aseismic areas represented by (i) the internal zone (Grand Paradis, Dent Blanche, Zone Briançonnaise) and (ii) a large part of the external zone of the western Alps: the Pelvoux and Grandes Rousses crystalline massifs, and the subalpine chains (Chartreuse, Vercors, Diois, Devoluy, Baronnies). It is worth noting that these aseismic areas are limited on both sides by important seismic alignments which are in close correlation with major tectonic alignments (Figure 1). The Canavese Line (in the east) and the Frontal Pennic Thrust (in the west) frame the internal aseismic area. The external aseismic area is limited by (i) the seismicity of the Durance fault, NE oriented, to the east; (ii) the seismic area of the Rhône valley to the west and by (iii) a more diffuse boundary to the north.

Since 1961, an earthquake sequence (20 earthquakes with $M_L \geq 3.5$, Table 1) has occurred south of Grenoble, centered on the previously aseismic subalpine massif of the Vercors (Figure 2). The largest earthquake of the sequence, the Corrençon

Table 1

Sequence of earthquakes ($M_L > 3.5$) that occurred in the French subalpine massifs during the 1960–1990 period

Number	Date	Felt Intensity	Depth (km)	Magnitude
1	03-03-1961 00h52	VI–VII	3	4.1[R]
2	04-12-1962 13h38	V	6	3.6[R]
3	04-25-1962 04h44	VIII–IX	5	5.3[R]
4	04-27-1962 04h17	V	6	3.6[R]
5	05-28-1962 16h21	VI	3	3.8[R]
6	06-07-1962 19h55	VI	3	3.8[R]
7	07-15-1962 04h46	V	—	3.5[e]
8	04-25-1963 13h36	VIII	3	4.9[R]
9	04-25-1963 20h24	—	—	4.0[R]
10	04-27-1963 05h28	—	—	4.5[R]
11	12-04-1963 11h26	VI	4	3.9[R]
12	12-07-1963 10h39	VI–VII	3	4.1[R]
13	12-12-1963 13h24	VI	4	3.9[R]
14	10-05-1964 15h15	V	—	3.5[e]
15	08-24-1966 20h47	V	5	3.6[R]
16	01-14-1971 03h05	V	—	3.5[e]
17	04-16-1979 12h27	VI	(20)	4.3
18	11-22-1979 07h24	VI	10	4.5
19	04-17-1984 08h54	VI	3–5	4.4
20	04-19-1984 20h41	V	3–5	4.2

[R] Magnitude from ROTHÉ (1972).
[e] Magnitude estimated from macroseismic map.

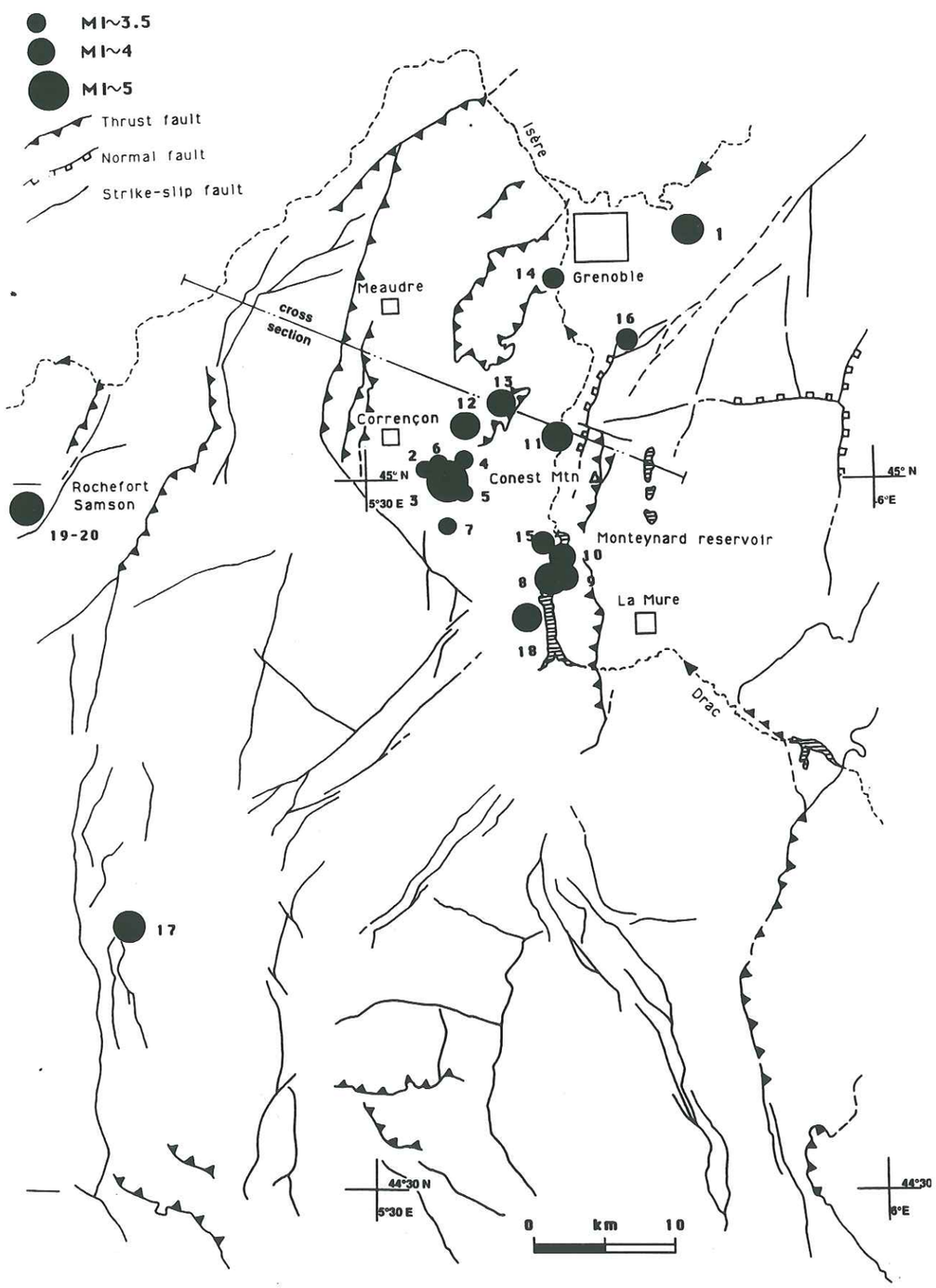

earthquake, in the Vercors massif, 04/25/62 $M_L \sim 5.3$, created significant damage with an intensity IX in the epicentral area (ROTHÉ, 1972). The second major shock, on April 25, 1963 ($M_L \sim 4.9$), occurred below the Monteynard dam on the Drac river, about ten kilometers distance from the 1962 Corrençon earthquake, only a few days after the water level of the Monteynard reservoir reached its maximum level. Two other shocks (events #9 and #10, Table 1) with $M_L \geq 4.0$ occurred a few kilometers below the reservoir during the following days. In the period December 1963–1966 five $M_L \geq 3.5$ events occurred within 10 km distance from the reservoir. The last major earthquakes of the sequence occurred in 1979 and 1984, 16 and 21 years later than the time of the first impoundment of the reservoir. These last earthquakes occurred either at greater distance from the dam, 35 km south of the reservoir for event #17 in April 1979, $M_L \sim 4.3$, 35 km west of the reservoir for events #19 and #20 in April 1984, $M_L \sim 4.4$–4.2, or at larger depth, $Z \sim 10$ km, for event #18 in November 1979, $M_L \sim 4.2$. However, one can notice that the sequence started in 1961, at the immediate onset of the reservoir filling, 30 km north of the reservoir and ended in 1984, 35 km westward from the reservoir. Therefore the possible interdependence of natural earthquakes and triggered seismicity must also be considered. Due to the paucity of the European seismological networks in the early 1960s, the regional catalog of instrumental earthquake locations is complete for $M_L \sim 3.5$ events. Because all of the $M_L \geq 3.5$ are felt earthquakes that are reported in the historical analysis, we used $M_L \geq 3.5$ as the threshold for this study. In the period 1960–1963 the nearest station was at a 100 km distance from the Monteynard reservoir. The earthquakes were located using a minimum of 8 stations within a 250 km radius. In the period August 1963 to December 1967 a local station within the dam was used. During this period the catalog is complete for $M_L \geq 1.5$ events within 6 km distance from the dam (ROTHÉ, 1972). It allows noting that the epicenter accuracy for the 1960–1963 period was of the order of a few kilometers. The misfit between the instrumental epicenters and the macroseismic epicenters ranges from a few kilometers in the 1960–1963 period (ROTHÉ, 1972), to less than 1 km in 1979 (B.C.S.F., 1984). For the $M_L \geq 4$ events in the 1960–1963 period, the order of magnitude of depth estimate is deduced from the macroseismic radii of different felt intensity levels. The #18 1979 event is located using 93 arrival times and the nearest station is at 25 km distance. A 10 km depth is obtained using either the whole data set or only the 5 stations with distance less than 100 km. The locations of the April 17 and 19, 1984 shocks were confirmed by local seismic network data from 6 stations that was

Figure 2

Seismic sequence (earthquakes with magnitude $M_L \geq 3.5$) located south of Grenoble in the 1960–1990 period. Numbers correspond to those of Table 1. The symbol size is proportional to the magnitude. Faults are adapted from BRGM (1979) geological map. A-A′ line locates the cross section of Figure 8. The dark area shows the extent of the Monteynard reservoir.

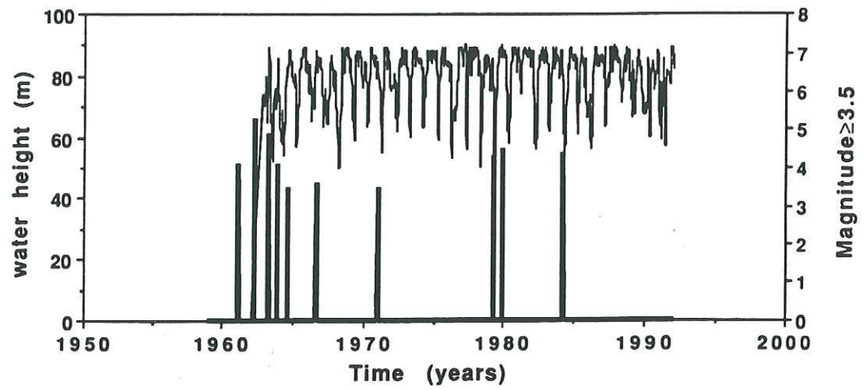

Figure 3
Water level and main earthquakes ($M_L \geq 4.5$) at Monteynard reservoir. Earthquakes occurred within a 15 km distance from the reservoir. They are plotted with thick vertical bars; numbers indicate magnitudes of largest events. Details of the water level and seismicity of each sequence are shown in Figures 5 to 7.

deployed 2 days after the April 19, 1984 shocks (THOUVENOT, 1984). Aftershock depth ranges in depth from 2.6 to 5.6 km, i.e., close to the 3 km depth of basement cover interface that is estimated from borehole data.

The main shocks that occurred in the 1962–1984 period and the water level of the reservoir are plotted versus time on Figure 3. Both (1) the large delay between the 1962–1963 earthquakes and the 1979–1984 earthquakes, and (2) the strong differences in focal mechanisms (vertical P axis for the 1963 event, horizontal P axes for 1979–1984 events; Figure 4), argue against a simple triggering mechanism for the whole sequence. We investigate the two types of mechanical processes, proposed by SIMPSON *et al.* (1988), that could trigger the main shocks of the 1962–1984 sequence in association with reservoir impoundments. The stress changes induced by human activity are modeled using the fluctuation of hydraulic load associated with artificial reservoir impoundment. We evaluate that the stress changes which trigger such seismic instabilities are small and we show that triggered earthquakes can be used as a stress gauge for assessment of the critical failure threshold within this area. In the last section we investigate the tectonic links between the triggered earthquakes and the local faults. Implication for the regional mapping of seismic fault in the Grenoble city area is presented.

Mechanics of Seismic Instabilities in the Neighborhood of the Monteynard Reservoir

Monteynard dam lies on the Drac river 25 km south of Grenoble. No historical seismic activity was reported south of Grenoble city either within the Pelvoux and

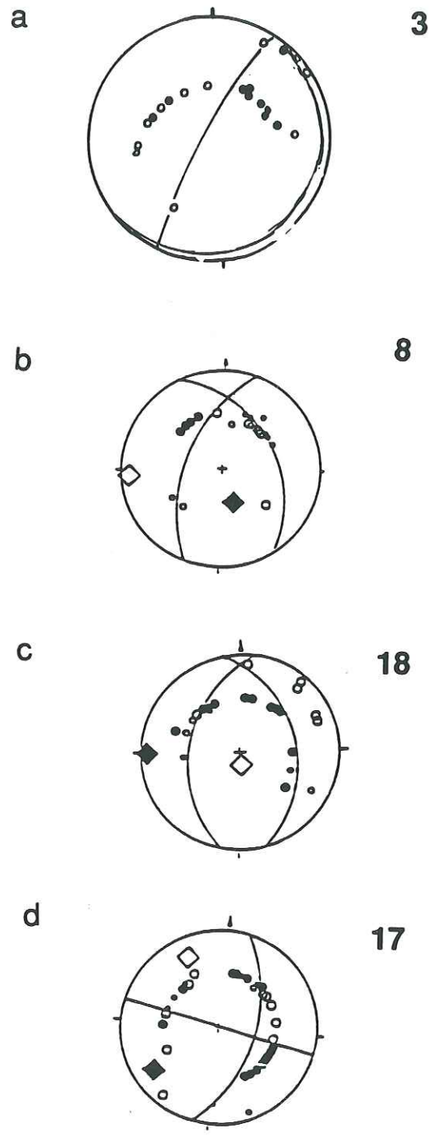

Figure 4
Focal mechanism for the main events of the Monteynard sequence. a) 04/25/1962, adapted from FRÉCHET (1978); b) 04/25/1963 from FRÉCHET (1978); c) 11/22/1979 from MÉNARD (1988); d) 04/16/1979, from MÉNARD (1988);- (dilatation, white circle; compression, black circle). The upper right number refers to the list of events in Table 1.

Grandes Rousses crystalline massifs which are located to the east of the Monteynard dam, or in the Vercors-Diois subalpine chains located to the west of the dam (Figure 1). The concrete arch dam is 153 m high and impounds a reservoir with a capacity of 0.27 km^3, at 490 m elevation, i.e., 127 m of effective water height corresponding to a 135 m water height above the river bed (GUERBERT and BALWAY, 1964). The arch is built on Lias limestone in a tectonically disturbed area. The Drac canyon contains a number of faults, fissures and joints which are parallel to the river and might have served as numerous possible shallow conduits for water to flow away from the reservoir (e.g., EDF, 1964; GUERBERT and BALWAY, 1964). The filling of the reservoir started in 1961 but no data are available before April 11, 1962, when the temporary diversion was closed at the 400 m water level elevation, i.e., 42 m above the river bed (ROTHÉ, 1972, p. 31). The first Vercors earthquake, $M_L \sim 5.3$, occurred on April 25, 1962. It was a shallow earthquake ($Z \sim 3$–5 km, ROTHÉ, 1972; ACHARD and GOULA, 1988) located 10 kilometers NW of the dam. The water level gradually increased during the period from April 1962 to April 1963 and reached its maximum (489.42 m) level on 04/25/1963. This maximum lake elevation (489.42 m) corresponds to a 135 m maximum water height. On the same day, 04/25/1963, a shallow earthquake, $Z \sim 3$ km, $M_L \sim 4.9$, followed by two shocks ($M_L \geq 4.0$) two days apart in the same area, was located in the immediate vicinity of the dam. This water level was never exceeded until the 489.79 m level on 10/22/79. One month after this absolute maximum water level was reached an earthquake, $M_L \sim 42$, occurred a few kilometers SW of the dam at 10 km depth below the reservoir. Then, until 1991, the reservoir level remained below this level. No other events ($M_L \geq 3.0$) were reported close to the reservoir since 1979, though annual variations of water level can reach 50 m (Figure 3). Previous works that studied the possible relation between local seismicity and the filling of the Monteynard reservoir (e.g., ROTHÉ, 1970; PLICHON *et al.*, 1979), focused on the earthquakes that occurred in the 1963–1966 period, excluding the analyses of 1962, 1979 and 1984 earthquakes. They used the data from the local seismic station that operated within the Monteynard dam from August 1963 to December 1967, and average monthly water levels. In the following section we use weekly water level data and $M_L \geq 3.5$ earthquakes during the 1961–1990 period. For each earthquake, triggering mechanisms are analyzed to test a possible causal association with pore-pressure changes and load effects induced by the Monteynard reservoir.

The April 25–27, 1963 Earthquake Sequence, $M_L \sim 4.9$–$M_L \sim 4.0$–$M_L \sim 4.5$

If we focus on the early stage of filling (Figure 5), we observe that a sequence of 3 earthquakes of magnitude $M_L \geq 4.0$ (Table 1) occurred a few days after the reservoir reached its maximum height for the first time, in the period April 25–27, 1963. The earthquakes are located in the immediate vicinity of the dam. Note that at many reservoirs larger events are clustered temporally (GUPTA *et al.*, 1972). At

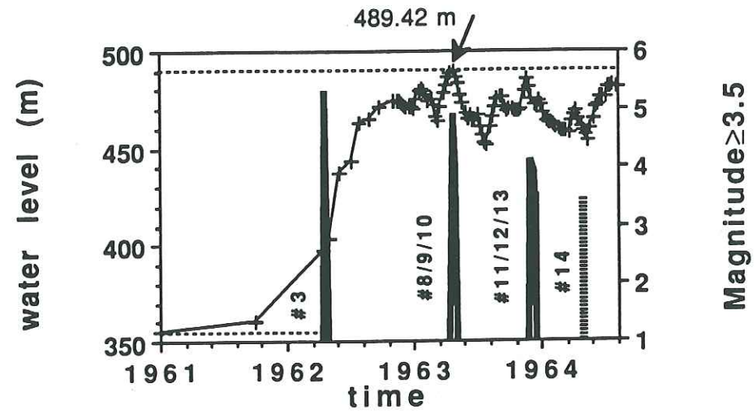

Figure 5
Weekly water level and earthquakes ($M_L \geq 3.5$) at Monteynard reservoir during the period 1962–1965. Earthquakes that occurred at 15 km maximum distance are plotted with thick vertical bars. The maximum 489.42 m elevation was reached 3 days before the 1963 events. Water levels provided by Electricité de France.

the Monteynard reservoir, there were no sufficient local stations to determine the depths or focal mechanisms with great accuracy for all events of this sequence. However, regional data and macroseismic estimations (ROTHÉ, 1972; ACHARD and GOULA, 1988) allow constraint of the depth of the largest shock to $Z \leq 3$ km ($M_L \sim 4.9$, #8, 04/25/1963, Table 1) and its focal mechanism to a normal fault type (Figure 4).

This kind of rapid seismic response, normal faulting earthquake at shallow depth in the immediate vicinity of a reservoir, is typical of the direct effect of elastic loading induced by reservoir impoundment, through either increased shear stress or by strength reducing by increased pore pressure at depth (e.g., SNOW, 1972; BELL and NUR, 1978; SIMPSON, 1986; ROELOFFS, 1988). Thus undrained conditions are necessary to produce fast pore pressure change during the rapid increase of the initial reservoir load. The 1963 sequence of $M_L \geq 4.0$ earthquakes agrees with the fast response mechanism in an undrained condition proposed elsewhere to explain reservoir-induced seismicity.

The November 22, 1979 Earthquake, $M_L \sim 4.5$

In terms of hydrological factors two significant facts summarize the Monteynard reservoir history before the 11/22/1979 earthquake. Each observation is related to a peculiar time scale. First, a short-term peak in water level was reported one month before the 1979 earthquake (Figure 6). This peak value (489.72 m) is the absolute maximum water height for the whole 1962–1991 reservoir history. The

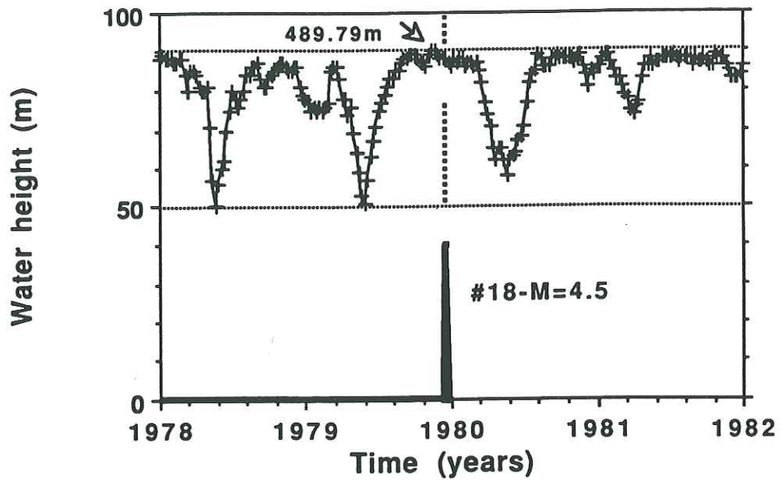

Figure 6
Weekly water level and the main earthquakes ($M_L \geq 3.5$) at Monteynard reservoir during the period 1978–1981. The earthquakes that occurred at 15 km maximum distance are plotted with thick vertical bars; numbers indicate magnitudes. The absolute maximum (489.79 m) of reservoir elevation was reached 20 days before the 1979 events. Water levels provided by Electricité de France.

second observation, which is the primary contribution in terms of spatial effect, is the gradual increase of average reservoir level since 1962 (Figure 7).

First, as previously noted, on October 22, 1979 the reservoir level exceeded for the first time its early April 1963 maximum, with a 489.72 m reservoir level. This type of association between the delayed maximum of water height and triggered earthquakes has been reported at least for two other reservoirs, Koyna dam (India) and Nurek dam (Tadjikistan). The largest of the Koyna earthquakes occurred in late 1967, $M_L \sim 6.2$ (GUPTA and RASTOGI, 1976). This earthquake is the largest known reservoir-induced earthquake despite the relatively small depth and volume of the Koyna reservoir (130 m, 2.8 km^3). This 1967 Koyna earthquake occurred at the time of the highest water level since the reservoir filling in 1962, although low seismic activity was observed in the period 1963–1966 (SIMPSON *et al.*, 1988). Following the 1967 event the water level was kept below the 1967 level until 1973. In 1973, although the water level exceeded that in 1967 by a maximum of only 1 m, the new peak in water level was associated with the highest energy release observed in the period 1968–1973, including an $M_L \sim 5.2$ earthquake. These effects are similar to the Kaiser effect observed with acoustic emission on rock core samples, where it has been observed that the previous stress maximum must be exceeded for acoustic emission to occur (DUNEGUN and TATRO, 1971; KURITA and FUJII, 1979). SIMPSON and NEGMATULLAEV (1981) and KEBEASY *et al.* (1987) also note

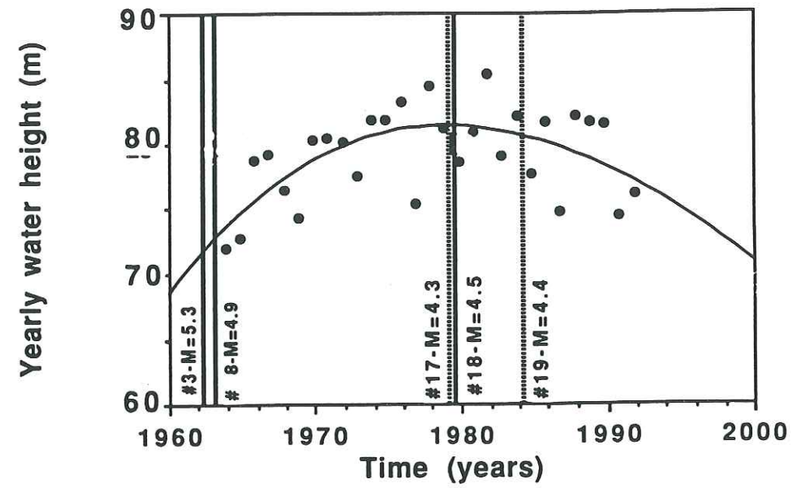

Figure 7
Annual average of water levels and main earthquakes ($M_L \geq 4.0$) at Monteynard reservoir. Earthquakes that occurred within 15 km distance from the reservoir are plotted with thick vertical bars; thick dotted bars are earthquakes that occurred at 20–40 km from the reservoir; numbers indicate magnitudes of largest events.

an increase of seismic activity when the water level exceeds its previous maximum at the Nurek and Aswan reservoirs. For the Koyna and Monteynard cases, the order of magnitude of the water level differences is one meter or less. Such a small critical stress change is of the same order of magnitude as that of the few tenths of bars modeled using poroelasticity to correlate the cyclic changes of a few meters of water reservoir height and locally triggered earthquakes (ROELOFFS, 1988). From a mechanical point of view, the 11/22/1979 Monteynard earthquake is a reverse fault type located at 10 km depth below the reservoir. The correlation between the peak water level of 10/22/1979 and the 11/22/1979 event would imply a 10 km fluid diffusion between the reservoir and hypocentral depth. One can note that such a type of delayed seismic response to reservoir impounding always occurs at larger distances from the reservoir than the rapid response type (SIMPSON *et al.*, 1988). This delayed response mechanism is dominated by the diffusion of pore pressure from the reservoir down to hypocentral depths (SNOW, 1972; BELL and NUR, 1978; SIMPSON, 1986; ROELOFFS, 1988). This process implies a short-term hydraulic diffusivity based on seismic diffusivity of 39 m^2/s (c_p, slope of L^2-T plot, T being the time delay between the peak of water level and the earthquake, Table 2), within the range of seismic diffusivities noted by TALWANI and ACREE (1985). Nevertheless the driving stress change is only a fraction of the pressure head that is defined at the bottom of the reservoir. Thus the mechanics of such types of seismic instability is not yet quantitatively solved.

Table 2

Estimates of seismic diffusivity using earthquakes ($M_L > 3.5$) that occurred in the vicinity of Monteynard reservoir during the 1960–1990 period

Number	Date	Depth (km)	Magnitude	Diffusivity (m^2/s)		
				c_i	c_p	direction
1	03-03-1961	3	4.1[R]	∞	<0	natural eq
2–7	04-25-1962	5	5.3	12–6	<0	W
8–10	04-25-1963	3	4.9[R]	0.2	∞	Z
11	12-04-1963	4	3.9[R]	1	43	NW
12–13	12-07-1963	3	4.1[R]	2	46	NW
14	10-05-1964	—	3.5[e]	4	300	NW
15	08-24-1966	5	3.6[R]	0.2	12	Z
16	01-14-1971	—	3.5	1.0	29	NE
17	04-16-1979	(20)	4.3	2.5	210	SW
18	11-22-1979	10	4.5	0.2	39	Z
19–20	04-17-1984	5	4.4	2.0	150	W

[R] Magnitude from ROTHÉ (1972).
[e] Magnitude estimated from macroseismic map.
c_i, c_p are seismic diffusivity estimated by $c_i = L^2/T_i$ (TALWANI and ACREE, 1985) where L is the distance between the earthquake and the reservoir and T_i is the time lag between onset of filling and earthquake occurrence. c_p corresponds to short-term diffusivity where T_p is the time lag between the peak of water level and the earthquake.

The second observation which enhances the possible short-term effect of the reservoir level peak on a global delayed response is the history of the reservoir average water height. The hydraulic reservoir load, in terms of annual average reservoir pressure, increased in the period 1963–1979, and decreased after 1980 (Figure 7). Accordingly, the volume affected by pore pressure diffusion increased with time. The reservoir-induced fault stability changes, at the focal depth of the 11/22/1979 event, can be resolved by the increased pore pressure, through decreased effective normal stress. The global pore-pressure diffusion is a long-term process that can trigger different faulting geometries (normal, reverse, thrust or strike-slip type) according to their location with respect to the reservoir (ROELOFFS, 1988). This process would give a hydraulic diffusivity of 0.2 m^2/s, for the #18, November 1979 Monteynard earthquake. This "initial diffusivity" is related to the time delay between the onset of the reservoir impoundment and the earthquake (c_i in Table 2). This value is both at the lower bound of the seismic diffusivity values proposed by TALWANI and ACREE (1985) and SIMPSON *et al.* (1988), and close to hydraulic diffusivity estimated on unfractured rock samples (e.g., RICE and CLEARY, 1976; HORATH, 1989). This value of diffusivity suggests moderate fracture permeability ($\sim$0.1 mD, i.e., 10^{-16} m^2), for a fluid flow path through depth within the crystalline basement (Figure 8).

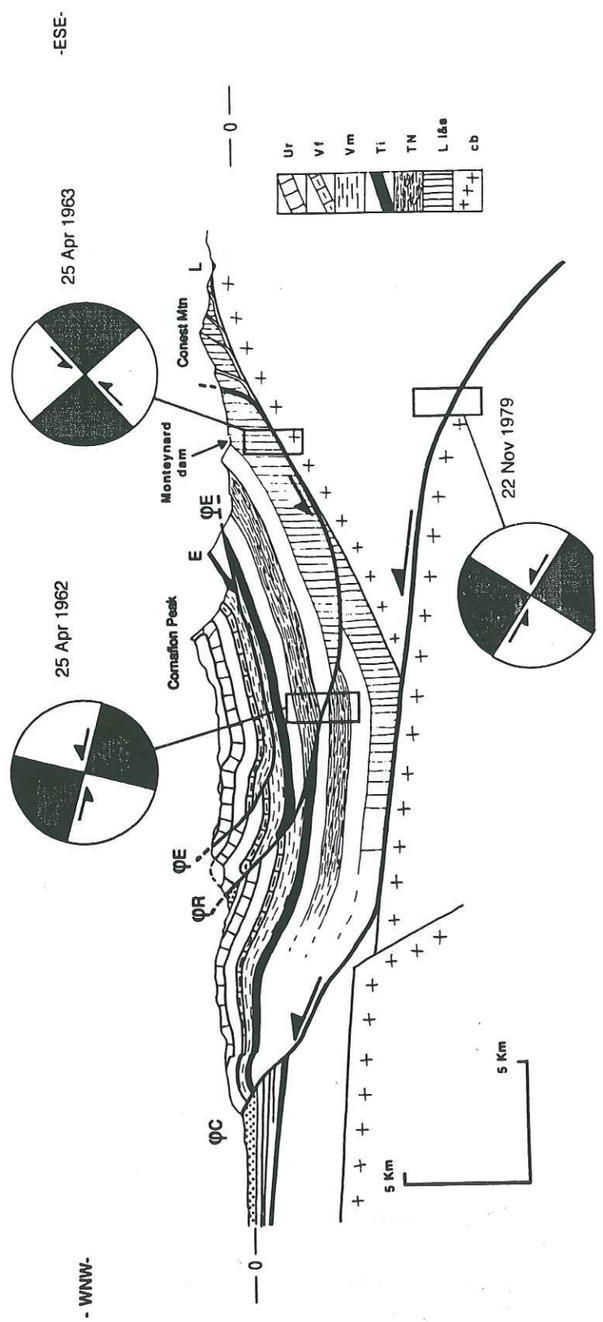

Figure 8
N 110 balanced cross section through northern Vercors and kinematics of seismic instabilities. On Figure 2, A-A' line locates the cross section. L, Laffrey lakes; D, Drac river; φE, Eperimont thrust, φR, Rencurel thrust; φC, Cherennes thrust. Key for shading: Ur = Urgonian limestones (Mid-Cretaceous); Vl = Valanginian limestones; Vm Valanginian marls (400 m–500 m thickness); Ti = Tithonian limestones (Upper Jurassic); TN = Terres Noires marls (800 m–1000 m thickness); $L_{l\&s}$ = Liassic limestones and shales; cb = crystalline basement. The kinematics of seismic slips are plotted using focal mechanisms that are presented in Figure 4. The depth and the magnitude of the earthquakes are reported (adapted from GAMOND, 1992).

We suggest that the loading was primarily in drained condition during the period 1962–1979 except in the localized zone of a shallow 1963 sequence. Diffusion at depth takes place slowly enough to avoid the production of excess pore pressure (diffusivity $c_i \sim 0.2\ m^2/s$). In a second step, the saturated zones have a high value of Skempton's constant B ($\Delta p = B\Delta\sigma$; Δp, induced incremental pore pressure; $\Delta\sigma$, incremental elastic stress; BELL and NUR, 1978), and the change in applied load leads to fast pore-pressure change at depth ($c_p \sim 40\ m^2/s$). Because $c \sim f(\nu, \mu, \eta, k, B^2)$, for the same mechanical constants, changes in Skempton's coefficient, from an unsaturated medium in the initial period (as low as 0.23 for 200 MPa effective stress, ROELOFFS, 1988) to a saturated medium with low effective pressure ($B \sim 1$), contribute to the explanation of the difference in the diffusivities. Moreover, the permeability, k, can increase between the two periods due to both pore-pressure increase (e.g., DAVID and DAROT, 1989) and to deviatoric stress effect on crack density. Thus, changes in Skempton's constant coupled to changes in permeability could bracket the estimated ratio between the two diffusivities and the November 1979 earthquake appears as typical of delayed seismic response to reservoir impoundment (e.g., SIMPSON *et al.*, 1988).

The April, 25 1962 Earthquake, $M_L \sim 5.3$

The relation between the level of the Monteynard reservoir and both the 1963 and 1979 earthquakes has been suggested in the previous sections, in terms of a change in the strength of the crust. These changes occur through two mechanisms. The first mechanism is an increase in elastic stress due to the surface load related to an increased pore pressure at hypocentral depths, resulting from undrained elastic compression during the loading. Such a mechanism explains the rapid seismic response of the April 1963 earthquake sequence to the initial filling of the reservoir. The second mechanism involves an increased pore pressure by diffusion from the bottom of the reservoir for the 1979 deep earthquake. Also, if we assume that diffusion played a role, a one-month delay implies a short-term diffusivity within saturated medium of $39\ m^2/s$.

The case of the April 1962 earthquake, the major earthquake within the Grenoble area for the last 5 centuries (FRÉCHET, 1978), cannot be simply considered as a triggered earthquake similar to the 1963 and 1979 earthquakes. The 1962 event occurred at a shallow depth, 10 km away from the reservoir, during the initial filling, with a 42 m water height (ROTHÉ, 1972, p. 31). Its focal mechanism is poorly constrained but could be either strike-slip or a low-angle thrust (Figure 4). Although triggered events were reported for water heights smaller than 50 m (e.g., Monticello reservoir, ZOBACK and HICKMAN, 1982), the associated earthquakes are usually shallow events in the immediate vicinity of the reservoir (a few km). Thus to relate the 1962 event to the reservoir impoundment it is necessary to involve the flow of water or pore pressure out of the reservoir. Evidence for the flow of water

within the left bank of the river (e.g., EDF, 1964; GUERBERT and BALWAY, 1964) and the existence of a shallow N 130 fault (Figure 2), added to the presence 4 km away of limestone formations (Malm and Cretaceous) which host karstic conduits, can be considered as positive arguments for rapid triggering of seismic instabilities at a moderate distance from the reservoir in the NW direction. The closure operation of the Monteynard reservoir started in November 1961 (GUERBET and BALWAY, 1964). Due to the lack of information for the water level before 04/11/1962, the causal effect of the short-term mechanism for the 1962 event is investigated as follows: if we assume that diffusion within fracture paths is the mechanism involved, the values for hydraulic diffusivity (c_i) on the order of $6–12\ m^2/s$ correspond respectively to 100 day (January 1962) and 200 day (November 1961) delays between the start of the filling and the April 1962 earthquake. It gives $0.6–1.2 \times 10^{-14}\ m^2$ estimates for the magnitude order of fracture permeability. This value appears to be a reasonable value for fracture permeability, as reported values exceed $10^{-12}\ m^2$, though intergranular permeability ranges from less than $10^{-20}\ m^2$ to $10^{-13}\ m^2$ (e.g., MOORE and VROLIJK, 1992). Because the seismicity occurs at some threshold, i.e., some value of the induced pore pressure changes, the seismic hydraulic diffusivity is within an order of magnitude of the material diffusivity (TALWANI and ACREE, 1985). The fast triggering process for the April 1962 earthquake involves a low threshold that can be associated with the lower bound of the hydrological characteristic of the fault path, i.e., a $0.6\ m^2/s$ hydraulic diffusivity and a $10^{-13}–10^{-12}\ m^2$ fracture permeability. It is worthwhile to note that the two foreshocks of the 04/25/1962 earthquakes occurred on April 12, 1962 and were located between the reservoir and the April 23, 1962 mainshock (ROTHÉ, 1972). Nevertheless, we cannot definitively determine if there have been any microearthquakes closer to the reservoir before the April 1962 events, or if the sequence started near the epicenter of the April 1962 event. Though no example of this type of triggered sequence has been reported in reservoir-induced seismicity, both the geological possibility for a fast fluid flow path within a karstic environment and the negative evidence against natural seismicity (shallow earthquake in an historically aseismic area), suggest that this 1962 event is not a pure tectonic event.

This possible earthquake triggering supports the two types of triggered seismicity induced by the Monteynard dam that we have proposed in the previous sections. Space and time analysis argues for triggered seismicity despite the small stress changes ($\Delta\sigma \sim 0.1–1$ MPa) estimated by the change in water height. These small stress changes agree with those proposed elsewhere to explain reservoir-induced seismicity. On such a basis, one can expect that pore-pressure diffusion from the reservoir could trigger a moderate earthquake ($M_L \sim 4–5$) at 30–40 km distance from the Monteynard reservoir, in the coming years. The #17, April 1979, and #19–20, April 1984, earthquakes, located 37 km apart from the reservoir, argue for the possibility of such events to occur. The probability for the occurrence of

such events is increased by (i) exceeding the previous maximum height of the reservoir and by (ii) the aftereffects of regional earthquakes on zones weakened by artificial reservoirs; such regional tectonic events have a high probability of occurrence within seismically active zones of the Belledonne massif and the Rhône valley (Figure 1).

Induced Earthquakes as a Stress Gauge for Natural Critical Thresholds

The seismicity that occurred at the Monteynard reservoir obviously falls into the two types of triggered seismicity observed worldwide (SIMPSON *et al.*, 1988): those occurring during and soon after the initial filling (1962–1963) and those in which the seismicity occurs years after the first filling (1979 event). Cases of mixed response at one site have been proposed at Koyna (GUPTA, 1983) and Lake Mead (CARDER, 1945). SIMPSON *et al.* (1988) reported that at Koyna, Oroville, and Aswan, the timing of the highest peak of delayed seismicity appears to be triggered by short-term changes in water level. This process can apply to the #18 1979 Monteynard event, in which the absolute maximum water height occurred one month before the event within the regular increase of the annual water level since 1963.

At the Monteynard dam the transition between the two types of response is supported by the analysis of the moderate ($M_L \sim 3.5$) events in the period that followed the April 1963 sequence. Between December 1963 and January 1971, 6 events with $M_L \geq 3.5$ occurred. In late 1963, 3 shallow earthquakes clustered at 8–10 km distance from the reservoir (#11–13, Table 1). They follow the 11/18/1963 peak water level (486.80 m) by 20 days and 25 days, respectively (Figure 9). The associated short-term diffusivities are 43 and 46 m^2/s. In 1966, 3 years after the initial impounding of the reservoir, a shallow earthquake (#15, Table 1) occurred close to the reservoir ($\Delta \leq 5$ km) 24 days after a short-term maximum (488.50 m; 08/01/1966) and still can be considered as a rapid response type (Figure 10). The next earthquake (#16, Table 1) occurred five years later. This event occurred in 1971, 5 months after a short-term maximum (489.25 m; 06/29/1971) but 17 km N-NE from the reservoir (Figure 9). The short-term diffusivities value is 29 m^2/s. As a delayed response-type earthquake ($L = 17$ km, $T = 8$ yrs) it would be triggered by the progressive migration of the pore-pressure front northward from the reservoir during the 1963–1971 period. The corresponding value for seismic diffusivity (L^2/T) is of the order of 1 m^2/s. This value agrees with the seismic diffusivity found for flow through fractures (TALWANI and ACREE, 1985; SIMPSON *et al.*, 1988) and is supported by geological observations in the area that show a N10 fault trace (Figure 2). One may note that the same diffusivity value accounts for the 1979 Diois earthquake (#17, Table 1), that occurred 37 km SW from the reservoir on a fault path defined as the SW continuation of the N10 fault (GRATIER *et al.*, 1989).

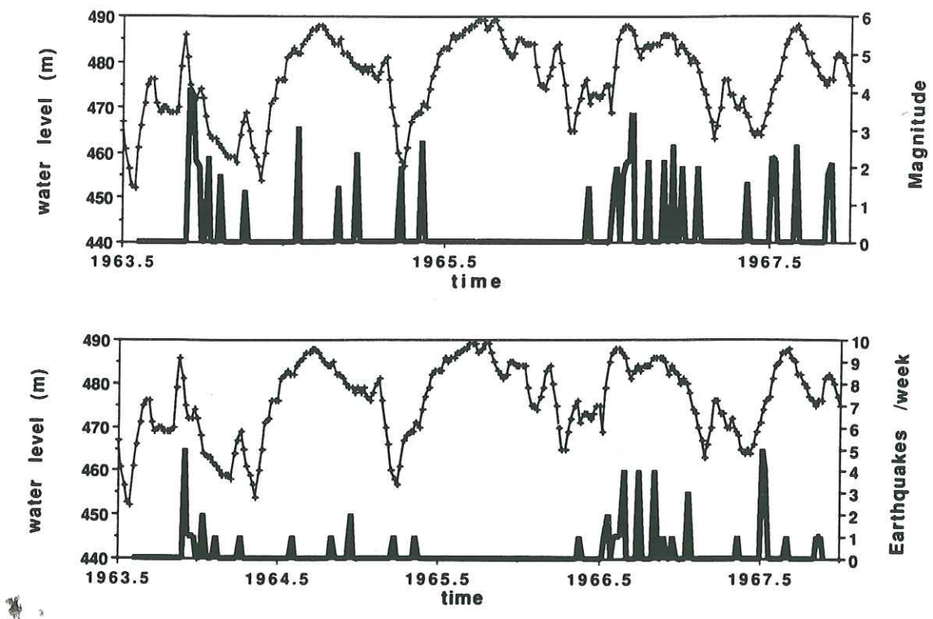

Figure 9(a)

Nevertheless, the last peak of water level occurred on 02/26/1979 (486.50 m) and if we assume the same possible causal association as for the previous events, we obtain 210 m^2/s for the short-term diffusivity. Note that the 5/10/1964 earthquake (#14, Table 1) occurred at a 20 km distance from the dam, 15 days after the 488.7 m peak water level that occurred on 09/21/1964. If we test the possibility for these events to be triggered by the Monteynard reservoir, the associated short-term diffusivity is 300 m^2/s for the 1964 event. The corresponding seismic diffusivity of the initial pore-pressure front migration would be 4 m^2/s. The last earthquakes of the sequence occurred on 04/17–19/1984, #19–20, at 37 km westward from the reservoir. The corresponding values for diffusivities are $c_i = 2\,m^2/s$ and $c_p \sim 150\,m^2/s$ (Figure 9).

Thus the two types of seismic response to the Monteynard reservoir impounding are supported by the analysis of most of the $M_L \geq 3.5$ earthquakes of the sequence under study. The scattering of the seismic diffusivity values shows the complexity of the fluid circulation in the heterogeneous poroelastic upper crust (Table 2). We can interpret the 1962 sequence and other events located to the N-NW of the reservoir, with $c_i \sim 1-10\,m^2/s$, by an inhomogeneous permeability model (BELL and NUR, 1978), in which more permeable zones intercept the reservoir in the W-NW direction but lie beyond the influence of the elastic stress increase caused by the reservoir. The earthquakes located NE-SW from the dam also correlate with fault

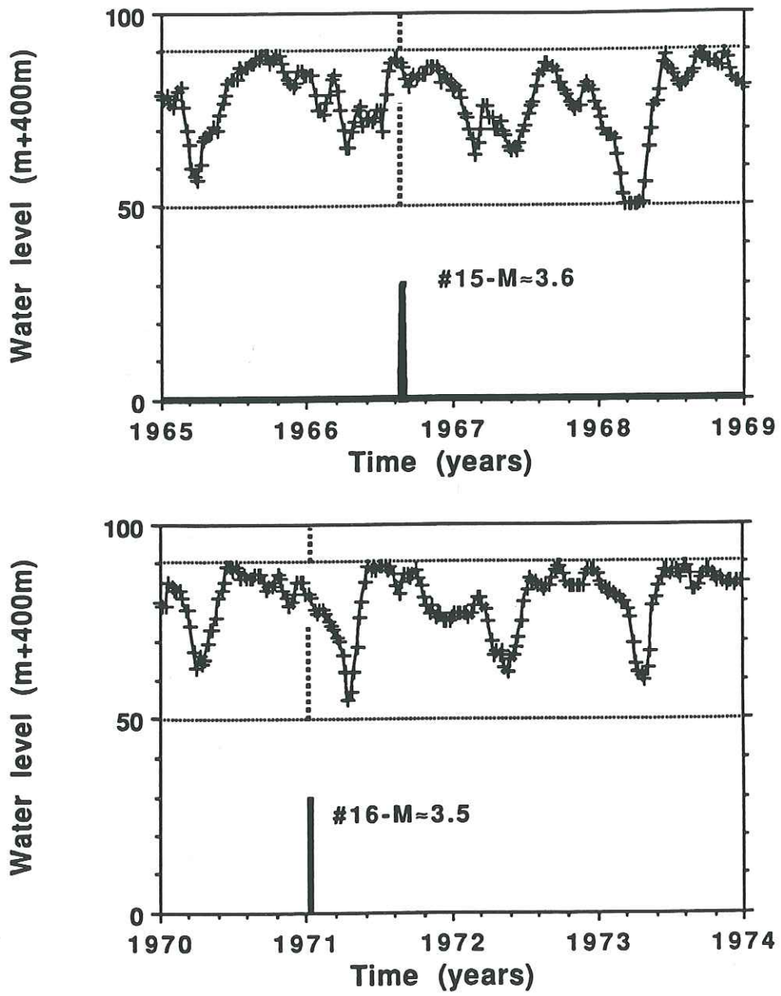

Figure 9(b)

paths. When the initial pore-pressure front evolves spatially the triggered $M_L \geq 3.5$ earthquakes appear to correlate with short time maxima. From each association between peak water level and earthquake we can estimate the order of magnitude of the short-term diffusivity (c_p on Table 2). The distant earthquakes ($\Delta > 20$ km, #14, 17, 19–20, Table 1) have homogeneous c_p diffusivities that are larger than c_p diffusivities of earthquakes that are located close to the reservoir (Table 2). This either implies another causal mechanism or rejects the possibility for these

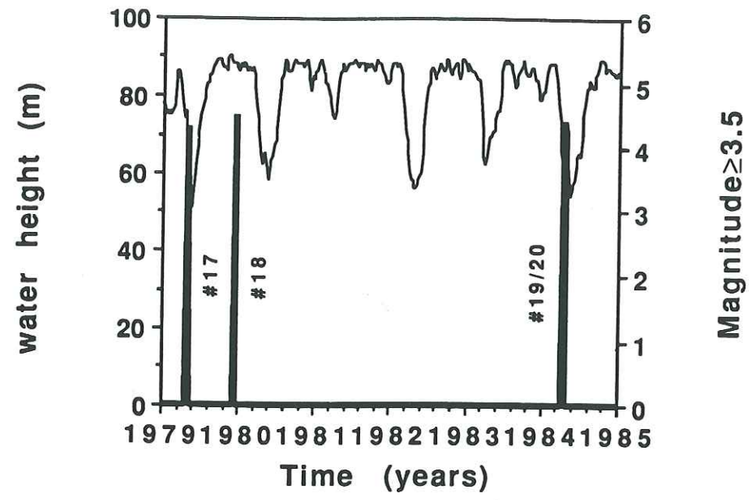

Figure 9(c)

Figure 9

(a) Weekly water level and earthquakes at Monteynard reservoir during the period 1963–1967. All earthquakes occurred at a shallow depth close to the reservoir ($\Delta \leq 5$ km). Water levels provided by Electricité de France. (b) Weekly water level and main earthquake activity at Monteynard reservoir during the period 1970–1973. The only $M_L \geq 3.5$ earthquake occurred at intermediate distance from the reservoir ($\Delta \sim 13$ km), 9 years after the first reservoir impoundment. The shallow depth of this earthquake is poorly constrained ($Z \geq 5$ km). (c) Weekly water levels and main earthquake activity at Monteynard reservoir during the period 1979–86. The 4 events are located at 37 km from the reservoir except #18 earthquakes that occurred at a 10 km depth below the reservoir. Water levels provided by Electricité de France.

distant earthquakes to be triggered. Note that the mechanical meaning of these short-term diffusivity values is not yet highlighted due both to the short delays between peak water level and earthquakes and to distance ranges between some earthquakes and the reservoir. Such spatial and temporal settings induce pore-pressure changes that are definitively a small fraction of the pressure head for all the events of the sequences, whatever their location relative to the reservoir. We suggest a summary of the mechanics of the 1962–1984 earthquake sequence as follows: (i) the analyses of events located close to the reservoir ($\Delta < 20$ km) fit the standard required to evaluate RIS (e.g., MEADE, 1982); (ii) on the basis of the diffusivity values estimated from the entire sequence of earthquakes the distant and time delayed earthquakes cannot be rejected as not related to the Monteynard reservoir water level; (iii) the possible correlation between peaks of water level and time delayed earthquakes confirms that the estimated diffusivity and induced stress change cannot resolve the mechanics of this type of seismic instability. Nevertheless, the maximum stress changes that could drive the 1962–1984 Monteynard seismic

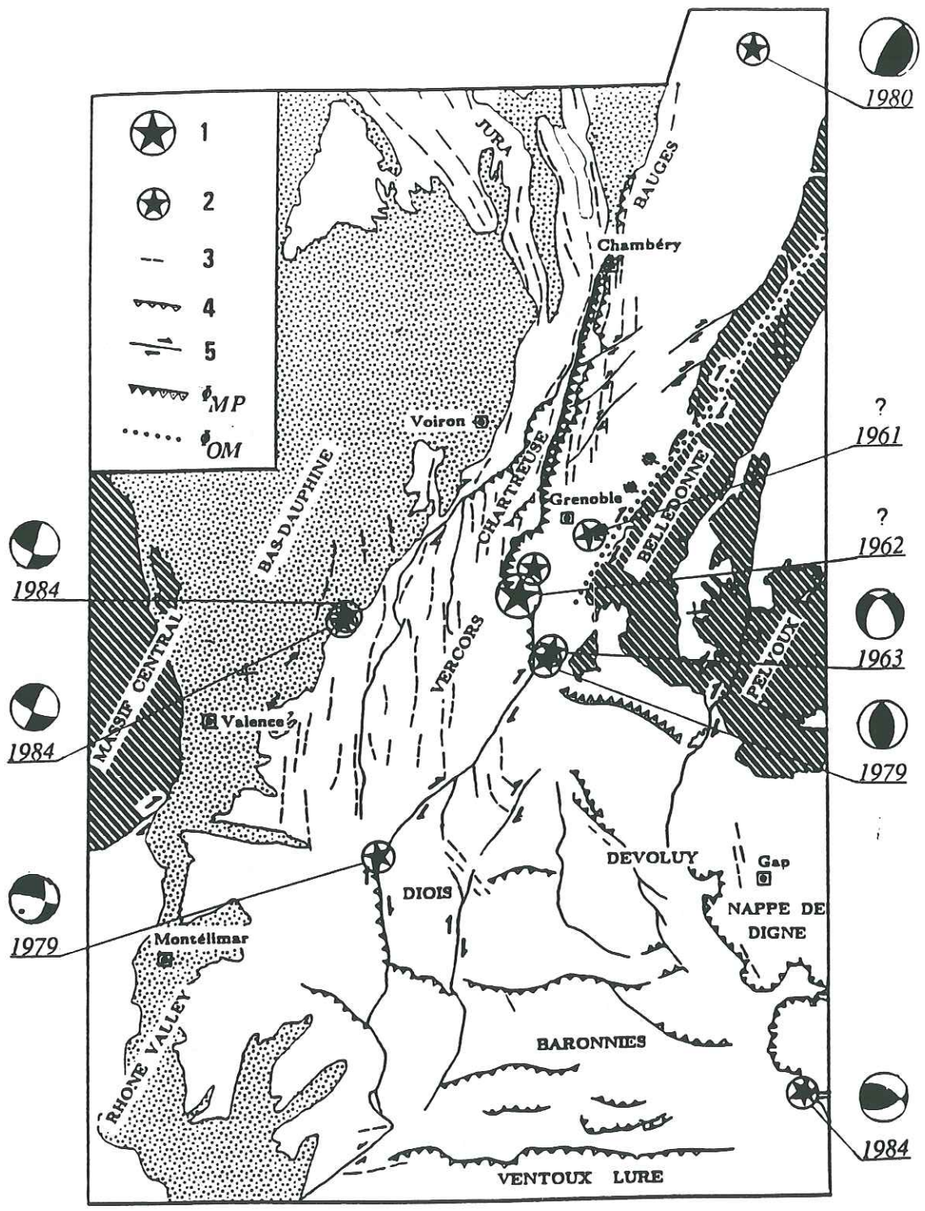

Figure 10
Seismotectonic map of the Grenoble area and major seismic events in the western Alps during the 1960–1990 period: (1) $M_L \geq 5$; (2) $5 > M_L \geq 4$. (3) Alpine fold axes (Miocene–Present); (4) main thrust faults; (5) main strike-slip faults; hatched area, basement; shaded area, Tertiary; Φ_{OM}, Oligo–Miocene basement thrust; Φ_{MP}, Miocene–Present basement thrust (with black triangles = outcrop, with dotted triangles = presumed basement thrust concealed by the sedimentary cover). Faults are adapted from GRATIER *et al.* (1989). Fault plane solutions for 1962–1979 period are from Figure 4. Other fault plane solutions are from NICOLAS *et al.* (1990). Dark quadrants contain compressional first motion, blank dilatational.

sequence are bounded by the $\Delta\sigma_{max} \sim 1$ MPa that trigger the 1963 shocks under an undrained condition.

The key point for the assessment of seismic risk in the Grenoble city area concerns the seismic instabilities associated with the delayed response type. As noted by SIMPSON *et al.* (1988), the diffusion of pore pressure from the reservoir to the hypocentral area allows the reservoir influence to extend to greater distances, affecting longer fault segments, prolucing lower stress gradients, and thus leading to larger magnitude earthquakes. Primary estimation of both seismic diffusivity and the location of regional faults is consistent with a faster migration time through faulted paths than in other directions. If the 1962 earthquake was triggered, it required open fluid flow northwestward from the reservoir. The N135 fault zone (Figure 2), close to the dam, is favorably oriented relative to the regional strain, to allow faster fluid connection to the NW of the reservoir than to the N and S directions (NICOLAS *et al.*, 1990; REBAI *et al.*, 1992). The actual existence of such a connection must be checked by independent hydrological information. Nevertheless, the 1962–1984 seismic sequence agrees with standard models that are used elsewhere to indicate reservoir-induced seismicity. The lack of *in situ* measurements of crustal hydrological properties in this area, shared by most of the RIS cases, prevents us from obtaining absolute evidence.

These observations and conceptual models attest that previous recurrence times for moderate natural shocks ($4.5 \leq M_L \leq 5.5$) estimated within this area using historic data, are modified by small stress changes. The apparently small changes in deviatoric stress imply that the upper curst in this area must be nearly everywhere at a state of stress near failure. Due to the location of chemical facilities 20 km north of the reservoir and a concentration of population at distances 25–35 km north of the dam, regional induced seismic risk must be readdressed. Note that the main triggered earthquakes of the sequence occurred in 1962, 1963 and 1979, within a $15 \times 10 \times 10$ km^3 volume from the reservoir. This earthquake area is bounded in space and time by the 1961, 1979 and 1984 shocks, respectively, 30 km north, 35 km south and 35 km west of the reservoir. All 18 earthquakes of the 1961–1979 sequence are located within a block that was relatively aseismic since early 1500. The 1961–1979 sequence of earthquakes defines a new seismically active geometry within the previously aseismic block (Figure 10).

Implications for Regional Mapping of Seismic Fault

Within the foreland of the western Alps, the convergence is still considered active and the thickening is realized through thrust faulting (ARPIN *et al.*, 1988; THOUVENOT and MÉNARD, 1990). The subalpine massifs (Figure 10), are located between a stable domain (Massif Central) in the West and a mobile domain (crystalline Belledonne and Pelvoux massifs) in the East which overthrusts westward the Chartreuse-Vercors-Diois subalpine chains (MÉNARD and THOUVENOT, 1984). The basement-cover interface is a major decollement surface on which the cover glides westward, pushed by the crustal thrust sheets of the external crystalline massifs. The shortening of the cover is achieved through a combination of the decollement and several thrust surfaces branching from it and cutting up the pile. As a result of this shortening, the uplift of the cover materials reaches 2000 m above S.L. in the Vercors massif (GRATIER *et al.*, 1989).

Due to the lack of both large earthquakes and a dense seismological network, particularly until the end of 1970, only a few focal mechanisms are available in this region. Although the major seismic instabilities of the studied area have negative evidence against natural events, the kinematics of the 3 largest shocks under study (1962, 1963, 1979) is consistent with the local tectonics as defined by the N110 balanced cross section through northern Vercors (Figure 8). Recent seismic profiles and geological data (MÉNARD and THOUVENOT, 1984; ARPIN *et al.*, 1988), constrain this balanced cross section with respect to the geometry of deep structures such as the decollement surfaces (GAMOND, 1992). According to GAMOND (1992), the westward tilting of the basement/cover interface on the Belledonne crystalline block has been occurring since Pliocene times. It has induced shallow gravity gliding processes in the cover and caused normal faulting to occur in the eastern part of the massif (Combes Normal Fault), below the reservoir dam. Thus the slip on the west dipping nodal plane of the 1962 Corrençon earthquake may correspond to such a gravity gliding process of the sedimentary pile. The driving process is the westward movement of crystalline massifs that is expressed by the deep thrust faulting for the 1979 event (Figure 8). The crystalline massifs act as an indenter and induce the shallow gravity gliding response of the Vercors massif; the small stress changes induced by the reservoir impoundment work as a trigger for the seismic instabilities. This local kinematics is coherent with the recent regional deformations.

The seismicity of the Alpine foreland occurs on crustal weakness zones which define the boundaries of aseismic blocks. The historical seismicity during the 1500–1990 period allows the location of seismic displacements on the boundaries of blocks. The map of the historic seismicity (Figure 1) clearly defines, along the western boundary of subalpine massifs (Bauges, Chartreuse, Vercors, Diois), the existence of a seismic alignment from Annecy to Montélimar. Four earthquakes have reached the intensity VIII on this block boundary in 1772, 1773, 1873 and 1901. To the southwest, the Rhône valley displays an important seismic alignment

between Montélimar and Cavaillon. The seismic alignment along the Durance valley, that bounds to the south the subalpine massifs, includes several destructive earthquakes (e.g., intensity IX, 1708, Manosque). These major seismic alignments presently have a very low activity but they bound the large Vercors-Diois block which was aseismic until 1960. We demonstrate in this study, that since 1961 a sequence of moderate earthquakes developed within this previously aseismic block. This sequence occurred close to the Grenoble valley and its geometry fits a NE-SW alignment that links together several faults previously considered to be subordinate faults (Figure 10). The activated structure could be a major crustal weakness boundary, cutting into two parts the previously aseismic mechanical entity of the Diois-Vercors massifs. The triggered characteristics of the earthquakes allow us to suggest that small stress changes were enough to drive the faults to failure. The importance of this newly activated structure for regional kinematics is confirmed by the southernmost event of the sequence, the Diois earthquake ($M_L \sim 4.3$, #17, Table 2). The dextral strike-slip movement obtained for the focal mechanism (NICOLAS *et al.*, 1990) is in close correlation with both local geologic observations and regional kinematics (Figure 10). This earthquake occurred 37 km SW from the reservoir, 16 years after the initial filling of the reservoir. It is located on the same fault as the 1971 event (#16, Table 2). Using as fault hydraulic diffusivity the value estimated from the 1971 earthquake, we could have predicated the 1979 Diois earthquake occurrence to within a few months.

The mapping of large faults and the understanding of their behavoir is a key point to the understanding of the seismicity within the Grenoble area. Zones where rocks are broken into lithic fragments attesting to recent seismic slip are fairly rare in the Alpine foreland, but evidence for large localized seismic slip in the past is newly recognized in the area. The cataclastic process is attested by observations of broken and kinked fibers, and by observations of euhedral crystals in the cavities opened by fault sliding (GRATIER and GAMOND, 1990). At least two sites are known: (i) the fault of Poliénas in the northern Vercors (GRATIER, pers. communication, 1991) where we can observe broken rocks (limestones) several meters wide, attesting to strong earthquakes in this area; (ii) the Cléry fault in the south of the Vercors, the location of the 1979 Diois event, shows on the same fault transitions between seismic (cataclastic) and aseismic (pressure solution) slips during the sliding period, associated with strike-slip motion. In this context, the triggered sequence of 1961–1984 earthquakes emphasizes that the area can be thought to be in a critical state for failure to occur.

Conclusion

During the 1961–1984 period, a seismic sequence of 20 moderate earthquakes, $3.5 \leq M_L \leq 5.3$, occurred south of the city of Grenoble within a large zone which had been aseismic for the last five centuries. The major earthquakes of the sequence

are located within ten kilometers of the Monteynard reservoir in the 1962–1963 period. The latest $M_L > 4$ earthquakes occurred in 1979 and 1984 at 35 km from the reservoir. Since the first shock of the sequence occurred in 1961, before the initial impoundment of the reservoir had started, we attempt to separate coincidental earthquake activity from induced activity. The two types of seismic responses to the filling of the Monteynard reservoir result from the two different mechanisms that are proposed to explain numerous cases of reservoir-induced seismicity (e.g., SIMPSON *et al.*, 1988).

The shallow 1963 earthquake (depth ≤ 3 km), with normal faulting, occurred a few days after the first filling of the reservoir and thus can be related to changes in elastic stress or changes in pore pressure coupled to the elastic stress. The effective stress change is $\Delta\sigma < 1$ MPa. The deeper 1979 earthquake (depth ≈ 10 km) occurred 16 years later than the initial filling of the reservoir but one month after the water height exceeded its previous 1963 maximum. The hydraulic reservoir load, in terms of annual average reservoir pressure, increased in the period 1963–1979, and decreased after 1980. Thus the volume affected by pore-pressure diffusion and the magnitude of the pore-pressure change increased with time during the period 1962–1980. The primary delayed process would give a vertical hydraulic diffusivity, c_i, based on seismic diffusivity (slope of L^2-T plot, TALWANI and ACREE, 1985) of 0.2 m^2/s close to hydraulic diffusivity estimated for rock samples (e.g., RICE and CLEARY, 1976). This value of diffusivity suggests moderate fracture permeability ($\sim$0.1 mD) in the vertical direction. Hence the primary delayed type for the 1979 earthquake shows a strong component of rapid response to short-term variations of water level that can be explained by the increased pore pressure, through decreased effective normal stress (e.g., SIMPSON *et al.*, 1988). The same process is also reported at Koyna (GUPTA, 1983), Oroville (TOPPOZADA and MORRISON, 1982) and Aswan (KEBEASY *et al.*, 1987). Although the water height difference between the previous maxima is small (less than 1 m and 0.5 m, respectively at Koyna and Monteynard), it drives major changes in seismicity. The weakness of the pore pressure changes at depth (see for example ROELOFFS, 1988), confirms that the mechanics of such earthquakes are not yet resolved. Horizontal seismic diffusivity of 1–4 m^2/s is estimated using earthquakes that occurred at larger distances from the reservoir (15–35 km) on known fault paths. This value roughly corresponds to a 10^{-15} m^2 fracture permeability and is consistent with the seismic diffusivity values estimated on other sites of RIS (e.g., TALWANI and ACREE, 1985; SIMPSON, 1986; SIMPSON *et al.*, 1988). The triggering mechanism of the 1962 instability, located ten kilometers from the dam during the initial filling, needs an open fluid flow path in the NW direction, i.e., $c_i \sim 10$ m^2/s. This process is supported by *in situ* knowledge of (i) the faulted zone, (ii) a fluid flow on the western bank of the reservoir in the NW direction, and (iii) by evidence of karstic medium located NW of the reservoir.

In this study we focused on the mechanics of seismic instabilities in an area where no seismic activity ($M_L \geq 3$) was reported for five centuries. Most of the

earthquakes are shallow events and correspond to changes of stress environment by increasing pore pressure through undrained or drained processes (artificial reservoir). When we assume that diffusion is a mechanism for delaying change in pore pressure, we explain the whole seismic sequence, except for one earthquake that occurred 30 km from the reservoir, before the initial impoundment started. Thus without completely answering the natural or triggered event question, which requires *in situ* knowledge of properties of the crust, we suggest that most of the sequence may be explained by a primarily poroelastic response of the upper crust to reservoir level history. The variability of the corresponding hydraulic diffusivity underlines the difficulty of the topic. The uppercrust has to be considered as a heterogeneous poroelastic medium. Thus, the permeability of rock matrices or fault, as well as the other poroelastic constants differ in space and time. Around Monteynard reservoir, we estimate significant changes between diffusivities associated with the initial pore-pressure front (unsaturated condition) and the short-term diffusivities associated with peak water level (saturated condition). Although knowledge of mechanical properties of the crust is minimal, the estimated value for diffusivity is either consistent on the same fault (e.g., 1 m^2/s on the NE-SW fault) or differentiated according to change in geological setting, 10 m^2/s on the NW area in a karstic medium versus 0.2 m^2/s within crystalline basement through depth below the reservoir.

The earthquake sequence under study and the two possible mechanisms of stress change argue that small stress changes trigger seismic instabilities. Although the evidence suggests a natural process for the 1961 event that occurred 30 km north from the Monteynard dam before the initial impoundment has started, the whole seismic sequence (1961–1979) maps a new seismically faulted zone within the previous aseismic block of the French subalpine massif. This structure links together several small scale faults. The kinematics of the seismic fracturing of the 1961–1984 sequence agrees with the regional tectonics. Thus the fault path mapped by the 1962–1979 triggered earthquakes could be a large regional fault. At present, it remains to be decided whether its behavior is mainly aseismic ($M_{max} \approx 5$) or if large seismic instabilities can occur on this newly proposed block boundary. The latest earthquakes up to 1992 occurred in 1984, 35 km west of the Monteynard reservoir. These two earthquakes, $M_L = 4.2$–4.3, occurred on the seismically active west boundary of the subalpine massif. They give evidence of the possible interrelation between natural seismicity, triggered earthquakes and fluid-induced perturbations. This study is one more case in a growing number of examples that strongly suggests that earthquake faulting occurs under low incremental shear stresses in the presence of high pore pressure.

Acknowledgements

This work was made possible by the use of accurate water level history of the Monteynard reservoir. We gratefully thank Electricité de France (Energie Alpes)

who provided this invaluable data. Two detailed reviews containing many excellent suggestions improved this study. R. Gibson and J.-P. Gratier reviewed an earlier version of the manuscript. This work was partially supported by Pôle Grenoblois d'Etudes et de Recherches pour la Prévision des Risques Naturels and Université Joseph Fourier, Grenoble, France.

References

ACHARD, V., and GOULA, X. (1988), *Contribution à un zonage sismotectonique de la France: Calcul des caractéristiques nécessaires à une évaluation probalistique de l'aléa sismique*, Commissariat à l'Energie Atomique, dept Analyse des Sites des Accidents et du Confinement, rapport SASC/88-58.

ARPIN, R., GRATIER, J.-P., and THOUVENOT, F. (1988), *Chevauchements en Vercors et Chartreuse déduits de l'équilibrage de données géologiques et géophysique*, Comptes Rendus de l'Académie des Sciences, Paris *307*, 1779–1789.

BELL, M. L., and NUR, A. (1978), *Strength Changes due to Reservoir-induced Pore Pressure and Stresses and Application to Lake Oroville*, J. Geophys. Res. *83*, 4469–4483.

B.C.S.F. (1984), *Observations sismologiques: sismicité de la France en 1978 et 1979* (eds. BCSF), I.P.G. Strasbourg, Strasbourg, France, 80 pp.

BRGM (1979), *Geological Map of the Alps 1/50000*, BRGM eds., Orléans, France.

CARDER, D. S. (1945), *Seismic Investigation in the Boulder Dam Area, 1940–1945, and the Influence of Reservoir Loading on Earthquake Activity*, Bull. Seismol. Soc. Am. *35*, 175–192.

DAVID, C., and DAROT, M., *Permeability and conductivity of sandstones*. In *Rocks at Great Depth* (eds. Maury, V., and Fourmaintraux, D.) (Balkema, Rotterdam 1989) pp. 203–210.

DUNEGAN, H. L., and TATRO, C. A., *Acoustic emission effects during mechanical deformation*. In *Techniques of Metal Research* (ed. Banshah, R. F.) 5, chap. 12 (Intersciences, New York 1971).

EDF (1964), *Chute de Monteynard: Dispositions générales de l'aménagement*, REHA1 *1*, 53 pp.

FRÉCHET, J. (1978), *Sismicité du Sud-Est de la France et une nouvelle méthode de zonage sismique*, Thèse 3ième cycle, Université de Grenoble, 159 pp.

GAMOND, J. F. (1992), *Normal Faulting and Tectonic Inversion Driven by Gravity in a Thrusting Regime*, J. Struc. Geol. (in press).

GRATIER, J.-P., MÉNARD, G., and ARPIN, R., *Strain-displacement compatibility and restoration of the Chaines Subalpines of the Western Alps*. In *Alpine Tectonics* (eds. Coward, M. P., Dietrich, D., and Park, R. G.) (Geological Society, London, Special Publications *45*, 1989) pp. 65–81.

GRATIER, J.-P., and GAMOND, J.-F., *Transition between seismic and aseismic deformation in the upper crust*. In *Deformation Mechanisms, Rheology and Tectonics* (eds. Knipe, R. J., and Rutter, E. H.) (Geological Society, London, Special Publications *54*, 1990) pp. 461–473.

GUERBET, R., and BALWAY, G. (1964), *Le barrage et l'Usine de Monteynard*, La technique des Travaux, mai–juin 1964, 1–40.

GUPTA, H. K., RASTOGI, B. K., and NARAIN, H. (1972), *Common Features of Reservoir-associated Seismicity*, Bull. Seismol. Soc. Am. *62*, 481–492.

GUPTA, H. K. (1983), *Induced-seismicity Hazard Mitigation through Water-level Manipulation at Koyna, India: A Suggestion*, Bull. Seismol. Soc. Am. *73*, 679–682.

GUPTA, H. K., and RASTOGI, B. K., *Dams and Earthquakes* (Elsevier, Amsterdam 1976) 229 pp.

HORATH, F. (1989), *Permeability Evolution in the Cascadia Accretionary Prism: Examples from Oregon Prism and Olympic Peninsula Melanges*, M.S. Thesis, Univ. of Calif., Santa Cruz, 104 pp.

KEBEASY, R. M., MAAMOUN, M., IBRAHIM, E., MEGAHED, A., SIMPSON, D. W., and LEITH, W. S. (1987), *Earthquake Studies at Aswan Reservoir*, J. Geodynamics *7*, 173–193.

KURITA, K., and FUJII, N. (1979), *Stress Memory of Crystalline Rocks in Acoustic Emission*, Geophys. Res. Lett. *6*, 9–12.

LEVRET, A., LOUP, C., and GOULA, X., *The provence earthquake of 11th June 1909 (France). A new assessment of near field effect*. In *Seismic Hazard in Mediterranean Regions* (eds. Bonnin, J., Cara, M., Cisternas, A., and Fantechi, R.) (Kluwer, Dordrecht 1988) pp. 383–399.

MÉNARD, G., and THOUVENOT, F. (1984), *Coupes équilibrées crustales: méthodologie et applications aux alpes occidentales*, Geodinamica Acta *1*, 34–45.

MÉNARD, G. (1988), *Structure et dynamique d'une chaine de collision: Les Alpes occidentales et centrales*, Doc. Etat. Thesis, Univ. of Grenoble.

MOORE, J. C., and VROLIJK, P. (1992), *Fluids in Accretionary Prisms*, Review of Geophys. *30*, 113–135.

NICOLAS, N., SANTOIRE, J. P., and DELPECH, P. Y. (1990), *Intraplate Seismicity: New Seismotectonic Data in Western Europe*, Tectonophysics *179*, 27–53.

PLICHON, J. N., GEVIN P., HOANG P., LONDE, P., and PETTERVILLE, P., *Sismicité des retenues de grands barrages*. In *Proceedings of the 13th Int. Comm. of Large Dams Congress, New Delhi* (ed. I.C.O.L.D.) 151 (Haussmann, Paris 1979) vol. 2, Q 51 R. 30, 1347–1362.

REBAI, S., PHILIP, H., and TABOADA, A. (1992), *Modern Tectonic Stress Field in the Mediterranean Region: Evidence for Variation in Stress Directions at Different Scales*, Geophys. J. Int. *110*, 106–140.

RICE, J. R., and CLEARY, M. P. (1976), *Some Basic Stress Diffusion Solutions for Fluid-saturated Elastic Porous Media with Compressible Constituents*, Rev. Geophys. Space Phys. *14*, 227–241.

ROELOFFS, E. (1988), *Fault Stability Changes Induced beneath a Reservoir with Cyclic Variations in Water Level*, J. Geophys. Res. *93*, 2107–2124.

ROTHÉ, J.-P. (1970), *Séismes artificiels*, Tectonophys. *9*, 215–238.

ROTHÉ, J.-P. (1972), *Annales de l'institut de Physique du Globe*, Nouvelle Série, Troisième partie, 9, Géophysique.

SIMPSON, D. W. (1986), *Triggered Earthquakes*, Ann. Rev. Earth Planet. Sci. *14*, 21–24.

SIMPSON, D. W., and NEGMATULLAEV, S. K. (1981), *Induced Seismicity at Nurek Reservoir*, Bull. Seismol. Soc. Am. *71*, 1561–1586.

SIMPSON, D. W., LEITH, W. S., and SCHOLZ, C. H. (1988), *Two Types of Reservoir-induced Seismicity*, Bull. Seismol. Soc. Am. *78*, 2025–2040.

SNOW, D. T., *Geodynamics of seismic reservoirs*. In *Proc. Symp. Percolation through Fissured Rock* (Ges. Erd und Grundbau, Stuttgart 1972) T2J, pp. 1–19.

TALWANI, P., and ACREE, S. (1985), *Pore Pressure Diffusion and the Mechanism of Reservoir-induced Seismicity*, Pure and Appl. Geophys. *122*, 947–965.

THOUVENOT, F. (1984), *Les séismes du Vercors ouest 17–19 avril 1984*, Rapport Institut Nationale Sciences Univers., 8 pp.

THOUVENOT, F., and MÉNARD, G. (1990), *Allochtony of the Chartreuse Subalpine Massif: Explosion-seismology Constraints*, J. Struct. Geol. *12*, 113–121.

TOPPOZADA, T. R., and MORRISON, P. W. (1982), *Earthquakes and Lake Levels at Oroville, California*, Calif. Geol. *35*, 115–118.

VOGT, J., *Les tremblements de terre en France*. In *Mémoires du BRGM* (eds. BRGM) (Orléans, France 1979) 215 pp.

ZOBACK, M. D., and HICKMAN, S. (1982), *In situ Study of the Physical Mechanisms Controlling the Induced Seismicity at Monticello Reservoir, South Carolina*, J. Geophys. Res. *87*, 6959–6974.

(Received October 4, 1992, revised/accepted April 20, 1993)

33

Activité sismique dans la zone de la séquence de séismes majeurs (3 M≥7) du gisement de Gasli (Ousbékistan).

submitted to B.S.S.A., Grasso et al., October 1992

Seismic activity in the 3 Ms≥7 Gasli sequence area: May-June 1991.

J.R. Grasso[1], L.M.Plotnikova[2], B.Nurtiev[2] and J. Frechet[1]

[1]LGIT, Grenoble Obervatory, B.P. 53X IRIGM, 38041 Grenoble Cedex France
[2]LIS, Academy of Sciences, 3 Kurshid Str.,700128, Tashkent, Uzbekistan

submitted to Bull. Seis. Soc. Am., November1992

Abstract

As a part of a collaborative programm between the University of Grenoble and the Academy of Sciences of Uzbek Republic, a reconnaissance of seismic activity in the area of the three Ms ≥ 7 Gasli earthquake sequence was performed during May - June 1991. 17 sites were instrumented which allowed for the location of more than 400 events, -0.2≤Ml≤4.5, which were recorded by at least 6 stations.

The prominent features of this activity are: (1) the seismic activity of the whole area is concentrated in a 20 km radius zone centered 30 km to the north of Gazli city; (2) the seismogenic zone is thick: the hypocenters range from 3 to 25 km in depth; (3) seismic activity delineates SW and SE dipping zones, implying concentric/convergent orientations of dipping planes toward the local shallow dome structure which trap the main hydrocarbon field of western Uzbekistan; (4) the thick seismogenic zone together with the concentric orientation of the dipping planes beneath the local dome structure and the possibility of numerous conjugate fault activations, suggest that the implied faults are relatively strong faults if not a newly faulted area; (5) the general pattern of seismic fractures, determined using focal mechanisms from local events, mimics the 3 main shock fault zones determined by teleseismic data, i.e. thrust faulting, despite newly faulted zone which appears to be seismically activated. Nevertheless NW and NE dipping planes for main shocks, as proposed elsewhere, are not supported by this two-month survey. These interpretations are supported by the two month survey, 7 years after the latest main shock. They provide new constraints on a model for the rupture sequence during and after the 3 main shocks, including a possible post-seismic activation of a subordonate conjugate plane set.

Introduction

In western Uzbekistan, in an area of previously estimated low seismic hazard (M.S.K. Intensity=5, Medvedev,1968), three severe earthquakes of Ms>7 (M.S.K. Intensity=9-10, Kasymov et al. 1977) occurred on April 8, 1976, May 17, 1976 and March 20, 1984. The 3 mainshock epicenters are located within 40 km distance of each others. This so called Gasli sequence occurred in an intraplate region that has exibited low seismic activity over the last few centuries (Kondorskaya and Shebalin, 1977). Starting from 1929, with the development of a network of seismic stations in the former USSR, regular seismological observations have been carried out which made it possible to register earthquakes with M_I=2 in the Central Kyzyl-Kums (Figure 1). The paucity of recent seismicity and the Quaternary cover of the Kyzyl-Kum sands do not allow for the identification of possible preexisting zones of weakness of the area, such as continental block boundaries or major faults. The area activated by the aftershocks of the 1976 major events was small compared to earthquakes of similar magnitude (Aptekman et al.,1978), and the rupture of the 1984 shock spread down-dip (Eyidogan et al. 1985), implying an unusual local state of stress. The presence of an active

hydrocarbon production close to the events raises the possibility they may have not a pure tectonic origin. Moreover, P axes of the major events of the Gasli sequence differ by more than 60° (Kristy et al.,1980; Eyidogan et al. 1985). Grasso et al. (1992) propose that the P axes of the M≥6 events are radially oriented around the local dome structure on the basis of smaller scale observations of seimic or aseismic deformations induced by fluid extraction (Grasso and Feignier, 1990, Teufel and Farwell, 1990). Simpson and Leith (1985) conjecture that these events could be induced by the gas exploitation, but the lack of geomechanical data does not allow one to confirm this hypothesis, nor the possible mechanism. A statistical model of induced seismicity for the hydrocarbon field proposed by Plotnikova et al.(1989), correlated production parameters to earthquakes. It is worth noting that none of the previous studies were able to choose the fault plane orientations for the major shocks, despite that all studies agree with the fact that the 3 main shocks and the largest aftershock (Ms=5.8, June, 4, 1978) were thrust events with depths between 10 and 20 km (Pletnev et al., 1977; Aptekman et al, 1978; Bezrodny, 1986; Hartzell 1980; Kristy et al., 1980; Eyidogan et al., 1985).

The purposes of this study was the following: (i) to test the capacity of monitoring seismic activity under adverse climatic constraints (Kyzyl-Kum desert: sand and storms, and temperatures up to 60°C) with a digital network; (ii) to obtain accurate imaging of seismic activity in order to understand the kinematic and dynamic behavior of this area; (iii) to better understand, using mechanical models, the possible temporal and spatial connections between earthquakes and fluid extraction/injection.

This study is a part of a collaborative project began in 1989, between the University of Grenoble, France and the Academy of Sciences of Uzbek Republic. In this first step of the cooperative work, we present 1) the locations of more than 200 events recorded by at least 6 stations, during the May-June 1991 field experiment; (2) focal mechanisms for larger shocks; (3) kinematic analysis and energy release analysis, with possible relation to the kinematic of the major Ms>7 events. These analyses provide constraints on a model for the rupture sequence during and after the 3 main shocks.

Field survey

The field work was carried out from May 17 to June 26, 1991, with equipement deployed and serviced by trucks out stationed at Gazli about 30km to the south. Storms and high temperatures led us to install stations underground, the digital stations having a 70° C operational limit. The equipment consisted of 8 MEQ-400 "smoked paper" seismographs and 10 digital CEIS lithoscope seismographs (Poupinet et al., 1989). The digital one-component seismic event detector is composed of a vertical 1hz seismometer, a gain-ranging amplifier and a micro computing board. The hardware can transmit to geostationnary satellites. Due to the poor satellite coverage of the region, we used these platforms as standard digital stations. A software program detects events, sorts them as a function of magnitude and stores them in a 1 megabytes storage module which complements the station. Each seismogramm is stored on 12 bytes and we use a digitization rate of 100 points per seconds because the network is

essentially installed to record local seismicity. 17 sites were set up with instruments, according to location of recent M_l>4.0 events provided by the Uzbek network (Figure 2). Battery supply for analog stations was provided by autonom energy group and the digital stations used solar panels. Common clock and absolute spatial positioning of the network was possible only using standard GPS receivers. Since all of the receivers were sited on "sand-loam", the seismometers were installedat an average depth of 1 m. More than 400 earthquakes were recorded by at least 6 stations. The largest events during the field survey were 4 events with local Richter magnitude $3.5 \leq M_l \leq 4.5$. Twenty seven events were magnitude 2.0 or larger. The stations operated stably over the entire period, except for the western point which has operated from May 25.

Geologic setting and hypocenter location

At an average elevation of 100 to 200 m, the Gasli region is underlain by a Tertiary basin filled with interbedded clay (shale) and sandstone overlying dense Paleozoic schist (Figure 3). The local subsurface geology was deduced from borehole data (CentrAsiaGaspetroleum Compagny, personnal communication, 1991). The depth to this basement gradually increases westward, from 1.2 km under the extreme eastern stations to 2.0 km beneath the western stations (Zunnonov et al., 1974; Krestinov et al., 1980). It should be noted that numerous stations were situated at either permanent local stations of the Uzbek Republic (since 1976), or temporal network stations deployed by the Institute for Earth Physics, formerly of the USSR Academy of Sciences, after the main 1976b and 1984 shocks. This allows for the potential localization of all $M_l \geq 4.0$ events that occured since 1976. For this study, our data base was extracted from more than 400 events recorded by at least 6 stations ($-0.20 \leq M_l \leq 4.5$) that were recorded in the May 17, 1991- June 26, 1991 period. The hypocenters were located using a modified HYPO71 code with a layered crust model based on "Deep Seismic Sounding" (Davydova,1975). The velocity model is shown in Table 1. Different subsets of data where analysed according to maximum location parameters ranging from 120-360° gap, 0.3-0.9s RMS residual, 2-10 km ERH, 2-20 km ERZ, 6-12 Nobs, without major changes. No time correction was applied to the digital station arrival times (± 0.05s) in this analysis, thus data described in the following section have an accuracy of smoked paper seismographs, i.e, ± 0.05s.

Earthquake distribution

The distribution of seismic activity determined by the May-June survey is shown in Figure 4, using events recorded by a minimum of 6 stations, with RMS residuals less than 0.3 s. The epicentral zone for this two month period is, without doubt, very small. It occupies a surface that roughly covers a 20 km radius zone centered 35 km to the north of Gasli. On Figure 4a, neither gap selection

nor strong RMS residual thresholds were performed in order to show that the majority of the activity, if not all, occurs in this area, thereby attesting for the aseismic (M_l<2) behavior of the surrounding region with a minimum radius of 80km. Within this cluster the epicenters are grouped in three zones. To the southwest is a distinct linear zone oriented N220°. Its length is close to 25 km with a possible discontinuity (seismic gap in the central part) within this general linear trend zone. This trend continues towards the north until it intersects the center of the cluster. The trend then changes direction to N340°. Less activity is observed in this northern zone of epicenters. To the east, there is a more diffuse N100° trend of epicenters, but this region was less-accurately monitored during the field survey due to the close eastern boundary of the local network. Nevertheless the strong stop of seimic activity on the eastern boundary is not an artifact due to network aperture. In this easternmost zone of epicenters, due to numerous events and a complex organization pattern, the N100° trend could intersect a NE-SW trend.

The general pattern of the locally monitored seismic activity follows in one part, the orientation of the focal mechanism nodal planes of the three 1976a, 1976b, 1984, Ms=7.0 shocks, i.e N100° and N220° (Hartzell, 1980 ; Kristy et al.,1980; Eyidogan et al. 1985). The N340° trend, in the northwestern part of the cluster, appears as a newly seismically activated zone.

To obtain more accurate imaging of seismic activity within the cluster, depth pattern and focal mechanisms are analysed by selecting quality epicenters within the network (gap<200°, RMS residual ≤ 0.3, ERH ≤ 3, ERZ ≤ 5). Figure 4b confirms the general epicemter trend deduced from the previous data base and Figure 5 shows the spatial distribution of the earthquakes, projected onto two cross sections. The NE-SW cross section runs parallel to the strike direction defined by seismic activity, and the focal mechanism of the 1976b and 1984 shocks (Figure 5a). In addition, this direction is roughly normal to the strike of the 1976a shock. On the northern boundary of this section the events dip steeply to the southwest (50°-60°), whereas the southern boundary of this cross section mimics a 30° dipping plane (Figure 5a). The cross section parallel to the strike of the 1976a event, with NW-SE orientation, shows a dip distribution of hypocenters that dip to the south (Figure 5b). The distribution is too diffuse to determine an unambiguous lineation. Nevertheless, these cross-sections attest that the NW and NE dipping zones, presented elsewhere as the fault planes for the mainshocks, are not the unique solution defined by this two-month survey.

In the eastern area, the seismic activity extends downwards between4 and 25 km depth. The seismic activity in itself is the deepest of the whole area in this time period. Due to the large width of the seismically active area (Figure 4 and Figure 5b), we propose the possibility of interaction between several subsets of faults in orderto explain the large lateral extension of the seismic zone. Note that the 1976b shock, with its complex faulting pattern (Aptekman et al. 1978, Hartzell 1980), is located within this area (Figure 6), and that dipping planes, defined with seismic activity in the eastern area are significantly steeper than the one of the N220° faulted zone (Figure 5). The activation of such steep reverse faults, which are severely misoriented relative to the regional stress field, argues for a probable fluid-assisted failure (e.g. Sibson, 1985).

With respect to energy release, the major events in this 2-month period (4 $M_l \geq 3.5$) occured on the eastern boundary of the N100° faulted zone (Figure 6), ranging in depth from 10 to 20 km. Other events with $2.0 \leq M_l \leq 2.7$, occur preferentially at the boundaries of the faulted areas previously described, i.e., extreme SW and extreme north in the seismically active area. One other feature of the May-June activity ditribution that merits attention is that the epicentral pattern of larger shocks significantly differs from that exibited by smaller shocks. The N100°and the N220° trends, if any could be defined by the larger shocks, are defined outside the area imaged with small scale ruptures. The area of smaller ruptures are mainly located close to the 1976b and 1984 main shock ruptures, whereas larger shocks either bound the lateral extension of the main event rupture or concentrate on the N340° new seismic lineament. The rupture sizes of the 1976a,b and 1984 main shocks are deduced from teleseismic models (Eyidogan et al. 1985; Hartzell 1980; Kristy et al.,1980) and from inversion of coseismic surface deformation for the 1984 event (Grasso and Briolle, 1992). If we focus on well located large shocks ($Ml \geq 2$, $RMS \leq 0.3$s, $Gap \leq 200°$, $ERHZ \leq 3$ km), the NW-SE cross section of seismic activity unambigously defines a SE 30° dipping zone (Figure 7).

Earthquakes kinematics

To investigate the kinematics of the three seismic branches more thoroughly, P-nodal solutions were determined for the thirty best constrained events. A two step criterion was used to select 28 focal mechanisms. First, a minimum 5 km depth was used in order to prevent possible depth mislocation of shallow events due to the station spacing. Second, a minimum of 10 first motions was required to constrain individual focal solutions. The 28 selected mechanisms are plotted on Figure 8. Two sets of mechanisms are defined by the individual mechanisms. 75 % of the individual solutions have an almost pure thrust mechanism. Note that the orientations of the P-axes of maximum compression span more than 90° of there maximum 180° (Figure 9). The strikes of the planes fit the mechanism of either the 1976b and 1984 main shocks or mimic the 1976a mechanism, altough the fault zone of the 1976a shock is at least 30 km apart and inactive in the May-June 1991 period. The second family, including only 7 events, involves strike-slip mechanisms and normal mechanisms.

In summary, the focal mechanisms indicate that faulting mechanics in the area are relatively simple and are dominated by thrust faulting. Nevertheless, fault orientations indicate a large azimutal range for fault planes, including 1976a, 1976b, 1984 mainshock orientations. Strike-slip and normal mechanisms are localized at the boundaries of the seismic branches previously defined (Figures 4). These fractures are second order internal deformation, linked with the apparent change in the orientation of epicenter lineament. The accomodation of both the majority of focal mechanisms and the distribution of hypocenters requires a set of concentric faults dipping towards the inner part of the local shallow anticline structure which trap the hydrocarbon reservoir. Nevertheless, the large extent of hypocenter locations is compatible, at least in the eastern area, with a set of *en echelon* fault

segments that could individualy dip towards the northeast within the overall south dipping orientation.

Relation with Major Shocks

In the May-June 1991 period, the predominant seismic activity delineates convergent planes dipping towards the local shallow dome structure (Figure 5). Teleseismic analysis of the main shocks from Harzell (1980) and Kristy et Al. (1980) specify that the choice of the fault plane was not possible. Nevertheless Eydogan et al. (1984) present results with NW dipping planes for the 1976b and 1984 shocks on the basis of leveling data, which concern neither the 1976b nor 1984 shocks, but the 1976a event. To the contrary we propose that the observations presented in our study argue for a southeast dipping plane at least for the 1984 shock (Figure 7). In the case of the 1976b shock we note that relocation from Eydogan et al. (1984) falls within the N100° branches of seismicity. Focal mechanisms deduced from regional data (Aptekman et al., 1978; Bezrodny, 1986) and teleseismic data do not constrain the azimuth of the 1976b fault. The width of the seismicity zone, in this area, deduced from our local survey observations, argue for a complex faulting process of the 1976b shock with subevents of different strikes, as was suggested by Aptekman et al. (1978) and Hartzell (1980). If one plane is oriented N40°, then the other one could be oriented N100°. Thus, the N100° observation of our temporary study could be related to the geometry of both the 1976b subevent and the 1976a event located 30 km apart (Figure 10). This could demonstrate the 40km continuity of the faulting geometry. One can also argue that our local data determined from a portable array study, 7 years after the latest main shock, could be regarded as a postseismic activation of a subordonate conjugate plane set (see e.g. Choy and Bowman, 1990). To constrain the kinematic and triggering processes of these compound earthquakes, a parallel study to investigate the constraints on fault planes of the three main shocks using the levelling data for 1976a,b and 1984 shocks is being done.

Relation with hydrocarbon recovery in 1991

The possible relation between local hydrocarbon recovery and the three Ms ≥7. Gasli sequence has been pointed out by Kristy et al (1980) and Simpson and Leith (1985). Without specific knowledge of the details of the hydrocarbon recovery procedure, it was impossible for these authors to investigate the possible mechanism. More recently a statistical model of induced seismicity for the Gasli hydrocarbon field was proposed by Plotnikova et al.(1989). Grasso (1992), reviewing the mechanics of seismic instabilities induced by fluid extraction, proposed three types of earthquakes induced by the recovery of hydrocarbons. Historically, the earthquakes triggered by subsurface fluid injection have been the first earthquakes associated with hydrocarbon recovery (e.g. Raleight et al.,

1972). These earthquakes are triggered within the reservoir itself by decreasing the effective stresses, according to a Mohr-coulomb failure criterion. More recently, large pore pressure drops (≥30 MPa) of depleted gas reservoirs have triggerred a second type of earthquakes above and below the gas reservoirs (Grasso 1992). These earthquakes are explained by poro-elastic stress being transferred from the reservoir to the surrounding levels (Segall, 1989). The change in horizontal stresses at the onset of seismic activity are less than 0.1 MPa for a minimum 30 MPa gas pressure drop within competent rock matrices (Grasso 1992). The third type of earthquakes are induced by the removal of load from the upper crust due to massive oil & gas recoveries. These earthquakes are both located at greater depth and are larger (Ml≥6) than the two other types. McGarr (1991) suggested a mechanical connection between the seismic moment of the seismic sequence and the mass removed by the hydrocarbon production. With this two-month-period data set, we could only investigate the possible relation between the present local fluid manipulations and the patterns of the moderate seismicity that we observe. Extraction in the Gasli reservoir (depth ranging from 0.5 to 1.5 km) ended in 1988, with an average reservoir pressure of 0.1 MPa. Since this date the reservoir has been used for regional gas storage (CAG, personnal communication 1991). Storage has taken place in 3 stages. The pressure fluctuation associated with this new activity is ± 2 bars, and no direct effect appears on the hypocentral pattern. The shallow events (z≤5km) have the same geometrical characteristics with the entire seismicity pattern. The lack of events close to or within the reservoir argue for a negative connection between either gas storage and seismicity or reservoir pressure drop and seismicity. Moreover the small initial 1MPa pore pressure of the Gasli field are negative argument against seismicity induced by poroelastic stressing. The most important observation deduced from this survey is that all the seismically active zones dip towards the hydrocarbon reservoir and that the largest events are located below the reservoir, 10km deeper. This pattern will aid in understanding the triggering mechanisms of the main shock sequence using the McGarr model (Grasso et al 1992b). The observed seismicity in the May-June 1991 period must then be explained by a residual stress release triggerred by the major stress change of the three Ms>7 shock sequences.

Discussion and conclusions

Accurate location of seismic activity in the area of the three Ms≥7 Gasli event sequence was performed during May-June 1991. The magnitude of recorded events ranged from -0.2 to 4.5. More than 400 events were recorded by a minimum of 6 stations. The prominent features of this activity are (1) the spatial concentration of the earthquakes in a 20 km radius area, (2) the trends of small events follow the main shock fault orientations despite a new faulted area being defined in the northern part of the cluster. The epicentral lineament clearly mimics the 1984 fault geometry. The correlation is poorer in the northern part, where the faulting splays and diffuses into a number of possibly conjugated fault segments in the area of the 1976b shock. These observations argue for a complex

faulting pattern of the 1976b shock both in terms of strike and dip, as was proposed elsewhere (Aptekman et al. 1978, Hartzell 1980). The lack of seismic activity in the area of the 1976a shock could imply that the stress release in the initial ruptures was complete in the sense that there were no residual stress concentration. This must be confirmed by an analysis of $M_l \geq 4$ events in the period 1976-1989. The newly faulted area, i.e., not related to the geometry of the 3 mainshocks, could be induced by the mechanics of fault junctions as was proposed by Andrews (1989); (3) the distribution of seismic activity as a function of depth is unusual for midplate earthquakes. The seismogenic zone is relatively thick; the hypocenters range from 3 to 25 km in depth; (4) the concentric orientation of dipping zones towards the local dome structure which traps the main hydrocarbon field of the Western Uzbekistan; (5) The thick seismogenic zone, the concentric orientation of the dipping planes beneath the local dome structure and the possibility of numerous conjugate fault activations, including possible triple junction, suggest that the implied faults are relatively strong faults, with the possibility of fresh fractures.

Acknowledgement

This field survey greatly benefited from the administrative support of the Laboratory of Induced Seismicity, Tashkent and the Academy of Sciences of Uzbekistan, which opened to us the Gasli area. We thank M. Iouldach, A. Olore, M. Lambert, P. Volant, F. Guyoton, R. Guiget, M. Gaillard for their key contributions during field experiments and R. Bossu who contributed to the data analysis. We thank G. Poupinet, head of Lithoscope polls, who rented to us the digital seismic stations, despite the negative opinions of numerous french colleagues. This study was partially supported by the DBT-Instability programm, contribution nº540 from INSU, France, the Uzbek Academy of Sciences, and Université Joseph Fourier, Grenoble, France.

REFERENCES

Andrews, D.J., (1989). Mechanics of fault junctions, Journ. Geophys. Res., 94, 9389-9397.

Aptekman, K. Y., V.M. Grayzier, K.G. Pletnev, D.N. Rustanovich, N.V. Shebalin and V. V. Shteinberg (1978). Data on processes in the epicentral zone of the 1976 Gasli earthquakes, in Epicentral zones of Earthquakes, vol. 19, Questions in Engineering Seismology, Nauka, Moscow, 149-166 .

Besrodny, E.M. (1986). The source mechanism of the Gazly earthquakes of 1976-1984, in Gazly earthquakes of 1976 and 1984, Tashkent, Fan, 94-105.

Choy, G.L. and J.R. Bowman (1990). Rupture process of a multiple main shock sequence: Analysis of teleseismic, local, and field observations of the Tennant Creek, Australia, earthquakes of January 22, 1988. Jour. Geophys. Res., 6867-6882.

Davydova, N.I., Y.F. Ivanstov, B.B. Tal'-Virskii, A.N. Fursov, and G.A. Yaroshevskaya (1975). Properties of the deep-seated seismic boundaries in western Uzbekistan, in Seismic properties of the Mohorovicic discontinuity, N.I. Davydova Editor, Jerusalem, Israel.

Eyidogan, H., Nabelek J. and N. Toksoz (1985). The Gazli, USSR, 19 march 1984 earthquake: the mechanism and tectonic implications, Bull. Seis. Soc. Am., 75, 661-675.

Grasso, J.-R. (1992). Mechanics of seismic instabiliies induced by the recovery of hydrocarbons. Submitted to Pageoph, Special Issue "Induced Seismicity".

Grasso, J.-R. and Feignier B. (1990). Seismicity induced by gas depletion: II Lithology correlated events, induced stresses and deformations, Pure Appl. Geophys,134, 427-450.

Grasso, J.-R. and P. Briolle 1992. Coseismic folding and geometrical constraint on the kinematic of the the Gasli earthquakes, internal report, LGIT, Observatoire de Grenoble.

Grasso, J-R., D. Fourmaintraux et V. Maury (1992a). Le role des fluides dans les instabilités de la croute supérieure: L'exemple des exploitations d'hydrocarbures, Bull., Soc. Geol. France, 163, 27-36.

Grasso, J.-R., Plotnikova, L.M., Nuteev, B. and R. Bossu (1992b). The largest seismic energy release by human activity: The 3 Ms≥7 Gasli sequence? Submitted to Pageoph, Special Issue "Induced Seismicity".

Hartzell, S. (1980). Faulting process of the May 17, 1976 Gazli, USSR, Earthquake, Bull. Seis. Soc. Am., 70, 1301-1310.

Kasymov,S.M, A. Dzhurayev and P. Madatov, (1977). Maps of the isoseismals of the Gazli earthquakes of april 8 and May 17, 1976, Information Bulletin,184, Taskent Fan .

Kondorskaya, N.V. and N.V. Shebalin (1977). New catalogue of strong earthquakes in the territories of the USSR from ancient times up to 1975, Kondorskaya, N.V. and N.V. Shebalin Editors, Nauka, Moscow, 535pp.

Krestinov, V.N., T.P. Belousov and D.V. Shtange (1980). Seismotectonic conditions of the occurence of the Gazli earthquakes of 1976, Bull. Acad. Sci. USSR., Earth Physics 16, 648-660.

Kristy, M.J., L.J. Burdick and D.W. Simpson (1980). The focal mechanisms of the Gazli, USSR, earthquakes, Bull. Soc. Seis. Am.,70, 1737-1750.

MacGarr, A. 1991. On a possible connexion between three major earthquakes in california and oil production. Bull. Seis. Soc. Am, 81, 948-970.

Medvedev, S.V. (1968). Seimic zoning of the USSR, Medvedev, S.V.Editor, Nauka, Moscow.

Pletnev K.G., N.V. Shebalin and V.V. Shteinberg (1977). Strong-motion records from the May 1976 Gazli, USSR earthquakes, U.S. Geol. Surv. Circular 762A, 3-5.

Plotnikova, L.M., Flynova, M.G., V.I. Machmudova (1989). Induced seismicity in gas field region. Proc. XXV IASPEI general assembly, Istambul, August 1989.

Poupinet, G., Pasquier, M., Vadell, M., and L. Martel (1989). A seismological platform traansmitting via meteosat, Bull. Seis. Soc. Am., 79, 1651-1661.

Raleigh, C.B., Healy J.H. and Bredehoeft J.D. 1972. Faulting and Crustal stress at Rangely, Colorado, A.G.U., Geophysical Monograph 16, 275-284.San Andreas fault.

Segall, P. 1989. Earthquakes triggered by fluid extraction. Geology, 17, 942-946.

Sibson, R.H. (1985). A note on fault reactivation, J. Struc. Geol., 7, 751-754.

Simpson D. W. and Leith W. (1985). The 1976 and 1984 Gazli, USSR, earthquakes - Were they induced ?, Bull. Seismol. Soc. Am.,75, 1465-1468

Teufel, L.W. and Farwell, H.E. (1990). Distribution of in situ stress and natural fractures in the Ekofisk field, North Sea, in Proc. Third North sea chalk Symp., Copenhagen, Denmark, June 11-12

Zunnonov F.K., M.A., Akhmedzhanov, O.M. Borisov and T. Ergeshev (1974). Geological and geophysical modelof the crust in the western Uzbekistan, Geotectonics, 1, 28-34.

FIGURE CAPTIONS

Table 1 : velocity model (adapted from Davydova et al., 1975).

Figure 1 : Seismicity map of the western Uzbekistan area, 1955-1985 (from Uzbek national network). The cluster located within the box is 400 km distant from both the Pamir-Hindou Kouch seismic zone and the Iran-Tadjik seismic zone, and is active since 1976.

Figure 2 : Temporary network that operated in the May-June, 1991 period. Lithosocope digital stations are black triangles. Analog stations are grey triangles. Small dots are active seismic zones during this period.

Figure 3 : Schematic SW-NE geological cross section throught Gasli field area.

Figure 4 : Seismicity map of the Gasli area deduced from the May-June, 1991 survey. a) No gap selections were performed in order to demonstrate that the seismic area is small in this time period. The 228 epicenters of this map have RMS≤0.3 s and NOBS≥6. b) Subset of 169 earthquakes selected with gap≤200°. Shaded areas are the local hydrocarbon field, estimated by CAG (Centrasia Gaspetroleum) Compagny.

Figure 5 : Hypocenter distribution projected on vertical cross sections. Earthquakes have been selected using RMS≤0.3 s, NOBS≥6, ERH≤5 km. a) NE-SW cross section. b) NW - SE cross section.

Figure 6 : Seismicity map of the major earthquakes, $M_l \geq 2$, that occured in the period May-June 1991. Shaded areas are the local gas field, estimated by CAG (Centrasia Gaspetroleum) Compagny. Rectangular boxes labelled 1 to 3 are the estimated projection of the fault size for respectivelly 1976a, b and 1984 M≈7 shocks. The locations of the earthquakes are from Eydogan et al. (1985); The geometry of the earthquakes is estimated using either teleseismic analyses or by levelling data for 1984 shocks only (Eydogan et Al., 1985; Grasso and Briolle, 1992).

Figure 7 : NW-SE vertical cross section of $M_l \geq 2$ earthquakes. Earthquakes have been selected using GAP≤200°, RMS≤0.3 s, NOBS≥6, ERH≤3 km.

Figure 8 : a) Single-event focal mechanism solutions (lower hemisphere equal-area projections) determined by FPFIT (Openheimer and Reasenberg,1984). Symbols: solid circle is compressionnal arrival; open circle is dilatationnal arrival; P and T are axes of maximun and

minimun compressive stresses, respectively. Selected events have a minimum depth of 5 km and a minimum of 10 first motions. b)map of focal mechanism (lower hemisphere equal-area). Symbols: solid dots are P -axes of maximun compressive stresses; open circle are P-axes of minimun compressive stresses. Non-thrust faulting solutions are articially grouped at the upper and lower part of the map. Their true locations are indicated by the black line.

Figure 9 : Relation between the geometry of the seismic activity located by the May-June, 1991 field survey and the geometry of the major earthquakes in the Gasli area (Uzbekistan). Black lines schematize local directions of the nodal planes for 1) 1976a (after Besrodny 1986, Eyidogan et al. 1987); 2) 1976b events (after Besrodny 1986, Eyidogan et al. 1987) 3) 1984 event (after Besrodny 1986, Eyidogan et al. 1985). The corresponding focal mechanisms are presented in the upper box.

Table 1 : velocity model.

P velocity (km/s)	Thickness (km)
2.5	1.4
5.9	10.6
6.1	13.0
6.3	10.0
6.4	6.0
8.0	.....

WESTERN UZBEKISTAN SEISMICITY 1955-1986 Z≤70 km SSR UZBEK NETWORK

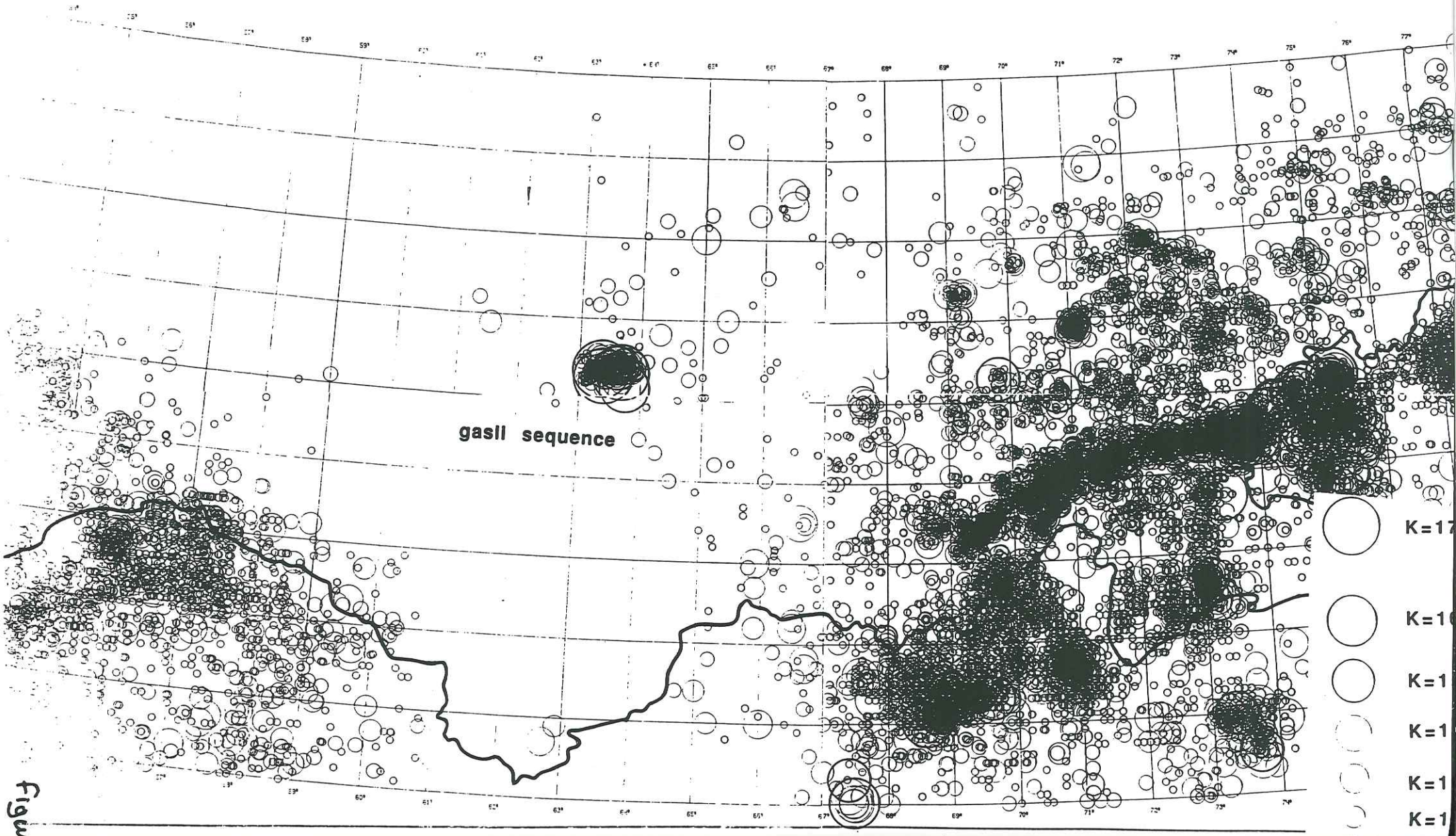

Figure

GASLI MAY-JUNE 1991: TEMPORARY NETWORK

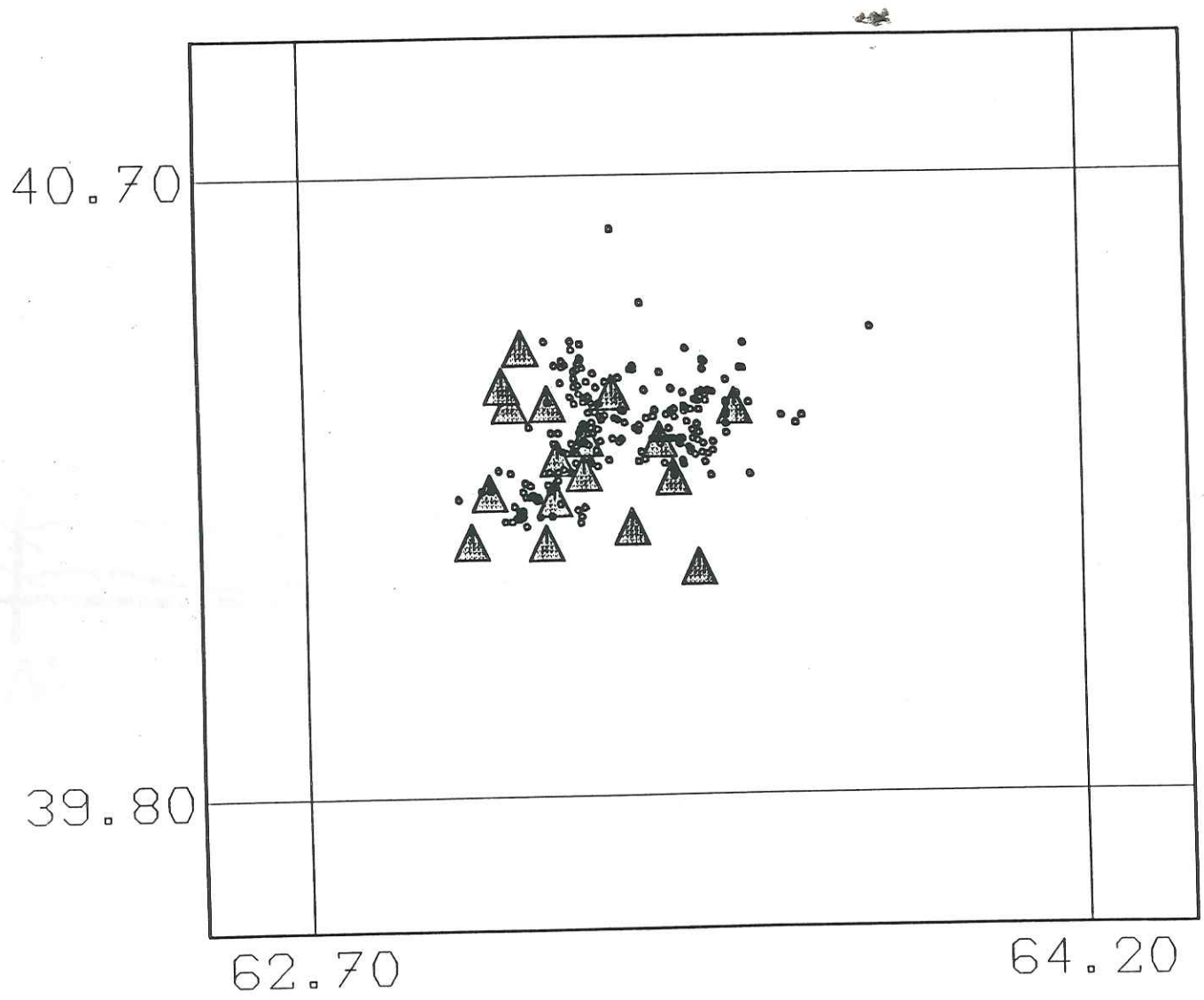

NOBS>6

RMS< 0.3s

GAP<360º

SCALE

Figure 2

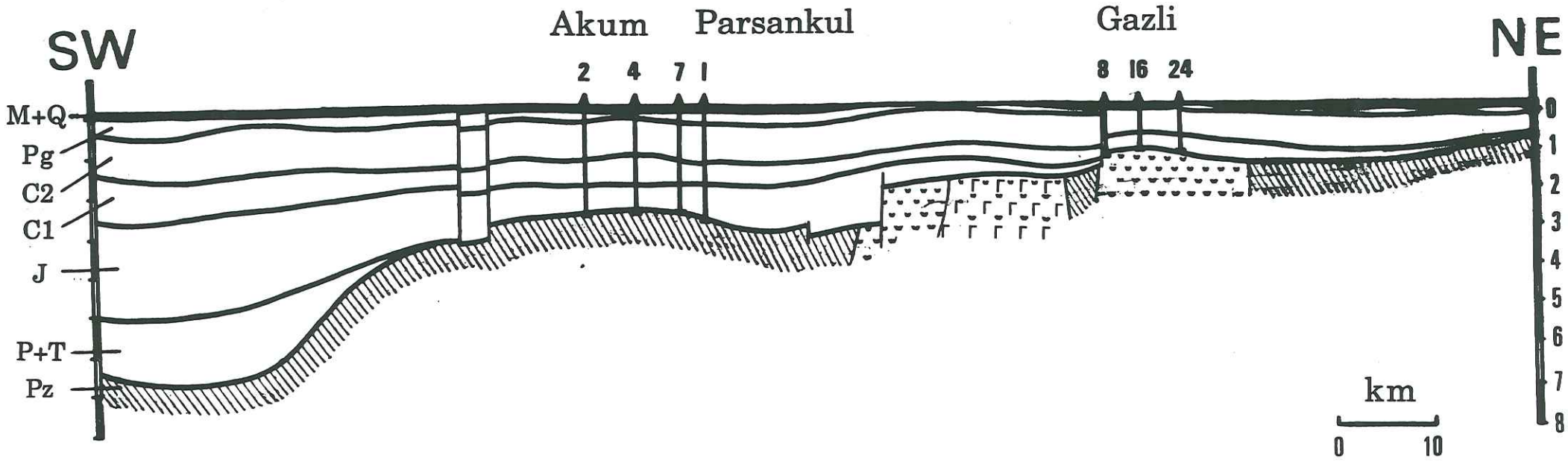

figure 3

GASLI MAY-JUNE 1991: DISTRIBUTION OF EPICENTERS

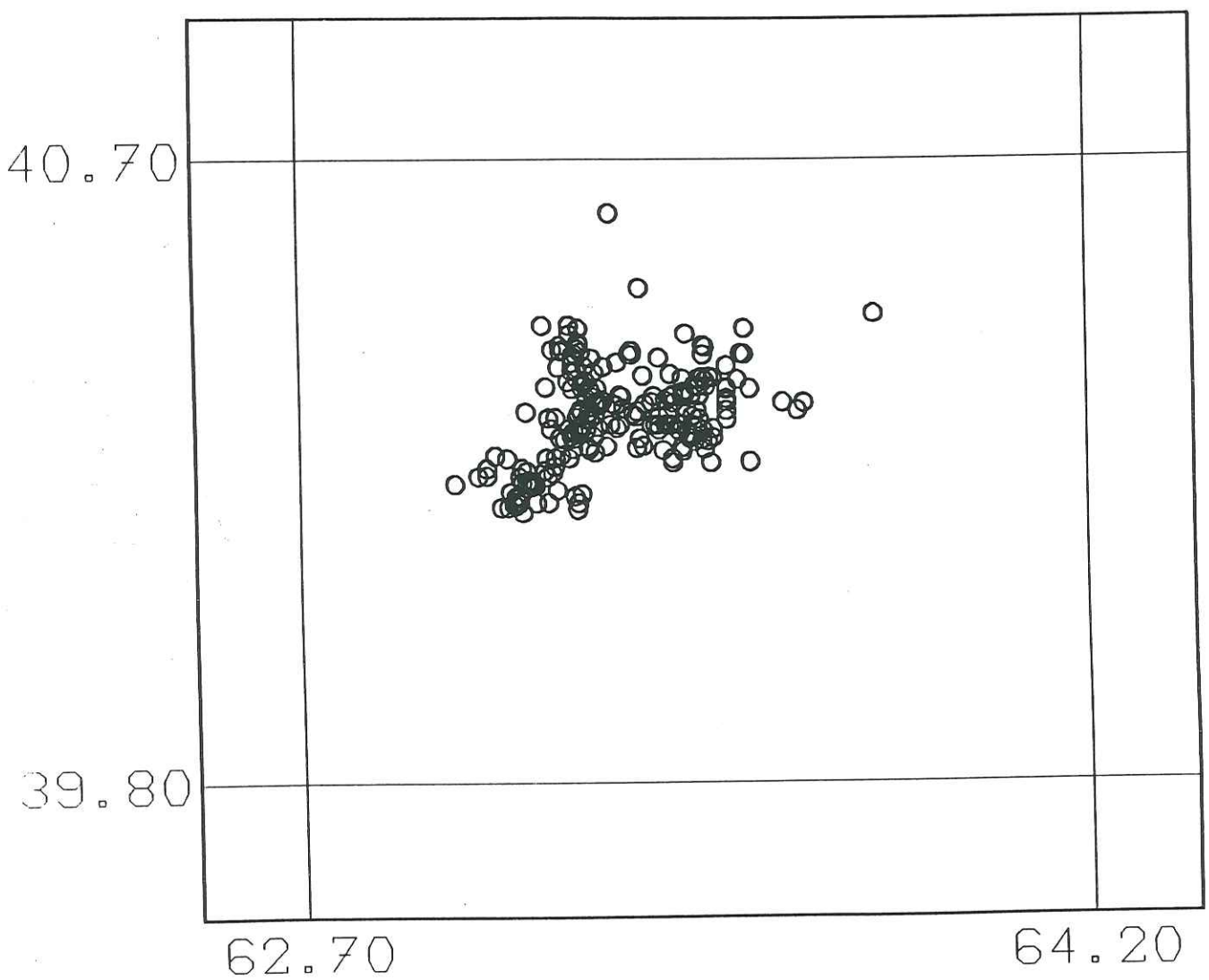

228 EVENTS

NOBS>6

RMS< 0.3S

GAP<360º

SCALE 05km

figure 4a

GASLI MAY-JUNE 1991: DISTRIBUTION OF EPICENTERS

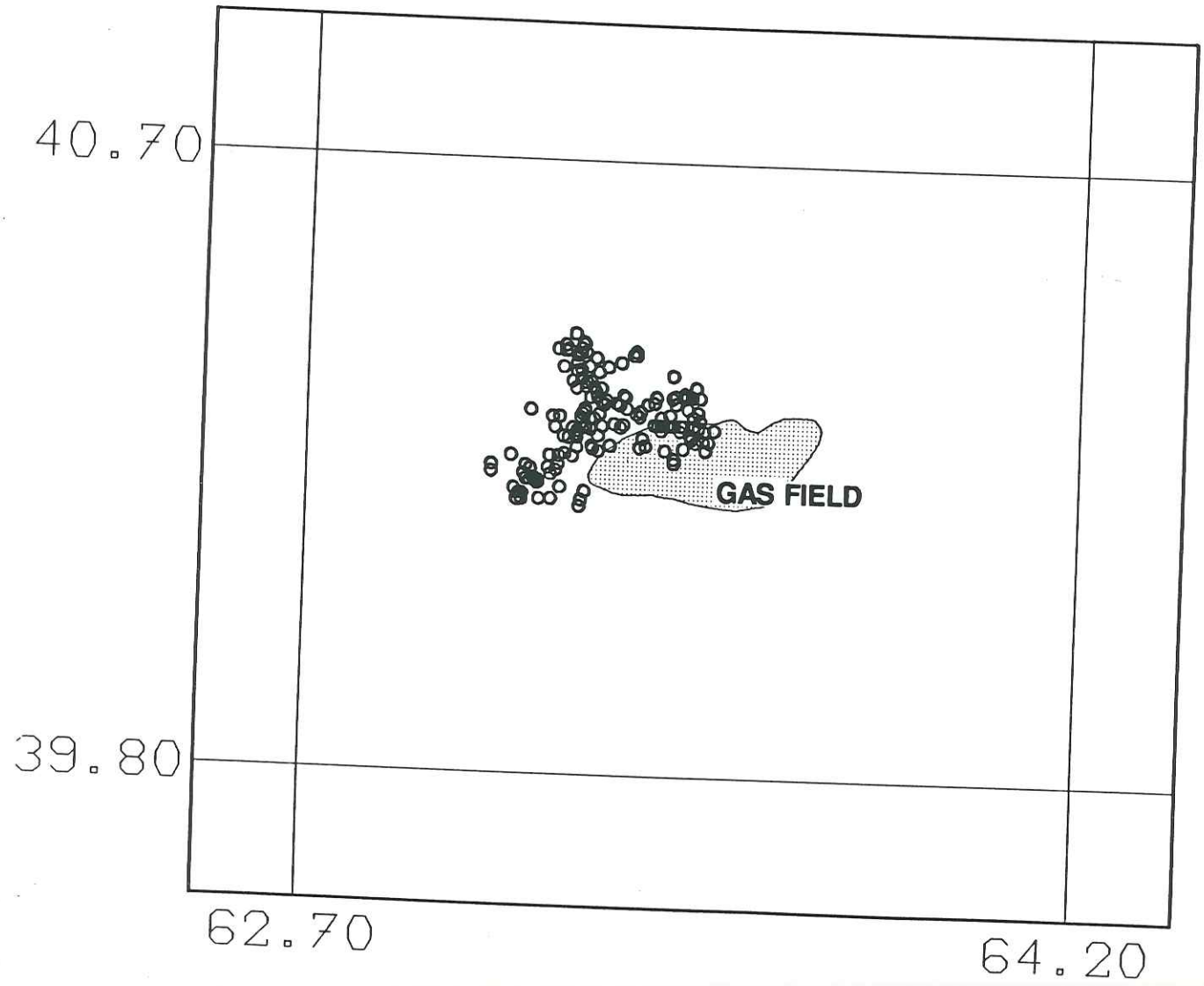

169 EVENTS

NOBS>6

RMS< 0.3S

GAP<200º

SCALE 05km

figure 4b

GASLI MAY-JUNE 1991: NE-SW CROSS SECTION

NOBS>6 **GAP<360º**

RMS< 0.3S **ERH<5 KM**

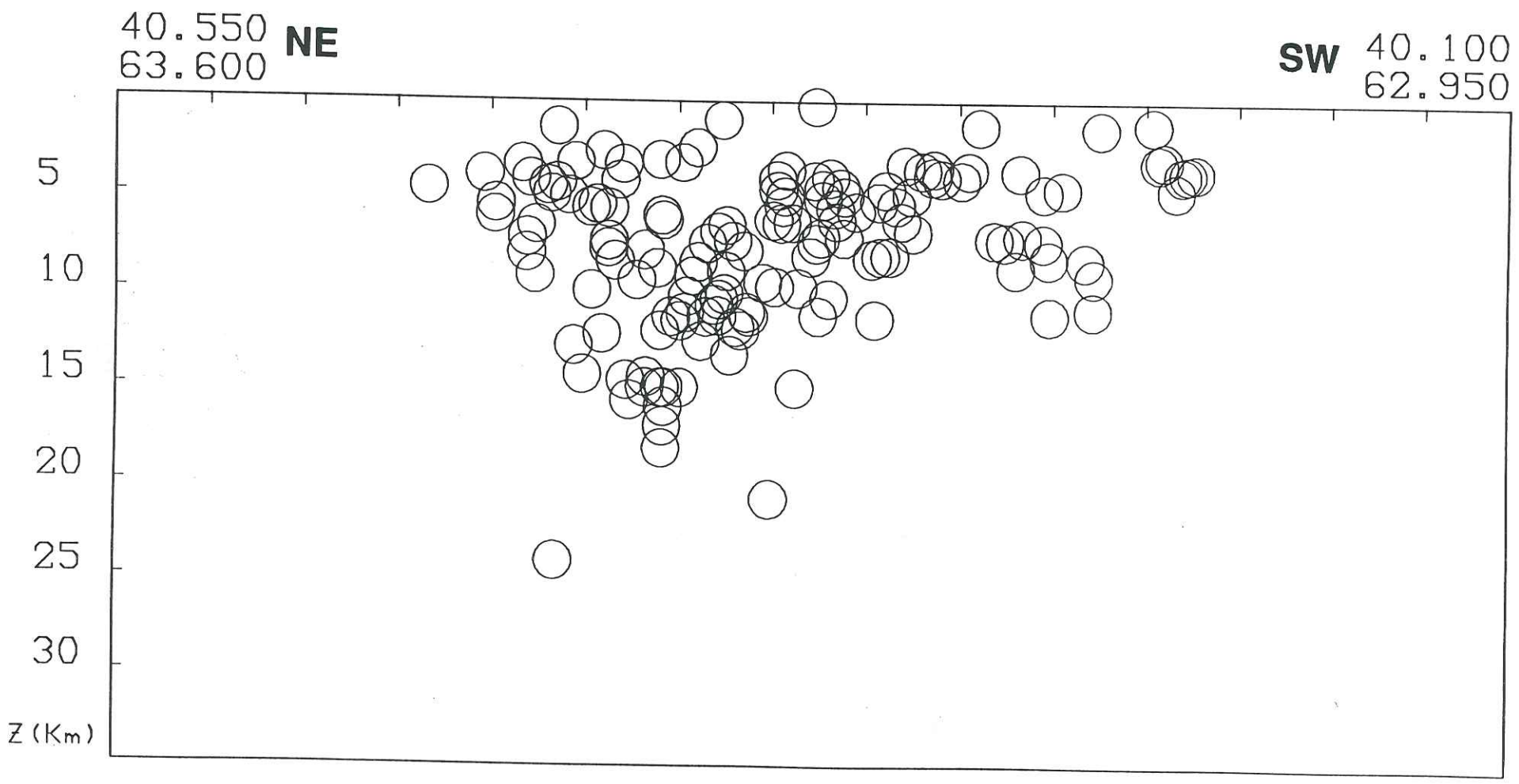

figure 5a

GASLI MAY-JUNE 1991: NW-SE CROSS SECTION

NOBS>6 GAP<360º

RMS< 0.3S ERH<5 KM

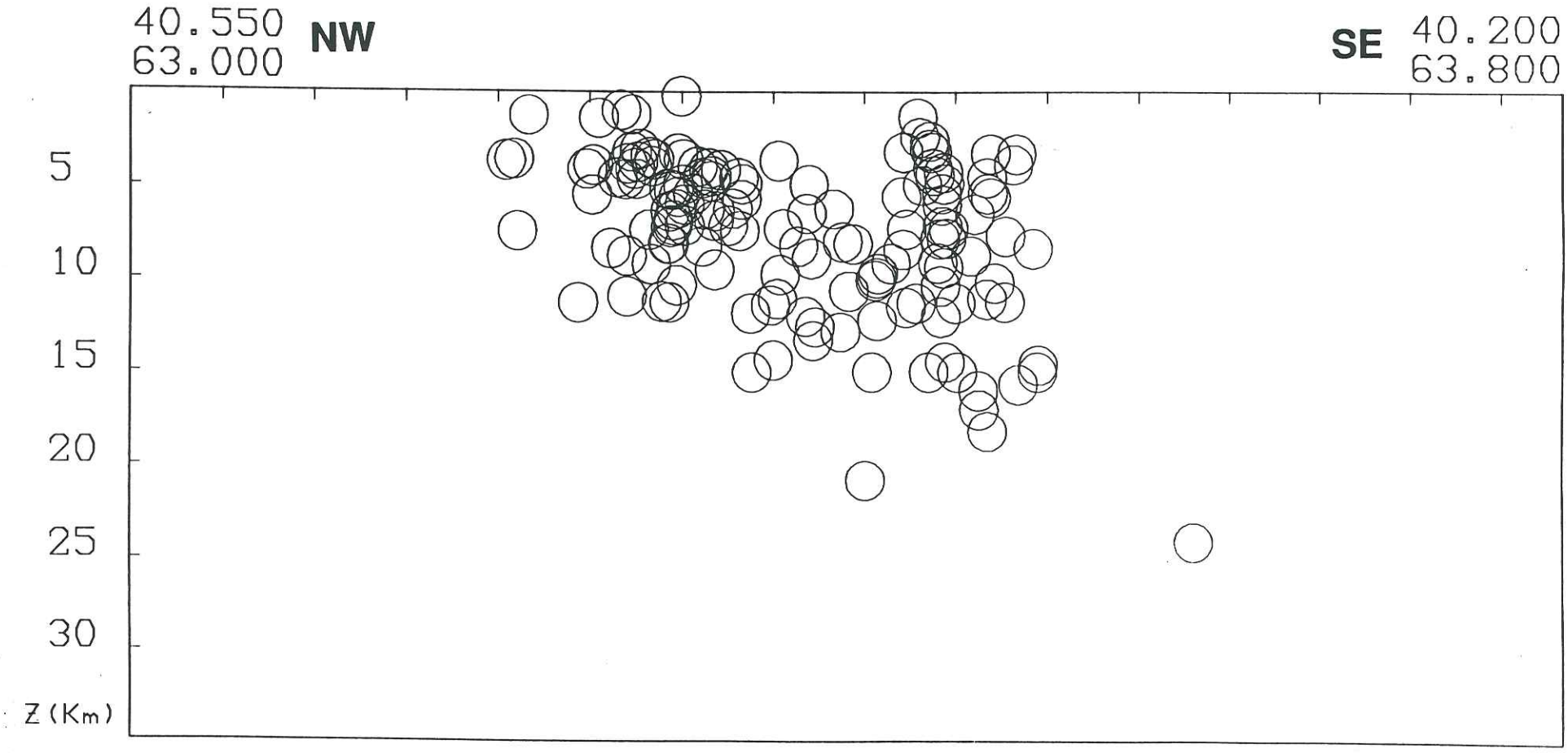

Figure 5 b

GASLI MAY-JUNE 1991: RELATION WITH MAINSHOCKS

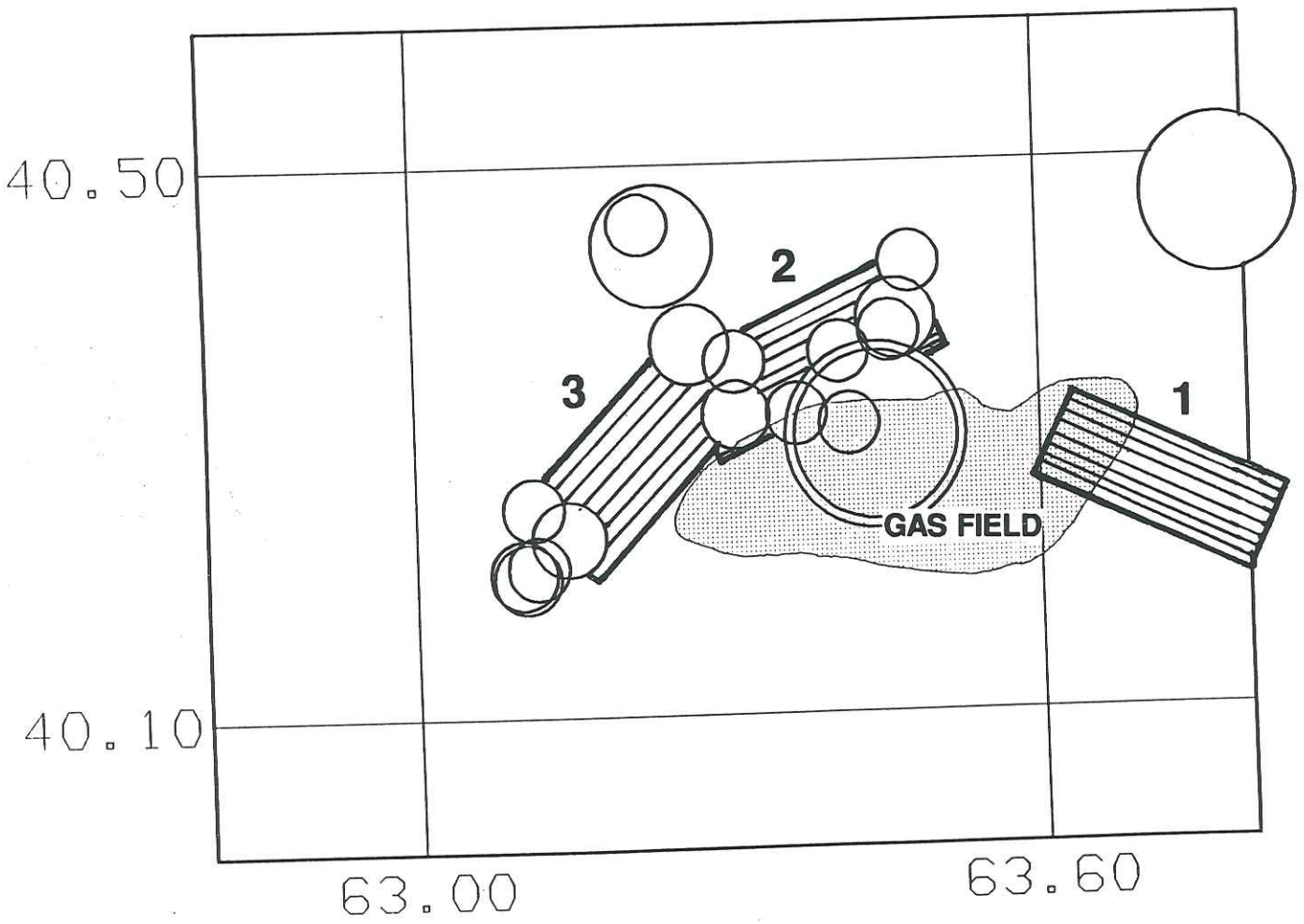

ML>2

NOBS>6

RMS< 0.3S

GAP<360º

SCALE 0 5 km

FAULT ORIENTATION

1=1976A
2=1976B
3=1984

Figure 6

GASLI MAY-JUNE 1991: NW-SE CROSS SECTION

NOBS>6 **GAP< 200º**

M*L*>2 **RMS< 0.3S** **ERH< 3 KM**

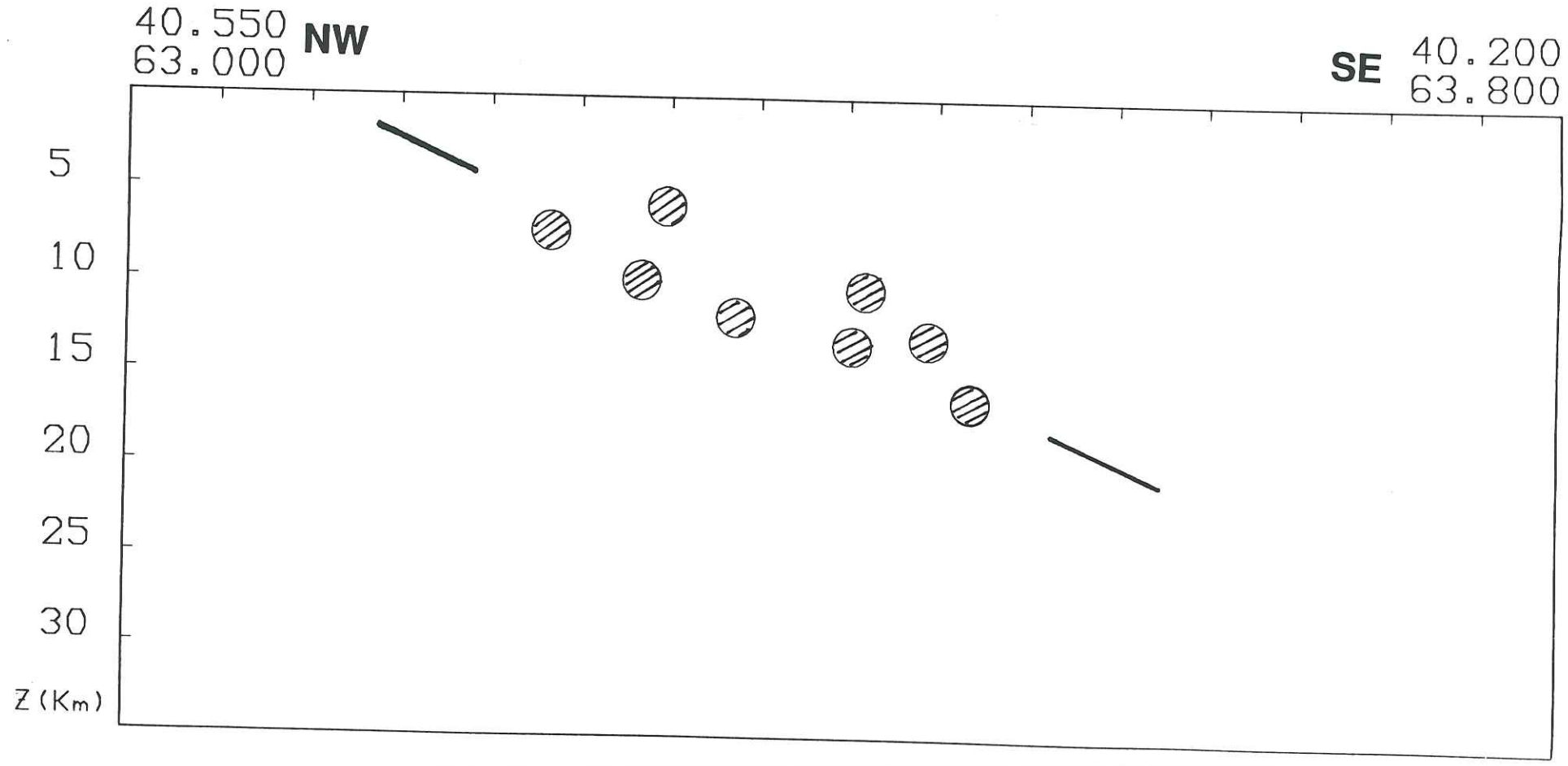

figure 7

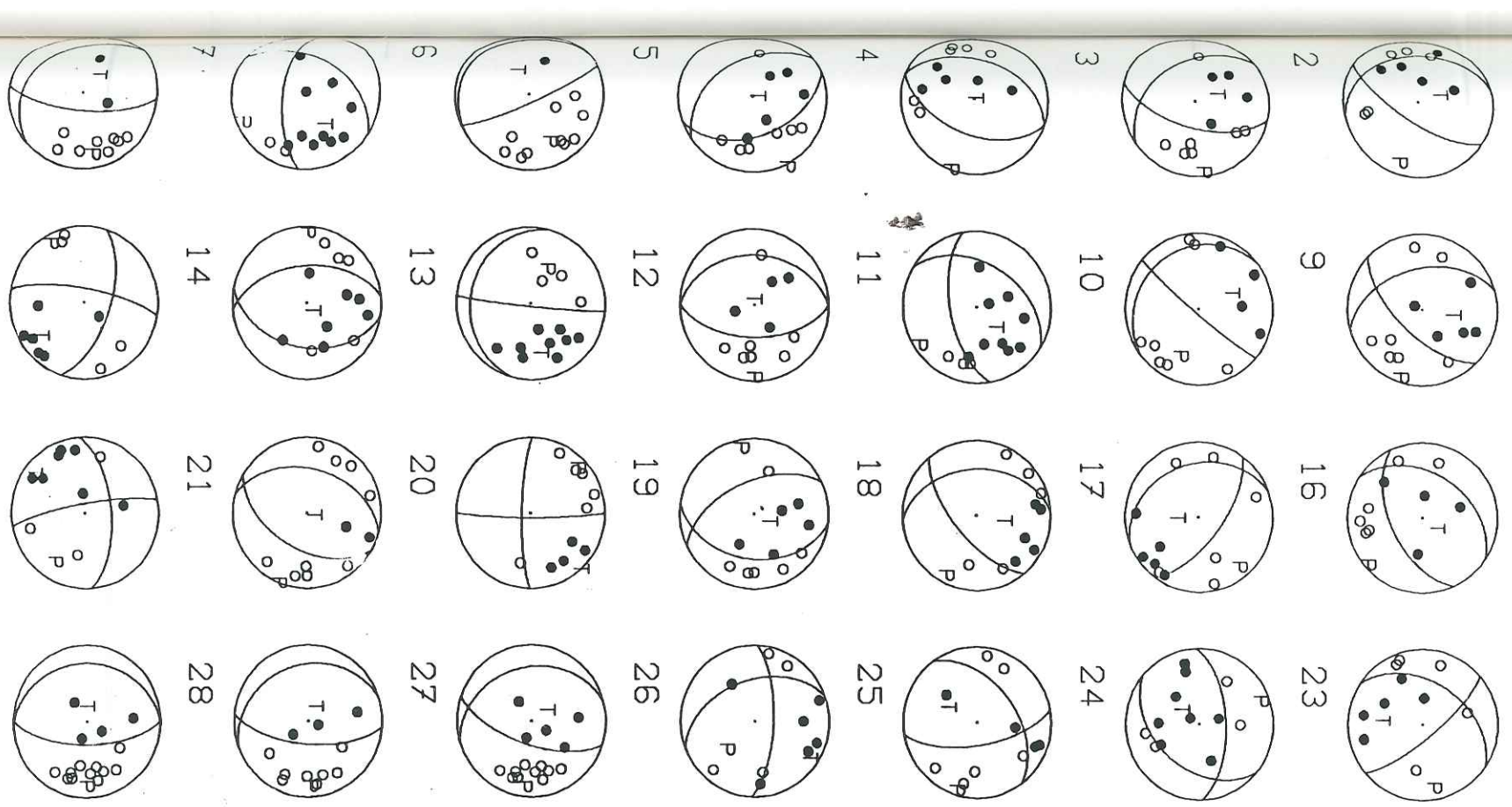

figure 8a

GASLI may-june 1991 nobs >10 Z>5 km selection mecanism

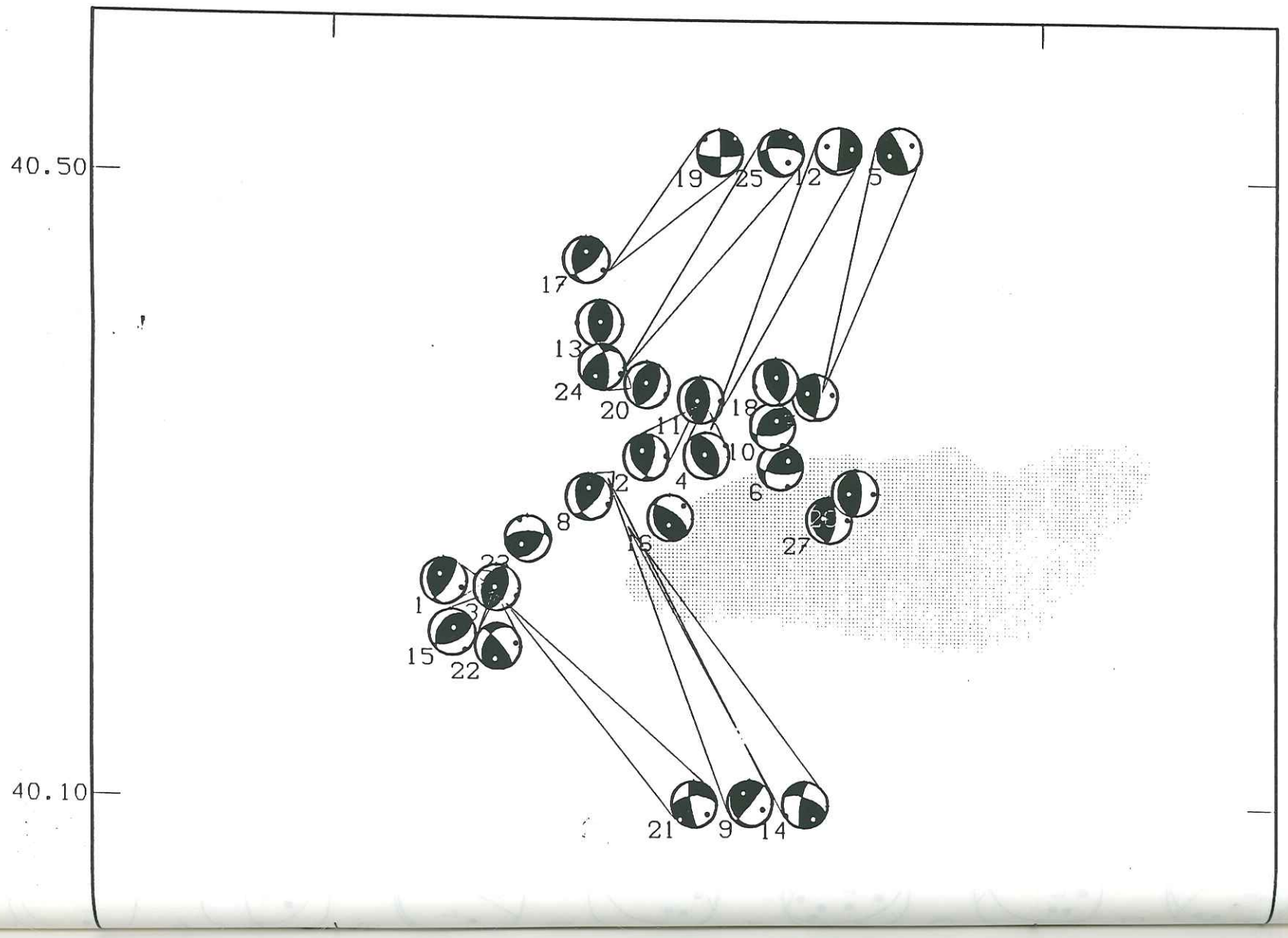

figure 8b

GASLI MAY-JUNE 1991: RELATION WITH MAINSHOCKS

France Group et al 1992 submitted SSA

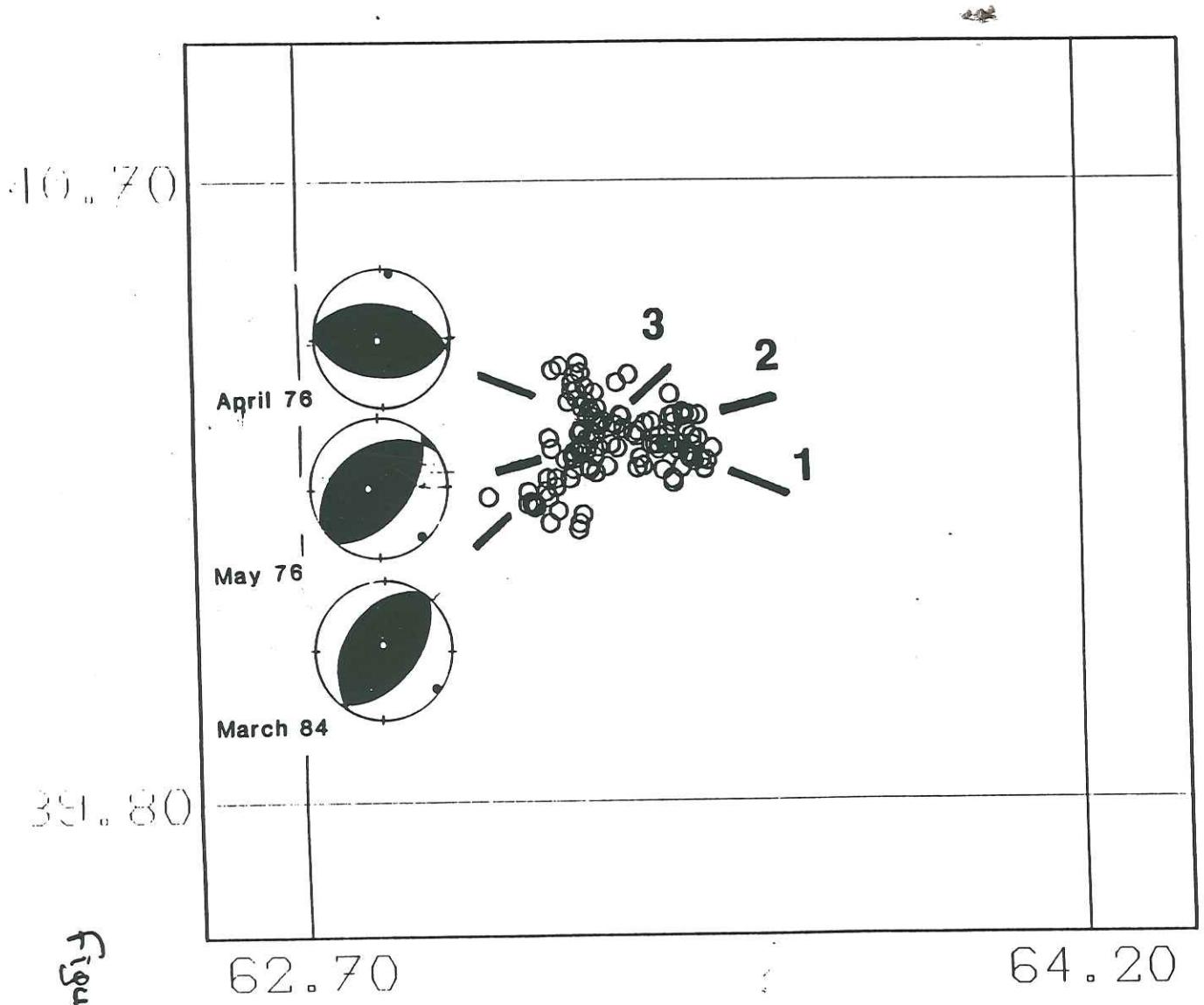

NOBS>6

RMS< 0.3S

GAP< 200º

ERH< 3 KM

SCALE 05km

FAULT ORIENTATION

1=1976A
2=1976B
3=1984

figure 9

4

MECANISMES DES RUPTURES INDUITES PAR L' EXPLOITATION D'HYDROCARBURE

Ce chapitre répertorie les réponses sismiques observées au voisinage d'exploitation d'hydrocarbures et propose 3 classes de cas types. Ces classes sont définies à la fois par la taille des ruptures sismiques induites et par leurs distances aux gisements. Pour chaque classe des modèles sont proposés pour valider les mécanismes possibles. Le couplage entre les différents phénomènes n'est pas envisagé à ce stade de l'étude. La validation des mécanismes ne pourra être effectuée que par apport de données supplémentaires, ce qui implique un partage de la connaissance géomécanique des sites sismiquement actifs avec les producteurs.

QUATRIEME ITERATION: Les failles du système deviennent de plus en plus significatives.
(Ian Malcolm)

PAGEOPH, Vol. 139, No. 3/4 (1992)

0033–4553/92/040507–28$1.50 + 0.20/0

Mechanics of Seismic Instabilities Induced by the Recovery of Hydrocarbons

J.-R. GRASSO[1]

Abstract—We review earthquake distributions associated with hydrocarbon fields in the context of pore pressure diffusion models, poroelastic stress transfer and isostasy theory. These three mechanisms trigger or induce seismic instabilities at both local scale ($D \leq 5$ km) and at regional scale ($D \geq 20$ km). The modeled changes in stress are small (≤ 1 MPa), whatever the tectonic setting. Each mechanism corresponds to different production processes. (1) Local hydraulic fracturing due to fluid injection induces seismic-slip on cracks ($M_L \leq 3$) within the injected reservoir through decreasing the effective stress. (2) Pure fluid withdrawal causes pore pressure to decrease within the reservoir. It triggers adjustments of the geological structure to perturbations related to the reservoir response to depletion. Poroelastic mechanisms transfer this stress change from the reservoir to the surrounding levels where $M_L \leq 5$ seismic instabilities occur either above or below the reservoir. (3) Massive hydrocarbon recovery induces crustal readjustments due to the removal of load from the upper crust. It can induce larger earthquakes ($M_L \geq 6$) at greater distance from the hydrocarbon fields than the two other mechanisms.

Due to the mechanical properties of the shallow rock matrices involved, seismic slip triggered either by mechanism (1) or (2), is a second-order process of the main elastoplastic deformation. For a minimum of 80% of commercially productive basins, most of the local deformation is reported as aseismic, i.e., there is no evidence for $M_L \geq 3$ earthquakes. Nevertheless, the induced stresses vary as a function of time in a manner that depends on the hydraulic diffusivity (i.e., permeability) of the reservoir and surrounding rocks. Because small earthquakes ($M_L \leq 3$) indicate changes in stress and pore pressure, monitoring of seismicity is a means of assessing *in situ* reservoir behavior.

The less constrained seismic response to hydrocarbon recovery is the possible connection between local fluid manipulations, triggered earthquakes and major regional earthquakes. Positive feedback mechanisms suggest that the region of seismic hazard changes is much larger than the area where hydrocarbons are extracted. These observations and models testify that fluid movement and pore pressure changes (increase or decrease) play important roles in the mechanics of earthquakes and in the triggering of natural earthquakes.

Key words: Induced seismicity, faulting, fluid, hydrocarbon, pore pressure.

Introduction

In most cases, the perturbation of the underground mechanical equilibrium due to rock and fluid manipulation (quarries, mines, dams, geothermal field, hydrocarbon recovery) induces deformation of the involved sites. The amplitude and the rate

[1] Observatoire de Grenoble, LGIT/IRIGM BP 53x 38041, Grenoble Cedex, France.

Microfracturing by fluid injection is a standard method used in geothermal fields for determining the reservoir properties and the evolution of the fields in space and time (see e.g., CORNET, 1977; PEARSON, 1981; BATCHELOR *et al.*, 1983). Its application to oil and gas fields is less common (e.g., POWER, 1977; HART *et al.*, 1984; CASSEL *et al.*, 1990). Observations made near Cold Lake, Alberta, of

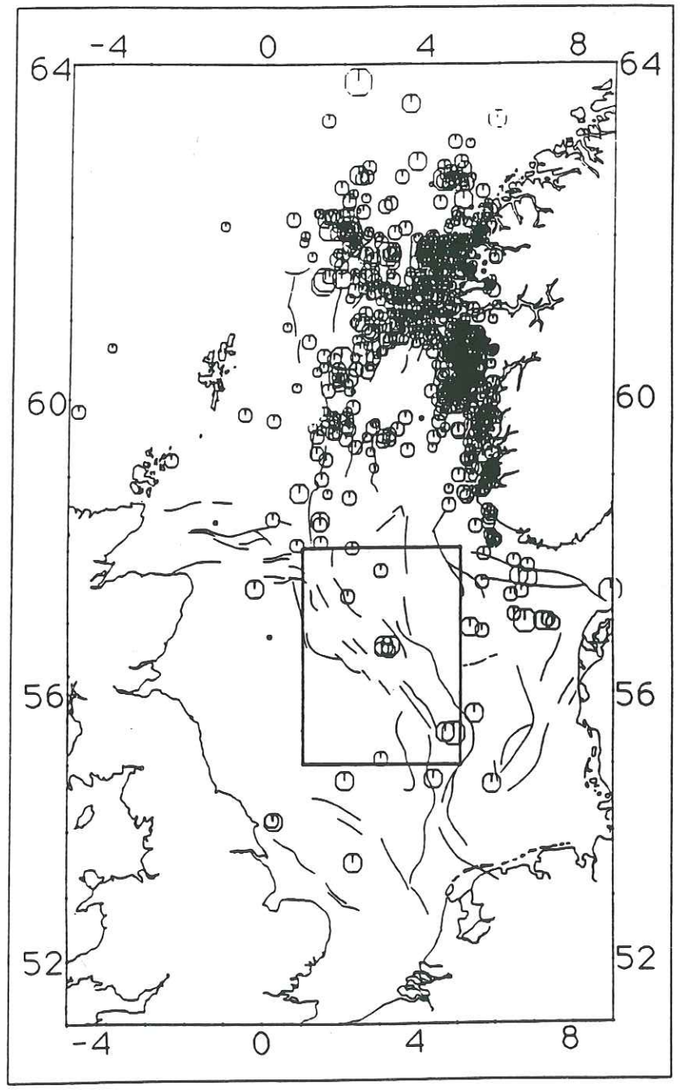

Figure 4(a)

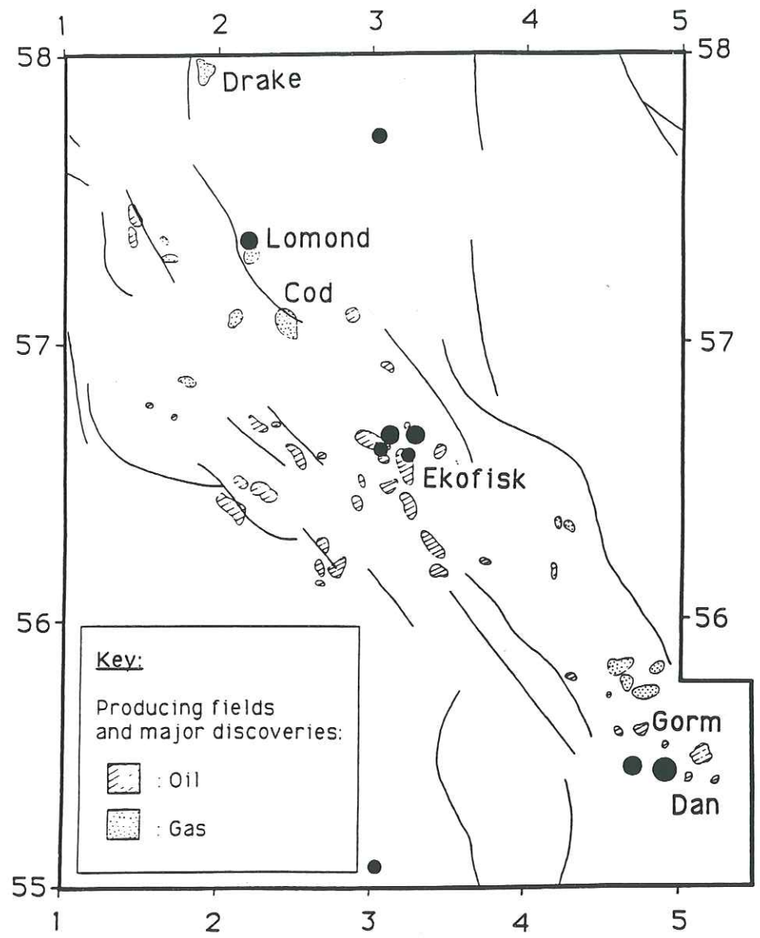

Figure 4(b)

Figure 4
a) Epicenters of North Sea earthquakes 1980–1989 located using British and Norwegian network (from British Geological Survey). b) Central North Sea seismicity map. The cluster located in the Central Graben is active since 1982 and is correlated in time and space with the major Norwegian and Danish gas field extraction (Ekofisk, Dan).

earthquakes with magnitudes between $M_L = -2.0$ and $M_L = 1.3$ (KAPOTAS and KANASEWICH, 1989) indicate microfractures due to induction of contaminated water for waste disposal. The time interval between injection and microfracturing is a function of pressure buildup time at the well bottom. Such fluid injection can give rise to fractures one meter to several tens of meters in size rocks initially devoid of fractures (maximum magnitude < 2). Note that the fracturing process itself, i.e.,

Table 1

Hydrocarbon fields and sedimentary basin where hydrocarbon recoveries induced $M_L \geq 3$ or felt earthquakes

Sedimentary Basin*	Area or Field	References for $M_L \geq 3$ Earthquakes
Alberta, Canada	Snipe lake field	MILNE, 1970
Alberta, Canada	Strachan field	WETMILLER, 1986
Appalachian, Canada	Gobles field	MEREU *et al.*, 1986
Aquitaine, France	Lacq field	ROTHÉ, 1977
Aquitaine, France	Meillon field	GRASSO, 1992a
Los Angeles, CA, USA	Wilmington field	RITCHTER, 1958; KOVACH, 1974
Los Angeles, CA, USA	Orcutt field	KANAMORI and HAUKSSON, 1991
Los Angeles, CA, USA	Montebello field	MCGARR, 1991
San Joaquin, CA, USA	Coalinga field	MCGARR, 1991
San Joaquin, CA, USA	Kettleman field	MCGARR, 1991
Caucasus, Tchetcheny	Grozny field	SMIRNOVA *et al.*, 1977
Central Asia, Uzbekistan	Gasli field	SIMPSON and LEITH, 1985
Midcontinent, OK, USA	El Reno	NICHOLSON, 1992
Rotliegendes, Netherlands	Assen field	HAAK, 1991
Rotliegendes, Netherlands	Groningen field	HAAK, 1991
Rotliegendes, Germany	Salzwedel field	LEYDECKER, 1992
North Sea, Norway	Ekofisk field	GRASSO, 1990
North Sea, Denmark	Dan field	GRASSO, 1990
Po Valley, Italy	Caviaga field	CALLOI *et al.*, 1956
Rocky Mountains, USA	Rangely field	RALEIGH *et al.*, 1972
West Texas, TX, USA	Fashing field	PENNINGTON *et al.*, 1986
West Texas, TX, USA	Cogdell field	DAVIS and PENNINGTON, 1989
West Texas, TX, USA	War-Wink field	DOSER *et al.*, 1991
Williston, NE, USA	Sleepy Hollow field	ROTHÉ and LUI, 1983

* Basin toponimy from PERRODON (1985).

the tensile events which are created during the propagation of the fracture, seems not to be the main cause of the recorded seismicity (e.g., TALEBI and CORNET, 1987). The events are essentially induced by slippage along a preexisting plane of weakness induced by the decrease of the effective stress around the hydraulic fracture. When recorded, tensile cracks are generated first at weak seams and then shear cracks follow on the opened joints (OHTSU, 1991).

The scale of observed phenomena is modified by massive injections used both as a secondary recovery method in oil reservoirs and to maintain the pore pressure in a reservoir while nearby wells are used for productions. In fact, many seismic events of magnitude between 3 and 4 were reported in the vicinity of fields stimulated by

fluid injection in regions previously considered as seismically inactive such as Colorado (RALEIGH *et al.*, 1972), New York (FLETCHER and SYKES, 1977), Nebraska (EVANS and STEEPLES, 1987), Ohio (NICHOLSON *et al.*, 1988), and Texas (DOSER *et al.*, 1991).

The basic mechanism of such instabilities is suggested by and tested on different case histories in Denver and Rangely (Colorado) and Dale (NY), using an effective stress approach with a Mohr-Coulomb type failure criterion. But the mechanism described above cannot directly explain the three major Denver earthquakes of magnitude $M_L > 5$ that took place at distances greater than 5 km from the injection well 14, 18 and 21 months after the injection (Figure 5). Instead, one may suggest a deferred stress transfer by propagation of fluid pressure along the preexisting fracture affected by the earliest seismic activity to an area where the preexisting stress is high and near failure. This stress transfer might have triggered the latest three major events (HSIEH and BREDEHOEFT, 1981). More recently, the case of a seismic sequence located at 5 and 10 km from an injection well in Ohio (NICHOLSON *et al.*, 1988) indicates that fluid pressure variations as small as a few MPa are able to initiate seismic fractures ($M_L \approx 3$–4) in an environment previously subjected to tectonic stresses near failure. Regional connections over horizontal distances of

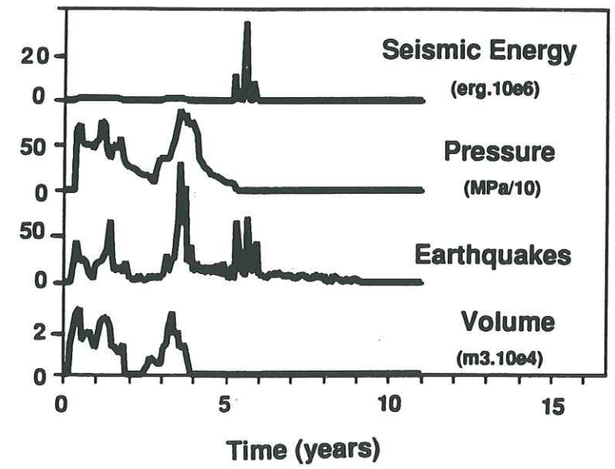

Figure 5

Denver earthquakes and fluid injection. From bottom to top: a) History of injected fluid volume; b) history of number of locally induced earthquakes; c) fluid pressure history; d) history of seismic energy release. Note the correlation between pressure history and the number of induced events during the first five years. Nevertheless, the correlation fails regarding seismic energy and pressure history. These major shocks ($M \approx 5$–5.5) occur respectively 18, 21 and 24 months after the injection ended, at larger distances from the injection well than the earliest small shocks (adapted from HEALY *et al.*, 1968).

some ten kilometers are possible, depending on the size and hydromechanical characteristics of preexisting fractures as well as on the amount and pressure of injected fluids. For the abovementioned Colorado and Ohio cases, the directions of the stresses measured *in situ* or inferred from seismic analyses of triggered events (RALEIGH *et al.*, 1972; EVANS, 1987; NICHOLSON *et al.*, 1988) correlate well with the *in situ* estimated regional directions.

Fluid pressure increase, in these cases, accounts only for a stress disturbance relative to the main initial tectonic loading causing seismic instabilities. These triggered instabilities are restricted to preexisting tectonic faults, thus contrasting with the new smaller-scale fractures produced by local hydraulic fracturing.

Fluid Extraction: Poroelastic Stress Transfer

Mechanical instabilities induced by fluid injection are understood to result from pore pressure increase, which causes the effective normal stress on the fault plane to be reduced, thus generating motion under the action of the unchanged shear stress (constant tectonic stress). Conversely, based on the same conventional arguments and on the fact that fluid extraction reduces pore pressure, the effective normal stress in the reservoir is increased and, thereby, recurrent faulting should be inhibited.

From the observations and studies of seismic events precisely recorded in Alberta (WETMILLER, 1986), and Aquitaine (GRASSO and WITTLINGER, 1990), it appears such instabilities do not occur in the depleted portions of the reservoir where gas pressure is on the decrease, but are located under or above the reservoir. In areas surrounding the Lacq field in Aquitaine, SW France, fluid connections between the reservoir and the overlying area are reduced due to the presence of impervious layers above the reservoir (GRASSO and FEIGNIER, 1990). There, the instability mechanism is not related to a rapid fluid pressure propagation. The direction of maximum *in situ* stress axes (inferred from focal mechanisms of induced seismic events) indicates a radial distribution of stresses around the reservoir which is quite different from the regional direction of *in situ* stresses determined from mechanisms at the foci of regional natural earthquakes and from borehole breakout measurements (GRASSO and FEIGNIER, 1990). SEGALL (1989) has suggested that poroelastic stresses resulting from production-generated decreases in pore pressure are responsible for earthquakes in these fields. He modeled the coupling between fluid flow and rock deformation using poroelasticity theory (BIOT, 1941; GEERTSMA, 1973; RICE and CLEARY, 1976) to explain the stresses induced in the levels surrounding the hydrocarbon reservoir. At the Lacq site where these events have been closely observed and studied for 18 years, seismic deformations are perceptible over distances of 5 km from the reservoir, meaning that the seismic area extends over a few kilometers (GUYOTON *et al.*, 1992). The linear relationship between pore pressure and subsidence on the Lacq area (Figure 6),

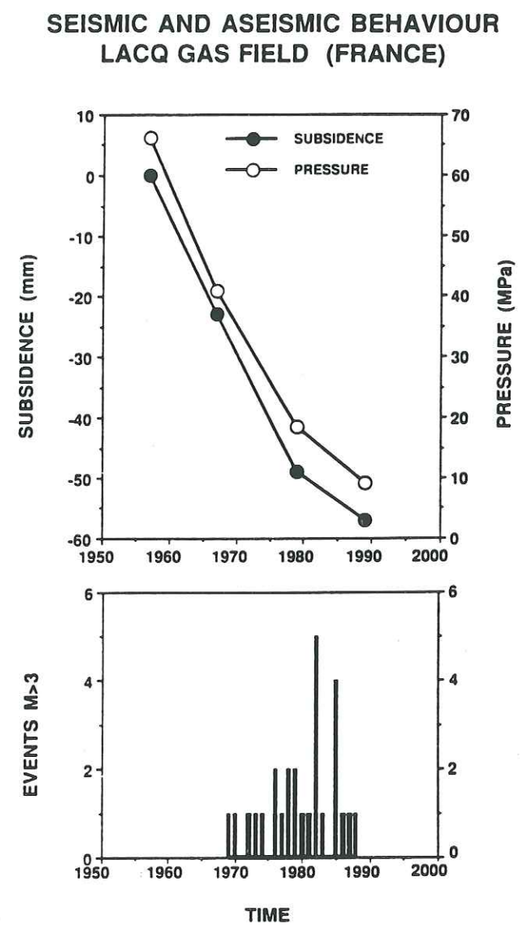

Figure 6
Seismic and aseismic deformation of the Lacq gas field (Pyrenees, France) as a function of pressure decrease within the gas reservoir.

supports the linear poroelastic modeling. A simplified analytical poroelastic model (Figure 7) helps, in that case, to evaluate the amount of induced stress variation in areas overlying the reservoir (<1 MPa, SEGALL and GRASSO, 1991). CHEN and NUR (1991) indicate that the structural anisotropy of rocks causes the pore pressure effect to be distinctive from that in isotropic rocks. The anisotropic effect may lead to the variation of directions and magnitudes of principal stresses. At other sites, where the quality of the measurements is not sufficient to draw conclusions as detailed as those reached for Lacq, it can however be observed that 30 MPa reservoir depletions at 3–4 km depth appear to be connected with seismic events of

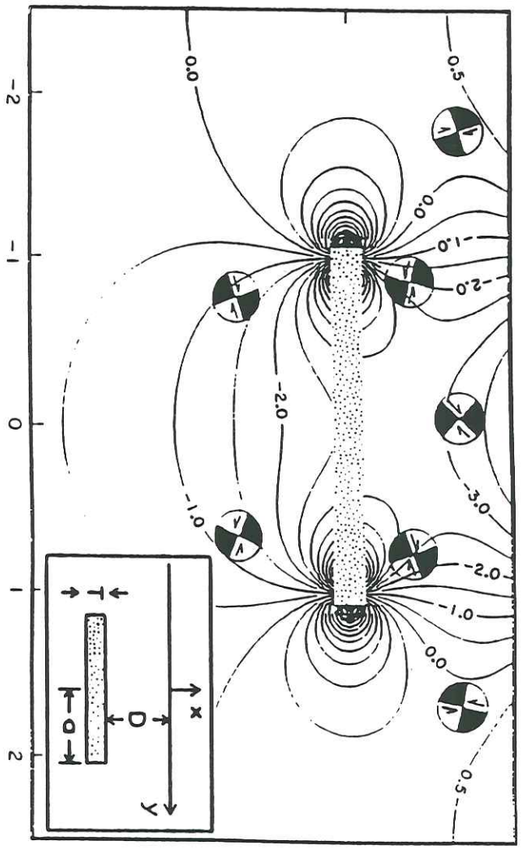

Figure 7

Relative changes in horizontal normal stress (relative tension positive) within a homogeneous elastic half-space (semi-infinite medium) where a poroelastic disk-shaped reservoir is embedded. The lower box indicates the reservoir geometry; a, D, T are respectively the radius, depth and thickness of the reservoir. Vertical and horizontal scales are the depth and the distance from the reservoir in units of reservoir depth. Stress contoured in units of $\alpha[(1-2\nu)/2\pi(1-\nu)] \cdot T/D \cdot \Delta P(t)$; the parameters are defined in Table 2. Simulated focal mechainsm indicates planes of maximum shear stress when reservoir is depleted (adapted from SEGALL, 1989).

maximum magnitude between 3 and 4 under a great variety of regional tectonic conditions (Table 2): stable in the Netherlands and Texas; extension in the North Sea, in Norway and Denmark; compression in Caucasus, Uzbekistan, France and Canada. At the Lacq site, locations of seismic events show that seismic fractures occur on preexisting discontinuities (either tectonic or lithological discontinuities, FEIGNIER and GRASSO, 1990), according to the mechanical properties of the rock matrices. Deduced from the spectral analysis of seismic recordings, the amplitude of the fault slip is of the order of a few millimeters (FEIGNIER and GRASSO, 1992). This may be the reason why, in spite of the obvious nonelastic behavior of the seismic events, the regional response of the rock mass is an elastic response.

Because the size of earthquakes induced by poroelastic stress transfer appears to follow a scaling law for size distributions as that observed for natural events (e.g., ROTHÉ and LUI, 1983; VOLANT *et al.*, 1992), we can expect that even though no earthquakes ($M_L \geq 3$) are recorded, small seismic instabilities have probably occurred

Table 2

Hydromechanical setting of earthquakes triggered by poroelastic stressing caused by hydrocarbon extraction. Average reservoir characteristics are defined as follows: T, thickness; ϕ, porosity; φ, matrix permeability; μ, shear modulus; ν Poisson's ratio; α is a coefficient related to the bulk moduli of saturated rock (K) and the grains in the rock (K_s) by $\alpha = 1 - K/K_s$. Displacement and pressure history are defined by: the onset of production and the date of the first induced event; P_{init}, the initial pressure in the reservoir; ΔP, the pressure drop at the onset of seismicity; pressure values are from the yearly bottom of well measurements, with a few bars of accuracy; ΔH is the maximum depth of the subsidence bowl; m_1 is the magnitude of the first reported induced event and m_2 is the maximum magnitude of induced events. $\Delta\sigma_{max}$, the order of magnitude of the induced stress at the onset of the seismicity, is estimated using the poroelastic stress model as follows: (i) For the 8 fields we reported a rough value depending on pressure drop and reservoir geometry: $\Delta\sigma_{max} \approx \alpha[(1-2\nu)/2\pi(1-\nu)] \cdot T/D \cdot \Delta P \cdot F_{max}$, where ΔP, F_{max} are respectively the reservoir pressure drop and a dimensionless function of position and reservoir geometry. A maximum stress change value above the reservoir is $F_{max} \sim 3$ (SEGALL, 1989); for limestone reservoir rocks of fields 1–2 and 4 we assume that $\alpha[(1-2\nu)/2\pi(1-\nu)] \sim 0.1$. (ii) If the subsidence and shear modulus of the rocks involved are known (field 3, 6–7), we check the above estimates by using $\Delta\sigma_{max} \approx [4\mu/(1-\nu)\pi D] \cdot \Delta H_{max}$), where μ, ν, D, H_{max}, are respectively the shear modulus, the Poisson's ratio of the rock matrix, the depth of reservoir and the maximum depth of the subsidence bowl

Area or Field Country	Strachan° Alberta	Fashing[a] Texas	Lacq[b] France	Grozny[c] Tchecheny	Assen[d] Groningen[d] Netherlands		Ekofisk[e] Norway	Dan[f] Denmark
Reservoir characteristics								
Size (km^2)	25	10	150	70	50	900	130	24
Depth (km)	3–5	3.4	3.5	4.0	3.0	2.9	3.0	1.8
T (km)	0.1	0.05	0.25	0.4	0.2	0.15	0.2	0.15
Φ (%)	—	15	3	4	15	18	30	30
φ (mD)	—	13	0.5	—		$0.1-10^3$	$1-10^2$	0.1–1
μ (GPa)	—	—	23	—	10	10	0.07	—
ν	—	—	0.25	—	0.25	0.26	0.3	(0.3)
α	—	—	0.25	—	0.9	0.9	1.0	(1.0)
Displacement and pressure histories at the onset of Eqs.								
Onset Prod. (year)	1971	1958	1959	1964	1972	1964	1973	1972
Onset Eqs. (year)	1976	1974	1969	1971	1986	1991	1982	1985
P_{init} (MPa)	50	35	66	69	37	35	48	26
ΔP (MPa)	25	23	30	25	30	15	24	18
ΔH (m)	—	—	0.05	—	—	0.16	3.5	—
m_1	3.0	3.1	4.0	3.5	2.8	2.5	2.2	4.0
$\Delta\sigma_{max}$ (MPa)	0.25	0.1	0.6	0.7	0.5	0.2	0.4	0.45
m_2	3.4	3.4	4.2	4.1	2.8	2.5	3.4	4.0

°from WETMILLER (1986); [a]from PENNINGTON *et al.* (1986); [b]from SEGALL and GRASSO (1991) and GRASSO and FEIGNIER (1990); [c]from SMIRNOVA (1977); [d]reservoir characteristics from PRICE *et al.* (1990), Netherlands Induced Seismicity Commission (pers. commun., 1992); [e]reservoir characteristics from TEUFEL *et al.* (1991); [f]reservoir characteristics from CONLIN *et al.* (1990).

on numerous hydrocarbon production sites. The induced stresses vary as a function of time in a manner that depends on the hydraulic diffusivity (i.e., permeability) of the reservoir and surrounding rocks. By recording the microseismicity, it is possible to monitor changes in stress and pore pressure as a function of space and time. Spectral analysis of seismic waves can give an estimate of the seismic source radii which in turn give an indication of the size of the blocks to be considered in the reservoir engineering models (MAURY *et al.*, 1992). Monitoring of such small seismic instabilities is therefore an efficient tool which allows the well operators to follow the *in situ* reservoir behavior.

We propose that the temporal behavior of levels surrounding the depleted reservoirs has to be modeled in a two-step mechanism. First, a primary homogeneous poroelastic stressing helps to predict the threshold that triggers the onset of the seismicity (Table 2). In this situation the preexisting discontinuities are not activated and the deformation is spread within the whole structure. Note that the involved reservoirs are 3–5 km deep. This mechanism involves competent rock matrices within levels above or below the reservoir where stress can be transferred. From the crude estimates of critical stress changes it appears that the critical threshold stands in the order of magnitude of a few bars (Table 2). Few observations constrain the *in situ* stress/strain history of the different hydrocarbon fields. Therefore few data are available to test the current models. For the Lacq gas field, the analytical poroelastic solution for an axisymmetric geometry fits the surface deformation (SEGALL and GRASSO, 1991), but fails to fit the decrease of seismic activity since 1980. GRASSO and FEIGNIER (1990) proposed that aseismic slip (energy release below the threshold of the measuring equipment used on the site, i.e., small earthquakes or low frequency events) occurred and that seismic instabilities are a second-order contribution for the deformation of the local sturcture. VOLANT *et al.* (1992) further argue that the aseismic instabilities explain the *b*-value decrease. At the Ekofisk field, the seismic activity began in 1985, and the critical stress estimated by poroelastic stressing falls within the same order of magnitude as that observed in other fields (Table 2). On the contrary, in the following period (1985–1990) the stress path deduced from *in situ* measurements in the neighborhood of the Ekofisk field is not compatible with the poroelastic behavior (TEUFEL *et al.*, 1991; TEUFEL, 1992, pers. communication).

During the second step of the reservoir deformation, we propose that the rock mass be modeled as a set of blocks with localized movements between some blocks causing the induced seismicity. At the Lacq field, slip on 3 faults, defined both by borehole observations and seismic activity, fits the surface subsidence, as well as the poroelastic model (Figure 8). More observations are needed to differentiate the homogeneous stressing and deformation of the whole structure from possible localized slip on few faults. It appears that the volume of formation compaction due to gas production, measured geodetically (GRASSO and FEIGNIER, 1990) causes mostly aseismic, instead of seismic, deformation. Thus, the seismic deformation

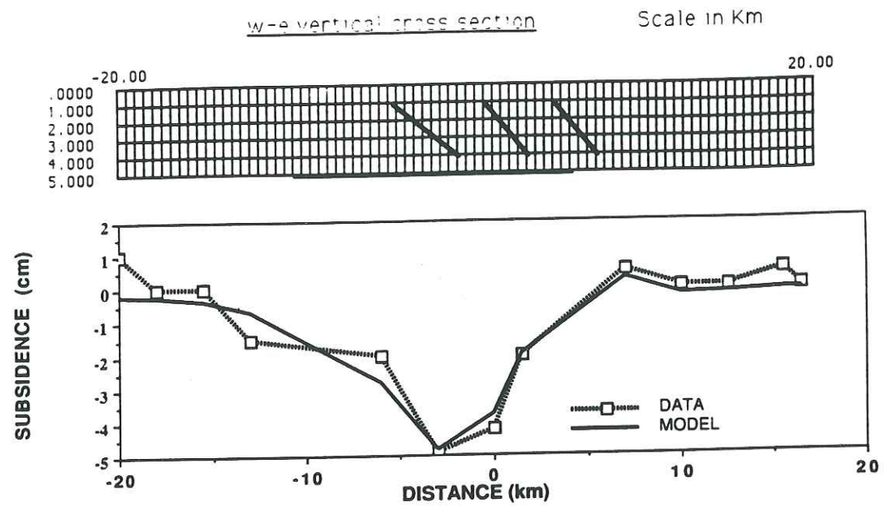

Figure 8

Comparison between observed and calculated surface displacements due to fault slips on the Lacq field test site. a) the model is built using 3 faults F1, F2, F3 over a horizontal reservoir within a homogeneous half-space. The geometries and kinematics of the faults are the ones defined by the 3 major seismically activated faults in the period 1976–1979 (FEIGNIER and GRASSO, 1990). The horizontal faults F4, F5, mimic the Lacq gas reservoir as defined by GRASSO and WITTLINGER (1990). Black arrow indicates the fixed movements on the faults. b) Dashed line is the observed subsidence in the period 1957–1979 corresponding to 22 years of gas extraction (GRASSO and FEIGNIER, 1990). Thick line is the subsidence calculated with the model defined in (a) and the boundary element technique (CROUCH and STARFIELD, 1983; BILHAM and KING, 1989). On the western part of the field, where the fit is poor, we have no seismic constraint on fault geometries. Note that the slips on the 3 faults are at least one order of magnitude larger than the cumulative seismic slips determined on the basis of spectral analysis of seismic signals (FEIGNIER and GRASSO, 1992). It implies that seismic slips are second-order displacements of the main aseismic deformation of the Lacq field site.

anticipated on the basis of this volume reduction (MCGARR, 1976) is much greater than that observed. The size of the induced events is controlled by both the rheology of the rock matrices and the preexisting fractures. Because this type of seismic instability occurred close to the oil and gas reservoirs ($D \leq 5$ km), the size of structural faults around a site (often components of oil and gas entrapments), and the mechanical properties of rock matrices close to the reservoir, impose a limit on the size of possible seismic fractures. These data are essential to understand and determine the possible seismicity.

Mass Transfer and Fluid Circulation

The observed cases of seismicity induced by fluid manipulations in the vicinity of oil and gas production sites cannot be classified and identified as easily as those

previously analyzed. The reservoirs are not only affected by a pressure decrease caused by depletion, but also by more complex fluid manipulations. Indeed, there is another type of disturbance caused by extraction. It is observed in reservoirs on the periphery of which fluid is injected to drive oil or gas toward the production well, and thus enhance the secondary recovery (DAVIS and PENNINGTON, 1989). Lack of balance between the depleted zone and the injection-receiving zone generates fractures in areas where imbalances are maximum. Such effects have been reported in Caucasia (SMIRNOVA *et al.*, 1975), in Ontario (MEREU *et al.*, 1986) and in Texas (DAVIS and PENNINGTON, 1989). Poroelastic stress transfer adds to the fluid pressure increase effect, and causes fracturing in places where both effects are combined. DAVIS and PENNINGTON (1989) propose a similar cumulative effect for some observations made in Texas fields. Seismic and aseismic responses are more or less deferred, depending on the tectonic conditions and the material rheology. Note that water injection for enhanced oil recovery often generates thermal stresses. Thermoelasticity could be used the same way as poroelasticity to explain some induced seismicity. Obviously this needs to be quantified to estimate the amount of stress drop, but it is not negligible. It could explain what we previously called imbalances (e.g., DAVIS and PENNINGTON, 1989) and would correspond to the cold front.

In some areas, instabilities may well be exclusively aseismic (energy release below the threshold of the measuring equipment used on the site) with large-scale deformations produced by an extended depletion without any earthquake activity. In many areas, the energy is released in the frequency domain above and below the artificial thresholds of the measuring equipment used on the site, i.e., "slow" or "quiet" earthquakes characterized by low frequency seismic signals (e.g.,Wilmington field, KOVACH, 1974; Orcutt field, KANAMORI and HAUKSSON, 1991) or high-frequency microruptures $M_L \leq 1$ associated with creep processes (MCEVILLY, 1992). This deformation can develop over many years and become widespread over the entire system before the first earthquakes $M_L \geq 3$ are detected. For instance at Groninguen in the Netherlands, 30 years of aseismic deformation, measured geodetically (see for example PRICE *et al.*, 1991) preceded the first earthquake, $M_L = 3$, that occurred in December 1991. On the contrary, these large aseismic deformations can be localized by a simple fault as in Buena Vista, California (NASON *et al.*, 1968). This point is not considered here although aseismic instabilities are of major importance to an operator (MAURY and SAUZAY, 1989; BRUNO, 1992).

Returning to the case where seismic fractures are recorded, it should be noted that the area affected by the reservoir induced poroelastic stress disturbance is the order of a few kilometers from the hydrocarbon reservoir. Most of the abovementioned cases are related to large (≥ 30 MPa) pore pressure drops, although the poroelastic stress changes are in the range 0.1–1 MPa. Such pore pressure drops are restricted to gas reservoirs.

In a broader context, MCGARR (1991) adds another category of earthquakes related to hydrocarbon production in terms of the removal of load induced by

massive oil extraction. Whether in California (MCGARR, 1991) or in Uzbekistan (SIMPSON *et al.*, 1988; PLOTNIKOVA *et al.*, 1989), the list is not exhaustive and identical situations are currently observed in Italy (CALLOI *et al.*, 1956), in Alberta (MILNE, 1970), in Oklahoma (NICHOLSON, 1992) and in Ecuador (GRASSO *et al.*, 1992c). Major events are related to upper crustal hydromechanical disturbances produced by subsurface fluid extraction from the upper levels. In these cases the stimulated zones are fault zones buried under reservoir-containing anticlines. In California, a region subjected to tectonic compression, McGarr proposes a connection between the seismic moment of earthquakes with the mass removal resulting from oil extraction corrected for the thickness of the earthquake-producing portion of the regional crust. This work is based on the analysis of recent seismic events near Coalinga (1983, $M_s = 6.5$), Kettleman North Dome (1985, $M_s = 6.1$) and Whittier Narrows (1987, $M_s = 5.9$). In western Uzbekistan, considered to be an aseismic region until the 3 $M_s \geq 7$ Gasli events, the relation $\sum M_o = 2\mu \cdot \Delta m \cdot H_s / \rho_c H$, where Δm is the mass of fluid removed due to hydrocarbon production, $\sum M_o$ the sum of seismic moments of the induced earthquakes, μ the shear modulus of the crust, ρ_c the average upper crustal density, H the thickness of the upper crust and H_s the thickness of the seismogenic part of the upper crust (MCGARR, 1991), might be considered as a trigger for the Gasli seismic sequence. Mass withdrawal can explain 30–40% of the seismic moment cumulation (GRASSO *et al.*, 1993). Note that the uncertainties on the estimated seismic moment make equality possible between mass withdrawal and seismic moment. Moreover, a local seismic survey (GRASSO *et al.*, 1992b) demonstrates that the seismic activity of the Gasli area clusters around this major hydrocarbon field. The hypocenters define concentric fault planes dipping beneath the gas field structure in agreement with MCGARR's analysis (Figure 9). Note the divergence of major instability stress axes from regional directions (Figure 10). Such abnormal directions can be illustrative of either local stress anomaly (radially spread around the reservoir as a result of an extended depletion area) or provide evidence for fluid contribution to fracturing, i.e., weak faults. The unusual geometry of seismically active fault planes; the concentration of regional seismic instabilities around the gas reservoir; the radial pattern of stress around the dome structure which traps the gas reservoir; and the significant contribution of the local mass withdrawal with respect to the seismic moment of the earthquakes, are all key factors which rule out the possibility that the three earthquake sequences at Gasli are simply natural tectonic events (GRASSO *et al.*, 1993).

Regional Stress Transfer

From all three mechanisms studied, it appears that relatively small stress variations, a few tenths of an MPa both for poroelastic stressing (Table 2) and the mass effect model (Table 3), can trigger seismic fractures in the neighborhood of

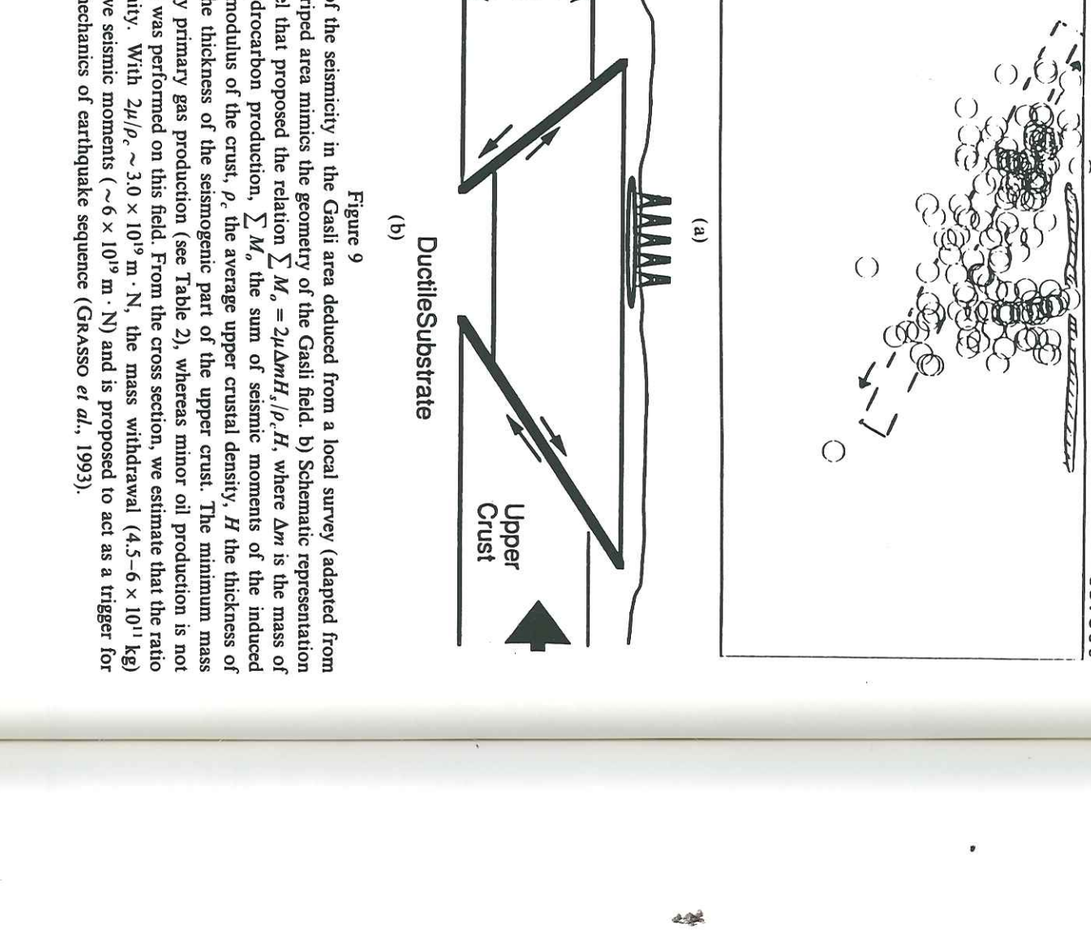

Figure 9

a) NW-SE cross section of the seismicity in the Gasli area deduced from a local survey (adapted from GRASSO *et al.*, 1992b). Striped area mimics the geometry of the Gasli field. b) Schematic representation of MCGARR (1991) model that proposed the relation $\sum M_o = 2\mu\Delta m H_s/\rho_c H$, where Δm is the mass of fluid removed due to hydrocarbon production, $\sum M_o$ the sum of seismic moments of the induced earthquakes, μ the shear modulus of the crust, ρ_c the average upper crustal density, H the thickness of the upper crust and H_s the thickness of the seismogenic part of the upper crust. The minimum mass withdrawal is estimated by primary gas production (see Table 2), whereas minor oil production is not yet available. No injection was performed on this field. From the cross section, we estimate that the ratio H_s/H is close to the unity. With $2\mu/\rho_c \sim 3.0 \times 10^{19}$ m · N, the mass withdrawal ($4.5–6 \times 10^{11}$ kg) explains 30% of cumulative seismic moments ($\sim 6 \times 10^{19}$ m · N) and is proposed to act as a trigger for the mechanics of earthquake sequence (GRASSO *et al.*, 1993).

Table 3

Hydromechanical setting of earthquakes triggered by the unloading of the uppercrust caused by hydrocarbon extraction. Column 3 is the year when extraction began and the date of the first induced event. Column 6 is the maximum magnitude of induced events. Mass deficit is reported on column 5. Assuming that mass withdrawal at these sites is related to the major earthquake, we estimate the induced stress, augmenting failure by multiplying the seismic stress drop by the ratio of stiffness of the loading system (the vertical force change) to the stiffness of the circular crack model according to MCGARR (1991)

Area or Field	Reservoir Depth	Onset of Prod. – Eqs.	Initial Pressure	Mass Removal	Maximum Magnitude	Induced Stress
Coalinga field[a] California, USA	2 km	1940–1983	25 MPa	2.7×10^{11} kg	$M = 6.5$	~0.01 MPa
Kettleman field[a] California, USA	1.5 km	19??–1985	—	1.2×10^{11} kg	$M = 6.1$	~0.01 MPa
Montebello field[a] California, USA	1.5 km	1924–1987	—	1.3×10^{11} kg	$M = 5.9$	~0.01 MPa
Gazli field[b] Kyzyl-Koum, Uzbekistan	1.5 km	1962–1976	10 MPa	2×10^{11} kg	$M \approx 7.0$	~0.04 MPa
Gazli field[b] Kyzyl-Koum, Uzbekistan	1.5 km	1976–1984	3 MPa	2×10^{11} kg	$M \approx 7.0$	~0.05 MPa

[a]from MCGARR (1991); [b]from GRASSO *et al.* (1993).

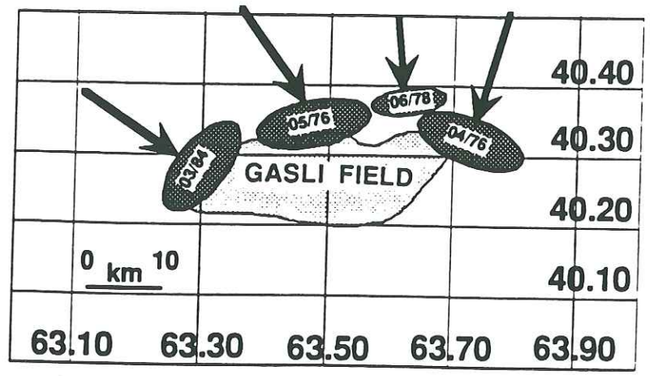

Figure 10
Major seismic events in the Gasli area (Uzbekistan), $M_s \geq 7$ except for 1978: $M_s = 5.9$. Black ellipses indicate positions and estimated size of seismic events determined by seismic analysis (HARTZELL, 1980; EYIDOGAN *et al.*, 1985) and levelling data GRASSO, 1992b). Black lines schematize local directions of the maximum horizontal stress (after BESRODNY, 1986; EYIDOGAN *et al.*, 1985).

hydrocarbon reservoirs. In areas where triggered events occur at larger distances from the hydrocarbon reservoirs, regional connections of pore pressure changes and stress transfer mechanisms require investigation. The case of the Grozny field (Caucasia) is noteworthy because from a seismological point of view, it illustrates the effects of pore pressure change on preexisting weak zones and the possible relationships between oil and gas production and active faults (SMIRNOVA, 1977). In a first stage of gas production (6 years), the 30 MPa fluid pressure decrease (gas reservoir) caused the tectonic seismic instabilities to be stabilized (Figure 11). These instabilities are restricted to a fault close to the reservoir (<5 km) and more precisely to a finite portion of the fault. As a result, stresses are enhanced near the ends of the "locked" portion of the fault. After 6 years, the shear strength is maximum and seismic recurrence is observed. Other observations of a possible correlation between the regional seismicity and the subsurface reservoir pressure history have been made at a larger scale near the Gasli field, Uzbekistan (PLOTNIKOVA *et al.*, 1989) and the Lacq field (Pyrenees, France). A preliminary hydraulic model, applied in the Lacq area to test the plausibility of these correlations (Figure 12), shows that the gas reservoir depletion can affect the aquifer pressure of the area and transmit significant pore pressure changes ($\sim$0.5 MPa, GRASSO *et al.*, 1992a), at 20–30 km distance on the regional active faults. The seismicity change of the main active fault of the Lacq field region (North Pyrenean Fault) can be explained by a pore pressure change that diffuses from the Lacq reservoir toward the regional Pyrenean fault. GRASSO *et al.* (1992a) propose that such connections are possible at distances ranging from 20 to 40 km, with time delays of less than 10 years. The small stress changes involved appear to be of the same order as the one proposed

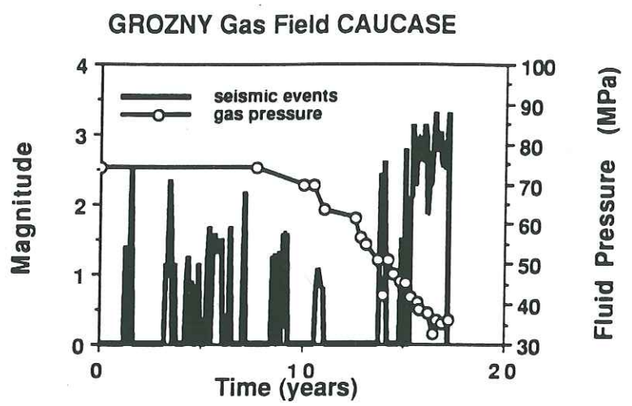

Figure 11
Seismicity and gas pressure decrease due to gas extraction (Grozny field, Tchechen Republic, Caucasus) from 1956–1974 (SMIRNOVA, pres. commun., 1990). Origin of the time axis corresponds to 1956. Pressure values are the average gas reservoir presure. Earthquake magnitudes are local magnitude.

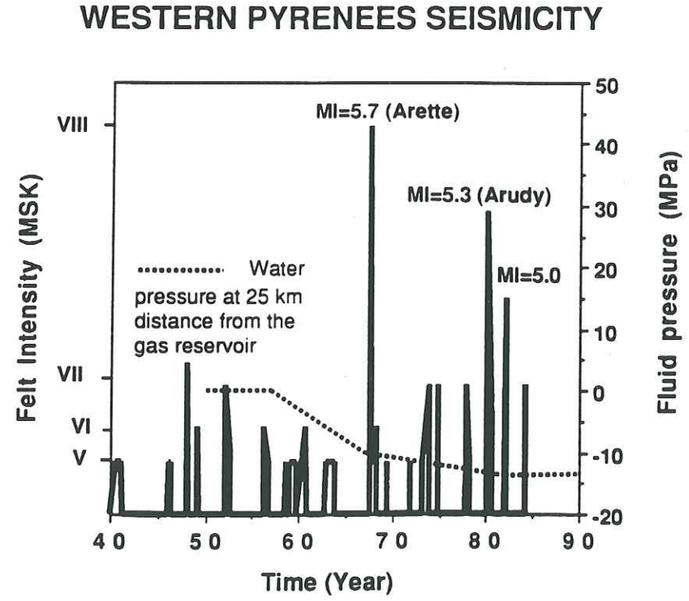

Figure 12
Historic seismicity of the Western Pyrenees and the estimated pressure change induced by the Lacq reservoir depletion on the North Pyrenean Fault (dotted line) at 20 km distance from the Lacq reservoir. The values are estimated with a strip flow model. Zero value on the time axis corresponds to the year 1940. Earthquake magnitudes are local magnitudes (adapted from GRASSO *et al.*, 1992a).

to explain reservoir-induced seismicity in the vicinity of an artificial water reservoir (SIMPSON, 1986; ROELOFFS, 1988). Correlation distances and time delays in the modification to the regional seismicity depend on the preexisting state of stress, the tectonic deformation rate and the estimated *in situ* hydrologic properties.

The final kind of observations we must consider are the possible earthquake aftereffects, triggered by major regional events, in areas weakened by fluid withdrawals. Both the co- and postseismic effects of regional earthquakes are possible triggers for local seismicity around hydrocarbon recovery sites. The postseismic process has been proposed at a larger scale (100–200 km connections) by ELSASSER (1969), THATCHER *et al.* (1980), RICE and GU (1983), and tested by RYDELEK and SACKS (1990). Stress diffusion, modeled by viscoelastic coupling in the upper crust (using well-defined rocksalt beds instead of the asthenospheric level as the viscoelastic layer) could trigger a delayed response (1–6 years), at distances ranging from 10 to 60 km (GRASSO *et al.*, 1992a). The coseismic effect itself can stimulate a short-lived increase of bed pressure and a slight increase of output in hydrocarbons (see for example, SMIRNOVA, 1968; SEGALL and YERKES, 1990). In southwestern France, GRASSO *et al.* (1992a) observed that the main Pyrenean earthquakes ($M_L \geq 5$) lead the changes in seismicity in the neighborhood of the Lacq gas field, located 30 km apart, by roughly 2 years. Such a possible aftereffect of the regional events on the Lacq field seismicity is consistent with a viscoelastic model, where salt rock acts as a viscoelastic channel below the sedimentary elastic bed (GRASSO *et al.*, 1992a). More generally, this mechanism could be effective in triggering "induced" seismic instabilities (in areas weakened by water reservoir impoundments and surface or subsurface extractions) in an area where the tectonic plates are close to failure.

Conclusion

Earthquakes occur in response to a buildup of the stress pattern imposed by the tectonic activity and controlled by various boundary conditions. The arrangement in space and time of the occurrences of events is a direct reflection of the local space and time properties which permit triggering when and where necessary conditions are met. A careful examination of the time/space seismicity pattern in the neighborhood of hydrocarbon recovery sites where stress changes and mechanical properties of the invloved medium are constrained and known, provides unique opportunities to interpret seismic instabilities. These earthquakes, triggered or induced by subsurface fluid manipulations, result either from pore pressure changes or from mass transfers. The sites where these shallow earthquakes occur are worldwide, located in different tectonic settings. The stress concentration from different possible mechanisms is small (< 1 MPa). This estimate of the change in driving stress, a few bars, regardless of the tectonic setting, confirms that the continental crust must be nearly

everywhere at a state of stress near failure (see the review of other types of triggered earthquakes by SIMPSON (1986) and the theoretical approach of structuration of the lithosphere as a self-organized critical phenomenon by SORNETTE and SORNETTE (1989)). The hydrocarbon recovery can trigger earthquakes on sites that are often located near major industry and toxic chemical facilities and hence the understanding of the care of these events is of great importance. For some of them, fluid pressure variations, induced by hydrocarbon recovery, trigger earthquakes that change the previous seismic risk assessment, deduced from the analysis of natural events. It is therefore necessary to investigate the possible occurrence of seismic instabilities in the neighborhood of hydrocarbon extraction to prevent potential instabilities when the production parameters can be optimized. These local behaviors require inclusion in the hazard assessment analysis.

Although coupling between different processes is prone to occur, three basic mechanisms have been isolated to explain the seismic response of hydrocarbon reservoirs to fluid extraction in terms of spatial, temporal and size distribution: (1) Local fluid injection decreases the effective stress and induces seismic cracks $M_L \leq 3$ within the hydrocarbon reservoir itself. (2) Pure fluid withdrawal causes pore pressure to decrease within the reservoir. For an ~ 25 MPa pore pressure decrease, a poroelastic mechanism transfers this stress change to the surrounding region where seismic instabilities, $M_L \leq 5$, occur above or below the reservoir, within distances of a few kilometers. The induced stress in the earthquake area is less than 1 MPa. This mechanism of earthquake triggering is predominant in the neighborhood of gas reservoirs. Mechanisms (1) and (2) are often mixed due to the recovery techniques employed. (3) Massive hydrocarbon recovery also corresponds to a removal of load from the upper crust. It appears to have induced a large earthquake $M_L \geq 6$ at a greater distance from the hydrocarbon field than the two other mechanisms. Due to the mechanical properties of the shallow rock matrix involved, seismic slip triggered by either mechanism (1) or (2), is a second-order process of the main nonbrittle deformation. Aseismic slip, if present, can suppress the occurrence of large earthquakes. The seismic effects that are induced by the unloading of the uppermost crust are proposed to involve the entire brittle crust (MCGARR, 1991) and thus could explain the large size of earthquakes associated with this mechanism. By constant recording of perennial microseismicity, induced by mechanisms (1) and (2), we have a tool to monitor changes in stress and pore pressure as a function of space and time. Therefore, monitoring of such local small seismic instabilities is an efficient tool for use by oil and gas producers to monitor reservoir behavior.

A less constrained seismic effect of hydrocarbon recovery is the possible connection between local fluid manipulations, triggered earthquakes and major regional earthquakes. Positive feedback mechanisms suggest that the region where the seismic hazard changes is much larger than the area from which hydrocarbons are extracted. The models reviewed in this study have been developed from

experience with the observations of some twenty reservoirs that triggered or induced seismic instabilities. It suggests future work must emphasize the value and type of far-field boundary conditions (stress or displacement boundary conditions) that are critical for the interpretations, whether or not a tectonically active zone is considered. The *known* associations between seismic instabilities and hydrocarbon recovery constitute 10% of the basins that provide commercial hydrocarbon production. To know how good these models are, it would be necessary to explain both the 90% of sedimentary basins where the hydrocarbon recovery is aseismic ($M_L \leq 3$) and to test these basic models on new data sets to predict both the type of seismic instabilities and the magnitudes of the induced earthquakes.

Acknowledgements

I am grateful to A. McGarr who invited me to present this study as a Keynote Address, Workshop on Induced Seismicity, 33rd U.S. Rock Mechanics Symposium, Santa-Fe, June 1992, and encouraged me to write this paper. I thank P. Segall, for discussions on poroelasticity as well as L. Plotnikova and L. Teufel for fruitful comments. The reviews of an anonymous reviewer and the editorial assistance of A. McGarr greatly clarify the final version of the manuscript. D. Haak and P. Marrow provided locations for northern Europe earthquakes. M. Thiercelin, M. Dietrich and Art McGarr provided helpful comments on an early version of the manuscript. I thank may authors cited in this review for supplying me with reprints, preprints, and beneficial comments. This study benefited from the open collaboration with petroleum companies: Cag, Elf, Nam, Petroland, Phillips, Shell provided geomechanical data of the fields studied in this work, but the opinions expressed in this study are the author's own. KNMI (Holland), the British Geological Survey (Scotland), the Federal Institute for Geoscience (Germany) and the Uzbek Academy of Sciences, kindly provided seismological data. This research was partially supported by the University Joseph Fourier, Grenoble, the Elf company under contract Risk reassessment within the Lacq Industrial Facilities and the French DBT-INSU Instability Program, contribution INSU-DTB no. 608.

References

BATCHELOR, A. S., BARIA, R., and HEARN, K. (1983), *Monitoring the Effects of Hydraulic Stimulation by Microseismic Event Location: A Case Study*, Paper presented at the 58th Technical Conf., San Francisco, CA. SPE 12109.

BESRODNY, E. M., *The source mechanism of the Gazly earthquakes of 1976–1984.* In *Gazly Earthquakes of 1976 and 1984* (Tashkent, Fan 1986) pp. 94–105.

BILHAM, R., and KING, G. (1989), *The Morphology of Strike-slip Faults: Examples from the San Andreas Fault California*, J. Geophys. Res. *94*, 10204–10216.

BIOT, M. A. (1941), *General Theory of a 3-dimensional Consolidation*, J. Appl. Phys. *12*, 155–164.

BRUNO, M. S. (1992), *Subsidence-induced Well Failure*, SPE Drilling Engineering *7* (1), SPE 20058.

CALLOI, P., DEPANFILIS, M., DIFILIPPO, D., MARCELLI, I., and SPADEA, M. C. (1956), *Terremoti della val Padana del 15–16 Maggio 1951*, Ann Geofis. *9*, 63–105.

CARDER, D. S. (1945), *Seismic Investigation in the Boulder Dam Area, 1940–1945, and the Influence of Reservoir Loading on Earthquake Activity*, Bull. Seismol. Soc. Am. *35*, 175–192.

CASSEL, B., BOL, G. M., and STEWART, L. (1990), *Acoustic Emission Monitoring during Hydraulic Fracturing*, SPE 20970, Paper presented at Europec 90, The Hague, Netherlands, 22–24 October 1990.

CHEN, Q., and NUR, A. (1991), *Pore Pressure Effects in Anisotropic Porous Rocks*, Paper presented at Int. Conf. Earthquake Prediction, State of the Art, Oct. 16–18, Strasbourg, France.

CORNET, F. H. (1977), *Study of Acoustic and Microseismic Emissions Associated with Hydraulic Frature*, Paper presented at Seminar on Geothermal Energy, Brussels, Dec. 1977, Eds. Commission of the European Communities, EUR 5920, pp. 685–691.

CONLIN, J. M., HALE, J. L., Maersk Oil & Gas, and SABATIER, J. C., FAURE, F., and MAS, D., Franlab (1990), *Multiple-fracture Horizontal Wells: Performance and Numerical Simulation*, SPE 20960, Paper presented at Europec 90, The Hague, Netherlands, 22–24 October 1990.

CROUCH, S. L., and STARFIELD, A. M., *Boundary Element Methods in Solid Mechanics* (Allen Unwin, London 1983).

DAVIS, S. D., and PENNINGTON, W. D. (1989), *Induced Seismic Deformation in the Codgell Oil Field of West Texas*, Bull. Seismol. Soc. Am. *79*, 1477–1497.

DOSER, D. I., BAKER, M. R., and MASON, D. B. (1991), *Seismicity in the War-Wink Gas Field, Delaware Basin, West Texas, and its Relationship to Petroleum Production*, Bull. Seismol. Soc. Am. *81*, 971–986.

ELSASSER, W. M., *Convection and stress propagation in the upper mantle.* In *The Application of the Modern Physics to the Earth and Planetary Interiors* (ed. Runcorn) (Wiley Interscience, NY 1969) pp. 223–246.

EYIDOGAN, H., NABELEK, J., and TÖKSÖZ, N. (1985), *The Gasli, USSR, 19 March 1984 Earthquake: The Mechanism and Tectonic Implications*, Bull. Seismol. Soc. Am. *75*, 661–675.

EVANS, M. D. (1966), *Man-made Earthquakes in Denver*, Geotimes *10*, 11–17.

EVANS, K. (1987), *In situ Stress Discontinuity across the Appalachian Plateau Decollement*, Paper presented AGU Spring Meeting, 1987.

EVANS, D. G., and STEEPLES, D. W. (1987), *Microearthquakes near the Sleepy Hollow Oil Field, Southwestern Nebraska*, Bull. Seismol. Soc. Am. *77*, 132–140.

FEIGNIER, B., and GRASSO, J.-R. (1990), *Seismicity Induced by a Gas Depletion: I. Correlation of Focal Mechanisms and Dome Structure*, Pure Appl. Geophys. *134*, 405–426.

FEIGNIER, B., and GRASSO, J.-R. (1992), *Characteristics of Seismic Fractures as a Function of Geomechanical Setting*, Pure Appl. Geophys. *137*, 175–199.

FLETCHER, J. B., and SYKES, L. R. (1977), *Earthquakes Related to Hydraulic Mining and Natural Seismic Activity in Western New York State*, J. Geophys. Res. *82*, 3767–3780.

GEERTSMA, J. (1973), *Land Subsidence above Compacting Oil and Gas Reservoir*, J. Petrol. Techn. *25*, 734–744.

GOUGH, D. I., and GOUGH, W. I. (1970), *Stress and Deflection in the Lithosphere near Lake Kariba*, Geophys. J. Roy. Astro. Soc. *21*, 65–101.

GRASSO, J.-R. (1990), *Hydrocarbon Extraction and Seismic Hazard Assessment*, EOS Transactions, Am. Geophys. Union *71*, 1454.

GRASSO, J.-R., and FEIGNIER, B. (1990), *Seismicity Induced by Gas Depletion: II. Lithology Correlated Events, Induced Stresses and Deformations*, Pure Appl. Geophys, *134*, 427–450.

GRASSO, J.-R., and WITTLINGER, G. (1990), *Ten Years of Seismic Monitoring over a Gas Field Area*, Bull. Seismol. Soc. Am. *80*, 450–473.

GRASSO, J.-R. (1992a), *Effects of the Gas Extraction on the Seismic and Aseismic Slips in the Neighborhood of Meillon-St-Faust Gas Field*, Report to EIF-Aquitaine Company, Feb. 1992, 60 pp.

GRASSO, J.-R. (1992b), *Coseismic Folding and Geometrical Constraint on the Kinematics of the Gasli Earthquakes*, Internal Report, LGIT, Observatoire de Grenoble.

GRASSO, J.-R., GRATIER, J. P., GAMOND, J. F., and PAUMIER, J.-C. (1992a), *Stress Diffusion Triggering of Earthquakes in the Upper Crust*, Special Issue on Mechanical Instabilities in Rocks and Tectonics, J. Struc. Geol. *14*, 915–924.

GRASSO, J.-R. PLOTNIKOVA, L. M., NURTIEV, B., and FRÉCHET, J. (1992b), *Seismic Activity in the Three $M_s \geq 7.0$ Gasli Sequence Area: May–June 1991*, submitted to Bull. Seismol. Soc. Am.

GRASSO, J.-R., CHATELAIN, J.-C., EYREDARD, J., and YEPES, H. (1992c), *Anomalous Seismicity in the Lago-Agrio Area, Ecuador Fluid-induced Earthquakes?* Report to EIF-Aquitaine Company, 10 pp.

GRASSO, J.-R., PLOTNIKOVA, L. M., NURTIEV, B., and BOSSU, R. (1993), *The Three $M_s \geq 7$ Gasli Sequence: the Largest Seismic Energy Release by Human Activity*, in preparation.

GUPTA, H. K., and RASTOGI, B. K., *Dams and Earthquakes* (Elsevier, Amsterdam 1976) 229 pp.

GUYOTON, F., GRASSO, J.-R., and VOLANT, P. (1992), *Interrelation between Induced Seismic Instabilities and Complex Geological Structure*, Geophys. Res. Lett. *19* (7), 678–684.

HAAK, H. W. (1991), *Seismiche Analyse van de Aardbeving bij Emmen op 15 februari 1991*, Koninklijk Nederlands Meteorologisch Instituut eds., Ministerie van Verkeer en Waterstaat, 14 pp.

HART, C., ENGI, D., FLEMING, R., and MORRIS, H. (1984), *Fracture Diagnostics Results for the Multiwell Experiment's Paludal Zone Simulation*, Paper SPE 12852, presented at the 1984 Unconventional Gas Recovery Symposium, Pittsburg.

HARTZELL, S. (1980), *Faulting Process of the May 17, 1976 Gasli Earthquake*, Bull. Seismol. Soc. Am. *70*, 1715–1736.

HEALY, J. H., RUBEY, W. W., GRIGGS, D. T., and RALEIGH, C. B. (1986), *The Denver Earthquakes*, Science *161*, 1301–1310.

HSIEH, P. A., and BREDEHOEFT, J. D. (1981), *Reservoir Analysis of the Denver Earthquakes. The Case of Induced Seismicity*, J. Geophys. Res. *86*, 903–920.

KANAMORI, H., and HAUKSSON, E. (1991), *A Slow Earthquake in Sediments in the Santa Maria Basin, California*, EOS Transactions, Am. Geophys. Union *72* (44), 293.

KAPOTAS, S., and KANASEWITCH, E. R. (1989), *Microseismicity and Stress Orientations in Cold Lake, Alberta*, Report to Esso Resources Canada Ltd. and Alberta Environment.

KOVACH, R. L. (1974), *Source Mechanisms for Wilmington Oil Field, California, Subsidence Earthquakes*, Bull. Seismol. Soc. Am. *64*, 699–711.

LEYDECKER, G. (1992), *The seismological surveillance of Gorbelen site and its surroundings*. In *Proceeding of OECD-NEA Workshop on Long-term Observation of the Geological Environment*, Helsinki, 9–11 September 1991, in press.

MCGARR, A. (1976), *Seismic Moments and Volume Changes*, J. Geophys. Res. *81*, 1487–1494.

MCGARR, A. (1991), *On a Possible Connection between Three Major Earthquakes in California and Oil Production*, Bull. Seismol. Soc. Am. *81*, 948–970.

MCEVILLY, T. V. (1992), *High-frequency Observations of Microearthquakes in Active Fault Zones*, Seismol. Res. Lett. *63*, 41.

MAURY, V., and SAUZAY, J.-M., *Oil well collapse due to fault shearing: a case study and some comments*. In *Proc. of the Int. Symp. Rock at Great Depth, Pau* (eds. Maury, V., and Fourmaintraux, D.) (Balkema, Rotterdam 1989) pp. 871–880.

MAURY, V., GRASSO, J. R., and WITTLINGER, G. (1992), *Lacq Gas Field (France): Monitoring of Induced Subsidence and Seismicity, Consequences on Gas Production and Field Operation*, Engineering Geology *32*, 123–135.

MEREU, R. F., BRUNET, J., MORRISSEV, K., PRICE, B., and YAPP, A. (1986), *A Study of the Microearthquakes of the Gobles Oil Field Area of Southwestern Ontario*, Bull. Seismol. Soc. Am. *76*, 1215–1223.

MILNE, W. G. (1970), *The Snipe Lake, Alberta, Earthquake of March 8, 1970*, Can. J. Earth. Sci. *7*, 1564–1567.

NASON, R. D., COPPER, A. K., and TOCHER, D. (1986), *Slippage on the Buena Vista Thrust Fault*, 43rd Annual Meeting Guidebook, AAPG, SEG, SEMP. Am. Ass. of Pet. Geol., Pac. Sect., 100–101.

NICHOLSON, C., ROELOFFS, E., and WESSON, R. L. (1988), *The Northeastern Ohio Earthquake of 31 January 1986: Was it Induced?* Bull. Seismol. Soc. Am. *78*, 188–217.

NICHOLSON, C., *Earthquakes associated with deep well activities: Comments and case histories*. In *Rock Mechanics* (eds. Tillerson & Wavesik) (Balkema, Rotterdam 1992) pp. 1079–1086.

NUR, A. (1972), *Dilatancy, Pore Fluids, and Premonitory Variation of t_s/t_p Travel Times*, Bull. Seismol. Soc. Am. *62*, 1217–1222.

OHTSU, M. (1991), *Simplified Moment Tensor Analysis and Unified Decomposition of Acoustic Emission: Application to Hydrofracturing Test*, J. Geophys. Res. *96*, 6211–6221.

PEARSON, C. F. (1981), *The Relationship between Microseismicity and High Pore Pressures during Hydraulic Stimulation Experiments in Low Permeability Granitic Rocks*, J. Geophys. Res. *86*, 7855–7864.

PENNINGTON, D. W., DAVIS, S. D., CARLSON, S. M., DUPREE, J., and EWING, T. E. (1986), *The Evolution of Seismic Barriers and Asperities Caused by the Depressuring of Fault Planes in Oil and Gas of South Texas*, Bull Seismol. Soc. Am. *76*, 939–948.

PERRODON, A., *Géodynamique pétrolière* (ed. Masson) (Paris 1985) 385 pp.

PLOTNIKOVA, L. M., FLYNOVA, M. G., MACHMUDOVA, V. I. (1989), *Induced Seismicity in Gas Field Region*, Proc. XXV IASPEI General Assembly, Istanbul, August 1989.

PRICE, D. G., VAN VEEN, F. R., SCHOKKING, F., ROSET, J. P. A., and HOUWINK, H., Proceedings of the *Bodemdaling in Netherlands* (eds. Price *et al.*) Symposium Verslag, Nov. 1990 (Tech. University Delft, Netherlands 1991).

POWER, D. V., *Acoustic emission following hydraulic fracturing in a gas well*. Paper presented at Conference on *Acoustic Emission/Microseismic Activity in Geologic Structures and Materials*, Penn. State Univ., June 1975 (eds. Hardy, H., and Leighton, F. W.) (Aedermannsdorf, Switzerland; Trans. Tech. Publications 1977) pp. 291–308.

RALEIGH, C. B., HEALY, J. H., and BREDEHOEFT, J. D. (1972), *Faulting and Crustal Stress at Rangely, Colorado*, A.G.U., Geophysical Monograph *16*, 275–284. San Andreas Fault, EOS Transactions, Am. Geophys. Union *71*, 1652.

RICE, J. R., and CLEARY, M. P. (1976), *Some Basic Stress Diffusion Solution for Fluid Saturated Elastic Porous Media with Compressible Constituents*, Rev. Geophys. Space Phys. *14*, 227–241.

RICE, J. R., and GU, C. (1983), *Earthquake Aftereffects and Triggered Seismic Phenomena*, Pure Appl. Geophys. *121*, 187–219.

RICHTER, C. F., *Elementary Seismology* (W. H. Freeman and Co., San Francisco 1958) 768 pp.

ROELOFFS, E. (1988), *Fault Stability Changes Induced beneath a Reservoir with Cyclic Variations in Water Level*, J. Geophys. Res. *93*, 2107–2124.

ROTHÉ, J.-P. (1977), *Séismes artificiels et exploitation pétrolières: L'exemple de lacq, France*, Annali di Geofisicia *30*, 369–383.

ROTHÉ, G. H., and LUI, C. Y. (1983), *Possibility of Induced Seismicity in the Vicinity of the Sleepy Hollow Oil Field, SW Nebraska*, Bull. Seismol. Soc. Am. *73*, 1357–1367.

RYDELEK, P. A., and SACKS, I. S. (1990), *Asthenospheric Viscosity and Stress Diffusion: A Mechanism to Explain Correlated Earthquakes and Surface Deformations in the N.E. Japan*, Geophys. J. Int. *100*, 39–58.

SEGALL, P. (1989), *Earthquakes Triggered by Fluid Extraction*, Geology *17*, 942–946.

SEGALL, P., and YERKES, R. F. (1990), *Stress and fluid pressure changes associated with oil-fields operations: A critical assessment of effects in the focal region of the earthquake*. In *The Coalinga, California, Earthquake of May 2, 1983*, U.S. Geol. Sur. Prof. Paper *1487*, 259–272.

SEGALL, P., and GRASSO, J.-R. (1991), *Poroelastic Stressing and Induced Seismicity near the Lacq Gas Field (France)*, EOS Trans. AGU *72* (44), 331.

SIMPSON, D. W. (1986), *Triggered Earthquakes*, Ann. Rev. Earth Planet. Sci. *14*, 21–42.

SIMPSON, D. W., and LEITH, W. (1985), *The 1976 and 1984 Gasli, USSR, Earthquakes—Were they Induced?* Bull. Seismol. Soc. Am. *75*, 1465–1468.

SIMPSON, D. W., LEITH, W. S., and SCHOLZ, C. H. (1988), *Two Types of Reservoir-induced Seismicity*, Bull. Seismol. Soc. Am. *78*, 2025–2040.

SMIRNOVA, M. N. (1968), *Effect of Earthquakes on the Oil Yield of the Gudermes Field (Northeastern Caucasus)*, *Izvestia*, Earth Physics *12*, 760–763.

SMIRNOVA, M. N., *Earthquakes induced by hydrocarbon recovery*. In *Seismicity Changes Induced by Human Activity* (Nauka, Moscow 1977) pp. 128–140 (in Russian).

SORNETTE, A., and SORNETTE, D. (1989), *Self-organized Criticality and Earthquakes*, Europhys. Lett. *9*, 197–202.

TALEBI, S., and CORNET, F. H. (1987), *Analysis of the Microseismicity Induced by a Fluid Injection in a Granitic Rock Mass*, Geophys. Res. Lett. *14* (3), 227–230.

TEUFEL, L. W., RHETT, D. W., and FARRELL, H. E. (1991), *Effect of reservoir depletion and pore pressure drawdown on in situ stress and deformation in the Ekofisk Field, North Sea*. In *Proceeding of the 32nd US Rock. Mech. Symposium* (ed. Roegiers, J. C.) (Balkema, Rotterdam 1991) pp. 63–72.

THATCHER, W., MATSUDA, T., KATO, T., and RUNDLE, J. B. (1980), *Lithospheric Loading by the 1896 Riku-u Earthquake, Northern Japan: Implications for Plate Flexure and Asthenosphere Rheology*, J. Geophys. Res. *85*, 6429–6435.

VOLANT, P., GRASSO, J. R., CHATELAIN, J. C., and FROGNEUX, M. (1992), *b-Value, Aseismic Deformation and Brittle Failure within an Isolated Object: Evidences from a Dome Structure Loaded by Fluid Extraction*, Geophys. Res. Lett. *19*, 1149–1152.

WETMILLER, R. J. (1986), *Earthquakes near Rocky Mountain House, Alberta, and Relationship to Gas Production*, Can. J. Earth Sciences *32* (2), 172–181.

YERKES, R. F., and CASTLE, R. O. (1976), *Seismicity and Faulting Attributable to Fluid Extraction*, Engin. Geol. *10*, 151–167.

(Received October 6, 1992, revised/accepted April 10, 1993)

5

LES SEISMES COMME JAUGES DE CONTRAINTE DE LA CROUTE SUPERIEURE

Lorsque l'objet étudié est bien cerné et les cas de charge contraints, les séismes peuvent être utilisés comme capteur de contrainte. La robustesse de ces estimateurs est fortement dépendante de la qualité des modèles. Dans le cas de zone de subduction, où les conditions de déplacements apparaissent moins obscures que dans les domaines continentaux, les corrélations spatiales et temporelles entre l'activité sismique de plusieurs essaims sur des distances atteignant 200 km permettent de définir des entités mécaniques au comportement homogène (partie 1). Dans la seconde partie, on tente d'éclairer l'aspect physique du concept de système critique auto-organisé. Ce concept est proposé à l'échelle de la lithosphère pour expliquer l'organisation spatiale et temporelle des séismes tectoniques. Les séismes induits apparaissent comme des sous-systèmes des précédents, où les ruptures de lois d'échelles reflètent des caractéristiques géomécaniques locales. Les conditions d'apparition, de pérennité ou de disparition de ces systèmes critiques auto-organisés, pourront peut être permettre de progresser dans l'utilisation des fractales pour comprendre et prévoir une sismicité. Dans ce sens prévoir un séisme tectonique revient à comprendre le chaos qui maintient l'activité sismique, au voisinage de barrage ou de réservoir d'hydrocarbures, pendant plus de 20 ans, sans migration de l'activité sismique et pour des variations de charge d'un à deux ordres de grandeur inférieurs à la charge qui a déclenché la première instabilité sismique. On remarquera bien sûr que l'instabilité majeure correspond rarement au premier maximum de la charge.

FITH ITERATION: "The extreme sensitivity of chaotic systems to tiny perturbations can be used both to stabilize regular dynamic behaviors and to direct chaotic trajectories rapidly to a desired state" (Shinrot et al., Nature 363, 411-417, 1993). When will this apply for earthquakes?

51

CORRELATION SPATIALE ET TEMPORELLE D'ESSAIMS SISMIQUES DANS L'ARC DES NOUVELLES-HEBRIDES: HOMOGENEITE MECANIQUE SUR PLUS DE 200 KM?

GEOPHYSICAL RESEARCH LETTERS, VOL. 19, NO. 11, PAGES 1157-1160, JUNE 2, 1992

SPATIAL AND TEMPORAL SEISMIC ENERGY RELEASE IN THE EFATE REGION (CENTRAL NEW HEBRIDES ISLAND ARC) : EVIDENCE FOR BUCKLING ?

Jean - Luc Chatelain [1] and Jean - Robert Grasso

Laboratoire de Géophysique Interne et Tectonophysique, Grenoble, France.

Abstract. A study of the spatial and temporal distributions of the seismicity in the central New Hebrides island arc shows that the Efate region (including the interplate boundary and the upper plate) can be considered as a single block under stress. Repeated activation of very specific zones within this block as indicated by seismic clusters is temporally correlated with larger than average energy release rates. These relative high rates are associated with main shocks with magnitude (Ms, mb) > 5.0 in the upper part of the interplate boundary and indicate that slip at the plate boundary is not steady. No correlation is found with main shocks located in the lower part of the interplate boundary, where slip occurs more freely. We propose that these observations are consistent with a buckling process with a wavelength of about 170 km within the overriding plate. Buckling or bending of the upper plate may be due to the impingement of a seamount on the subduction system, elevating the stress level of the Efate region, which behaves like a single mechanical entity.

Introduction

Numerous investigations of the connection between major interplate earthquakes and outer rise events show that the connections are time delayed (5 to 40 years) and suggest that visco-elastic processes may be involved [e.g. Li and Kisslinger, 1985 ; Rydelek and Sacks, 1990]. Corresponding models predict that occurrence of outer rise events varies both spatially and temporally. In a few cases (Kuriles, New Hebrides), a change in state of stress in the outer rise from extension to compression is temporally observed [Christensen and Ruff 1988], and some authors have proposed using this pattern for moderate term earthquake prediction [e.g. Dwomska and Lovison, 1988]. While the effect of coupling on the regional stress field is also evident in the overriding plate and in the subducting plate below the interplate coupled zone, its study requires preliminary identification of the processes involved as well as accurate hypocenter locations [e.g. Astiz and Kamamori, 1986; Dewey and Spence, 1979; Dwomska and Lovison, 1988, Dwomska et al., 1988; Lay et al., 1988; McNally et al., 1986; Seno, 1979; Spence, 1977, 1986, 1987]. In this study we focus on a possible connection between interplate events and events in the overriding plate using data from a local network located in the central part of the New Hebrides island arc. The events within the overriding plate are clusters of events occurring few months before or after the main energy release in the coupled part of the interplate boundary.

The central New Hebrides island arc can be divided into at least four segments (northern Santo, southern Santo-northern Malekula, southern Malekula, Efate) [Taylor et al., 1980]. A network of 19 seismograph stations was established in 1978-1979 in this part of the arc as a joint project between ORSTOM and Cornell University. As the focus of this paper is the seismicity of the Efate segment, the zone covered by the network has been divided in 3 regions, which for convenience we call the Efate region, the northern region, and the southern region without further distinction of blocks north or south of the Efate region (Figure 1). The edges of the Efate region are marked by two barriers limiting the development of aftershock zones, designated as boundary 1 and boundary 3 (boundary 2 located in the northern region is not considered in this study) [Chatelain et al. 1986]. These are roughly located at 17.2°s and 18.1°S respectively (Figure 1).

On a large scale, the Efate region is a transition zone between subduction to the south and a portion of the plate boundary that might be locked to the North [Chatelain et al., 1986] . At a smaller scale, the Efate region shows an interruption of the deepest part of the trench coinciding with the arrival of the ORSTOM seamount in the subduction system (Figure 1). These features together with the difference in seismicity regimes up-dip and down-dip are in favour of a stick-slip motion in the up-dip part of the interplate boundary, while the down-dip part slips more freely.

Using data collected by the local ORSTOM/Cornell network (detecting events with magnitude > 1.9) from

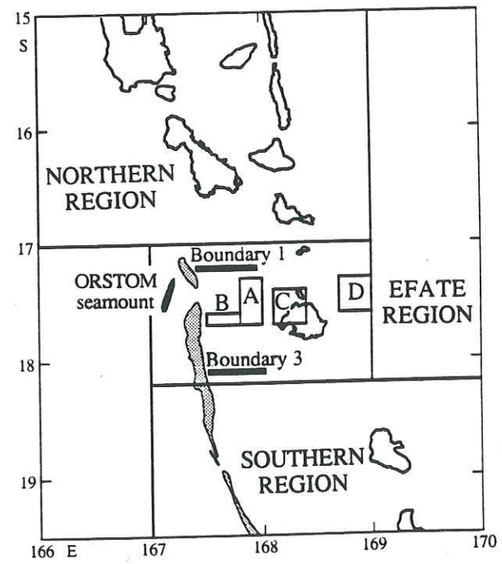

Fig. 1. Map of the central New Hebrides island arc, showing the northern, Efate and southern regions, as defined in this study. The black area represents the 4000 meter contour of the ORSTOM seamount. The grey area represents the 6000 meter contour of the trench. The two thick black lines represent boundaries 1 and 3, and the boxes represent the four zones (A, B, C, D) repeatedly activated by clusters of earthquakes, from Chatelain et al. [1986].

[1]Also at ORSTOM, Noumea, New Caledonia.

Paper number 92GL00975
0094-8534/92/92GL-00975$03.00

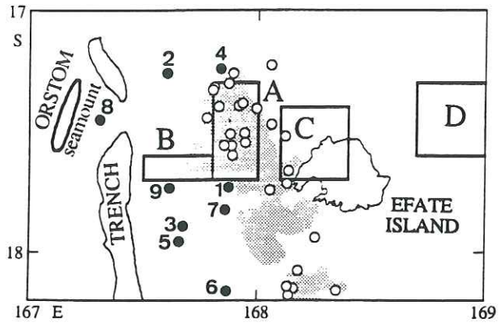

Fig. 2. Map of the Efate region, as defined in this study. The shaded area represents the down-dip zone with high background seismicity level. Boxes represent the four cluster zones from Chatelain et al. [1986]. ORSTOM seamount and trench contours as in Figure 1. The magnitude (M_S, mb) > 5.0 main shocks that occurred during the period 1978-1990 are shown by open circles in the down-dip zone, and by solid circles numbered by chronological order in the up-dip zone. Magnitudes of up-dip main shocks: 6.2 (1); 7.1 (2); 5.1 (3); 6.7 (4); 5.6 (5); 6.3 (6); 5.1 (7); 5.1 (8); 6.2 (9).

October 1978 to 1984, Chatelain et al. [1986] have shown that most of the seismicity is concentrated in the Efate region and that two regimes of seismicity characterize the Efate region. Next to the trench (termed the up-dip part of the contact zone), the background seismicity level is low, and main shocks (magnitude Ms, mb > 5.0) are followed by large aftershock zones. Nearer to the island arc (termed the down-dip part of the contact zone), the background level is very high, and main shocks are followed by small aftershock zones or no aftershocks at all. Most clusters of seismicity are located in the Efate region and are not randomly distributed. Instead, they occur in four distinct well determined zones: one is located up-dip (Zone B), one down-dip (Zone A), and two in the upper plate (Zones C and D) (Figure 2). These observations, revealed by the study of the seismicity from 1978 to 1984 are still observed through 1990. From 1978 to 1990, the station distribution in the Efate region remained the same, there is thus no variation of network sensitivity with time.

In this paper we investigate the temporal and spatial relationship between peaks of energy release in the up-dip part of the contact zone and occurrence of clusters in the Efate region, indicating that (1) this region behaves like a single mechanical entity and (2) the distribution of clusters in the upper plate can be explained by buckling process.

Data Analysis

From October 1978 (when the network started operating) to December 1990, 36 earthquakes with magnitude (Ms, mb) > 5.0 occurred in the Efate region (for seismicity crisis, only events with the largest magnitude were considered). Nine of these earthquakes occurred in the up-dip part, while the others occurred in the down-dip part (Figure 2). The nine up-dip main shocks can be correlated to the major seismic episodes in the larger region comprised between 15°S and 19.5°S, as well as in the Efate region, while activity North of the Efate region can be connected only to event 2 and activity South of the Efate region to event 6 (Figure 3). These observations attest that the main energy release in this time period is located in the Efate region.

We calculated the seismic energy released in the Efate region by earthquakes shallower than 80 kilometers in six

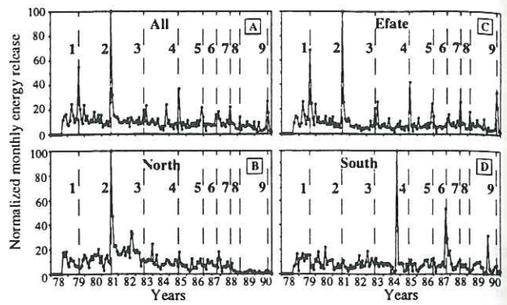

Fig. 3. Monthly energy release in the regions delimited in Figure 1: (A) entire region, (B) northern region, (C) Efate region, and (D) southern region. Occurrences of up-dip magnitude (M_S, mb) > 5.0 main shocks are shown by dotted numbered lines. Numbering for main shocks as in Figure 2. Energy has been calculated with the formula Log(E) = 11.4 + 1.5*M. For each month the summation of Log(E) is represented rather than summation of E, in order to avoid squeezing of the scale by the highest peaks. For each region, the energy release has been normalized to the highest peak of the given region. Energy values for the highest peaks are (in ergs) : 1.20 10 **22, 5.64 10**21, 1.17 10**22 and 8.00 10**21 for the entire, northern, Efate and southern regions respectively.

distinct zones : up-dip, down-dip, and zones A,B,C,D. Whereas zones A and B overlap the up-dip and down-dip zones, zones C and D are totally separate (Figure 2). Peaks in energy release in these 6 zones are closely related within a few month time lag. Moreover, energy release in the different zones are correlated in time with magnitude (Ms, mb) > 5.0

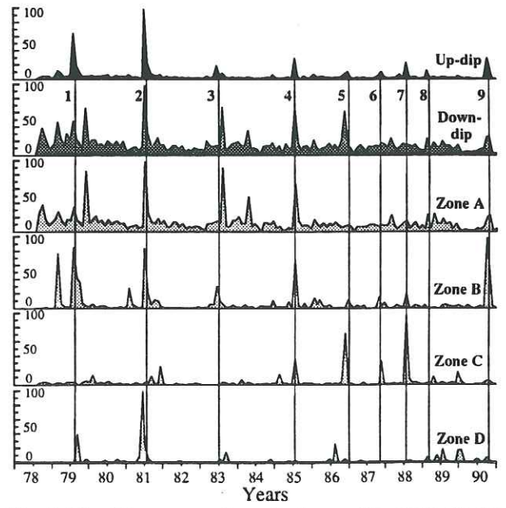

Fig. 4. Monthly energy release in the up-dip, down-dip and cluster zones A, B, C, D of the Efate region. For each zone the energy release has been normalized to the highest peak of the given zone. Numbered lines show the occurrences of magnitude > 5.0 up-dip main shocks in the Efate region. Numbering as in Figure 2. Maximum energy release are (in ergs) : 1.15 10**22, 2.81 10**21, 1.85 10**20, 5.37 10**20, 4.45 10**19, 2.87 10**19 for the up-dip, down-dip, A, B, C, and D zones respectively.

events located in the up-dip zone (Figure 4), but no correlation is apparent with the magnitude (Ms, mb) > 5.0 events that occur in the down-dip zone. No consistent cycle appears in the spatial distribution of energy release. The delay between energy release in the different zones is also variable from almost instantaneously to few months before and/or after the up-dip main shock occurrences (Figure 4). Thus, the activity in none of the 6 zones appears to control the triggering of seismic activity in the others, and no reproducible seismic migration can be observed. Rather, the Efate region (comprising the contact zone between the two plates and the upper plate east to zone D) behaves like a single entity under stress.

Discussion and Conclusion

Kanamori [1971] suggested that the great and apparently systematic variations in the size of large interplate earthquakes from one subduction zone to another correlates with the degree of compression across the plate boundary. Different idealized subduction types have been proposed according to their seismic coupling efficiency as estimated by the maximum earthquake size [Ruff and Kanamori, 1980] or by summing seismic moments [Petterson and Seno, 1984]. Thus, variations in seismic coupling along arcs can be related to variations in the mean normal stress that act across the subduction zone plate interfaces. At a smaller scale, in comparing arcs with different seismic coupling, Lay and Kanamori [1981] assumed that stresses are inhomogeneously distributed on the interface and that the areas of concentrated moment release are the most highly stressed regions and probably the most strongly coupled zones. In absolute value the New Hebrides subduction zone is of type 3, following Kanamori's classification, i.e. moderate coupling. In this study, at distances of the order of 100 km we work with, the Efate region is the highest coupled region of this part of the New Hebrides arc. Assuming the asperity model, we expect that this region undergoes the highest regional stress. This description points out the importance of the scale factor in investigating the mechanics of a tectonic area. This scale factor is fundamental to determine what are the driving forces of the object (Efate region) we study in this paper.

To explain the observations presented in the previous section, it is necessary to focus on the interface between the two plates. Sykes and Quittmeyer [1981] propose possible down-dip variations of seismic coupling in individual subduction zones. Our up-dip and down-dip seismicity zones correspond, respectively, with areas of strong and weak coupling. The correlation between energy release in the strongly coupled zone (up-dip events) and swarm activity eastward of this zone in the upper plate are indicative of high stress in the whole area. Earthquake clusters occur selectively in comparatively weak zones within the crust and sensitively reflect the state of crustal stress. Locations of such weak zones at different scales have been reported [e.g., Xu and Shen 1981]. The clusters located within the overriding plate occur in time intervals spanning a few months before and after the main energy release in the coupled part of the interplate boundary (up-dip zone). The correlation between the up-dip events and the clusters is neither the result of a propagation process nor the effect of faults as found in other regions [e.g., Li and Kisslinger, 1985 ; Mogi, 1981 ; Tsukuda, 1988]. Rather, this correlation is interpreted as the result of forces applied simultaneously to the whole Efate region, with small temporal separation (from almost instantaneously to 1-3 months: see Figure 4) being only a manifestation of differences in rheological responses.

The seismicity defines the Efate region as a block of homogeneous behavior. The east-west extent of the block (about 200 km) is bounded by the development of clusters of seismicity. The north-south extent of the block (about 150

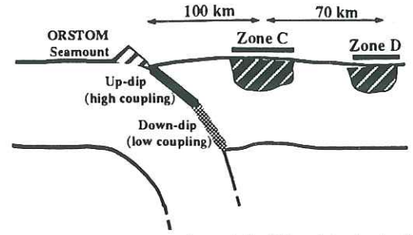

Fig. 5. Schematic cross section of the Efate block. In the up-dip part of the interplate boundary the subduction process is perturbated by the arrival of the ORSTOM seamount. As a consequence, the Efate region behaves like a single mechanical entity, leading to buckling process in the upper plate with repeated activation of weak zones in the upper plate linked to episodes of main energy release along the up-dip part of the interplate boundary.

km) is bounded by major events locations, background seismicity level, and aftershocks migration.

The localization of the clustered activity in front of the most strongly coupled area (Figure 5), is induced by high stress in this zone, despite the fact that it is usually assumed that in subduction zones, earthquakes are result of slip instabilities that depend on the contrasting stiffnesses of the fault and the coupled plate system [e.g. Stuart and Mavko, 1979; Li and Rice, 1983a,b]. To solve this apparent paradox we need to describe the local source of stress, which is able to perturb the transient subduction slip. The geometry of the sea floor exhibits (1) an interruption of the trench in front of the Efate zone and (2) the ORSTOM seamount located westward of this interruption (Figure 2) . These two features may explain the local high coupling between the two plates and the collision-like behavior of the overriding plate. Note also that these two features and the cluster zones are aligned in the direction of plate convergence (Figure 2) .

We propose that a buckling process within the overriding plate explains the spacing between the cluster zones. This process is observed in different tectonic setting using either seismic activity or deep seismic imaging or geodesy [Sacks et al. 1978 ; Xu and Shen 1981 ; Awata and Kakimi 1985, Bull 1990]. The proposed models investigate different rheologies of the lithosphere to fit the available observations, i.e. plastic rheology or recoverable elastic properties [e.g., Turcotte and Schubert, 1982 ; Martinod and Davy, 1992]. The model of Martinod and Davy [1992] can be used to estimate the wavelength of oceanic buckling as a function of the lithosphere age in the New-Hebrides area. Unfortunately no estimate of the age of the upper plate in the Efate region is available. However, the spacing of weak areas deduced either from cluster activity (D=l/2≈70 km), or from the distance to the trench of the first cluster l/2≈100 km), imply a wave length, l, of about 170 km (Figure 5). Such a wavelength dimension is in agreement with a 35 Myr old plate, which is within the range of estimates of the age of the plate in the northern region [Recy et al., 1990].

Such correlation distances are observed with other tools (e.g. water level change). As with our observations, changes are not always coseismic (either few months before or after major events) and poroelastic effects fail to explain long distance correlation [e.g. Sadovsky et al., 1984; Roeloffs, 1988]. Thus, the model proposed here may have a general meaning and can apply in other settings.

Acknowledgements. We thank all the people involved in the data collection and analysis operations. We thank two anonymous reviewers and P. Molnar for their constructive

criticisms and help in improving the manuscript. This work was supported by ORSTOM and Université Joseph Fourier.

References

Astiz,L., and H. Kanamori, Interplate Coupling and Temporal Variation of Mechanisms of intermediate-depth earthquakes in Chile, *Bull. Soc. Am.*, 76, 1614-1622, 1986.

Awata Y. and T. Kakimi, Quaternary tectonics and damaging earthquakes in northeast Honshu, Japan, *Earthq. Predict. Res.*, 3, 231-251, 1985.

Bull J.M., Structural style of intraplate deformation, Central Indian Ocean basin: evidence for the role of fracture zones, *Tectonophysics*, 184, 213-228, 1990.

Chatelain J.-L., B.L. Isacks, R.K. Cardwell, R. Prévot, M. Bevis, Patterns of Seismicity Associated with Asperities in the Central New Hebrides Island Arc, *J. Geophys. Res.*, 91, 12,497 - 12,519, 1986.

Christensen D.H., and L.J. Ruff, Seismic Coupling and Outer Rise Earthquakes,*J. Geophys. Res.*, 91, 13,421 - 13,444, 1988.

Dewey, J.W. and W. Spence, Seismic gap and sources zones of recent large earthquakes in coastal Peru, *Pure and Appl. Geophys.*, 117,1148-1171, 1979.

Dwomska, R. and L.C. Lovison, Intermediate term seismic precursors for some coupled subduction zones,*Pure and Appl. Geophys.*, 126, 643-664, 1988.

Dwomska, R., J.R. Rice, L.C. Lovison and D. Josell, Stress transfer and seismic phenomena in coupled subduction zones during the earthquake cycle, *J. Geophys. Res.*, 93,7869-7884, 1988.

Kanamori, H., Great earthquakes at island arcs and the lithosphere, *Tectonophysics*, 12, 187-198, 1971.

Lay, T. and H. Kanamori, The asperity model of earthquake sources and its implications for triggering and seismic gap discrimination, *in Earthquake Prediction, Maurice Ewing Series*, 4, D. Simpson and P. Richards, Eds., American Geophysical Union, Washington D.C., 579-592, 1981.

Lay T., L. Astiz, H. Kanamori, and D. Christensen, Temporal variation of large intraplate earthquakes in coupled subduction zones, *Phys. Earth Planet. Inter.*, 112-132,1988.

Li V.C. and C. Kisslinger, Stress transfer and nonlinear stress accumulation at subduction-type plate boundaries-application to the Aleutians, *Pure and Appl. Geophys.*, 122, 812-830, 1985.

Li V.C. and J.R. Rice, Preseismic rupture progression and great earthquake instabilities at plate boundaries, *J. Geophys. Res.*, 88, 4231-4246, 1983a.

Li V.C. and J.R. Rice, Precursory surface deformation in great plate boundary earthquake sequences, *Bull. Seism. Soc. Am.*,73, 1415-1434, 1983b.

Mc Nally K.C., J.R. Gonzales-Ruiz and C. Stolte, Seismogenesis of the 1985 great (Mw=8.1) Michoacan, Mexico earthquake, *Gephys. Res. Lett.*, 13, 585-588, 1986.

Martinod J. and P. Davy, Periodic instabilities during compression or extension of the lithosphere: 1. deformation modes from an analytical calculation method, *J. Geophys. Res.*, 97, 1999-2014, 1992.

Mogi K., Earthquake prediction program in Japan, *in Earthquake Prediction, Maurice Ewing Series*, 4, D. Simpson and P. Richards, Eds., American Geophysical Union, Washington D.C., 635-666a, 1981.

Peterson E.T. and T.Seno, Factors affecting seismic moment release rates in subduction zones, *J. Geophys. Res.*, 89,10,233-10,248, 1984.

Recy J., B. Pelletier, P. Charvis, M. Gerard, M.C. Monjaret and P. Maillet, Structure, age et origine des fossés arrière-arc des Nouvelles-Hébrides, *Oceanologica Acta*, 10, 165-182,1990.

Roeloffs, E. , Hydrological precursors to earthquakes: A review.*Pure and Appl. Geophys.*, 126,177-209, 1988.

Ruff L. and H. Kanamori, Seismicity and the subduction process, *Phys. Earth Planet. Inter.*, 23, 240-252,1980.

Rydelek P.A., and I.S. Sacks, Asthenospheric viscosity and stress diffusion: a mechanism to explain correlated earthquakes and surface deformations in the N. E. Japan, *Geophys. J. Int.* 100, 39-58, 1990.

Sacks I.S., A.T. Linde, B.A. Rodriguez and J.A. Snoke, Shallow seismicity in subduction zones, *Geophys. Res. Lett.*,5, 901-903, 1978.

Sadovsky, M.A., Monakov, F.I., Kissin, I.G., Shirokov, B.D., Short term hydrogeodynamic precursors of earthquakes, *in Earthquake prediction*, Terrapub Unesco, Paris, pp 233-243, 1984.

Seno T., Pattern of intraplate seismicity in south-western Japan before and after great interplate earthquakes, *Tectonophysics*, 57, 267-283, 1979.

Spence W., The Aleutian arc: Tectonic blocks, episodic subduction, strain diffusion and magma generation, *J. Geophys. Res.*, 82, 213-230, 1977.

Spence W., The 1977 Sumba earthquake series: Evidence for slab pull force acting at a subduction zone, *J. Geophys. Res.*, 91, 7225-7239, 1986.

Spence W., Slab pull and the seismotectonics of subducting lithosphere, *Rev. Geophys.*, 25, 55-69, 1987.

Stuart W.D. and G.M. Mavko, Earthquake instability on a strike slip fault,*J. Geophys. Res.*, 84, 2153-2160, 1979.

Sykes L.R. and R.C. Quittmeyer, Repeat times of great earthquakes along simple plate boundaries, *in Earthquake Prediction, Maurice Ewing Series*, 4, D. Simpson and P. Richards, Eds., American Geophysical Union, Washington D.C., 217-247, 1981.

Taylor F.W., B. L. Isacks, C. Jouannic, A. L. Bloom, J. Dubois, Coseismic and Quaternary vertical tectonic movements, Santo and Malekula islands, New Hebrides island arc, *J. Geophys. Res.*, 85. 5367-5381, 1980.

Tsukuda T., Linked activities at the adjacent seismic spots, *Seis. Res. Lett.*, 59, 6, 1988.

Turcotte D.L. and G. Schubert, *Geodynamics Applications of continuum Physics to Geological Problems*. John Wiley and Sons Eds, New-York, 1982.

Xu S. and P. Shen, Seismicity patterns in China, *in Earthquake Prediction, Maurice Ewing Series*, 4, D. Simpson and P. Richards, Eds., American Geophysical Union, Washington D.C., 117-125, 1981.

J.-L. Chatelain and J.-R. Grasso, IRIGM-LGIT, Domaine Universitaire, BP 53X, 38041 Grenoble CEDEX, France.

(Received November 25, 1991;
revised March 30, 1992;
accepted April 21, 1992.)

IS THE UPPERMOST CRUST IN A SELF-ORGANIZED CRITICAL STATE ? EVIDENCES FROM INDUCED SEISMICITY

Abstract

Characterizing the crust structures and unravelling the basic mechanisms controlling their origin and more generally the crust behavior from short time scales (earthquakes) up to long time scales (tectonic deformations) is one of the most important problem in geophysics. Recently (Sornette and Sornette, 1989; Bak and Tang, 1989; Sornette et al., 1990; Scholtz 1991; Sornette, 1991), it has been proposed that the structuration of the crust is a self-organized critical (SOC) phenomenon (Bak et al., 1987). Within this concept, many observations are rationalized, such as the existence of power laws (Gutenberg-Richter law, earthquake epicenter fractal distributions, fractal fault patterns, etc...), exemplifying the "critical" state of the crust. However, other observations seem at variance with the SOC idea : 1) the diffuse seismic activity implicit in the original SOC picture is in contrast with the observed seismic clustering, due to fault structures and crust heterogeneity; 2) Within the sandpile paradigm of SOC, one expects that essentially any disturbance may trigger avalanches of all sizes. In contrast, some perturbations does not seem to destabilize the crust. Here, we reexamine the relevance of SOC and show how to reconcile these facts with the idea of self-organized criticality. In this goal, we first review major reported cases of induced seismicity in various parts of the world. Earthquakes induced by human activity, in otherwise historically aseismic areas, provide direct evidences that both pore pressure changes ($\pm\Delta p$) and mass transfers ($\pm\Delta m$), corresponding to incremental deviatoric stresses of the order of 1 MPa regardless of the tectonic setting, trigger seismic instabilities in the uppermost crust with magnitude ranging from 3.0 to 7.0. Once triggered, stress variations of at least one order of magnitude less than the triggering stress change, but larger than the ~0.005 MPa of tidal stress, still sustain seismic activity. We then summarize the basic ingredients of SOC, as applied to the crust problem and show how these observations constitute a dramatic illustration of the fact that the crust is in a "critical" state, in which small external perturbations may lead to large responses of the system. Furthermore, a careful analysis of the geological setting and tensorial nature of the human induced perturbations allows us

to reconcile the paradoxes mentioned above. We show in particular that seismic clustering is not in contradiction with SOC and that induced seismicity reflects the potential of many regions to be activated at stress thresholds which may be slightly higher than in other parts due to screening and/or incoherence of the stress perturbation with respect to the local tectonic stress. The existence of breaks in self-similarity in the measured Gutenberg-Richter power laws is not in contradiction with the SOC concept either and reflects solely finite-size effects : these breaks correlate well with the width of the local seismogenic beds, ranging in sizes from that of mines pillars in the case of Mining Induced Seismicity, to the thickness of brittle sedimentary beds in the vicinity of dams or depleted hydrocarbon reservoirs. This mimics the effect the schizosphere plays for tectonic earthquakes (Scholz 1991; Sornette, 1992a). The earthquake size being locally bounded by the thickness of seismogenic beds, there is no paradox why the major induced earthquakes ($m \geq 6$) occur in so called "stable" shield provinces where thick shallow seismogenic bed (>10 km) is available. Our analysis suggests that the region of possible seismic hazard is much larger than the area where earthquakes are common.

INTRODUCTION

Most of the world's seismically active faults are concentrated along plate boundaries, and slip on them results from the relative movements between essentially rigid plates. Stress accumulates continuously as one plate move past another until an earthquake occurs. Yet, many earthquakes occur within the generally aseismic rigid plates, and little is known about the processes causing intraplate seismic instabilities in continental setting. The details of what triggers seismogenic failures well away from plate boundaries, at a particular place and time are generally unclear, despite numerous studies (see for example Byerlee, (1967); Nur (1972); Costain,et al. (1987); Sibson (1989)) that rely, by indirect evidence, on changes in fluid pressure and movements of fluids. An opportunity to test and quantify these possible mechanisms by direct evidence is offered where and when changes in hydro-mechanical parameters of the crust are known, i.e. in areas where earthquakes are induced by human intervention.

Six stress indicators are usually used to infer the orientation and the relative magnitudes of the contemporary in-situ tectonic stress field in the Earth's lithosphere: earthquake focal mechanisms, well bore breakouts, hydraulic fracturing and overcoring, and young geologic data including fault slips and volcanic alignments (e.g. Zoback and Zoback, 1980). Most of the types of data previouly described give an indication of the orientation of some components of the stress tensor without information on the magnitude of the stress components. The hydraulic fracturing stress measurements is the only technique that ideally provides information on both horizontal stress magnitudes and orientations (e.g. Haimson and Faihrhurst,1970; Zoback and Haimson, 1983). On the other hand, when the mechanics of earthquakes induced by certain types of human activity can be isolated, an estimation of the perturbation of the stress field that drive faulting is possible in term of driven shear stress. Previous works related seismic stress parameters (stress drops from induced earthquakes) to the relevant in situ stress and rock properties (Wyss and Molnar, 1972; McGarr et al., 1979; Fletcher 1982; Simpson 1986).

In this paper, we review major reported cases of Induced Seismicity including Reservoir Induced Seismicity and seismicity that is triggered by subsurface fluid manipulations. A special emphasis is given to so-called "stable" tectonic settings, i.e. area where the deformation rate is slower than in the so called "active" areas where most of the seismicity takes place. Source mechanisms of triggered earthquakes are used to quantify local critical stress thresholds. Observations reported in Zambia (Gough and Gough 1970), in SE China and in SW India (Gupta and Rastogi, 1976), in western Uzbekistan (Simpson and Leith, 1985), in northern Holland, in Norway and in SW France (Grasso, 1993) show examples of untypical seismicity relatively to low historical seismicity in the vicinity of either water reservoir impoundments or hydrocarbon extractions.

In the second part of this study, we analyze the relevance of the SOC concept to these observations. In this goal, we first review the basic ingredients of SOC, as applied to the crust problem. We then show how the observations on induced seismicity

constitute a dramatic illustration of the fact that the crust is in a "critical" state, in which small external perturbations may lead to large responses of the system. Each previously low seismicity area is treated as an isolated system, in which external forces that are applied at the boundaries of the regions are relatively constant by comparison to the fast fluid induced changes in internal forces that have altered the stress and the stability of the regions. We report observations where the induced seismicity, once triggerered, is sustained over years and obey a power law size distribution. Then, local uppermost crustal blocks are moved to criticality as a response to pore pressure changes and mass transfers. It is shown that seismic clustering is not in contradiction with SOC, but reflects the natural long-term organization of the crust in response to the on-going seismic activity. This organization is responsible for local screening of regions which thus present low activity. Induced seismic instabilities ranging in magnitude from 3.0 to 7.0 reflects the potential for any such screened region to be brought to a critical state, due to the action of a local stress perturbation of the right tensorial nature. The importance of the tensorial nature of the crust deformation is underlined with an emphasis on the relation between the human perturbation and the local tectonic setting. This allows us to undertand why some perturbations does not seem to destabilize the crust, in contradiction with the naive expectation based on the uncorrect idea that self-organized criticality implies that the crust is everywhere on the verge of rupturing.

Overview of Mechanics of Fluid Induced Earthquakes

Historically, two types of earthquakes were suggested to be associated with fluid manipulations: those produced by the filling of an artificial reservoir (Carter, 1945; Gupta and Rastogi, 1976; Simpson, 1986), and those associated with fluid injections under pressure greater than hydrostatic (Evans, 1966; Healy et al. 1968; Raleigh et al. 1972). Reservoir impoundments trigger seismicity either by direct loading effects or by coupled poro-elastic effect (Simpson 1986). The direct effects of the load can be divided into an elastic effect and an undrained porelastic effect. The elastic effect will change the radius of the Mohr circle depending of the tectonic environment and modify the seismicity

accordingly with respect to the Coulomb failure envelop: induced seismic activity in normal faulting area and triggered seismic quiescence in thrust faulting area (i.e. Bufe 1976; Jacob et al. 1979). The second direct load effect, the increase of pore pressure immediatly below the reservoir, will always favor induced seismicity by moving the Mohr circle towards the origin. This way, many seismic events of magnitude between 3 and 4 have been reported in the vicinity of subsurface fluid injections, e.g. hydrocarbon fields stimulated by fluid injection or waste storage (Colorado, (Evans, 1966; Healy et al. 1968; Raleigh et al. 1972); N.Y., (Fletcher and Sykes, 1977); Nebraska (Evans and Steeples, 1987); Ohio (Nicholson et al. 1988). Delayed seismic responses to reservoir impoundment correspond to more gradual diffusion of water from the reservoirs to hypocentral depths (Simpson et al. 1988a). Similar possible connections between fluid manipulations and earthquakes at distances of tens of kilometers were also proposed at Denver and Lacq fields on the basis of pore pressure diffusion associated to deep well activities (Hsieh and Bredehoeft 1981; Grasso et al. 1992a). The delayed mechanisms for induced seismicity are not well constrained due to the lack of knowledge of hydrological properties at depth and will not be used in this work.

Earthquakes induced by fluid loading are understood to result from an increase in pore pressure, causing an effective normal stress reduction on the fault plane. However, there is an apparent paradox with the review of Grasso (1992) on numerous cases where simple hydrocarbon extractions had triggered seismic activity. From the observations of seismic events recorded by local networks in areas surrounding hydrocarbon fields, e.g. in Alberta, Canada (Wetmiller 1986), in SW France (Grasso and Wittlinger, 1990; Guyoton et al. 1992) and in northern Holland (Haak 1991), it appears that such earthquakes have not occurred in the depleted portions of the reservoir where gas pressure has decreased, but instead above or below the actual gas reservoir. These observations are explained by a poroelastic stress transfer from the depleted reservoir to the levels surrounding the hydrocarbon reservoir (Segall, 1989). The linear relation between the decrease in pore pressure and subsidence near Lacq (Grasso et al. 1992b) supports the poroelastic modelling of the local strain and stress fields. At other sites

where the available measurements do not permit to identify unambigously the rock mass rheology, Grasso (1992) propose a two step mechanism in which poroleastic stressing occurs before the in-situ faults, that localize displacements, had been reactivated. In these cases, seismic slips (m_{max}~4) are a second order pattern of a main aseismic displacement. In a broader context, massive hydrocarbon recovery reduces the vertical load which can trigger earthquakes in a thrust faulting environment. The same basic relation explains the magnitude of seismic energy which is released by earthquakes induced by mining (McGarr 1976). McGarr (1991) suggests a mechanical connection between the mass withdrawal and the earthquake size: the seismic deformation (estimated from the seismic moment) is that required to offset the force imbalance caused by hydrocarbon production (proportionnal to the mass withdrawal). The other types of seismicity induced by mass withdrawal include those due to quarrying (e.g. Pomeroy et al 1976; Yerkes et al,1983) and those associated with the removal of ice sheets (Stein et al., 1979; Johnston, 1987,1989).

INDUCED EARTHQUAKES AS STRESS GAUGES

Stress changes induced by pore pressure changes:

An upper bound of the amplitude of the pore pressure variation necessary to cause Reservoir Induced Seismicity is given by the water height of the reservoir. The values stand around 1-2 MPa for most of $m \geq 2.5$ RIS (see for example Table 1 of Gupta, 1985). In some area, fluctuations of a few meters of water level correlate with seismicity in agreement with model of coupled pore pressure field beneath the reservoir (Simpson and Negmatullaev 1981; Roeloffs, 1988). Roeloffs's analysis argues for a 0.1 MPa size of the stress step needed to trigger seismicity. Similarly, upon fluid injection performed for washing for salt removal purposes in Dale (NY), a monthly rate of 80 earthquakes was observed against a background of one natural earthquake per month (Fletcher and Sykes, 1977). Downhole pressures ranged from 5.2 to 5.5 MPa at 450 m (Plitho/Pfluid ≈1.9), but for pressures below 5 MPa, there was no seismic activity.

Application of the poro-elastic stressing model to the Lacq gas field where hydromechanical parameters are constrained by numerous subsurface data (porosity, bulk and elasticity moduli, Biot coefficient, pore pressure history, surface subsidence are in-situ estimated) predicts that a variation in shear stress of few bars trigger seismicity above and below the gas reservoir (Segall and Grasso, 1991; Segall 1993). At other sites, we estimated the maximum induced stress at the onset of seismicity either using the subsidence and shear modulus of the rocks involved, or using a rough value depending on pressure drop and reservoir geometry as proposed by Grasso (1993). In the first case, we can make an order-of-magnitude estimate of the expected stress changes using

$$(1)\quad \Delta\sigma_{max} \approx (4\mu/(1-\nu)\pi D)\ \Delta H_{max})$$

where μ, ν, D, H_{max}, are respectively the shear modulus, the poisson coefficient of the rock matrix, the depth of reservoir and the maximum depth of the subsidence bowl. In the second case, we use

$$(2)\quad \Delta\sigma_{max} \approx ((1-2\nu)/2\pi(1-\nu))\ \Delta p\ F_{max}(a/D),$$

or

$$(3)\quad \Delta\sigma_{max} \approx 0.1.(T/D)\ \Delta p\ F_{max}(a/D),$$

for standart (limestones) reservoir rock type. Δp and $F_{max}(a/D)$ are respectively the reservoir pressure drop and a dimensionless function of position and reservoir geometry. a is the reservoir radius and D is the reservoir depth (the maximun value is $F_{max}(1) \approx 3$, Segall 1989). For all the sites where estimates can be performed, stress changes smaller than 1 MPa appears to trigger seismic instabilities (Table 1). The stress variation that triggers seismicity appears to be roughly of the order of those estimated to trigger

seismicity in the surrounding of artificial water reservoir impoundments. Moreover, these seismic instabilities occur under a great variety of regional tectonic conditions: stable in the Netherlands and Texas; stable or/and extension in the North Sea, Norway and Denmark; compression in the Caucasus, France and Canada. Due to the mechanical properties of most of shallow rock matrix involved, this type of seismic slip is a second order process of the main non-brittle deformation (Grasso 1993). In Table 1a, we present local seismicity changes induced by deep well pore pressure fluctuations. Either increases or decreases of pore pressure have triggered $m < 5$ seismicity that is located a few kilometers away from well activities. We have selected those cases of seismicity induced by fluid manipulations in the vicinity of oil/gas production sites that can be related to pure injection or pure extraction of fluid (Grasso 1993). When secondary recovery is performed using fluid injection on the periphery of the depleted reservoirs, mixed mechanisms generate fractures (e.g. Davis et al. 1988). In these cases, the estimates of the critical induced stress are not accurate, and we do not use this data.

Stress changes induced by perturbations of the loading system of the upper crust : it is worth mentioning the proposed relationships between some major earthquakes ($m \geq 6$) and hydrocarbon production sites. Both in California (McGarr 1991) and in Uzbekistan (Grasso,1993), major events can be related to upper crustal hydromechanical disturbances produced by subsurface fluid extraction from shallow geological formations. Despite the smaller fluid pressure changes observed on these sites compare to those previously described to trigger events by pore pressure effect, larger seismic response and greater distance to the reservoir are observed (McGarr, 1991; Grasso, 1993). The stimulated zones are deep fault zones buried under anticlines containing hydrocarbon reservoirs. Following McGarr's (1991) analysis that mass withdrawal at these sites is related to the major earthquakes sequences, we can obtain a rough estimate for each sequence stress change. We multiply the seismic stress drop by the ratio of the loading system stiffness (the vertical force change) to the stiffness of a circular crack model (Table 1b). Although less direct and reliable than the values extracted from the pore

pressure effects, these estimates suggest that earthquake faulting occurs under low shear stress perturbations (<1 MPa). Note that (Figure 1) for the $m \geq 6$ earthquakes that occurred in the Gasli field area, the orientations of the P-axes of maximum compression span nearly half (i.e. 90º) of their maximal range (180º). Such abnormal variations in orientation can either indicate a local stress anomaly induced by the hydrocarbon production or provide evidence for fluid contributions to fracturing, i.e. weak faults stimulated by hight fluid seals that decrease the apparent friction coefficient (Blanpied et al. 1992).

One may note that a critical mass of some 10^{11} kg (Table 1b) appears to be sufficient to induce the large thrust events in compressive setting. Such a value raises two remarks.

First, the same critical mass has been reached in other hydrocarbon fields where $S_1 \neq S_H$ and the poro-elastic response by itself had triggered only moderate seismicity ($m<5$) closed to the depleted reservoirs (e.g. Lacq field western pyrennees foreland; Groningen field northern Holland; Ekofisk field, central graben Norway, Table 1a). In agreement with admitted standard tectonic setting for the three areas given as examples (e.g. Zoback 1992), the lack of thrust faulting setting in these three regions has not permitted the generation of large seismic failures in response to mass withdrawal. In absence of thrust faulting, only the poroelastic stressing effect, which is independant of the preexisting tectonic stress, can induce earthquakes. On this basis, we propose that the comparison between seismicity triggered by poroelastic stress change and seismic response of the crust to mass transfer is a robust indicator of the local tectonic setting.

Second, the crude value of the critical mass withdrawal that induces thrust events is at the lower limit of the value of the increases in load that trigger fast normal faulting response to reservoir impoundment (Gupta and Rastogi, 1976; Simpson et al. 1988). Accordingly, normal faulting types of reservoir induced seismicity are also indicators that confirm the regional extension setting of the african midplate stress field (Kariba), the local extension state of deformation of different foot hills massifs (Sierra Nevada, Oroville; french subalpine massif, Monteynard) and the western anatolian stress province

(Kremasta). These earthquakes are the only four normal faulting type of the top nine $m>5.0$ RIS listed on Table 2. Note that in the Himalayan thrust region, load increase inhibits thrust earthquakes to occur. Accordingly numerous reservoir impoundements, for water height ≥ 100m, had not triggered fast seismic response within Himalayan areas (Gupta 1985). For the other fast seismic responses to reservoir impoundments, the observed reverse slip or strike slip events are associated to local increase pore pressure in undrained conditions that are independant of the tectonic setting, as well as the delayed response type observed for large Reservoir Induced Seismicity (Gupta and Rastogi, 1976; Simpson, 1976, 1986; Gupta, 1985). Whatever is the mechanism of pore pressure change (drained or undrained), the water height is the key paramater to bound the maximum stress changes. Despite a minimum 100 m water height which is admitted to be a critical threshold that triggers RIS (e.g. Rothé, 1970), there is no correlation between water height and the size of largest RIS (Figure 2). This observation and the unusually hight b-values reported for RIS (Gupta and Rastogi, 1976), i.e. larger number of small shocks in the frequency-magnitude diagram, support the hypothesis that the size of the Reservoir Induced Earthquakes is bounded by the size of seismogenic bed of the uppercrust. Accordingly, the largest Induced earthquakes must occur in an area where the largest seismogenic beds stand, i.e. shield area. This appears to be verified for the top four largest Induced Earthquakes that activates fault lengths larger than 10 km in midplate area (Gasli, Koyna, Hsingfenkiang, Kariba, Table 2).

Synthesis of the observations of induced seismicity : From the observed cases of induced seismicity and for the two proposed mechanisms, pore pressure effect and mass effect, it appears that small stress variations (1-2 MPa), trigger seismic failures in the upper crust in the vicinity of water reservoir impoundments and subsurface fluid manipulations (Table 1 and 2). Observations and models of these phenomena allow us to extend to general tectonic settings the determination of the critical stress threshold previously observed and modelled at tectonic plate boundaries. It is worth mentioning that small stress transfer (~0.1MPa) has been proposed to explain coseismic slip-

triggered or slip-locked by an earthquake on neighbouring faults (Jones et al. 1982; Simpson et al. 1988b) in area prone to failure, i.e. for natural activated seismicity. Recent models of coseismic after effects of Lander's California earthquake support that 0.1-1 MPa stress change affects seismicity 30-100 km away from the main ***m***~7.4 shock (Harris and Simpson 1992, Stein et al. 1992, Jaumé and Sykes, 1992). For the same distance range, regional effects of fluid manipulation are reported either to increase or to decrease the regional seismicity depending on the sign on the fluid pressure variations (Grasso et al. 1992a). Grasso et al. (1992a) use an analytical approach to calculate the poro-elastic stress change using the hydromechanical values measured on rock sample from deep borehole observations. Although the final numbers are somewhat model dependent, the effective stress variations range in all cases between 0.1-1 MPa. In the cases of induced seismic instabilities after the principal effect had locally moved the area to criticality, small variations in stresses (~0.1 MPA), related to variations either in surface water level storage (Figure 3) or in subsurface fluid pressure drop (Figure 4), control the on-going seismic slips occurring on pre-existing discontinuities. Thus in several areas, smooth and slow stress changes of at least one order of magnitude smaller than the triggering stress variation, sustain induced seismicity over months or years.

From seismic nests that are repetitively activated on volcanoes by moon tides (Rydeleck et al.1988), the minimum stress changes that induce seismicity can be estimated to a fews hundredth of MPa. Althought searches for RIS/tide correlation are weak, due to the poor number of data, tidal-stress triggering of RIS has been proposed as significant in a few sites (Klein, 1976). For the cases reviewed in our study, changes in stress of a few 0.1 MPa change previous risk assessment based on natural seismicity (e.g. northern Holland; Aquitaine bassin, France; SW India, SE China; western Uzbekistan, Grasso (1993)). Note that volcanic activity represents another class of induced seismicity which has been studied recently in the context of SOC (Diodati et al., in press; Sornette, 1992b).

INDUCED SEISMICITY AS A PROBE OF THE SELF-ORGANIZED CRITICAL STATE OF THE UPPERMOST CRUST

We now discuss how these observations enter into the framework of self-organized criticality. We first make this notion as precise as possible in the context of earthquakes and tectonic deformations of the brittle crust and then articulate the different data within this picture.

Self-organized criticality and induced seismicity. For the sake of clarity and precision, it is useful to restrict the term SOC to the class of phenomena occurring in continuously driven out-of-equilibrium systems made of many interactive components, which possess the two following fundamental properties : 1) a highly non-linear behavior, namely a *threshold* response and 2) a *very slow driving*. For the crust, the first ingredient corresponds to the rupture threshold for the rapid nucleation and growth of the dynamical rupture associated to an earthquake. The second ingredient reflects the slow tectonic driving force. The extreme separation of time scales between the driving tectonic velocity (cm/year) and the rupture front velocity (10^3 m/s) makes the crust problem maybe the best natural example of self-organized criticality, in this sense.

It is fundamental to realize that these two ingredients must come together. Let us imagine a system composed of elements with threshold dynamics but which is driven at a finite rate compared to the typical time scale of its response. In the earthquake problem, this would correspond to imagine plates moving at a velocity which is not much smaller than the brittle rupture velocity. In this case, the crust would rupture incessantly, with earthquakes which could not be individualized and which would create an average rapid flow deformation of the crust. The frequency size distribution would disappear and the system would not be in a SOC state. Artificial block-spring models of seismicity rapidly driven can be used to illustrate this idea (Burridge and Knopoff, 1967; Carlson et al., 1991). Alternatively, consider a system driven very slowly but with elements which do not possess a threshold but only a strong but continuous non-linear response. Due to the very slow driving implying a small increasing sollicitation, the system will respond

adiabatically without any interesting behavior such as earthquakes with brittle rupture ("slow" earthquake regime). Thus, it is the existence of the threshold that enables the system to accumulate the slowing increasing stress until the instability is reached and earthquakes are triggered. In turn, the slow driving permits a response which is uncoupled from the driving itself and reflects the "critical" organization of the crust.

It is important to realize that the nature of the criticality which organizes itself in this class of systems is fundamentally different from the standard criticality found in thermodynamics critical phase transitions. This remark is quite important in view of the common tendancy to amalgamate these different problems. Various numerical discrete toy models of the brittle crust organization, presenting these two basic ingredients (threshold and slow driving), have been proposed to illustrate and make progress in the theory of crust tectonic deformations and earthquakes (Bak and Tang, 1989; Zhang, 1990; Chen et al., 1991; Cowie et al., submitted) as well as in the understanding of the fundamentals of SOC.

In the standard thermodynamic critical phase transitions, the systems are submitted to rapidly fluctuating driving forces (the thermal fluctuations induced by the rapid motion of the atoms at a finite temperature) and respond very slowing on the approach to the critical point. This dynamical behavior, which is characteristic of the system reaching the critical point, is usually coined "critical slowing down". The slowing down of the response reflects the divergent growth of the correlation length which measures the size of the domains which behave progressively as single entities. Note that this behavior is in strong constrast with the very slow driving of tectonic crust and fast response of earthquakes. Furthermore, in standard thermodynamic critical transitions, the spatial correlation can progressively establish itself and grow from a nucleus until it invades the total system. This is a type of "local" growth of correlations by "proximity" effects which is also completely different from the nature of the spatial correlation which builds up in the crust. In this latter case, the spatial correlations between different parts of the system cannot emerge as a result of the growth of cooperativity from a localized region but emerge only as a global phenomenon, where no parts of the system can be

left out : it is by the repetitive action of earthquakes that the crust has globally organized itself into its present state. In other words, different portions of the crust become correlated at long distance by the action of earthquakes which progressively link the stress field in various parts of the crust. This is essentially the physical picture which emerges from various numerical and analytical studies of toy model of the crust (Bak and Tang, 1989; Zhang, 1990; Chen et al., 1991; Cowie et al., submitted).

As a consequence, one of the most relevant property of SOC systems is the delicate nature of the spatial correlation of the corresponding critical state. It is useful to be more precise, using the understanding brought by an exact solution of a simpler abelian version of sandpile models (Dhar, 1990). Dhar has shown that the critical state is not a single state but the union of a complete set of metastable states (analogous to the set of microstates which constitute a macrostate in statistical thermodynamics). In the earthquake language, these metastable states are visited when an earthquake is triggered, which changes the system from a metastable state to another one belonging to the whole critical set. In this framework, the frequency-magnitude earthquake Gutenberg-Richter distribution reflects somehow the hierarchical structure of the set of metastables states constituting the global critical state. An understanding of the critical state therefore needs a careful study of each of these metastable state. It has been shown (Dhar and Ramaswamy, 1989; Dhar, 1990) that the spatial correlation of the stress-stress fluctuations around the average stress is long range and decays as a power law, thus exhibiting the special nature of the organization of the stress field. A similar conclusion on the related strain field fluctuations has been obtained within a different mathematical formalism (Sornette and Virieux, 1992). It is therefore the delicate and subtle balance of stress fluctuations which controls the properties of the SOC state. In this context, it is important to realize that this does not imply that "the crust is almost everywhere on the verge of rupture", as often believed. Numerical simulations (Zhang, 1989) and analytical arguments (Pietronero et al., 1991) show that in discrete models made of interacting blocs carrying a continuous scalar stress variable, the average stress is around 0.6 times the threshold stress at rupture: this clearly shows that the model crust is far, on the

average, from rupture. However, it exhibits strong fluctuations such that a *finite* subset of space is very close to rupture. These facts are not in contradiction with SOC : the power law dependence of the Gutenberg-Richter frequency-magnitude relationship reflects the special spatial correlation between the stress field in different regions of the system. A very small perturbation will thus have a finite chance of triggering a local instability in a place where the stress was very close to the rupture threshold. This local rupture may then propagate and form a large event (earthquake), depending upon the local spatial correlation of the stress field, in a way similar to a branching domino cascade.

This is essentially the basic framework which allows us to rationalize the induced seismicity which has been reviewed in previous sections : not all parts of the crust but a substantial portion (whose precise quantification depends on the specificity of the model) may be brought to instability as a result of a very small perturbation. We thus view the phenomenon of induced seismicity as the signature of the self-organized critical state of the crust, and more precisely of the delicate spatial correlation of the stress field which characterizes its state. We also note that the observed large fluctuations in amplitude of stress perturbations (in the ratio 1 to 10 typically), which have been observed to trigger induced seismicity, can be naturally explained as resulting from the stress fluctuations within the crust around an average tectonic stress. On Figure 5, direct evidences for induced earthquake self-similarity are presented, this being an important criterion for the SOC hypothesis. From Mining Induced Seismicities, where induced seismic instabilites disappear the no-worked days (see for example Cook (1976)), we can estimate that the shortest time life for to activate SOC system by induced seismicity is a few tens of hours time duration.

Not all perturbations, even when strong, induce seismicity. For the same distance range, regional effects of fluid manipulation are reported either to increase or to decrease the regional seismicity depending on the sign on the fluid pressure variations (Grasso et al. 1992a). In the Himalayan thrust region, load increase inhibits thrust earthquakes to occur. Accordingly numerous reservoir impoundements, for water height $\geq$ 100m, had not triggered fast seismic response (Gupta 1985). This is not in

contradiction to the previous physical picture. Indeed, in order to induce seismicity, a perturbation must of the correct "sign" and of the correct tensorial nature. It is clear that the elastic effect induced by fluid loading will change the radius of the Mohr circle depending of the tectonic environment and modify the seismicity accordingly with respect to the Coulomb failure envelop: induced seismic activity in normal faulting area and triggered seismic quiescence in thrust faulting area (i.e. Bufe 1976; Jacob et al. 1979). In the toy models of SOC, this last situation corresponds to an effective deloading of the system. The example of the Himalayan thrust region illustrate the importance of the direction of the stress tensor perturbation in comparison with that of the natural stress field. Another vivid example is provided by the south american subduction belt for which no induced seismicity has been observed as a response to the fluid impoundments in a large number of reservoirs (Madariaga, pers. communication 1993). Here again, load increase inhibits thrust earthquakes to occur and stabilize the system.

Finally, we discuss the relationship between the SOC picture and the ubiquitous observation of seismic clustering. An illustrative example of interelation between geological structure, induced stress change and mechanical localization that trigger self-similarity of seismic activity is observed during the depletion of the Lacq gas field (Figure 6). The dynamics is thus of the SOC type on faults that localize seismic instabilities, i.e. nests of earthquakes. The remaining diffuse activity does not follow the same scaling law that the nest seismicity (Volant and Grasso 1993). We would like to make clear the notion that SOC is not incompatible with mechanical localization. In fact, the fractal fault patterns observed at the surface of the crust already offer an example of the self-similar organization of the crust at large times and long scales (Sornette et al., 1990; Davy et al., 1990; Sornette, 1991). However, seismic clustering and mechanical localization seem in contradiction with the idea that most parts of the crust can be brought to an active state, as observed in the examples of induced seismicity discussed above. The paradox cannot be resolved within the toy models of SOC discussed in the litterature.

However, a new model has recently been introduced, which can be used to understand and solve the paradox. The model is sufficiently simple to allow for a careful

analysis while being sufficiently rich to capture both the complexity of fault spatial structure localization and complex seismic activity (Miltenberger, Sornette and Vanneste, submitted; Cowie, Vanneste and Sornette, submitted; Sornette D., Cowie, Sornette A. and Vanneste, 1993). In its simplest version, it incorporates long-range scalar elasticity, a stress rupture criterion, a deloading associated with slip concurrent with the "earthquake" corresponding to the appearence of a dipole force (or double dipole in tensorial elasticity). The system is driven slowly at its boundaries at a finite strain rate. Furthermore, a small scale featureless uncorrelated heterogeneity is assumed : the system is divided into many (typically 10^2 by 10^2) elements whose stress thresholds are taken out of a distribution. Based on the detailled analysis of this simple 2D dynamical model of a tectonic plate, the interplay between the nonlinear chaotic dynamics of earthquake activity and the quenched featureless small-scale heterogeneity gives rise to the spontaneous formation of fractal fault structures by repeated earthquakes and an interesting spatio-temporal dynamics of earthquakes. It has been shown that fault localization can be mapped onto a minimal interface problem, which in 2D corresponds to the random directed polymer (RDP) problem. Individual faults are thus predicted and observed to be self-affine with a roughness exponent 2/3. The global fault network weighted by the local cumulative fault slips is found multifractal. This result allows to rationalize many reported fractal fault studies.

Basically, what happens in this model is that the earthquake dynamics "contracts" itself from the initial large space provided by the total system to a small subset, corresponding to the faults. On these faults, the earthquake frequency-magnitude distribution is well-described by the Gutenberg-Richter power law. The dynamics is thus of the SOC type on the fault structure. Elsewhere, essentially no activity is observed due to screening by the optimal fault structures. However, if we were to apply a local perturbation to such a screened zone, induced seismicity would appear for a quite small amplitude of the perturbation, due to the fact that the screening created by faults is small and that the stress field is not far from rupture in many other regions that on the fault systems. In other words, in this model, the geometry exemplified by the faults constitutes

a large exageration and amplification of small stress differences existing in the system. Therefore, other parts of the system which are quiescient can be easily brought into an active state by small local perturbations. A quantitative analysis of these aspects of the model response is left for a future work.

Finite size effects in induced seismicity. The size of the induced earthquakes, that occur in previously low seismic area, can be used to assess the size of intraplate seismicity that is otherwise difficult to predict using the poor historical seismicity in intraplate area. The largest induced events ($M_0 \geq 10^{18}$ N.m) triggered either by water reservoir impoundements or hydrocarbon recoveries are located where thick seismogenic beds are reported close to the surface, i.e. shield area for the top four induced events that occurred in low seismicity area: Gasli, central Asia; Hsinfengian, Southeast China; Kariba, Zambia-Zimbabwee; Koyna, SouthWest India. In other area of reported $m>3$ induced seismicity, the thickness of the larger brittle sedimentary bed (for seismicity induced by impoundment (RIS) or depletion of reservoir (EIS)) or the geomechanical setting (dimension of the mine pillars in the case of MIS) bounds the upper size of the earthquakes in agreement with the break in self-similarity (see Figure 7 for example on recurent break slope in self-similarity) . This could be checked more closely by analysis of the break slope in both b-values and fractal dimensions of induced earthquakes (Figure 6) as proposed by Volant and Grasso (1993). This characteristic dimension for the uppermost crust mimics the concept of characteristic dimension proposed for the whole brittle schizosphere by Scholz (1982) and observed as the upper boundary of different scaling laws (e.g. McGarr 1986, Shimazaki 1986, Pacheco et al. 1992). On others sites with induced seismicity, break of slopes in either b value or seismic moment release have been proposed to correlate with the local geomechanical setting (Figures 8 and 9). The concept of characteristic earthquakes has also been proposed by Jin and Aki (1989) to explain anomalies of b-value that are induced by a large number of earthquakes with the same size. Such subsets of characteristic dimensions would help in

determining locally the magnitude and depth of the possible shallow energy release, which occurrence is critical for damage estimates.

Concludind Remarks

Major reported cases of induced seismicity in various parts of the world have been reviewed. Earthquakes induced by human activity, in otherwise historically aseismic areas, occur in neighboring hydrocarbon fields that share the same extraction pattern, as shown by the following cases that we have studied more specifically, i.e. three Northern Holland fields, two fields located within the central north sea graben, two field in Aquitaine Bassin and two neighbouring field of South Texas (Grasso, 1993; Pennington et al. 1986). These studies provide direct evidences that both pore pressure changes ($\pm\Delta p$) and mass transfers ($\pm\Delta m$), corresponding to incremental deviatoric stresses of the order of 1 MPa regardless of the tectonic setting, trigger seismic instabilities in the uppermost crust with magnitude ranging from 3.0 to 7.0. Moreover, with stress steps of amplitude around 0.1 MPa, at least one order of magnitude smaller than the the trigger step, sustained induced seismic activity is often observed over long period of times.

We have shown of these observations provide a vivid confirmation that the crust is in a self-organized critical state, such that a finite fraction of the crust may be put out of a quiescent state in reponse to a perturbation, as a result of the subtle spatial correlations of the stress field which characterize the self-organized critical state. We have attempted to make clearer the notion of self-organized criticality and to solve some apparent contradictions between this concept and some observations. In particular, the importance of the sign and tensorial nature of the perturbation, in comparison to the local tectonic stress field, has been underlined. This allows us to explain why not any perturbation can induce seismicity, as a naive expectation would lead to believe on the basis of the study of scalar "sandpile" models of self-organized criticality.

We have also demonstrated that the thickness of the largest local seismogenic bed is the characteristic dimension of each self-organized critical system. This characteristic dimension mimics the effect that the schizosphere plays for tectonic

earthquakes (Scholz 1991). This dimension is defined by the break slope in self-similarity from small to moderate earthquakes. It ranges from the pillar size in MIS to thickness of britlle sedimentary beds in the vicinity of RIS and EIS. These dimensions control the size and the location of the shallow earthquakes which can be triggered. Thus, sedimentary basin with soft material which are prone to local destructive amplification of seismic waves are less strongly subject to shallow earthquake. Reversely, thick cratonic or shield area have localized the largest induced earthquakes ($m \geq 6$) and are candidate for future large shallow earthquakes. The identification and study of such isolated object within actual low seismicity area (e.g. intraplate area) helps both to estimate the size of largest possible earthquake and to understand the behavior of SOC systems, in particular in relation to the subtle spatial correlation of the stress field in the critical state. In terms of seismic risks, estimates of earthquake sizes, that use the characteristic dimension of local induce self-organized critical systems, are complementary to the analysis of Boatwright and Choy (1992) who focussed on acceleration source spectra of large cratonic earthquakes.

An important consequence of our study extended to the scale of the whole lithosphere is to focus attention on the large scale spatial correlation of the stress field. Indeed, relatively small stress changes may trigger seismic activity at large distances, a signature of the mechanical correlations over distance larger than hundred of kilometers (e.g. Sornette et al. 1990). The resulting seismic and aseismic instabilities correspond to the earthquake precusory phenomena and these instabilities have been used for several years in China and in the the former USSR to calibrate the preparation zone of the major shock (Dobrovolsky et al., 1979). Small stress changes, with the same amplitude range than the ones that sustain induce seismicity, can explain large distance anomalies in precusor phenomena to earthquakes associated to hydrological changes (e.g Roeloffs, 1989, Silver and Valette-Silver 1992) and electrical changes (e.g. Bernard 1992) and are now proposed to be driven by local fluid induced instabilities.

For most induced seismicity cases, seismicity occurs both in the pressure (or stress) diffusing front and behind the rising pore pressure (or stress). Only if the

distribution of preexisting local strenghs is narrow will there be a simple relationship between the movements of an isobaric front and the location of events near it (Byerlee and Lockner 1977; Krantz et al. 1990). Fractal spatial patterns of induced seismicity can thus help to determine the local distribution of geomechanic strengths in both magnitude and position and we intend to test this idea in the future, notably by a quantitative analysis of simple statistical physics models. We also note that not all deformations are by far uniquely associated to earthquakes and that aseismic instabilities (slow or quiet earthquakes) are a source of discrepency when comparing deformations that rely on the fractal geometry of faults and those estimated from the fractal geometry of earthquake sets. Earthquakes and faults are not uniquely associated in observations (see however Davy et al. (1990) for a first attempt to provide such a link). Monitoring induced seismicity provides a very important opportunity to observe and understand the nature of the crust organization, and to characterize the distribution of strengths within geological objects. In a way, induced seismicity provides a unique mechanism to "perturb" the system in a way similar to well-controlled systems in experimental laboratories, a method which always constitutes the best strategy to probe and study the system.

Acknowledgements: One of us (J.-R. G.) thank D. Simpson for discussions on RIS as well as A. McGarr and P. Volant for fruitful comments. P. Molnar and J.L. Chatelain and O. Coutant provided helpful comments on an earlier version of the manuscript. This study benefited from the open collaboration with petroleum compagnies: Cag, Elf, Nam, Petroland, Phillips, Shell provided geomechanical data of the fields studied in this work, but the opinions expressed in this study are the authors' own. This research was partially supported by the University Joseph Fourier, Grenoble, the Elf company under contract Risk re-assesment within the Lacq Industrial Facilities and the french DBT-INSU Instability Program.

REFERENCES

Bak P. and Tang C., Earthquakes as self-organised critical phenomenon, J. Geophys. Res., 94, 15635-15637, 1989.

Bak P., Tang C. and Weisenfeld K., Self-organised criticality : an explanation of 1/f noise, Phys. Rev A 38, 364-374, 1987.

Bernard P., Plausibility of long distance electrotelluric precursors to earthquakes. J. Geophys. Res., 97, 17531-17546, 1992.

Besrodny, E.M., The source mechanism of the Gazly earthquakes of 1976-1984, in Gazly earthquakes of 1976 and 1984, Tashkent, Fan, 94-105, 1986.

Blanpied M.L., Lockner, D.A. and J.D. Byerlee, An earthqauke mechanism based on rapid sealing of faults, nature,13 08 92, 1992.

Boatwright J. and G.L. Choy, Acceleration spectra anticipated fpr large earthquakes in NE north america,Bull. Seis. Soc. Am., 82, 660-682, 1992.

Bufe,C.G., The Anderson Reservoir seismic gap - Induced aseismicity? Engineering Geology, 10, 255-262, 1976.

Burridge, R. and Knopoff L., Model and theoretical seismicity, Bull. Seis. Soc. Am., 57, 341-371., 1967.

Byerlee, J. D., Frictionnal characteristics of granite under high confining pressure. J. Geophys. Res. 72, 3639-3648 1967.

Byerlee, J.D. and D. Lockner, Acoustic emision during fluid injection into rock.Paper presented at first Conference on acoustic emission/microseismic activity in geologic structures and materials,Penn. Stae Univ.,june 1975, eds, H.Hardy and F.W. Leighton, Aedermannsdorf, Switzerland; Trans. Tech. Publications, pp 87-98, 1977.

Calloi,P., Depanfilis, M., DiFilippo, D., Marcelli, L. and Spadea,M.C., Terremoti della val Padana del 15-16 Maggio 1951:Ann. Geofis., 9, 63-105 1956.

Carder, D.S., Seismic investigation in the boulder dam area, 1940-1945, and the influence of reservoir loading on earthquake activity, Bull. Seism. Soc. Am. 35, 175-192., 1945.

Carlson, J.M., J.S. Langer, B. Shaw and C. Tang, Intrinsic properties of the Burridge_Knopoff model of a fault, Physical Review A, 44, 884-897,1991.

Chen, K., Bak, P., and Okubov, S.P., Self-organized Criticality in Crack-propagation Model of Earthquakes, Phys. Rev., A43, 625-630, 1991.

Chung-Kang, S., Hou-Choun C., Li-Sheng, H., Tzu-Chiang, L., Cheng-Yung, Y. Ta-Chun, W. and L. Hsueh-hai,Earthquakes induced by the reservoir impounding and their effect on the Hsinfengkiang Dam, Sci Sin., 17, 239-272,1974.

Cook, N.G.W., Seismicity associated with Mining. Engineering Geology, 10, 99-122, 1976.

Costain, J. K., Bollinger, G. A., Speer, J. A., Hydroseismicity : a hypothesis for the role of water in the generation of intraplate seismicity. Seismol. Res. lett. 58, 41-63, 1987.

Cowie P., Vanneste C. and Sornette D., Statistical physics model of complex fault pattern organization and earthquake dynamics, J.Geophys.Res. submitted, 1993.

Davis, S.D. and W.D. Pennington, Induced seismic deformation in the Cogdell oil field of West Texas. Bull. Seis. Soc. Am., 79 1477-1494, 1989.

Davy, Ph., Sornette A. and D. Sornette, Some consequences of a proposed fractal nature of continental faulting, Nature, 348, 56-58, 1990.

Davy P., Sornette A. and Sornette D., Experimental discovery of scaling laws relating fractal dimensions and the length distribution exponent of fault systems, Geophys.Res.Lett.19 n°4, 361-364, 1992.

Deliac E.P. and N.C. Gay, The influence of stabiizing Pillars on seismicity and rockbursts at ERPM, in N.C. Gay and E.H. Wainwright (eds) Proceeding of the 1 Int. Congress on Rockburst and Seismicity in Mines, Johannesburg, 1982, SAIMM, Johannesburg, 1984.

Dhar D. and Ramaswamy R., Exactly Solved Model of Self-organized Critical Phenomena, Phys.Rev.Lett. 63, 1659-1662, 1989.

Dhar D., Phys.Rev.Lett. 64, 1613, 1990.

Dobrovolsky, I.P., Zubkov S.I. and V.I. Miachkin, Estimation of the size of the earthquake preparation zones, Pure Appl. Geophys.,117, 1025, 1979.

Evans D.G. and Steeples D. W., Microearthquakes near the Sleepy Hollow oil field, southwestern Nebraska, Bull. Seis. Soc. Am., 77,132-140, 1987.

Eyidogan, H., Nabelek J. and N. Toksoz,The Gazli, USSR, 19 march 1984 earthquake: the mechanism and tectonic implications, Bull. Seis. Soc. Am., 75, 661-675, 1985.

Fabre D., J.R. Grasso and Y. Orengo., Mechanical behaviour of deep rock core samples from a seismically active gas field, Pure Appl. Geophys., 137, 200-220, 1992.

Feignier, B.and Grasso J.R., Characteristics of seismic fractures as a function of geomechanical setting, Pure Appl. Geophys., 137, 175-199, 1992.

Fernandez, L.M., Seismic energy released by the deep mining operations in the Tranvaal and Orange Free State during 1971. S. Afr. Dep. Mines Geol. Survey, 1973.

Fletcher, J.B., A comparison between the tectonic stress measures in situ and stress parameters from induced seismicity at Monticelleo Reservoir, South Carolina, J. Geophys. Res, 87,6931-6944, 1982.

Fletcher, J.B. and L.R. Sykes, Earthquakes related to hydraulic mining and natural seismic activity in western New-York State, J. Geophys. Res., 82, 3767-3780, 1977.

Gough, D.I. and Gough W.I., Stress and deflection in the lithosphere near lake Kariba. Geophys. Journ. Roy. Astro. Soc., 21, 65-101, 1970.

Grasso, J.-R., Mechanics of seismic instabilities induced by the recovery of hydrocarbons, Special Issue Induced Seismicity, Pure Appl. Geophys., in press, 1993.

Grasso, J.R. and Wittlinger G., Ten years of seismic monitoring over a gas field area, Bull. Seism. Soc. Am.,80, 450-473, 1990.

Grasso, J.-R. and Feignier B., Seismicity induced by gas depletion: II Lithology correlated events, induced stresses and deformations, Pure Appl. Geophys,134, 427-450.32, 1990.

Grasso, J.-R., Gratier J.-P., Gamond J.F. and J.-C. Paumier, Stress diffusion triggering of earthquakes in the upper crust., Special Issue Mechanical Instabilities In Rocks and Tectonics, Journ. Struc. Geol., 14, 915-924, 1992a..

Grasso, J-R., D. Fourmaintraux et V. Maury,Le role des fluides dans les instabilités de la croute supérieure: L'exemple des exploitations d'hydrocarbures, Bull., Soc. Geol. France, 163, 27-36, 1992b.

Grasso, J.-R., Guyoton F., J. Frechet and J.F. Gamond, Triggered earthquakes as stress gauges: Implication for risk re-assessment in the Grenoble area, France, Special Issue Induced Seismicity, Pure Appl. Geophys., in press, 1993.

Gupta, H.K. and Rastogi B.K., Dams and earthquakes, 229 pp., Amsterdam, Elsevier, 1976.

Gupta, H.K., The present status of Reservoir induced seismicity: investigations with a special emphasis on Koyna earthquakes, Tectonophysices,118, 257-279, 1985.

Guyoton,F., Grasso, J.R. and P. Volant, Interrelation between induced seismic instabilities and complex geological structure, Geophys. Res. Lets., 19, 7, 1992.

Haak H.W., Seismiche Analyse van de Aardbeving bij Emmen op 15 februari 1991, Koninklijk Nederlands Meteorologisch Instituut eds., Ministerie van Verkeer en Waterstaat, 14 pp., 1991.

Haimson B.C. and C. Faihrhurst, Insitu stress determination at great depth by means of hydraulic fracturing, Proc. U.S. Symp. Rock Mech., 11th, 559-584, 1970.

Harris R.A. and Simpson R.W., Changes in static stress on southern California faults after the 1992 Landers earthquake.Nature, 360,251-254, 1992.

Healy, J.H., Rubey W.W., Griggs D.T. and Raleigh C.B., The Denver earthquakes, Science, vol. 161, 1301-1310, 1968.

Hsieh P. A. and J.D. Bredehoeft, Reservoir analysis of the Denver earthquakes. The case of induced seismicity. Journ. Geophs. Res., 86, 903-920, 1981.

Jacob, K.H., Armbuster, J., Seeber, L. and W Pennington, Tarbela reservoir, Pakistan: aregion of compressionnal tectonics with reduced seismicity upon initial reservoir filling, Bull.. Seis. Soc. Am., 69, 1175-1182, 1979.

Jaumé S.C. and Sykes L.R., Changes in state of stress on the southern San Andreas fault resulting from the california earthquake sequence of April to June 1992, Science, 2581325-1328, 1992.

Johnston, A.C., Suppression of earthquakes by large continental ice sheets, Nature, 330,467-469, 1987.

Johnston, A.C., The seismicity of "stable continental interiors", in Earthquakes at north atlantic passive margins: Neotectonics and post glacial rebound, S. Gregersen and P.W. Basham (eds), Kluwer, Dordrecht, The netherlands, 740 pp., 1989.

Jones L.M., Wang B., Xu S. and T. J. Fitch , Journ. Geophys. Res., 87, 4575-4584, 1982.

Krantz R.L., T. Satoh, O. Nishizawa, K. Kusunose, M. Takahashi, K.Masuda and A. Hirata, Laboratory study of fluid pressure diffusion in rock using acoustic emission. J. Geophys. Res., 95, 21593-21607, 1990.

Klein F.D., Tidal triggering of reservoir-associated earthquakes. Engineering Geology,10, 197-210, 1976.

Kusznir N.J. and N.H. Al-Saigh, Some observation on the influence of pillars in Mining-Induced-seismicty, in N.C. Gay and E.H. Wainwright (eds) Proceeding of the 1 Int. Congress on Rockburst and Seismicity in Mines, Johannesburg, 1982, SAIMM, Johannesburg, 1984.

Lukk A.A. and S.L. Yunga, In "Geodynamics and stress strain state of the lithosphere of the Central Asia., Ed. Donish, Duschambe, 1988.

MacGarr, A., Seismic moments and volume changes. J. Geophys. Res., 81,1487-1494, 1976.

McGarr, A., Some observations indicating complications in the nature of earthquake scaling, in S.Das, J. Boatwight and C. Scholtz (eds), Earthquake source mechanics, A.G.U. Geophysical Monograph 37, whasshington D.C., A.G.U., 217-225, 1986.

MacGarr, A., On a possible connexion between three major earthquakes in california and oil production. Bull. Seis. Soc. Am, 81, 948-970, 1991.

McGarr A., S.M. Spottiswoode, N.C. Gay and W.D. Ortlepp, Observations relevant to seismic driving stress, stress drops and efficeincy, J. Geophys. Res., 84, 2251-2261, 1979.

McGarr A., Green, R.W.E and S.M. Spottiswoode, Strong ground motion of mines tremors: some implication for near source ground motion parameters, Bull. Seis. Soc. Am., 71, 295-309, 1981.

Nason R.D., Copper A.K., and Tocher D., Slippage on the Buena Vista thrust fault, 43rd annual meeting guidebook, AAPG, SEG, SEPM. Am. Ass. of Pet. Geol., Pac. Sect., 100-101, 1968.

Nicholson, C., Roeloffs, E. and R.L. Wesson, The northeastern Ohio earthquake of 31 january 1986 : Was it induced? Bull. Seis. Soc. Am., 78, 188-217, 1988.

Nicholson, C., Earthaquakes induced by deep well activity, Special Issue Induced Seismicity, Pure Appl. Geophys., in press, 1993.

Nur, A., Dilatancy, pore fluids, and premonitory variation of ts/tp travel times. Bull. Seim. Soc. Am. 62, 1217-1222, 1972.

Pacheco J.F., Scholtz C.H., and L.R. Sykes, Changes in frequancy-size relationship from small to large earthquake, Nature ,355, 71-73, 1992.

Pennington D.W, Davis S.D, Carlson S M, Dupree J. and Ewing T.E., The evolution of seismics barriers and asperities caused by the depressuring of fault planes in oil and gas fields of south Texas, Bull. Seismol. Soc. Am., 939-948, 1986.

Pietronero L., Tartaglia P., and Zhang Y.C., Physica, 173,22, 1991.

Plichon, J.N., Gevin P., Hoang P., Londe P. and P. PettervilleQ 51 R. 30, Sismicité des retenues de grands barrages, *Proceeding of the 13th Int.Comm. Of Large Dams Congress,* New-Delhi, I. C. O. L. D. editor,151, Bd Haussmann, Paris, vol. 2 ,1347-1362, 1979.

Pomeroy P.W., D.W.Simpson and M.L. Sbar, Earthquakes triggered by syrface quarrying: The Wappingers Falls, New-York, sequnece of June 1974, Bull. SEis. Soc. Am., 66, 685-700, 1976.

Raleigh, C.B., Healy J.H. and Bredehoeft J.D., Faulting and Crustal stress at Rangely, Colorado, A.G.U., Geophysical Monograph 16, 275-284, 1972..

Roeloffs, E., Fault stability changes induced beneath a reservoir with cyclic variations in water level. J. Geophys. Res. 93,2107-2124, 1988.

Roeloffs, E., Hydrologic precursors to earthquakes: areview, Pure Appl. Geophys., 126, 177-209, 1989.

Rothé J.P., Séismes artificiels (man-made earthquakes). Tectonophysics, 9, 215-238, 1970.

Rydelek, P.A., P.M. Davis and R. Koyanagi, Tidal triggering of earthquake swarms at Kilauea volcano, Hawaii, Jour. Geophys. Res.,93, 4401-4411, 1988.

Segall, P., Earthquakes triggered by fluid extraction. Geology, 17, 942-946, 1989.

Segall, P. and J.-.R Grasso, Poroelastic stressing and induced seismicity near the Lacq gas field (France). Eos transactions, Am. Geophys. Union,72, 44, 293, 1991.

Sibson R.H., High-angle reverse faulting in northern New-Brunswick, canada, and its implication for fluid pressure levels. Jour. Struc. Geol. 11, 873-877, 1989.

Silver P.G. and Valette-Silver N.J., Detection of hydrothermal precursors to large california earthquakes. Science, 257, 1363-1368, 1992.

Simpson D.W., Reservoir Induced Sesismicity, Engineering Geology, 10, 87-110, 1976..

Simpson D.W., Triggered earthquakes. Ann. Rev. Eath Planet. Sci., 14, 21-4, 1986.

Simpson and Negmatullaev S.K., Induced seismicity at Nurek reservoir, Tajikistan. USSR. Bull. Seis. Soc. Am.,71, 1561-1586, 1981.

Simpson D. W. and Leith W., The 1976 and 1984 Gazli, USSR, earthquakes - Were they induced ?, Bull. Seismol. Soc. Am.,75, 1465-1468, 1985.

Simpson D. W., Leith W. S. and Scholz C. H., Two types of reservoir-induced seismicity, Bull. Seismol. Soc. Am., 78, 2025-2040, 1988a.

Simpson, R.W., Schulz, S.S., Dietz, L.D. and Budford R.O., The response of creeping parts of the San Andreas fault to earthquakes on nearby faults: two examples. Pure and Applied Geophys., 126, 665-685, 1988b.

Sornette A. and Sornette D., Self-Organized criticality and earthquakes, Europhys. Lett, 9, 197-202, 1989.

Sornette, D., Davy P. and Sornette A., Structuration of the lithosphere in plate tectonics as a Self-Organized Critical phenomena. Jour. Geophys. Res., 95, 17353-17361, 1990.

Sornette D. and Davy P., Fault growth model and the universal fault length distribution, Geophys.Res.Lett. 18, 1079-1081, 1991.

Sornette D., Self-organized criticality in plate tectonics, in the proceedings of the NATO ASI "Spontaneous formation of space-time structures and criticality", Geilo, Norway 2-12 april 1991, edited by T. Riste and D. Sherrington, Kluwer Academic Press, p.57-106, 1991.

Sornette D. and Virieux J., A theory linking large time tectonics and short time deformations of the lithosphere, Nature 357, 401-403, 1992..

Sornette D., Volcanic tremors given mathematical foundation, Physics World, January 1992, p.23-24, 1992a.

Sornette D., Self-organized criticality, earthquakes and plate tectonics, Phys.Rev.Lett. 69, 1287, 1992b.

Scholtz C.H., Scaling laws for large earthquakes: consequences for physical models, Bull. Seis. Soc. Am. 72, 1-14, 1982.

Scholtz C.H., Earthquakes and Faulting: self-organized critical phenomena with characteristic dimension.; in Triste and D. Sherrington (eds), Spontaneous formation of space-time structures and criticality,Kluwer Academic Publishers, Netherlands, 41-56, 1991.

Shimazaki, K., Small and largeearthquakes:the effects of the thickness of the seismogenic layer and the free surface, in S.Das, J. Boatwight and C. Scholtz (eds), Earthquake source mechanics, A.G.U. Geophysical Monograph 37, whasshington D.C., A.G.U., 209-216, 1986.

Spottiswoode S.M., Source mechanism of mine tremors at Blyvooruitzicht gold mine. In N.C. Gay and E.H. Wainwright (eds) Proceeding of the 1 Int. Congress on Rockburst and Seismicity in Mines, Johannesburg, 1982, SAIMM, Johannesburg, 1984, pp 29-37, 1984.

Spottiswoode S.M. and A. McGarr, Source parameters of tremors in a deep-level gold mine. Bull. Seis. Soc. Am.,65, 93-112, 1975.

Stein S., Sleep, N.H., Geller R.J., Wang, S.C. and G.C. Kroeger, Earthquakes along the passive margin of eastern canada, Geophys. Res. Lett., 6, 537-540, 1979.

Stein R.S., King, G.C.P. and Lin J., Chnage in failure stress on the southern san andreas fault system caused by the 1992 M=7.4 Landers earthquake, Science, 255, 1687-1690, 1992.

Volant P. and Grasso, J.R., Interrelation between fractal dimension, b-value and the geomehanical setting of shallow earthquakes. Paper presented at EGS meeting, Wiesbaden, May 2-5, 1993.

Volant P., Grasso, J.R., Chatelain, J.C. and M. Frogneux, b-value, aseismic deformation and brittle failure within an isolated object: evidences from a dome structure loaded by fluid extraction, Geophys. Res. Letters, 19, 1149-1152, 1992.

Wetmiller R.J., Earthquakes near Rocky Mountain House, Alberta, and relationship to gas production. Can. Journ. of Earth Sciences, 32, 2,172-181, 1986.

Wyss M. and P. Molnar, Efficiency, stress drops, effective stress and frictinal stress of Denver (USA) earthqaukes, J. Geophys. Res., 77, 1433-1438, 1972.

Yerkes R.F., Ellsworth,W.L. and J.C. Tinsley. Triggered reverse fault and earthquake due to crustal unloading, northwest Tranverse ranges, California, Geology,11, 287-291.

Zhang Y.-C., Phys.Rev.Lett. 59, 2125, 1987.

Zhang Y.-C., Scaling Theiry of Self-organized Criticality, Phys. Rev. Lett., 63, 470-473, 1989

Zoback M.D. and B.C. Haimson, Hydraulic fracturing stress measurements, US. National Comittee for Rock Mecahnics, National Academic press, Washington D.C., 270 pp., 1983.

Zoback, M. D.and Zoback, M., State of stress in the conterminous United States. J. Geophys. Res. 85, 6113-6156, 1980.

Zoback M.L., First- and second-order patterns odf stress in the lithosphere: The world stress map project, J. Geophys. Res., 97, 11703-11728, 1992.

Figure Captions

Figure 1 : Major seismic events in Gasli area (Uzbekistan), $m \geq 7$ except for 1978 : $m = 5.9$. Black ellipses indicate positions and estimated size of seismic events determined by seismic analysis (Eydogan et al. 1985 and levelling data (Grasso 1993). Black lines that schematize local directions of the major compressionnal axis inferred from earthquakes, diverge from regional NW-SE orientation as determined by Lukk and Yunga, 1988.

Figure 2 : Size of Induced Earthquakes as a function of water height of the reservoir.Data are $m \geq 2.5$ RIS from Table 1 of Gupta (1985)

Figure 3 : Self Organized Critical systems induced by reservoir impoundments.

-a) Monticello reservoir, USA; number of events per day and cumulative number of events versus lake level (adapted from Talwani et al. 1979; Flecher 1982).

-b) Lake Mead, Hoover dam, USA; water level (curve) versus monthly frequency of earthquakes (vertical bars); adapted from Roeloffs (1988). The m~5 largest earthquake occurs in 1939. Data from Carder (1970).

-c) Nurek reservoir, Tadjikistan; same as (b) except that the number of $m \geq 1.5$ earthquakes are monthly reported. The two m~4.5 largest earthquake occur in 1972. (from Simpson and Negmatullaev (1981).

-d) Koyna, India; same as (b).The m~6.2 largest earthquake occur in 1967. The second largest earthquake, m~5.2 occur in 1973 when the water level was allowed to increase for 1 meter beyond the1967 maximun, (from Simpson et al. 1988).

-e) Monteynard reservoir, France; same as (b) except that the number of $m \geq 3.5$ earthquakes are monthly reported. The m~5.3 largest earthquake occur in 1962. The second largest earthquakes, m~4.5 occur in 1963 and 1979. The 1979 water level exceed that in 1963 by less than one meter, (from Grasso et al. 1993).

The time duration of ISOC systems ranges from few months after the maximun water level had been reached at Monticello (a) to tens of years at Lake Mead (b). For the above RIS cases the earthquake donot move with an elevated isobaric front. Because local in-situ strenghs have unkown magnitude and spatiall distribution, events occur both along and behind the preceding lower front pressure. For cases (c), (d), (e), the latest seismic energy released are within 10 km distance from the reservoir. The stress change can be read by transforming the water height to pressure i.e. 100 m ~ 1 MPa.

Figure 4 : Self-Organized Critical systems induced by subsurface reservoir depletions .

-a) Strachan field, Canada; number of earthquakes recorded per years and decline in average gas reservoir pressure, adapted from Segall (1989). The m~4 largest earthquake occurs in 1974. Data from Wetmiller (1986).

-b) Lacq field, France; number of m≥3.0 earthquakes recorded per years and decline in average gas reservoir pressure. The m~4.2 largest earthquake occurs in 1981; adapted from Grasso and Wittlinger (1990).

-c) Ekofisk field, Norway; number of m≥2.5 earthquakes recorded per years and decline in average gas reservoir pressure. The m~3.8 largest earthquake occurs in 1988.Pressure data from Phillips (perso. communication 1992).

-d) Assen field, Northern Holland; number of m≥2.5 earthquakes recorded per years and decline in average gas reservoir pressure. The m~2.8 largest earthquake occurs in 1986. Data for earthquakes (Haak 1991).

-e) Fashing field, Souththern Texas; number of m≥2 earthquakes recorded per years and decline in average gas reservoir pressure. The m~3.4 largest earthquake occurs in 1983. Data from Pennington et al (1986).

-f) Imogene field, Souththern Texas; number of m≥2 earthquakes recorded per years and decline in average gas reservoir pressure. The m~3.9 largest earthquake occurs in 1984. Data from Pennington et al (1986).

The induced stress ((a) to (f)) at a time t, is roughly related to the gas reservoir pressure as follow (see text for details):

$\Delta\sigma \sim 3\ 10^{-3}\ (P_{init}-P_t)$.

Note that if seismicity emerge with $\Delta\sigma$~1 MPa for all the case-studies, it is further sustained by $P_{init}-P_t \leq 10$ MPa, i.e. $\Delta\sigma \leq 0.1$ MPa.

Figure 5 : Example of power law size distribution relation for Induced earthquakes.

-a) Mining Induced Seismicity, South Africa gold mines. Seismic moment as a function of corner frequency for mines earthquakes in South Africa. Data from Spottiswoode and McGarr (1975) - Circles, McGarr et al. (1981) - Diamonds, and Spottiswoode (1984) - squares. Adapted from Spottiswoode (1984).

-b) Fluid Extraction Induced Seismicity, Lacq gas field, France. Seismic moment as a function of source radii. Source radii is calculated using the a rupture velocity of 0.9β, R=0.32β /f0. From Feignier and Grasso (1992).

-c) Reservoir Induced Seismicity at Oroville reservoir USA. Peak-velocity parameter (Rv) as a function of seismic moment. Note that Rv scale to source radii for constant stress-drop scaling, i.e. $Rv \sim M_0^{1/3}$. Adapted from McGarr (1986).

Figure 6 : Characteristic dimension of ISOC systems.

a) Frequency-size relation ship for Induced earthquakes in the vicinity of Lacq gas field.

b) fractal dimension of the same data set. adapted from (Volant and Grasso 1993).

c) geomechanical cross section of the local structure where deep brittle calcareous beds (E=50 GPa , σc= 100 MPa) and ductile marly beds (E= 30 GPa, σc= 70 MPa) are reported. Mechanical properties are from Fabre et al. 1992.

Note the correlation between the break slope point in both b value and fractal dimension at a common 500 m distances (m~3) that is roughly the thickness of seismogenic beds.

Figure 7 : Time duration of Self-Organized Critical systems induced by subsurface Mining Example of a South Africa gold mine and constant break slope in self-similarity (adapted from McGarr 1976).

Figure 8 : Characteristic dimension of ISOC systems: Minig Induced Seismcity.

a) Break slope in b value reported in Coal Mining Induced seismicity, data from Kusznir and Al-Saigh (1984).

b) Break slope in b value reported in Gold Mine Induced Seismicity from underground seismic observations, (data from Deliac and Gay (1984)).

Figure 9 : Characteristic dimension of ISOC systems: Reservoir Induced Seismcity.

a) Break slope in b value reported in RIS, Monteynard Reservoir, France. Data (squares) are from the seismic station that operated within the dam during the 12/1963-12/1967 period. Note that both the m=4.3 shock that occur in August 1966 and the sequence of 3 m≥4 earthquakes that occured in the April 25-27 1963 period are shifted relatively to the number the small shocks (3.1≥m≥1). All the earthquakes are within 7 km distance from the reservoir (data from Plichon et al. 1979).

b) Number of events having an average normalized peak amplitude greater than A (in units of mV/mm) before and after borehole pressurisation in rock sample experiments. (from Krantz et al.1990)

c) geological cross section of the local structure where brittle calcaerous beds and ductile marly beds (Vm and TN levels) are reported. The main shocks and their focal mechanisms are plotted. Adapted from Grasso et al. (1992).

Note that the observed pattern on frequency - size relationship of Monteynard earthquakes (a) mimics the laboratory observations (b) of Krantz et al. (1990). Accordingly the low number of large earthquakes in the 12/1963-12/1967 period could correspond to fractures within a non fluid-pressured area whereas the m≥4 shocks could be a direct effect of pore pressure-induced seismicity.

Table 1 :

a) Mechanical constant used to estimated the poro-elastic stress change that triggered seismicity in the neighboring of hydrocarbon extraction. Column 1-4 are the reservoir characteristic used (depth (D), thickness (T), shear modulus (μ) and Poisson coefficient (ν). Column 5 is the maximum depth of the subsidence bowl at the onset of the seismicity. Initial reservoir pressure and pressure drop at the onset of seismicity are reported on column 6 and 7. Column 8 and 9 are respectively the onset of production and the onset of seismicity. Column 10 is the maximun magnitude reported of the field. The maximum

induced stress at the onset of the seismicity is estimated using poroelastic stressing in Column 11. Exponant [1] indicates that the subsidence and shear modulus of the rocks involved are known and we used the equation (1) in order to estimate $\Delta\sigma max \approx (4\mu/(1-\nu)\pi D) \times \Delta H max$, where μ, ν, D, $H max$, are respectively the shear modulus, the poisson coefficient of the rock matrix, the depth of reservoir and the maximum depth of the subsidence bowl. When subsidence value or rock properties are not reported (exponant [2]) we estimated $\Delta\sigma max$ using equation (2); $\Delta\sigma max \approx ((1-2\nu)/2\pi(1-\nu)) \times \Delta p \times F max(a/D)$, where Δp, $F max(a/D)$ are respectively the reservoir pressure drop and a dimensionless function of position and reservoir geometry, a, reservoir radius, D, reservoir depth, see text for details. Note that for the all reservoirs the poroelastic stress change is one order of magnitude larger than the vertical stress change induced by mass discharge , $-\Delta mg/A$; A being the effective reservoir area. Modified from Grasso (1993).

b) Hydromechanical Hydromechanical setting of earthquakes triggered by unloading of the uppercrust causes by hydrocarbon extraction. Column 2 is the year when extraction began and the date of the first induced event. Column 5 is the size of the largest induced event. Mass deficit is reported on column 4. Assuming that mass withdrawal at these sites is related to the major earthquake, we estimate the induced stress augmenting failure by multiplilying the earthquake stress drop by the ratio of stiffness of the loading system (the vertical force change) to the stiffness of circular crack model according to McGarr (1991). Note that the initial pressures of the reservoirs induce poro-elastic stress changes that are one order of magnitude less than the stress change induced by mass removal. For the Coalinga field, the poroelastic stress change and the stress change due to unloading have a value of the same magnitude order at the hypocentral depth of the mainshock (Segall, 1985; McGarr 1991).

Table 2 : M>5 induced earthqukes. For each events the pressure change and the mass change at noted. Pressure data are respectively the maximum water heigths for Reservoir induced Seismicity (RIS), the hydrocarbon pressure change for Extraction induced Seismicity (EIS). $\sigma 1$ orientation are estimated from focal mechanisms of induced earthquakes; for tectonic setting see e.g. Zoback 1992.

Area or field	reservoir characteristic used				Subsi.	Pressure		Onset of	Maximum	Induced Stress	Mass	Reservoir	Vertical stress
	D km	T km	μ GPa	ν	max.[e] m	Init. MPa	Change MPa	Prod-eqs years	Magnitude *m*	(Poro-elastic) MPa	Change 10^{11} kg	Area km^2	change (Unloading MPa
Strachan field[o] Alberta, Canada	3-5	0.1	-	-	-	50	-25	1971-1976	3.4	≤0.7 MPa[2]	0.18	25	0.007
Fashing field[a] Texas, USA	3.4	0.03	-	-	-	35	-23	1958-1974	3.4	≤0.7 MPa[2]	<0.1	10	<0.01
Imogene field[a] Texas, USA	2.4	0.03	-	-	-	25	-13	1938-1973	3.9	≤0.4 MPa[2]	<0.1	20	<0.005
Lacq field[b] Aquitaine, France	3-6	0.25	23	0.25	.005	66	-30	1959-1969	4.2	≤0.5 MPa[1]	2.0	150	0.01
Grozny field[c] Tchetcheny,Caucasus	4-5	0.67	-	-	-	69	-25	1964-1971	4.1	≤0.7 MPa[2]	1.5	70	0.02
Assen field[d] Netherland	3.0	0.1	10	0.25	-	30	-25	1972-1986	2.8	≤0.7 MPa[1]	<0.1	50	0.002
Groningen field[d] Netherland	2.9	0.2	10	0.26	0.16	35	-30	1964-1991	2.5	≤0.4 MPa[1]	9.0	900	0.01
Ekofisk field[e] Offshore, Norway	3-5	0.2	0.07	0.30	3.50	48	-24	1973-1982	3.4	≤0.4 MPa[1]	0.2	130	0.002
Dan[f] Offshore, Danemark	1.8	0.15	0.30	-	-	26	-18	1972-1985	4.0	≤0.45 MPa[1]	<0.1	24	0.004

[o] from Wetmiller 1986; [a] from Pennington et al 1986; [b] from Grasso and Wittlinger (1990); [c] from Smirnova(1976);
[d] data from Price et al.(1990) and Netherland Induced Seismicity commission (pers. commun. 1992); [e] data from Teufel et al. (1991) and from Phillips (pers. commun. 1992); reservoir characteristics from Conlin et al. (1990);

TABLE 1a

Area or field	Reservoir Depth km	Reservoir Area km^2	Onset of Prod.- Eqs. years	Initial Pressure MPa	Mass Removal 10^{11}kg	Eqs Size Magnitude *m-Mo*(mN)	Induced Stress (Unloading) MPa	Vertical stress change (Unloading) MPa
Caviaga field[g] Po valley, Italy	1.5		19..-1951	13	-	5.5 - 10^{17}	-	-
Coalinga field[h] California, USA	2	110	1940-1983	25	2.7	6.5- 4.10^{18}	0.01 MPa	0.024
Kettleman field[h] California, USA	1.5	50	19..-1985	-	1.2	6.1- 2.10^{18}	0.01 MPa	0.024
Montebello field[h] California, USA	1.5	6	1924-1987	-	1.3	5.9 -1.10^{18}	0.01 MPa	0.21
Gazli field[i] Kyzyl-Koum, Uzbekistan	1.5	300	1962-1976	10	1.9	7.0 -2.10^{19}	0.04 MPa	0.006
Gazli field[i] Kyzyl-Koum, Uzbekistan	1.5	300	1976-1984	3	1.8	7.0 -2.10^{19}	0.05 MPa	0.006

[g] data from Caloi et al. (1956); [h] data from McGarr (1991); [i] from Grasso (1993);

TABLE 1b

Table 2: M > 5.0 induced earthquakes

Dam/reservoir or hydrocarbon field	ΔP (MPa)	ΔM (10^{11}kg)	Maximum Magnitude	Regional seismicity	σ1 orientation (from induced eqs) and Tectonic setting.
Gazli field, EIS Uzbekistan	≤0.	-2.	M=7.3	low	Horizontal - Midplate,
Koyna, RIS India	+1.	+27.	M=6.5	low	Horizontal - Midplate,
Coalinga field, EIS USA	≤0.	-2.7	M=6.5	high	Horizontal - Plate boundary
Kremasta[D], RIS Greece	+1.6	+47.	M=6.3	high	Vertical - Back arc extension
Hsinfengkiang, RIS China	+1.	+1.0 10^{2}	M=6.1	low	Horizontal - midplate
Kettleman field, EIS USA	≤0.	-1.2	M=6.1	high	Horizontal - Plate boundary
Montebello field, EIS USA	≤0.	-1.3	M=5.9	high	Horizontal - Plate boundary
Oroville, RIS USA	+2.4	+43	M=5.9	low	Vertical - Sierra Nevada foothills
Kariba, RIS Zambia/Zimbabwee	+1.3	+1.7 10^{3}	M=5.8	low	Vertical - Midplate
Marathon[D], RIS Greece	+0.7	+0.4	M=5.7	high	n.a - Plate boundary
Aswan[D], RIS Egypt	+1.1	+1.6 10^{3}	M=5.5	low	Vertical - Midplate
Eucumbene, RIS Australia	+1.1	+4?	M=5.5	low	n.a - Midplate
Hoover, RIS USA	+2.2~	+3.7 10^{2}	M=5.5	low	Vertical - Colorado plateau
Denver, IIS USA	+3.5*	+10^{-3}	M=5.5	low	Vertical - Colorado plateau
Caviaga, EIS Italy	≤0.	-??	M=5.5	low	Horizontal - midplate
Lake County, IIS USA	+0.5**	-0.	M=5.3	low	Horizontal - midplate
Monteynard, RIS France	+1.3	+2.7	M=5.3	low	Vertical - Alps foothills
El Reno, EIS USA	≤0.	-??	M=5.2	low	Horizontal - midplate
Snipe Lake, EIS Canada	≤0.	-??	M=5.1	low	Horizontal - midplate

n.a., no-available information;
RIS, EIS and IIS are respectively reservoir, extraction and injection induced seismicity.
see references for RIS, EIS and IIS, respectively within Gupta 1985, Grasso 1993 and Nicholson 1993;
D Disagree with decision diagramm for Corps of Engineers study of RIS (Meade, 1990);
* Modeled fluid pressure increase (Hsieh and Brehoeft, 1981);
** Modeled fluid pressure increase (Nicholson et al. 1988);

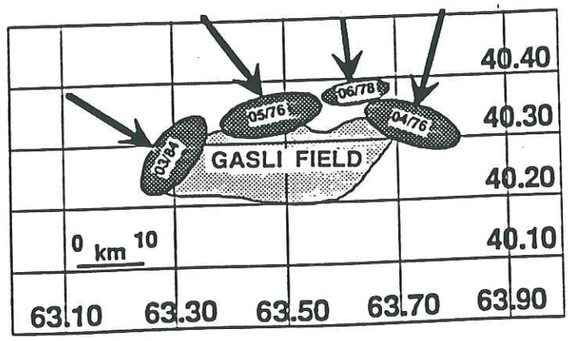
40.40
40.30
40.20
40.10
03/84
05/76
06/78
04/76
GASLI FIELD
0 km 10
63.10
63.30
63.50
63.70
63.90

Fig 1

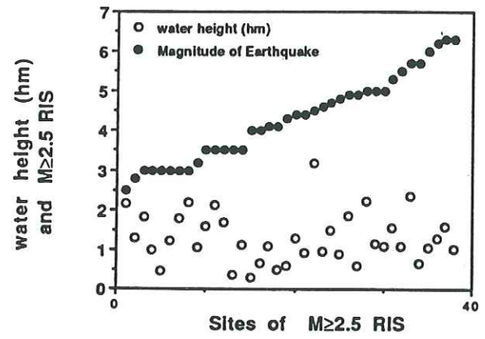
water height (hm)
Magnitude of Earthquake
water height (hm) and M≥2.5 RIS
Sites of M≥2.5 RIS
0
1
2
3
4
5
6
7
40

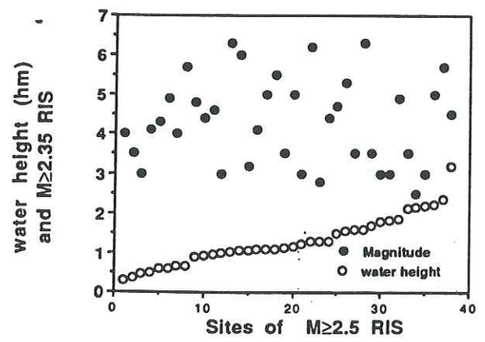
water height (hm) and M≥2.35 RIS
Magnitude
water height
Sites of M≥2.5 RIS
0
1
2
3
4
5
6
7
10
20
30
40

Fig 2

a)

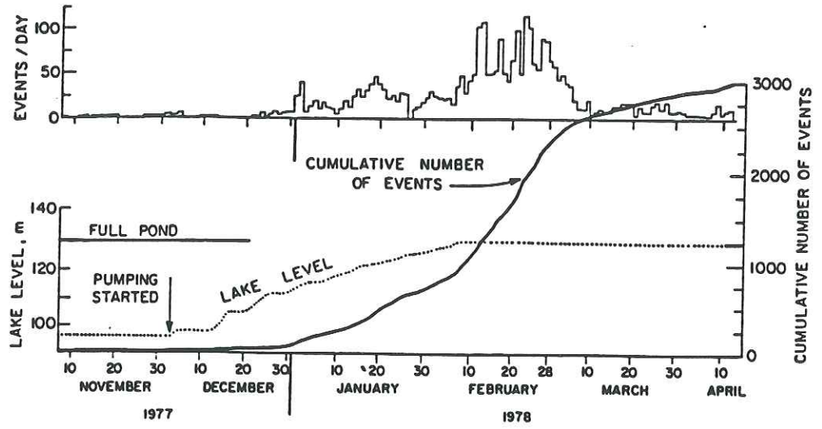

b)

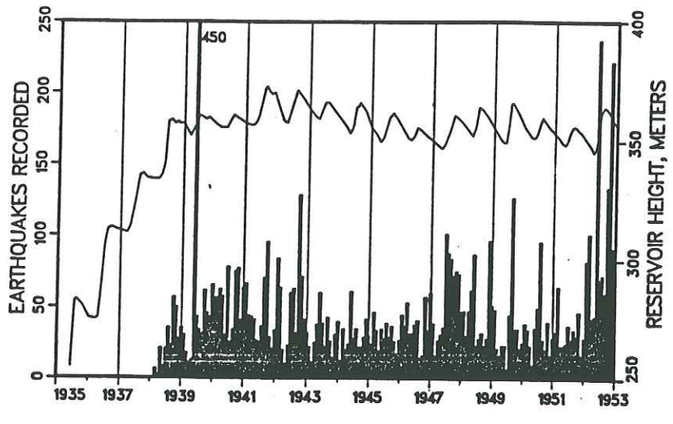

c)

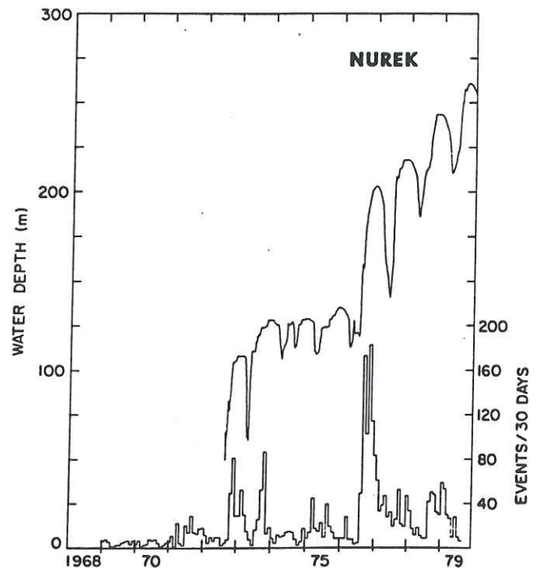

Fig 3

d)

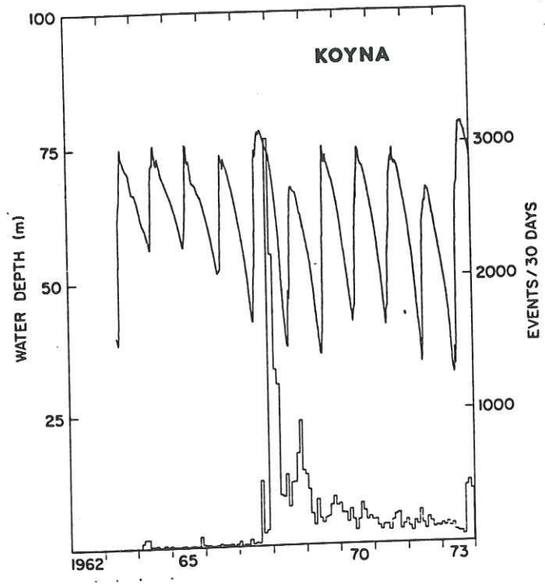

e)

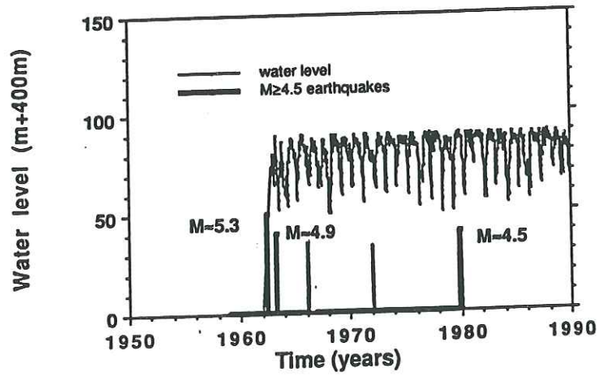

Fig 3

a)

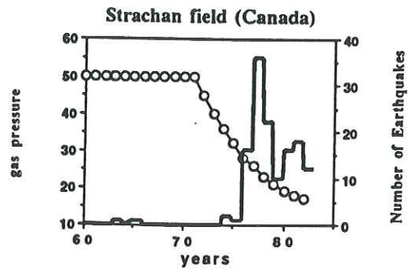

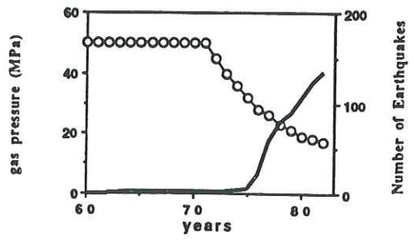

b)

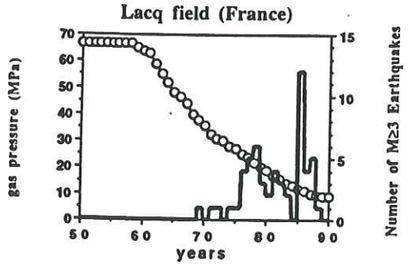

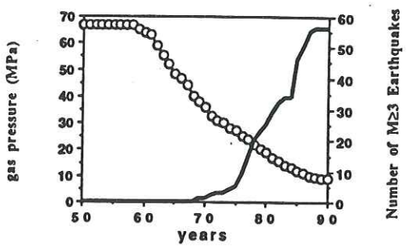

c)

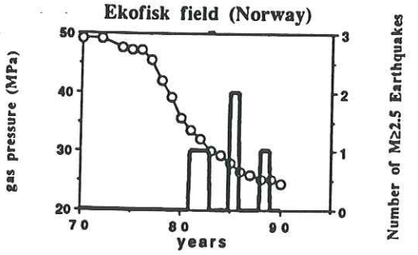

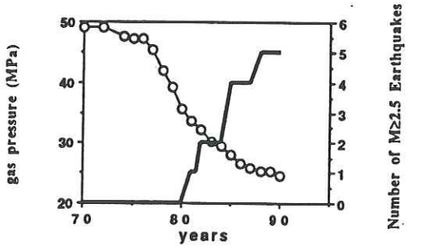

Fig 4

d)

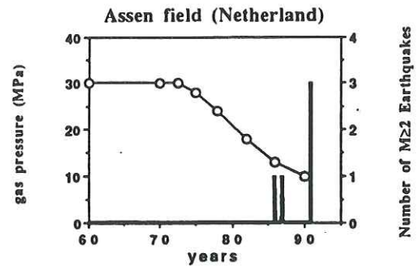

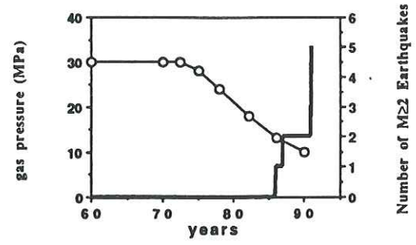

e)

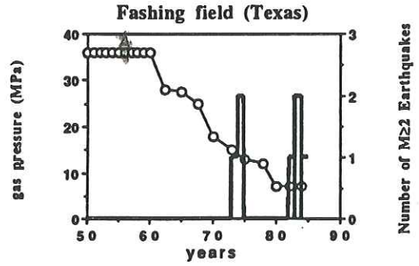

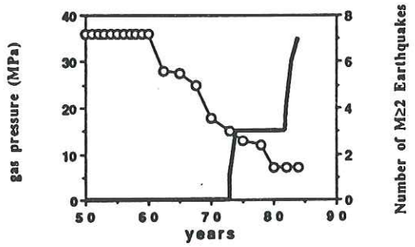

f)

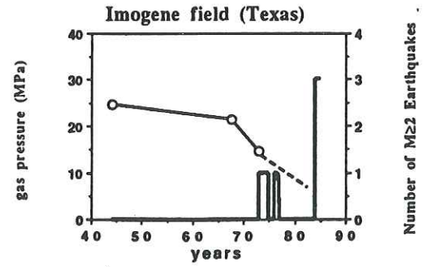

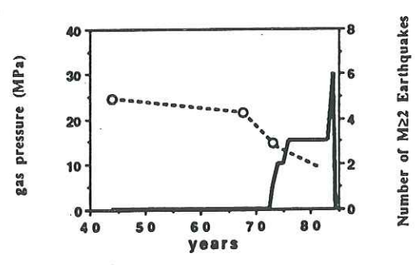

Fig 4

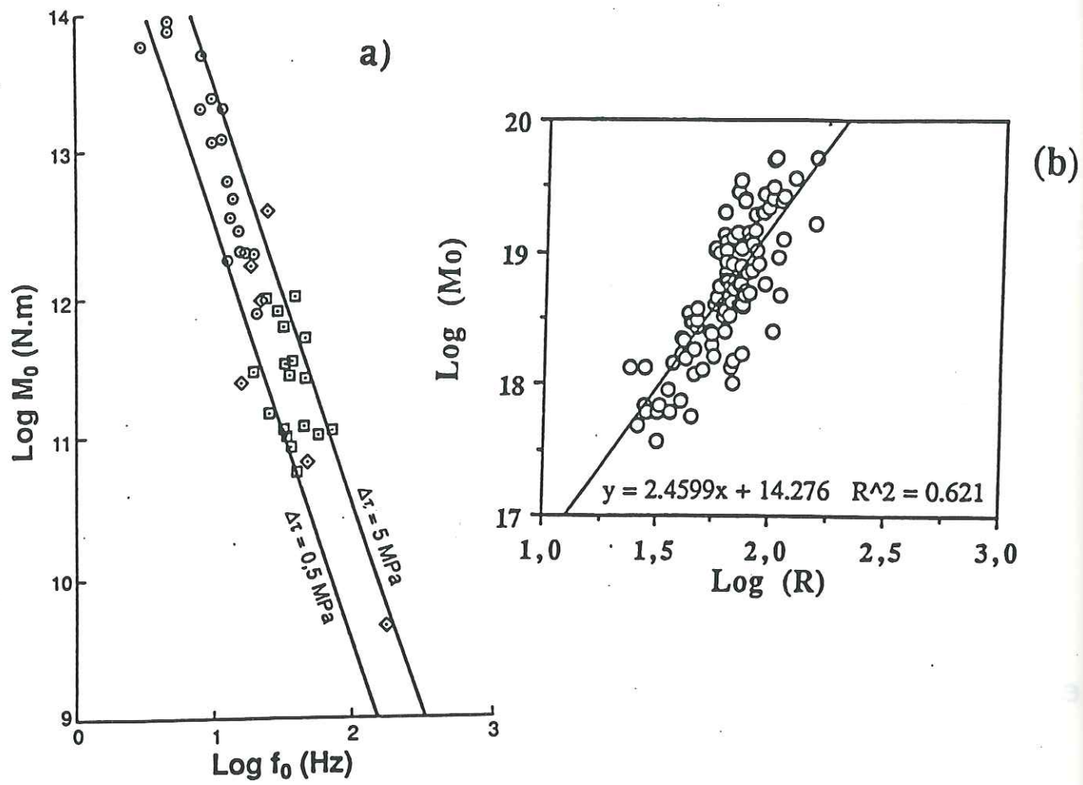
a)
Log M_0 (N.m)
Log f_0 (Hz)
$\Delta\tau$ = 5 MPa
$\Delta\tau$ = 0,5 MPa
(b)
Log (Mo)
Log (R)
y = 2.4599x + 14.276 R^2 = 0.621

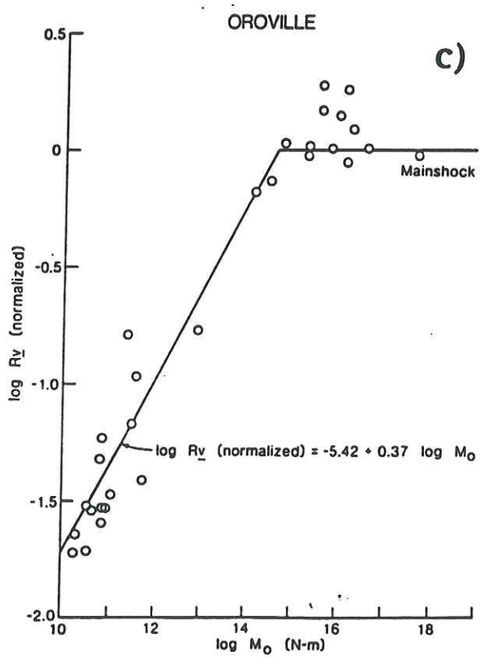
OROVILLE
c)
Mainshock
log $R_{\bar{v}}$ (normalized)
log $R_{\bar{v}}$ (normalized) = -5.42 + 0.37 log M_0
log M_0 (N-m)

Fig 5

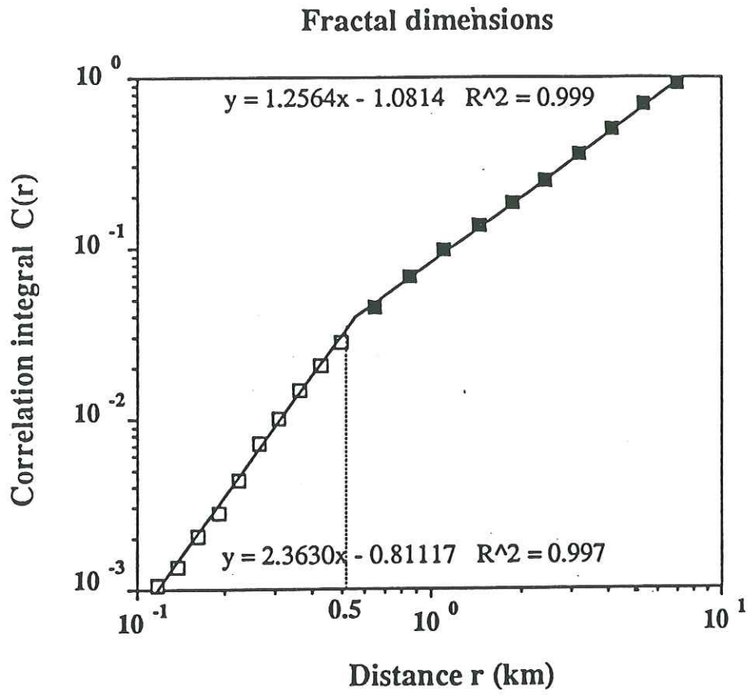
b)
Fractal dimensions
y = 1.2564x - 1.0814 R^2 = 0.999
y = 2.3630x - 0.81117 R^2 = 0.997
Correlation integral C(r)
Distance r (km)

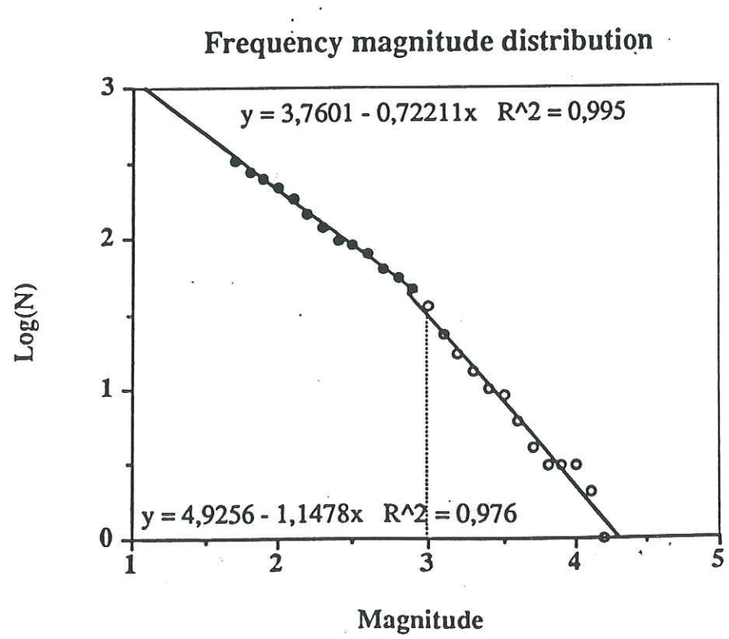
a)
Frequency magnitude distribution
y = 3,7601 - 0,72211x R^2 = 0,995
y = 4,9256 - 1,1478x R^2 = 0,976
Log(N)
Magnitude

Fig 6

c)

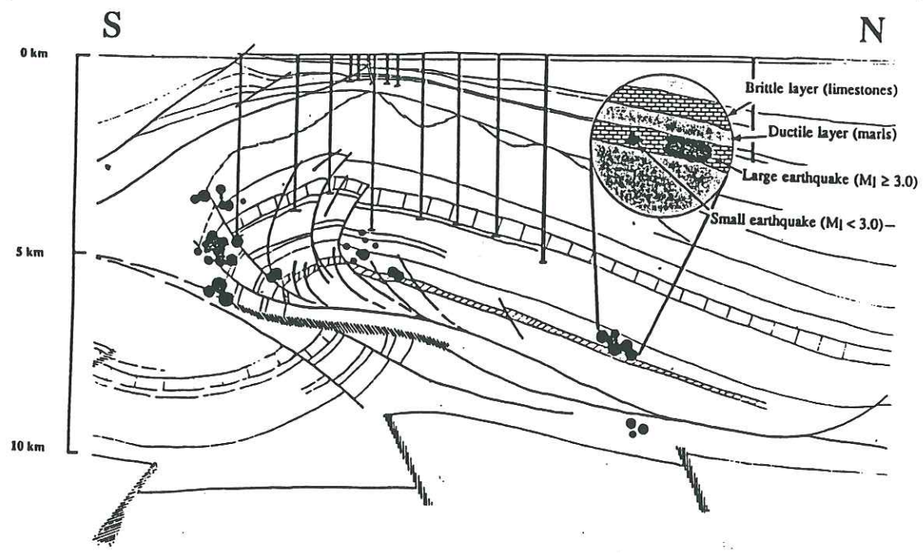
S
N
0 km
5 km
10 km
Brittle layer (limestones)
Ductile layer (marls)
Large earthquake (Ml ≥ 3.0)
Small earthquake (Ml < 3.0)

Fig 6

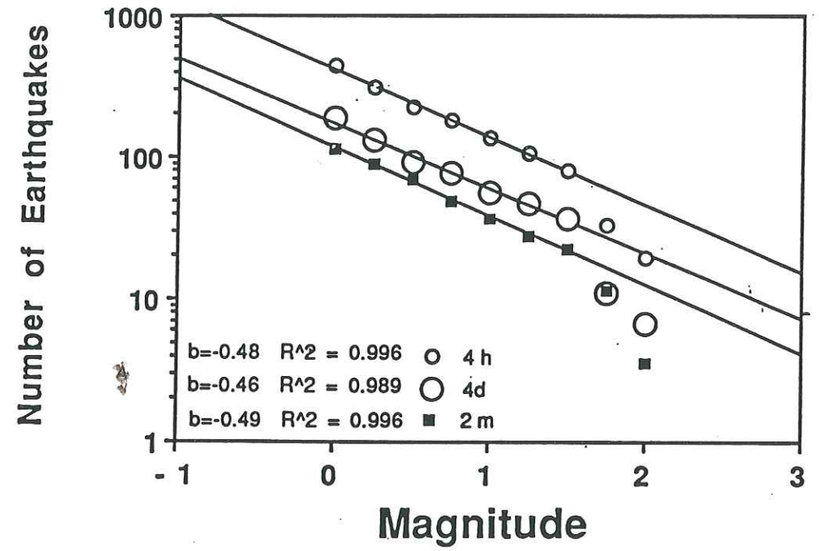
Number of Earthquakes
1000
100
10
1
b=-0.48 R^2 = 0.996 4 h
b=-0.46 R^2 = 0.989 4d
b=-0.49 R^2 = 0.996 2 m
- 1
0
1
2
3
Magnitude

Fig 7

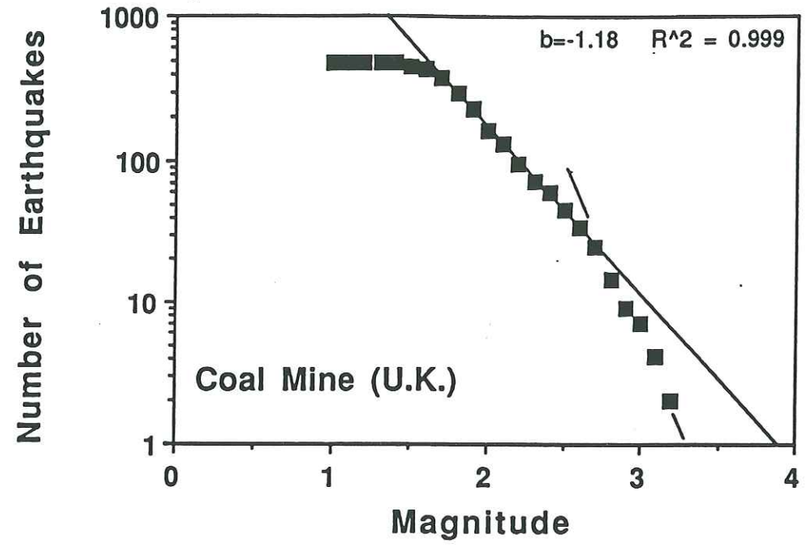

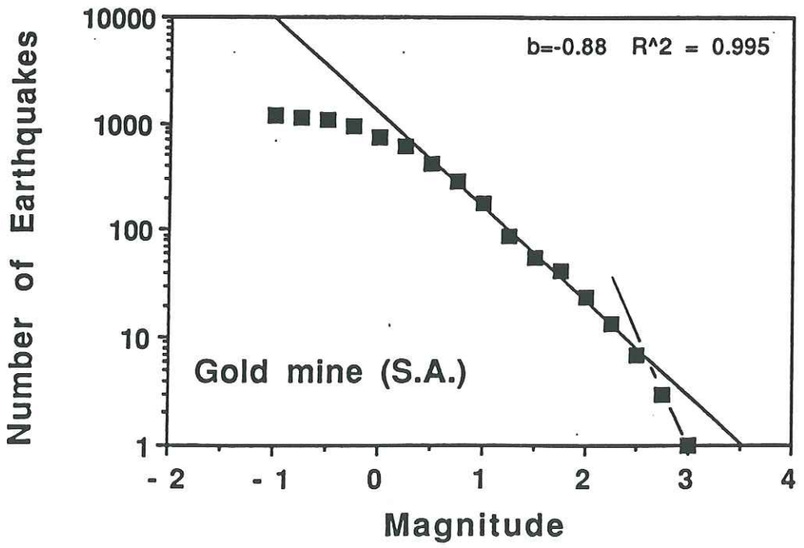

Fig 8

a)

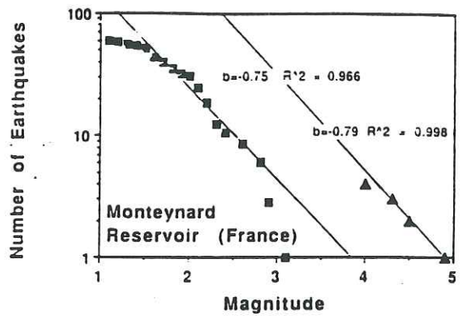

b)

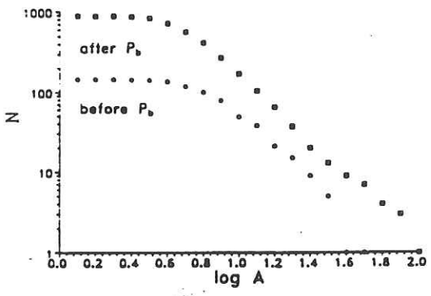

c)

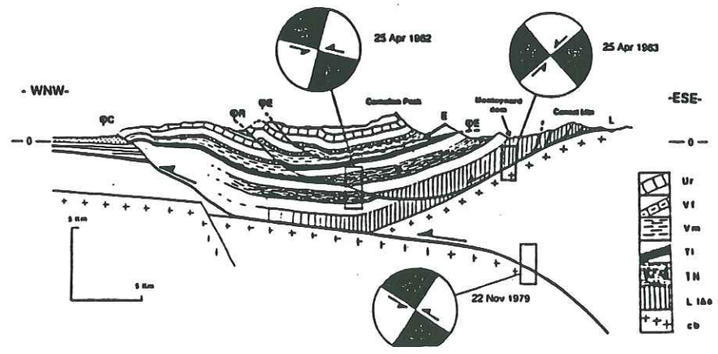

Fig 9

SYNTHESE

HIERARCHIE SPATIALE ET TEMPORELLE DES INSTABILITES SISMIQUES DECLENCHEES DANS LA CROUTE SUPERIEURE

Par l'ensemble des travaux réunis ici, notre contribution à l'analyse du comportement mécanique de la croûte superficielle éclaire des domaines qui intéresseront à la fois les ingénieurs de compagnies pétrolières ou ceux concernés par des problèmes de stockages de déchets, et des géophysiciens impliqués dans la compréhension de la mécanique des instabilités sismiques.

En terme de recherche appliquée, l'analyse mécanique des instabilités sismiques déclenchées par la récupération d'hydrocarbures doit permettre à l'opérateur de dimensionner ses outils de production pour minimiser l'impact possible d'un potentiel de sismicité. Ce dimensionnement peut s'envisager, avant la production par une analyse géomécanique du site qui peut déboucher à la fois sur une géométrie d'implantation des forage, pour éviter les zones de concentrations de contrainte liées par exemple aux fortes déplétions, et sur la définition d'un taux de production qui doit influencer la mise en charge de la structure et le déclenchement des instabilités. Si le contexte tectonique n'exclue pas une réponse de type 3 (M>6) le problème du dimensionnement (prévention passive) pour se prévenir contre de tels mouvements du sol reste un choix de rentabilité financière. D'un point de vue statistique, si ce type de réponse parait possible, le taux d'occurrence ne peut pas, sur la base des données disponibles actuellement, être quantifié. De plus la distance au gisement est peu contrainte et nous devons utiliser de nouvelles données pour mieux définir ce mécanisme. En particulier, la collaboration avec l'industrie pétrolière doit nous permettre de comprendre l'aséismicité (M>3) de nombreuses exploitations, à l'aide d'études géomécaniques pluridisciplinaires.

Cependant certains producteurs, lors d'ouvertures de champs avec des perspectives de production importantes en Amériques du sud ou en Asie centrale (BP, Chevron) envisagent déjà le type séismicité potentiellement déclenchable sur ces sites et les études de risques de séismicité déclenchée sont incluses dans les projets d'exploitations. La rapidité de ce transfert d'information montre l'impact de ce travail dans le milieu industriel.

Le second aspect qui devrait sensibiliser les industriels est l'utilisation de la séismicité induite pour suivre le comportement des réservoirs au cours de leur exploitation. Actuellement les mesures de déformations de surface sont utilisées comme des indicateurs des déformations des extractions. Avec l'approfondissement des sites exploités ces indicateurs de surfaces deviennent

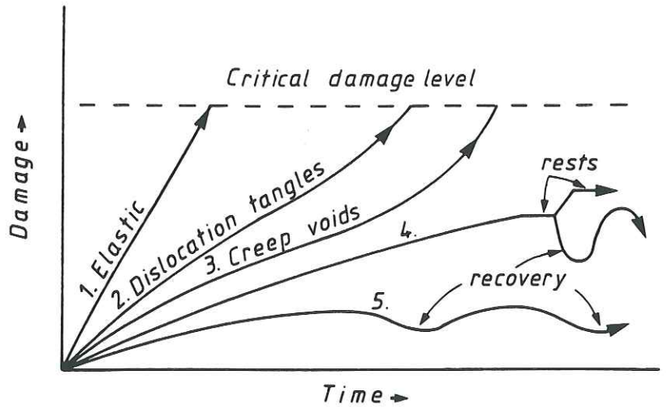

Diagram reviewing the different 'damage' processes which can contribute to failure at a critical damage level. The different paths shown (1–5) illustrate different mechanisms of pre-failure damage accumulation which range from elastic strain energy accumulation (path 1), through dislocation tangles (path 2), to creep void development (path 3). Paths 4 and 5 illustrate deformation paths where the damage build up is interrupted by rest periods or recovery periods when damage is reduced.

Figure C1

moins précis. Par contre, les microséismes sont des indicateurs localisés à proximité des niveaux réservoirs et sont présents (M~1) sur la plupart des réservoirs. Avec des instruments d'enregistrement disposés en fond de forage, une écoute passive des gisements exploités renseignera sur le comportement in-situ du réservoir d'une façon plus directe et complémentaires des mesures de déplacements de surface.

Dans un domaine plus proche de la communauté scientifique, notre contribution à l'analyse du comportement mécanique de la croûte superficielle peut s'évaluer sur un aspect observationnel, où des données pluridisciplinaires contribueront à l'études des différents couplages géomécaniques à partir de l'étude d'objets isolés, et sur un aspect méthodologique en proposant des réflexions sur les échelles d'interactions physiques dans la croûte superficielle (Figure 1, d'aprés Knipe 1987).

En particulier le faible changement de contrainte, qui, sur la base des modéles mécaniques actuels, parait déclencher des instabilités sismiques sur les objets que nous avons étudiés, permet une nouvelle approche des phénomènes précurseurs de séismes. Beaucoup de ces phénomènes, rejetés sur la base d'une mécanique classique trouvent une interprétation possible dans un contexte d'instabilité où la croûte supérieure est vue comme un système dans un état critique auto-organisé. Les études d'objets géologiques isolés où les vitesses de perturbation sont d'un ordre de grandeur supérieur aux sollicitations tectoniques permettent de quantifier les perturbations critiques. Ces conditions expérimentales permettent d'observer à la fois l'apparition, la pérennité et la disparition de système critique auto-organisé. En effet sur des objets de dimensions spatio-temporelles plus faible (échantillon de mécanique des roches) on ne peut observer que la mise en place du systéme critique, car dés la localisation de la rupture, une macro-fracture se développe jusqu'aux bornes géométriques du système. Par opposition dans les zones tectoniquement actives, l'étude de la séismicité renseigne seulement sur les caractéristiques d'un régime critique auto-organisé, régime établi depuis une échelle de temps très grande devant la durée d'observation.

D'un autre point de vue, l'utilisation des lois puissances en séismologie a été un relatif échec en ce qui concerne la mécanique de la rupture. En effet le lien entre la valeur de b , proposé sur la base d'essai en laboratoire, comme étant relié à la contrainte (Mogi, 1963, Scholtz, 1968), et l'occurrence d'un séisme ne s'est pas avéré statistiquement fiable depuis une vingtaine d'année. Par contre, les résultats que nous proposons ici laissent entrevoir des applications possibles

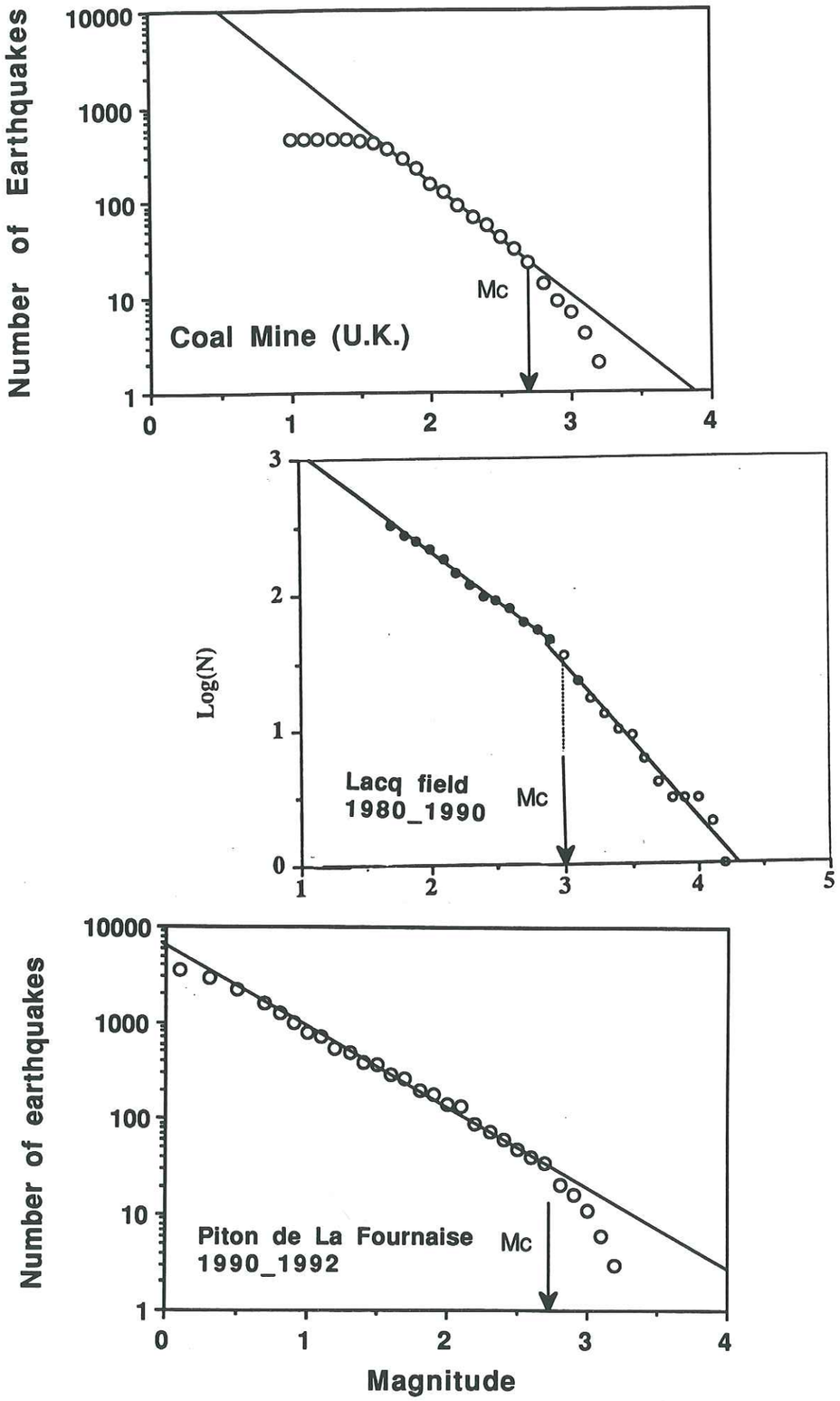

Figure C2

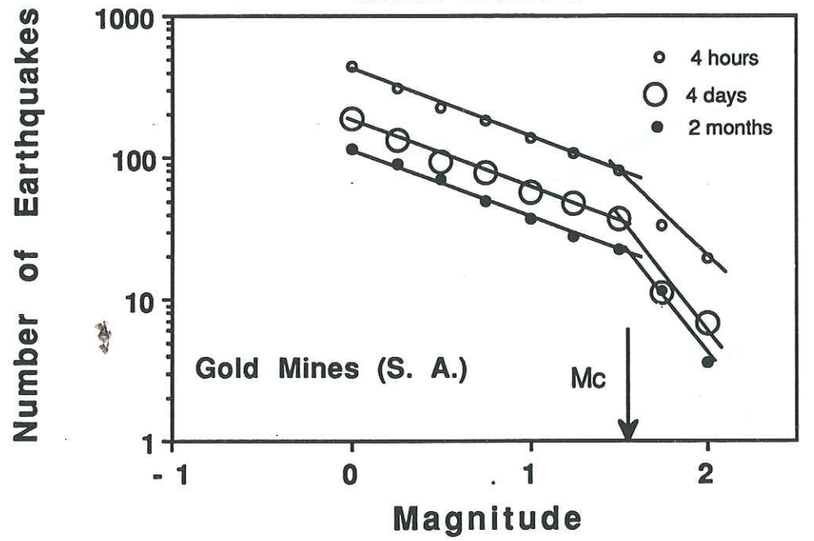

Figure C3

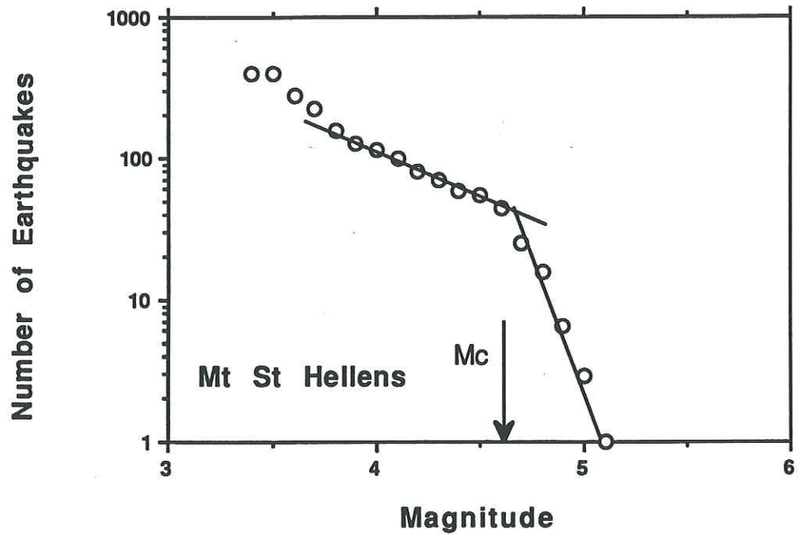

Figure C4

pour la compréhension des mécanismes de ruptures de la croûte terrestre, en utilisant non pas la valeur du coefficient de la loi puissance mais les limites de validité de la loi, par exemple les ruptures de pente. En effet, quels liens entre les magnitudes de coupure des plus forts séismes enregistrés sur des sites où la séismicité est induite par une extraction minière, un réservoir de gaz déplété ou la montée d'un dyke sur un édifice volcanique (Figure 2)? Une fois le problème du temps d'échantillonnage écarté, il y a pérennité de la magnitude de coupure indépendamment de l'intervalle de temps choisi (Figure 3), il nous restent deux possibilités: l'une relie la taille des séismes critiques au résultat de l'interaction entre la dimension de la perturbation mécanique (en terme géométrique ou énergétique) et la rhéologie du milieu (épaisseur des niveaux compétents); d'un autre point de vue, on peut envisager que l'interaction entre les dimensions et la répartition des discontinuités préexistantes dirige la répartition fréquence-taille des ruptures. Sur la base des observations effectués sur les objets géologiques précédemment cités, nous montrons que dans le cas du gisement de lacq, la brisure dans les lois d'échelles fréquence-taille des ruptures est lié à l'épaisseur des niveaux fragiles. Pour les mines, il semble que la géométrie du front de taille, de l'ordre de la centaine de métres corresponde à la brisure de la répartition fractale de la sismicité induite par l'extraction (M~2.5-3). Sur les volcans de type basaltique, cette brisure, M=2.8 sur le Piton de la Fournaise, peut être reliée elle aussi à la géométrie du dyke qui est injecté, typiquement entre 1-3 m d'épaisseur pour une centaine de métres d'extension latérale, donc de dimension proche de celle rencontrée en domaine minier. Enfin lors d'éruption de type explosive, Mt St Hellens par exemple, la brisure proche de M=4.5 (Figure 4), peut être encore reliée à l'épaisseur de la zone fragile (2 km environ sur la base des isothermes). La persistance de brisures dans les répartitions fréquence-taille des ruptures sur différents sites semble donc relier à la géomécanique du milieu. De plus, des déviations aux lois d'échelles sont présentes au second ordre sur de de nombreux diagrammes. On prendra comme exemple la Figure 5 où il est clair que deux mécanismes ou deux population de failles interagissent pour créer cette répartition. D'un autre point de vue, on peut proposer qu'il manque une famille de discontinuité pour que la répartition des ruptures suive les lois d'échelles. Soit la dimension spatiale du site, soit son histoire géomécanique, est trop courte et l'absence d'une répartition fractals de toutes les tailles de discontinuités conduit à l'absence de loi d'échelle pour les ruptures sismiques. Une autre alternative pour expliquer ces brisures et manques dans les lois d'échelles, que l'on doit considérer pour l'ensemble des objets géologiques étudiés ici, consiste en une compétition entre rejeux sismiques (ruptures fragiles) et rejeux

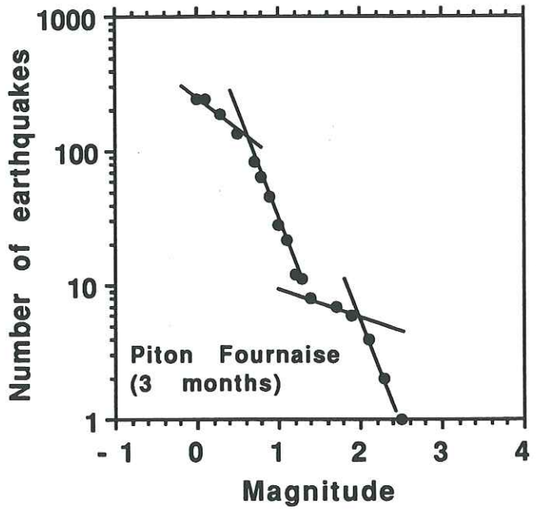

Figure C5

asismiques (déplacements lents). En effet si on considére qu'il a été proposé que l'épaisseur des niveaux fragiles limitait la répartition fractales des tailles de séismes tant à l'échelle de la lithosphére (Pacheco et al. 1992) que sur des objets superficiels (Volant et Grasso, 1993), on peut alors envisager que le changement de pente observé, correspondant à une diminution de la taille des gros séismes relativement à celle des petits, est en fait une mesure d'une modification de la contribution aséismique présente dans toute déformation et déjà observée dans les phase initiales et finales de gros séismes (précurseurs et relaxations lentes de la rupture). Dans ce sens, le manque de faibles magnitudes, sur ces mêmes diagrammes fréquence-taille de séismes, attribué à des problèmes instrumentaux peut aussi être considérer suivant les sites comme une contribution majeure de rejeux asismiques.

Pour conclure, à partir d'une dizaine d'années de contact avec des séismes déclenchés par des faibles perturbations, je proposerai quelques pistes de réflexions.

Les fluides sont vecteurs de transferts de contrainte puissants. En tant qu'indicateurs de perturbations de l'état de la croûte superficielle, ils s'avèrent des agents très intéressant pour la détection de phénomènes précurseurs (variations de niveaux d'eau inexpliquées à grandes distances de séismes), mais malheureusement pas toujours fréquents et souvent instables. Dans ce sens, les changement en contenu gazeux des eaux où les effets électriques de circulation de ces derniéres, sont des indicateurs d'une sensibilité beaucoup plus grande que la mesure du niveau d'eau lui-même et sont des mesures qui pourront potentiellement apporter de nouvelles contraintes sur les processus mécaniques qui sont à la base des observations actuelles.

On doit alors envisager que les modéles de rupture de type Mohr-Coulomb soient redéfinis dans ce nouveau contexte tant au niveau de la signification des paramétres (que représente par exemple les coefficients de friction actuels: statiques, dynamiques,..), que par le choix du critére de rupture: la perte de cohésion avec augmentation de la friction (pour permettre la phase de stabilisation aprés la rupture) lors de la déformation n'est elle pas récemment proposée pour expliquer certains phénomémes en mécaniques des roches?

Du point de vue de la modélisation mécanique, la compétition entre rejeux sismiques et asismiques, la mobilisation partielles ou totales des fractures existantes, sont de nouveaux challenges qui doivent permettre de mieux comprendre la complexité de la répartition des séismes, et leurs interactions à travers des systémes chaotiques.

THESE de DOCTORAT

Titre de l'ouvrage :

FLUIDES ET INSTABILITES SISMIQUES : IMPLICATIONS POUR LE COMPORTEMENT MECANIQUE DE LA CROUTE SUPERIEURE

Nom de l'auteur :

Jean-Robert GRASSO

Etablissement :

Université Joseph Fourier - Grenoble I

RESUME

Sur la base des faibles variations de contraintes poroélastiques qui sont à l'origine de la séismicité déclenchée localement par la baisse de pression du gisement de Lacq, on tente dans le chapitre 3 d'évaluer les échelles spatiales des connections fluides dans la croûte supérieure à l'aide de la migration des fronts de pression induits. Les séismes associés à la mise en eau d'une retenue artificielle (M 4-5, Monteynard, Vercors, France) permettent par exemple de cartographier des failles sismiques potentielles au sud de l'agglomération grenobloise, les séismes induits jouant alors le rôle de jauges de contrainte. Dans la région de Lacq, à l'aide de modélisations analytiques des transferts de contraintes visco-élastiques et poro-élastiques, on montre qu'on ne peut rejeter a-priori des interactions entre l'extraction du champ de Lacq, les séismes majeurs de la faille Nord-Pyrénéenne distants d'une trentaine de kilomètres, et les séismes locaux à l'aplomb du champ d'hydrocarbure.

Le chapitre 4 constitue une synthèse des mécanismes d'instabilités sismiques déclenchées par les exploitations d'hydrocarbures. On isole trois classes de mécanismes de déclenchements des séismes correspondant à des types d'exploitations et à des réponses sismiques (taille-temps-espaces) bien différenciés : augmentation de pression due à l'injection de fluide ; baisse de pression due à extraction de fluide, déficit de masse lors d'extraction massive. Les mécanismes de ruptures sont en accord avec les lois de contraintes effectives, et s'expliquent soit par des transferts poroélastiques soit par des compensations isostasiques. Si la sismicité induite par les extractions de fluides reste marginale par rapport au nombre de gisements exploités, la surveillance sismique fine effectuée sur les gisements montre que de nombreux petits séismes (M < 3) sont présents et permettent un suivi in-situ du comportement des réservoirs au cours de l'exploitation.

Notre approche de la séismicité à l'aide des séismes induits par des activités humaines montre les limites des lois de la mécanique classique qui, si elles permettent de comprendre et d'évaluer les seuils critiques qui déclenchent les instabilités sismiques, ne peuvent expliquer ni la durée des phénomènes d'instabilités qui sont entretenus durant de nombreuses années ni la taille des instabilités sismiques (Mmax 7). Sur la base des cas mondiaux de séismicité induite on propose la notion de Systèmes Critiques Auto-Organisés Induits où l'on peut observer la genèse, la pérennité et la disparition de systèmes critiques dans un contexte, proposé par ailleurs, d'état critique auto-organisé pour l'ensemble de la croûte supérieure.

MOTS CLES

Fluides et failles ; Fractales ; Gazli ; Hydrocarbures ; Lacq ; Mécanique de la croûte ; Monteynard ; Sismicité induite.